Institutional Repository - Research Portal
Dépôt Institutionnel - Portail de la Recherche
researchportal.unamur.be
University of Namur

THESIS / THÈSE

DOCTOR OF BIOMEDICAL AND PHARMACEUTICAL SCIENCES

Characterization of the anticancer properties of hydroxamate-based histone deacetylase inhibitors

Lernoux, Manon

Award date:
2019

Awarding institution:
University of Namur

Link to publication

General rights
Copyright and moral rights for the publications made accessible in the public portal are retained by the authors and/or other copyright owners and it is a condition of accessing publications that users recognise and abide by the legal requirements associated with these rights.

- Users may download and print one copy of any publication from the public portal for the purpose of private study or research.
- You may not further distribute the material or use it for any profit-making activity or commercial gain
- You may freely distribute the URL identifying the publication in the public portal ?

Take down policy
If you believe that this document breaches copyright please contact us providing details, and we will remove access to the work immediately and investigate your claim.

Download date: 02. May. 2026

Characterization of the anticancer properties of hydroxamate-based histone deacetylase inhibitors

Manon LERNOUX

Thèse présentée en vue de l'obtention du grade de Docteur en Sciences Biomédicales

Laboratoire de Biologie Moléculaire et Cellulaire du Cancer (LBMCC)
Fondation de Recherche « Cancer et Sang » (FRCS), Hôpital Kirchberg, Luxembourg

UNIVERSITÉ DE NAMUR

Characterization of the anticancer properties of hydroxamate-based histone deacetylase inhibitors

Manon LERNOUX

Thesis submitted for the purpose of obtaining the grade of PhD in Biomedical Sciences

Laboratoire de Biologie Moléculaire et Cellulaire du Cancer (LBMCC)
Fondation de Recherche « Cancer et Sang » (FRCS), Hôpital Kirchberg, Luxembourg

Jury members

Co-promoters:

Pr. Marc DIEDERICH (Seoul National University, South Korea)
Pr. Carine MICHIELS (URBC, UNamur, Belgium)

Supervisor:

Dr. Michael SCHNEKENBURGER (LBMCC, Luxembourg)

Pr. Thierry ARNOULD (URBC, UNamur, Belgium) – president
Pr. Pierre SONVEAUX (FATH, UCLouvain, Belgium)
Pr. Johan WOUTERS (UCPTS, UNamur, Belgium)
Pr. Jean-Pierre GILLET (URPhyM, UNamur, Belgium)
Pr. Mario DICATO (FRCS, Luxembourg)

The work presented in this PhD thesis has been performed

at « Laboratoire de Biologie Moléculaire et Cellulaire du Cancer »,

Hôpital Kirchberg, Luxembourg

This work would not have been possible without the financial support of:

« Télévie Luxembourg » (bourse de formation-recherche Télévie)

« Recherche Cancer et Sang (FRCS) » foundation,

« Recherches Scientifiques Luxembourg (RSL) » association,

Action Lions « Vaincre le Cancer » association and

« Een Häerz fir kriibskrank Kanner (A heart for cancer-sick children) » association

Acknowledgements

As the writing of this manuscript is coming to an end, I would like to thank all the persons who made my thesis possible and participated in the completion of this work.

The research reported in the following pages was performed at the « Laboratoire de Biologie Moléculaire et Cellulaire du Cancer » in Luxembourg. I am grateful to Pr. Marc Diederich, head of the lab and director of my thesis, for his involvement in all the steps of my traineeship and his advices that allowed me to widen my research from various perspectives. Thank you for giving me the great opportunity to carry out some experiments in Seoul, it was instructive in many aspects.

I cannot find words to express my gratitude to Pr. Carine Michiels for accepting the co-directorship of my thesis. A special thank you for your administrative help, availability, and support!

I wish to acknowledge my advisor Dr. Michael Schnekeburger for the continuous support throughout my 4-year PhD study and related research, for his patience and selfless time. His enriching and constructive scientific guidance, as well as his incredible attention to details helped me in the progression of my research, as well as in the writing of quality manuscripts.

During my thesis, I benefited from a Télévie grant essential to accomplish my thesis. I appreciate that Pr. Mario Dicato allowed me to work under a contract of the Foundation « Recherche Cancer et Sang » of which he is the president.

I am also indebted to the members of my thesis committee and jury: Pr. Carine Michiels, Pr. Yohan Wouters, Pr. Thierry Arnould, Pr. Jean-Pierre Gillet and Pr. Pierre Sonveaux for their interest in my work, and also for their insightful comments and suggestions. I also express my appreciation to Guy Bormans and his team for providing me with the compounds that were studied intensively for 4 years.

Finally, I am thankful to Pr. Christophe Pierreux and Dr. Mylah Villacorte, who welcomed me into their team as a master student and taught me with passion the basis of lab research.

Merci à mes collègues pour leur expérience scientifique, partagée avec plus ou moins d'enthousiasme. Plus particulièrement, merci à Hélène pour les mois passés à Séoul, pour nos innombrables discussions et ton soutien qui ont permis d'alléger les instants de doute et les périodes difficiles qui font partie intégrante d'un doctorat; à Marion et Esma qui, malgré leur départ avant la fin de ce travail de longue haleine, m'ont apporté de la positivité, de la motivation et de l'énergie indispensables pour tenir le coup ; à Cindy qui s'est donné la lourde tâche de me redonner confiance quoi qu'il arrive ; à Franck, Anthoula, Sébastien et Déborah pour nos conversations de toutes sortes lors des temps de midi et autres moments passés ensemble !

Merci à mes anciens collègues et amis du laboratoire Cell ! Malgré la distance qui s'est progressivement installée, je n'oublie pas les merveilleux instants partagés, pendant et après mon passage dans le laboratoire. Vous m'avez démontré que l'ambiance agréable au travail, les pauses non scientifiques, les soirées pour souder les liens sont une part non négligeable de la motivation à se lever pour aller bosser !

Merci à la meilleure équipe Mowha, ainsi qu'à Benoit, Céline et Sophie ! Il me faudrait plus de pages que ma thèse pour vous dire tout ce que vous représentez pour moi. Les repas, les voyages, vos sourires, votre présence sans faille, votre générosité, votre écoute, nos discussions en tous genres… en bref, votre inestimable amitié a contribué très fortement à me permettre de rester debout jusqu'à la fin de cette aventure !

Merci aux BIOMED / SBIM : Nora, Math, Sansan, Louise, Laurent, Gloria, Cha, pour ces neuf années d'étude intense, entrecoupée d'instants beaucoup plus légers tels que les voyages au ski, les vins chauds sur le marché de Noël, les heures passées à simplement se raconter nos vies et les nombreuses soirées dont certaines restent des histoires marrantes à raconter… enfin, ça dépend pour qui !

Merci à mes nombreux coloc's, et tout spécialement à Jansi, Cha, et Débo pour nos conversations quotidiennes, pour le sport en salle et la découverte des trails, pour les soirées détentes sur la terrasse, pour les fous rires, pour la Schueberfouer, pour la coupe du monde de foot, pour les gin to', et j'en passe ! Tant de super moments passés à Arlon et environs (oui, oui, c'est possible) qui resteront à jamais gravés dans ma mémoire !

The last but not least… Un énorme **merci** à mes parents et à mon frère d'avoir fait de moi qui je suis, de supporter mes humeurs, de me donner du courage afin que je ne baisse pas les bras, d'être présents pour moi en toutes circonstances, de me conseiller comme vous savez si bien le faire, et d'encourager mes projets depuis mes premiers jours sur cette planète. On ne choisit pas sa famille, mais je vous choisirais à chaque fois !

Table of Contents

List of abbreviations

List of figures

List of tables

Preamble

Introduction **1**

1. Histones **1**

1.1. From histones to chromatin 1

1.2. Histone modifications 1

2. Acetylation of histone and non-histone proteins **2**

3. Histone acetyltransferases **3**

3.1. HAT classification and structure 3

3.2. HAT families 4

3.3. HAT functions 5

4. Histone deacetylases **5**

4.1. Classification 5

4.2. Regulation of HDAC activities 6

4.3. HDAC and cancer 7

4.3.1. Cellular proliferation 8

4.3.2. Hematopoietic differentiation 8

4.3.3. Angiogenesis and metastasis 9

5. HDAC inhibitors **9**

5.1. Classification and structure 9

5.2. Consequences of HDAC inhibition 11

5.2.1. ER stress 13

5.2.2. Autophagy 15

5.2.3. Apoptosis 17

5.3. Most common HDACi 19

5.3.1. “Short-chain fatty acid” family: sodium butyrate and valproic acid 19

5.3.2. “Benzamide” family: MS-275 and MGCD103 20

5.3.3. “Hydroxamic acid” family: SAHA 20

5.3.4. “Depsipeptide” family: FK228 20

6. The isoenzyme HDAC6 22
6.1. From gene expression to protein structure 22
6.2. Regulation of HDAC6 activity 23
6.3. Physiological roles of HDAC6 24
6.3.1. Cytoskeletal dynamics 24
6.3.1.1. α-Tubulin 24
6.3.1.2. Cortactin 26
6.3.2. HDAC6 and misfolded proteins 26
6.3.2.1. Repair of misfolded proteins 27
6.3.2.2. Proteasomal degradation 28
6.3.2.3. Autophagic degradation 28
6.3.2.4. Unfolded protein response and cell death 29
6.3.3. Apoptosis 29
6.3.4. Transcriptional repression 31
6.3.5. Pro-oxidant activity 32
6.4. HDAC6 in cancer 32
6.4.1. Tumor progression 34
6.4.2. Angiogenesis 34
6.4.3. Epithelial-to-mesenchymal transition 35
6.4.4. Aggressiveness: migration, invasion and metastasis 35
6.4.5. Cancer resistance to therapeutic agents 36
7. HDAC6 inhibitors 36
7.1. Tubacin 37
7.2. Tubastatin A 37
7.3. ACY-1215 38
8. Cancers 40
8.1. Chronic myeloid leukemia 40
8.1.1. Classification of leukemia 40
8.1.2. Epidemiology 40
8.1.3. Pathophysiology 40
8.1.4. Current treatments 41
8.1.4.1. First-generation inhibitor: imatinib 42
8.1.4.2. Second-generation inhibitors: dasatinib, nilotinib, and bosutinib 43
8.1.4.3. Third-generation inhibitor: ponatinib 44
8.1.4.4. HDAC inhibitors 46

8.2. Multiple myeloma 47
8.2.1. Epidemiology 48
8.2.2. Diagnostic criteria 49
8.2.3. Pathophysiology 49
8.2.4. Current treatments 50
8.2.4.1. Proteasome inhibitors 51
8.2.4.2. HDAC and HDAC6 inhibitors 51
9. MAKV compounds 54
9.1. MAKV-8 and derived compounds 54
9.2. MAKV-15 compound 55
Objectives 56
Material and methods 58
1. Cell culture 58
1.1. Cell models 58
1.2. Healthy models 60
1.2.1. Proliferating and non-proliferating peripheral blood mononuclear cells 60
1.2.2. Platelets 62
1.2.3. RPMI-1788 cells 62
1.2.4. CD34+ cells 62
1.3. Transfections 63
1.4. Chemicals and cell treatments 64
1.5. Cell viability and proliferation test 65
2. Computational analysis of public CML datasets 65
3. Docking studies 65
4. Protein extractions 66
4.1. Total extraction 66
4.2. Acid extraction 66
4.3. Determination of protein concentration with Bradford method 66
5. Western blot 67
6. *In vitro* HDAC activity assay 69
7. Clonogenic assay 71
8. Evaluation of nuclear morphology by fluorescent microscopy 71
9. Study of mitochondrial membrane potential by flow cytometry 72

10. Assessment of apoptosis induction by flow cytometry 72
11. Analysis of cell morphology with Giemsa staining..... 73
12. Monitoring autophagy in live cells..... 73
13. Transmission electron microscopy 74
14. Cell cycle analysis by flow cytometry 74
15. Analysis of gene expression 75
15.1. RNA extraction 75
15.2. Reverse transcription..... 75
15.3. End-point polymerase chain reaction..... 76
15.4. Real-time PCR 77
16. Study of ALDH+ population 77
17. Tumor growth evaluation of xenografted cells in zebrafish..... 78
18. Statistical analysis 79

Results 80

1. Characterization of the anticancer properties of a new hydroxamate-based pan-HDACi: MAKV-8..... 80
1.1. *In vitro* inhibitory potential of MAKV-8 on HDAC isoenzymes 80
1.2. MAKV-8 significantly induces target protein acetylation 85
1.3. The potent pan-HDACi MAKV-8 displays cytotoxic properties in CML cells 88
1.4. MAKV-8 derivatives are less potent molecules than their parent compound 90
1.5. MAKV-8 induces cell cycle arrest and apoptotic cell death in CML cells..... 95
1.6. MAKV-8 triggers ER stress, stimulates autophagic flux, and provokes DNA damage 99
1.6.1. Evaluation of ER stress induction 99
1.6.2. Evaluation of autophagy induction 101
1.6.3. Evaluation of the induction of double strand breaks 106
1.7. MAKV-8 in combination with imatinib displays synergistic pro-apoptotic activity in imatinib-sensitive and -resistant CML cells, and mild toxicity in healthy cell models 107
1.7.1. Evaluation of MAKV-8-imatinib co-treatments in imatinib-sensitive CML cell lines . 107
1.7.2. Evaluation of MAKV-8-imatinib co-treatments in imatinib-resistant CML cell lines .. 117
1.7.3. Determination of MAKV-8-imatinib-mediated toxicity on healthy models 120
1.8. Beclin 1 knock-down reduces MAKV-8-imatinib combination-induced apoptosis..... 124
1.9. MAKV-8 and imatinib co-treatment synergistically lessens BCR-ABL-related signaling pathways involved in CML cell growth and survival 126
1.10. MAKV-8 and imatinib co-treatment reduces stem cell population 128

2. Characterization of the anticancer properties of MAKV-15, a new hydroxamate-based selective HDAC6i 130

2.1. *In vitro* inhibitory potential of MAKV-15 and tubastatin A on HDAC isoenzymes 130

2.2. *In cellulo* study of MAKV-15 and tubastatin A 133

2.2.1. Study of MAKV-15 in CML cells 133

2.2.1.1. MAKV-15 acts as a potent HDAC6i in CML cells 133

2.2.1.2. Selectively inhibiting HDAC6 is insufficient to reduce CML cell proliferation and viability 134

2.2.1.3. High concentrations of MAKV-15 induce cell cycle arrest and apoptotic cell death in CML cells 135

2.2.2. Study of MAKV-15 in MM cells 137

2.2.2.1. MAKV-15 acts as a potent HDAC6i in MM cells 137

2.2.2.2. Selectively inhibiting HDAC6 is insufficient to reduce MM cell proliferation and viability 139

2.2.2.3. HDAC6i in combination with bortezomib in MM 141

2.2.2.4. HDAC6i in a tri-therapy for MM 144

2.2.2.4.1. Screening of chemotherapeutical compounds for efficient tri-therapies in combination with HDAC6i and bortezomib 144

2.2.2.4.2. BCL-2 family protein inhibitors as a third compound for efficient tri-therapies in combination with HDAC6i and bortezomib 145

Discussion 151

1. Characterization of the anticancer properties of a new hydroxamate-based pan-HDACi: MAKV-8 151

2. Characterization of the anticancer properties of a new hydroxamate-based selective HDAC6i: MAKV-15 158

2.1. CML cells 159

2.2. MM cells 159

Conclusions and Perspectives 162

1. Characterization of the anticancer properties of a new hydroxamate-based pan-HDACi: MAKV-8 162

2. Characterization of the anticancer properties of a new hydroxamate-based selective HDAC6i: MAKV-15 166

3. "Take home" message 169

References 170

Annexes 197

Abbreviation List

ABC	ATP-binding cassette
ACTR	Activator of thyroid and retinoic acid receptor
ADP	Adenosine diphosphate
AF	Activation function
AIB	Amplified in breast
ALDH	Aldehyde dehydrogenase
ALL	Acute lymphocytic leukemia
AMBRA	Activating molecule in beclin 1-regulated autophagy protein
AML	Acute myeloid leukemia
AMP	Adenosine monophosphate
AMPK	AMP-activated protein kinase
ANOVA	Analysis of variance
APAF	Apoptotic peptidase activating factor
APL	Acute promyelocytic leukemia
AR	Androgen receptor
ARD1	Arrest-defective-1 protein
ATAT	α-tubulin acetyltransferase
ATCC	American Type Culture Collection
ATF	Activating transcription factor
ATG	Autophagy-related protein
ATP	Adenosine triphosphate
BAK	BCL-2 homologous antagonist/killer
BAX	BCL-2-associated X protein
BCL	B-cell lymphoma
BCL-xL	BCL-extra large
BCR-ABL	Breakpoint cluster region - Abelson murine leukemia viral oncogene homolog 1
BID	BH3 interacting domain death agonist
BM	Bone marrow
BMP	Bone morphogenetic protein
BMSC	BM stromal cell
BSA	Bovine serum albumin
BUZ	Ubiquitin-binding domain
CAD	Caspase-activated DNase
CBP	CREB-binding protein
CD	Cluster of differentiation
cdc	Cell-division cycle protein
CDK	Cyclin-dependent kinase
CDKN	CDK inhibitor
CDY	Chromodomain protein, Y-linked
CDYL	CDY-like
CFSE	5,6- carboxyfluorescein diacetate succinimidyl ester
CHOP	CCAAT/enhancer-binding protein homologous protein
CI	Combination index
CK	Casein kinase
CLIP	Cytoplasmic linker protein

CLL	Chronic lymphocytic leukemia
CML	Chronic myeloid leukemia
CREB	cAMP response element-binding protein
CrkL	Crk-like protein
CRM	Chromosome region maintenance
CTCL	Cutaneous T-cell lymphoma
CXCR	C-X-C chemokine receptor
CYLD	Cylindromatosis
CYP	Cytochrome P450
DD	Deacetylase domain
DEAB	Diethylaminobenzaldehyde
DISC	Death inducing signaling complex
DMB	Dynein motor binding
DMEM	Dulbecco's Modified Eagle's medium
DMSO	Dimethylsulfoxide
DNA	Deoxyribonucleic acid
DPBS	Dulbecco's PBS
DSB	Double strand break
DSMZ	Deutsche Sammlung für Mikroorganismen und Zellkulturen
EB	End-binding protein
EC	Effective concentration
ECe	Endothelial cell
EDTA	Ethylenediaminetetraacetic acid
EGFR	Epidermal growth factor receptor
eIF	Eukaryotic initiation factor
ELP	Elongator complex protein
EMT	Epithelial-to-mesenchymal transition
ER	Endoplasmic reticulum
EsR	Estrogen receptor
ERBB2	Erb-B2 receptor tyrosine kinase
ERK	Extracellular signal-regulated kinase
ERST	ER stress-tolerance
ESCO	Establishment of cohesion *N*-acetyltransferase
FADD	Fas-associated protein with death domain
FCS	Fetal calf serum
FDA	Food and Drug Administration
FGF	Fibroblast growth factor
FGFR	FGF receptor
FIP200	FAK family kinase-interacting protein of 200 kDa
FL2-A	FL2-area
FL2-W	FL2-width
FLICE	FADD-like IL-1 β-converting enzyme
FLIP	FLICE inhibitory protein
FLT	Fms-related tyrosine kinase
GAB	GRB2-associated-binding protein
GBM	Glioblastoma
GCN	General control non-derepressible
GNAT	GCN5 related *N*-acetyltransferase

GR	Glucocorticoid receptor
GRB	Growth factor receptor-bound protein
GRIP	Glutamate receptor-interacting protein
GRK	G protein-coupled receptor kinase
GRP78	78 kDa glucose-regulated protein
GSK	Glycogen synthase kinase
γH2AX	Phosphorylated histone H2AX
HAT	Histone acetyl transferase
HBO1	Human acetylase binding to ORC1
HCC	Hepatocellular carcinoma
Hda	Histone deacetylase (yeast)
HDAC	Histone deacetylase
HDAC6i	Histone deacetylase 6 inhibitor
HDACi	Histone deacetylase inhibitor
HIF	Hypoxia-inducible factor
HMGB	High mobility group box
HPF	HiPerFect Transfection Reagent
HSC	Healthy stem cell
HSF	Heat shock transcription factor
HSP	Heat shock protein
hTERT	Human telomerase reverse transcriptase
IAP	Inhibitor of apoptosis
IC	Inhibitory concentration
iCAD	Inhibitor of CAD
ICAM	Intercellular adhesion molecule
ICD	Immunogenic cell death
IGF	Insulin-like growth factor
IGH	Immunoglobulin heavy locus
IIp	Invasion inhibitory protein
IL	Interleukin
IMiD	Immunomodulatory drug
IMDM	Iscove's Modified Dulbecco's Medium
IRE	Inositol-requiring enzyme
IRF	Interferon regulatory factor
JAK	Janus kinase
JCRB	Japanese Collection of Research Bioresources
JNK	c-Jun N-terminal kinase
LC	MT-associated protein 1 light chain
LCoR	Ligand-dependent nuclear receptor co-repressor
LSC	Leukemic stem cell
MAPK	Mitogen-activated protein kinase
MCL	Myeloid cell leukemia
MDR	Multi-drug resistance protein
MGUS	Monoclonal gammopathy of undetermined significance
miR	Micro-RNA
MM	Multiple myeloma
MMP	Mitochondrial membrane potential
MOZ	Monocytic leukemia zinc finger protein

MORF	MOZ-related factors
mRNA	Messenger RNA
MT	Microtubule
MTOC	MT organizing center
mTOR	Mammalian target of rapamycin
MTT	3-(4,5-dimethylthiazol-2-yl)-2,5-diphenyltetrazoliumbromide
N-CoR	Nuclear receptor co-repressor
NAD	Nicotinamide adenine dinucleotide
NAT	Nα-acetyltransferase complex
NES	Nuclear export signal
NF-κB	Nuclear factor kappa-light-chain-enhancer of activated B cells
NLS	Nuclear localization signal
NOC	Nitrile oxide cycloaddition
OCT	Organic cation transporter
PARP	Poly (ADP-ribose) polymerase
PBMC	Peripheral blood mononuclear cell
PBS	Phosphate buffer saline
PCAF	p300/CBP-associated factor
pCIP	p300/CBP co-integrator-associated protein
PCR	Polymerase chain reaction
PDB	Protein Data Bank
PDGF	Platelet-derived growth factor
PE	Phosphatidylethanolamine
PERK	Protein kinase RNA-like ER kinase
PHA	Phytohaemoagglutinin
PI	Propidium iodide
Pi	Proteasome inhibitor
PI3K	Phosphoinositide 3-kinase
PIN	Peptidylprolyl cis/trans isomerase NIMA-interacting
PKA	Protein kinase A
PML	Promyelocytic leukemia
PP	Protein phosphatase
PPAR	Peroxisome proliferator-activated receptor
pRb	Retinoblastoma protein
Prx	Peroxiredoxin
PS	Phosphatidylserine
PTCL	Peripheral T-cell lymphoma
PTM	Post-translational modification
PTPN6	Protein tyrosine phosphatase non-receptor type 6
PVDF	Polyvinylidene difluoride
QSAR	Quantitative structure-activity relationship
RAC	Ras-related C3 botulinum toxin substrate
RAR	Retinoic acid receptor
RASSF	Ras association domain family member
RhoB	Ras homolog family member B
RNA	Ribonucleic acid
ROS	Reactive oxygen species
Rpd	Reduced potassium dependency (yeast)

RPMI	Roswell Park Memorial Institute
RRMM	Relapsed or refractory MM
RT	Room temperature
RUNX	Runt-related transcription factor
SAHA	Suberoylanilide hydroxamic acid
SCID	Severe combined immunodeficient
SCF	Stem cell factor
SCLC	Small cell lung cancer
SD	Standard deviation
SDS-PAGE	Sodium dodecyl sulfate polyacrylamide gel electrophoresis
SE14	Cytoplasmic retention domain
SERCA	Sarco/endoplasmic reticulum Ca2+ ATPase
Sir	Silent information regulator (yeast)
siRNA	Small interfering RNA
SIRT	Sirtuin
SLAM	Signaling lymphocyte activation molecule
SMAR	Scaffold/matrix attachment region binding protein
SMRT	Silencing mediator for retinoid or thyroid-hormone receptor
SOS	Son of sevenless
Sp	Specificity protein
SQSTM	Sequestosome
SRC	Steroid receptor cofactor
STAT	Signal transducer and activator of transcription
t-RA	All trans retinoic acid
TAFII250	TATA box binding protein-associated factor 250 kDa
Tau	Tubule-associated unit
TBL1X	Transducer beta-like 1, X-linked
TBP	Trx binding protein
TEM	Transmission electron microscopy
TFIIIC	Transcription factor IIIC 220 kDa subunit
TGF	Transforming growth factor
TGFβR	TGFβ receptor
TKi	Tyrosine kinase inhibitor
TIF	Transcriptional mediators/intermediary factor
TIP60	Type 1 interacting protein
TNF	Tumor necrosis factor
TP53	Tumor protein p53
TPPP	Tubulin polymerization-promoting protein
TRAF	TNF receptor associated factor
TRAM	Translocation associated membrane protein
TRIM	Tripartite motif containing
Trx	Thioredoxin
TSG	Tumor suppressor gene
ULK	Unc-51 like autophagy activating kinase
UPR	Unfolded protein response
UVRAG	Ultra-violet radiation resistance associated protein
VCP	Valosin-containing protein
VDR	Vitamin D receptor

VEGF	Vascular endothelial growth factor
VEGFR	VEGF receptor
VHL	von Hippel-Lindau
VPA	Valproic acid
VPS	Vacuolar protein sorting
XBP	X-box binding protein
XIAP	X-linked inhibitor of apoptosis protein
YY	Yin Yang
Z-VAD-FMK	Carbobenzoxy-valyl-alanyl-aspartyl-[O-methyl]- fluoromethylketone
ZBG	Zinc binding group

List of Figures

Figure 1: Reciprocal histone HDAC-mediated deacetylation and HAT-mediated acetylation..2
Figure 2: Reactions of HDAC-mediated deacetylation and HAT-mediated acetylation.....3
Figure 3: Prototypical pharmacophoric model of HDAC inhibitors (HDACi). 10
Figure 4: Consequences of HDAC inhibition. 12
Figure 5: ER stress induction elicits UPR signaling pathways. 14
Figure 6: Autophagic machinery. 16
Figure 7: Apoptosis pathways. 18
Figure 8: Molecular structures of Food and Drug Administration-approved HDAC inhibitors. 21
Figure 9: Schematic structure of HDAC6. 23
Figure 10: Role of HDAC6 in cell division and migration. 25
Figure 11: Reciprocal reaction of acetylation-deacetylation on lysine 40 of α-tubulin catalyzed by α-tubulin acetyltransferase (ATAT)1 and histone deacetylase (HDAC)6, respectively. 25
Figure 12: Role of HDAC6 in protein degradation. 27
Figure 13: HDAC6 possesses anti-apoptotic properties. 30
Figure 14: HDAC6 participates in gene regulation. 32
Figure 15: HDAC6 is involved in redox regulation. 32
Figure 16: Molecular structures of selected HDAC6 inhibitors. 39
Figure 17: CML pathogenesis and impact of treatment with tyrosine kinase inhibitor imatinib. 45
Figure 18: MM pathogenesis. 48
Figure 19: Chemical structures of MAKV-8 and derived compounds. 54
Figure 20: Chemical structures of tubastatin A and MAKV-15. 55
Figure 21: Principle of HDAC activity assay. 70
Figure 22: Effect of MAKV-8 on HDAC1, HDAC6 and total HDAC activities. 81
Figure 23: Docking of MAKV-8 into human HDAC isoenzymes. 84
Figure 24: Effect of MAKV-8 on the acetylation of histone H4 and α-tubulin in CML cells. 87
Figure 25: Effect of MAKV-8 on CML cell proliferation and viability. 88
Figure 26: Effect of MAKV-8 on CML colony formation capacity. 89
Figure 27: Effect of MAKV-8 derived compounds on HDAC6 and total HDAC activities. ..91
Figure 28: Effect of MAKV-8 derived compounds on the acetylation of histone H4 and α-tubulin in K-562 cells. 93
Figure 29: Effect of MAKV-8 derived compounds on cell proliferation and viability. 94
Figure 30: Effect of MAKV-8 on K-562 cell cycle. 96
Figure 31: Effect of MAKV-8 on K-562 cell death. 97
Figure 32: Effect of MAKV-8 on caspase and PARP-1 cleavage in K-562 cells. 98
Figure 33: Effect of MAKV-8 on ER stress induction in K-562 cells. 100
Figure 34: Effect of MAKV-8 on autophagy induction in K-562 cells. 102
Figure 35: Effect of MAKV-8 on double strand breaks induction in K-562 cells. 106
Figure 36: Expression levels of HDAC mRNA in stem cells from healthy and CML patients. 107
Figure 37: Effect of co-treatment with MAKV-8 and imatinib on the acetylation of histone H4 and α-tubulin in CML cells. 108
Figure 38: Effect of co-treatment with MAKV-8 and imatinib on K-562 cell death. 109
Figure 39: Effect of co-treatment with MAKV-8 and imatinib on K-562 cell death. 111
Figure 40: Effect of MAKV-8-imatinib co-treatment on KBM-5 and MEG-01 cell death.. 113

Figure 41: Effect of co-treatment with MAKV-8 and imatinib on caspase and PARP-1 cleavage in CML cells. 114
Figure 42: Effect of treatment with MAKV-8 and imatinib on CML colony formation. 116
Figure 43: Effect of MAKV-8-imatinib co-treatment on tumor growth in zebrafish. 117
Figure 44: Effect of MAKV-8-imatinib co-treatment on imatinib-resistant CML cell death. 118
Figure 45: Anticancer effects in KBM-5R cells co-treated with MAKV-8 and imatinib. 119
Figure 46: Effect of MAKV-8-imatinib combinations on the viability of healthy cell models. 121
Figure 47: Effect of combinations with MAKV-8 and imatinib on healthy platelet viability. 123
Figure 48: Effects of beclin 1 silencing on apoptotic cell death induced by MAKV-8 in combination with imatinib. 125
Figure 49: Effect of MAKV-8-imatinib co-treatments on proteins implicated in BCR-ABL-dependent signaling pathways in imatinib-sensitive and -resistant CML cells. 127
Figure 50: Effect of co-treatments with MAKV-8 and imatinib on ALDH activity in K-562 cells. 129
Figure 51: Effect of MAKV-15 and tubastatin A on the activity of total HDAC and HDAC isoenzymes. 131
Figure 52: Effect of MAKV-15 and tubastatin A on the acetylation of histone H4 and α-tubulin in K-562 cells. 134
Figure 53: Effect of MAKV-15 and tubastatin A on K-562 cell proliferation and viability. 135
Figure 54: Effect of MAKV-15 and tubastatin A on K-562 cell cycle (A) and cell death (B). 136
Figure 55: Effect of MAKV-15, ACY-1215, and tubastatin A on the acetylation of histone H4 and α-tubulin in U-266 and MOLP-8 cells. 138
Figure 56: Effect of MAKV-15, ACY-1215, and tubastatin A on proliferation and viability of U-266 and MOLP-8 cells. 140
Figure 57: Effect of co-treatment with MAKV-15 or tubastatin A, and bortezomib on MOLP-8 cell death. 142
Figure 58: Effect of co-treatments bortezomib-MAKV-15 or tubastatin A on the accumulation of poly-ubiquitinated proteins in MOLP-8 cells. 143
Figure 59: Effect of co-treatments with bortezomib, rapamycin and MAKV-15 or tubastatin A on MOLP-8 cell death. 145
Figure 60: Evaluation of the constitutive expression level of five proteins in 10 MM cell lines. 146
Figure 61: Effect of MAKV-15 on the acetylation of histone H4 and α-tubulin in MM cell lines. 148
Figure 62: Effects of tri-therapies with HDAC6i, proteasome inhibitor, and BCL-2 family protein inhibitors on MM cell death. 150
Figure 63: Mechanisms of action of MAKV-8 in combination with imatinib in CML cells. 163
Figure 64: Mechanisms of action of MAKV-15 in combination with bortezomib in MM cells. 166

List of Tables

Table 1: HDAC isoenzymes. 6
Table 2: HDAC6 expression is deregulated in various cancer subtypes. 33
Table 3: Selected clinical trials with HDACi in combination treatments in MM. 53
Table 4: Culture characteristics. 59
Table 5: Cytogenetic abnormalities of multiple myeloma cell lines. 60
Table 6: Compounds used in this study. 64
Table 7: Conditions for the use of antibodies in western blots. 68
Table 8: *In silico* prediction of the MAKV-8 druglikeness and oral bioavailability based on Lipinski's Rule of Five extended with Ghose filter and on Veber's Rule. 83
Table 9: Comparative molecular docking of MAKV-8 against selected HDACs. 85
Table 10: Comparative molecular docking of MAKV-8 derivatives against HDAC6. 92
Table 11: Selectivity ratio of MAKV-8-imatinib co-treatment for cancer cells versus healthy models. 122
Table 12: *In silico* prediction of the MAKV-15 druglikeness and oral bioavailability based on Lipinski's Rule of Five extended with Ghose filter and on Veber's Rule. 132

PREAMBLE

The two-meter-long DNA molecule, encoding our genetic heritage that is essential for the physiological functioning of every cell, is compacted into chromosomes that fit inside a nucleus of about 6 µM. To achieve that incredible level of compaction, DNA molecules are tightly wrapped around proteins called histones, whose "tails" can be "decorated" by many posttranslational modifications, including acetylation. This type of histone modification is executed in a highly regulated manner by key regulatory enzymes and is considered as one of the main epigenetic marks. These discrete chemical modifications control chromatin remodeling and are thus critical for the accessibility of highly specific DNA regions to the transcription machinery, precisely regulating gene expression. Conversely, the removal of acetyl groups from histone tails, which is catalyzed by histone deacetylases (HDACs), is associated with increased chromatin condensation and potent transcriptional repression.

Alterations of the epigenetic landscape, a term coined by the scientist and philosopher Waddington, largely contribute to the development of numerous cancers. More specifically, aberrant activation or overexpression of HDAC isoenzymes, triggering disruptions of the functional acetylation landscape, is truly a hallmark of cancer. Due to the reversible nature of epigenetic modifications, targeting one or multiple HDAC activities with small molecule inhibitors represent an attractive approach for cancer prevention and therapy. HDAC inhibitors (HDACi) regulate the acetylation states of histones and/or non-histone proteins, thus affecting gene expression and a plethora of essential cellular processes such as cell cycle progression, endoplasmic reticulum stress, modulation of autophagy, reactive oxygen species production and cell death induction.

Despite the existence of various treatment options, the occurrence of drug resistance remains a barrier to cure cancer, necessitating the discovery of innovating therapeutic approaches. In this work, we aimed to establish novel therapeutic strategies by combining so far unexplored hydroxamate-based pan-HDACi (MAKV-8) and specific HDAC6i (MAKV-15) with clinically-used targeted therapies against two hematological malignancies. First, the combination of tyrosine kinase inhibitors with epigenetic modulators has emerged as a potential strategy for improving the outcome of chronic myeloid leukemia (CML). For this project, we investigated the anticancer activity of the promising molecule MAKV-8 in combination with imatinib in CML models. Moreover, multiple myeloma (MM) cells are characterized by an excessive production and accumulation of cytoplasmic immunoglobulins. We thus targeted this uncurable disease with the combined inhibition of both proteasome and aggresome pathways in selected MM cell lines by the new compound MAKV-15 and the well-known proteasome inhibitor bortezomib, respectively.

INTRODUCTION

Epigenetics refer to changes in gene expression that do not involve deoxyribonucleic acid (DNA) sequence modifications. DNA methylation, histone modifications and small ribonucleic acid (RNA)-mediated gene silencing/non-coding RNA functions are considered as the three main epigenetic mechanisms (Schnekenburger *et al.*, 2016).

1. Histones

1.1. From histones to chromatin

Histones form the building blocks of an octamer protein core, which is surrounded by a segment of eukaryotic DNA to constitute nucleosomes. Nucleosomes, fundamental packing units of chromatin, are composed of one tetramer of histones H3 and H4 and two histone H2A-H2B dimers. Each histone contains positively charged amino acids that interact with negatively charged phosphate groups of DNA. Although most of the histone core is inaccessible to external proteins, the N-terminal chains of the histones, referred to as histone tails, protrude from the nucleosome allowing post-translational modifications (PTMs). Another histone named H1 functions as an anchor to attach DNA to the nucleosomes, and helps to tightly bundle neighboring nucleosomes together *via* its binding to the "linker DNA" region (Clapier *et al.*, 2009; Folmer *et al.*, 2010; Gardner *et al.*, 2011).

1.2. Histone modifications

Histone tails can be epigenetically modified by phosphorylation (Banerjee *et al.*, 2011), methylation (Sadakierska-Chudy *et al.*, 2015), ubiquitination (Fierz *et al.*, 2011), adenosine diphosphate (ADP)-ribosylation (Bartolomei *et al.*, 2016), sumoylation (Wilson *et al.*, 2016), and acetylation (Khan *et al.*, 2010). Together these PTMs of histones constitute the “histone code” and work in concert with other epigenetic mechanisms (Sadakierska-Chudy *et al.*, 2015) to dictate the chromatin accessibility for transcription machinery to promoter regions of their target genes, establishing a specific pattern of gene expression required for normal physiological cell functions and a wide variety of biological processes (Berger, 2007).

Various enzymes regulate covalent histone modifications affecting their chemical properties and influencing the chromatin condensation level, which is a critical factor determining whether genes are transcribed or silenced (Kouzarides, 2007). For instance, two classes of proteins determine the acetylation status of histones: histone acetyltransferases (HATs) and histone deacetylases (HDACs) are the “writers” and “erasers”, respectively, that

work in association with proteins containing a bromodomain specifically recognizing the acetyl-lysine moiety referred as "readers" (Verdin *et al.*, 2015). HAT-mediated acetylation of the ε-amino group of lysine residues on histones tails correlates with a relaxation of chromatin and gene expression, whereas, the reverse process, which is catalyzed by HDACs, is associated with chromatin condensation and transcriptional repression (Figure 1).

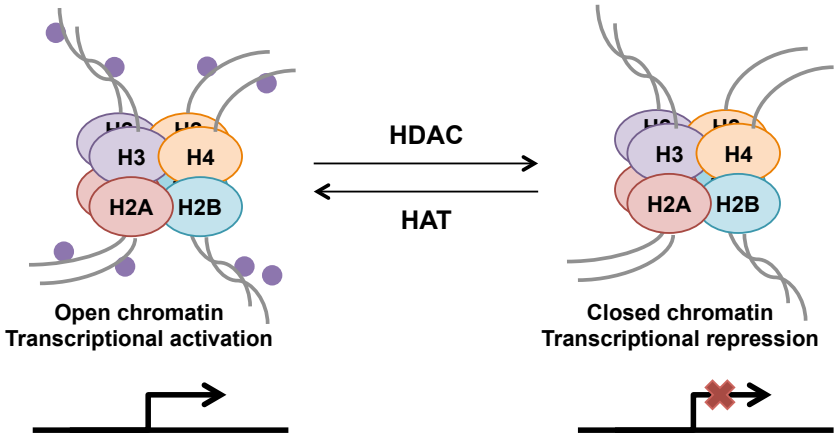

Figure 1: Reciprocal histone HDAC-mediated deacetylation and HAT-mediated acetylation. Histone acetyl transferase (HAT)-mediated acetylation of lysine residues on histone tails is associated with an open chromatin and transcriptional activation, whereas histone deacetylase (HDAC)-mediated deacetylation of histones is related to closed chromatin and transcriptional repression. Acetyl groups are represented by purple beads.

2. Acetylation of histone and non-histone proteins

Growing evidence highlights the essential role of histone and non-histone protein lysine acetylation in the coordination of highly regulated cell functions. This PTM neutralizes the positive charge of the ε-amino group of lysine residues or introduces steric hindrance, resulting in the modulation of protein interactions with nucleic acids or with other proteins (Hodawadekar *et al.*, 2007; Florean *et al.*, 2011). In addition, acetylation can regulate the catalytic activity of metabolic enzymes through directly neutralizing the positive charge of lysine residues in the active site, influencing their interactions with negative regulatory proteins, or causing allosteric changes (Xiong *et al.*, 2012; Choudhary *et al.*, 2014).

As previously mentioned, the acetylation status of lysine residues in histones, as well as non-histone proteins, results from a balance between the addition and removal of the acetyl group by HATs and HDACs, respectively (Figure 2). All HAT enzymes use acetyl coenzyme A as a cofactor, transferring the acetyl moiety of the latter to lysine residues of target proteins (Sadoul *et al.*, 2011). Since acetyl coenzyme A is a key metabolic intermediate in essential carbon catabolic pathways, protein acetylation links metabolism to diverse cellular signaling pathways (Choudhary *et al.*, 2014).

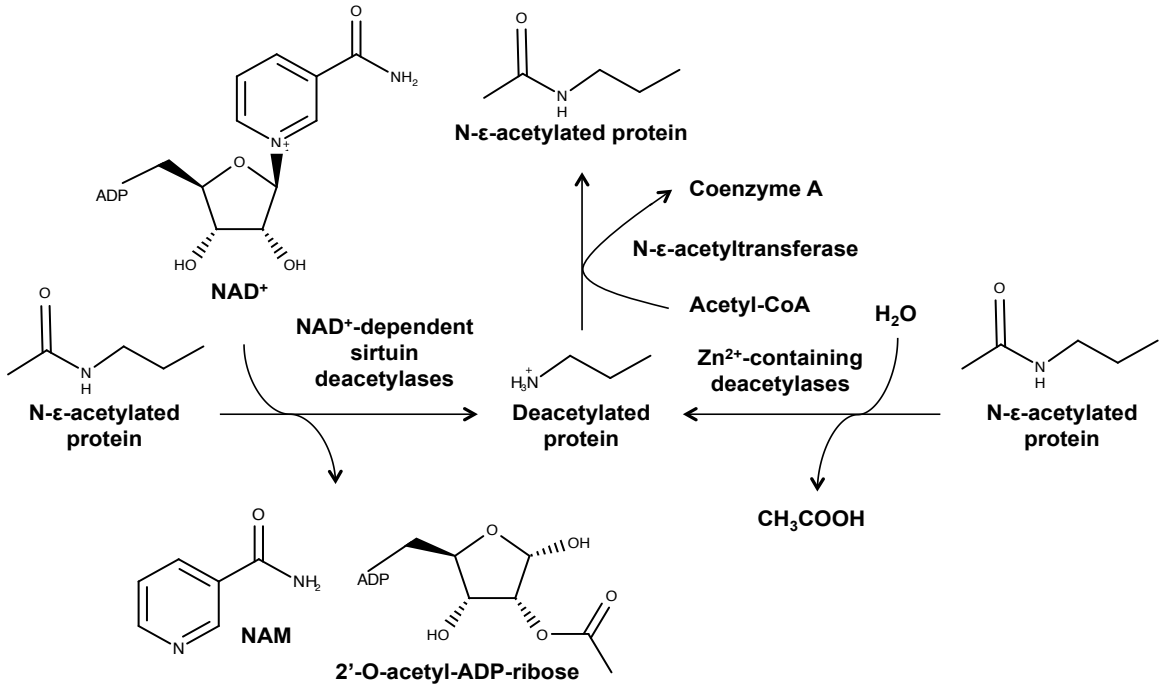

Figure 2: Reactions of HDAC-mediated deacetylation and HAT-mediated acetylation.
ADP: adenosine diphosphate; CoA: coenzyme A; NAD^+: nicotinamide adenine dinucleotide; NAM: nicotinamide.

Initially, HATs and HDACs were considered to target only histones; however, mass spectrometry-based investigations of the acetylome in various cell models revealed that such enzymes control the acetylation of a large and continuously growing list of many non-histone targets in different cellular compartments (Spange *et al.*, 2009). Accordingly, lysine acetylation is a major PTM regulating many cytoplasmic and nuclear protein functions including enzymatic activity, subcellular localization and protein-protein interactions, and affecting a wide variety of vital cellular processes such as pluripotency, cellular signaling, protein turnover, cell differentiation and cell survival (Choudhary *et al.*, 2014; Seidel *et al.*, 2014; Y.C. Wang *et al.*, 2014).

3. Histone acetyltransferases

3.1. HAT classification and structure

In mammals, over 30 HATs are categorized in two general classes according to their cellular localization: group A is primarily nuclear thus mainly carrying out transcription-related acetylation, whereas group B is essentially cytoplasmic, acetylating *de novo* synthesized free histones, promoting their nuclear localization and deposition onto newly synthesized DNA. Despite a high diversity among HATs, such enzymes are further classified based on their functions, as well as sequence and structural similarities in five distinct

subfamilies: general control [GC]N5 related *N*-acetyltransferase (GNAT), cAMP response element-binding protein (CREB)-binding protein (p300/CBP), MYST (MOZ, Ybf2/Sas3, SAS2 and TIP60), TATA box-binding protein-associated factor 250 kDa (TAFII250) and steroid receptor cofactor (SRC) (Spange *et al.*, 2009; Friedmann *et al.*, 2013).

Each of these HAT subfamilies contains a structurally conserved core region that has little to no sequence homology between the different HAT subfamilies (Friedmann *et al.*, 2013). Moreover, the different HAT subfamilies contain structurally divergent regions that flank the core region and also use different catalytic strategies to acetylate their substrates, which is involved in HAT-specific activities such as regulation by cofactor proteins and substrate-specific binding (Yuan *et al.*, 2013).

3.2. HAT families

The GNAT family is composed of KAT2A (GCN5, general control non-derepressible); KAT2B (PCAF, p300/CBP-associated factor); KAT1 (HAT1, histone acetyltransferase 1); elongator complex protein (ELP)3; establishment of cohesion *N*-acetyltransferase (ESCO)1 and 2; chromodomain protein, Y-linked (CDY)1, 2A and 2B; CDY-like (CDYL) and L2; N^{α}-acetyltransferase complex (NAT)10 as well as transcription factor IIIC (TFIIIC). Those enzymes are implicated in the deposition of histones on newly synthetized DNA strands (Burgess *et al.*, 2010) and in DNA repair *via* homologous recombination (X. Yang *et al.*, 2013). PCAF is important for transcriptional initiation, ELP3 is involved in transcriptional elongation and HAT1 is implicated in histone deposition and telomeric silencing (Hawkes *et al.*, 2002; Campos *et al.*, 2010). NAT10 or arrest-defective-1 protein (ARD1) stimulates human telomerase reverse transcriptase (hTERT) transcription, increasing telomerase activity, and participates in the nuclear envelope formation at the end of mitosis.

p300/CBP is composed of p300 and CBP, both possessing a bromodomain, which is an evolutionarily conserved protein module specifically recognizing acetyl-lysine residues and directing chromatin-associated proteins to acetylated histones. p300 seems to have the broadest substrate acceptance for histones and non-histone proteins (Kimura *et al.*, 2005).

Members of the MYST family, Esa1, type 1 interacting protein (TIP60), TAF250 serve as catalytic subunits in human acetylase binding to ORC1 (HBO1) and monocytic leukemia zinc finger protein/MOZ- related factor (MOZ/MORF) complexes (K.K. Lee *et al.*, 2007).

The enzymes SRC-1, translocation associated membrane protein (TRAM)-1/activator of thyroid and retinoic acid receptor (ACTR)/amplified in breast (AIB)1/p300/CBP co-integrator-associated protein (pCIP)/Ras-related C3 botulinum toxin substrate (RAC3), SRC-

3, transcriptional mediators/intermediary factor (TIF)-2, glutamate receptor-interacting protein (GRIP)1 and activating transcription factor (ATF)2 form the SRC family.

Other enzymes are not classified in a family, such as alpha tubulin acetyltransferase (ATAT)1 responsible of α-tubulin acetylation (Friedmann *et al.*, 2012).

3.3. HAT functions

HAT enzymes catalyze the highly dynamic transfer of an acetyl group from their co-substrate, acetyl-coenzyme A, to the ε-NH2 group of the amino acid side chain of lysine residues. Many HATs show a distinct pattern of substrate specificity for histones and non-histone proteins depending on the subunit composition of HAT complexes and the specific recruitment to the target sites of acetylation (Spange *et al.*, 2009).

4. Histone deacetylases

4.1. Classification

In mammals, 18 HDACs were identified and subdivided in four classes according to their catalytic activity, sequence similarity, and cellular localization (Table 1). Class I includes HDAC1, 2, 3, and 8; class II is divided in two subclasses: subclass IIa corresponds to HDAC4, 5, 7, and 9, and subclass IIb encompasses HDAC6 and 10; class III contains seven members, sirtuins (SIRT) 1 to 7; and class IV comprises only HDAC11 (de Ruijter *et al.*, 2003; Seto *et al.*, 2014).

Classes I, II, and IV metalloenzymes possess a zinc ion at the bottom of their catalytic pocket essential for the deacetylation reaction, whereas class III isoforms (sirtuins) depend on the cofactor nicotinamide adenine dinucleotide (NAD^+) for their catalytic activity. Members of classes I and IIa are characterized by a single deacetylase domain at their C-terminus, whereas class IIb enzymes, HDAC6 and 10, also present a second deacetylase domain on their N-terminus that is only active in HDAC6 (Seto *et al.*, 2014). Notably, the substrate specificity of HDAC isoforms may be influenced by the amino acid sequence of the substrate, second site modifications of the peptidic substrate sequence, as well as other proteins interacting with HDACs within transcriptional co-repressor complexes (Riester *et al.*, 2007).

Class I and II HDACs show homology to yeast reduced potassium dependency (Rpd)3 and yeast histone deacetylase (Hda)1, respectively (Gregoretti *et al.*, 2004). Ubiquitously expressed class I enzymes are mainly detected in the nucleus of cells owing to the presence of a nuclear localization signal (NLS). Except HDAC9 and HDAC10, class II isoenzymes possess both a NLS and a nuclear export signal (NES), conferring them with the remarkable

capability to shift back and forth between the nucleus and the cytoplasm. Notably, the expression of class IIa HDAC is tissue specific. The only member of class IV, HDAC11, is homologous to class I and II HDACs. Class III members, known as sirtuins by analogy with the yeast silent information regulator 2 (Sir2), can be located either in the nucleus, mitochondria, or cytoplasm (Gregoretti *et al.*, 2004; Florean *et al.*, 2011).

Table 1: HDAC isoenzymes.

Family	Class	Protein (*S. cerevisiae*)	Subclass	Protein (human)	Cellular localization	Chromosomal localization
Histone deacetylase	I	Rpd3, Hos1, Hos2, Hos3	NA	**HDAC1**	Nuclear	1p34
				HDAC2	Nuclear	6q21
				HDAC3	Nuclear	5q31
				HDAC8	Mainly nuclear	Xq13
	II	Hda1	Class IIa	**HDAC4**	Nucleo-cytoplasmic shuttle	2q37.3
				HDAC5		17q21
				HDAC7		12q13.1
				HDAC9	Nuclear	7p21.1
			Class IIb	**HDAC6**	Mainly cytoplasmic	Xp11.23
				HDAC10	Nuclear and cytoplasmic	22q13.31
	IV		NA	**HDAC11**	Nuclear	3p25.1
Sir2 regulator	III	Sir2, Hst1, Hst2, Hst3, Hst4	I	**SIRT1**	Mainly nuclear	10q21.3
				SIRT2	Nuclear and cytoplasmic	19q13
				SIRT3	Mitochondrial	11p15.5
			II	**SIRT4**	Mitochondrial	12q
			III	**SIRT5**	Mitochondrial	6p23
			IV	**SIRT6**	Nuclear	19p13.3
				SIRT7	Mainly nuclear	17q25

Hda: yeast histone deacetylase, HDAC: histone deacetylase, NA: non-applicable, Rpd: yeast reduced potassium dependency, Sir: yeast silent information regulator, SIRT: sirtuin.

4.2. Regulation of HDAC activities

Very few studies report the transcriptional and/or post-transcriptional mechanisms implicated in the regulation of HDAC expression. For instance, the transcription factor Yin Yang (YY)1, involved in cancer progression, promotes HDAC1 expression by binding to its promoter (Dong *et al.*, 2017). In addition, selected regulatory microRNAs (miR) govern HDAC expression levels (Kim *et al.*, 2015). HDAC enzymatic activities are highly regulated at the post-translational level. Two well-characterized mechanisms of HDAC regulation are protein-protein interactions within stable large multi-subunit complexes and PTMs such as

phosphorylation, sumoylation, acetylation, ubiquitination and glycosylation. Moreover, the regulation of some HDAC activities includes also subcellular localization, alternative RNA splicing, proteolytic processing and availability of metabolic cofactors (Seto *et al.*, 2014).

Examples of HDAC regulation by protein-protein interaction were reported in studies on class I HDACs. At least three distinct multi-protein complexes called the CoREST, the NuRD, and the Sin3 complexes function as recruitment platforms for HDAC1 and HDAC2 (Ayer, 1999). In addition, HDAC3 exists in a complex constituted of silencing mediator for retinoid or thyroid-hormone receptor (SMRT) and nuclear receptor co-repressor (N-CoR) (Wen *et al.*, 2000).

All HDACs possess phosphorylation sites targeted by specific kinases, and their status of phosphorylation, which is the most extensively studied PTM for controlling HDAC functionality, affects enzymatic activity and protein complex formation. Regarding class I HDACs, phosphorylation enhances HDAC1-3 activities, but inhibits HDAC8 (de Ruijter *et al.*, 2003; Seto *et al.*, 2014). The enzymatic activity of phosphorylated class IIa HDAC4 is modulated partly through subcellular localization, as the binding of 14-3-3 proteins to phosphorylated HDAC4 results in its cytoplasmic sequestration (Z. Wang *et al.*, 2014).

4.3. HDAC and cancer

Disruption of the functional acetylation pattern contributes to tumorigenesis. Accordingly, HDAC overexpression is usually detected in cancer, resulting in a global hypoacetylation. Alternatively, mutations in the sequences encoding HDAC isoforms are detected in different cancer subtypes leading to a loss of function of the mutated isoform or a disruption of its cellular localization (Clocchiatti *et al.*, 2011). A third mechanism involves fusion proteins responsible for an aberrant recruitment of HDACs to target gene promoters, leading to deregulation of gene transcription that may involve both an abnormal silencing of tumor suppressor genes (TSGs) and activation of developmental genes that sustain cancer progression. Moreover, aberrant activation or overexpression of HDACs promotes tumorigenesis *via* the arrest of normal hematopoietic cell differentiation (Florean *et al.*, 2011; Seidel *et al.*, 2012a).

Class IIa HDACs reportedly display a weak catalytic activity *in vitro*, and their presence in complexes with other HDACs suggests a recruitment function (Lahm *et al.*, 2007; Jones *et al.*, 2008). Therefore, the following chapters will describe some examples of the implications of class I HDACs in tumorigenesis, and the roles of class IIb HDAC6 in cancer will be described with more details in chapter 6.4.

4.3.1. Cellular proliferation

Cyclin-dependent kinase inhibitor 1A (CDKN1A, p21) promotes cell-cycle arrest primarily by binding to and inhibiting cyclin/cyclin-dependent kinase (CDK) complexes (Abbas *et al.*, 2009). Multiple HDACs repress p21 transcription through deacetylation of histones H3 and H4 in its promoter region (Richon *et al.*, 2000). In normal development, loss of HDAC1 activity causes early embryonic lethality due to a lack of proliferation caused by increased p21 expression (Lagger *et al.*, 2002). Many cancer cell types overexpress HDAC1, HDAC2, and/or HDAC3 as compared to the normal counterpart, which correlates with lowered p21 expression (Halkidou *et al.*, 2004; Hrzenjak *et al.*, 2006; Wilson *et al.*, 2006).

In addition, the loss of tumor suppressor scaffold/matrix attachment region binding protein (SMAR)1 in cancer correlates with overexpression of the cell cycle activator cyclin D1. SMAR1 normally binds to cyclin D1 promoter and recruits the HDAC1/mSin3 repression complex, leading to reduced cyclin D1 expression through histone deacetylation and restrained cell growth (Rampalli *et al.*, 2005).

Furthermore, HDAC1-containing complexes interact with and induce deacetylation of the tumor suppressor p53 at C-terminal lysine residues K320, K373 and K382, strongly reducing p53 stability and transcriptional activity, thereby reversing p53-mediated cell growth arrest, senescence and apoptosis (Reed *et al.*, 2014).

HDAC1 is also associated with Sp1/Sp3 at the promoter of transforming growth factor (TGF)β receptor (TGF-βR)I, decreasing histone H3 and H4 acetylation levels. The subsequent loss of TGF-βRI expression, frequently observed in many cancer types, renders tumor cells unresponsive to TGFβ allowing unfettered cell growth (Ammanamanchi *et al.*, 2004).

4.3.2. Hematopoietic differentiation

Chromosomal translocations in leukemia and lymphoma often result in an aberrant HDAC recruitment to regulatory regions of promoters, preventing the appropriate expression of target genes involved in differentiation. For instance, the oncogenic fusion protein promyelocytic leukemia (PML)-retinoic acid receptor (RAR)α resulting from the t(15;17) translocation is the main driver of acute promyelocytic leukemia (APL) development. Accordingly, different class I HDAC-containing repressor complexes associate with PML-RARα, which leads to the blockage of physiological all trans retinoic acid (t-RA) signaling, thereby preventing complete remission (Puccetti *et al.*, 2004). Additionally, the chimeric protein runt-related transcription factor (RUNX)1-ETO, product of the t(8;21) translocation, interacts with HDAC1-3 as well as the co-repressors mSin3a, SMRT and N-CoR, preventing transcription of target genes

implicated in myeloid differentiation, thus allowing for continued proliferation of undifferentiated progenitor cells and initiation of acute myeloid leukemia (AML) (Lam *et al.*, 2012).

4.3.3. Angiogenesis and metastasis

Hypoxic regions of tumors increase HDAC1 expression and activity, resulting in enhanced angiogenesis *via* the repression of the tumor suppressor genes p53 and von Hippel–Lindau (VHL), and associated with the induction of genes promoting new vessel formation such as hypoxia-inducible factor (HIF)-1α and vascular endothelial growth factor (VEGF). Casein kinase (CK)2 may be a key mediator for HDAC activation under hypoxia through increased protein phosphorylation (Pluemsampant *et al.*, 2008).

Class I HDACs are involved in the loss of extracellular matrix-related gene expression. For instance, HDAC1 inhibits the expression of cystatin, a peptidase inhibitor that suppresses tumor invasion (Whetstine *et al.*, 2005). In addition, the repressor Snail recruits HDAC1 and HDAC2, as well as the co-repressor mSin3A to the E-cadherin promoter, directly silencing its gene expression, which is essential to lower cell–cell adhesion and stimulate the invasiveness of cells (Peinado *et al.*, 2004). Similarly, the HDAC3 and peroxisome proliferator-activated receptor (PPAR)γ complex repress E-cadherin gene transcription through binding to its promoter in prostate cancer cells (Annicotte *et al.*, 2006). Furthermore, HDAC inhibitors (HDACi) down-regulate the expression of the C-X-C chemokine receptor (CXCR)4 in acute lymphocytic leukemia (ALL) cells, resulting in impaired cell migration (Crazzolara *et al.*, 2002). Importantly, the HDACi-mediated increase in intercellular adhesion molecule (ICAM)1 expression on tumor-derived endothelial cells prevents the escape of tumor cells from the immune response by restoring leukocyte-vessel wall interactions and leukocyte infiltration into the tumors (Hellebrekers *et al.*, 2006).

5. HDAC inhibitors

Owing to the reversible nature of epigenetic modifications, considerable efforts have been undertaken to generate small molecules inhibiting proteins involved in epigenetic regulation like HDACs. Thus, over the years, HDACi have become a promising strategy for the treatment of multiple malignancies (Florean *et al.*, 2011; Seidel *et al.*, 2015).

5.1. Classification and structure

Based on their chemical structures, HDACi were initially sub-divided in five classes,

namely hydroxamic acids, carboxylates (short-chain fatty acids), benzamides, depsipeptides and cyclic peptides (Li *et al.*, 2013; P.H. Yang *et al.*, 2013). Moreover, a long list of other compounds with a broad range of chemical structures was reported to inhibit HDAC activities. A multitude of these HDACi was discovered in nature, whereas derivatives have been synthesized by rational design or the modification of natural compounds (Losson *et al.*, 2016). Although most of them are pan-HDACi (*i.e.* targeting multiple non-sirtuin HDACs), an increasing number of molecules are designed to be selective for one class or even for a single isoform (Seidel *et al.*, 2012a).

Three domains characterize the prototypical pharmacophoric model shared by HDACi (Figure 3): the zinc binding group (ZBG), which is a metal-binding moiety that chelates the catalytic zinc ion; the hydrophobic linker region that mimics the substrate's lysine chain and fits the catalytic site channel; and the cap group that blocks the access of the substrate to the active site by targeting the channel rim, mainly responsible for HDAC isoform selectivity (Li *et al.*, 2013). HDACi specificity arises not only from interactions with residues in the cap region, which is adjacent to the catalytic site (Bertrand, 2010; Li *et al.*, 2013), but also from π-π interactions (Ahamed *et al.*, 2016).

HDACi mainly exert their inhibitory effect by chelating the zinc cofactor, which is stabilized by two aspartate and one histidine residues at the active site of the enzyme. Despite toxicity due to non-specific metal binding, hydroxamic acid is the most commonly used ZBG for its strong coordination of the zinc ion. In addition, the sulfhydryl group exposed upon reduction of the depsipeptide disulfide bond is also a potent zinc chelator. In benzamides, the amino group is responsible for the chelation of the zinc ion but the distance between the carbonyl oxygen and zinc indicates weak interactions. Nevertheless, introduction of novel ZBGs is still necessary for improving the pharmacokinetic and safety issues of current HDACi (Wu *et al.*, 2011; Zhang *et al.*, 2018).

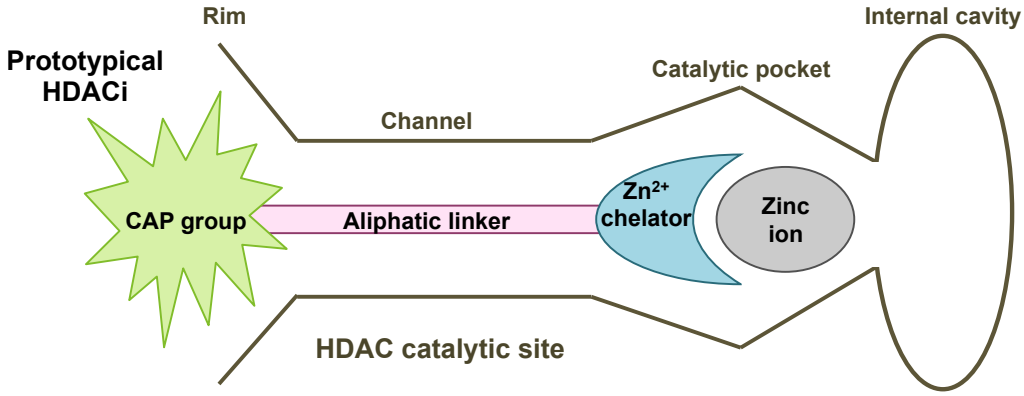

Figure 3: Prototypical pharmacophoric model of HDAC inhibitors (HDACi).

5.2. Consequences of HDAC inhibition

The inhibition of HDAC enzymes in cancer cells leads to hyperacetylation of histone and non-histone proteins, resulting in various anticancer properties through many different mechanisms (Figure 4) (Mrakovcic *et al.*, 2019). Interestingly, deacetylation of histones H3 and H4 was reported in genomic regions close to transcription start sites of genes down-regulated upon HDACi exposure, suggesting that such therapeutic compounds may display additional mechanisms of action (Rada-Iglesias *et al.*, 2007).

Some HDACi display the potency to restore impaired differentiation processes in certain tumor types (Schnekenburger *et al.*, 2006), whereas others inhibit aberrant cell-cycle progression through increased p21 expression levels (Kumagai *et al.*, 2007). In addition, many HDACi induce apoptotic cell death *via* the restoration of apoptotic pathways, and the transcriptional induction or inhibition of pro-apoptotic (*e.g.* BIM) or anti-apoptotic (*e.g.* survivin) proteins, respectively (Bhatnagar *et al.*, 2009; Xargay-Torrent *et al.*, 2011). Furthermore, DNA damage induction implicated in HDACi toxicity toward transformed cells has been imputed to reactive oxygen species (ROS) generation (Rosato *et al.*, 2008). Accordingly, HDAC inhibition may result in the up-regulation of thioredoxin (Trx) binding protein (TBP)2, which binds and inhibits the activity of the ROS antioxidant scavenger Trx (Xu *et al.*, 2007). Lethal consequences of ROS production may be strengthened by HDACi that interfere with DNA repair processes *via* the acetylation or transcriptional down-regulation of DNA repair proteins such as Ku70 or RAD50, respectively (Miller *et al.*, 2010). Finally, some HDACi promote endoplasmic reticulum (ER) stress *via* 78 kDa glucose-regulated protein (GRP78) acetylation (Rao *et al.*, 2010) or disruption of the aggresome pathway (Nawrocki *et al.*, 2006). Such compounds also induce autophagy by inhibiting mammalian target of rapamycin (mTOR) (Mrakovcic *et al.*, 2019) or acetylating autophagy-related proteins (ATGs) for instance (Banreti *et al.*, 2013). Notably, HDACi usually target preferentially cancer cells with moderate effects on normal cells (Seidel *et al.*, 2014).

The nature of response induced by HDACi in cancer cells, as well as the molecular mechanisms underlying HDACi-mediated anticancer effects seem to depend on the cancer context, along with the HDAC inhibitory profile, the concentration and the time of exposure to the inhibitor. In order to facilitate the comprehension, only the cellular processes mentioned in the results will be shortly described in the following chapters.

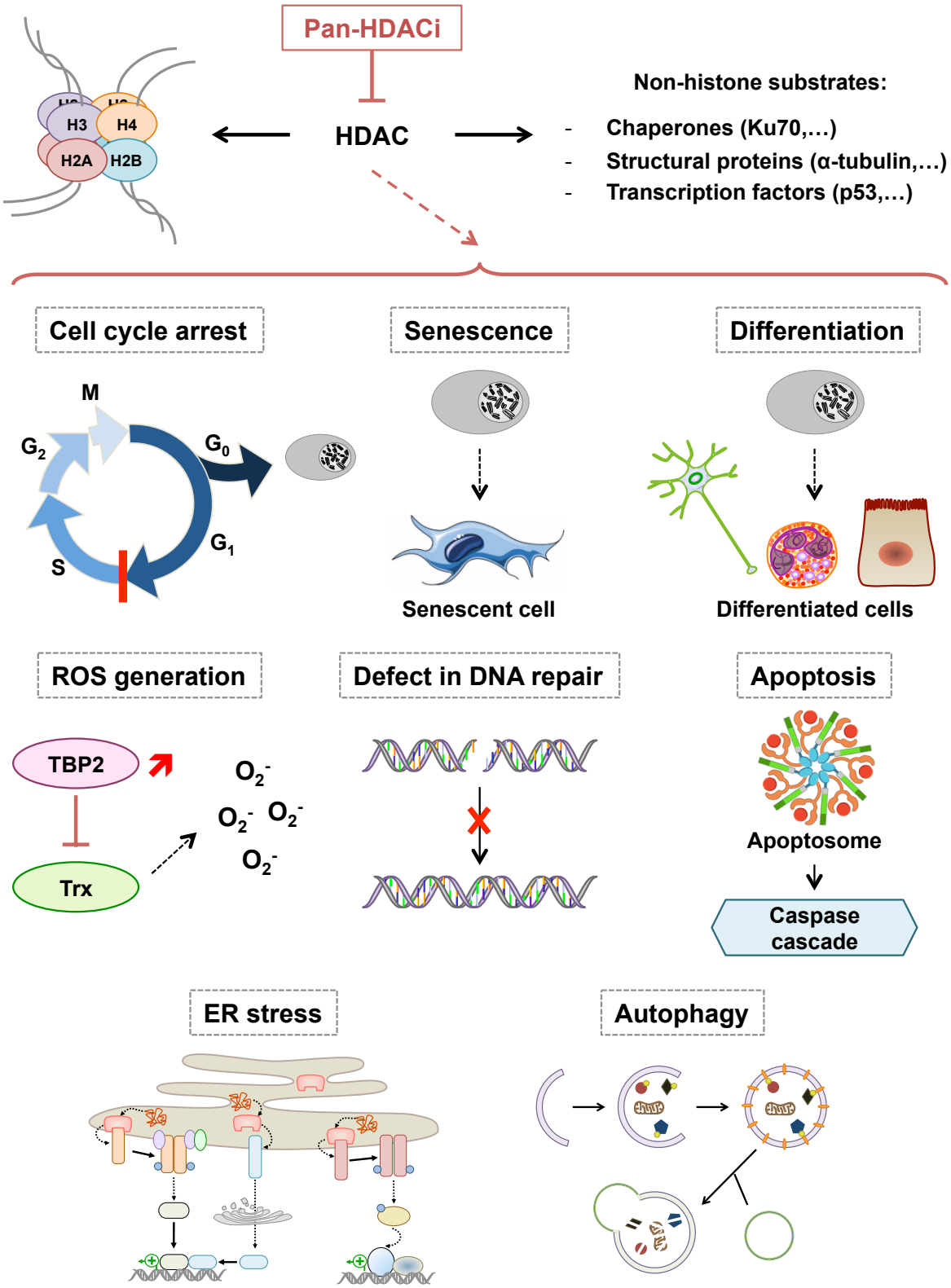

Figure 4: Consequences of HDAC inhibition.
Through the inhibition of HDACs targeting numerous histone and non-histone proteins, pan-HDAC inhibitors (HDACi) display many anticancer properties. Trx: thioredoxin; TBP: Trx binding protein.

5.2.1. ER stress

The ER is an essential intracellular organelle of the secretory pathway involved in the synthesis, folding, post-translational modifications, and transport of proteins (Cao *et al.*, 2012). Upon impairment of ER function by physiological and pathological insults, immature defective proteins accumulate within this sensitive organelle, triggering a condition called ER stress. In response to stress, the ER initiates a tightly orchestrated collection of intracellular signal transduction reactions, termed the unfolded protein response (UPR), in attempt to restore protein homeostasis (Senft *et al.*, 2015).

The UPR restructures transcriptional, translational and degradation pathways in order to resolve protein misfolding disorders. These actions are accomplished through the activation of three trans-membrane ER sensor proteins, namely protein kinase RNA-like ER kinase (PERK), inositol-requiring enzyme (IRE)-1α and ATF6, with distinct but overlapping functions (Figure 5). Under physiological conditions, the luminal domains of PERK and ATF6 proteins are bound to the ER resident chaperone GRP78, which keeps them inactive. When misfolded proteins accumulate in the ER, GRP78 is released from these complexes to assist with the proper folding of accumulated proteins, resulting to the activation of the two ER sensor proteins. In contrast to PERK and ATF6, IRE1α activation is GRP78-independent but requires the direct binding of unfolded proteins to its luminal domain (Adams *et al.*, 2019). Upon activation, the UPR modulators PERK, IRE1α and ATF6 induce signal transduction events that alleviate the accumulation of misfolded proteins in the ER by (*i*) increasing transcriptional activation of cytosolic and ER-resident chaperones such as GRP78 or the heat shock protein (HSP)90-like protein GRP94, (*ii*) inhibiting protein entry into ER by arresting messenger RNA (mRNA) translation, and (*iii*) stimulating retrograde transport of misfolded proteins from the ER into the cytosol for ubiquitination and destruction by a process named ER-assisted degradation (Sano *et al.*, 2013; Bruning *et al.*, 2015; Kaneko *et al.*, 2017). The timing of induction of UPR pathways and their mutual interactions are important issues and ultimately determine the cell response to stress. If the UPR fails to reestablish ER homoeostasis, ER stress causes cell dysfunctions leading to cell death (Lindholm *et al.*, 2017).

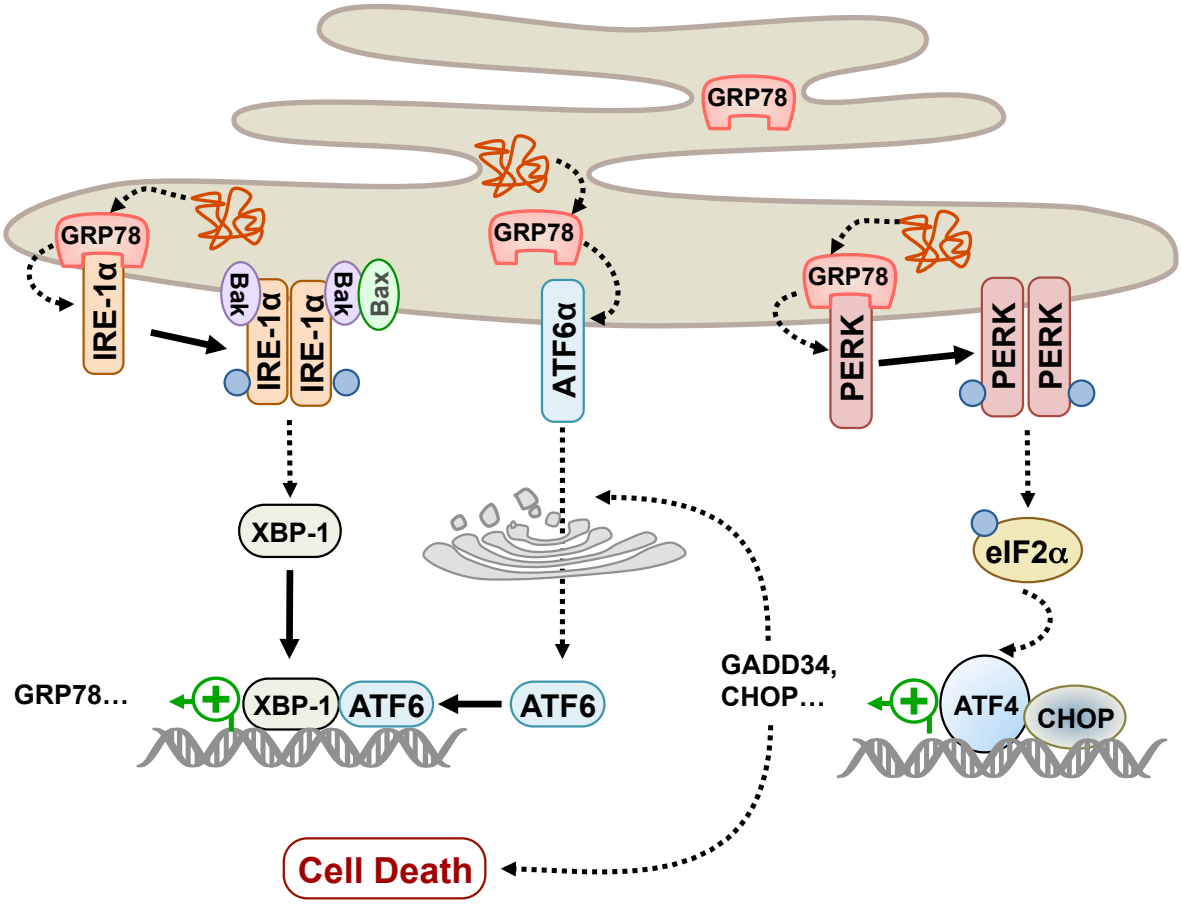

Figure 5: ER stress induction elicits UPR signaling pathways.
Three ER stress sensors [protein kinase RNA-like ER kinase (PERK), activating transcription factor (ATF)6, and inositol-requiring enzyme (IRE)-1α] initiate UPR signaling. Upon sensing the presence of unfolded or misfolded proteins, IRE-1α undergoes dimerization and autophosphorylation to become active, resulting in the splicing of X-box binding protein (XBP)-1 mRNA. Spliced XBP-1 mRNA encodes a transcription factor that up-regulates a wide range of UPR target genes, including genes that orchestrate ER-assisted degradation or protein folding. When activated through oligomerization and autophosphorylation, PERK directly phosphorylates the Ser51 of the α subunit of eukaryotic initiation factor (eIF)2, which then subsequently prevents the formation of ribosomal initiation complexes leading to global mRNA translational attenuation. In contrast, some mRNAs, such as the one encoding ATF4, require eIF2α phosphorylation for translation. The transcription factor ATF4 regulates several UPR target genes including those involved in ER stress-mediated apoptosis such as CCAAT/enhancer-binding protein homologous protein (CHOP). Upon ER stress conditions, ATF6α transits to the Golgi, where it is cleaved by site 1 and site 2 proteases, generating an activated β-ZIP factor. This processed form of ATF6α translocates into the nucleus to activate UPR genes involved in protein folding, processing, and degradation.

5.2.2. Autophagy

Macro-autophagy (or autophagy) is an evolutionarily ancient catabolic process, highly conserved across eukaryotic cells for degradation and recycling of cellular components (Levy *et al.*, 2017). The two types of autophagy are referred to as (*i*) non-selective autophagy, a bulk degradation pathway responsible for the clearance of long-lived or aggregated proteins, as well as excess, unneeded or damaged organelles, and (*ii*) selective autophagy that recognizes and removes specific cargos (Farre *et al.*, 2016). In both types, the autophagic process begins with the expansion of a unique membrane, called phagophore or isolation membrane, through the activity of specific autophagy effectors (Figure 6). The nascent membrane then engulfs a portion of cytoplasm including soluble proteins, aggregates or organelles. Complete sequestration of cytoplasmic constituents within the elongating phagophore eventually results in formation of an autophagosome, a double membrane-bounded vesicle. On the autophagosomal inner membrane, MT-associated protein 1 light chain (LC)3 under its phosphatidylethanolamine (PE)-conjugated form reportedly functions as a receptor for sequestosome (SQSTM)1, a selective substrate that binds to LC3, as well as specific cargos *via* its ubiquitin-binding domain, and is preferentially degraded by autophagy. The autophagosomal structure then moves along microtubules towards lysosomes for fusion, leading to autophagolysosome formation. The inner membrane of the autophagosome and the cytoplasm-derived materials packed into the autophagosome are finally degraded by lysosomal hydrolytic enzymes such as lipases, proteases and nucleases (Levy *et al.*, 2017; Singh *et al.*, 2018).

Diverse physiological purposes of autophagy have been described, including the maintenance of cellular homeostasis and quality control of cytoplasmic components, as well as the utilization of degradation products, which are recycled back to the cytoplasm as monomeric units for macromolecular synthesis and/or energy production (Singh *et al.*, 2018). Consequently, defects in autophagic elimination of cellular contents are associated with various pathologies, including cancer (Kroemer, 2015). Although autophagy is frequently demonstrated as a survival mechanism for tumor cells, many reports highlight autophagy as a tumor suppressor process depending on cell type, properties of drug, as well as duration of treatment. For instance, allelic loss of beclin 1, a subunit of the class III phosphoinositide 3-kinase (PI3K) complex, promotes tumorigenesis (Qu *et al.*, 2003).

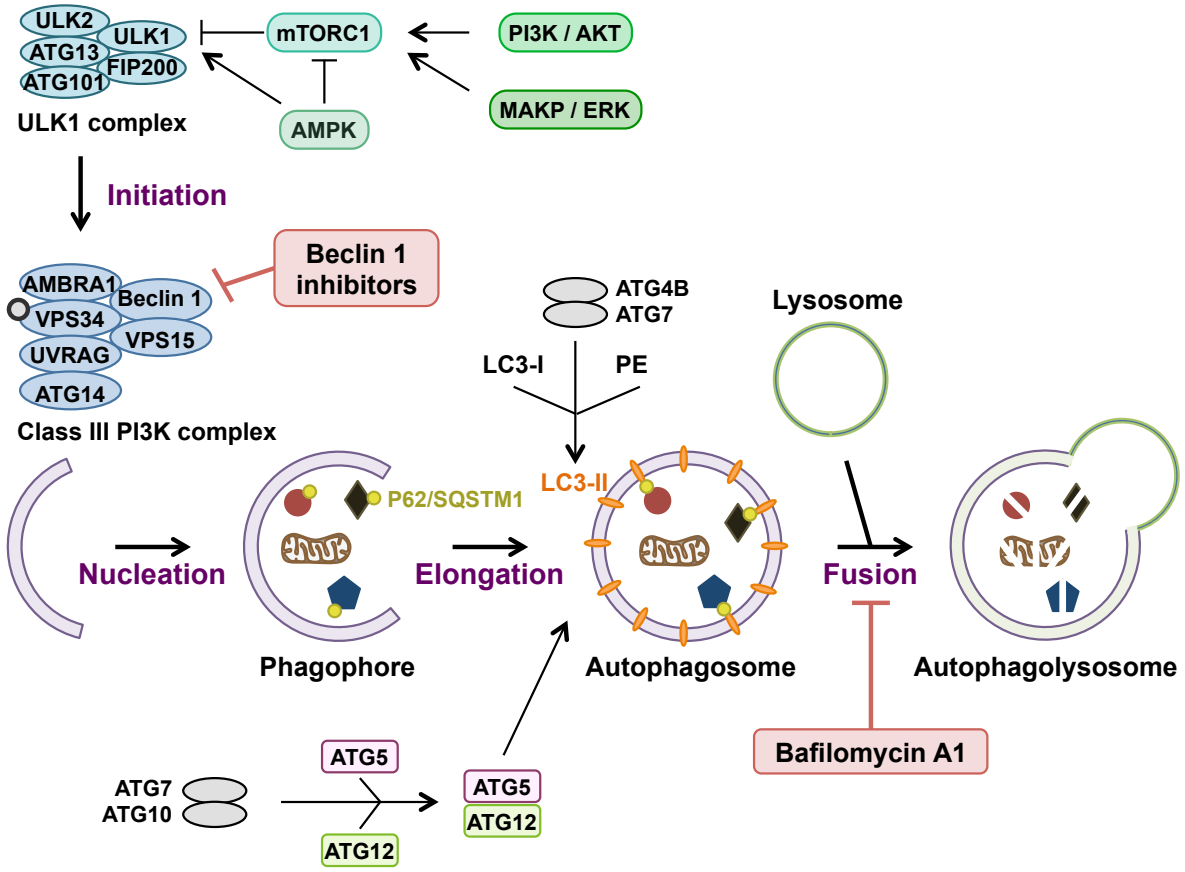

Figure 6: Autophagic machinery.
Depending on the signal transduced to mammalian target of rapamycin complex 1 (mTORC1) through various pathways including phosphoinositide 3-kinase (PI3K)/AKT, mitogen-activated protein kinase (MAPK)/extracellular signal-regulated kinase (ERK), or adenosine monophosphate (AMP)-activated protein kinase (AMPK), the induction of autophagic flux starts with the assembly of Unc-51 like autophagy activating kinase (ULK)1 complex comprising ULK1 and 2, proteins encoded by autophagy-related protein (ATG)13 and 101, and FAK family kinase-interacting protein of 200 kDa (FIP200). ULK1-mediated phosphorylation events regulate autophagy. Concomitantly, membranes of various organelles contribute to the formation of an isolation membrane known as the phagophore. Nucleation of the isolation membrane involves class III PI3K complex constituted of beclin 1, ATG14, vacuolar protein sorting (VPS)34 and 15, activating molecule in beclin 1-regulated autophagy protein (AMBRA)1, UV radiation resistance associated protein (UVRAG). This complex assembly is promoted by ULK1 complex translocation to the phagophore. Beclin 1 inhibitors block the autophagic process at that stage. Elongation of the isolation membrane is driven by ATG12–ATG5 conjugation mediated by ATG7 and 10, as well as microtubule-associated protein 1 light chain (LC)3 processing. Cytoplasmic LC3-I is cleaved by ATG4B to generate a C-terminal-exposed glycine residue to which ATG7 and 3 conjugate a phosphatidylethanolamine (PE) moiety. Lipidated LC3-II is then recruited to the autophagosomal membranes. Sequestration of cargo bond to sequestosome (SQSTM)1 and closure of the membrane result in the completion of double-membrane autophagosome, which fuse with lysosomes to form single-membrane autolysosomes. Lastly, enzymatic degradation of cargo inside lysosomes is followed by release of biomolecules in the cytosol for reuse. Late-stage autophagy inhibitor bafilomycin A1 prevents the fusion between autophagosomes and lysosomes *via* vacuolar H^+-ATPase inhibition. Adapted from (Levy *et al.*, 2017).

5.2.3. Apoptosis

Apoptosis is a programmed cell death first described by Kerr *et al.* (Kerr *et al.*, 1972), and characterized by specific morphological and biochemical changes of dying cells, including cell shrinkage, nuclear condensation and fragmentation, dynamic membrane blebbing and loss of adhesion to neighbours or to extracellular matrix. Three apoptotic pathways exist: the extrinsic pathway *via* the activation of cell death receptor by an extracellular ligand, the intrinsic pathway induced by DNA damage, for example, and the granzyme pathway triggered by the entrance of granzyme B into the cytoplasm (Figure 7) (Taylor *et al.*, 2008).

To trigger the extrinsic pathway, extracellular death ligands engage their cognate plasma-membrane death receptor, leading to the formation of death-inducing signaling complex (DISC), which promotes the auto-processing and activation of initiator caspases 8 and 10. Active caspase 8 then proteolytically processes and activates executioner caspases 3 and 7. In some cases, the extrinsic pathway can also crosstalk with the intrinsic pathway, *via* caspase 8-mediated cleavage of pro-apoptotic BH3 interacting domain death agonist (BID). Truncated form t-BID is required for oligomerisation of B-cell lymphoma (BCL)-2-associated X protein (BAX) and BCL-2 homologous antagonist/killer (BAK), promoting mitochondrial cytochrome *c* release (Taylor *et al.*, 2008; Czabotar *et al.*, 2014). In the intrinsic pathway, diverse cytotoxic stimuli provoking cell stress or damage typically activate one or more members of the BH3-only family members. When the inhibitory effect of the pro-survival BCL-2 proteins is overcome, the assembly of BAK–BAX oligomers is enabled within mitochondrial outer membranes. These oligomers drive mitochondrial permeabilization, allowing the efflux of cytochrome *c* into the cytosol. On release from mitochondria, cytochrome *c* can seed apoptosome assembly, which is composed of cytochrome c, pro-caspase 9 and apoptotic peptidase activating factor (APAF)-1. Active caspase 9 then propagates a proteolytic cascade of further caspase activation events, such as the cleavage of executioner caspases 3, 6 and 7. Finally, the degradation of inhibitory protein inhibitor of caspase-activated DNAse (iCAD) by caspases allows the activation and nuclear translocation of the nuclease CAD that induces DNA fragmentation (Czabotar *et al.*, 2014).

Among proteins implicated in the regulation of apoptotic mechanisms, two main families have been characterized. The first one is BCL-2 family divided in three classes: anti-apoptotic proteins [BCL-2, BCL-extra large (BCL-xL), BCL-W, myeloid cell leukemia (MCL)-1, DIVA...], multi-domain pro-apoptotic proteins (BAX, BAK, BOK...), and BH3-only pro-apoptotic proteins (BID, BAD, BIK, BIM, NOXA, PUMA...). The second family is the inhibitor of apoptosis (IAP) family composed of proteins such as X-linked inhibitor of

apoptosis protein (XIAP), cIAP or survivin (Taylor *et al.*, 2008).

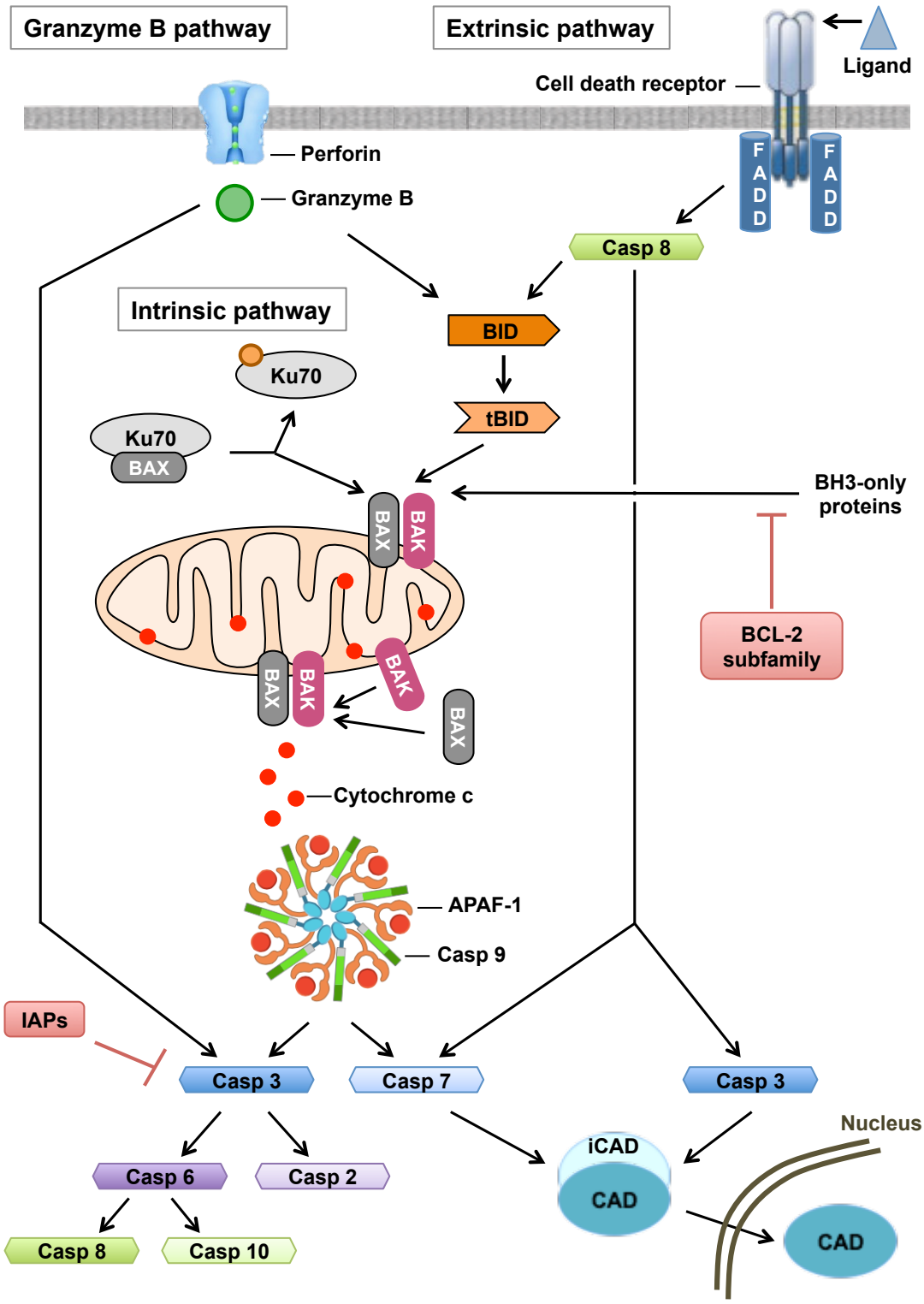

Figure 7: Apoptosis pathways.
Apoptosis, or programmed cell death, is triggered by various stimuli, leading to the activation of the intrinsic, extrinsic or granzyme pathways. APAF: Apoptotic protease activating factor, BAK: BCL-2 homologous antagonist/killer, BAX: BCL-2-associated X protein, BID: BH3 interacting domain death agonist, iCAD: inhibitor of caspase-activated DNAse, Casp: caspase, FADD: Fas-associated protein with death domain, IAP: inhibitor of apoptosis protein. Adapted from (Taylor *et al.*, 2008).

Importantly, mitochondrial calcium overload, due to acute release of this sensitizing signal from the ER for instance, is one of the pro-apoptotic mechanisms inducing the swelling of mitochondria, with perturbation or rupture of the outer membrane, and in turn the release of mitochondrial apoptotic factors into the cytosol (Giorgi *et al.*, 2012; Sano *et al.*, 2013)

5.3. Most common HDACi

Many pan-HDACi have been developed in the last years, some of which have entered clinical trials and are currently investigated in different phases against a variety of diseases, including different types of cancer [reviewed in (Schnekenburger *et al.*, 2016)]. Hematological malignancies reacted well to most of the pan-HDACi already tested clinically, but the efficacy on solid tumors was disappointingly poor and also associated with intolerable side effects (Bruning *et al.*, 2015).

Besides studies using HDACi as a single agent, a growing number of completed or ongoing clinical trials employ HDACi in combination with other chemotherapeutic drugs in order to achieve improved anticancer activities (Seidel *et al.*, 2012a). Thus, the combination of 'classical' anticancer agents with epigenetic modulators appears to be a promising future strategy against cancer (Seidel *et al.*, 2015).

5.3.1. "Short-chain fatty acid" family: sodium butyrate and valproic acid

Within the class of short-chain fatty acids, the two most characterized HDACi are valproic acid (VPA) and sodium 4-phenylbutyrate (Seidel *et al.*, 2012a). The latter is derived from sodium butyrate, a prototypical compound of the "short-chain fatty acid" family initially reported to induce differentiation in cultured erythroleukemic cells (Leder *et al.*, 1975) and whose short half-life limits its therapeutic application (Florean *et al.*, 2011). Sodium 4-phenylbutyrate shows selective toxicity against leukemia cells compared to healthy blood cells (Batova *et al.*, 2002) and underwent a phase II trial for the treatment of pediatric brain tumors (www.clinicaltrials.gov). VPA, a branched derivative of valeric acid, is commonly used for its antiepileptic properties (Chateauvieux *et al.*, 2010) and shows selective inhibition against class I and IIa HDACs. Moreover, VPA induces the differentiation of AML cells and increases responsiveness of Philadelphia-positive chronic myeloid leukemia (CML) and promyelocytic leukemia (PML) cell lines to cytarabine (N. Liu *et al.*, 2016). This compound was tested in a phase I trial for the treatment of solid tumors and central nervous system tumors in children (Su *et al.*, 2011), and in a phase II trials for treatments in combination with 5-azacytidine in hematological malignancies (Schnekenburger *et al.*, 2016).

5.3.2. "Benzamide" family: MS-275 and MGCD103

The group of benzamides, a class of molecules showing specificity for class I HDACs, comprises mainly MS-275 (Entinostat) and MGCD0103 (Mocetinostat) (Seidel *et al.*, 2012a). Both of them have entered clinical trials against hematological malignancies and some solid tumors. Indeed, MS-275 and MGCD0103 were evaluated in two clinical phase II trials for the treatment of patients with refractory chronic lymphocytic leukemia (CLL) and metastatic melanoma, respectively (Hauschild *et al.*, 2008; Blum *et al.*, 2009). Moreover, MS-275 was used together with 5-azacytidine to generate improved cytotoxic effects against AML and ALL (Gao *et al.*, 2008). Interestingly, MGCD0103 possesses two main advantages: an oral mode of administration and a long half-life, the latter allowing less frequent drug administration but preventing dose escalation or re-treatment (Seidel *et al.*, 2012a). Treatment with MS-275 did not achieve any objective responses. However, MS-275 could be evaluated as part of a combination therapy to enhance its efficacy (Schnekenburger *et al.*, 2016).

5.3.3. "Hydroxamic acid" family: SAHA, PXD101 and LBH589

The group of hydroxamate-based HDACi contains several compounds tested in clinical trials. Suberoylanilide hydroxamic acid (SAHA; vorinostat) is a pan-HDACi approved by the Food and Drug Administration (FDA) in 2006 for the treatment of cutaneous T-cell lymphoma (CTCL) (Duvic *et al.*, 2007). Moreover, SAHA has been tested in phase II clinical trials against numerous solid cancer types, including breast cancer (Luu *et al.*, 2008), non-small cell lung cancer (Traynor *et al.*, 2009), ovarian epithelial cancer (Modesitt *et al.*, 2008), primary peritoneal cavity cancer and thyroid cancer (Woyach *et al.*, 2009). Two other compounds belonging to the class of hydroxamic acids recently obtained FDA approval: PXD101 (belinostat) was approved in 2014 for the treatment of patients with relapsed or refractory peripheral T-cell lymphoma (PTCL) (Bodiford *et al.*, 2014) and LBH589 (panobinostat) was approved in 2015 for patients with multiple myeloma (MM) who received at least two prior regimens including the proteasome inhibitor bortezomib and an immunomodulatory agent (Atadja, 2009; Wahaib *et al.*, 2016). In addition, both LBH-589 and PXD101 have undergone different phase clinical trials for the treatment of solid and non-solid tumors (Giles *et al.*, 2006; Steele *et al.*, 2008; Ramalingam *et al.*, 2009).

5.3.4. "Depsipeptide" family: FK228

The depsipeptide FK228 (romidepsin), an epigenetic drug from natural origin, received

FDA approval in 2009 for the treatment of CTCL based on two studies, sponsored by Gloucester Pharmaceuticals Incorporated and the National Cancer Institute, which highlighted the benefits of using FK228, including a response rate of approximately 35%, the duration of the response, as well as low and reversible toxicity (Whittaker *et al.*, 2010). Notably, FK228 has undergone phase II clinical trials for various solid cancers including metastatic breast cancer, metastatic renal cell carcinoma, ovarian epithelial or peritoneal cavity cancer, prostate cancer and small cell lung cancer (SCLC) (Seidel *et al.*, 2012a).

The four compounds that have received FDA approval (Figure 8) are class I selective (FK-228) or pan-HDAC inhibitors (SAHA, LBH-589, and PXD-101).

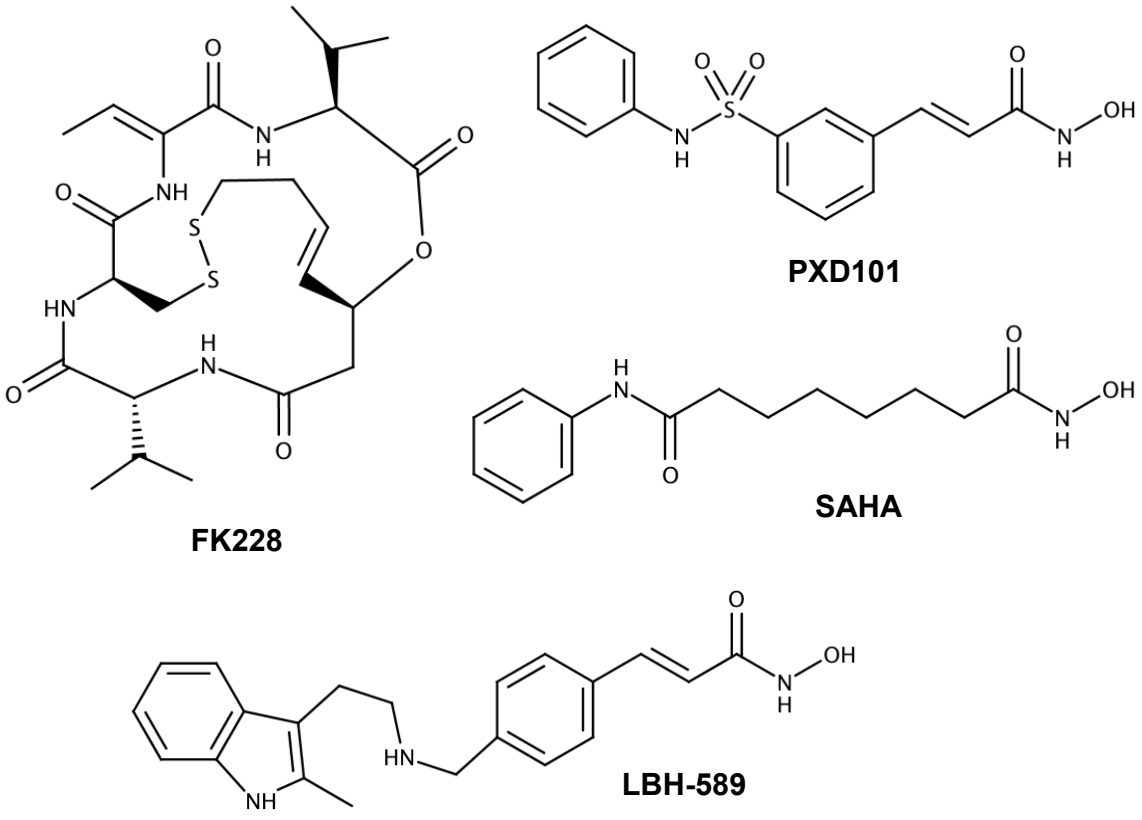

Figure 8: Molecular structures of Food and Drug Administration-approved HDAC inhibitors. SAHA: suberoylanilide hydroxamic acid.

6. The isoenzyme HDAC6

Over the past few years, there has been a significantly increasing interest for the class II deacetylase HDAC6 due to its critical role in multiple biological functions through deacetylase-dependent and -independent mechanisms regulating many vital cellular regulatory processes essential to cell growth, migration and survival. Despite its key implication in cell homeostasis, the regulation of HDAC6 as well as its substrate interactions and specific functions are not totally unraveled yet (L. Zhang *et al.*, 2015).

6.1. From gene expression to protein structure

The gene coding for HDAC6 covers 21923 base pairs on chromosome X p11.22–23 (Voelter-Mahlknecht *et al.*, 2003) and its transcription results in a 3648-bp mRNA encompassing 28 exons. Within its promoter, binding sites for nuclear factor kappa-light-chain-enhancer of activated B cells (NF-κB) and the glucocorticoid receptor (GR) were identified (Ding *et al.*, 2013). In addition, the transcription of HDAC6 is regulated by epigenetic mechanisms. Commonly, DNA hypermethylation correlates with heterochromatin formation and transcriptionally inactive genes. Accordingly, higher methylation levels of the CpG islands of the HDAC6 promoter are associated with lower HDAC6 mRNA expression in systemic lupus erythematosus patients (Fang *et al.*, 2016), whereas promoter hypomethylation is associated with HDAC6 overexpression in patients with chronic obstructive pulmonary disease (Lam *et al.*, 2013). Moreover, HDAC6 expression is also down-regulated by miR such as miR-22 (Sibbesen *et al.*, 2015), -433 and -548 (Seidel *et al.*, 2015), which post-transcriptionally target the 3'-untranslated region of HDAC6 mRNA.

HDAC6 is a structurally unique isoenzyme of the HDAC family as it is the only member harboring two potentially functional active sites (Figure 9). From N-terminal to C-terminal, this enzyme is composed of the following domains: a NLS rich in arginine and lysine sequences; a leucine-rich NES; two catalytic sites, deacetylase domain (DD)1 and 2 (Hubbert *et al.*, 2002); a cytoplasmic retention signal called SE14, which is a repeated sequence of eight consecutive Ser-Glu tetradecapeptides (Bertos *et al.*, 2004); and a zinc finger ubiquitin-binding domain (BUZ) (Seigneurin-Berny *et al.*, 2001) that binds poly-ubiquitinated misfolded proteins through the C-terminal Gly-Gly residues of ubiquitin (Pai *et al.*, 2007). Up to now, it is controversial whether both DD1 and DD2 of HDAC6 are fully functional. Initial studies reported that both domains are catalytically active toward histone substrates, with only DD2 displaying tubulin deacetylase activity (Haggarty *et al.*, 2003), whereas more recent studies suggested that only DD2 is catalytically active (Zou *et al.*, 2006). In 2016,

crystallographic structures of both catalytic domains of zebrafish HDAC6, and of human DD2 were reported. The two catalytic domains are structurally highly conserved with a similar active site. In zebrafish, both DD1 and DD2 are functional, although DD1 has a weaker activity and displays much more stringent selectivity towards substrates bearing C-terminal acetyl-lysine residues (Hai *et al.*, 2016; Y. Liu *et al.*, 2016). Despite several dissimilarities between zebrafish and human HDAC6 proteins, an overall analysis revealed that the structure of zebrafish HDAC6 is a valid model to characterize the human enzyme (Miyake *et al.*, 2016).

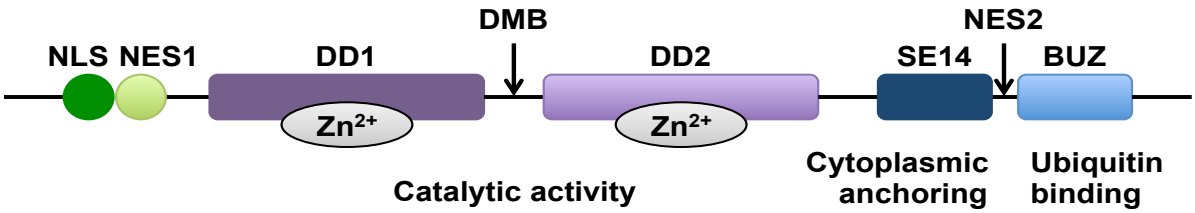

Figure 9: Schematic structure of HDAC6.
Figure adapted from (Li *et al.*, 2013). DD: Deacetylase domain; DMB; Dynein motor binding; NLS: Nuclear localization sequence; NES: Nuclear export sequence; SE14: Cytoplasmic retention domain; BUZ: Ubiquitin binding domain.

6.2. Regulation of HDAC6 activity

Multiple levels of regulation are required to achieve well-tuned HDAC6 activity. The first one is related to its localization within cells. In undifferentiated cells (*e.g.* embryonic stem cells, neuronal cells and some cancer stem cell lines), HDAC6 is mainly localized in the nucleus where it regulates TIP60-p400, a chromatin-remodeling complex in which TIP60 functions as a HAT and p400 mediates exchange of histone dimers in nucleosomes (Chen *et al.*, 2013). Upon cell differentiation, HDAC6 translocates to the cytoplasm thanks to its NES sequence. The cytoplasmic localization of HDAC6 depends on chromosome region maintenance (CRM)1 and an inhibition of this nuclear export protein triggers HDAC6 nuclear re-localization (Verdel *et al.*, 2000). Moreover, its retention in the cytoplasm results from an inhibition of HDAC6-importin-α interaction due to p300-mediated acetylation at the NLS. Notably, the SE14 domain also serves as an important sequence element to stably retain HDAC6 in the cytoplasm (Bertos *et al.*, 2004). Within the cytoplasm, HDAC6 has the capacity to translocate through its association with HSP90α, along with Ras-related C3 botulinum toxin substrate (RAC)1. This displacement to actin-enriched membrane ruffles follows platelet-derived growth factor (PDGF) stimulation and results in signaling-dependent actin remodeling and cell migration (Gao *et al.*, 2007).

HDAC6 functions are also regulated by PTMs such as phosphorylation and acetylation by specific kinase or HAT, respectively (Kramer *et al.*, 2014). For instance, glycogen synthase kinase (GSK)-3β (Chen *et al.*, 2010) and CK2 (Watabe *et al.*, 2011) promote HDAC6 activity through enhanced phosphorylation, potentially at Ser22 and at Ser458, respectively, resulting in decreased α-tubulin acetylation, whereas human epidermal growth factor receptor (EGFR)-mediated phosphorylation of HDAC6 on Tyr570 leads to increased acetylated α-tubulin (Deribe *et al.*, 2009). In addition, under certain conditions p300 interacts with and acetylates HDAC6 resulting in the inhibition of its deacetylase activity (Han *et al.*, 2009).

Finally, HDAC6 activity is modulated through its direct or indirect interactions with various partners, such as the membrane-associated protein dysferlin (Di Fulvio *et al.*, 2011), invasion inhibitory protein (IIp)45 (Wu *et al.*, 2010), tubulin polymerization-promoting protein/p25 (TPPP/p25) (Tokesi *et al.*, 2010) or farnesyltransferase (Zhou *et al.*, 2009). HDAC6 deacetylase activity is inhibited through direct interaction with dysferlin, IIp45 or TPPP/p25, as well as *via* the disruption of the tripartite protein complex composed of HDAC6 and farnesyltransferase together with microtubules (MTs), promoting subsequent acetylation of the MT network.

6.3. Physiological roles of HDAC6

Unlike most other members of the lysine deacetylase family, HDAC6 does not modify histones but controls the acetylation status of many non-histone substrates such as chaperones and cytoskeletal proteins (Spange *et al.*, 2009). Consequently, HDAC6 plays a critical role in many cellular processes, which are explained in greater details below.

6.3.1. Cytoskeletal dynamics

The cytoskeletal network is composed of MTs (α- and β-tubulin polymers), intermediate filaments (consisting of fibrillar proteins) and filamentous actins (F-actin polymers of globular or G-actin). The cytoskeleton controls a wide range of cellular mechanisms, such as the maintenance of cellular morphology and polarity, as well as the modulation of intracellular transport, endocytosis, mitosis, cell migration and angiogenesis (Aldana-Masangkay *et al.*, 2011b; Seidel *et al.*, 2015).

6.3.1.1. α-Tubulin

The acetylation level of α-tubulin is essential for MT structure and functions (Figure 10) and is mostly governed by the balance between the actions of ATAT1 (Friedmann *et al.*,

2012) and HDAC6 (Hubbert *et al.*, 2002) on lysine 40 (Figure 11). This modification site of α-tubulin, located on the luminal side of MTs, is also targeted by SIRT2 (Misawa *et al.*, 2013; Nagai *et al.*, 2013) and various HATs (*e.g.* ELP3, ARD1, NAT10, and GCN5) that have only a minor impact on its global level of acetylation (L. Li *et al.*, 2015; Seidel *et al.*, 2015).

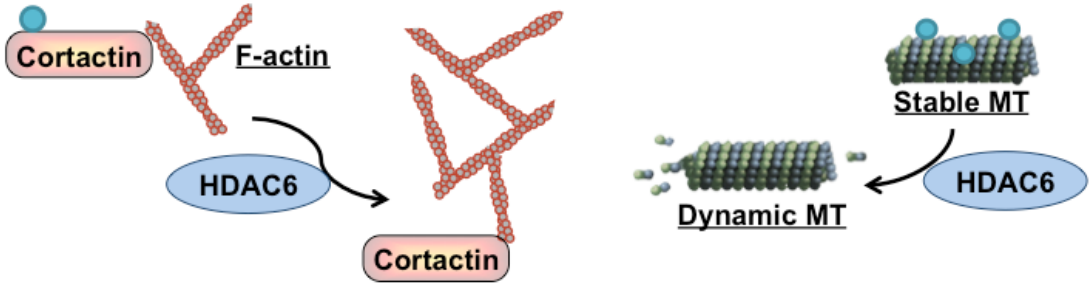

Figure 10: Role of HDAC6 in cell division and migration.
HDAC6 participates in F-actin assembly and microtubule (MT) dynamic through the regulation of the acetylation of cortactin and α-tubulin, respectively. acetyl.

Although α-tubulin acetylation mainly occurs on stable MTs resistant to depolymerization, this might rather be a consequence of MT stability. Indeed, the level of bound HDAC6, and not tubulin acetylation, determines the stability of MTs. Notably, HDAC6-mediated enhancement of cellular motility is due to decreased tubulin acetylation leading to reduced MT stability (L. Li *et al.*, 2015).

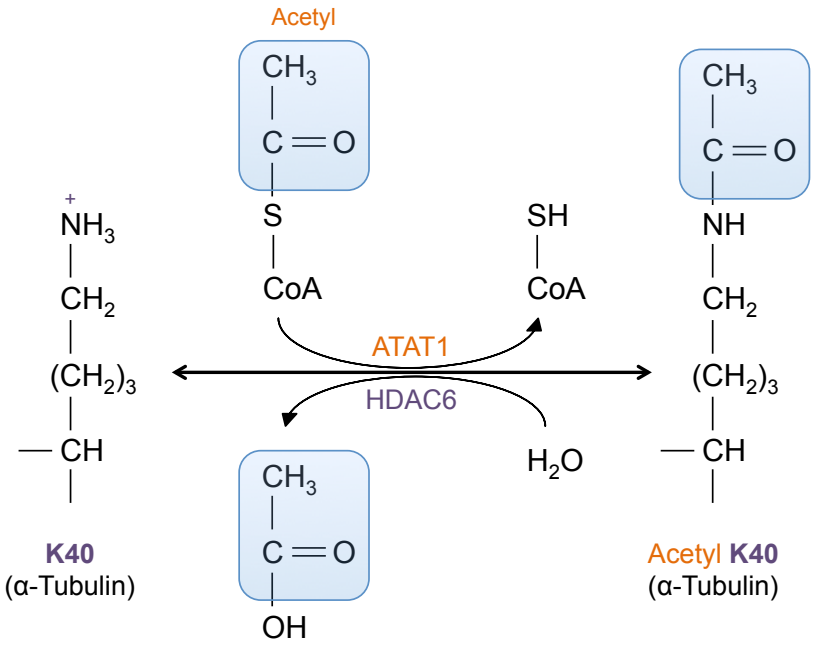

Figure 11: Reciprocal reaction of acetylation-deacetylation on lysine 40 of α-tubulin catalyzed by α-tubulin acetyltransferase (ATAT)1 and histone deacetylase (HDAC)6, respectively.
Adapted from (L. Li *et al.*, 2015).

HDAC6-dependent α-tubulin deacetylation contributes to the regulation of endocytic transport and degradation of receptor tyrosine kinases, such as EGFR, in various cancer subtypes (Gao *et al.*, 2010; W. Liu *et al.*, 2012). HDAC6 prolongs EGFR signaling by delaying its degradation in gastric cancer cells (Park *et al.*, 2014), whereas decreased HDAC6 expression leads to an increase in EGFR protein turnover in lung cancer cells (Kamemura *et al.*, 2008). Thus, the loss of HDAC6 activity causes a decrease in the steady-state level of EGFR due to the deregulation of the MT-dependent trafficking of EGFR-containing endosomal vesicles and the subsequent delivery of endocytosed EGFR to the lysosome for degradation (Deribe *et al.*, 2009; Gao *et al.*, 2010).

6.3.1.2. Cortactin

Cortactin is a protein involved in the rearrangement of the F-actin cytoskeleton through the promotion of F-actin polymerization and crosslinking. The balance between the catalytic activities of the acetyltransferase PCAF on one side, and HDAC6 and SIRT1 on the other side determines the level of acetylation of lysine residues within F-actin-binding repeats of cortactin (Figure 10). Upon deacetylation, cortactin binds to F-actin and enhances its polymerization, stimulating cell motility (Zhang *et al.*, 2007; Zhang *et al.*, 2009).

6.3.2. HDAC6 and misfolded proteins

The accumulation of misfolded proteins leads to the formation of toxic protein aggregates and disturbs protein homeostasis by interacting with normal native proteins and inhibiting their function and activity. Therefore, cells need to continuously protect themselves against misfolded proteins. Interestingly, HDAC6 appears both as a sensor of stressful stimuli and as an effector, which mediates and coordinates appropriate cell responses to manage the cellular stress induced by cytotoxic assaults (Matthias *et al.*, 2008). Depending on the physio-pathological situation, cells are able to counteract the toxic effects of misfolded proteins by activating different defense mechanisms involving HDAC6 thanks to unique cytoprotective functions dependent and independent of its deacetylase activity (Bruning *et al.*, 2015) (Figure 12).

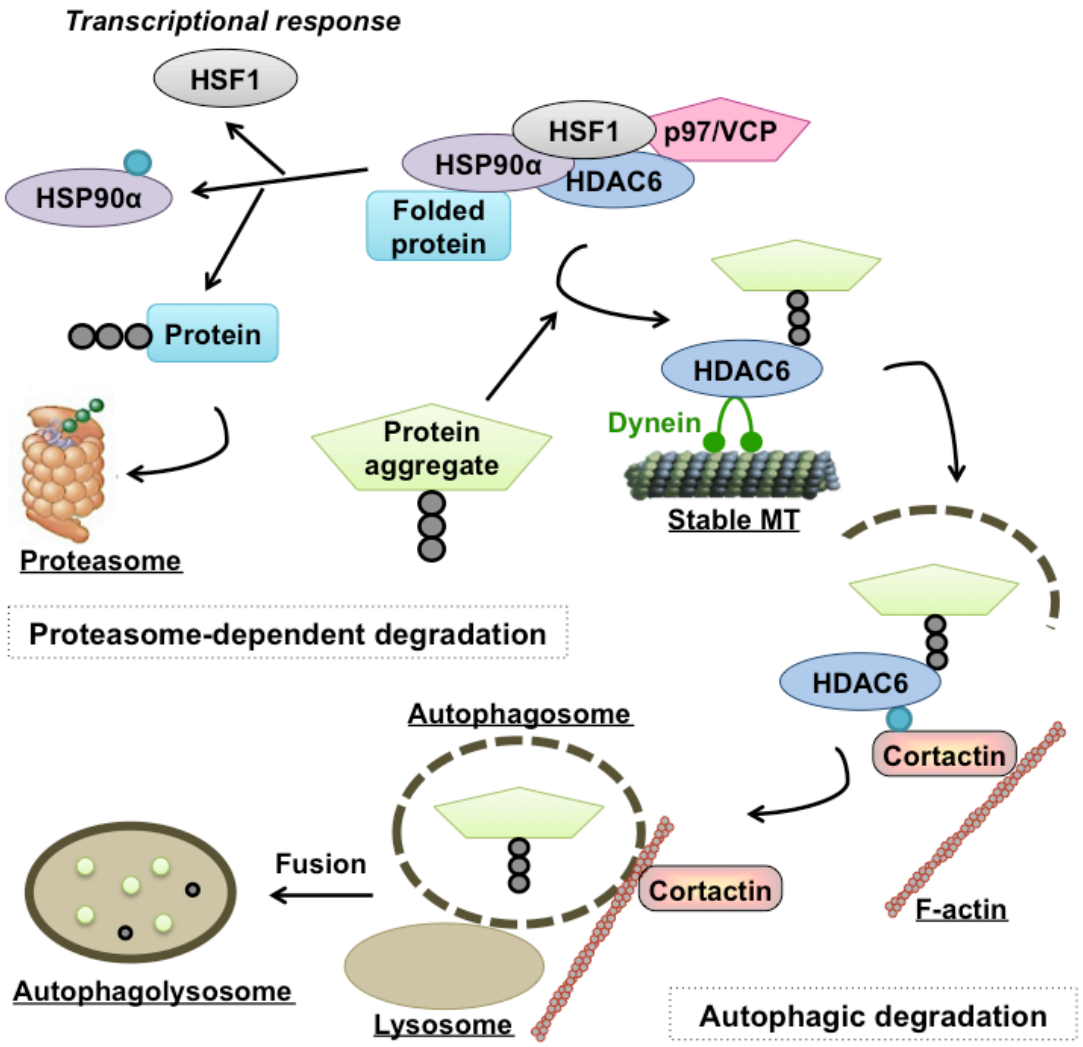

Figure 12: Role of HDAC6 in protein degradation.
HDAC6 is implicated in protein degradation that is either proteasome-independent by forming aggresomes or proteasome-dependent based on the acetylation status of the chaperone heat shock protein (HSP)90α. acetyl, ubiquitin. HSF: heat shock factor; MT: microtubule; VCP: valosin-containing protein.

6.3.2.1. Repair of misfolded proteins

HDAC6 is implicated in protein renaturation through its interaction with the chaperone HSP90α (Bali *et al.*, 2005; Kovacs *et al.*, 2005) (Figure 12), which is the most common and abundantly expressed HSP in eukaryotic cells (Miyata *et al.*, 2013). Upon deacetylation by HDAC6, HSP90α binds client proteins, which rely on its chaperoning activity to maintain a stable and favorable conformation allowing physiological activities (Bruning *et al.*, 2015; Seidel *et al.*, 2015) and protein homeostasis (Kramer *et al.*, 2014). Acetylation of HSP90α impedes its chaperone activity and therefore triggers proteasome-mediated degradation of its pro-growth and pro-survival client oncoproteins, including the breakpoint cluster region

(BCR)-V-Abl Abelson murine leukemia viral oncogene homolog (ABL), androgen receptor (AR), p53, Erb-B2 receptor tyrosine kinase (ERBB)2, AKT, RAF1, EGFR, fms related tyrosine kinase (FLT)3 (Bali *et al.*, 2005; Bolden *et al.*, 2006; Kim *et al.*, 2009), GR (Jochems *et al.*, 2015), fibroblast growth factor (FGF)-3 (Ota *et al.*, 2016) and HIF-1α (Ryu *et al.*, 2017b).

6.3.2.2. Proteasomal degradation

HDAC6 regulates proteasome-dependent protein degradation and elimination (Figure 12). In unstressed cells, HDAC6 recruits a partner, the adenosine triphosphate (ATP)-dependent chaperone p97/valosin-containing protein (VCP), to a complex in which HSP90α interacts with the major heat shock transcription factor (HSF)1 to maintain it in an inactive form. When poly-ubiquitinated proteins accumulate, they recruit and bind HDAC6 triggering the disruption of the repressive HDAC6/HSP90α/HSF1 complex (Boyault *et al.*, 2007b), resulting in increased HSF1-mediated gene transcription of various cytoprotective chaperone proteins (*e.g.* HSPs). The chaperone p97/VCP contributes to the specific separation of HSP90α and HSF1 by its "segregase" activity (Boyault *et al.*, 2006). Furthermore, p97/VCP dissociates poly-ubiquitinated proteins bound to HDAC6, and is implicated in the binding and remodeling of proteins before their delivery to the proteasome (Boyault *et al.*, 2006; Boyault *et al.*, 2007b).

6.3.2.3. Autophagic degradation

HDAC6 is involved in the aggresome–autophagy pathway through an adaptor role in a deacetylase-independent manner (Figure 12). Upon inhibition or physiological overload of the proteasome machinery, specific ubiquitin-binding proteins such as HDAC6 detect and recruit individual poly-ubiquitinated proteins and small ubiquitinated aggregates, *via* their zinc finger ubiquitin-binding domain (Olzmann *et al.*, 2007). Intriguingly, the unusual structural feature of its BUZ domain suggests that HDAC6 exclusively recognizes and binds unanchored K63-linked ubiquitin chains in aggregates. Accordingly, HDAC6 appears to pair with two different deubiquitinases, aggregate-associated ataxin 3 and proteasomal Poh1, to control aggresome formation and clearance, respectively (Ouyang *et al.*, 2012; Hao *et al.*, 2013). By serving as an adaptor protein between ubiquitinated protein aggregates and dynein, HDAC6 facilitates the loading of aggregated proteins onto the MT motor protein complex, which is important for addressing misfolded proteins to the MT-organizing center (MTOC) (Kawaguchi *et al.*, 2003). Upon α-tubulin deacetylation, HDAC6 mediates retrograde transport of aggregate-

containing inclusion bodies along the microtubular network towards the MTOC (Kawaguchi *et al.*, 2003; Iwata *et al.*, 2005), where intermediate filaments surround and sequester the misfolded and deposited proteins to form aggresomes (Rodriguez-Gonzalez *et al.*, 2008). Aggresomes recruit proteasomes and a large amount of functional chaperones, which help to resolubilize these aggregates, or further maturate through engulfment into autophagosomes (Aldana-Masangkay *et al.*, 2011b). HDAC6 subsequently recruits and deacetylates cortactin, thereby promoting F-actin remodeling essential for efficient autophagosome–lysosome fusion and protein aggregate autophagic clearance (J.Y. Lee *et al.*, 2010a).

Thanks to its ability to bind ubiquitin, HDAC6 also plays a role in the elimination of damaged and poly-ubiquitinated mitochondria by mitophagy. Together with the ubiquitin-binding protein SQSTM1, also called p62, HDAC6 is recruited to mitochondria marked by parkin-mediated ubiquitination to form mito-aggresomes (J.Y. Lee *et al.*, 2010b). Moreover, HDAC6 and SQSTM1 colocalize with the E3 ubiquitin ligase tripartite motif containing (TRIM)50 to aggregate formation sites (Fusco *et al.*, 2012; Fusco *et al.*, 2014). Interestingly, a specific binding domain of SQSTM1, localized in an undefined region between the ZZ-type zinc finger domain of SQSTM1 and tumor necrosis factor (TNF) receptor associated factor (TRAF)6 binding region (*i.e.* residues 164-225), interacts with DD2 of HDAC6 to modulate HDAC6-mediated deacetylation of α-tubulin, which controls MT stability (Yan *et al.*, 2013). Disruption of the SQSTM1-HDAC6 interaction blocks the autophagosome-lysosome fusion, which triggers different types of cell death through oxidative stress and lysosomal rupture (Chen *et al.*, 2015). Of note, HDAC6 and SQSTM1 have also been associated with the clearance of non-ubiquitinated substrates through the aggresome pathway (Watanabe *et al.*, 2011). Additionally, HDAC6 regulates autophagic degradation of misfolded proteins by deacetylation of ATGs. For example, it induces the deacetylation of LC3B-II, a key regulator of autophagy (Liu *et al.*, 2013), concomitant with SQSTM1 degradation.

6.3.2.4. Unfolded protein response and cell death

HDAC6 is implicated in ER stress by deacetylating GRP78. This ATP-dependent chaperone is located in the ER where it helps protein folding and assembly. When GRP78 is acetylated, it dissociates from PERK, initiating UPR followed by cell death (Rao *et al.*, 2010).

6.3.3. Apoptosis

HDAC6 regulates apoptosis by controlling the acetylation status of Ku70, a DNA repair nuclear factor also localized in the cytoplasm, where it interacts with the pro-apoptotic BAX

protein (Figure 13). Deacetylated Ku70 leads to BAX sequestration, which inhibits apoptosis, whereas acetylated Ku70 causes the dissociation of the complex and thereby the release of BAX, which subsequently triggers apoptosis (Subramanian *et al.*, 2011). Moreover, Ku70 acetylation disrupts its interaction with the anti-apoptotic protein Fas-associated death domain protein (FADD)-like IL-1 β-converting enzyme (FLICE) inhibitory protein (FLIP), which is then degraded by the proteasome, resulting in apoptosis induction (Kerr *et al.*, 2012). HDAC6 also controls apoptosis through its implication in PI3K/AKT and mitogen-activated protein kinase (MAPK)/extracellular signal-regulated kinases (ERK) signaling pathways (Figure 13). After inhibition, HDAC6 detaches from protein phosphatase (PP)1 (Balliu *et al.*, 2015), promoting the dephosphorylation of its targets phospho-AKT and phospho-ERK, which leads to reduced cell proliferation and an induction of cell death in cancer cells. Moreover, phosphorylated AKT and ERK levels are decreased upon HSP90α hyperacetylation, triggered by HDAC6 inhibition (Lee *et al.*, 2008; Seidel *et al.*, 2015).

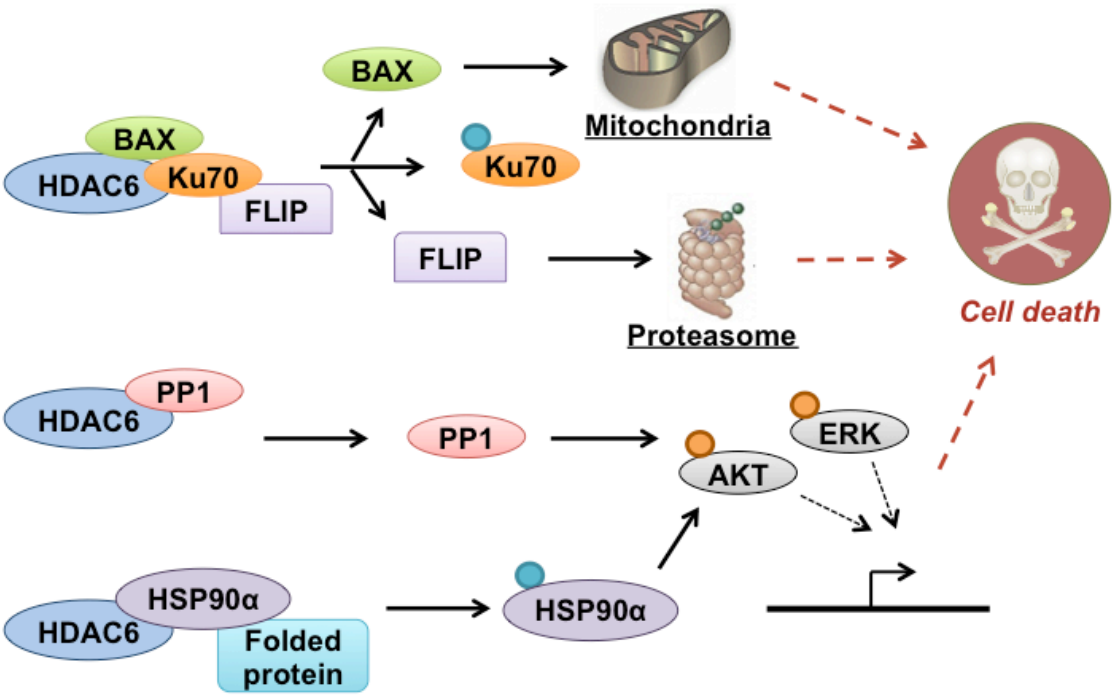

Figure 13: HDAC6 possesses anti-apoptotic properties.
HDAC6 deacetylates Ku70, which sequesters BCL-2-associated X protein (BAX) and Fas-associated death domain protein (FADD)-like interleukin-1β-converting enzyme (FLICE) inhibitory protein (FLIP), as well as plays a role in the phosphoinositide 3-kinase (PI3K)/AKT and mitogen-activated protein kinase (MAPK)/extracellular signal-regulated kinase (ERK) signaling pathways. acetyl, phosphate. HSP: heat shock protein; PP: protein phosphatase.

6.3.4. Transcriptional repression

Upon localization in the nucleus, HDAC6 recruitment to regulatory sequences of target gene promoters may result in their transcriptional repression (Figure 14). For instance, at the c-MYC promoter, HDAC6 is retained in a protein complex whose critical components appear to be repressing factors such as SMRT and HDAC11. Authors point out that the dynamic association of those nuclear proteins, along with vitamin D receptor (VDR) and transducer beta-like 1, X-linked (TBL1X), may sufficiently explain the mechanisms of c-MYC down-regulation by the nuclear hormone 1α,25-dihydroxyvitamin D_3 (Toropainen *et al.*, 2010).

Upon ligand stimulation, GR forms a complex with HDAC6, which directly interacts with the GR activation function (AF)-1 domain *via* a L*XX*LL motif leading to histone H3 and H4 deacetylation. The subsequent chromatin remodeling orchestrates GR gene expression by a negative feedback regulation (Govindan, 2010).

In osteoblasts, HDAC6 and RUNX2 directly interact with each other and with chromatin. This interaction suggests a contribution of HDAC6 to RUNX2-mediated repression of the cyclin-dependent kinase inhibitor p21 (Westendorf *et al.*, 2002). In addition, the sequestration of p53 in a complex along with RUNX2 and HDAC6 prevents its transcriptional activities (Ozaki *et al.*, 2013), likely through HDAC6-mediated deacetylation at lysine 381/382 (Ryu *et al.*, 2017a).

Co-localization experiments established a direct association and co-recruitment of ligand-dependent nuclear receptor co-repressor (LCoR) and HDAC6 to promoters of genes under estradiol regulation. Here, HDAC6 acts as a cofactor of LCoR-mediated transcriptional repression of estrogen target genes in breast cancer cells. However, it is unclear whether they also enhance the expression of a subset of estrogen-stimulated genes. Notably, LCoR and HDAC6 seem to be associated with distinct complexes within bone morphogenetic protein (BMP)7 promoter (Palijan *et al.*, 2009).

HDAC6 was reported to interact with the promoter of Ras homolog family member B (RhoB) and repress its expression. Upon HDAC6 inhibition, RhoB transcription could be regulated *via* p300-mediated acetylation of HDAC6, which would result in decreased HDAC6 deacetylase activity. The subsequent tubulin deacetylation would indirectly suppress specificity protein (Sp)1 transcriptional activity that promotes the expression of oncogenes (Marlow *et al.*, 2015).

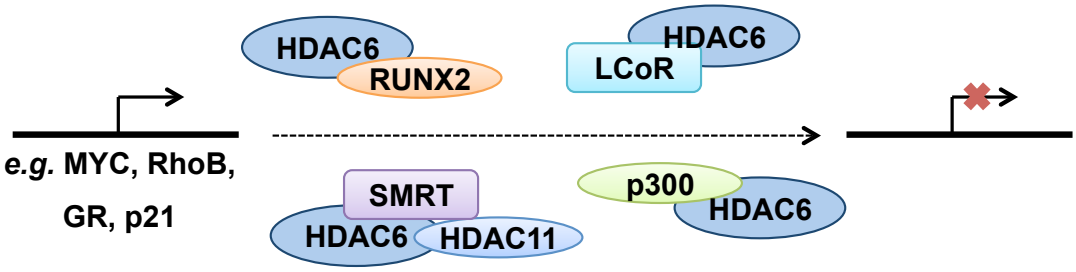

Figure 14: HDAC6 participates in gene regulation.
HDAC6 regulates genes through the formation of various transcriptional repressor complexes. GR: glucocorticoid receptor; LCoR: ligand-dependent nuclear receptor co-repressor; RhoB: Ras homolog family member B; RUNX: runt-related transcription factor; SMRT: silencing mediator for retinoid or thyroid-hormone receptors.

6.3.5. Pro-oxidant activity

The redox regulatory proteins peroxiredoxins (Prxs) are thiol-dependent peroxidases, which detoxify H_2O_2, organic hydroperoxides and peroxynitrite to protect cells against free radical accumulation. Prx 1 and 2 are specific substrates of HDAC6 deacetylase activity, which thus plays an essential role in redox regulation and cellular stress response. Upon HDAC6 inhibition, increased acetylation of the antioxidant enzymes Prx 1 and 2 on Lys197 and Lys196 residues, respectively, is associated with enhanced H_2O_2-reducing activity, leading to an increased cellular resistance to H_2O_2-induced cell death (Figure 15). Remarkably, this effect may contribute to cancer cell resistance to chemotherapy (Parmigiani *et al.*, 2008).

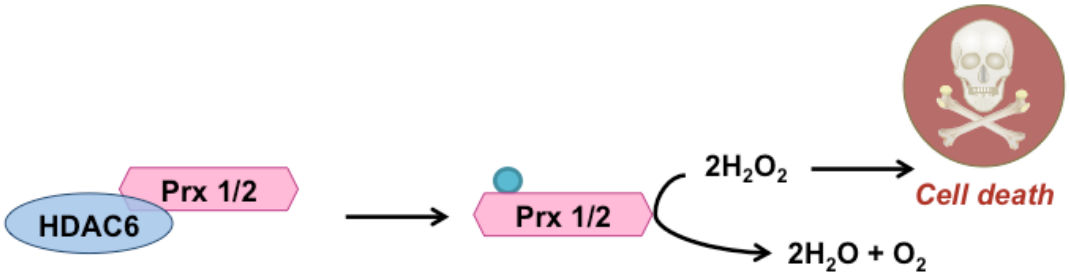

Figure 15: HDAC6 is involved in redox regulation.
HDAC6 possesses pro-oxidant properties *via* the deacetylation of peroxiredoxin (Prx)1/2. acetyl.

6.4. HDAC6 in cancer

Nowadays, it is well established that HDAC6 exerts functions in various disease processes, such as in neurodegenerative and chronic diseases (Batchu *et al.*, 2016), in viral infections by affecting viral replication (Zheng *et al.*, 2017), or in autoimmune diseases by their capacity to decrease the immunosuppressive potential of regulatory T cells (Kalin *et al.*,

2012). We will focus on the critical implications of HDAC6 in diverse mechanisms related to cancer including tumor initiation, development and metastasis (Lee *et al.*, 2008; P.H. Yang *et al.*, 2013). HDAC6 expression is up- or down-regulated in several cancer subtypes (Table 2) in which it can play a role as tumor inducer or suppressor depending on cancer type and stage (de Ruijter *et al.*, 2003; Seidel *et al.*, 2015). In cancer, aberrant HDAC6 overexpression correlates with advanced cancer stages and increased neoplastic transformation (Aldana-Masangkay *et al.*, 2011b; Bruning *et al.*, 2015).

Table 2: HDAC6 expression is deregulated in various cancer subtypes.

Cancer	Expression-comments	Reference
ALL	Overexpressed - expression increased in advanced stage	(Bradbury *et al.*, 2005; Moreno *et al.*, 2010)
AML	Overexpressed relative to adult	(Bradbury *et al.*, 2005)
Brain cancer	Overexpressed	(de Ruijter *et al.*, 2003)
Breast cancer	Overexpressed - correlated with better or poor prognosis	(Yoshida *et al.*, 2004; Zhang *et al.*, 2004; Saji *et al.*, 2005)
Cholangiocarcinoma	Overexpressed	(Gradilone *et al.*, 2013)
CLL	Overexpressed - correlated with longer survival	(Van Damme *et al.*, 2012)
CTCL	Overexpressed - correlated with longer survival	(Marquard *et al.*, 2008)
GBM	Overexpressed	(S. Li *et al.*, 2015)
HCC	Overexpressed - expression increased in advanced stage Under expressed - correlated with poor prognosis	(Jung *et al.*, 2012; Kanno *et al.*, 2012; Ding *et al.*, 2013; Lv *et al.*, 2016)
Lung adenocarcinoma	Overexpressed	(Wang *et al.*, 2016b)
Melanoma	Overexpressed	(Bai *et al.*, 2015)
Oral squamous cell carcinoma	Overexpressed - expression increased in advanced stage	(Sakuma *et al.*, 2006; Witt *et al.*, 2009)
Ovarian cancer	Overexpressed - expression increased in advanced stage	(de Ruijter *et al.*, 2003; Bazzaro *et al.*, 2008)
Pancreatic cancer	Overexpressed	(Li *et al.*, 2014)
Urothelial cancer	Overexpressed	(Rosik *et al.*, 2014)

ALL: acute lymphocytic leukemia, AML: acute myeloid leukemia, CLL: chronic lymphocytic leukemia, CTCL: cutaneous T-cell lymphoma, GBM: glioblastoma, HCC: hepatocellular carcinoma.

6.4.1. Tumor progression

It has been demonstrated that HDAC6 regulates cell proliferation at distinct cell-cycle phases. HDAC6 interacts with and is inhibited by the deubiquitinating enzyme cylindromatosis (CYLD) in the perinuclear region, significantly delaying the G_1-to-S-phase transition, and in the midbody where it regulates the rate of cytokinesis in a deubiquitinase-independent manner (Wickstrom *et al.*, 2010). Moreover, HDAC6 regulates the c-Raf-PP1-ERK signaling pathway and inhibition of HDAC6 activity contributes to early M-phase cell-cycle transition arrest *via* sustained ERK activation in prostate cancer (Chuang *et al.*, 2013). Additionally, cancer developmental steps such as the sustained activation of growth factor signaling and cellular proliferation are achieved through the modulation of specific HDAC6-related pathways, such as (*i*) the HDAC6-peptidylprolyl cis/trans isomerase NIMA-interacting (PIN)1 axis, whose activation underlies the positive effects of G protein-coupled receptor kinase (GRK)2 in both luminal and basal breast cancer cells (Nogues *et al.*, 2016); (*ii*) HDAC6-mediated attenuation of TGFβ receptor signaling promoting glioblastoma growth (S. Li *et al.*, 2015); (*iii*) HDAC6-p53 molecular network that controls hepatocellular carcinoma development (Ding *et al.*, 2013).

6.4.2. Angiogenesis

HDAC6 is implicated in various mechanisms underlying angiogenesis, which is an essential process for tumor progression and metastatic spread. First, HDAC6, whose mRNA and protein expression levels are up-regulated by hypoxia in endothelial cells (ECes) (Kaluza *et al.*, 2011), increases HIF-1α stability in cancer cells *via* direct deacetylation, and also indirectly through the modulation of HSP90α chaperone function (Ryu *et al.*, 2017b). HIF-1α protein accumulation stimulates its transcriptional activity towards target genes promoting angiogenesis such as VEGF (Qian *et al.*, 2006). Additionally, HDAC6-mediated HSP90α deacetylation ensures adequate binding to VEGF receptor (VEGFR)-1 or VEGFR-2, which transduces angiogenic signaling upon VEGF-A stimulation (Park *et al.*, 2008). Furthermore, pro-angiogenic effects of HDAC6 in ECes are achieved *via* HDAC6-modulated (*i*) stimulation of membrane ruffling at the leading edge to promote cell polarization, (*ii*) regulation of ECe migration and generation of capillary-like structures in a MT end-binding protein (EB)1-dependent manner (Li *et al.*, 2011), and (*iii*) deacetylation of the actin-remodeling protein cortactin, which is necessary for ECe migration and sprouting (Kaluza *et al.*, 2011). Surprisingly, hypoxia-induced suppression of HDAC6 promotes angiogenesis in hepatocellular carcinoma by significantly up-regulating HIF-1α/VEGF-A expression levels

(Lv *et al.*, 2016). Although the mechanisms underlying hypoxia-induced modulation of HDAC6 expression have not been extensively described, one study showed that HDAC6 down-regulation by hypoxia was mediated by increased expression of miR-26a that directly targeted the 3'-untranslated region of HDAC6 mRNA (Lee *et al.*, 2015).

6.4.3. Epithelial-to-mesenchymal transition

Type-3 epithelial-to-mesenchymal transition (EMT) is a hallmark of metastatic cancer, promoting tumor cell motility and invasiveness (Kalin *et al.*, 2013). TGFβ-mediated EMT induction is accompanied with HDAC6-dependent loss of α-tubulin acetylation, supporting that HDAC6 represents a key regulator of this process (Gu *et al.*, 2016). In non-small cell lung cancer, HDAC6 regulates the TGFβ-induced Notch-1 signaling cascade activation *via* deacetylation of HSP90α (Deskin *et al.*, 2016), whereas in lung adenocarcinoma, HDAC6 interplays with the TGFβ-SMAD3 signaling cascade and is required for the maximal expression of various TGFβ-induced EMT markers, such as the proteins E-cadherin and vimentin (Shan *et al.*, 2008).

6.4.4. Aggressiveness: migration, invasion and metastasis

Thanks to its influence on the acetylation status of α-tubulin and other cytoskeletal proteins such as cortactin [reviewed by Boyault *et al.* (Boyault *et al.*, 2007a)], HDAC6 promotes cell motility and contributes to the invasiveness and metastasis of many cancers including breast cancer (Saji *et al.*, 2005), prostate cancer (Hou *et al.*, 2015), Burkitt's lymphoma (Ding *et al.*, 2014), neuroblastoma (Zhang *et al.*, 2014) and hepatocellular carcinoma (HCC) (Kanno *et al.*, 2012). In other cancer types, HDAC6 stimulates tumor cell aggressiveness by acting synergistically with other partners such as SIRT2 in bladder cancer (Zuo *et al.*, 2012), cytoplasmic linker protein (CLIP)-170 in pancreatic cancer cells (Li *et al.*, 2014), HDAC5 in melanoma cells (J. Liu *et al.*, 2016), and estrogen receptor (EsR)α ligand in EsRα-positive breast cancer cells (Azuma *et al.*, 2009). Interestingly, stress signals can stimulate the migration of cancer cells by enhancing HDAC6 gene transcription through a protein kinase A (PKA)/Epac/ERK-dependent signaling pathway in lung and other cancer cells (Lim *et al.*, 2016). Accordingly, HDAC6 inhibition or depletion increases acetylated α-tubulin levels (Miyake *et al.*, 2016), which enhances MT stability and reduces cancer cell growth and migration (Hubbert *et al.*, 2002). For example, Ras association domain family member (RASSF)1A regulates cell migration through inhibition of HDAC6 activity (Jung *et al.*, 2013).

6.4.5. Cancer resistance to therapeutic agents

HDAC6 is implicated in cancer cell resistance to various chemotherapeutic agents. HDAC6 overexpression, resulting in EGFR stabilization and activation, confers resistance to the EGFR inhibitor gefitinib in lung adenocarcinoma (Wang *et al.*, 2016b), and to the VEGF inhibitor sorafenib in non-small lung cancer cells (Wang *et al.*, 2016a). Furthermore, the balance of HDAC6-p97/VCP influences HDAC6-facilitated autophagic clearance of ubiquitinated misfolded proteins, which is crucial to ER stress-tolerance (ERST)-associated temozolomide resistance in glioma (Li *et al.*, 2017). In contrast, HDAC6 inhibition or depletion sensitizes cancer cells to chemotherapeutic compounds such as doxorubicin and etoposide in transformed but not in normal cells (Namdar *et al.*, 2010; Lee *et al.*, 2013); placlitaxel (Marcus *et al.*, 2005) and cisplatin (Wang *et al.*, 2012) in non-small cell lung cancer; vincristine and bortezomib in ALL (Aldana-Masangkay *et al.*, 2011a).

7. HDAC6 inhibitors

Since epigenetic mechanisms are virtually involved in all signaling pathways, non-selective HDACi alter many cellular processes leading to many side effects for patients during cancer therapy. Nowadays, an increasing number of investigations are focusing on the development of isotype-selective HDACi (Balasubramanian *et al.*, 2009; Qin *et al.*, 2017) to target cancer cells more specifically and reduce side effects (Gryder *et al.*, 2012).

Considering its unique physiological function and structure, as well as its implication in cancer progression, HDAC6 isoenzyme became an interesting and important pharmacological target for cancer therapy (P.H. Yang *et al.*, 2013; Seidel *et al.*, 2015). Diverse HDAC6i have been synthetized with the hope of designing a highly selective and potent compound, with suitable pharmacological properties. However, the selectivity and potency for most of them have only been characterized *in vitro* and tested on a limited number of cancer cell lines in which they display an anti-proliferative activity and promote cancer cell death. In addition, some molecules were tested on mouse tumors, decreasing tumor size without affecting animal weight, which suggests that HDAC6 inhibition would not cause major side effects (Bruning *et al.*, 2015; Seidel *et al.*, 2015). Up to now, only tubacin and tubastatin A were intensively reported in the literature as selective HDAC6 inhibitors (HDAC6i), while ACY-241 and ACY-1215 are undergoing clinical trials (Figure 16).

7.1. Tubacin

The hydroxamate-based tubacin, whose name is shortened from 'tubulin acetylation inducer', is considered as the first HDAC6-selective inhibitor and has been isolated through a high-throughput screening based on a multidimensional chemical genetic screen of 7392 small molecules and cell-based assays. Tubacin is characterized by a 1,3-dioxane structure and specifically inhibits α-tubulin deacetylation in a dose-dependent manner with no cross-reactive histone deacetylase activity (Haggarty *et al.*, 2003). Since tubacin possesses non-drug-like qualities such as a high lipophilicity and elaborate synthesis, it is used mainly as a pharmacological tool in *in vitro* fundamental research to discern the biological functions of HDAC6 in numerous cellular processes rather than as a potential drug for clinical applications.

Tubacin alone is neither able to alter gene expression in microarray analysis, nor does it induce any changes in cell cycle progression and cause aberrant mitotic spindle formation. Combining tubacin with other chemotherapeutic agents that stimulate stress response pathways in cancer cells, such as doxorubicin (topoisomerase II inhibitor), bortezomib (proteasome inhibitor) or 17-AAG (HSP90α inhibitor), enhances the inhibition of proliferation and viability of cancer cell lines (Li *et al.*, 2013; Seidel *et al.*, 2015). In addition, the combined use of bortezomib with tubacin results in an accumulation of cytotoxic proteins and aggregates in cancer cells. Indeed, these two drugs display a synergistic effect against MM cell lines with no detectable toxic effect on normal noncancerous peripheral blood mononuclear cells (PBMCs) (P.H. Yang *et al.*, 2013; Bruning *et al.*, 2015). Different studies also revealed the efficacy of tubacin as a single agent against leukemia cells and a chemo-sensitizing effect to cytotoxic drugs in breast and prostate cancer cells (Bruning *et al.*, 2015).

7.2. Tubastatin A

Butler *et al.* synthetized molecules following the canonical HDACi structure constituted of a hydroxamic acid, a linker and a carbazole system as an aromatic cap group. In order to find drug-like compounds with decreased lipophilicity, a tertiary amino moiety was added to the carbazole moiety to form salts improving the solubility of compounds. The resulting derivative called tubastatin A is another selective HDAC6i thanks to its tricyclic cap group, large and rigid enough to occupy the wider channel rim in the catalytic domain of HDAC6 compared to that of HDAC1. Tubastatin A was initially considered as a promising anticancer drug (Butler *et al.*, 2010); however, it displays apparently limited efficacy on solid cancer cells (P.H. Yang *et al.*, 2013; Bruning *et al.*, 2015; Seidel *et al.*, 2015).

7.3. ACY-1215

Among HDAC6 inhibitors, the hydroxamic acid-based compound ACY-1215 (rocilinostat) is currently undergoing clinical trials (www.clinicaltrials.gov). *In cellulo*, this molecule induces α-tubulin acetylation, as well as ER stress and caspase-dependent apoptosis, in synergy with bortezomib in MM cell lines. Accordingly, a preclinical study was conducted in a MM mouse model using ACY-1215 in combination with the proteasome inhibitor bortezomib resulting in increased α-tubulin acetylation associated with delayed tumor growth and improved mouse survival (Santo *et al.*, 2012). Similarly, ACY-1215 sensitizes a BRAF-mutant melanoma cell line to the anticancer effects of the BRAF inhibitor vemurafenib, which occur partly through stimulation of ER stress and inactivation of ERK (Peng *et al.*, 2017).

The promising pre-clinical data and the oral applicability of this compound have led to several clinical studies. Those trials are mainly conducted by Acetylon Pharmaceuticals, Inc. to test the efficacy of ACY-1215 either as a single agent or in combination with bortezomib and dexamethasone in patients with MM and other lymphoid malignancies (Vogl *et al.*, 2017).

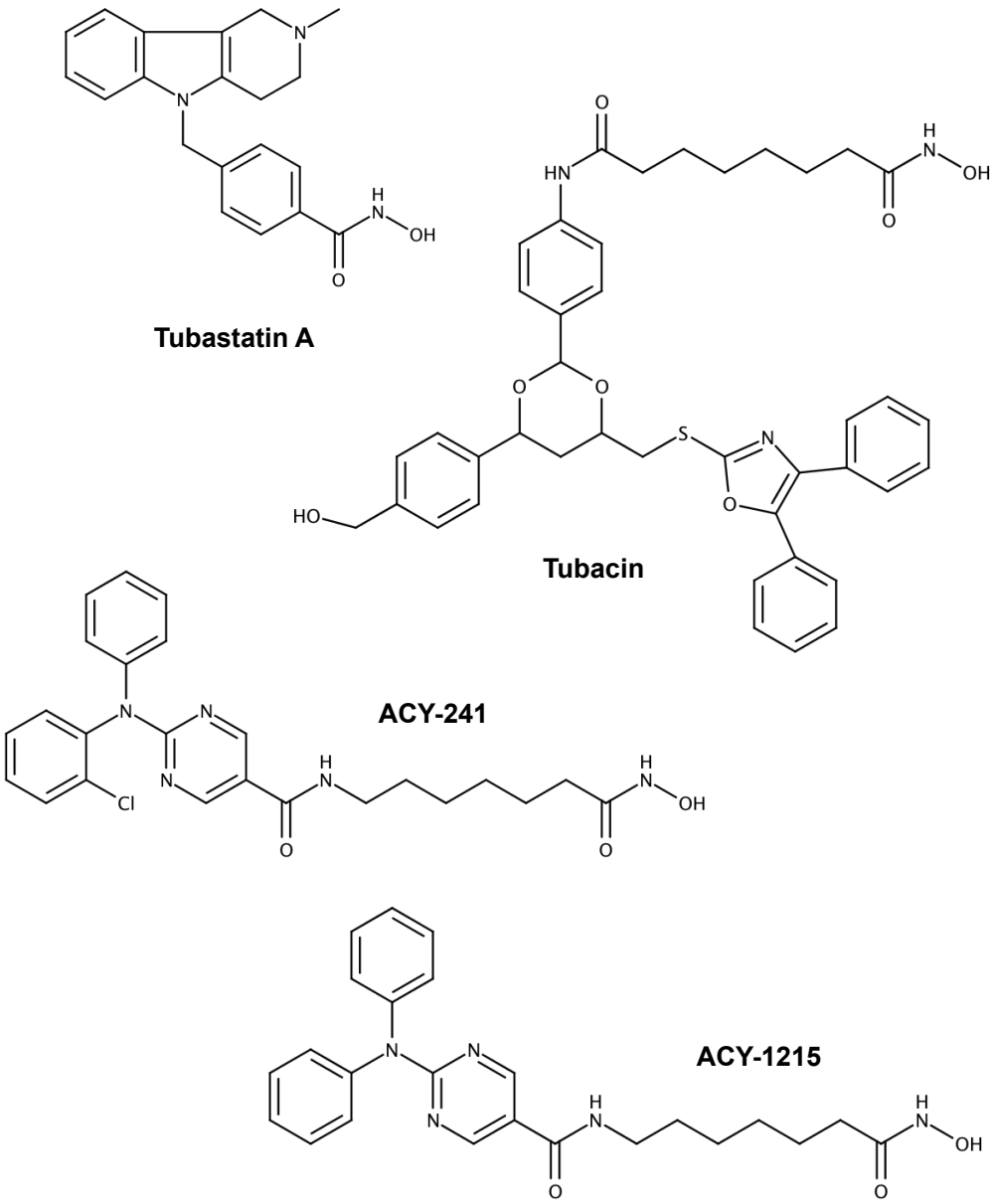

Figure 16: Molecular structures of selected HDAC6 inhibitors.

8. Cancers

8.1. Chronic myeloid leukemia

8.1.1. Classification of leukemia

The term *leukemia* describes abnormal proliferation and development of one or more cell lines in the bone marrow (BM). The broad classification of leukemia is still based on the cell origin (myeloid versus lymphoid) and the rapidity of the clinical course (acute versus chronic), resulting in four main types of leukemia. In chronic leukemia, slowly progressive accumulation (rather than proliferation) of cells in the BM and peripheral tissues predominates. Replacement of the normal hematopoietic tissue in the BM by tumor cells can occur before the onset of overt leukemia (Arber *et al.*, 2016).

CML is a hematological disorder characterized by an abnormal accumulation of clonal pluripotent hematopoietic stem cells in peripheral blood, BM and the spleen. Patients with CML consequently display symptoms such as anemia, extreme blood granulocytosis with immaturity, basophilia, thrombocytosis, and splenomegaly. Without treatment, CML ultimately progresses from a chronic phase that is primarily asymptomatic and characterized by an increase in granulocytes, to an accelerated phase, with a rapid expansion of granulocytes, and terminal blast crisis that resembles acute leukemia, leading to metastasis, organ failure and death (Thompson *et al.*, 2015).

8.1.2. Epidemiology

Worldwide, 1.2 to 1.5 million people are currently living with CML. In the United States, CML has an incidence of 1-2 cases per 100,000 adults, and accounts for approximately 15% of newly diagnosed cases of leukemia in adults (Jabbour *et al.*, 2018). While the number of patients diagnosed each year has stayed relatively constant, survival rates have more than doubled owing to advances in treatment.

The associated risk factors that may affect CML initiation include age (increased risk after 65 years of age), gender (higher genetic predisposition in males), obesity, and heavy exposure to radiation (Kabat *et al.*, 2013).

8.1.3. Pathophysiology

In 95% of patients, CML pathogenesis is driven by a cytogenetic abnormality known as the Philadelphia chromosome resulting from the reciprocal translocation t(9;22)(q34;11) between BCR and ABL genes (Figure 17). The resulting BCR-ABL fusion gene is translated in different BCR-ABL proteins that vary in size and pathogenicity depending on the location

of the breakpoint in the BCR gene. Three breakpoint cluster regions in the BCR gene have been described to date: major (M-BCR; p210), minor (m-BCR; p230), and micro (μ-BCR; p190) (Mughal *et al.*, 2016). The majority of patients with CML display breakpoints in exon a2 of the ABL gene and either in exons 13 (b2) or 14 (b3) of the BCR gene, resulting in fusion genes that are transcribed either to a b2a2 or b3a2 mRNA. The final product of this genetic rearrangement is a 210-kDa cytoplasmic fusion protein that is essential and sufficient for the malignant transformation of CML. Less frequently, CML is induced by atypical BCR-ABL transcripts, involving for instance, ABL exon a3 instead of a2 or transcripts with an e1a2, e19a2, or e6a2 junction (Pane *et al.*, 2002).

The oncogenic BCR-ABL protein, displaying abnormal constitutive tyrosine kinase activity, interacts with a variety of effector proteins involved in oncogenic pathways, which leads to the disruption of key cellular processes (Figure 17). Among these effectors, STAT5 is a transcription factor aberrantly activated through BCR-ABL-mediated constitutive phosphorylation, which then up-regulates the expression of BCL-xL and MCL-1, two anti-apoptotic BCL-2 family members. Another effector is growth factor receptor-bound protein (GRB)2 that binds to a tyrosine-phosphorylated site of BCR-ABL *via* its SH2 domain. The BCR-ABL/GRB2 complex recruits son of sevenless (SOS), which induces the activation of GRB2-associated binding protein (GAB)2. Consequently, the GRB2/GAB2/SOS complex causes constitutive activation of PI3K and Ras signaling pathways. The latter stimulates the activation of MAPK proteins, which results in the up-regulation of c-MYC expression. This proto-oncogene then regulates the expression of survivin, a member of the IAP family that inhibits caspase activation, thereby leading to a negative regulation of apoptosis (Cilloni *et al.*, 2012). Subsequently, the activation of these signaling pathways leads to uncontrolled cell proliferation, impaired transcriptional activity, decreased adherence of leukemia cells to the BM stroma, malignant expansion of hematopoietic stem cell populations, and stimulated survival of tumor cells owing to a reduced apoptotic response to mutagenic stimuli (Bose *et al.*, 2013; Apperley, 2015).

8.1.4. Current treatments

The development of tyrosine kinase inhibitors (TKi), including imatinib, more than 10 years ago helped to transform Philadelphia chromosome-positive CML from a life-threatening disease to, in most cases, a chronic condition when managed with appropriate treatments (Novartis, Basel, Switzerland) (Garcia-Gutierrez *et al.*, 2019).

8.1.4.1. First-generation inhibitor: imatinib

Imatinib consists in a typical bisarylanilino core comprising a phenyl ring and a pyridine-pyrimidine moiety, containing a benzamide-piperazine group in the meta-position of the aniline-type nitrogen atom (Rossari *et al.*, 2018). Imatinib is a type II TKi that only binds to the inactive state of BCR-ABL, which is characterized by a specific DFG (Asp-Phe-Gly)-out conformation of the unphosphorylated activation loop, in which the DFG motif is being folded away from the conformation required for ATP phosphate transfer. Imatinib interactions with BCR-ABL are mediated by (*i*) a unique hydrogen bond donor-acceptor pair and hydrophobic 'tail' moiety that form van der Waals interactions with the hydrophobic site of BCR-ABL, also referred to as the 'allosteric site', that is directly adjacent to the ATP binding pocket created by the DFG-out conformation, and (*ii*) a 'head' group that extends to the adenine region and forms a single hydrogen bond with the kinase hinge residue (Schindler *et al.*, 2000; Liu *et al.*, 2006). Notably, imatinib is most efficacious in the chronic phase of CML when a majority of patients achieve durable complete cytogenetic response.

Nevertheless, such therapeutic regimens are associated with TKi resistance and severe side effects, which represent barriers to effective treatments. Clinical resistance to imatinib can be elicited by various BCR-ABL-dependent and -independent mechanisms. The BCR-ABL-dependent mechanisms include selection of sub-clones containing point mutations, and the over-expression or amplification of the BCR-ABL gene. Mutations in BCR-ABL are present in 40 to 90% of imatinib-resistant patients, depending on the sensitivity of the detection method and the stage of CML (Balabanov *et al.*, 2014). Over a hundred mutations have been identified (Meenakshi Sundaram *et al.*, 2019) and the seven most common mutations, accounting for about 66% of all mutations discovered to date, comprise G250A/E, Y253F/H and E255D/K/R/V located in the ATP binding P-loop, T315I located at the imatinib binding site, M351T and F359C/L/V/R located in the catalytic C-loop and finally H396P located at the activation A-loop (Jabbour *et al.*, 2013). The "gatekeeper" T315I mutation, representing 4 to 15% of the mutations described, leads to the loss of an oxygen molecule and the creation of a steric hindrance, which prevent the hydrogen bond between imatinib and the tyrosine kinase domain, as well as the binding of such inhibitor (Bixby *et al.*, 2009; Linev *et al.*, 2018). Mutations at the P-loop result in a conformational change whereas mutations occurring at A-loop stabilize BCR-ABL in active conformation, both impeding imatinib from binding to BCR-ABL (An *et al.*, 2010; Jabbour *et al.*, 2013).

The BCR-ABL-independent mechanisms involve factors influencing the intracellular concentration of imatinib and activation of BCR-ABL independent pathways (Roychowdhury

et al., 2011; Nestal de Moraes *et al.*, 2012). The transformation of imatinib to its main circulating metabolite, the pharmacologically active N-desmethyl piperazine derivative, is mediated by cytochrome P450 (CYP) family, and in particular the CYP3A4 isoform, whose expression may vary among patients, resulting in distinct drug responses (Balabanov *et al.*, 2014; Ankathil *et al.*, 2018). Alterations in drug influx and efflux are also reported to affect imatinib intracellular concentration. Accordingly, a polymorphism of the organic cation transporter (OCT)1, responsible for the influx of imatinib into cells, is associated with imatinib resistance (Jabbour *et al.*, 2013). In addition, imatinib is a substrate of the ATP-binding cassette (ABC) efflux transporter P-glycoprotein, also known as multi-drug resistance protein (MDR)1, whose overexpression has been associated with chemotherapy failure in leukemia (Holohan *et al.*, 2013).

Furthermore, the quiescent population of leukemic stem cells (LSCs), characterized by a high activity of aldehyde dehydrogenase (ALDH) enzymes that catalyze the oxidation of intracellular cytotoxic aldehydes into their corresponding carboxylic acids (Marcato *et al.*, 2011), constitutes a possible reservoir for the development of therapeutic resistance or disease progression through escape mechanisms of altered self-renewal, differentiation, and survival pathways (Roychowdhury *et al.*, 2011; Zhou *et al.*, 2015).

Therefore, it is critical to explore novel therapeutic approaches to address these limitations (Thompson *et al.*, 2015). The need for alternative or additional treatment for imatinib-resistant BCR-ABL-positive leukemia has guided the design of second generation TKi (see chapters 8.1.4.2. and 8.1.4.3. for more details) (Weisberg *et al.*, 2007). Additionally, treatment of cancerous cells with imatinib combined with another drug such as HDACi (see chapter 8.1.4.4. for more details) could sensitize cells to the cell killing effects of imatinib and allow lessening the concentration of each compound, thus reducing side effects.

8.1.4.2. Second-generation inhibitors: dasatinib, nilotinib and bosutinib

Dasatinib is a smaller TKi than imatinib, establishing fewer interactions with its targets, and binding BCR-ABL very versatility, in both active and inactive conformations. Nevertheless, the inactive DFG-out conformation has higher entropy than the DFG-in active conformation, the latter being thus preferentially inhibited by dasatinib. Conversely, nilotinib binds to the DFG-out inactive conformation of the BCR-ABL protein (Rossari *et al.*, 2018). *In vitro*, dasatinib and nilotinib display 325-fold and 10- to 50-fold greater potency against native BCR-ABL, respectively, in comparison to imatinib, as well as activity against all currently described imatinib-resistant BCR-ABL mutations except T315I (Wei *et al.*, 2010).

Therefore, dasatinib and nilotinib became FDA-approved for the second-line treatment of CML, *i.e.* for the treatment of patients with chronic or accelerated phase CML associated with resistance or intolerance to prior therapy, including imatinib. Despite this, dasatinib- and nilotinib-insensitive BCR-ABL mutations have been identified *in vitro* (Stein *et al.*, 2010).

Bosutinib is a potent dual SRC/ABL kinase inhibitor with considerable activity against BCR-ABL and most imatinib-resistant BCR-ABL mutants except T315I and V299L (Cortes *et al.*, 2018b). Bosutinib is approved for the treatment of CML in patients previously treated with one or more TKi and for whom imatinib, nilotinib, and dasatinib are not considered as appropriate treatment options, or in patients resistant or intolerant to prior therapy. More recently, bosutinib was approved for first-line treatment of patients with newly diagnosed chronic phase CML (Cortes *et al.*, 2018a).

8.1.4.3. Third-generation inhibitor: ponatinib

To date, the only approved third-generation TKi is ponatinib, a dual SRC/ABL inhibitor designed to overcome the gatekeeper T315I mutation. Ponatinib is indicated for the treatment of CML patients in every phase of the disease resistant and/or intolerant to dasatinib and nilotinib and for whom imatinib is not indicated anymore, or for patients with T315I mutation (Massaro *et al.*, 2018). Structurally, ponatinib closely overlaps nilotinib despite several differences such as the insertion of an ethynyl linker to accommodate isoleucine side chain without any steric interference also in inactive conformation (Rossari *et al.*, 2018).

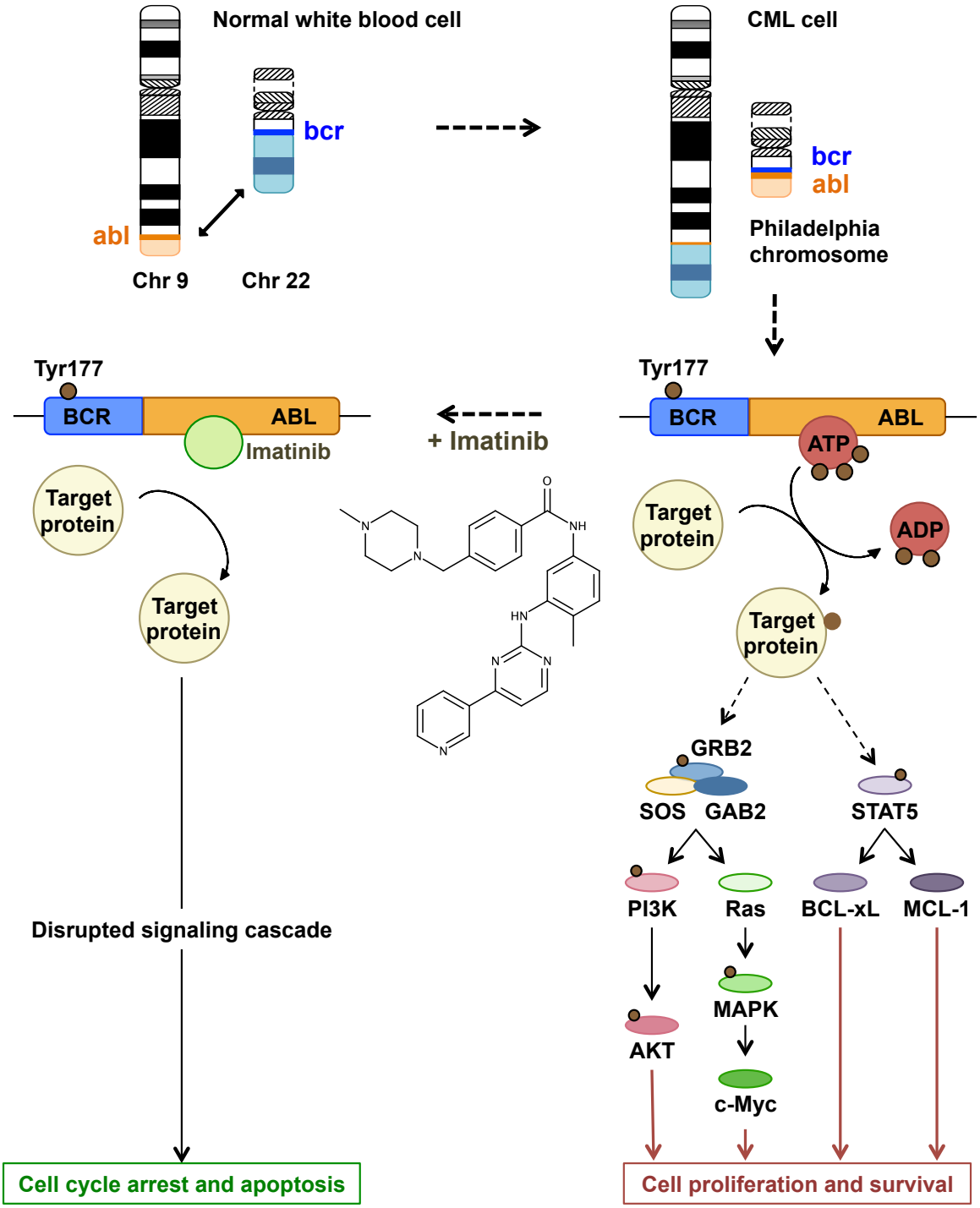

Figure 17: CML pathogenesis and impact of treatment with tyrosine kinase inhibitor imatinib. Breakpoint cluster region-Abelson murine leukemia viral oncogene homolog 1 (BCR-ABL)-dependent signaling pathways are activated upon phosphorylation of the tyrosine (Tyr) 177 of BCR-ABL. Growth factor receptor-bound protein (GRB)2, phosphorylated by BCR-ABL, is associated to Son of Sevenless (SOS) and GRB2-associated-binding protein (GAB)2, leading to the activation of phosphatidylinositol 3-kinase (PI3K) and Ras signaling pathways. The latter is responsible of the expression of c-MYC gene *via* mitogen-activated protein kinases (MAPK). BCR-ABL also induces phosphorylation of signal transducer and activator of transcription (STAT)5, which is responsible of the expression of Bcl-xL et MCL-1 genes. Those BCR-ABL dependent signaling pathways are implicated in cell proliferation and survival. Imatinib induces cell cycle arrest and apoptotic cell death by preventing the binding of BCR-ABL target proteins (*e.g.* GRB2 and STAT5) in its active site.

8.1.4.4. HDAC inhibitors

The regulation of HDAC1 and 2 is essential in maintaining CML cell survival (Chen *et al.*, 2019). Alteration of the normal balance between HATs and HDACs, partly owing to the up-regulation of class I HDACs, leads to aberrant acetylation status of apoptosis-related non-histone proteins p53 and Ku70, which promotes BCR-ABL-independent imatinib resistance (S.M. Lee *et al.*, 2007). Accordingly, the HDACi AR-42 may increase the sensitivity of CML cells to imatinib and reverse imatinib resistance by regulating HDAC1 expression, which is up-regulated in imatinib-resistant cells (Wei *et al.*, 2018). Furthermore, low protein tyrosine phosphatase non-receptor type 6 (PTPN6) expression level, correlated with CML progression and observed in cell lines and patients with advanced phase CML, results from its regulation by HDAC1 through direct binding (Zhang *et al.*, 2017).

Mechanistically, HDACi-mediated HSP90α hyperacetylation leads to the inhibition of the interaction between this chaperone and BCR-ABL, thereby promoting BCR-ABL proteasomal degradation (Nimmanapalli *et al.*, 2003). Some HDACi also reduce the ratio of anti-apoptotic exon 3- to pro-apoptotic exon 4-containing BIM transcripts in CML cell lines and primary CML progenitors with the BIM deletion polymorphism, inducing apoptotic cell death and restoring TKI-sensitivity (Rauzan *et al.*, 2017). Finally, HDACi target the AKT-mTOR signaling pathway, down-regulating the level of phosphorylated eIF4E that participates in the translation of tumor-associated proteins such as c-MYC, cyclin D1, and MCL-1 (Jia *et al.*, 2019).

It has already been shown that combining HDACi with TKi or dual BCR-ABL and Aurora kinase inhibitors synergistically induce anti-CML effects like induction of apoptosis in imatinib-sensitive and -resistant cells, as well as primary cells from patients expressing wild-type and imatinib-resistant mutant forms of BCR-ABL (Morotti *et al.*, 2006; Dai *et al.*, 2008; Fiskus *et al.*, 2008; Matsuda *et al.*, 2016). Noteworthy, cell mortality is not increased in normal cells incubated with such co-treatments (Nguyen *et al.*, 2011). In addition, HDACi-TKi combination induces apoptosis in pro-B Ba/F3 murine cells expressing either wild-type BCR-ABL in an ectopic manner, or the imatinib-resistant T315I and E255K point-mutated BCR-ABL (Fiskus *et al.*, 2006b). Such combination also exhibited antitumor activity *in vivo* (Okabe *et al.*, 2014), significantly prolonging the survival of mice xenografted with imatinib-resistant BCR-ABL$^+$ leukemic cells (Nguyen *et al.*, 2011).

HDACi in combination with TKi exert anticancer properties through various mechanisms. First, their synergistic effect involves reduction of cyclin D1 levels, as well as induction of

p21 and p27 expression (Fiskus *et al.*, 2006b; Kim *et al.*, 2007). Additionally, such therapies enhance the activation of mitochondria-dependent caspase cascades (Bu *et al.*, 2014), ROS generation and DNA damage induction (Nguyen *et al.*, 2011), accompanied by up-regulated and decreased expression of BIM and anti-apoptosis proteins, such as MCL-1 and XIAP, respectively (Bu *et al.*, 2014). Finally, combined treatments induce stronger depletion of BCR-ABL, p-Crk-like protein (p-CrkL), p-STAT5, p-ERK1/2, c-MYC, and BCL-xL levels (Fiskus *et al.*, 2006a; Fiskus *et al.*, 2006b).

TKi-HDACi combinations display also the potential to eliminate LSCs responsible for TKi resistance (Al Baghdadi *et al.*, 2012) by up-regulating hsa-miR-196a expression (Bamodu *et al.*, 2018) or suppressing γ-catenin, which displays a β-catenin-independent role in survival and self-renewal of LSCs (Jin *et al.*, 2016). Interestingly, therapeutic activity against LSCs was reproduced in *in vivo* mice models (Bamodu *et al.*, 2018).

8.2. Multiple myeloma

MM is a hematological malignancy derived from post-germinal center B cells (Harada *et al.*, 2016). Physiologically, B cells originate from pluripotent hematopoietic stem cells in the BM. Once the B cell pathway has been selected, B cell development and differentiation occurs in a series of stages, progressing from pro- to pre-, to immature B cells (Regna *et al.*, 2016). MM is characterized by a clonal proliferation of malignant plasma cells that accumulate primarily in a favorable microenvironmental *niche* of the BM and produce high levels of immunoglobulin (Raab *et al.*, 2009; He *et al.*, 2016). The progression of MM almost always occurs from an asymptomatic pre-malignant stage known as monoclonal gammopathy of undetermined significance (MGUS) through smoldering MM to active MM and then plasma cell leukemia (Figure 18) (Abramson, 2016; Harada *et al.*, 2016).

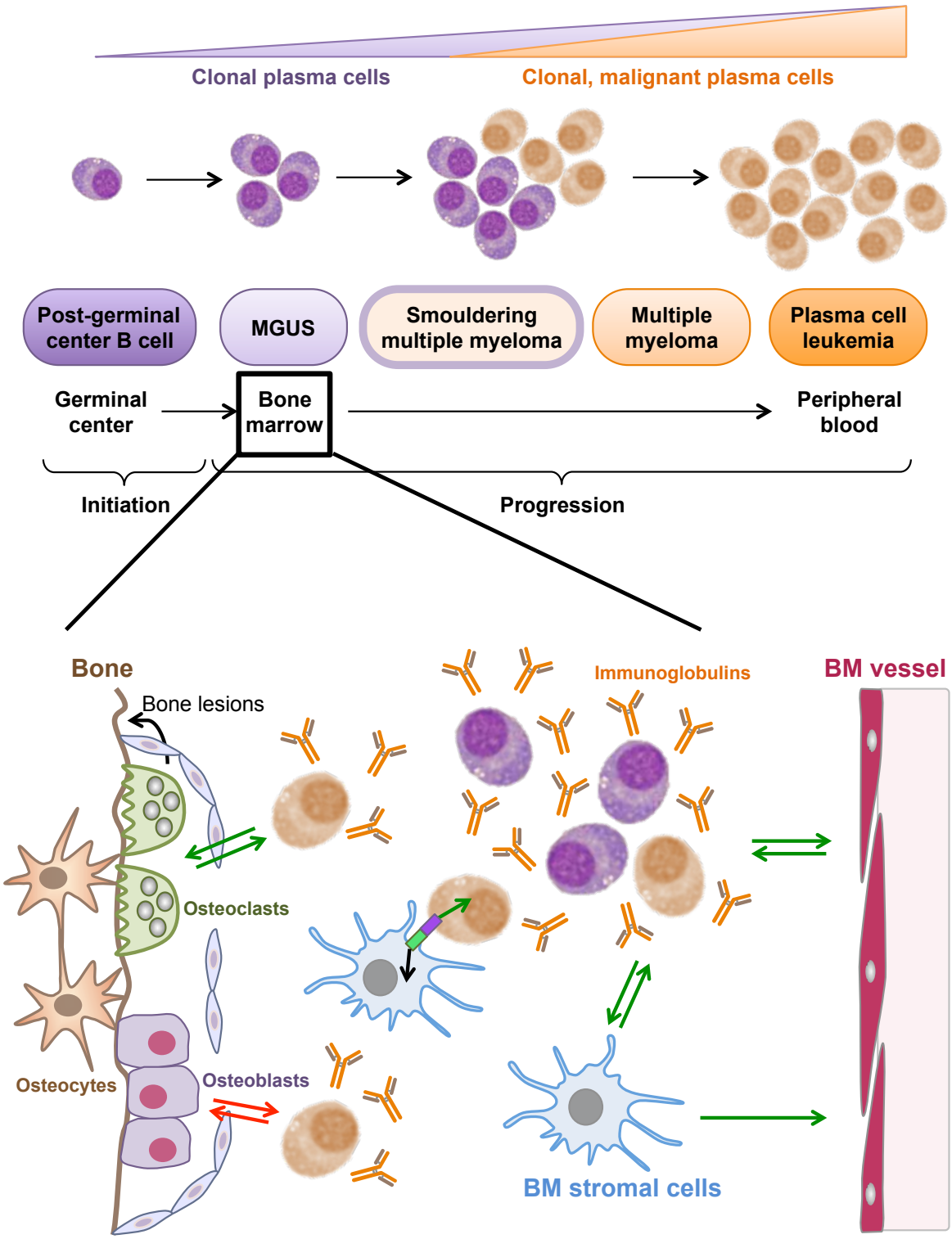

Figure 18: MM pathogenesis.
MM cell interactions with cellular components of the surrounding BM microenvironment are essential for the disease progression. Green and red arrows represent positive and negative interactions, respectively. BM: bone marrow, IGH: immunoglobulin heavy locus, IL: interleukin, MGUS: monoclonal gammopathy of undetermined significance. Adapted from (Kumar *et al.*, 2017).

8.2.1. Epidemiology

Ranking second in terms of diagnostic frequency among all blood cell disorders, MM

accounts for 1.8% of all new cancer cases and more than 10% of all hematological malignancies in the United States (Abramson, 2016; Tandon *et al.*, 2016). So far, the outcome of MM patients has not been satisfactory, with a median survival of 2 to 5 years and a 5-year overall survival rate of only 45% for patients with MM at distant stage, which accounts for 95% of all new diagnosed cases (Cottini *et al.*, 2015; Tandon *et al.*, 2016). Consequently, MM is still an incurable pathology in most cases.

The etiology of MM is poorly deciphered partly due to low frequency of the disease making its investigation difficult, as well as the fact that the risk factors playing a major role for malignant diseases, such as tobacco consumption and diet, have not been found obviously implicated in MM pathogenesis. Nevertheless, few risk factors may affect MM initiation, such as age (increased risk after 65 years old), race (incidence 2 times higher among African Americans than Caucasian population), gender (slightly more prevalent in males) and family history (Becker, 2011).

8.2.2. Diagnostic criteria

For several decades, the major clinical features of MM corresponded to increased blood calcium level, renal insufficiency, anemia, and bone lesions (CRAB) (He *et al.*, 2016). In addition to this classic tetrad, the diagnostic criteria for MM were expanded to include validated biomarkers predictive of myeloma-related end organ damage (Rajkumar *et al.*, 2014). For instance, another feature of MM is the accumulation of high levels of monoclonal immunoglobulins or paraproteins in blood and/or urine, which is considered as an important contributor to renal damage (Afifi *et al.*, 2015; Tandon *et al.*, 2016).

8.2.3. Pathophysiology

MM is a biologically complex disease that can exhibit marked heterogeneity in terms of cytogenetic alterations, thereby leading to individual variations in overall response and survival of patients under identical therapeutic strategies (Tandon *et al.*, 2016). Initiation and progression of MM is associated with genetic abnormalities such as point mutations, deletions (*e.g.* del(17p)), or chromosomal translocations (*e.g.* t(11;14), t(4;14), t(14;16), t(6;14) affecting CCND1, MMSET/FGFR3, c-MAF, CCND3 expression, respectively), as well as epigenetic alterations including global DNA hypomethylation, histone hypermethylation (*e.g.* histone H3 lysine 9 mono-methylation, lysine 36 di-methylation or lysine 27 tri-methylation) and hypoacetylation, or aberrant miR expression (Alzrigat *et al.*, 2018). Those lesions may result in activation or deregulation of critical oncogenic signaling pathways including NF-κB,

Wnt/β-catenin, CDK/retinoblastoma protein (pRb), Janus kinase/signal transducer and activator of transcription protein (JAK/STAT) and ERK pathways, which contribute to the pathogenesis of MM (Harada *et al.*, 2016; Tandon *et al.*, 2016).

Evidence indicates that the BM microenvironment surrounding tumor cells has a pivotal role in myeloma pathogenesis, mediating cell survival, proliferation and resistance to anticancer drugs (Raab *et al.*, 2009; Harada *et al.*, 2016). Drug resistance is acquired through functional and physical interactions of MM cells with the BM microenvironment *via* two overlapping mechanisms. First, BM stromal cells (BMSCs) produce soluble factors, such as interleukin (IL)-6 and insulin-like growth factor (IGF)-1, to activate signal transduction pathways resulting in drug resistance. Second, BMSCs up-regulate the expression of cell cycle inhibitors, anti-apoptotic members of the BCL-2 family and ABC drug transporters in myeloma cells upon direct adhesion (Furukawa *et al.*, 2016).

8.2.4. Current treatments

For several decades the standard-of-care drugs for treating MM were alkylating agents, primarily melphalan, in combination with corticosteroids. Over the past decade, this treatment paradigm has shifted dramatically with the introduction of chemotherapy, steroids, immunomodulatory drugs (IMiDs) and proteasome inhibitors (Pi). Conjunction of MM therapy with autologous stem cell transplantation has further extended the range of therapeutic options for combatting this disease (Abramson, 2016). Despite remarkable advances in MM therapies and the consequent improvement in clinical outcomes, nearly all patients eventually relapse and become refractory to treatment, likely due to a continuous selection of more biologically aggressive sub-clones (Lopez-Iglesias *et al.*, 2016; Pogue *et al.*, 2016; Manni *et al.*, 2017). As a result, MM remains an incurable disease, justifying an urgent need for novel therapeutic agents and combinations with conventional treatments that may further inhibit important survival pathways for these tumor cells and overcome acquired or intrinsic drug resistance (He *et al.*, 2016; Hideshima *et al.*, 2016; Lopez-Iglesias *et al.*, 2016).

A new generation of Pi and IMiDs is already demonstrating efficacy in relapsed or refractory MM (RRMM). Multiple additional strategies are currently incorporated in the MM therapeutic platform, consisting of molecules interfering with protein catabolism such as HDAC6-specific inhibitors, epigenetic therapies including HDACi, immune-based therapeutic strategies and agents targeting various signaling pathways (*e.g.* AKT, CRM1, c-MYC and NF-κB) (Cottini *et al.*, 2015).

8.2.4.1. Proteasome inhibitors

MM displays a unique biology characterized by high rates of protein synthesis, resulting in ER stress and activation of the UPR. Plasma cell differentiation and survival depend on UPR activation, which results in up-regulation of protein degradation by the 26S proteasome. Accordingly, the introduction of Pi into MM therapies has led to a dramatic enhancement of clinical outcomes (Vogl *et al.*, 2017).

The FDA-approved Pi bortezomib (Velcade®) blocks the degradation of poly-ubiquitinated misfolded proteins, amplifies ER stress, and triggers apoptosis of MM cells. Consequently, it has rapidly been tested in preclinical and clinical studies demonstrating remarkable anti-MM efficacy (Hideshima *et al.*, 2001). Although most MM patients receiving continuous bortezomib-containing therapy do not develop severe adverse events, the number of cases with acquired resistance to bortezomib therapy has increased continuously, mainly due to point mutations or over-expression of the gene coding for the proteasome β5 subunit. The majority of the substituted amino acid residues are located around the S1 specificity pocket of the proteasome β5 subunit, leading to conformational changes that may disrupt the affinity between the chymotrypsin-like active site and bortezomib. Notably, drug efflux *via* P-glycoprotein appears to only mediate a low level of bortezomib resistance (Lu *et al.*, 2013).

Several clinical studies of bortezomib treatment for RRMM showed that the median duration of response ranged from 6 to 12 months with or without dexamethasone, which supports the theory that MM cells eventually develop resistance to bortezomib, leading to relapse of disease in the majority of patients within a year. To explore effective treatment strategy for overcoming bortezomib resistance, several clinical trials using new agents or combination therapy with bortezomib have been performed (Hideshima *et al.*, 2016). Alternatively, the second-generation Pi carfilzomib, ixazomib, and marizomib also show improved pharmacological properties, offering benefits in terms of increased efficacy and reduced toxicity as off-target effect, as well as displaying promising anti-tumor responses (Hideshima *et al.*, 2016; Ri, 2016). Furthermore, the efficacy of second-generation Pi is not affected by bortezomib resistance as they offer a different chemical structure, mechanism of action and biological properties (Chhabra, 2017).

8.2.4.2. HDAC and HDAC6 inhibitors

Multiple HDACi inhibit myeloma cell survival and proliferation by various mechanisms. Treatments with non-selective or class I HDACi induce cell cycle arrest in the G_0/G_1 phase through reduced expression of cell cycle-dependent cyclins and CDKs, or up-regulation of the

cell cycle inhibitors, p21 and/or p53 (Afifi *et al.*, 2015; Harada *et al.*, 2016). Early preclinical data revealed that SAHA induces cell growth arrest as a result of increased levels of p21, p53 and hypophosphorylated pRb, in addition to decreased levels of cyclin D1 and CDK4 (Afifi *et al.*, 2015). HDACi can also induce both apoptotic and non-apoptotic cell death, overcoming drug resistance mediated by the BM environment. In addition, HDACi-induced apoptosis can be mediated *via* the intrinsic and extrinsic pathways by stimulating mitochondrial cytochrome *c* translocation and release, up-regulating APAF-1, and inducing cleavage of caspases 3 and 9 (Afifi *et al.*, 2015; Harada *et al.*, 2016). Interestingly, GRP78 was identified as a novel non-histone target of HDACi (Rao *et al.*, 2010). Upon inhibition of class 1 HDACs, acetylated GRP78 activates UPR and contributes to the antitumor activity of HDACi such as SAHA (Kahali *et al.*, 2012).

The pan-HDACi panobinostat has shown significant clinical benefit and is the first one approved for use in combination with bortezomib and dexamethasone for the treatment of patients with relapsed or relapsed and refractory MM who have received ≥2 prior regimens including bortezomib and an IMiD (Richardson *et al.*, 2017). Caspase-8-mediated post-translational Sp1 degradation appears to be among major mechanisms for synergistic anti-MM effects of panobinostat and Pi in combination (Bat-Erdene *et al.*, 2016).

Non-selective HDACi induce potent cytotoxicity against MM cells in the preclinical setting (Harada *et al.*, 2016). Clinical trials with pan-HDACi in combination with bortezomib and dexamethasone have shown improved outcomes, but also substantially increased toxicity (Vogl *et al.*, 2017). Indeed, pan-HDACi induce unfavorable side effects due to the broad range of modulation of histone and non-histone protein functions (Harada *et al.*, 2016). To minimize these side effects, research has focused on the development isoform-selective HDACi. To date, HDAC6i are the only class of isoform-selective HDACi whose significance in MM biology has well been documented due to the unique role of HDAC6 in the aggresome/autophagy pathway (Harada *et al.*, 2016).

HDAC6 mediates trafficking of cytosolic poly-ubiquitinated misfolded proteins to the aggresome/autophagy pathway, which serves as an alternative route for protein degradation upon proteasome inhibition and thereby contributes to therapeutic resistance towards proteasome inhibitor therapy (see chapter 6.3.2.3. for more details). Therefore, the selective inhibition of HDAC6, leading to increased α-tubulin acetylation and accumulation of poly-ubiquitinated proteins in MM cells, may yield improved efficacy and synergistic cytotoxicity when combined with proteasome inhibition (Vogl *et al.*, 2017). Furthermore, it has been reported that the simultaneous targeting of the integrated networks of aggresome, proteasome,

and autophagy-lysosome system potently enhances efficient ER stress-mediated apoptosis in MM cells (Moriya *et al.*, 2015).

Selected clinical trials evaluating the efficacy of HDACi and HDAC6i in combination treatment in patients with MM are summarized in Table 3.

Table 3: Selected clinical trials with HDACi in combination treatments in MM.
The more advanced phase for each co-treatment was selected from online database provided by the U.S. National Library of Medicine.

Selectivity	Name	Combination treatments	Phase
Pan HDACi	**Vorinostat (SAHA)**	Bortezomib – dexamethasone	2
		Bortezomib	3
		Marizomib	1
		Dexamethasone – lenalidomide	2
		Bortezomib – dexamethasone – lenalidomide	1
		Carfilzomib – dexamethasone – lenalidomide	2
		Lenalidomide	1
		Bortezomib – doxorubicin	1
		Bortezomib – dexamethasone – doxorubicin	2
		Melphalan – Prednisone	2
		Bortezomib – carfilzomib – thalidomide – lenalidomide	3
	Panobinostat (LBH589)	Bortezomib – dexamethasone	4
		Bortezomib – dexamethasone – thalidomide	2
		Everolimus	2
		Carfilzomib	2
		Bortezomib	1
		Bortezomib – dexamethasone – lenalidomide	2
		Carfilzomib – dexamethasone	2
		Carfilzomib – dexamethasone – lenalidomide	2
		Melphalan	2
		Dexamethasone – lenalidomide	2
		Busulfan – dexamethasone – gemcitabine – melphalan – Palifermin	2
		Dexamethasone – ixazomib	2
	Belinostat (PXD101)	Dexamethasone	2
		Bortezomib	2
	Romidepsin	Pralatrexate	2
	AR-42	Pomalidomide	1
	JNJ-2641585	Bortezomib – dexamethasone	1
HDAC6i	**ACY-1215**	Dexamethasone – lenalidomide	2
		Bortezomib – dexamethasone	2
		Dexamethasone – pomalidomide	2
	ACY-241	Dexamethasone – pomalidomide	1
		PVX-410 – lenalidomide	1

HDACi: histone deacetylase inhibitor, HDAC6i: HDAC6 inhibitor, SAHA: suberoylanilide hydroxamic acid.

9. MAKV compounds

MAKV-8 and its derivatives, as well as MAKV-15, have been synthetized in the laboratory of Guy Bormans (Laboratory of Radiopharmacy, KU Leuven, Leuven, Belgium).

9.1. MAKV-8 and derived compounds

The synthesis of compound MAKV-8, characterized by a linker of 6-methylene units and a CAP group with arylisoxazole, was accomplished through the chemistry of nitrile oxide cycloaddition (NOC), assembling related building blocks, namely the 5-arylisoxazole-3-carboxylic acid ethyl esters (Kozikowski *et al.*, 2008; P.H. Yang *et al.*, 2013). The activity of this compound has been tested with isolated enzymes and pancreatic cancer cell lines *in vitro* in order to understand the structure-activity and structure-selective relationships. Their results showed that compound 3 (MAKV-8) displayed an IC_{50} value of 2 pM towards HDAC3 and HDAC6 and its *in vitro* anti-proliferative activity against pancreatic cancer cell lines was similar to the one of SAHA (Kozikowski *et al.*, 2008; P.H. Yang *et al.*, 2013). The four MAKV-8 derived compounds, synthetized by the group of Guy Bormans, were named MAKV-6, -7, -10 and -12; the two first ones lack the linker, whereas the hydroxamate group of the two last ones is substituted by a methylester group (Figure 19).

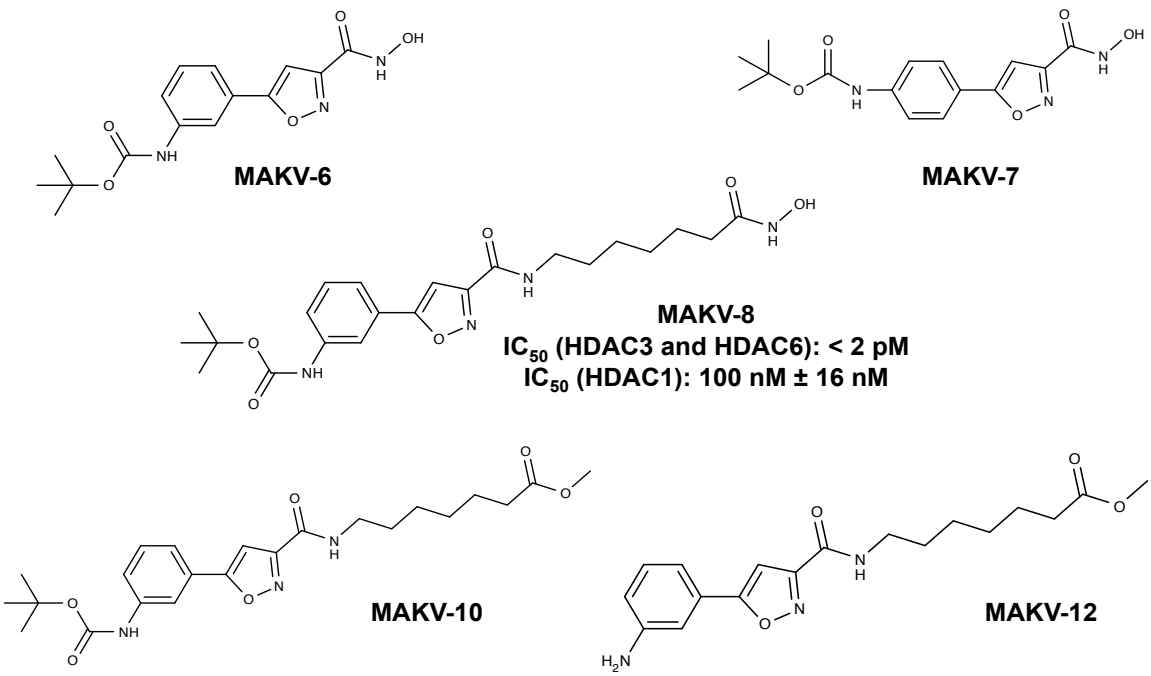

Figure 19: Chemical structures of MAKV-8 and derived compounds.
IC_{50} values from (Kozikowski *et al.*, 2008).

9.2. MAKV-15 compound

Compounds MAKV-15 and tubastatin A (Figure 20) were synthesized using structure-based drug design combined with homology modeling techniques (Butler *et al.*, 2010). In the paper from Butler *et al*., compound 6 (tubastatin A) and 7 (MAKV-15), characterized with tetrahydro-γ-carboline and tetrahydro-β-carboline moiety, respectively, were obtained through modification of the tricyclic. Based on the *in vitro* results from the literature, this small change between the two molecules has an impact on the potency and selectivity towards HDAC6. Indeed, both of the compounds displayed higher selectivity for HDAC6 over HDAC1 compared to tubacin. Tubastatin A and MAKV-15 displayed an IC_{50} value of 15 and 1.4 nM towards HDAC6 and about a 1000- and 3500-fold selectivity for HDAC6 over HDAC1, respectively (Butler *et al.*, 2010; P.H. Yang *et al.*, 2013).

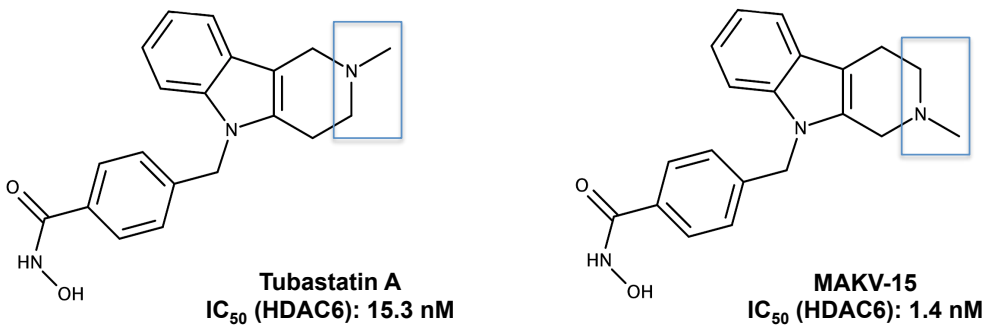

Figure 20: Chemical structures of tubastatin A and MAKV-15.
The blue rectangles highlight the change in the N-position. IC_{50} values from (Butler *et al.*, 2010).

OBJECTIVES

HDACs play a role in the modulation of the acetylation status of proteins. Disruptions of the functional acetylation patterns contribute to tumorigenesis and can be triggered by various mechanisms such as aberrant activation or overexpression of HDAC isoforms. Targeting HDAC activities with small molecule inhibitors thus represents a promising anticancer strategy for hematological malignancies. However, through their implications in many cell processes, treatment of cancer with pan-HDACi is associated with unwanted side effects, leading to the research of more potent and selective HDACi.

The main goal of this project is to develop **efficient therapeutic approaches for the treatment of hematological malignancies** based on the use of **HDACi in combination with targeted drug therapies**. To achieve our objectives, the research project consists on the following specific aims:

1. To identify new synthetic pan- or selective HDACi with **improved inhibitory properties *in vitro*** using a fluorimetric HDAC activity assay and ***in cellulo*** by analyzing the acetylation status of HDAC target proteins.

2. To characterize the **anticancer properties** of selected HDACi **alone** or **in combination with targeted drug therapies.**

- HDACi-TKi in CML

First, we intend to assess the effects of those inhibitors on cell proliferation and viability by Trypan blue exclusion test. The effect on cell cycle distribution will be studied using flow cytometry and the type of induced cell death evaluated *via* nuclear morphology analysis and flow cytometric assessment of phosphatidylserine (PS) exposure. The effects of compounds on proteins implicated in cell death pathways will be investigated by performing western blotting to analyze caspase and poly (ADP-ribose) polymerase (PARP)-1 cleavage. To determine whether co-treatments display a synergistic effect on cell mortality, the combination index will be calculated using the CompuSyn software. Finally, the replicative ability of tumor cells in a 3D model will be evaluated by clonogenic assay. Importantly, the toxicity of co-treatments will be studied on CML cells by comparison to healthy cell models.

To further describe the HDACi anticancer potential, GRP78 expression level will be analyzed as a marker of ER stress. Accordingly, the activation of UPR sensor pathways including PERK/eIF2α/ATF4; ATF6; as well as the amount of spliced XBP1 mRNA will be studied. In addition, compound-mediated induction of the autophagic process will be evaluated by (*i*) analysis of cellular structures by transmission electron microscopy (TEM), (*ii*) cell morphology assessment after GIEMSA staining, (*iii*) visualization and quantification of autophagy-associated vacuoles after Cyto-ID® staining, and (*iv*) analysis by western blotting of autophagic markers. Finally, the effect of MAKV-8 on histone H2AX phosphorylation (γH2AX) levels will be studied by western blotting as the earliest marker for DNA damage localized at double strand breaks (DSBs).

- HDAC6i-proteasome inhibitor-common chemotherapeutic drug or BCL-2 family protein inhibitors in MM.

We aim to assess the effects of those inhibitors on cell proliferation and viability by Trypan Blue exclusion test and the type of induced cell death *via* nuclear morphology analysis. The effect on cell cycle distribution will also be studied by flow cytometry.

3. To understand the **mechanisms of action** underlying most effective drug combinations with MAKV-8 and imatinib. Since CML pathogenesis is mainly driven by BCR-ABL fusion oncoprotein that displays constitutive tyrosine kinase activity leading to aberrant downstream signaling, the effects of co-treatment will be examined on the expression and phosphorylation of BCR-ABL and its downstream targets. Furthermore, we will evaluate whether a MAKV-8-imatinib treatment could reduce the ALDH-positive cell population representing a subset of hematopoietic stem cells that are implicated in TKi resistance and relapse in CML patients.

4. Test the potency of most promising combinational strategies in ***in vivo*** **models.** For that purpose, we will visualize tumor growth thanks to xenografted fluorescent CML cell lines in zebrafish.

MATERIAL AND METHODS

1. Cell culture

1.1. Cell models

Human CML and MM cell lines were purchased from various culture collections (Table 4). Human CML KBM-5 cells were kindly provided by Dr. Bharat B. Aggarwal. Imatinib-resistant K-562 cells (K-562R) were a gift from of the Catholic University, Seoul and imatinib-resistant KBM-5 cells (KBM-5R) were established as previously described (Mazumder *et al.*, 2018). The human MM MM1.S cell line was kindly provided by Wim Vanden Berghe (University of Antwerpen, Belgium). Of note, the MM cell lines used in the experiments (Table 5) were representative of the molecular heterogeneity described in patients (www.keatslab.org/myeloma-cell-lines/hmcl-characteristics).

Cells were cultured in the appropriate medium (BioWhittaker, Lonza, Verviers, Belgium) supplemented with heat-inactivated fetal calf serum (FCS) and 1% antibiotic-antimycotic (BioWhittaker) at 37°C in a humid atmosphere and 5% CO_2, and sub-cultured to the appropriate concentration every two or three days (Table 4).

Table 4: Culture characteristics.

Cells were purchased from American Type Culture Collection (ATCC; Manassas, Virginia, USA); Deutsche Sammlung für Mikroorganismen und Zellkulturen (DSMZ; Braunschweig, Germany); Japanese Collection of Research Bioresources (JCRB; Osaka, Japan).

Cancer	Cell line	Provider	Medium	FCS[1]	Seeding density
CML	K-562	DSMZ	RPMI 1640	10%	2×10^5 cells/ml
	K-562R	CU	RPMI 1640	10%	3×10^5 cells/ml
	KBM-5	MDACC	IMDM	10%	2×10^5 cells/ml
	KBM-5R	NA	IMDM	10%	3×10^5 cells/ml
	MEG-01	DSMZ	RPMI 1640	10%	2.5×10^5 cells/ml
MM	AMO-1	DSMZ	RPMI 1640	20%	5×10^5 cells/ml
	JJN-3	DSMZ	DMEM (40%) + IMDM (40%)	20%	3×10^5 cells/ml
	KMS-12-PE	DSMZ	RPMI 1640	20%	5×10^5 cells/ml
	KMS-28-BM	JCRB	RPMI 1640	10%	5×10^5 cells/ml
	KMS-34	JCRB	RPMI 1640	10%	3×10^5 cells/ml
	MM1.R[2]	ATCC	RPMI 1640	10%	3×10^5 cells/ml
	MM1.S[2]	KUL	RPMI 1640	10%	3×10^5 cells/ml
	MOLP-8	DSMZ	RPMI 1640	20%	4×10^5 cells/ml
	OPM-2	DSMZ	RPMI 1640	10%	3×10^5 cells/ml
	U-266	DSMZ	RPMI 1640	10%	4×10^5 cells/ml

[1] All cells were cultured in medium supplemented with heat-inactivated FCS from BioWhittaker except KMS-34 cells, for which FCS is provided by BioWest (Nuaillé, France).

[2] The parental MM1.S cell line and the subline MM1.R are sensitive and resistant to dexamethasone, respectively.

CML: chronic myelogenous leukemia; CU: Catholic University; DMEM: Dulbecco's Modified Eagle's medium; FCS: fetal calf serum; IMDM: Iscove's Modified Dulbecco's Medium; KUL: University of Leuven; MDACC: M.D. Anderson Cancer Center; MM: multiple myeloma; NA: not applicable; RPMI: Roswell Park Memorial Institute.

Table 5: Cytogenetic abnormalities of multiple myeloma cell lines.

Cell line	Translocation	Gene	Cytogenetic characteristics
AMO-1	t(12;14)	KRAS	Heterozygous A146T
		NRAS, TP53	Wild type
		TRAF3	Heterozygous A484Afs
JJN-3	t(14;16) + t(8;14)	KRAS, TRAF3	Wild type
		TP53	Homozygous deletion
KMS-12-PE	t(11;14)	CDKN2C	Homozygous deletion
		KRAS, NRAS, TRAF3	Wild type
		FGFR3	Heterozygous S321C
		TP53	Homozygous R337L
KMS-28-BM	t(4;14)	FGFR3	Expressed
		KRAS	Homozygous G12A
		TRAF3	Wild type
KMS-34	t(4;14)	FGFR3	Expressed
		TP53	Homozygous W146X
		TRAF3	Heterozygous S352N
MM.1R	t(14;16) + t(8;14)	CDKN2C	Homozygous deletion
MM.1S		KRAS	Heterozygous G12A
		NRAS, TP53	Wild type
		TRAF3	Homozygous K536-N545delinsD
MOLP-8	t(11;14)	KRAS	Heterozygous deletion K179
		NRAS	Heterozygous Q61L
OPM-2	t(4;14)	CDKN2C	Homozygous deletion
		FGFR3	Heterozygous K650E
		KRAS, NRAS, TRAF3	Wild type
		TP53	Homozygous R175H
U-266	t(11;14)	BRAF	Heterozygous K601N
		KRAS, NRAS	Wild type
		pRb	Homozygous E419X and K228R
		TP53	Homozygous A161T
		TRAF3	Homozygous K550IfsX3

CDKN: cyclin-dependent kinase inhibitor, FGF: fibroblast growth factor, FGFR: FGF receptor, pRb: retinoblastoma protein, TNF: tumor necrosis factor, TP53: tumor protein p53, TRAF: TNF receptor-associated factor.

1.2. Healthy models

1.2.1. Proliferating and non-proliferating peripheral blood mononuclear cells

PBMCs were isolated from fresh blood of healthy human donors (Red Cross, Luxemburg, Luxemburg) with their consent and respect of anonymity. Blood was diluted eight times in sterile Dulbecco's Phosphate Buffered Saline (DPBS; BioWhittaker) supplemented with 2 mM ethylenediaminetetraacetic acid (EDTA; MP Biomedicals, Illkirch, France), then carefully added to 30% Ficoll-Paque™ Premium (GE Healthcare, Roosendaal, The Netherlands). The following centrifugation at 400 *g* for 30 minutes allowed the formation of

layers based on a density gradient, containing from bottom to top: erythrocytes/granulocytes, Ficoll-Paque media, mononuclear cells, and plasma. PBMCs were collected, washed twice in 1X DPBS-2 mM EDTA, counted and seeded at $5x10^6$ cells/ml in RPMI 1640 supplemented with 10% heat-inactivated FCS and 1% antibiotic-antimycotic (BioWhittaker). Treatments with indicated compounds were performed 24 hours later on PBMCs seeded at a concentration of 10^6 cells/ml.

PBMCs were induced to proliferate by using a cocktail of mitogens and cytokines including phytohemagglutinin (PHA) and IL-2. After isolation by density gradient, PBMCs were transferred into a culture flask pre-conditioned with heat-inactivated human AB serum (BioWhittaker) at a concentration of $2x10^6$ cells/ml in RMPI-1640 supplemented with 1% antibiotic-antimycotic and 10% inactivated human AB serum. After an overnight incubation at 37°C, floating lymphoid cells were collected and resuspended at 10^6 cells/ml in RMPI-1640 supplemented with 1% antibiotic-antimycotic, 1% HEPES (Invitrogen, Tournai, Belgium), 1% sodium pyruvate (Invitrogen), 0.1% 2-mercaptoethanol (Invitrogen), 1% non-essential amino acids (Invitrogen), 5% FCS, 10% human AB serum; 1µg/ml PHA (Gentaur, Kampenhout, Belgium) and 50 units/ml IL-2 (Miltenyi Biotec, Utrecht, The Netherlands).

Concomitantly, two samples of 10^7 PBMCs were resuspended in 10 ml of phosphate buffer saline (1X PBS: 137 mM NaCl ; 2.7 mM KCl ; 10 mM Na_2HPO_4 ; 1.8 mM KH_2PO_4 ; pH7.4) supplemented with or without 0.1 µM 5,6-carboxyfluorescein diacetate succinimidyl ester (CFSE ; CellTraceTM, Thermofisher, Waltham, Massachusetts, USA) and incubated in the dark for 20 minutes. To remove any free dye remaining in the solution, PBMCs underwent a 5-minute incubation with additional 40 ml of RPMI 1640 supplemented with 10% FCS. After washing with 1X PBS, cells were resuspended at 10^6 cells/ml in RMPI-1640 supplemented with 1% antibiotic-antimycotic, 1% HEPES, 1% sodium pyruvate, 0.1% 2-mercaptoethanol, 1% non-essential amino acids, 5% FCS and 10% human AB serum. CFSE-stained and unstained PBMCs were then split in two flasks, followed by addition of 1µg/ml PHA and 50 units/ml IL-2 in one of the flasks. After 72 hours, the blastogenic response of T-cells lymphocytic sub-populations was validated by a multiparametric and comparative analysis between stimulated versus non-stimulated cells. First, cell proliferation was determined using the Trypan Blue exclusion method (see chapter 1.5 for more details) and counting non-stimulated versus stimulated PBMCs under bright field microscope. Then, two samples of 2×10^5 cells from non-stimulated and stimulated PBMCs were washed once with 1X PBS. Pellets of cells were resuspended in 50 µl of 1X PBS supplemented with 3 µl of FITC-conjugated mouse anti-human CD (cluster of differentiation)3 (BD Pharmingen,

Erembodegem, Belgium) in first sample and 3 µl of FITC-conjugated mouse IgG 2a, κ isotype control (BD Pharmingen) in second one. After a 20-minute incubation in the dark, 200 µl of Annexin V Binding Buffer (see chapter 10 for more details) was added to cells. Stained and unstained samples were processed through a cytometer (FACS Calibur, BD Biosciences, San Jose, CA, USA) and data were recorded statistically (10,000 events/sample) using the CellQuest Pro software (BD Biosciences). Morphological cellular changes associated with cell activation, replicative ability of T-cell lymphocytes and the purity of the T-cell lymphocytic proliferating population were monitored by assessment of FSC-H versus SSC-H parameters, CFSE and anti-CD3-associated intensity of fluorescence, respectively. Data were analyzed using the Flow-Jo 8.8.5 software (Tree Star, Inc., Ashland, OR, USA).

Once the blastogenic response was confirmed, cells were resuspended in fresh RPMI-1640 medium, completed and supplemented with mitogens/cytokines as reported above, at the concentration of 10^6 cells/ml prior to treatments with indicated compounds.

1.2.2. Platelets

Fresh human platelets at a concentration of 1.2 to $1.5x10^9$ cells/ml (Red Cross) were obtained from healthy human donors with their consent and respect of anonymity. On the day of reception, platelets were diluted 10X in RPMI 1640 supplemented with 1% antibiotic-antimycotic and treated with indicated compounds.

1.2.3. RPMI-1788 cells

Human RPMI-1788 cells, which are derived from B lymphocytes, were purchased from ATCC. They were cultured in RPMI 1640 (BioWhittaker) supplemented with 20% heat-inactivated FCS and 1% antibiotic-antimycotic (BioWhittaker), and subcultured at a seeding concentration of 3×10^5 cells/ml every two or three days.

1.2.4. $CD34^+$ cells

Umbilical cord blood was kindly provided by Clinique Bohler (Luxemburg, Luxemburg) and collected in 50-ml tubes containing 20 units/ml of heparin (Ratiopharm, Ulm, Germany). Donor's written informed consent was in agreement with the National Committee of Research Ethics in Luxemburg. PBMCs were first isolated as previously described and washed twice in 1X DPBS-2 mM EDTA. Then, $CD34^+$ cells were purified by magnetic cell sorting following manufacturer's instructions. For 10^8 PBMCs, 300 µl of magnetic cell sorting (MACS) solution (1X DPBS ; 2 mM EDTA ; 0.5% (v/v) bovine serum albumin (BSA) solution

(Sigma, Bornem, Belgium) were added to PBMCs without resuspension, as well as 100 µl of FcR Blocking Reagent Human and 100 µl of CD34 Microbeads Human (CD34 MicroBead Kit Human, Miltenyi Biotec). After a 30-minute incubation at 4°C, cells were diluted in 10 ml of MACS solution, centrifuged for 7 minutes at 340 *g*, and resuspended in 500 µl of MACS solution. Magnetically-labeled $CD34^+$ cells were successively isolated on two LS MACS separation columns (Miltenyi Biotec) pre-activated with 2 ml of MACS solution, the first one supplemented with pre-separation filter (Miltenyi Biotec) to eliminate red blood cells. After magnetic selection of $CD34^+$ cells that are held in suspension within each column, three-time washing with 3 ml of MACS solution was followed by an elution of cells from the column using 4 ml of MACS solution and piston. $CD34^+$ cells were finally seeded at $2x10^5$ cells/ml in serum-free condition in Stem Line Medium II (Sigma) supplemented with 2% (v/v) L-glutamine, 1% antibiotic-antimycotic (BioWhittaker), 10 ng/ml IL-3 (ReliaTech, Wolfenbüttel, Germany) and 50 ng/ml stem cell factor (SCF; ReliaTech), and cultivated for 3 days before treatment.

1.3. Transfections

Transfections were performed with HiPerFect Transfection Reagent (HPF; Qiagen, Venlo, The Netherlands), which is a blend of cationic and neutral lipids allowing efficient introduction of small interfering RNAs (siRNAs) into cells.

siRNAs targeting beclin 1 (BECN1) gene were obtained from Qiagen: Hs_BECN1_2 (si00055580) or non-targeting siRNA (AllStars Negative Control siRNA). K-562 cells were transfected with 1 nM siRNA using 1.5 µl of HPF according to manufacturer's instructions. Briefly, 100 µl of cells were seeded at a concentration of 1.2×10^6 cells/ml in culture medium with 10% FCS and incubated at 37°C and 5% CO_2 during the following steps. In a final volume of 100 µl, appropriate amount of siRNA corresponding to a final concentration of 1 nM was diluted in RPMI 1640 without FCS, then 1.5 µl HPF was added to the diluted siRNA. After vortexing the samples, 10-minute incubation at RT enabled the formation of transfection complexes, which were then added dropwise onto the cells and uniformly distributed by gentle agitation of the vial. After 6-hour incubation in normal growth conditions, 400 µl of culture medium with 12.5% FCS were added to the cells. Notably, all the volumes need to be scaled up based on the number of cells required for subsequent experiments. Cell number and viability were evaluated 24 hours post-transfection, and then cells were harvested to analyze gene silencing or treated for subsequent experiment.

1.4. Chemicals and cell treatments

Cells were treated in their exponential phase. Compounds MAKV-6, -7, -8, -10, -12 and -15 were provided by Guy Borman's laboratory (Laboratory of Radiopharmacy, University of Leuven, Belgium) and dissolved in dimethylsulfoxide (DMSO). The descriptions of the other compounds used to treat the cells are presented in Table 6. These compounds were used in the concentrations indicated in each experiment, and treatment with the appropriate solvent alone corresponded to the vehicle.

Table 6: Compounds used in this study.

Compounds were purchased from various companies: Adooq Bioscience (Irvine, CA, USA); ApexBio Technology (Houston, TX, USA); Cayman Bio-connect (Ann Arbor, MI, USA); Millipore (Merck, Brussels, Belgium); Selleckchem Bio-connect (Munich, Germany); Sigma (Bornem, Belgium); Teva Pharma (Antwerpen, Belgium).

Compound	Provider	Solvent	Purpose	Storage
A1210477	Selleckchem Bio-connect	DMSO	MCL-1 inhibitor	-80°C
ABT-199	Selleckchem Bio-connect	DMSO	BCL-2 inhibitor	-80°C
ACY-1215	Adooq Bioscience	DMSO	HDAC6i	-20°C
Bortezomib	Selleckchem Bio-connect	DMSO	Proteasome inhibitor	-80°C
Cisplatin	Teva Pharma	Saline solution	Alkylating-like agent	RT
Dexamethasone	Sigma	Ethanol	Immunomodulatory agent	-20°C
Doxorubicin	Sigma	Water	Topoisomerase II inhibitor	-20°C
Imatinib	Sigma	DMSO	TKi	-20°C
Rapamycin	Selleckchem Bio-connect	DMSO	mTOR inhibitor	-80°C
S63845	ApexBio Technology	DMSO	MCL-1 inhibitor	-20°C
SAHA	Cayman Bio-connect	DMSO	HDACi	-20°C
Thapsigargin	Sigma	DMSO	SERCA inhibitor	-20°C
Tubastatin A	Sigma	DMSO	HDAC6i	-20°C
Z-VAD-FMK	Millipore	DMSO	Caspase inhibitor	-20°C

BCL: B-cell lymphoma, DMSO: dimethyl sulfoxide, HDACi: histone deacetylase inhibitor, mTOR: mammalian target of rapamycin, RT: room temperature, SAHA: suberoylanilide hydroxamic acid, SERCA: sarco/endoplasmic reticulum Ca^{2+} ATPase, TKi: tyrosine kinase inhibitor, Z-VAD-FMK: carbobenzoxy-valyl-alanyl-aspartyl-[O-methyl]-fluoromethylketone.

At the end of treatments, cells were used for further experiments or collected by centrifugation at 350 *g* for 7 minutes, washed twice in cold 1X PBS and stored at -80°C prior subsequent analysis.

1.5. Cell viability and proliferation test

Cell viability was evaluated using the Trypan Blue exclusion method (BioWhittaker). This method is based on the capacity of viable cells to actively reject the dye in the extracellular medium, appearing in white under the microscope, while dead cells turn blue because they have lost this ability of expulsion.

Cells were processed using a semi-automated image-based cell analyzer (Cedex XS Innovatis, Roche, Luxembourg, Luxembourg), which provided the cell number as well as cell viability based on this Trypan Blue exclusion method.

2. Computational analysis of public CML datasets

The gene expression microarray datasets E-MTAB-2581 from (Scott *et al.*, 2016) and GSE97562 (Aviles-Vazquez *et al.*, 2017) were downloaded from the ArrayExpress database (Kolesnikov *et al.*, 2015) and the Gene Expression Omnibus repository, respectively. The datasets were normalized using the Robust Multichip Average algorithm from the oligo R package (version 1.48.0) (Carvalho *et al.*, 2010) and was batch corrected using the function *removeBatchEffect* from the limma R package (version 3.40.2) (Ritchie *et al.*, 2015). The *ggboxplot* function from the ggpubr package (version 0.2.1) (Kassambara, 2018) was used to draw the boxplots in R 3.6.0 (R Development Core Team, 2010) and RStudio (RStudio Team, 2015).

3. Docking studies

Docking studies were carried out using AutoDock Vina software (The Scripps Research Institute, CA, USA) (Trott *et al.*, 2010). Initial structures of HDAC1, HDAC2, HDAC3, HDAC4, HDAC6, HDAC7 and HDAC8 were obtained from the Protein Data Bank (PDB; PDB codes: 4BKX, 4LY1, 4A69, 2VQM, 5EDU, 3C10, and 3EW8, respectively), and coordinates for MAKV-6, -7, -8, -10 and -12, and SAHA were generated using ChemDraw Professional software (version 15.0, PerkinElmer Informatics). To prepare the structure for docking, the ligand and all water molecules were removed. The size of the docking grid was 40 Å × 40 Å × 40 Å, which encompassed most of the entire structures of the HDAC isoforms.

AutoDock Vina program was run with four-way multithreading, and the other parameters were default settings in AutoDock Vina program. Figures were generated using PyMol (The PyMOL Molecular Graphics System, version 2.0 Schrödinger, LLC).

4. Protein extractions

4.1. Total extraction

Cell pellets were resuspended in 10% (v/v) Mammalian Protein Extraction Reagent solution (MPER®, Thermofisher, Erembodegen, Belgium) supplemented with 1X protease inhibitor cocktail (Complete EDTA-free, Roche). After a constant agitation of 10 minutes at room temperature which allowed the mild detergent present in the solution to dissolve cell membranes, the samples were centrifuged at 14,000 *g* for 10 minutes at 4°C. Supernatants containing total soluble proteins were collected and stored at -80°C.

4.2. Acid extraction

Cell pellets were resuspended in 1 ml of hypotonic lysis buffer (10 mM Tris-HCl pH8 ; 1 mM KCl ; 1.5 mM $MgCl_2$; 1 mM DTT ; 1X Complete EDTA-free) supplemented with 10 µM SAHA, and incubated for 30 minutes at 4°C under a constant and gentle agitation. All the following steps were done at 4°C. After a centrifugation at 10,000 *g* for 10 minutes, nuclei were lysed by resuspension in 400 µl of 0.4 N sulfuric acid and gentle agitation for 30 minutes. The samples were then centrifuged at 16,000 *g* for 10 minutes, and trichloroacetic acid was added drop by drop to the supernatant up to a final concentration of 25%. The precipitation of proteins, mainly composed of histones, progressed overnight.

On the second day, the samples were centrifuged at 16,000 *g* for 10 minutes to collect principally histones in the pellets, which were then washed twice with 500 µl of cold acetone. When pellets were dry and devoid of acetone, they were dissolved in pure water, then transferred into fresh tubes and stored at -80°C.

4.3. Determination of protein concentration with Bradford method

The Bradford method is a colorimetric assay used to determine protein concentration and based on the absorbance of a Commassie dye solution turning from red to blue color in the presence of proteins. When proteins are very concentrated, the bound fraction of the dye is high, and the blue color is intense.

To measure the protein concentration of samples, 160 µl of appropriately diluted samples were added to 40 µl of Bradford reagent (BioRad, Temse, Belgium), this being done in

duplicates. After 5 minutes of incubation, the absorbance of each well was read at a 590 nm wavelength in a spectrophotometer (SpectraCount, Canberra Packard, Schwadorf, Austria) conducted by the Plate-reader software. The mean of the duplicate values was calculated and put into the equation coming from the standard curve of BSA to calculate concentration of proteins.

5. Western blot

The western blot is an analytical technique allowing the specific detection of proteins in a cell lysate. Protein samples in Laemmli buffer (125 mM Tris-HCl pH6.8 ; 20% glycerol ; 4% SDS ; 5% 2-β-mercapto-ethanol ; 0,005% bromophenol blue) are denaturated at 100°C for 5 minutes and loaded into a discontinuous polyacrylamide gel constituted of two parts: the upper staking gel (125 mM Tris-HCl pH6,8 ; 0,1% SDS ; 0,1% ammonium persulfate ; 0,1 % TEMED (v/v) ; 4% acryl/bisacry 37,5:1) in which proteins were concentrated thanks to the difference of pH and salinity, and the lower running gel (373 mM Tris-HCl pH8,8 ; 0,1% SDS ; 0,1% ammonium persulfate ; 0,1 % TEMED (v/v) ; acryl/bisacry 37,5:1) whose final concentration was adjusted depending on the size of the proteins to detect.

Electrophoresis gels were immerged in electrophoresis buffer (25 mM Tris ; 0.192 mM glycine ; 0.1% SDS), and, thanks to an electrical field of 200 volts/cm^2, proteins were separated according to their molecular weight in denaturing conditions by a method called sodium dodecyl sulfate-polyacrylamide gel electrophoresis (SDS-PAGE). Proteins surrounded by SDS, a strong anionic detergent, were denatured and gained a negative global charge identical for all proteins. After migration, proteins were transferred onto methanol-activated polyvinylidene difluoride (PVDF) membranes (GE Healthcare), thanks to a constant transversal electrical field of 100 volts/cm^2 in cold transfer buffer (25 mM Tris ; 0,192 mM glycine ; 5% methanol for all proteins except LC3 that required 10% methanol).

On the membrane, proteins are analyzed by immunodetection consisting in the use of a primary antibody, directed against an epitope of the target protein, which is then recognized by the secondary antibody coupled to a system of detection. To limit unspecific binding of the primary antibody, the membranes were incubated with a blocking solution – 1X PBS-0.1% Tween® with 5% milk or BSA (Table 7) – for one hour at room temperature. After an incubation overnight at 4°C with the suitable blocking solution and the primary antibody (Table 7), the membranes were incubated for one hour at room temperature with the secondary antibody in PBS-Tween® with 5% of blocking agent. This secondary antibody is coupled to a Horseradish peroxidase which, in presence of an oxidative agent and luminol,

oxidates the latter. The signal given by this highly sensitive chemiluminescent detection reagent (kit ECL Plus Western Blotting Detection System, GE Healthcare) was acquired by a CCD-based imaging system (ImageQuant LAS 500; GE Healthcare). Quantifications of western blots were performed with ImageQuant TL software (GE Healthcare) and the corresponding fold-change values reported to control are indicated underneath western blot pictures, unless otherwise specified. EC_{50} values, which represent 50% of the maximum effect, were calculated using Prism software.

In addition to the protein of interest, β-actin or α-tubulin, and histone H1 were detected on the membranes as loading control for total proteins and histone extract, respectively.

Table 7: Conditions for the use of antibodies in western blots.

Dilutions of primary and secondary antibodies were performed in 1X PBS-0.1% Tween® with 5% blocking agent. Primary antibodies were purchased from various companies: BD Biosciences (San Jose, CA, USA); Cell Signaling (Leiden, The Netherlands); Millipore (Merck, Brussels, Belgium); Santa Cruz Biotechnology (Boechout, Belgium). Secondary antibodies were obtained from Santa Cruz except in cases reported in Table 7.

Target (kDa)	Company	Blocking	Primary antibody dilution – blocking agent	Secondary antibody dilution – blocking agent	Host of primary antibody
Acetylated α-tubulin (K40) (55)	Santa Cruz	Milk	1/1000 - Milk	1/5000 - Milk	Mouse
Acetylated histone H4 (11)	Millipore	BSA	1/50,000 - Milk	1/5000 - Milk	Rabbit
β-actin (42)	Sigma	Milk	1/20,000 - Milk	1/10,000 - Milk	Mouse
BCL-2 (25)	Calbiochem	Milk	1/2000 - Milk	1/5000 - Milk	Mouse
BCL-xL (32)	Santa Cruz	Milk	1/1000 - Milk	1/2000 - Milk	Mouse
BCR-ABL/ABL (210/120)	Santa Cruz	Milk	1/1000 - BSA	1/2500 - Milk	Mouse
Beclin 1 (60)	Cell Signaling	Milk	1/1000 - BSA	1/4000 - BSA	Rabbit
c-MYC (62)	BD Biosciences	Milk	1/250 - Milk	1/1000 - Milk	Mouse
Caspase 3 (17/19, 35)	Cell Signaling	Milk	1/1000 - Milk	1/4000 - Milk	Mouse
Caspase 7 (20, 30, 35)	Cell Signaling	Milk	1/1000 - Milk	1/2000 - Milk	Mouse

Caspase 8 (18, 43, 57)	Cell Signaling	Milk	1/1000 - BSA	1/4000 - Milk	Mouse
Caspase 9 (10, 35, 47)	Cell Signaling	Milk	1/1000 - Milk	1/10,000 - Milk	Rabbit
eIF2α (37)	Cell Signaling	Milk	1/2000 - Milk	1/4000 - Milk	Rabbit
γ-H2AX (Ser139) (15)	Millipore	Milk	1/500 – Milk	1/2500 – Milk	Mouse
GRP78 (78)	Santa Cruz	Milk	1/1000 - Milk	1/4000 - Milk	Rabbit
HDAC6 (160)	Santa Cruz	Milk	1/2500 - Milk	1/1000 - Milk	Rabbit
Histone H1 (30)	Millipore	Milk	1/2000 - BSA	1/2500 - Milk	Mouse
LC3 (16-18)	Sigma	Milk	1/1000 – Milk (2h RT)	1/5000 – Milk (Amersham)	Rabbit
MCL-1 (40)	Cell Signaling	Milk	1/1000 - BSA	1/4000 - Milk	Rabbit
SQSTM1 (62)	Santa Cruz	Milk	1/1000 - Milk	1/2000 - Milk	Mouse
PARP-1 (24, 89, 116)	Cell Signaling	Milk	1/1000 - Milk	1/4000 - Milk	Rabbit
PERK (140)	Cell Signaling	Milk	1/1000 - Milk	1/4000 - Milk	Rabbit
Phosphorylated BCR (Tyr177) (210)	Cell Signaling	Milk	1/1000 - BSA	1/5000 - Milk	Rabbit
Phosphorylated eIF2α (Ser51) (37)	Cell Signaling	BSA	1/2000 - BSA	1/4000 - Milk	Rabbit
Phosphorylated PERK (Thr981) (140)	Santa Cruz	BSA	1/1000 - BSA	1/4000 - Milk	Rabbit
Phosphorylated STAT5 (Tyr694) (90)	Cell Signaling	Milk	1/1000 - Milk	1/20000 - Milk	Rabbit
STAT5 (90)	Cell Signaling	BSA	1/5000 - BSA	1/1000 - Milk	Rabbit
Ubiquitin	Santa Cruz	BSA	1/200 - BSA	1/5000 - Milk	Mouse

BCL: B-cell lymphoma; BCR-ABL: Breakpoint cluster region-Abelson murine leukemia viral oncogene homolog 1; BSA: bovine serum albumin; eIF: eukaryotic initiation factor; GRP78: 78 kDa glucose-regulated protein; HDAC: histone deacetylase; LC3: MT-associated protein 1 light chain 3; PARP: poly (ADP-ribose) polymerase; PERK: protein kinase RNA-like ER kinase; RT: room temperature; SQSTM: sequestosome; STAT: signal transducer and activator of transcription.

6. *In vitro* HDAC activity assay

The HDAC fluorimetric assay allows *in vitro* measurement of either whole or one specific deacetylase activity. A synthetic peptide-like substrate containing an acetylated lysine side chain, a fluorophore and a quencher is incubated in presence of a source of HDAC activity. Only the deacetylated substrate becomes sensitive to cleavage by a "developer", allowing the

release of a fluorescent molecule. The fluorophore has an emission wavelength of 460 nm when excited with a 360 nm light (Figure 21).

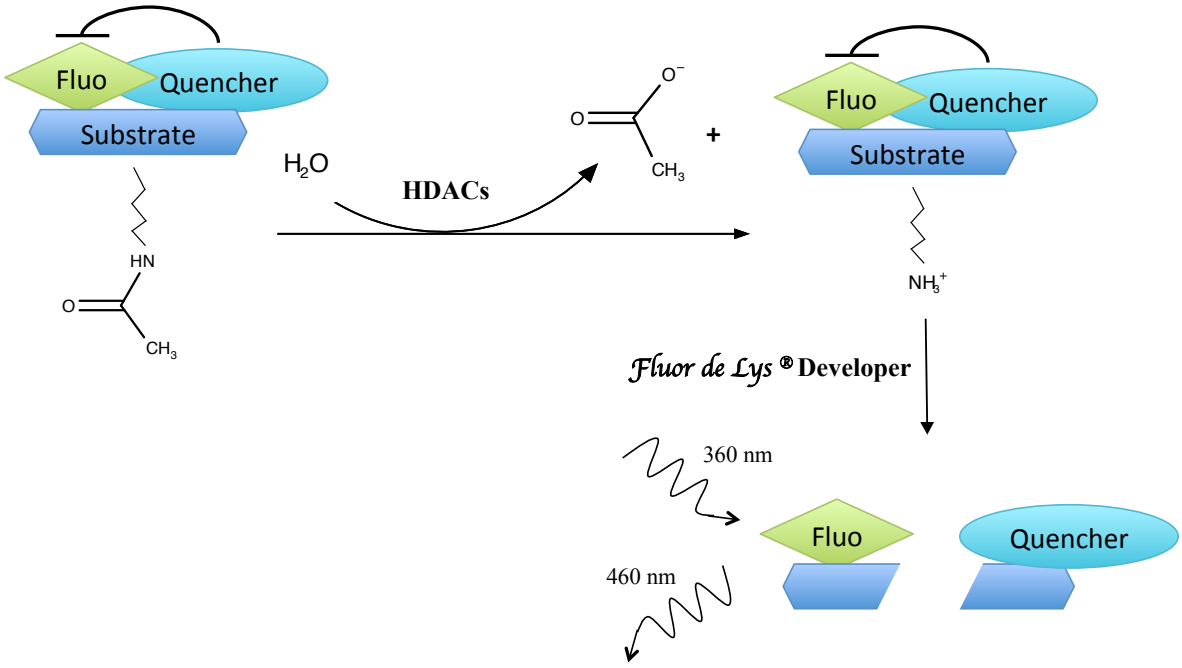

Figure 21: Principle of HDAC activity assay.
An acetylated substrate is bound to a quencher inhibiting the fluorophore (Fluo). In presence of HDAC enzymatic activity, the substrate is deacetylated, becoming recognizable for the "developer". The developer-mediated cleavage of the deacetylated substrate allows the release of the fluorophore whose fluorescence is measured. Fluor-de-Lys®: Fluorogenic Histone Deacetylase Lysyl.

In vitro total HDAC activity (classes I, II and IV) was measured using total protein extracts from K-562 cells. Using a 96-well plate, 50 µM Fluorogenic Histone Deacetylase Lysyl (Fluor-de-Lys®) substrate (Enzo Life Sciences, Antwerpen, Belgium) was incubated with 10 µg of proteins and increasing concentrations of the compound tested for its potential inhibitory effect. After 45 minutes of incubation at 37°C, a developing solution containing 1X Fluor-de-Lys® developer I concentrate (Enzo Life Science) and 2 µM SAHA was added to the previous mixture and incubated for 10 minutes at 37°C to stop the reaction and generate a molecule whose fluorescent signal was measured on a fluorescence microplate reader (Spectra MAX Gemini, Molecular devices, INC. Sunyvale, CA, USA) using the Soft Max Pro software. All reagents were diluted in a buffer containing 50 mM Tris-HCl, pH8 ; 137 mM NaCl ; 2,7 mM KCl and 1 mM $MgCl_2$.

Specific *in vitro* HDAC activities were measured using 1 unit of recombinant proteins (HDAC1 or HDAC6, Enzo Life Science) incubated with 10 µM Fluor-de-Lys®-Sirt1 substrate (Enzo Life Science) and increasing concentrations of the compound tested for its potential

inhibitory effect. After 1 hour of incubation at 37°C, the developing solution consisting of 1X Fluor-de-Lys® developer II concentrate (Enzo Life Science) supplemented with 2 µM SAHA was added to stop the reaction. After 10 minutes of incubation at 37°C, fluorescence was measured as for total HDAC activity. All tested compounds were diluted in a buffer containing 50 mM Tris-HCl, pH8 ; 137 mM NaCl ; 2,7 mM KCl ; 1 mM $MgCl_2$ and 1 mg/ml BSA.

The potential inhibitory activity of tested compounds was determined in three steps. First, the amount of fluorescence generated by the deacetylated substrate itself was established by subtracting the basal fluorescent signal generated by the substrate in absence of HDAC activity. Then, the percentage of activity for each dilution of the compounds was calculated by comparing their amount of fluorescence with the one generated by the vehicle control. Finally, the IC_{50}, representing the drug concentration that causes 50% inhibition of a specified individual target, were determined using Prism software (GraphPad Software, Inc., La Jolla, CA, USA).

7. Clonogenic assay

Clonogenic assay, also referred as colony formation assay, is a cell culture method allowing the study of single cell capacity to form colonies in a 3-dimensional matrix. Colonies are detected thanks to 3-(4,5-dimethylthiazol-2-yl)-2,5-diphenyltetrazoliumbromide (MTT), which is reduced into purple-colored insoluble formazan by NAD(P)H-dependent oxidoreductase enzymes of metabolically active cells.

1000 cells were grown in 1 ml of semi solid methylcellulose medium (Methocult H4230; StemCell Technologies Inc., Grenoble, France) supplemented with 10% heat-inactivated FCS (BioWhittaker) in a 12-well plate well. Colonies were detected after 10 days of culture by adding 300 µl of MTT reagent (5 mg/ml ; Sigma) and incubating for 15 minutes at 37°C. Pictures were taken with the GelDoc XR+ System (BioRad) driven by Quantity One® software (BioRad) and quantifications were conducted using Image J software (U.S. National Institute of Health, Bethesda, MD, USA).

8. Evaluation of nuclear morphology by fluorescent microscopy

The identification of the type of cell death (apoptosis versus necrosis) is possible after the staining of cells with two fluorescent dyes: Hoechst 33342 and propidium iodide (PI). Both molecules intercalate between the bases of the DNA, allowing the study of the nuclear

morphology, but reach the nucleus in different conditions. Hoechst 33342 enters all cells and stains their nucleus in blue, while PI stains the nucleus in red only if the cells have lost the integrity of their membrane either by going through necrosis or being in a stage of late apoptosis. Therefore, this double staining is necessary to differentiate alive, necrotic and apoptotic cells.

To perform nuclear morphology analyses, cells were incubated at 37°C for 15 minutes with a Hoechst 33342 (Invitrogen) solution (1 µg/ml). After centrifugation at 350 *g* for 5 minutes, cell pellets were resuspended in 1X PBS supplemented with 1 µg/ml PI (Sigma). Finally, a few microliters of cells suspension were dropped on a microscope slide and visualized under an IX81 (MT10) fluorescent microscope (Olympus, Aartselaar, Belgium) allowing the counting of the different cell populations after each treatment.

9. Study of mitochondrial membrane potential

Mitochondrial membrane potential (MMP) was assessed thanks to MitoTracker® Red Chloromethyl-X Rosamine (Thermofisher), which stains active mitochondria in live cells since its accumulation is dependent upon MMP. The chloromethyl moiety covalently reacts with intra-mitochondrial thiols on peptide or proteins to form a thioester bond and generate fluorescent aldehyde conjugates whose excitation and emission wave lengths are 579 nm and 599 nm, respectively.

To label healthy mitochondria, 1 µl of 0.1 mM MitoTracker® Red CMXRos was added to 1 ml of cell suspension, which was then incubated for 30 minutes at 37°C. Stained samples were processed through a cytometer (FACS Calibur, BD Biosciences) and data were recorded statistically (20,000 events/sample) using the CellQuest Pro software. Data were analyzed using the Flow-Jo 8.8.5 software (Tree Star, Inc., Ashland, OR, USA). A two-dimensional dot plot (SSC *vs.* FL2-H) was produced in order to delineate cells with high *vs.* low MMP.

10. Assessment of apoptosis induction by flow cytometry

Fluorescent Annexin V conjugates are commonly used to detect apoptotic cells thanks to their strong and specific affinity for PS, which are exposed to the external cellular environment upon apoptosis induction.

FITC Annexin V Apoptosis Detection Kit I (BD Biosciences) was used according to supplier's instructions. Briefly, 5 µl of Annexin V and 5 µl of PI were added to 100 µl of 1X Annexin V Binding Buffer containing 10^5 cells. After 15 minutes of incubation at RT in the

dark. 400 µl of 1X Binding Buffer were added to the samples. Of note, platelets were only stained with Annexin V since they are devoid of nucleus.

Stained samples were processed through a cytometer (FACS Calibur, BD Biosciences) and data were recorded statistically (10,000 events/sample) using the CellQuest Pro software. Compensation was needed because of a contamination of the green signal (Annexin V) in the red signal (PI). Data were analyzed using the Flow-Jo 8.8.5 software. A two-dimensional dot plot (FL1-H *vs.* FL2-H) was produced in order to distinguish Annexin V-negative/PI-negative (alive) and Annexin V-positive (apoptotic) cells.

11. Analysis of cell morphology with Giemsa staining

The technique used to visualize global cell morphology is a modified May-Grünwald-Giemsa staining that is based on differential staining properties of two dyes, eosin and methylene blue. The first one is acid, selectively fixing acidophilic cell constituents, while the second one is basic and selectively fix basophilic cell constituents.

Around 200,000 cells resuspended in 100 µl of 1X PBS were spun down onto a microscope slide by centrifugation at 700 rpm for 4 minutes using a cytofuge (Shandon Cytospin 4, Thermofisher). Slides were then air-dried and soaked successively for a few seconds in the 3 solutions constituting the Differential Quik Stain kit (Dade Behring SA, Brussels, Belgium): the first solution fixes the cells, the second one stains the cytoplasm in red and the third one stains the nucleus in blue. Slides are finally washed in Giemsa water (1 liter of distilled water supplemented with one buffer tablet pH6.8, Millipore), air-dried and observed under the microscope Leica DM2000 (Lecuit, Howald, Luxembourg) equipped with a DFC420C camera. Images were acquired with Leica FireCam software.

12. Monitoring autophagy in live cells

The Cyto-ID® Autophagy Detection Kit (Enzo Life Science) was used to evaluate the autophagic activity of cells by monitoring the appearance of autophagic vesicles highlighted by a 488 nm-excitable green fluorescent cationic amphiphilic tracer dye that becomes brightly fluorescent in vesicles produced during autophagy (details not provided by supplier).

Briefly, 10^6 cells were resuspended in 100 µl of Microscopy Dual Detection Reagent solution [*i.e.* 1X Assay Buffer supplemented with 5% FCS, 0.2% Cyto-ID® Green Detection Reagent (v/v) and 0.1% Hoechst 33342 Nuclear Stain (v/v)], incubated for 30 minutes at

37°C in the dark, washed in 1X Assay Buffer, and visualized under an IX81 (MT10) fluorescent microscope.

13. Transmission electron microscopy

TEM is a method in which an electron beam is transmitted through a sectioned sample to form an image with a significantly higher resolution than light microscopes.

Before TEM analysis, samples were subjected to different steps:

- (*i*) For primary fixation, $5x10^6$ cells were resuspended in 1 ml of ice-cold 0.1 M sodium cacodylate solution pH7.2 (Sigma) supplemented with 2.5% glutaraldehyde (Electron Microscopy Science, Hatfield, PA, USA) and incubated for 8 hours at 4°C. Fixed cells were then washed twice in 500 µl of ice-cold 0.1 M sodium cacodylate solution and stored at 4°C until the following step.

- (*ii*) For resin embedding, cells were first incubated in a mixture constituted of 1 ml of 2% osmium tetroxide and 1 ml of 0.1 M cacodylate buffer for 2 hours at 4°C and then washed twice in cold distilled water. After being en bloc stained thanks to an incubation with 0.5% uranyl acetate over night at 4°C, cells were dehydrated thanks to successive incubations of 10 minutes in 30, 50, 70, 80, 90 % ethanol solutions, followed by three incubations in 100% ethanol. The transition between dehydration and infiltration steps was done by incubating cells twice in 2 ml of 100% propylene oxide for 10 minutes.

- (*iii*) For the infiltration step, cells were incubated for 2 hours in a mixture composed of 1 ml of propylene oxide and 1 ml of Spurr's resin, followed by an overnight and a 2-hour incubations in 2 ml of Spurr's resin. In order to allow polymerization of the resin, cells were incubated in 2 ml of Spurr's resin for at least 24 hours in a dry oven at 70°C.

After being sectioned with an ultramicrotome (MT-X, RMC, Tucson, AZ, USA), samples were stained with 2% uranyl acetate for 7 min then with Reynolds' lead citrate for 7 minutes. Observation was realized under a transmission electron microscope (LIBRA 120, Carl Zeiss, Germany).

14. Cell cycle analysis by flow cytometry

Cell cycle analysis by flow cytometry is based on the fluorescence intensity emitted by cell nuclei stained with PI, a dye that intercalates between the two DNA strands. This intensity is therefore proportional to the amount of DNA.

One million of cells were fixed by adding cold 70% ethanol drop by drop while gently vortexing. After 30 minutes incubation at 4°C, cells were washed twice with cold 1X PBS and incubated 20 minutes in 500 µl of 1X PBS supplemented with RNase A (100 µg/ml, Roche) and PI in solution (1 µg/ml).

Stained samples were processed through a cytometer (FACS Calibur, BD Biosciences) and data were recorded statistically (10,000 events/sample) using the CellQuest Pro software. Data were analyzed using the Flow-Jo 8.8.5 software. A two-dimensional dot plot (FL2-A *vs.* FL2-W) was produced in order to only select the cells of interest by discriminating doublets and eliminating dead cells. The gated cells were then plotted in a histogram based on fluorescence intensity, which showed cell repartition in the phases of the cycle. The percentage of cells in each phase of cycle was determined by the Dean-Jet-Fox algorithm.

15. Analysis of gene expression

15.1. RNA extraction

Total RNA are extracted with the NucleoSpin® RNA plus kit (Macherey-Nagel, Hoerdt, France) according to manufacturer's instructions. Briefly, a maximum of 4×10^6 cells were first lysed by incubation in a chaotropic ion lysis buffer solution, which immediately inactivated RNases. After clarifying the lysate and removing contaminating gDNA, the RNA was bound to silica columns. Two subsequent wash steps removed salts, metabolites, and macromolecular cellular components. Finally, RNA was eluted with RNase-free water and stored at -80°C.

The RNA concentration was calculated with a microspectrophotometer (NanoDrop ND 1000, Thermo Scientific). By measuring the optical density of samples at a wavelength of 260 nm, the device allowed the determination of RNA concentration thanks to Lambert-Beer law. It also calculated two ratios of absorbance A_{260}/A_{280} et A_{260}/A_{230} that give additional indication about the quality and purity of samples, respectively.

15.2. Reverse transcription

Reverse transcription allows the transformation of single strand RNA into complementary double strand DNA thanks to a viral reverse transcriptase, in presence of nucleotidic primers and nucleotides.

RNA (1 µg) was denatured at 70°C for 10 minutes in presence of 0.5 µg oligo$(dT)_{15}$ primers that subsequently hybridized to the denatured RNA. Denatured RNA was then rapidly transferred on ice to prevent secondary structure reformation. To each sample was added a

reaction mixture composed of 1X reverse transcriptase buffer, 10 mM DTT, 0.5 mM of each dNTP, 40 units of RNAsein® Ribonuclease inhibitor and 50 units of M-MLV (Moloney-Murine Leukemia Virus) reverse transcriptase, RNase (H-), point mutant (Promega, Leiden, The Netherlands). The synthesis of the cDNA strands then took place for 1.5 hour at 42°C, and ended with 15 minutes at 70°C to inactivate the reverse transcriptase. Finally, the reaction mixture was incubated with 2.2 units of RNase H at 37°C for 20 minutes to digest RNA. After addition of RNase free water to reach a concentration of 4 ng/µl cDNA, newly synthesized cDNA strands were stored at -20 ° C.

15.3. End-point polymerase chain reaction

Polymerase chain reaction (PCR) is a technique producing a high number of copies of a DNA sequence defined by the pair of sense and antisense synthetic oligonucleotides. Products of end-point PCR are detected on a polyacrylamide gel stained with ethidium bromide, a DNA intercalating agent that fluoresces under UV light.

cDNA (4 ng) were used as template for amplification by PCR in a reaction mixture composed of 0.4 µM of preliminarily validated primer forward and reverse (Eurogentec, Liege, Belgium; XBP-1: forward 5'-GGAGTTAAGACAGCGCTTGG-3', reverse 5'-ACTGGGTCCAAGTTGTCCAG-3'), 1.25 units of HotStart Taq® DNA polymerase (Qiagen), 1X buffer and 0.2 mM of each dNTP (Invitrogen). Amplification of the target gene was realized in a Mastercycler® gradient (Eppendorf, Aarschot, Belgium) and started with an initial 15-minute incubation at 95°C to activate the HotStart Taq® DNA polymerase, followed by 35 successive repetitions of three phases: denaturation at 94°C for 30 seconds, hybridization at 60°C for 1 minute and elongation at 72°C for 2 minutes. Amplification ends with an additional elongation phase of 10 minutes at 72°C.

PCR products in GBX DNA loading buffer (50 mM Tris-HCl pH7.6 ; 50 mM EDTA ; 50% glycerol ; 0.005% xylene cyanol ; 0,005% bromophenol blue) were loaded on a continuous 15% acrylamide gel [1X Tris Borate EDTA (TBE) buffer: 90 mM Tris, 90 mM boric acid, 2.5 mM EDTA pH8 , 0.1% ammonium persulfate, 0.1% TEMED (v/v) ; 15% acryl/bisacry 37.5:1]. Gels were immerged in 1X TBE buffer and, thanks to an electrical field of 200 volts/cm^2, PCR products migrated according to their size.

After migration, gels were immerged in ethidium bromide (Promega) solution (0.5 µg/ml) for 10 minutes, and then exposed to UV light to reveal stained PCR product. Pictures were taken with GelDoc XR+ System (BioRad) driven by Quantity One® software.

15.4. Real-time PCR

In real-time PCR, the amplification of the transcript can be followed over time thanks to the measurement of the fluorescence emitted at each cycle by SYBR Green, a molecule that fluoresces only when intercalated between the two amplified DNA strands.

In 96-well plates, 8 ng of cDNA were mixed with 1X Power SYBR® Green PCR Master Mix (Applied Biosystems, Halle, Belgium) and 0.1 µM of preliminarily validated primers (Eurogentec; β-actin: forward 5'-CTCTTCCAGCCTTCCTTCCT-3', reverse 5'-AGCACTGTGTTGGCGTACAG-3'; DDIT3: forward 5'-TGGAAGCCTGGTATGAGGAC-3', reverse 5'-AAGCAGGGTCAAGAGTGGTG-3').

Amplification of the target gene and detection of fluorescence were realized in a 7300 Real Time PCR System (Applied Biosystems) driven by the 7300 System software. During the PCR reaction, cDNA went through 40 successive repetitions of three phases: denaturation at 95°C for 15 seconds, then hybridization and elongation at 60°C for 60 seconds. The second step at 60°C allowed the specific pairing of the sense and antisense primers on their complementary sequence on the cDNA and polymerase-mediated elongation of a strand complementary to the cDNA from the 3'-OH ends of hybridized primers. Additionally, melt curve was produced to verify the quality of the target gene amplification, *i.e.* absence of non-specific product amplification or primer dimer formation.

Based on the amplification curve, the software determined a cycle threshold (Ct) where (*i*) the fluorescence exceeded the background noise, and (*ii*) the amplification curve was in the linear phase, which allowed their comparison. Results were analyzed thanks to the following equations: $\Delta Ct = Ct_{\text{(gene of interest)}} - Ct_{\text{(housekeeping gene)}}$, in which the amount of target gene was normalized to the endogenous level of β-actin; and $2^{-\Delta Ct}$, allowing the comparison of target gene expression in the different conditions of treatment.

16. Study of ALDH+ population

To identify progenitor cells on the basis of their ALDH activity, ALDEFLUOR™ kit (StemCell Technologies Inc.) was used according to manufacturer's procedures. Briefly, 10^6 cells were resuspended in 1 ml of ALDEFLUOR™ Assay Buffer. Immediately after addition of 5 µl of activated ALDEFLUOR™ Reagent, a fluorescent substrate for ALDH that freely diffuses into viable cells, 0.5 ml of the cell suspension was transferred into another tube containing 5 µl of diethylaminobenzaldehyde (DEAB), a specific inhibitor of ALDH used to set up the threshold of background fluorescence. Samples were incubated at 37°C for 40

minutes, then centrifuged at 250 *g* for 5 minutes. Cells were resuspended in 0.5 ml of ALDEFLUOR^{TM} Assay Buffer and stored on ice.

Stained samples were processed through a cytometer (FACS Calibur, BD Biosciences) and data were recorded statistically (100,000 events/sample) using the CellQuest Pro software. Data were analyzed using the Flow-Jo 8.8.5 software. After excluding dead cells and debris from the analysis, a two-dimensional dot plot (FL1-H *vs.* SSC) was produced in order to delineate cells with high *vs.* low ALDH activity by comparison to the corresponding DEAB-treated control cells.

17. Tumor growth evaluation of xenografted cells in zebrafish

Wild type zebrafish (*Danio rerio*) were obtained from the Zebrafish International Resource Center (ZIRC, University of Oregon, OR, USA), and maintained according SNU guidelines at 28.5°C with 10-hour dark/14-hour light cycles.

One male and one female zebrafish were separated in a partition tank filled with UV-sterilized and filtered tap water at 28.5°C in the dark. After 24 hours of separation, fishes of both genders were mixed to initiate mating. Fertilized eggs were directly transferred from mating tank to a 55 cm^2 Petri dish containing 5 ml of fresh 1X Danieau's solution (58 mM NaCl ; 0.7 mM KCl ; 0.4 mM $MgSO_4$; 0.6 mM $Ca(NO_3)_2$; 5 mM HEPES solution ; pH7.6), washed three times with 5 ml of 1X Danieau's solution and incubated for 8 hours at 28.5°C. Eggs were then incubated in 1X Danieau's solution supplemented with 0.03% 1-phenyl-2-thiourea (PTU) to inhibit pigmentation. Opaque eggs, representing unfertilized eggs or containing undeveloped embryos, were sort out to prevent contamination. Twenty-four hours post fertilization, embryos were dechorionated using forceps under a microscope and hatching embryos were incubated in 1X Danieau's solution-0.03% PTU at 28.5°C until 48 hours post fertilization.

In the meantime, cells were treated with compound for the indicated period of time in order to maintain viability but commit cells towards cell death. Two hours before the end of treatment, cells were stained with 2 µM CM-Dil (Invitrogen), a fluorescent cell tracker dye.

Micropipettes for injection and anesthesia were generated from a 1.0-mm glass capillary (World Precision Instruments, FL, USA) by using a micropipette puller (Shutter Instrument, USA). Zebrafishes were anesthetized in a 0.02% (w/v) tricaine solution (Sigma, St. Louis, MO, USA) for 5 minutes and immobilized on an agar plate. Prior to injection, 10^6 cells were diluted in 50 µl of 1X PBS supplemented with 1% phenol red sodium salt solution. Micropipettes were then loaded with 20 µl of cells suspension and 200 cells were injected into

the yolk sac of the zebrafish through 5 injections of 2 nl each using a PV820 microinjector (World Precision Instruments). Subsequently, fishes were allowed to recover for 15 minutes in 5 ml of 1X fresh Danieau's solution-0.03% PTU and were then dispatched in 24-well plates with 1 ml of 1X fresh Danieau's solution-0.03% PTU. After a 72-hour incubation at 28.5°C, fishes were anesthetized in a 0.02% (w/v) tricaine solution and immobilized on a glass slide with a drop of 1X Danieau's solution supplemented with 3% (w/v) methylcellulose (Sigma). Pictures of sided fishes were taken under Leica DE/DM 5000B fluorescent microscope driven by the LAS V4.2 software and the size of fluorescent tumors was quantified by Image J software.

18. Statistical analyses

All histograms represent the mean ± standard deviation (SD) of at least 3 independent experiments. Significant differences were determined using one-way or two-way analyses of variance (ANOVA) followed by the Holm-Sidak's multiple comparison tests in the Prism 8.0 software. Variations between patient and Cyto-ID-stained samples were evaluated using Welch *t*-test in the R 3.6.0 software and paired *t*-test in the Prism 8.0 software, respectively. Statistical significances were evaluated with *p*-values below 0.05 and represented by the following legend: * $p \leq 0.05$, ** $p \leq 0.01$, *** $p \leq 0.001$. In all experiments, results of treated samples were statistically compared to the corresponding vehicle unless otherwise specified.

The combination index (CI) was calculated according to Chou and Talalay (Chou, 2006) using Compusyn Software (ComboSyn, Inc., Paramus, NJ, USA). This method for drug combination is based on the median-effect equation, which is derived from the mass-action law principle and encompasses the Michaelis-Menten, Hill, Henderson-Hasselbalch and Scatchard equations (Chou, 2010). CI values below or above 1 indicate synergism or antagonism, respectively, whereas the effect is determined to be additive if the CI is equal to 1.

RESULTS

HDACs became promising targets for anticancer therapy due to the deregulation of their expression and/or activity in various cancers. More specifically, the isoenzyme HDAC6 is closely implicated in cancer progression, mainly through its overexpression.

In this work, we evaluated the anticancer properties of new hydroxamate-based (*i*) pan-HDACi and (*ii*) HDAC6i, alone or in combination with targeted therapies. For that purpose, we first tested their potential inhibitory activity for total HDAC or specific HDAC isoenzymes *in vitro* and *in cellulo*. Then, we studied the effect of the compounds alone or in combination on cell proliferation and viability to orientate further investigations on their anticancer potential and underlying mechanisms of action.

1. Characterization of the anticancer properties of a new hydroxamate-based pan-HDACi: MAKV-8

In the initial study, authors synthetized new potential HDACi by use of NOC chemistry, and evaluated their selectivity on isolated enzymes (HDAC1, 2, 3 and 8 from class I, and HDAC6 and 10 from class II). In their data, the molecule 3 (MAKV-8) was reported to act as a selective HDACi as it displayed IC_{50} values of 100 nM and 2 pM against HDAC1 and HDAC3 or HDAC6, respectively, and showed anti-proliferative activity against pancreatic cancer cell lines (Kozikowski *et al.*, 2008).

Based on those data, the group of Prof. Guy Bormans synthetized the molecule and derived four other molecules. MAKV-6 and MAKV-7 lack the linker chain, whose length plays a role in the selectivity and potency of inhibition, whereas MAKV-10 and MAKV-12 lack the hydroxamate group that represents a metabolic liability as it is directly implicated in the mechanism of HDAC inhibition by chelating the zinc ion (Figure 19).

1.1. *In vitro* inhibitory potential of MAKV-8 on HDAC isoenzymes

First, we assessed the inhibitory potential of MAKV-8 against HDAC activities *in vitro*, using a fluorimetric HDAC activity assay. Notably, an inhibition of total HDAC activity can be due to a strong inhibition of one important HDAC isoenzyme, or a weaker inhibition of several HDAC isoenzymes. This analysis reveals that MAKV-8 inhibits total HDAC activity as well as that of recombinant HDAC1 and HDAC6 with IC_{50} values of 5.8, 2.6, and 11.4 nM, respectively. IC_{50} values within the same concentration range suggest that multiple activities

are inhibited *in vitro*. Moreover, the potency of the inhibition was evaluated by comparison with SAHA, used as a positive control for the inhibition of selected enzyme activity. MAKV-8 appears to be a stronger HDACi *in vitro* than the reference compound SAHA, as about 10% of the total HDAC activity remains following incubation with 2 µM SAHA and 0.1 µM MAKV-8 (Figure 22).

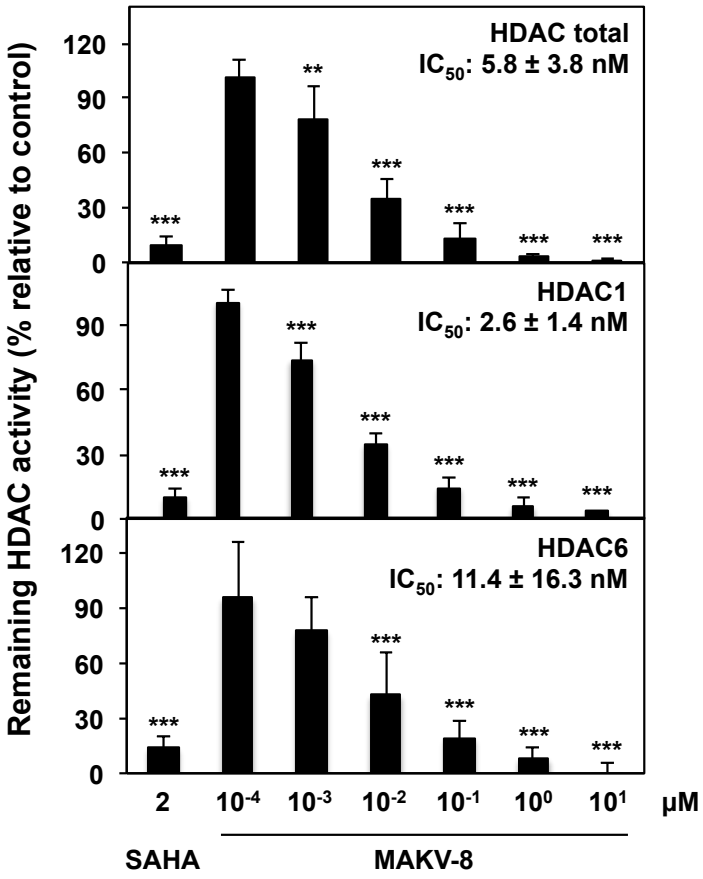

Figure 22: Effect of MAKV-8 on HDAC1, HDAC6 and total HDAC activities.
In vitro HDAC activity assays were performed with increasing concentrations of MAKV-8. Relative activities of total HDAC, HDAC1 and HDAC6 were determined by comparison to the vehicle, and IC_{50} values for each HDAC activities were calculated using nonlinear regression from Prism software. SAHA (2 µM) was used as a reference HDACi. Results correspond to the mean ± SD of at least three independent experiments. IC_{50}: concentration inhibiting 50% of enzymatic activity.

Lipinski's rule of five is an experimental and computational approach to estimate the solubility and permeability in discovery and development settings (Lipinski, 2004). Over the years, those features have been improved with various extensions such as the Ghose filter (Ghose *et al.*, 1999) or the Veber's Rule. (Veber *et al.*, 2002). *In silico* predictions showed that MAKV-8 has low lipophilicity, as characterized by a Log*P* coefficient below 5 and a $logD_{7.4}$ of 2.8, which is a major criterion for orally active drugs. Unlike the other pan-HDACi, the molecular flexibility for membrane permeation, as defined by the number of rotatable bonds, and the drug transport properties predicted by topological polar surface area are not favorable for MAKV-8, which displays values that are nevertheless close to the defined limits and imply free diffusion over the cell membrane. Indeed, this compound expresses a topological polar surface area of 142.79 combined with a molecular weight of 446.5 Da; further 4 and 10 hydrogen bond donors and acceptors, respectively, are recognized. Interestingly, MAKV-8 displays a favorable intestinal absorption parameter and plasma protein-binding potential based on comparison to PXD-101, which has a high plasma protein binding percentage that predicts a limited bioavailability (Table 8). Altogether, MAKV-8 globally displays favorable druglikeness parameters and a low predicted risk of toxicity, similar to FDA-approved pan-HDACi.

Concerning the pharmacokinetics of HDACi, some of them are reportedly metabolized by CYP biotransformation enzymes. In addition, such compounds have the ability to modulate CYP enzymatic activities and/or expression (Lin *et al.*, 2015). Several HDACi have also been found to increase P-glycoprotein expression levels in various cancer cells (Lee *et al.*, 2012). According to *in silico* predictions, MAKV-8 is a weak substrate of CYP3A4 and inhibits CYP2D6, but not CYP2C19, CYP2C9 and CYP3A4. Additionally, MAKV-8 is not predicted to be an inhibitor of P-glycoprotein-mediated drug efflux mechanisms.

Table 8: *In silico* prediction of the MAKV-8 druglikeness and oral bioavailability based on Lipinski's Rule of Five extended with Ghose filter and on Veber's Rule.

Method	Parameter (unit)	Values				
		Theoretical	**MAKV-8**	**SAHA**	**PXD-101**	**LBH-589**
Lipinski's rule of five	Volume ($Å^3$)	NA	411.02	255.64	266.11	330.62
	Log*P*	≤5	3.49	2.47	2.19	3.19
	MW (Da)	≤500	446.5	264.32	318.35	349.43
	n-OHNH	≤5	4	3	3	4
	n-ON	≤10	10	5	6	5
Ghose filter	n-atoms	20≤ x ≤70	32	19	22	26
Veber's Rule	n-rotb	≤10	12	8	5	7
	TPSA ($Å^2$)	≤140	142.79	78.42	95.5	77.14
Absorption	BBBP	0.1≤ MA ≤2	0.12	0.22	0.18	1.16
	IA (%)	≥70	76.68	84.53	89.94	89.23
	PPB (%)	<90	82.82	72.16	94.26	78.3
Toxicity	Rat	NA	Negative	Negative	Negative	Negative

BBBP: blood-brain barrier penetration; IA: intestinal absorption; MA: middle absorption; Log*P*: octanol-water partition coefficient; MW: molecular weight; n-: number of; OHNH: hydrogen bond donors; ON: hydrogen bond acceptors; rotb: rotatable bonds; NA: not applicable; PPB: plasma protein binding; TPSA: topological polar surface area.

In order to gain insight into the modes of interaction between MAKV-8 and human HDACs, we implemented a docking simulation on a panel of HDAC isoforms frequently associated with tumorigenesis. Results indicate that the hydroxamate group and hydrophobic linker region of MAKV-8 can establish efficient interactions in the ligand-binding pocket of all HDAC isoenzymes, whereas the CAP group of MAKV-8 interacts with loops around the ligand-binding pocket (Figure 23). Noteworthy, HDAC4 loop bends outwards allowing an interaction with MAKV-8 *via* a broader interface.

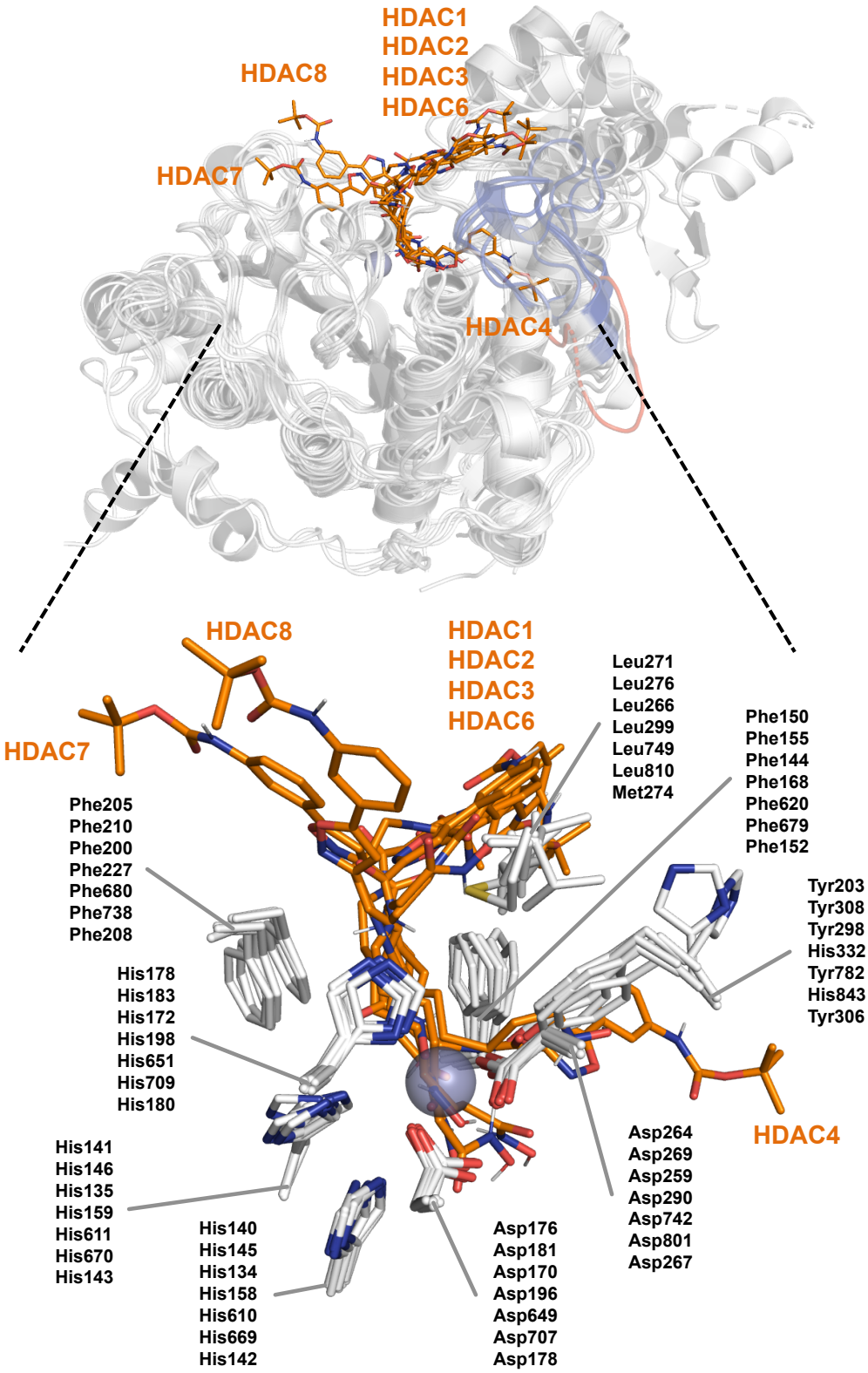

Figure 23: Docking of MAKV-8 into human HDAC isoenzymes.
Docking poses of MAKV-8 molecule, represented as stick model (orange), on the crystal structure of the indicated HDAC isoenzymes that are superposed (white; PDB codes: 4BKX, 4LY1, 4A69, 2VQM, 5EDU, 3C10, and 3EW8 for HDAC1, HDAC2, HDAC3, HDAC4, HDAC6, HDAC7 and HDAC8, respectively). Residues forming hydrophobic effects in the binding sites are shown as stick representation with residue numbering corresponding to HDAC1 to 8 from top to bottom. Zinc atom is shown as a purple sphere; nitrogen and oxygen are colored in blue and red, respectively.

Moreover, comparative molecular analysis demonstrates that MAKV-8 displays lower binding affinity energy values than SAHA for all tested HDACs, with average values of -6.2 and -7.1 kcal/mol, respectively. Interestingly, the two compounds present similar binding affinities for HDAC2, HDAC3 and HDAC8, whereas distinct binding affinities are obtained for HDAC1, HDAC4, HDAC6 and HDAC7 (Table 9). Altogether, our results suggest more potent binding affinities and moderately different pan-HDAC inhibitory profile for MAKV-8 compared to SAHA, which is in line with our *in vitro* results.

Table 9: Comparative molecular docking of MAKV-8 against selected HDACs.

HDAC (PDB code)	MAKV-8	SAHA
HDAC1 (4BKX)	-6.7	-5.4
HDAC2 (4LY1)	-7.2	-6.7
HDAC3 (4A69)	-6.9	-6.5
HDAC4 (2VQM)	-7.7	-5.6
HDAC6 (5EDU)	-7.2	-6.1
HDAC7 (3C10)	-7.1	-6.0
HDAC8 (3EW8)	-7.0	-6.9
Average	**-7.1**	**-6.2**

Binding affinity energy values (kcal/mol) for the indicated Protein Data Bank (PDB) codes were calculated using AutoDock Vina program. SAHA was used as a reference pan-HDACi.

1.2. MAKV-8 significantly induces target protein acetylation

Results from enzymatic assays are not sufficient to evaluate the inhibitory potential of a compound as it could act differently in cells due to their pharmacokinetic properties. To determine whether MAKV-8 also acted as a HDACi *in cellulo*, we next analyzed by western blot the effect of increasing concentrations of compound compared to the reference drug SAHA on the acetylation of histone H4, a nuclear substrate of class I, II and IV HDACs, and α-tubulin, a cytoplasmic substrate of HDAC6. In K-562 cells, MAKV-8 strongly induces the acetylation levels of α-tubulin and histone H4 in a concentration-dependent manner, observed from 5 and 1 µM, respectively, with the maximal acetylation level reached between 15 and 25 µM for both protein targets (Figure 24A). SAHA increases α-tubulin and histone H4 acetylation levels from 0.5 and 0.25 µM, respectively, in a similar manner to that observed with MAKV-8, albeit at lower concentrations. Nevertheless, the EC_{50} values determined for MAKV-8 and SAHA against acetyl α-tubulin and acetyl histone H4 suggest distinct HDAC

inhibitory profiles (Figure 24A). Indeed, MAKV-8 displays increased selectivity against nuclear HDACs targeting histone H4 compared to HDAC6 (EC_{50} values of 5.9 and 12.1 µM, respectively), whereas SAHA acts similarly on both targets (EC_{50} values of 2.6 and 1.9 µM, respectively). Notably, concentrations of compounds near the EC_{50} values have been used for subsequent experiments. In KBM-5 and MEG-01 cells, MAKV-8 exposure also enhances α-tubulin and histone H4 acetylation detected from a concentration of 1 and 5 µM, respectively (Figure 24B).

Additionally, kinetic analysis of the acetylation status of α-tubulin and H4 shows a rapid and time-dependent increase in histone H4 and α-tubulin acetylation noted from 2 hours following MAKV-8 treatment, with the peak occurring between 8 and 24 hours. With SAHA, similar effects are observed with acetyl α-tubulin, but the acetylation of histone H4 is maintained at a later time (Figure 24C).

In conclusion, MAKV-8 acts as a more potent HDACi than SAHA *in vitro*, which is in agreement with docking poses within the ligand-binding pocket of all HDAC isoenzymes associated with stronger binding affinities. Additionally, MAKV-8 inhibits multiple HDAC activities *in cellulo*, seemingly with a distinct HDAC inhibitory profile compared to SAHA.

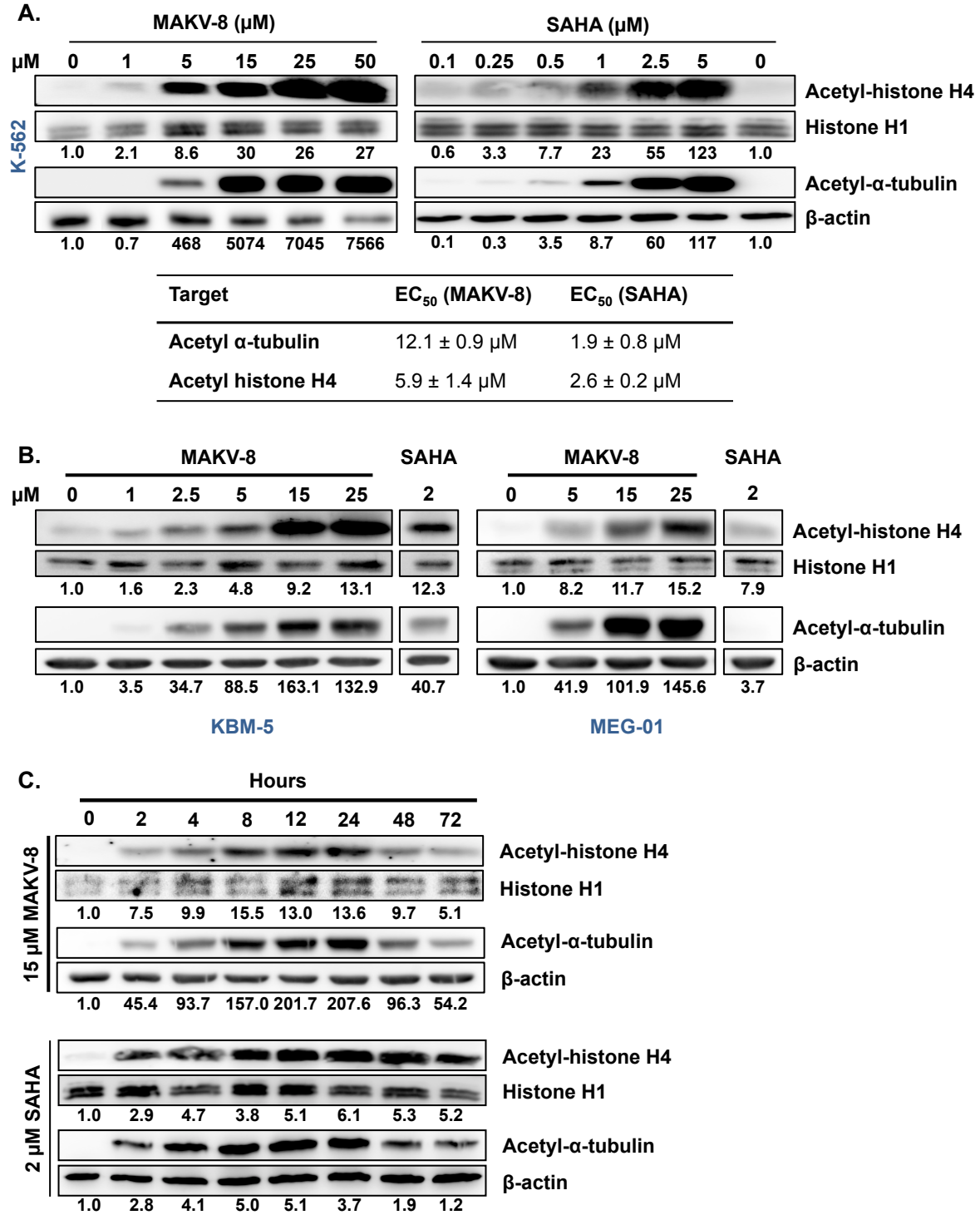

Target	EC_{50} (MAKV-8)	EC_{50} (SAHA)
Acetyl α-tubulin	12.1 ± 0.9 μM	1.9 ± 0.8 μM
Acetyl histone H4	5.9 ± 1.4 μM	2.6 ± 0.2 μM

Figure 24: Effect of MAKV-8 on the acetylation of histone H4 and α-tubulin in CML cells.
(A) K-562, (B) KBM5 and MEG-01 cells were treated with increasing concentrations of MAKV-8 for 24 hours. (C) K-562 cells were treated with 15 μM MAKV-8 for the indicated period of times. Acetylation of histone H4 and α-tubulin was assessed by western blot, with β-actin and histone H1 as loading controls for α-tubulin and histone H4, respectively. SAHA was used as a reference HDACi. Quantification values are indicated underneath corresponding blots that are representative of three independent experiments. EC_{50} values (*i.e.* 50% of the maximum effect) were determined using prism software and represent the mean ± SD of three independent experiments.

1.3. The potent pan-HDACi MAKV-8 displays cytotoxic properties in CML cells

We further evaluated whether MAKV-8 treatments exert anticancer properties against CML cells. CML cell lines were incubated with increasing concentrations of MAKV-8, and their proliferation and viability were assessed after up to 72 hours of treatment using a Trypan blue assay. In K-562 cells, the inhibition of proliferation is triggered beginning at 3.33 µM MAKV-8 after 48 hours of treatment whereas an increase of cell death is detected only after 72 hours of treatment starting at 10 µM MAKV-8. After 48 and 72 hours of treatment with 33.3 µM MAKV-8, cell viability is reduced of 30 and 70%, respectively. Similarly, in KBM-5 and MEG-01 cell lines, decreased proliferation is noted after 48 hours of treatment with MAKV-8 starting from a concentration of 3.33 µM, whereas cell death is induced at 10 µM MAKV-8. After 72 hours of treatment with 10 µM MAKV-8, cell viability is reduced of 70 and 30% in KBM-5 and MEG-01 cells, respectively (Figure 25).

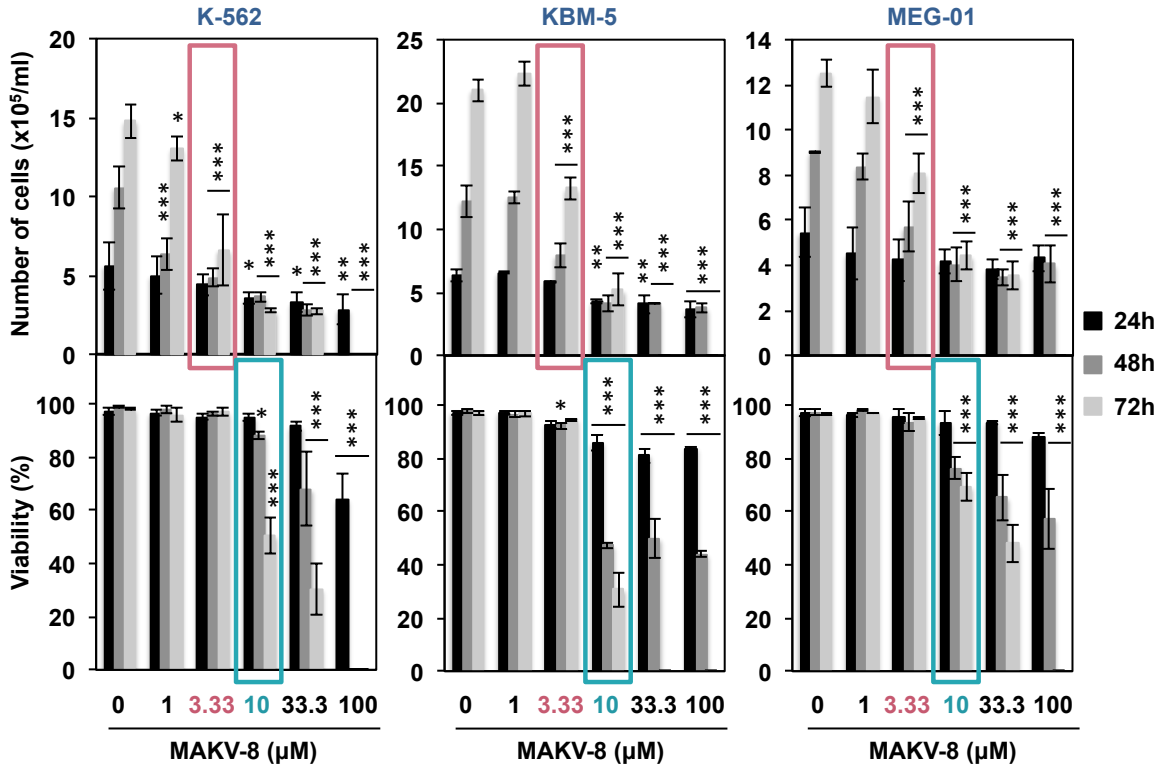

Figure 25: Effect of MAKV-8 on CML cell proliferation and viability.
CML cells were treated with increasing concentrations of MAKV-8 for up to 72 hours, and cell proliferation and viability were assessed based on the Trypan Blue exclusion method. Results correspond to the mean ± SD of three independent experiments and were analyzed by a two-way ANOVA with *, **, *** indicating $p < 0.05$, $p < 0.01$, $p < 0.001$, respectively. Pink and blue rectangles highlight the concentrations of MAKV-8 from which a decrease of proliferation and an induction of cell death are detected, respectively.

To evaluate the potential of MAKV-8 to impair the replicative ability of cancer cells in a 3D model, CML colony formation assays were performed in a semi-solid medium in the presence of increasing concentrations of compound. Results demonstrate that the colony forming capacity of cells is strongly reduced by MAKV-8 exposure detected from 5 µM in K-562 and MEG-01 cells, and 10 µM in KBM-5 cells (Figure 26).

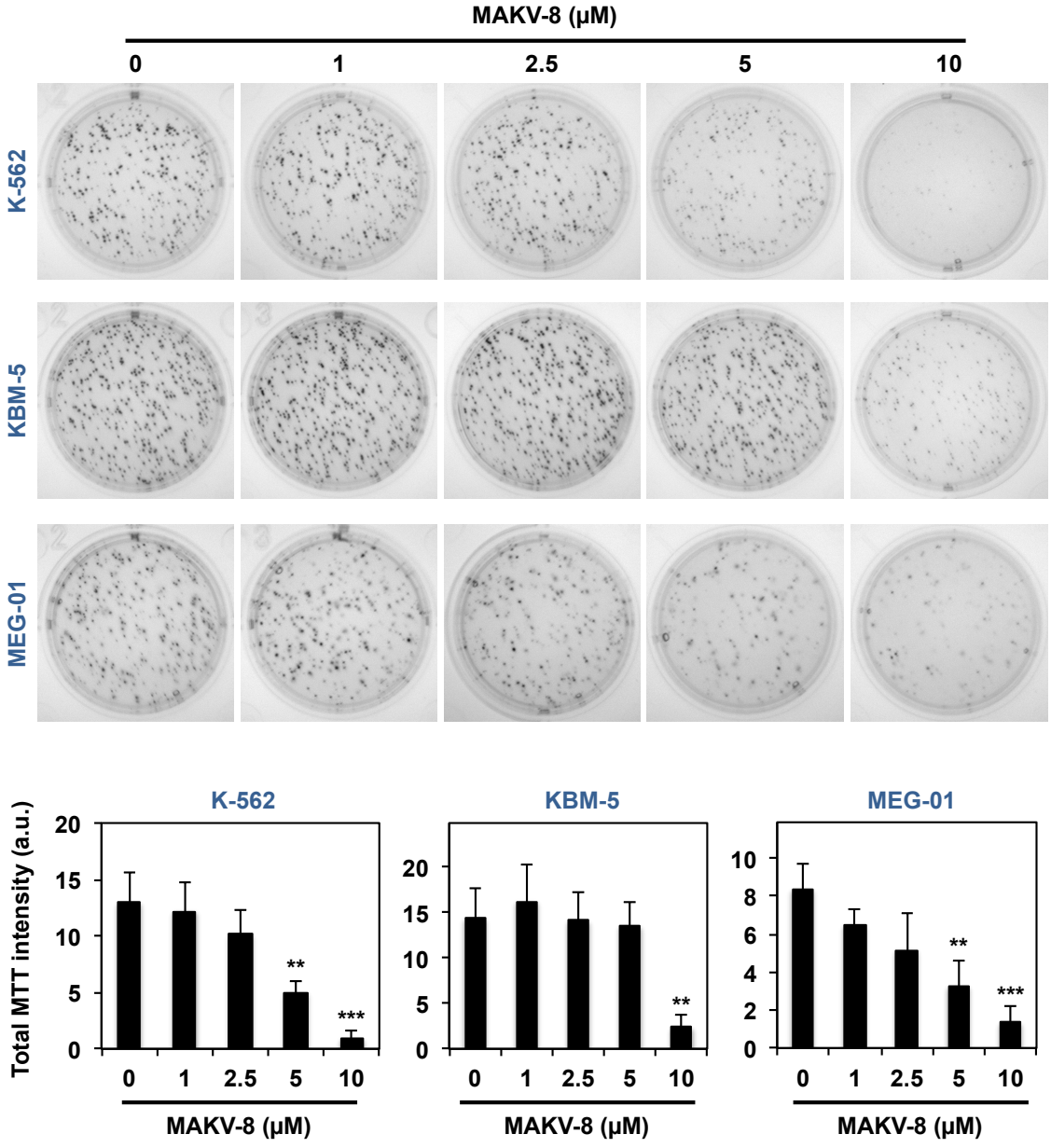

Figure 26: Effect of MAKV-8 on CML colony formation capacity.
CML cells were grown in the presence of increasing concentrations of MAKV-8 for 10 days and colonies were then detected after addition of MTT. Representative pictures (upper panel) and quantifications corresponding to the mean of total MTT intensity ± SD (lower panel) from three independent experiments are provided. Results were analyzed by a one-way ANOVA with **, *** indicating $p < 0.01$, $p < 0.001$, respectively.

In conclusion, MAKV-8 inhibits CML cell replicative and survival abilities.

1.4. MAKV-8 derivatives are less potent molecules than their parent compound

In order to gain insight into the relationship between the structure of MAKV-8 and its deacetylase inhibiting activities, we tested the HDAC inhibitory potential against total HDAC or HDAC6 activities of four derivatives: MAKV-6 and -7 lack the linker part, whereas the hydroxamate group of MAKV-10 and -12 is substituted with a methylester group. *In vitro*, MAKV-6 and MAKV-7 inhibit total HDAC and HDAC6 activities, with IC_{50} values ranging in the low µM, demonstrating a lower potency than MAKV-8. Such compounds have an IC_{50} inhibitory activity against total HDAC of 1.05 and 22 µM, respectively, and HDAC6 of 1.94 and 3.14 µM, respectively. In contrast, MAKV-10 and MAKV-12 fail to inhibit HDAC activities with concentrations up to 100 µM (Figure 27A).

Accordingly, docking analyses of MAKV-8 derivatives highlights moderate binding to HDAC6, but with lower affinity than MAKV-8. Compounds MAKV-6 and -7 cannot bind properly in the HDAC6 ligand-binding pocket, whereas the pose of MAKV-10 and -12 in the ligand-binding pocket do not allow suitable interaction with the zinc atom. The docking results are therefore in line with the *in vitro* results (Figure 27B, Table 10).

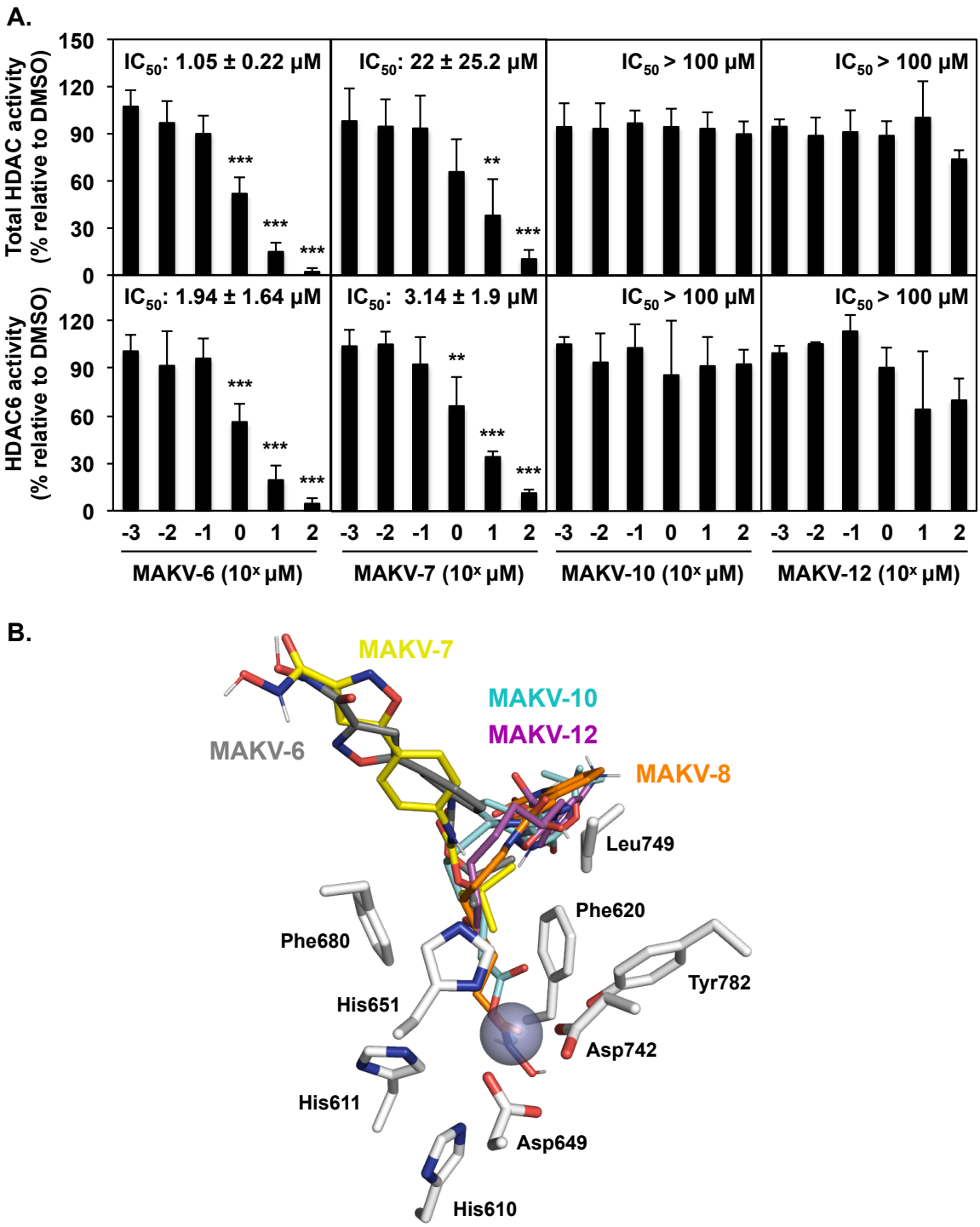

Figure 27: Effect of MAKV-8 derived compounds on HDAC6 and total HDAC activities.
(A) *In vitro* HDAC activity assays were performed with increasing concentrations of MAKV-8 derived compounds. Relative activities of total HDAC and HDAC6 were determined by comparison to the vehicle, and IC_{50} values for each HDAC activities were calculated using nonlinear regression from Prism software. Results correspond to the mean ± SD of at least three independent experiments. IC_{50}: concentration inhibiting 50% of enzymatic activity. (B) Docking poses of MAKV-8 derivatives, superposed and represented as stick model, on the crystal structure of HDAC6 (white; PDB code: 5EDU). Residues forming hydrophobic effects in the binding sites are shown as stick representation with residue numbering. Zinc atom is shown as a purple sphere; nitrogen and oxygen are colored in blue and red, respectively.

Table 10: Comparative molecular docking of MAKV-8 derivatives against HDAC6.

Compounds	Binding affinity (kcal/mol)
MAKV-6	-5.9
MAKV-7	-6.4
MAKV-8	-7.2
MAKV-10	-6.9
MAKV-12	-6.1

Binding affinity energy values for Protein Data Bank (PDB) code 5EDU were calculated using AutoDock Vina program.

We also tested whether MAKV-8-derived compounds have the ability to modulate protein acetylation. K-562 cells were treated with increasing concentrations of MAKV-6, -7, -10 and -12 compounds for 24 hours and α-tubulin and histone H4 acetylation levels were evaluated by western blots. Results show that MAKV-6 and 7 increase only histone H4 acetylation at higher concentrations compared to MAKV-8, detected from 15 μM and 25 μM, respectively, but fail to increase α-tubulin acetylation, suggesting a preferential inhibition of HDACs targeting histones but with a much lower potency than MAKV-8. Compounds MAKV-10 and -12 do not augment α-tubulin and histone H4 acetylation levels even at the highest concentrations tested, confirming *in vitro* results (Figure 28).

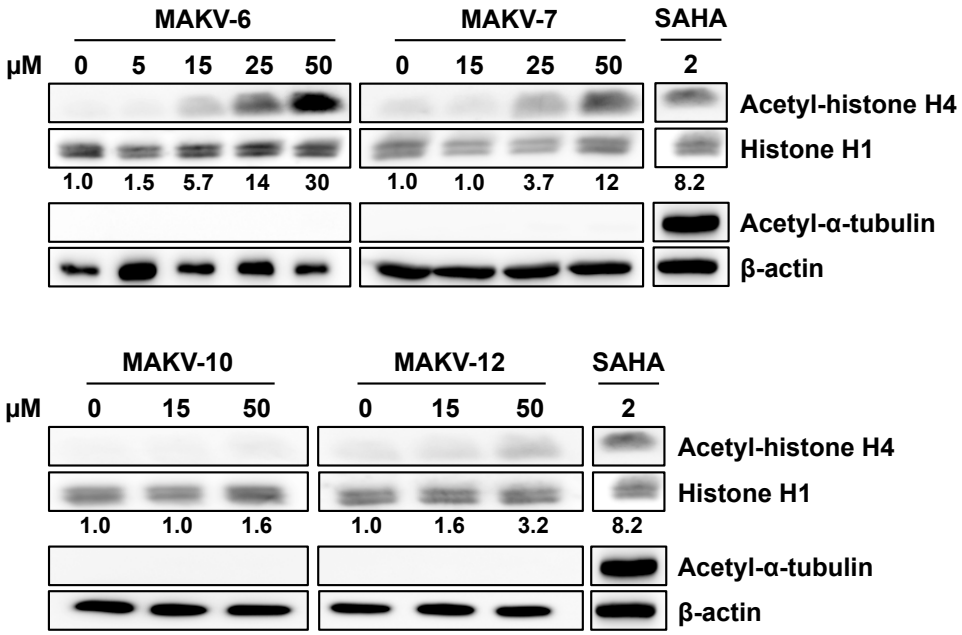

Figure 28: Effect of MAKV-8 derived compounds on the acetylation of histone H4 and α-tubulin in K-562 cells.

K-562 cells were treated with increasing concentrations of the indicated MAKV-8 derived compounds for 24 hours and acetylation levels of histone H4 and α-tubulin were assessed by western blot, with β-actin and histone H1 as loading controls for α-tubulin and histone H4, respectively. SAHA was used as a reference HDACi. Quantification values are indicated underneath corresponding blots that are representative of three independent experiments.

Finally, we measured the proliferation and viability of K-562 cells treated with increasing concentrations of MAKV-8 derived compounds for up to 72 hours. After 48 hours of treatment, we detect a diminution in K-562 cell proliferation starting at 5 μM MAKV-6 or 10 μM MAKV-7, and a reduction in cell viability of 45 and 25% starting at 25 μM MAKV-6 and MAKV-7, respectively. In contrast, neither MAKV-10 nor MAKV-12 has any impact on cell proliferation and viability (Figure 29), suggesting that the anticancer effects of MAKV-8 are associated with the inhibition of HDAC activities.

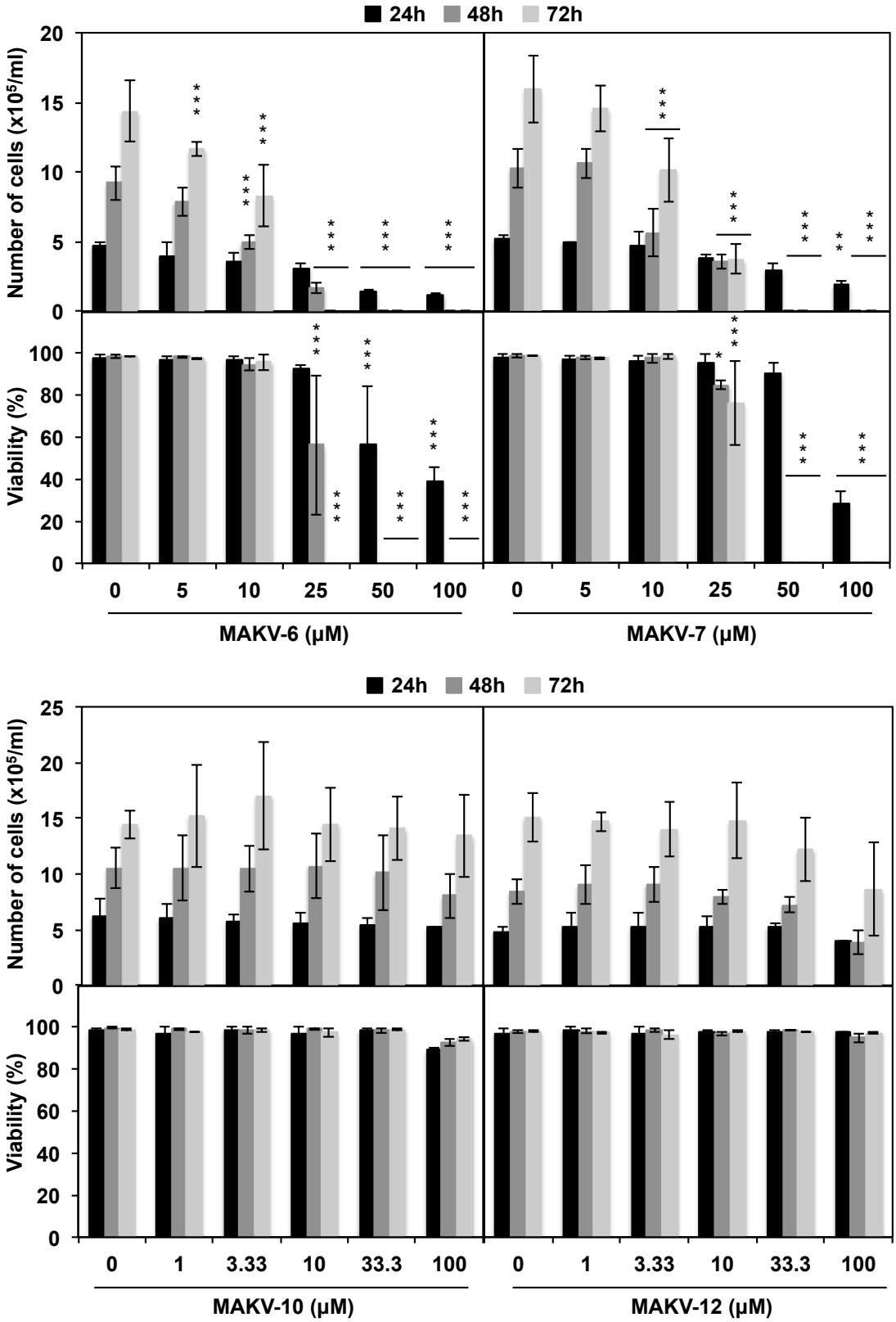

Figure 29: Effect of MAKV-8 derived compounds on cell proliferation and viability.
K-562 cells were treated with increasing concentrations of the indicated MAKV-8 derived compounds for 24, 48 and 72 hours, and cell proliferation and viability were assessed based on the Trypan Blue exclusion method. Results correspond to the mean ± SD of three independent experiments and were analyzed by a two-way ANOVA with **, *** indicating $p < 0.01$, $p < 0.001$, respectively.

In conclusion, MAKV-8 derived molecules are less effective against HDAC activity *in vitro* and less active against cancer cells.

Characterization of MAKV-8 derived molecules, lacking the linker (MAKV-6 and -7) or the hydroxamate group (MAKV-10 and -12), was stopped because they present a lower potency as HDACi. Therefore, the hydroxamate group, as well as the length of the linker, can be considered as valuable lead structures in the pursuit of novel potent HDACi *in vitro* and *in cellulo*.

1.5. MAKV-8 induces cell cycle arrest and apoptotic cell death in CML cells

Many pan-HDACi have the ability to modulate and stop cell cycle, leading to an accumulation of cells in one of the three G_0/G_1, S, or G_2 phases. Generally, cancerous cells accumulate in the G_0/G_1 phase upon treatment with a pan-HDACi. Since treatment of cells with MAKV-8 hampers CML cell proliferation, the effect of compound on K-562 cell cycle distribution was studied by flow cytometry after 24 and 48 hours of treatment. In order to focus only on aspects of cell cycle modulation, we used MAKV-8 concentrations for which we observed growth inhibition without cell death induction. Results presented in Figure 30 demonstrate that K-562 cell repartition in the three phases of cell cycle is time and concentration-dependent. A progressive increase in the cell population is observed in the G_1 phase at 1 and 5 µM at both 24 and 48 hours, while at 10 µM, the decrease in the cell population in S phase at 24 hours is followed by an accumulation in G_1 after 48 hours. Overall, accumulation of cells in G_1 phase reaches its maximum at 48 hours, following a treatment with 5 µM MAKV-8. Treatments with 5 or 10 µM MAKV-8 also induce a decrease in cell accumulation in S phase up to 9% whatever the time compared to 30-35% in untreated cells (Figure 30). By comparison, treatment of cells with 2 µM SAHA induces a progressive accumulation in G_1 phase, as reported in literature (Nimmanapalli *et al.*, 2003).

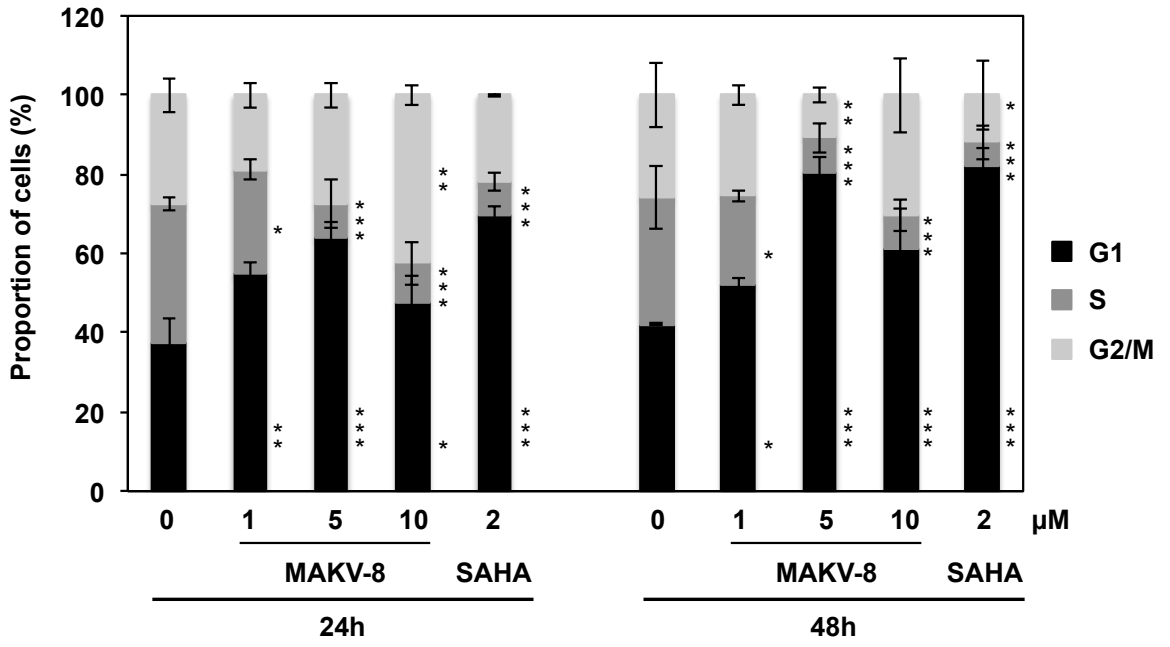

Figure 30: Effect of MAKV-8 on K-562 cell cycle.
K-562 cells were treated with 1, 5 and 10 µM of MAKV-8 for 24 and 48 hours. Distribution of cells in the three phases of cell cycle was obtained after their staining with propidium iodide and analysis by flow cytometry. SAHA was used as a reference HDACi. Results correspond to the mean ± SD of three independent experiments and were analyzed by a two-way ANOVA with *, **, *** indicating $p < 0.05$, $p < 0.01$, $p < 0.001$, respectively.

Since treatment of cells with 10 µM MAKV-8 induces a decrease in cell viability detected at 48 hours, we next evaluated the type of cell death occurring upon MAKV-8 treatment. K-562 cells treated with MAKV-8 for two periods of time were stained with Hoechst-PI, and the type of cell death induced was first characterized by analysis of nuclear morphology under a UV-microscope. Cell counting shows a time and concentration-dependent increase in apoptotic cells accompanied by a moderate increase in PI-positive cells (<15%). Accordingly, when cells are concomitantly incubated with 50 µM of the pan-caspase inhibitor Z-VAD-FMK and 25 µM MAKV-8 for 48 hours, the induction of apoptosis is almost completely prevented, going from 50 to 2% (Figure 31). K-562 cells treated with 50 µM cisplatin for 24 hours are used as a positive control of apoptosis induction.

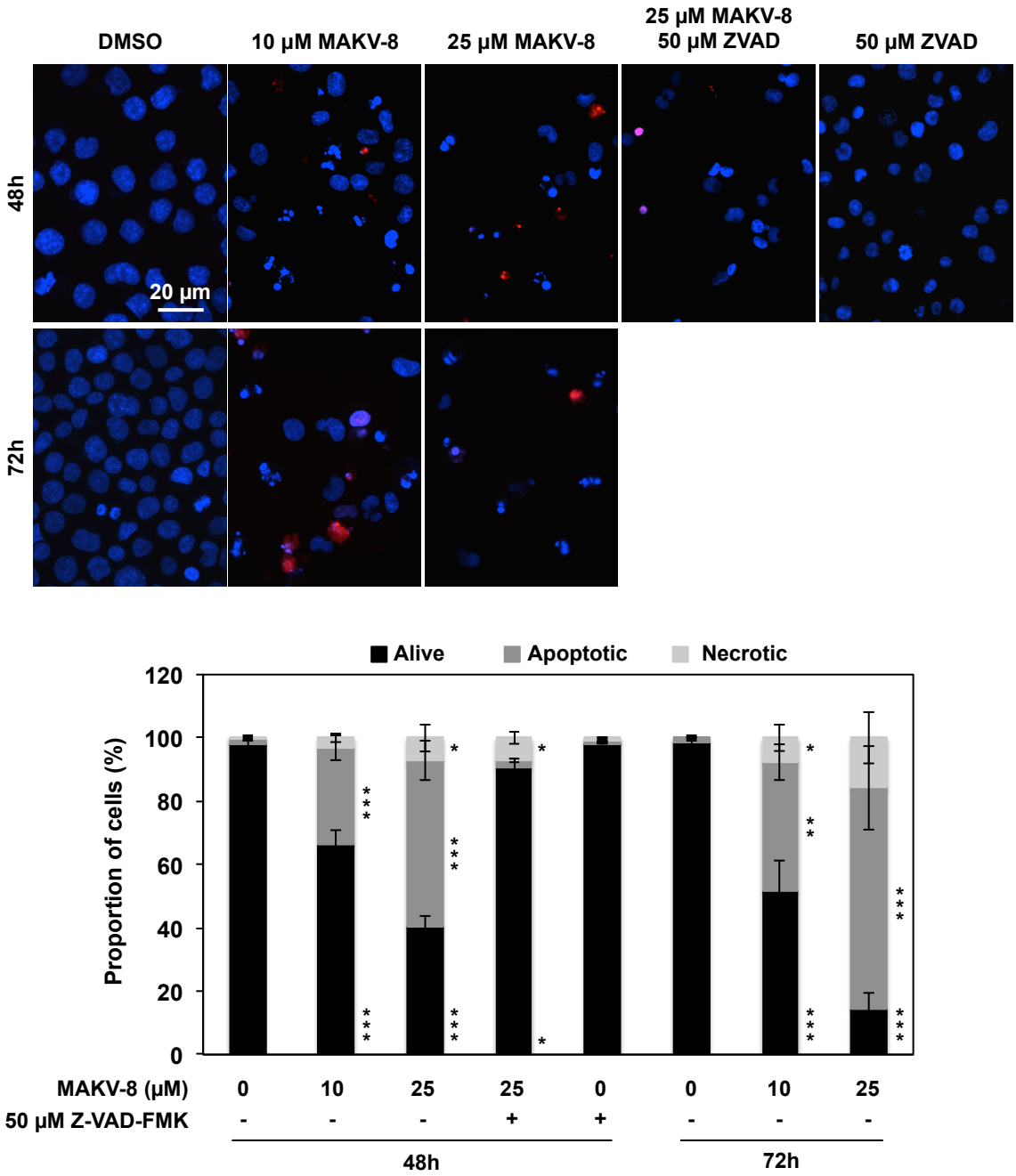

Figure 31: Effect of MAKV-8 on K-562 cell death.
K-562 cells were treated with 10 and 25 µM of MAKV-8 for 48 and 72 hours. Where indicated, cells were pre-incubated for 1 hour with the caspase inhibitor Z-VAD-FMK. The study of nuclear morphology was performed by fluorescence microscopy after Hoechst-propidium iodide staining. Representative pictures (upper panel) and quantification corresponding to the mean ± SD (lower panel) from three independent experiments are provided. Results were analyzed by a two-way ANOVA with *, **, *** indicating $p < 0.05$, $p < 0.01$, $p < 0.001$, respectively.

To characterize the apoptotic pathway leading to cell death after the treatment of K-562 cells with high concentrations of MAKV-8, we first assessed by western blotting the effects of two MAKV-8 concentrations on the cleavage of caspases 3, 7, 8, 9 and PARP-1 after 24

and 48 hours. Notably, PARP-1 is a target of caspase 3, which inactivates it by cleavage. Treatment with 5 µM MAKV-8 induces the cleavage of caspase 9 after 24 hours, and more importantly after 48 hours. The resulting cleavages of caspases 3 and 7, as well as that of PARP-1, display the same time pattern. After treatment with 10 µM MAKV-8, caspase 8 is cleaved at 24 hours in addition to the cleavage of caspases 3, 7, 9 and PARP-1. At this concentration, cleavage of all proteins is also more important after 48 hours of treatment (Figure 32). Overall, results correspond to the induction of caspase-dependent apoptosis. In cells treated with 50 µM cisplatin for 24 hours, we observe a cleavage of caspases 3, 8, 9, and PARP-1, which is in correlation with apoptosis induction (Dasari *et al.*, 2014).

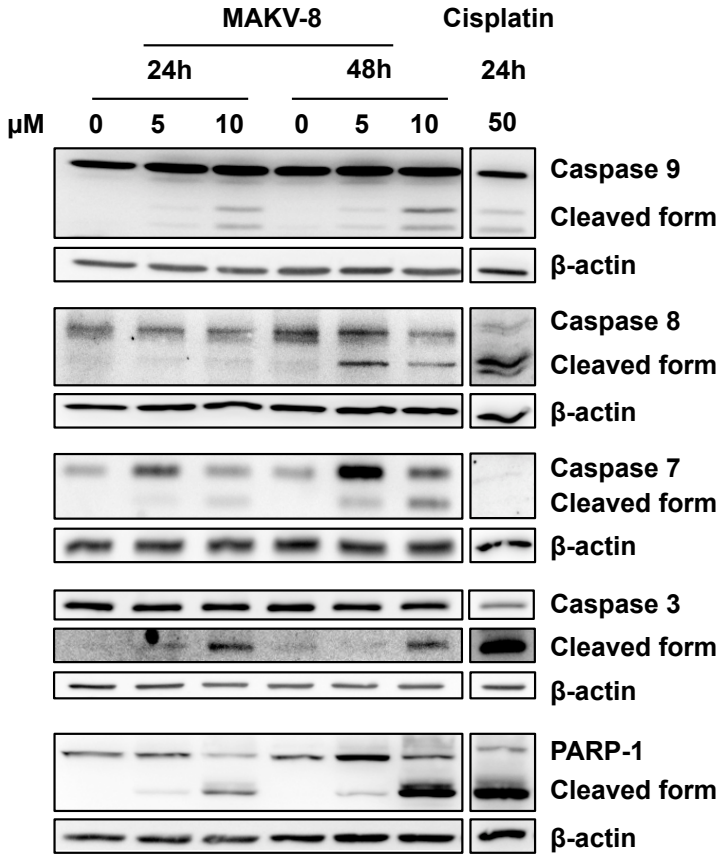

Figure 32: Effect of MAKV-8 on caspase and PARP-1 cleavage in K-562 cells.
K-562 cells were treated with 5 and 10 µM of MAKV-8 for the indicated period of time, and the cleavage of caspases 3, 7, 8 and 9, as well as PARP-1, was analyzed by western blot, with β-actin as a loading control. Cisplatin was used as the positive control for caspase and PARP-1 cleavage. Blots are representative of three independent experiments.

In conclusion, K-562 cells treated with low concentrations of MAKV-8 accumulate in the G_1 phase of cell cycle and die by caspase-dependent apoptosis.

1.6. MAKV-8 triggers ER stress, stimulates autophagic flux and, provokes DNA damage

Depending on their HDAC inhibitory profiles, pan-HDACi can elicit a broad range of biological responses that impede the growth and/or survival of tumor cells (Schnekenburger *et al.*, 2016).

1.6.1. Evaluation of ER stress induction

Inhibited cell cycle progression could be due to the activation of ER stress-induced UPR to prevent exacerbated misfolded protein-mediated toxicity (Y. Liu *et al.*, 2012). To evaluate whether MAKV-8 induces ER-stress, K-562 cells were treated with the compound for increasing periods of time, and the expression levels of an ER stress marker, the chaperone GRP78, was assessed by western blot by comparison to the canonical ER stress inducer thapsigargin. Results reveal that GRP78 protein expression is up-regulated after 8 hours of treatment, which is maintained over time independent of the concentration. Furthermore, increased phosphorylation levels in PERK and eIF2α are detected from 24 and 8 hours after treatment with 5 and 10 µM MAKV-8, respectively (Figure 33A). Accordingly, treatment of K-562 cells with 10 µM MAKV-8 results in a 1.75-fold increase in DDIT3 mRNA expression after 24 hours (Figure 33B). In addition, XBP1 mRNA splicing, detected after migration of PCR products in a polyacrylamide gel, is observed from 4 hours of treatment with 10 µM MAKV-8 (Figure 33C). Altogether, our results demonstrate that MAKV-8 triggers the activation of UPR signaling.

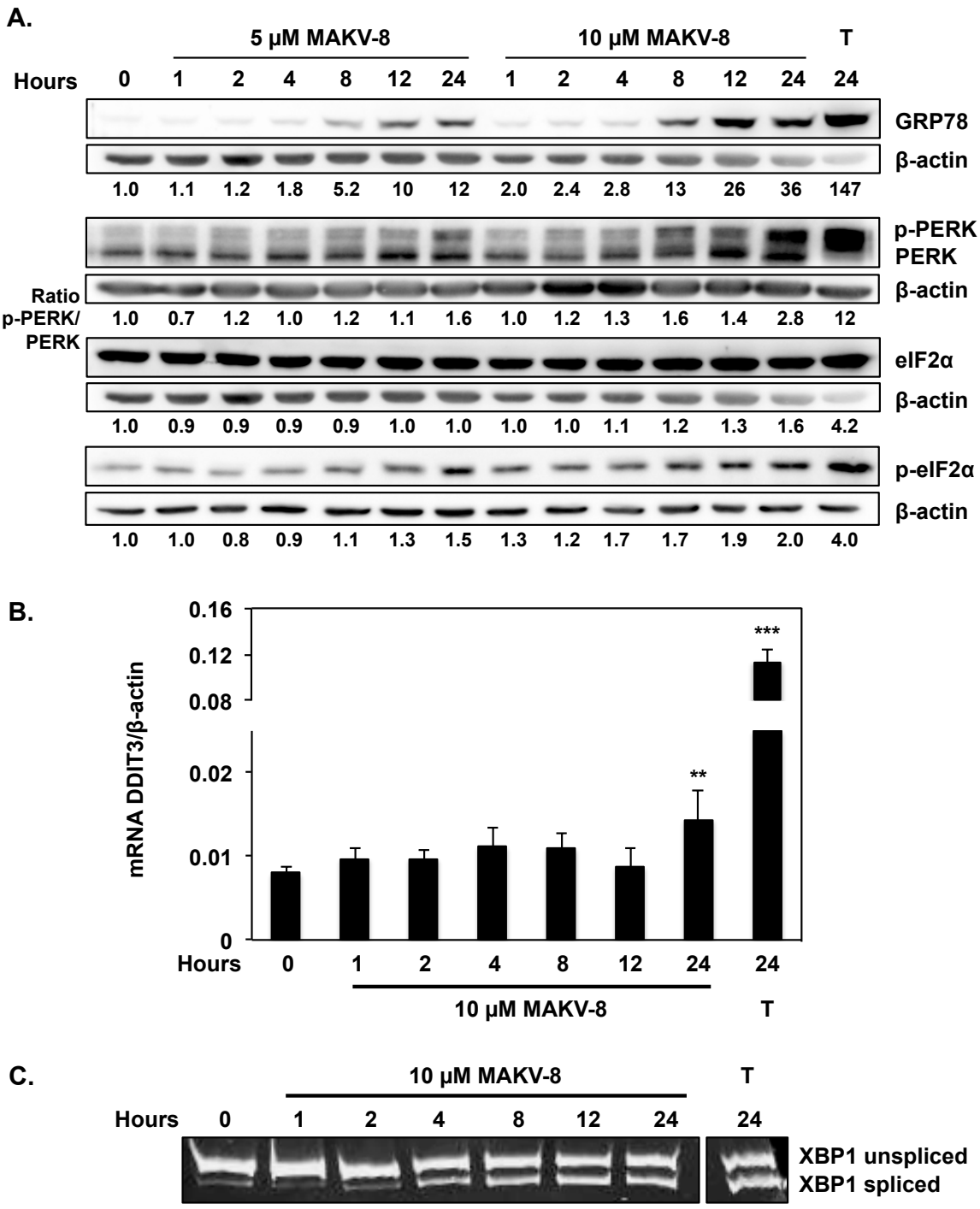

Figure 33: Effect of MAKV-8 on ER stress induction in K-562 cells.

K-562 cells were treated with 5 and 10 µM of MAKV-8 for the indicated time points. (A) The expression level of UPR-associated proteins was assessed by western blot, with β-actin as a loading control. Quantification values are indicated underneath corresponding blots. (B) DDIT3 mRNA expression levels was quantified by real-time PCR and normalized to the housekeeping gene β-actin. (C) The cleavage of XBP1 mRNA was detected under a UV light on acrylamide gels stained with ethidium bromide. Blots and gels are representative of three independent experiments. Results correspond to the mean ± SD of three independent experiments and were analyzed by a one-way ANOVA with **, *** indicating $p < 0.01$, $p < 0.001$, respectively. Thapsigargin (T, 4 µM) was used as a positive control for ER stress induction.

1.6.2. Evaluation of autophagy induction

UPR pathways are able to activate the autophagic machinery to clear the ER from accumulated protein aggregates (Song *et al.*, 2018), and accumulating evidence show that autophagy modulation contributes to the anticancer effect exhibited by HDACi (Gammoh *et al.*, 2012). We thus aimed to determine whether MAKV-8 modulated the autophagic pathway. In order to further analyze cell morphology, K-562 cells treated with 5 and 10 µM MAKV8 for 48 hours were stained with modified GIEMSA. The nucleus of control cells is surrounded by a thin cytoplasm whereas MAKV-8-treated cells undergo size increase due to a swollen cytoplasm enriched with numerous vacuoles of various sizes (Figure 34A). In addition, K-562 cells treated with 10 µM MAKV-8 for 8 hours and stained with Cyto-ID® were observed under a fluorescent microscope to visualize and quantify vacuoles associated with the autophagic pathway. In MAKV-8 treated cells, the dotted fluorescent pattern indicates the presence of autophagic vesicles compared to control cells, which display a homogeneous signal. The percentage of cells displaying autophagic vesicles is three times higher in MAKV-8-treated cells than in control cells (Figure 34B). These results prompted us to detect by western blot the presence of two markers of the autophagic process, *i.e.* the appearance of the converted LC3-II form and reduced SQSTM1 abundance. Treatment of K-562 cells with 10 µM MAKV-8 for 8 hours stimulates the conversion of LC3-I to LC3-II and down-regulates SQSTM1 expression. Concomitant addition of the late-phase autophagy inhibitor, bafilomycin A1, to MAKV-8 treatment further enhances LC3-II and SQSTM1 accumulation, and strongly decreases the percentage of living cells, suggesting that MAKV-8 induces protective autophagy (Figure 34C). Accordingly, the study of cellular structures by TEM reveals a more extensive autophagocytic vacuolization in MAKV-8-treated cells in comparison with control cells (Figure 34D).

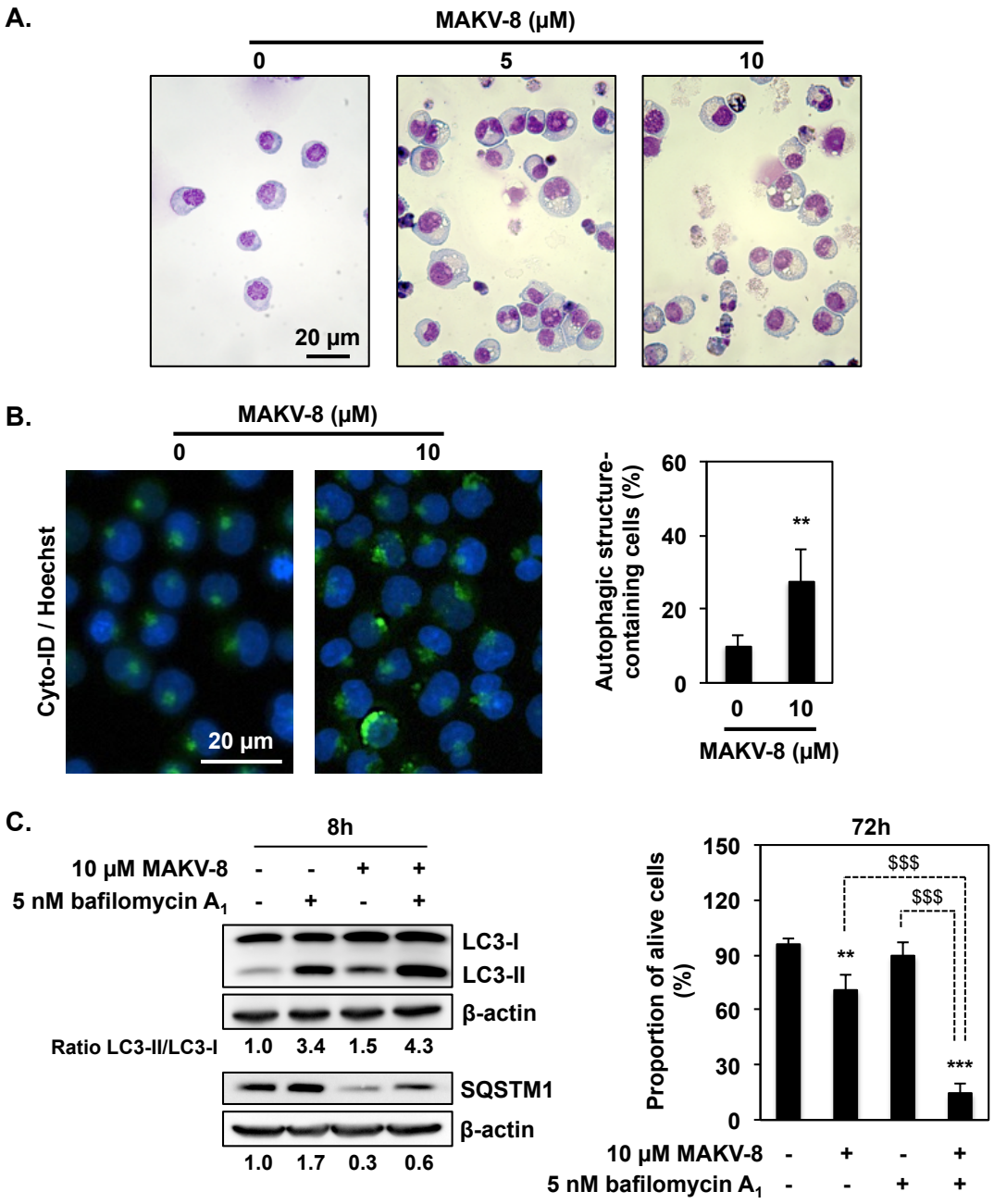

Figure 34: Effect of MAKV-8 on autophagy induction in K-562 cells.

(A) K-562 cells were treated with 5 and 10 µM of MAKV-8 for 48 hours, and cell morphology was analyzed after a modified GIEMSA staining. Pictures were acquired by bright-field microscopy. (B) K-562 cells treated with 10 µM MAKV-8 for 8 hours were stained with Cyto-ID® Green dye. Appearance of autophagosome-related vesicles was quantified by counting (right panel) after visualization by fluorescence microscopy (left panel). (C) K-562 cells were treated with 10 µM MAKV-8 for indicated periods of time with or without addition of 5 nM bafilomycin A_1. LC3-I to LC3-II conversion and SQSTM1 expression were analyzed by western blot, with β-actin as a loading control; quantification values are indicated underneath corresponding blots. The study of nuclear morphology was performed by fluorescence microscopy after Hoechst-PI staining. (B-C) Results correspond to the mean ± SD of three independent experiments and were analyzed by a one-way ANOVA with **, *** indicating $p < 0.01$, $p < 0.001$, respectively. (D) CML cells were treated with MAKV-8 for indicated periods of time and studied by TEM: (1) phagophores, (2) autophagolysosomes. Pictures and blots are representative of three independent experiments.

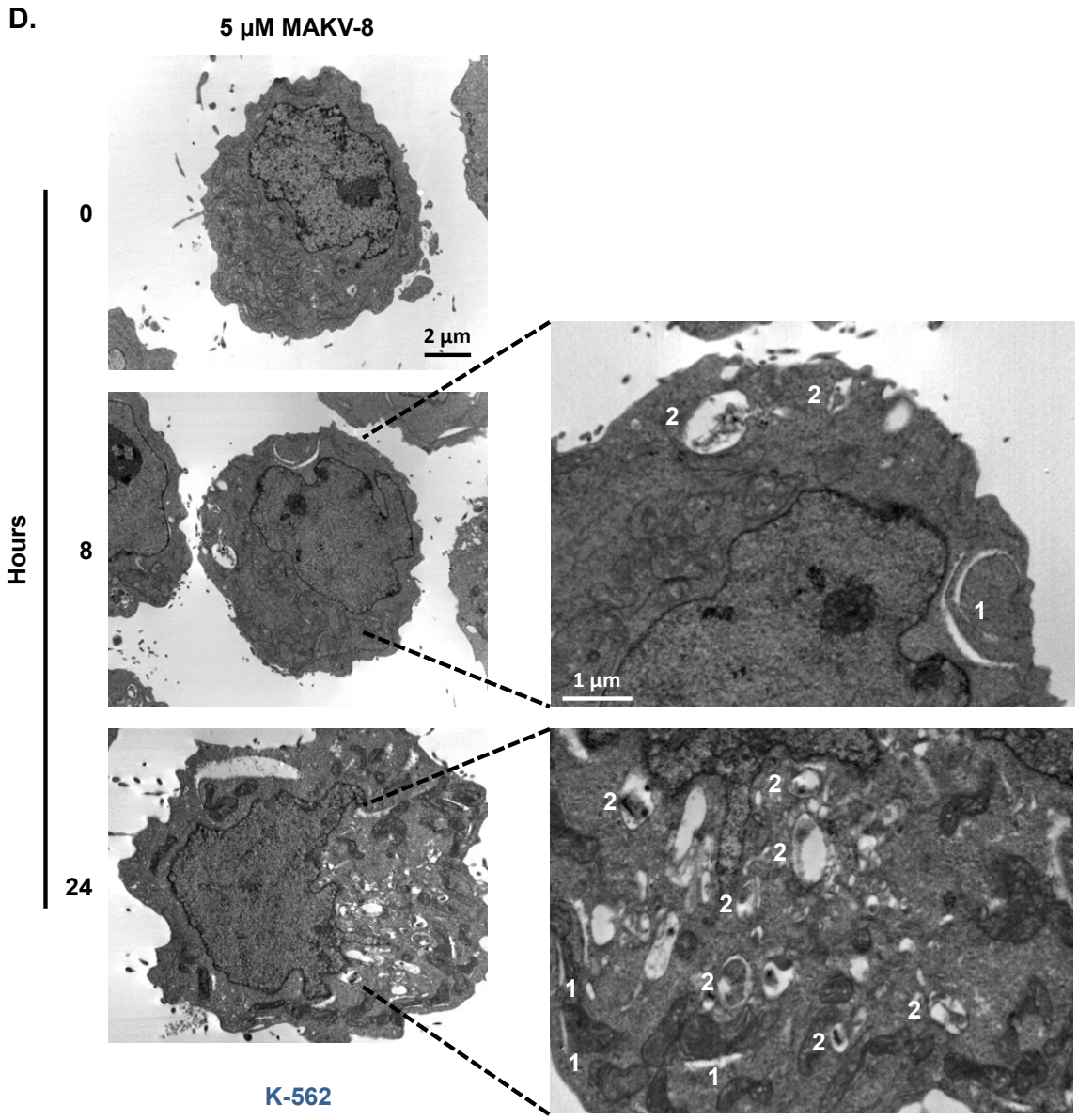

Figure 34 (Continued)

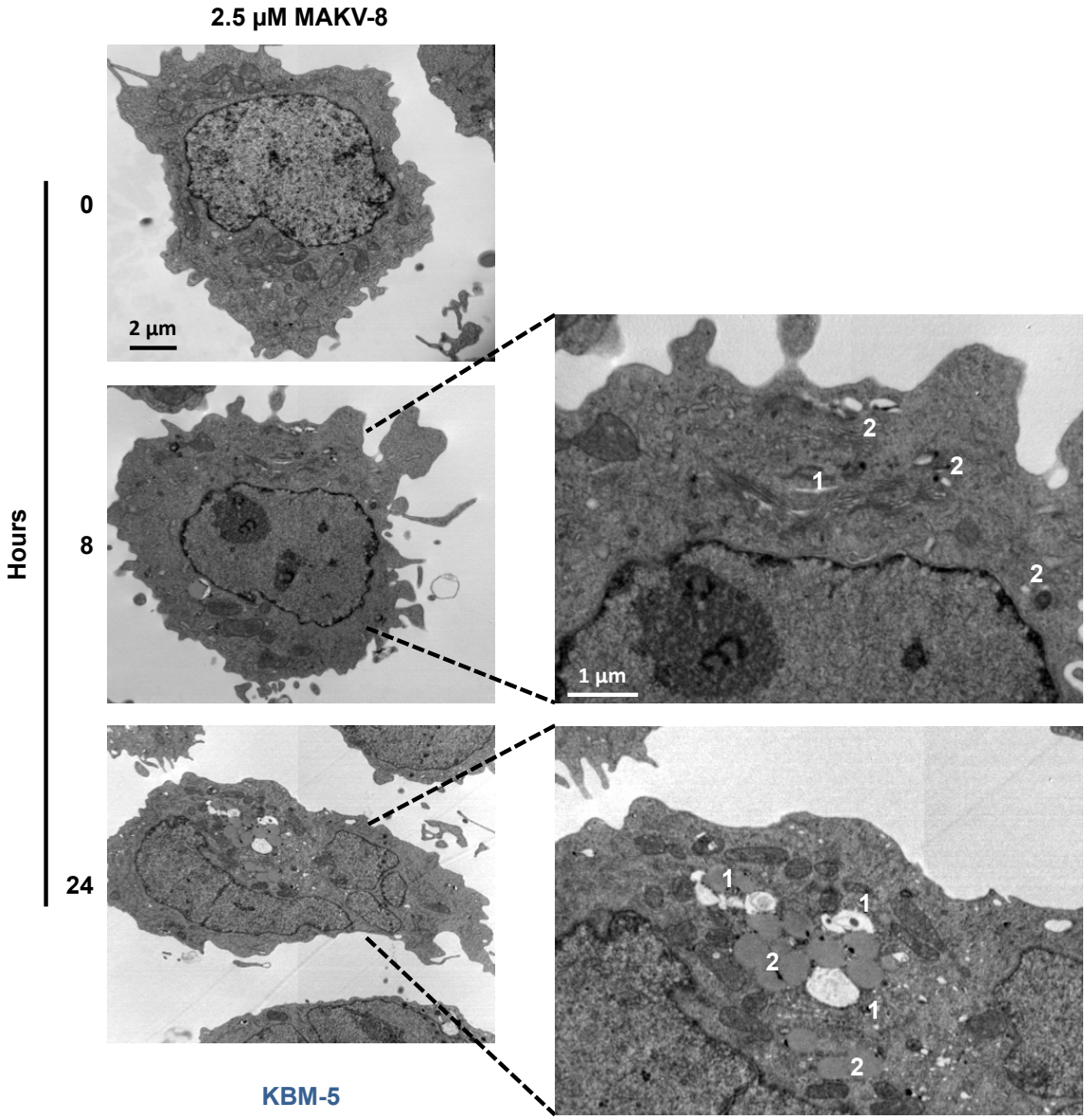

Figure 34 (Continued)

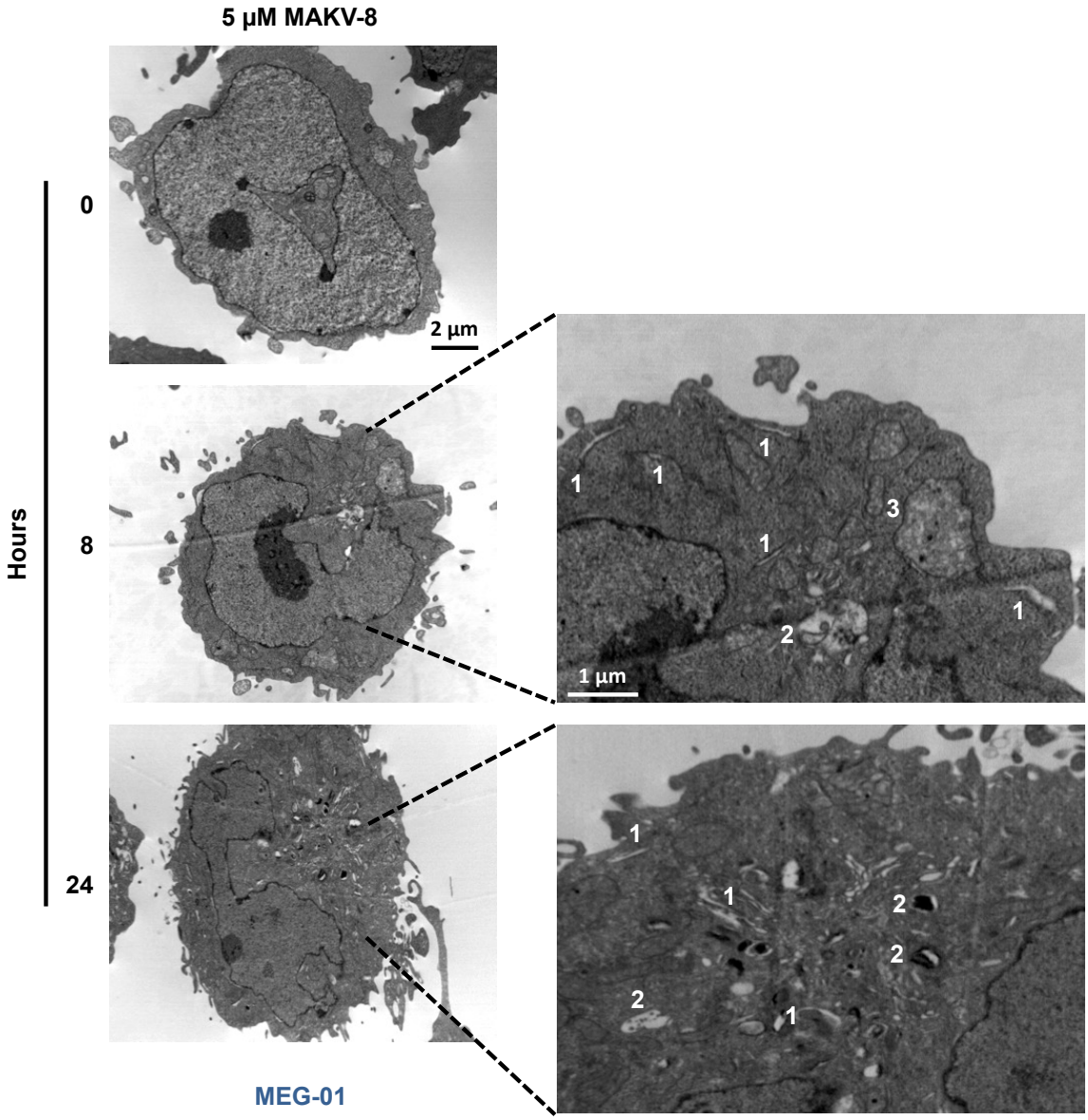

Figure 34 (Continued)

1.6.3. Evaluation of the induction of double strand breaks

HDACi treatments reportedly cause DNA damage, including DSBs, which partly underlies the induction of apoptosis (Petruccelli *et al.*, 2011). DSBs in chromatin initiate the phosphorylation of the histone H2A variant, H2AX, at serine 139 to generate γH2AX (Kinner *et al.*, 2008). To determine whether treatment with MAKV-8 leads to an induction of DNA DSBs, K-562 cells were treated with 5 and 10 µM MAKV-8 for increasing periods of time, and the expression of γH2AX was assessed by western blot. Results reveal that 5 µM MAKV-8 enhances γH2AX levels only after a 24-hour incubation and the effect is more pronounced with 10 µM (Figure 35A), albeit not reaching that observed with cisplatin, a well-known DNA damaging agent (Galluzzi *et al.*, 2012). When cells are pre-treated with 50 µM Z-VAD-FMK for 1 hour, the MAKV-8-mediated induction of histone H2AX phosphorylation is almost completely abrogated. Surprisingly, similar results are obtained after a 1-hour pre-treatment with 50 µM Z-VAD-FMK followed by treatment with 50 µM cisplatin (Figure 35B).

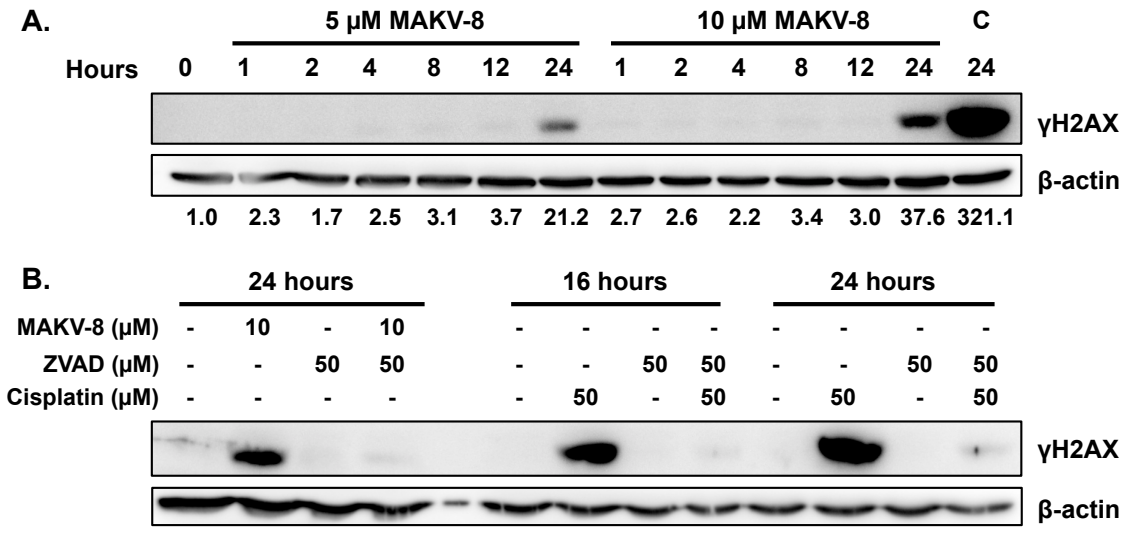

Figure 35: Effect of MAKV-8 on double strand breaks induction in K-562 cells.
K-562 cells were (A) treated with 5 and 10 µM of MAKV-8 for the indicated time points or (B) treated with or without Z-VAD-FMK for 1 hour and then incubated for 24 hours in presence or absence of 10 µM MAKV-8. The expression level of γH2AX was assessed by western blot, with β-actin as a loading control. Cisplatin (C, 50 µM) was used as a positive control for double strand break induction. Quantification values are indicated underneath corresponding blots that are representative of three independent experiments.

In conclusion, MAKV-8 treatment results in the activation of UPR signaling pathways and autophagic process, as well as DSB induction in K-562 cells.

1.7. MAKV-8 in combination with imatinib displays synergistic pro-apoptotic activity in imatinib-sensitive and -resistant CML cells

1.7.1. Evaluation of co-treatments in imatinib-sensitive CML cell lines

Despite the outstanding therapeutic results obtained with TKi in CML, the occurrence of imatinib resistance in over 30% of CML patients clearly necessitates the discovery and investigation of additional therapeutic approaches. For instance, treatment of cancerous cells with imatinib combined with another drug could sensitize cells to the cell killing effects of imatinib. The analyses of transcriptomic data from patients revealed that HDAC1 and HDAC2 mRNA expression levels are significantly up-regulated and associated with a trend towards increased HDAC3 mRNA levels in LSCs compared with healthy stem cells (HSCs) (Figure 36). Notably, other HDAC isoenzymes are similarly or less expressed in LSCs (data not shown). The importance of HDAC1 and 2 in tumor survival provides a good rational for treating CML cells with imatinib in combination with a pan-HDACi (Chen *et al.*, 2019).

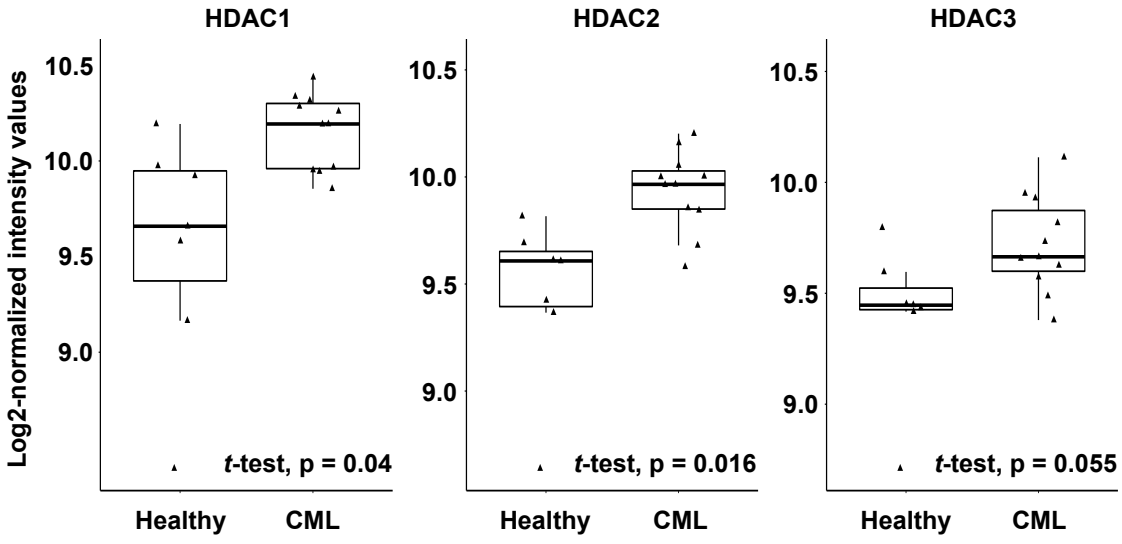

Figure 36: Expression levels of HDAC mRNA in stem cells from healthy and CML patients. Boxplots including outliers illustrating fold change (log2) of HDAC1, 2 and 3 mRNA expression levels in $CD34^{+}CD38^{-}$ stem cells isolated from healthy (n=7) and CML (n=11) patients (represented by triangles).

Considering computational results, we sought to determine the ability of MAKV-8 in combination with imatinib to exert anti-tumor effects against CML cells. Accordingly, we selected MAKV-8 and imatinib concentrations that induced only moderate toxicity (*i.e.* less than 10-20% of cell death) against CML cells.

First, the effects of co-treatments were monitored on histone H4 and α-tubulin acetylation levels in CML cells to test whether concomitant treatment with imatinib affected MAKV-8-

mediated HDAC inhibition. In the tested CML cell lines, the acetylation of α-tubulin is similarly induced after 24 hours of exposure to MAKV-8-imatinib co-treatment compared to MAKV-8 treatment alone, whereas the level of acetylated histone H4 is further enhanced. In contrast, CML cells co-treated with SAHA and imatinib display lower and increased levels of α-tubulin and histone H4 acetylation, respectively, compared to treatment with SAHA alone (Figure 37). Of note, those results suggest a different HDAC inhibitory profile between MAKV-8 and SAHA.

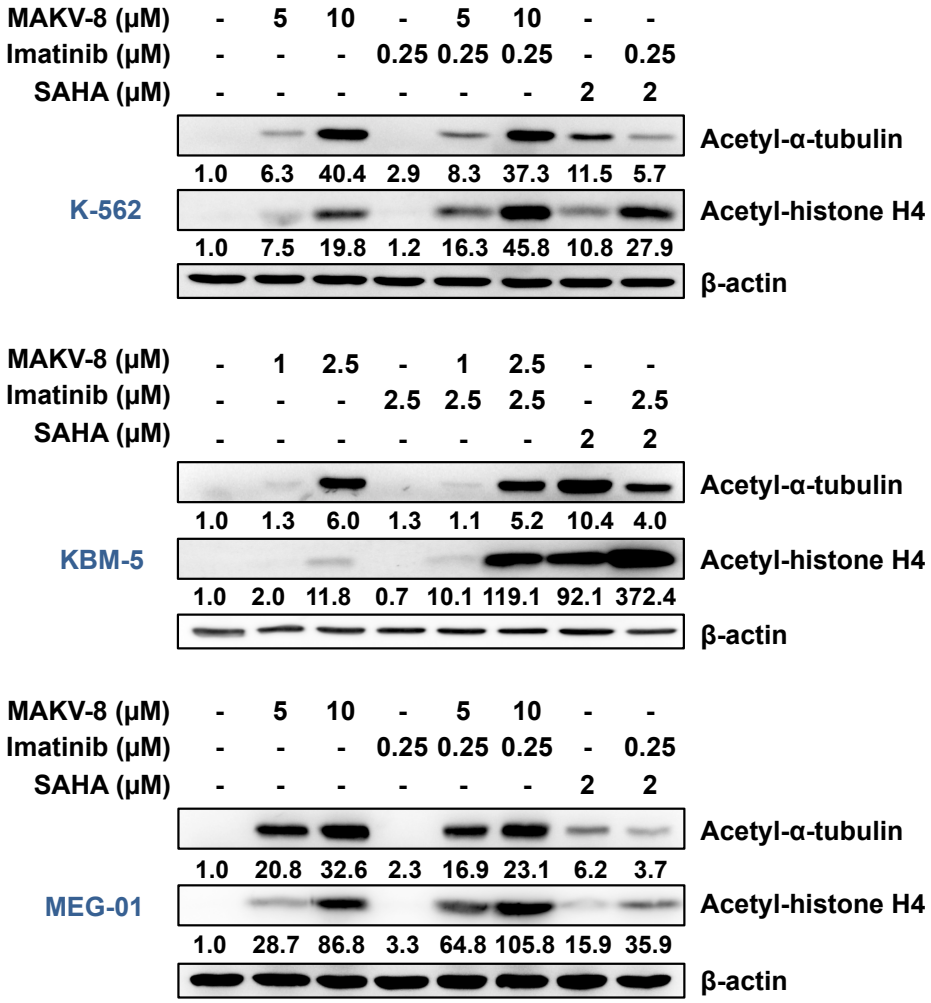

Figure 37: Effect of co-treatment with MAKV-8 and imatinib on the acetylation of histone H4 and α-tubulin in CML cells.
CML cells were treated with either MAKV-8 or imatinib alone, or in combination. After 24 hours of incubation the acetylation levels of histone H4 and α-tubulin were assessed by western blot, with β-actin as loading control. SAHA was used as a reference HDACi. Quantification values are indicated underneath corresponding blots that are representative of three independent experiments.

We then tested the effect of MAKV-8-imatinib combination on CML cell viability by nuclear morphology analysis. In that purpose, K-562 cells were treated with increasing

concentrations of imatinib or MAKV-8 or co-treated with increasing concentrations of MAKV-8 and 0.25 µM imatinib for 48 and 72 hours. The reduction in viability mediated by the co-treatment is greater than that induced by either compound alone, with a 75% decrease in living cells after treatment with the highest MAKV-8 concentration combined with imatinib. By analogy, co-treatment with 2 µM SAHA presents similar results to those exhibited by co-treatment with 5 µM MAKV-8. In combination treatments, CI values below 1 indicate synergism for each concentration of MAKV-8 combined with 0.25 µM of imatinib at both 48 and 72 hours, with the maximal effect using 10 µM of MAKV-8 (Figure 38). Of note, no effect is detected on K-562 cell viability after 24 hours of MAKV-8 and/or imatinib (co-) treatments (Annex A1).

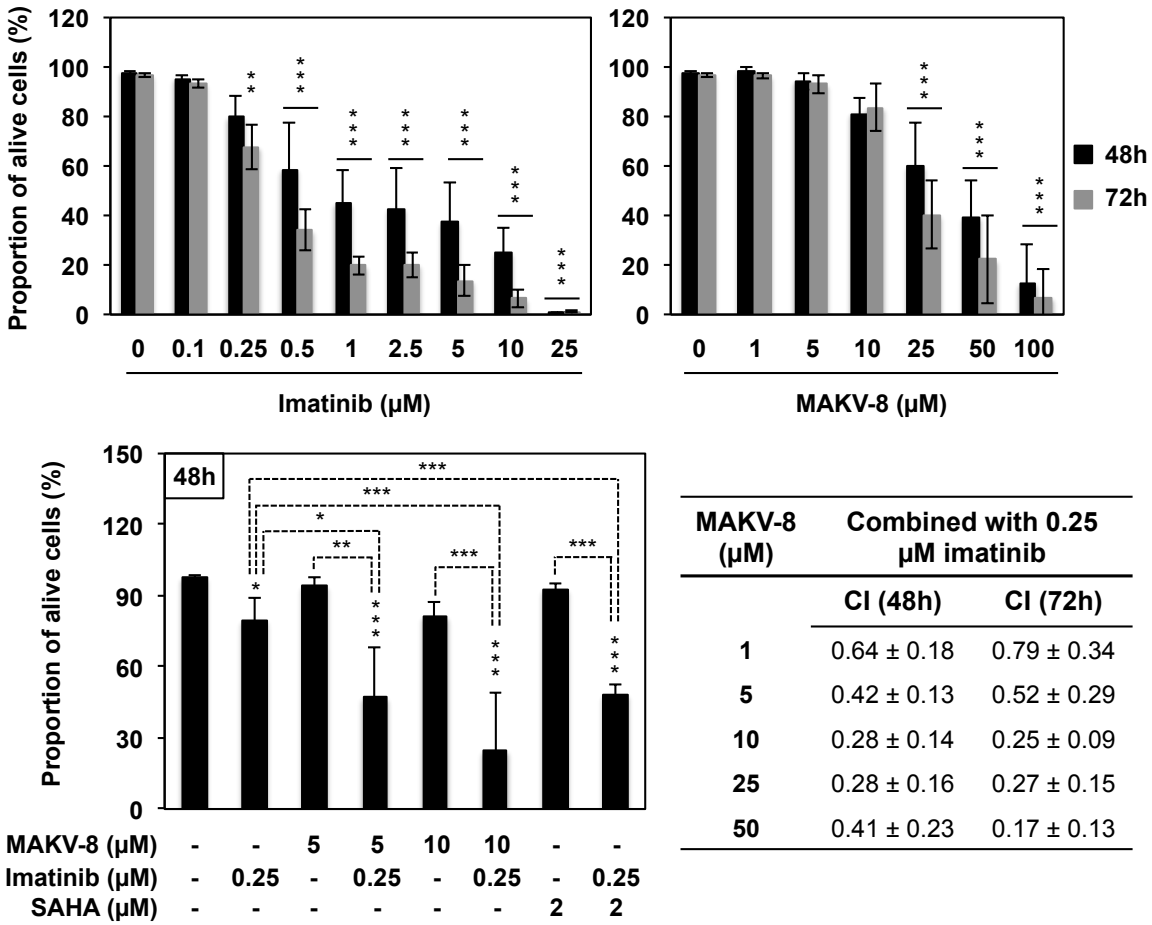

MAKV-8 (µM)	Combined with 0.25 µM imatinib	
	CI (48h)	CI (72h)
1	0.64 ± 0.18	0.79 ± 0.34
5	0.42 ± 0.13	0.52 ± 0.29
10	0.28 ± 0.14	0.25 ± 0.09
25	0.28 ± 0.16	0.27 ± 0.15
50	0.41 ± 0.23	0.17 ± 0.13

Figure 38: Effect of co-treatment with MAKV-8 and imatinib on K-562 cell death.
K-562 cells were treated with increasing concentrations of MAKV-8 or imatinib alone, or combination of increasing concentration of MAKV-8 and 0.25 µM imatinib for 48 and 72 hours. The study of nuclear morphology was performed by fluorescence microscopy after Hoechst-PI staining. Results correspond to mean ± SD of three independent experiments and were analyzed by a two-way ANOVA (compounds alone) or a one-way ANOVA (combinations) with *, **, *** indicating $p < 0.05$, $p < 0.01$, $p < 0.001$, respectively. Combination index (CI) values (mean ± SD, N=3) were determined with CompuSyn software.

Disruption of MMP precedes the release of pro-apoptotic factors from mitochondria such as cytochrome *c* and nuclear signs of apoptosis (Macho *et al.*, 1996). In addition, PS flips from the inner to the outer leaflet of the plasma membrane during the intermediate stages of apoptosis, allowing its detection with fluorescent Annexin V conjugates (Duensing *et al.*, 2018). Therefore, K-562 cells co-treated with 5 or 10 μM MAKV-8 and 0.25 μM imatinib were stained with either MitoTracker Red, or Annexin V and PI. The fluorescence of those dyes was then quantified by flow cytometry.

MAKV-8-imatinib combinations trigger MMP loss and increase the proportion of annexin V-positive cells, reaching approximately 83% of cells displaying low MMP and annexin V positivity, respectively, after co-treatment with 10 μM MAKV-8 compared to 7 and 20% in untreated cells. Furthermore, the effect in combination treatment is increased compared to the treatment with each drug alone. Interestingly, co-treatment with 2 μM SAHA gives similar results than those obtained after co-treatment with 5 μM MAKV-8. Cells treated with 50 μM cisplatin for 24 hours were used as a positive control for MMP disruption and apoptosis induction (Figure 39).

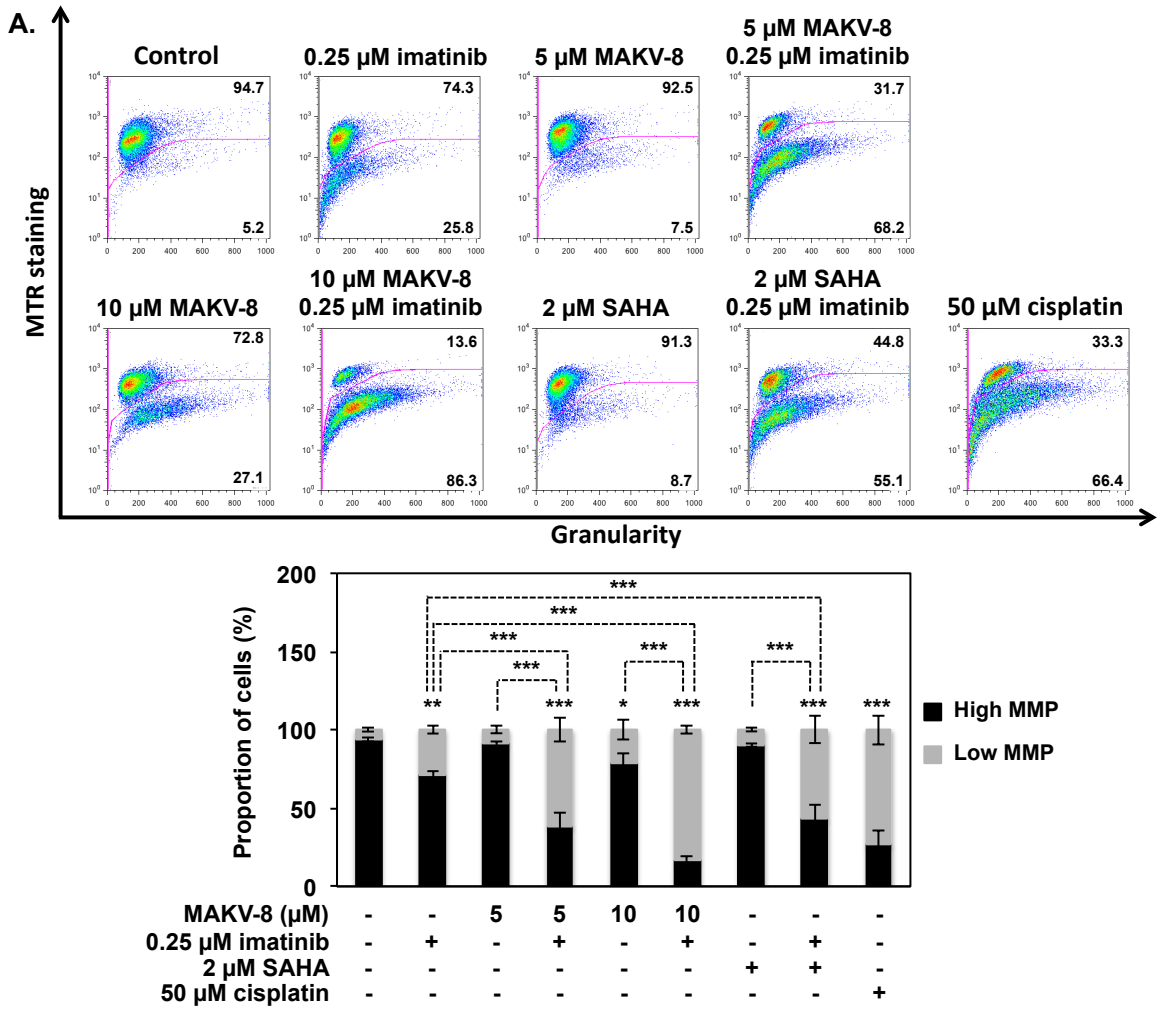

Figure 39: Effect of co-treatment with MAKV-8 and imatinib on K-562 cell death.
K-562 cells were treated with either MAKV-8 or imatinib alone, or in combination for 48 hours. The study of MMP disruption or apoptosis induction was performed by flow cytometry after (A) MitoTracker Red or (B) annexin V and PI staining, respectively. SAHA was used as a reference HDACi. Cisplatin (24 hours) was used as a positive control for MMP disruption and apoptosis induction. Representative dot plots (upper panel) and quantifications corresponding to the mean ± SD (lower panel) from three independent experiments are provided. Results were analyzed by a one-way ANOVA with *, **, *** indicating $p < 0.05$, $p < 0.01$, $p < 0.001$, respectively.

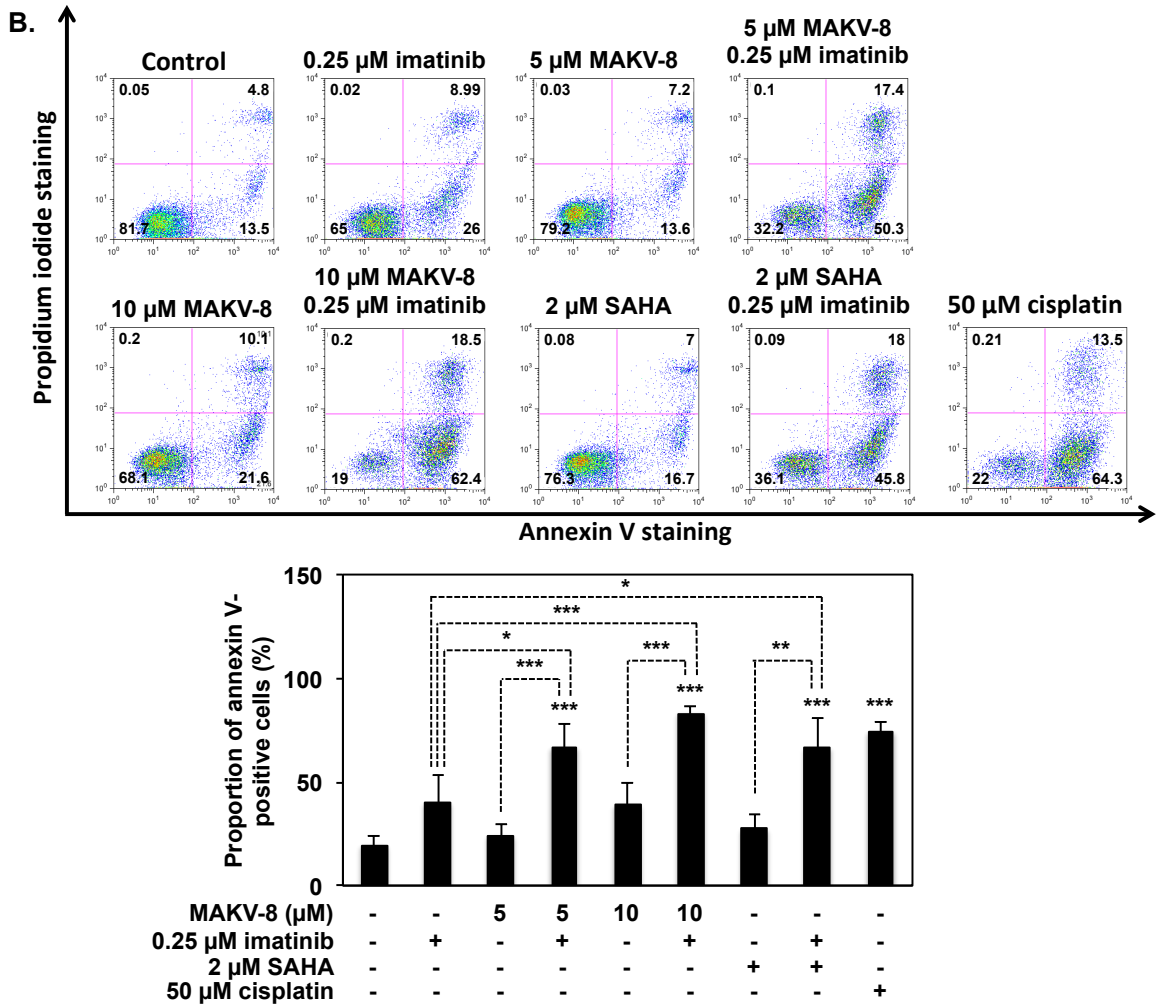

Figure 39 (Continued)

To evaluate the effects of combination treatments with imatinib and MAKV-8 on additional BCR-ABL-positive CML cell death, KBM-5 and MEG-01 cells were treated with imatinib and MAKV-8 alone or in combination, and nuclear morphology analyses were performed after 48 hours of treatment. We extended our findings by showing that treatments with MAKV-8 in combination with imatinib have also a synergistic effect on KBM-5 and MEG-01 cell viability, with a reduction of 88 and 69% of alive cells, respectively, after a treatment with the highest concentration of MAKV-8 (Figure 40).

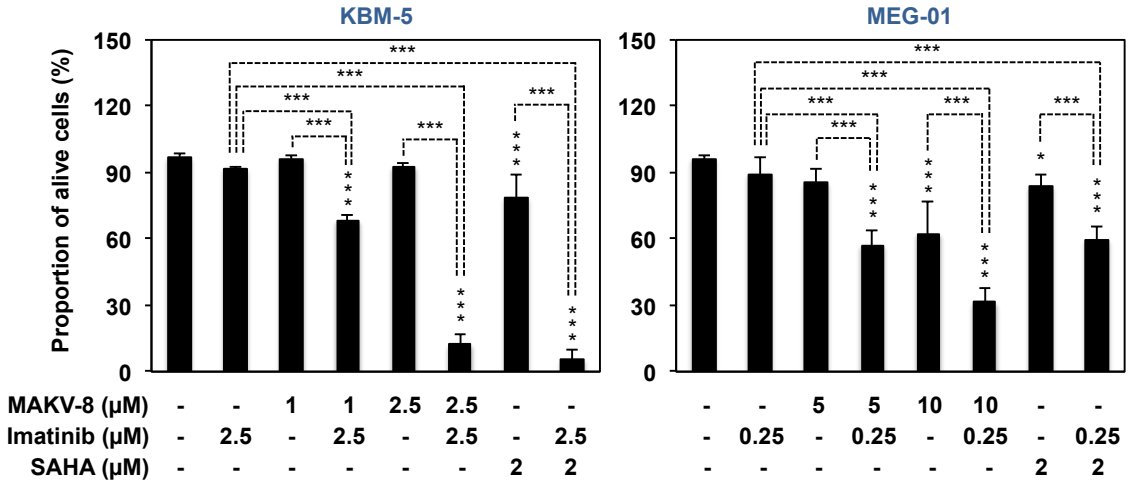

Cell line	MAKV-8 (µM)	Imatinib (µM)	CI (48h)
KBM-5	1	2.5	0.46 ± 0.06
	2.5	2.5	0.05 ± 0.03
MEG-01	5	0.25	0.77 ± 0.16
	10	0.25	0.37 ± 0.07

Figure 40: Effect of MAKV-8-imatinib co-treatment on KBM-5 and MEG-01 cell death.
KBM-5 and MEG-01 cells were treated with either MAKV-8 or imatinib alone, or in combination for 48 hours. The study of nuclear morphology was performed by fluorescence microscopy after Hoechst-PI staining. Results correspond to mean ± SD of three independent experiments and were analyzed by a one-way ANOVA with *, *** indicating $p < 0.05$, $p < 0.001$, respectively. Combination index (CI) values (mean ± SD, N=3) were determined using CompuSyn software.

Those results prompted us to investigate the type of cell death occurring in CML cells upon treatment with MAKV-8 and imatinib. Accordingly, the effects of MAKV-8 alone or in combination with imatinib were assessed by western blot on the cleavage of caspases and PARP-1 after 24 hours of treatment. In K-562 cells, such co-treatment causes a stronger cleavage of caspase 3, 8, 9, and PARP-1 than that observed due to single treatments. Similar results are observed for caspase 3 and PARP-1 cleavage in KBM-5 and MEG-01 cells (Figure 41). By comparison, co-treatments with 2 µM SAHA offer results close to those obtained after co-treatment with 2.5 and 5 µM MAKV-8 in KBM-5 cells and K-562 or MEG-01 cells, respectively. In cells treated with 50 µM cisplatin for 24 hours, the cleavage of caspases and PARP-1 is in correlation with apoptosis induction, as reported in the literature (Galluzzi *et al.*, 2012). Collectively, our results highlight an activation of apoptotic pathways, which was more important upon treatment with MAKV-8 and imatinib compared to the one triggered by each drug alone.

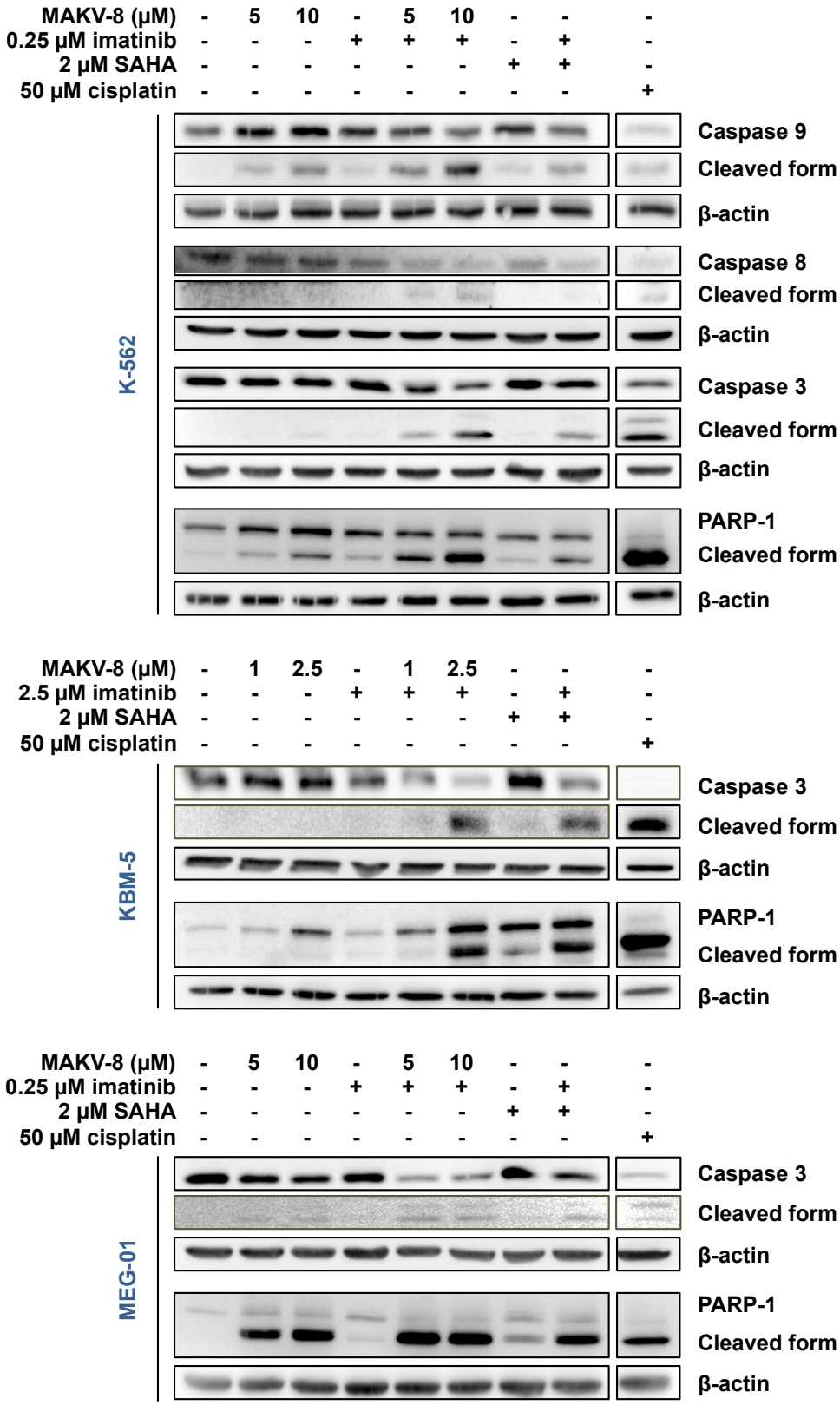

Figure 41: Effect of co-treatment with MAKV-8 and imatinib on caspase and PARP-1 cleavage in CML cells.

CML cell lines were treated with either MAKV-8 or imatinib alone, or in combination for 24 hours. The cleavage of caspases 3, 7, 8 and 9, as well as PARP-1 was analyzed by western blot, with β-actin as a loading control. SAHA was used as a reference HDACi. Cisplatin was used as the positive control for caspase and PARP-1 cleavage. Blots are representative of three independent experiments.

Next, we investigated the ability of CML cells pre-treated with MAKV-8 for 8 hours to form colonies in a semi-solid medium in the presence of imatinib in order to verify the potential of compounds to impair the replicative ability of cancer cells in a 3D model. The concentrations of imatinib used in those experiments were preliminarily determined by performing clonogenic assays on cells treated with a range of imatinib concentrations and selecting one that does not impact colony formation (Annex A2). In the three tested CML cell lines, results demonstrate that combinations exert more potent effects on reducing colony formation than either agent alone, suggesting that MAKV-8 sensitizes CML cells to imatinib treatment (Figure 42).

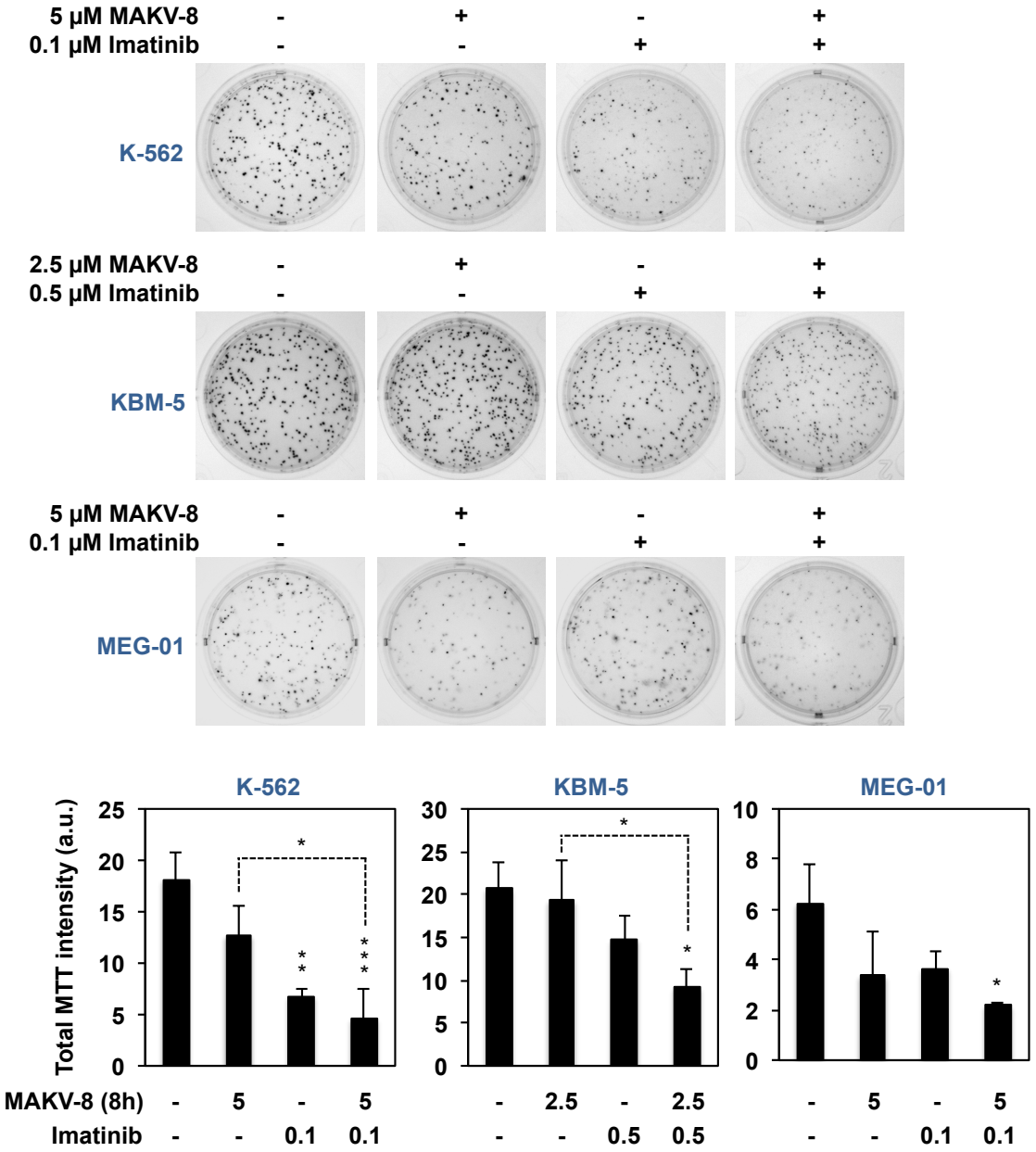

Figure 42: Effect of treatment with MAKV-8 and imatinib on CML colony formation.
CML cells pre-treated with MAKV-8 for 8 hours were then grown in the presence or absence of imatinib for 10 days. Colonies were detected after addition of MTT. Representative pictures (upper panel) and quantifications corresponding to the mean of total MTT intensity ± SD (lower panel) from three independent experiments are provided. Results were analyzed by a one-way ANOVA with *, **, *** indicating $p < 0.05$, $p < 0.01$, $p < 0.001$, respectively.

To extend our *in cellulo* results to an *in vivo* setting, we evaluated the capacity of MAKV-8 and imatinib, alone or in combination, to prevent tumor formation in a zebrafish xenograft model. Pre-treatment of xenografted K-562 cells with MAKV-8 and imatinib in combination fully abrogates tumor growth in zebrafish, whereas injection of K-562 cells pre-treated with single agent alone results in formation of tumors with 50%-reduced size compared to control (Figure 43, Annex A3).

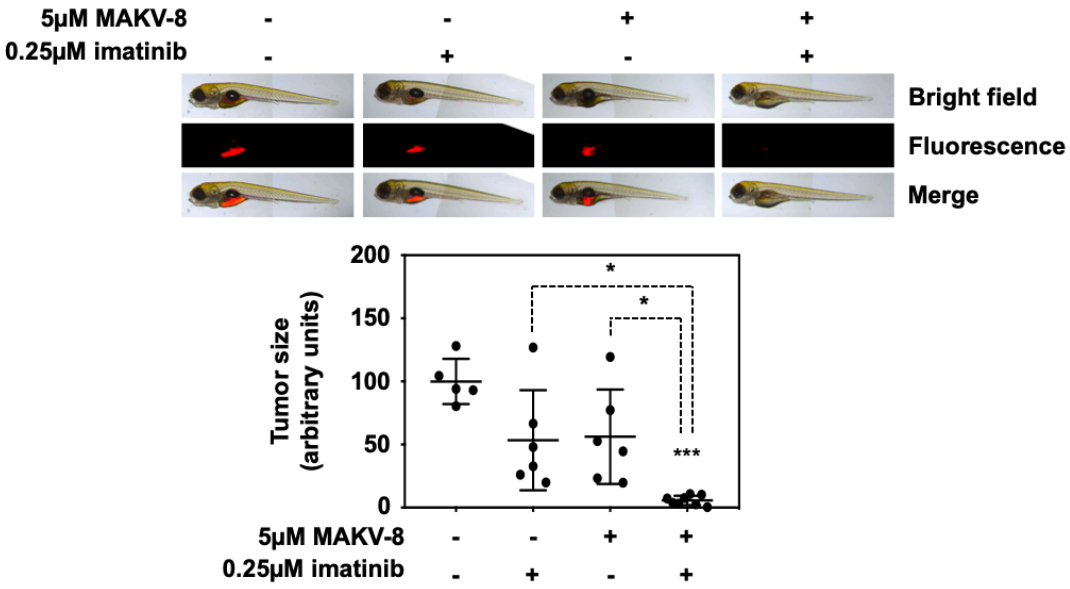

Figure 43: Effect of MAKV-8-imatinib co-treatment on tumor growth in zebrafish.
K-562 cells were treated for 24 hours, fluorescently labeled, and then injected in the zebrafish yolk sac. Three days post-injection, pictures of 5 to 8 fishes (one representative set of pictures is presented) were taken. Graph corresponds to the mean ± SD of fluorescence intensity quantification and were analyzed by a one-way ANOVA with *, *** indicating $p < 0.05$, $p < 0.001$, respectively.

1.7.2. Evaluation of co-treatments in imatinib-resistant CML cell lines

Despite the success of TKi to manage CML patients, imatinib resistance remains one of the major therapeutic challenges. Accordingly, we tested whether a combination imatinib-MAKV-8 could be effective against resistant CML cell models. The optimal concentration of imatinib used in combination with MAKV-8 was preliminarily determined by treating imatinib-resistant K-562 and KBM-5 cell lines (K-562R and KBM-5R, respectively) with a range of imatinib concentrations and selecting one that induces low cell mortality, *i.e.* less than 10-20% of cell death (Annex A4). Considering that K-562R and KBM-5R cells begin to die in response to 10 µM imatinib, we used this concentration for subsequent experiments.

To evaluate whether treatment with MAKV-8 is able to overcome imatinib resistance, the effect of combination was assessed on K-562R and KBM-5R cell viability after 48 hours of treatment. The study of nuclear morphology shows that K-562R cell mortality is not impacted by co-treatments; however, the decrease in KBM-5R cell viability is further enhanced by co-treatments compared to treatments with either drug alone, and a synergistic loss of 65% of living cells occurs after a combination with 2.5µM MAKV-8 and 10µM imatinib. Therefore, CI was determined for each co-treatment and a mild synergistic effect is detected for 2.5µM MAKV-8 in combination with imatinib (Figure 44).

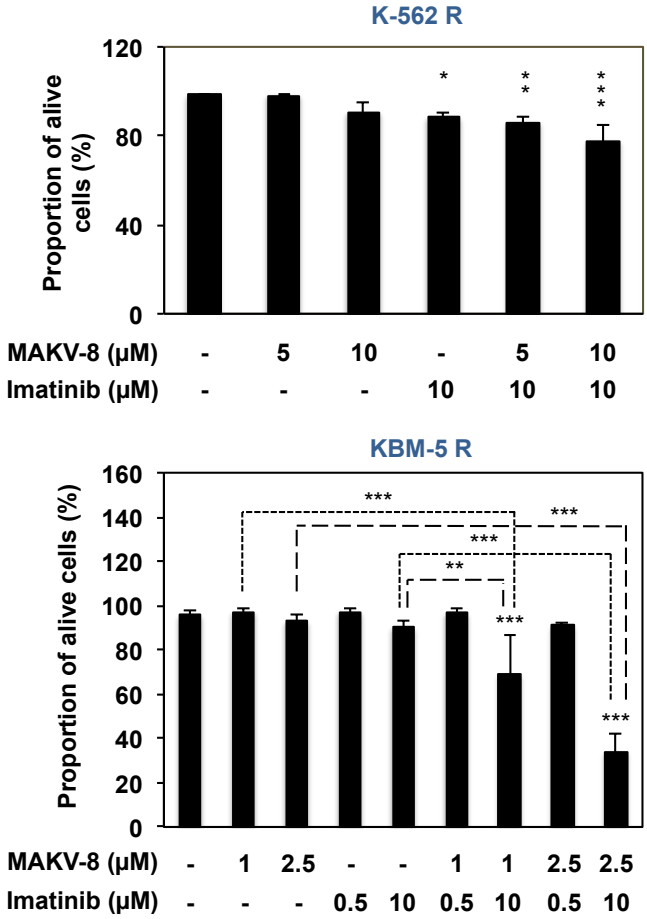

MAKV-8 (µM)	Imatinib (µM)	CI (48h)
1	10	1.42 ± 0.58
2.5	10	0.78 ± 0.16

Figure 44: Effect of MAKV-8-imatinib co-treatment on imatinib-resistant CML cell death.
K-562R and KBM-5R cells were treated with MAKV-8 and imatinib alone or in combination for 48 hours. The study of nuclear morphology was performed by fluorescence microscopy after Hoechst-PI staining. Results correspond to the mean ± SD of three independent experiments and were analyzed by a one-way ANOVA with *, **, *** indicating $p < 0.5$, $p < 0.01$, $p < 0.001$, respectively. Combination index (CI) values (mean ± SD, N=3) were determined using CompuSyn software.

Since co-treatments with MAKV-8 plus imatinib do not impact K-562R cell mortality, the anticancer effects of compounds were further characterized only in KBM-5R cells. As in imatinib-sensitive KBM-5 cells, α-tubulin acetylation is similarly induced after MAKV-8-imatinib co-treatment compared to treatment with MAKV-8 alone, whereas the level of acetylated histone H4 is enhanced (Figure 45A). In addition, after co-treatments, the cleavage of PARP-1 is more important compared to the one induced by treatments with each drug alone (Figure 45B), revealing an activation of apoptotic pathways also in imatinib-resistant cells. Finally, MAKV-8 pre-treatment followed by imatinib treatment is more effective at reducing colony formation than either single agent alone, suggesting that MAKV-8 is likely to overcome imatinib resistance in CML cells (Figure 45C, Annex A2).

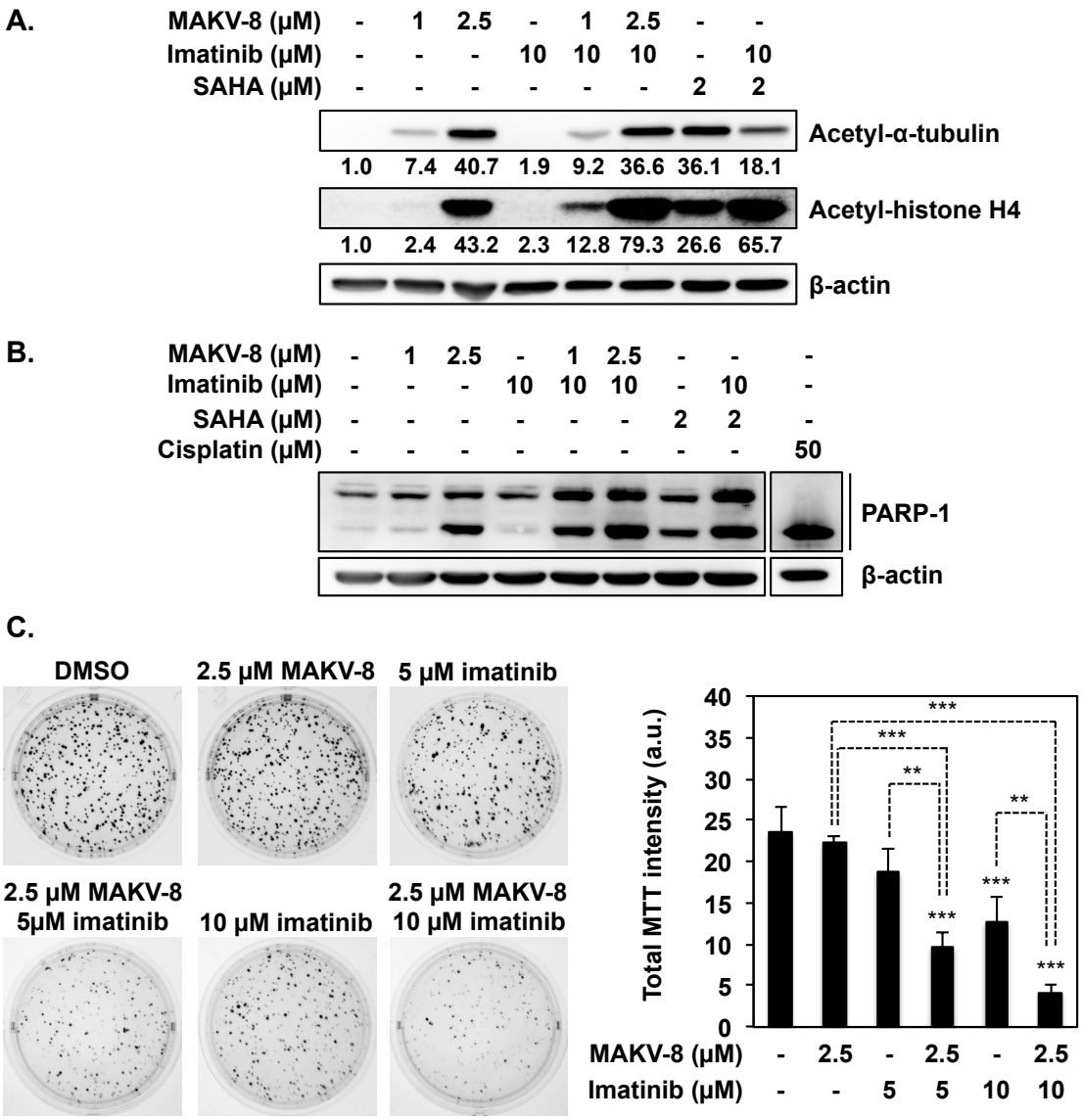

Figure 45: Anticancer effects in KBM-5R cells co-treated with MAKV-8 and imatinib.
KBM-5R cells were treated with either MAKV-8 or imatinib alone, or in combination for 24 hours and (A) acetylation levels of histone H4 and α-tubulin or (B) PARP-1 cleavage were assessed by western blot. Cisplatin was used as the positive control for PARP-1 cleavage. β-actin and SAHA were used as a loading control and a reference HDACi, respectively. Quantification values are indicated underneath corresponding blots that are representative of three independent experiments. (C) KBM-5R cells pre-treated with MAKV-8 for 8 hours then grown in the presence or absence of imatinib for 10 days. Colonies were detected after addition of MTT. Representative pictures (upper panel) and quantifications corresponding to the mean of total MTT intensity ± SD (lower panel) from three independent experiments are provided. Results were analyzed by a one-way ANOVA with **, *** indicating $p < 0.01$, $p < 0.001$, respectively.

In conclusion, MAKV-8 combined with imatinib synergistically triggers apoptotic cell death in imatinib-sensitive and -resistant BCR-ABL-positive CML cells. Furthermore, tumor growth of xenografted K-562 cells in zebrafish is completely abrogated upon combined treatment with MAKV-8 and imatinib.

1.7.3. MAKV-8–imatinib combination displays a mild toxicity in healthy cell models

When administrating a novel therapeutic compound to patients, it is essential to guarantee restrained side effects thanks to a differential toxicity of the treatment towards cancer versus healthy cells. In order to facilitate the comparison of the toxicity between healthy and cancerous blood cells, the concentrations of MAKV-8 and imatinib used for the treatments in healthy models and CML cells were identical.

We started by incubating non-proliferating and proliferating PBMCs in presence of MAKV-8 and/or imatinib for 48 hours. Notably, the blastogenic response of PHA/IL-2-stimulated PBMCs was preliminarily evaluated (Annex A5). Using a Trypan blue exclusion test on non-proliferating PBMCs, we observe a moderate effect of treatments with MAKV-8 either alone or in combination, with a maximum decrease of 30% of viable cells after 48 hours of treatment, whereas imatinib alone fails to trigger any cell mortality (Figure 46A). Unfortunately, in proliferating PBMCs stained with Hoechst-PI, 5 µM MAKV-8 induces a strong decrease of cell viability, reaching 15% of alive cells following a treatment with 10 µM MAKV-8. Of note, this diminution is not further enhanced upon addition of imatinib (Figure 46B). By comparison, treatments with SAHA alone or in combination with imatinib fail to impact cell viability either in non-proliferating or proliferating PBMCs (Figure 46A and B).

Next, we tested the effect of MAKV-8 in combination with imatinib on the viability of pluripotent $CD34^+$ stem cells. Nuclear morphology analyses reveal that 48-hour treatments with MAKV-8 alone or in combination stimulate a robust reduction of $CD34^+$ cell viability, reaching 10% of alive cells with 10 µM MAKV-8. Importantly, the FDA-approved SAHA also severely decreases viable cell population (Figure 46C).

Finally, the impact of MAKV-8-imatinib combinations on the viability of lymphocytic RPMI-1788 cell line was evaluated by analysis of nuclear morphology. Although RPMI-1788 cells undergo a reduction of about 55% of alive cells following a 48-hour treatment with 10 µM MAKV-8, the decrease in cell viability is not further enhanced upon the addition of imatinib. Noteworthy, similar concentrations of MAKV-8 and SAHA show comparable results (Figure 46D).

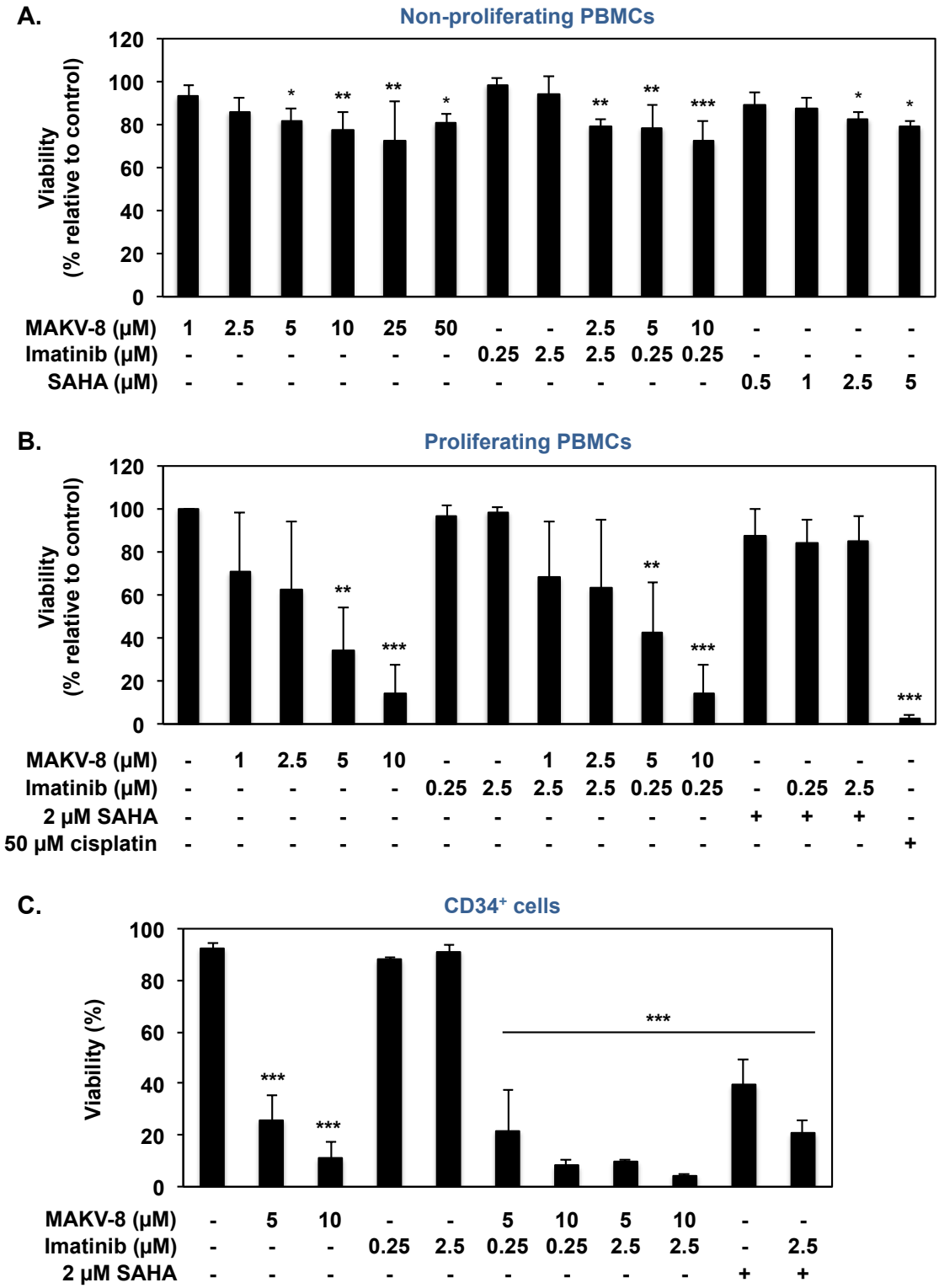

Figure 46: Effect of MAKV-8-imatinib combinations on the viability of healthy cell models. (A) Non-proliferating and (B) proliferating PBMCs, as well as (C) $CD34^+$ cells from healthy donors, and (D) RPMI-1788 cells were treated with either MAKV-8 or imatinib alone, or in combination for 48 hours. Cell viability was assessed based on the Trypan Blue exclusion method and the study of nuclear morphology after Hoechst-PI staining for non-proliferating PBMCs and proliferating PBMCs, $CD34^+$ cells or RPMI-1788 cells, respectively. SAHA was used as a reference HDACi. Results correspond to the mean ± SD of three independent experiments and were analyzed by a one-way ANOVA with *, **, *** indicating $p < 0.05$, $p < 0.01$, $p < 0.001$, respectively.

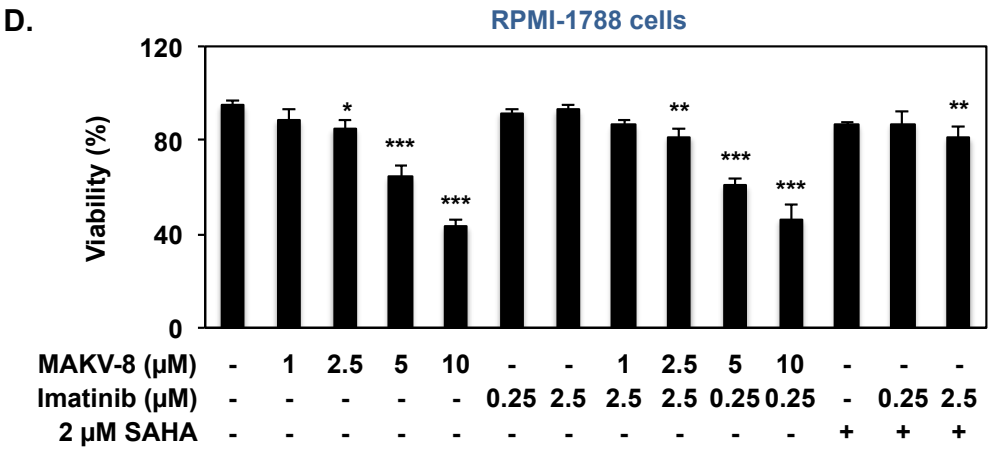

Figure 46 (Continued)

Consequently, the ratio of cell death induced by MAKV-8-imatinib co-treatments, calculated from the mean of cancer versus normal cell death reported to control, is attesting of a stronger toxicity against cancer cells by comparison to non-proliferating PBMCs and RPMI-1788 cells (Table 11).

Table 11: Selectivity ratio of MAKV-8-imatinib co-treatment for cancer cells versus healthy models.

CML cells	Selectivity ratio	
	PBMCs	RPMI-1788
K-562	5.8	3.9
KBM-5	8.5	9.2
MEG-01	2.2	1.5

Next, PS exposure of platelets from healthy donors incubated in presence of increasing concentrations of MAKV-8 or co-treated with MAKV-8 and imatinib for 48 hours was assessed by flow cytometry. MAKV-8 neither alone nor in co-treatments elicits any significant cytotoxicity in platelets, as compared to the positive control (Figure 47).

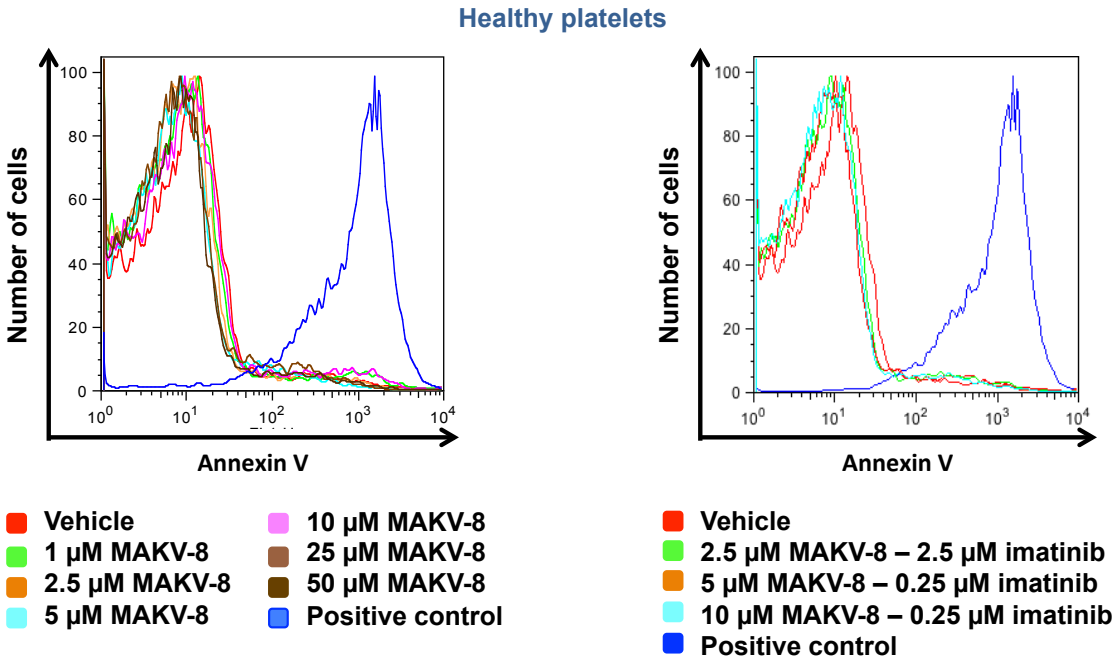

Figure 47: Effect of combinations with MAKV-8 and imatinib on healthy platelet viability. Platelets from healthy donors were treated with increasing concentrations of MAKV-8 or co-treated with MAKV-8 and imatinib for 48 hours. Cell viability was assessed by flow cytometry after annexin V staining. Vehicle and positive control are represented by 0.1 and 50% DMSO (v/v), respectively. Results are representative of three independent experiments.

In conclusion, our results strongly suggest that the combination MAKV-8-imatinib displays an increased toxicity against cancer cells accompanied by a promising safety profile against non-proliferating healthy models.

1.8. Beclin 1 knock-down reduces MAKV-8-imatinib combination-induced apoptosis

Since MAKV-8 treatment induces autophagy, we tested whether this process would be implicated in the synergistic cell death observed with the combination. Transfection of K-562 cells with siRNA targeting the gene coding for beclin 1 (*i.e.* BECN1), a protein involved in initiating autophagic flux, expectedly leads to a knock-down of the gene, which is maintained up to the end of treatments (Figure 48A). Of note, optimal transfection conditions for this specific siRNA had been preliminarily determined. Interestingly, we observe after 48 hours of treatment with the combination that the proportion of viable K-562 cells is significantly augmented from 15 and 20% in cells transfected with or without non-targeting siRNA, respectively, to 40% in BECN1-silenced cells. Finally, the reduction in PARP-1 cleavage (*i.e.* the ratio between the cleaved and uncleaved forms) in BECN1-silenced cells further confirms the previous observation of reduced apoptotic cell death (Figure 48B). Surprisingly, down-regulation of beclin 1 expression does not result in prevention of MAKV-8-mediated down-regulation of SQSTM1 expression or LC3-I to LC3-II conversion after 8 hours. In addition, no difference is observed in GRP78 expression upon transfection with or without siRNA targeting BECN1 (Figure 48C).

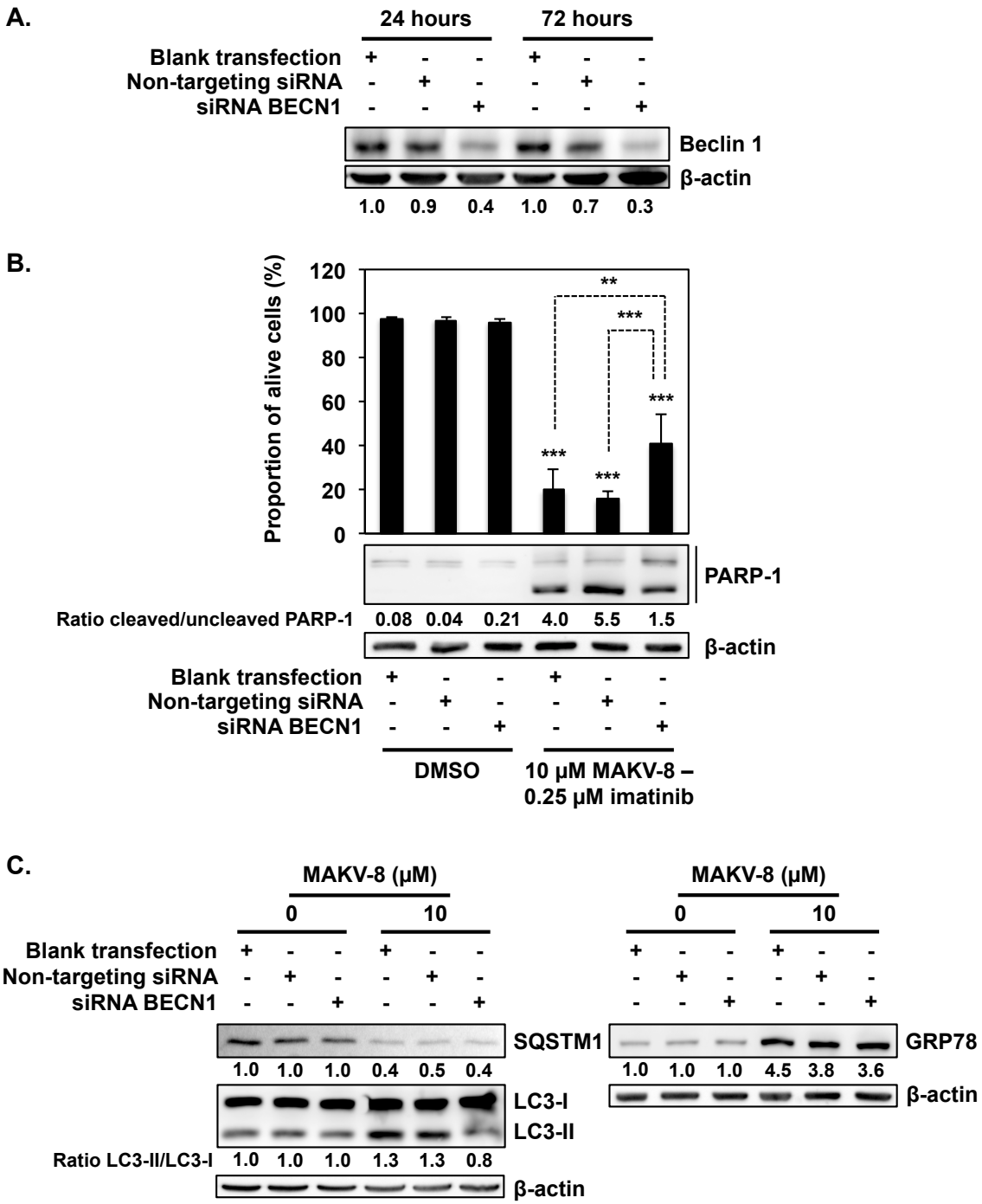

Figure 48: Effects of beclin 1 silencing on apoptotic cell death induced by MAKV-8 in combination with imatinib.

K-562 cells were transfected with or without non-targeting siRNA or a siRNA targeting BECN1 for 24 hours, then (A) the expression level of beclin 1 was assessed by western blot 24 and 72 hours post transfection; (B) the study of nuclear morphology was performed by fluorescence microscopy after Hoechst-PI staining and the cleavage of PARP-1 was analyzed by western blot in cells treated with MAKV-8 and imatinib for 48 hours; (C) LC3 conversion, and the expression of SQSTM1 and GRP78 were evaluated by western blot in cells treated with MAKV-8 for 8 hours. Results correspond to the mean ± SD of three independent experiments and were analyzed by a one-way ANOVA with **, *** indicating $p < 0.01$, $p < 0.001$, respectively. Quantification values are indicated underneath corresponding blots, representative of three independent experiments, with β-actin as loading control.

1.9. MAKV-8 and imatinib co-treatment synergistically lessens BCR-ABL-related signaling pathways involved in CML cell growth and survival

The increase of cell death observed after the co-treatment imatinib-MAKV-8 can be due to the disruption of many different pathways, such as the ones regulated by BCR-ABL activity. The BCR-ABL fusion oncoprotein displays constitutive tyrosine kinase activity through its phosphorylation on tyrosine 177 and therefore aberrant downstream signaling pathways leading to proliferation and survival. Accordingly, we examined by western blotting the repercussion of co-treatments with MAKV-8 and imatinib on the expression and phosphorylation of BCR-ABL and its downstream targets in K-562 cells. Although MAKV-8-imatinib treatment does not impact BCR-ABL expression, it leads to a drastic decrease in its phosphorylation accompanied by a similar effect on STAT5 phosphorylation. Notably, MAKV-8 further down-regulates STAT5 protein levels and provokes a striking decrease in c-MYC expression, which is maintained by co-treatment with imatinib. Conversely, MCL-1 expression is not markedly impacted by the combination due to oppositional effects exhibited by each drug. Despite a MAKV-8-mediated increase in BCR-ABL expression, treatments with MAKV-8 and imatinib result in decreased BCR-ABL phosphorylation in KBM-5, MEG-01, and KBM5-R cells. In all CML cell lines, treatments with SAHA, either alone or in combination with imatinib, exhibit results comparable to that of the highest MAKV-8 concentration on the expression and phosphorylation of BCR-ABL and downstream targets (Figure 49).

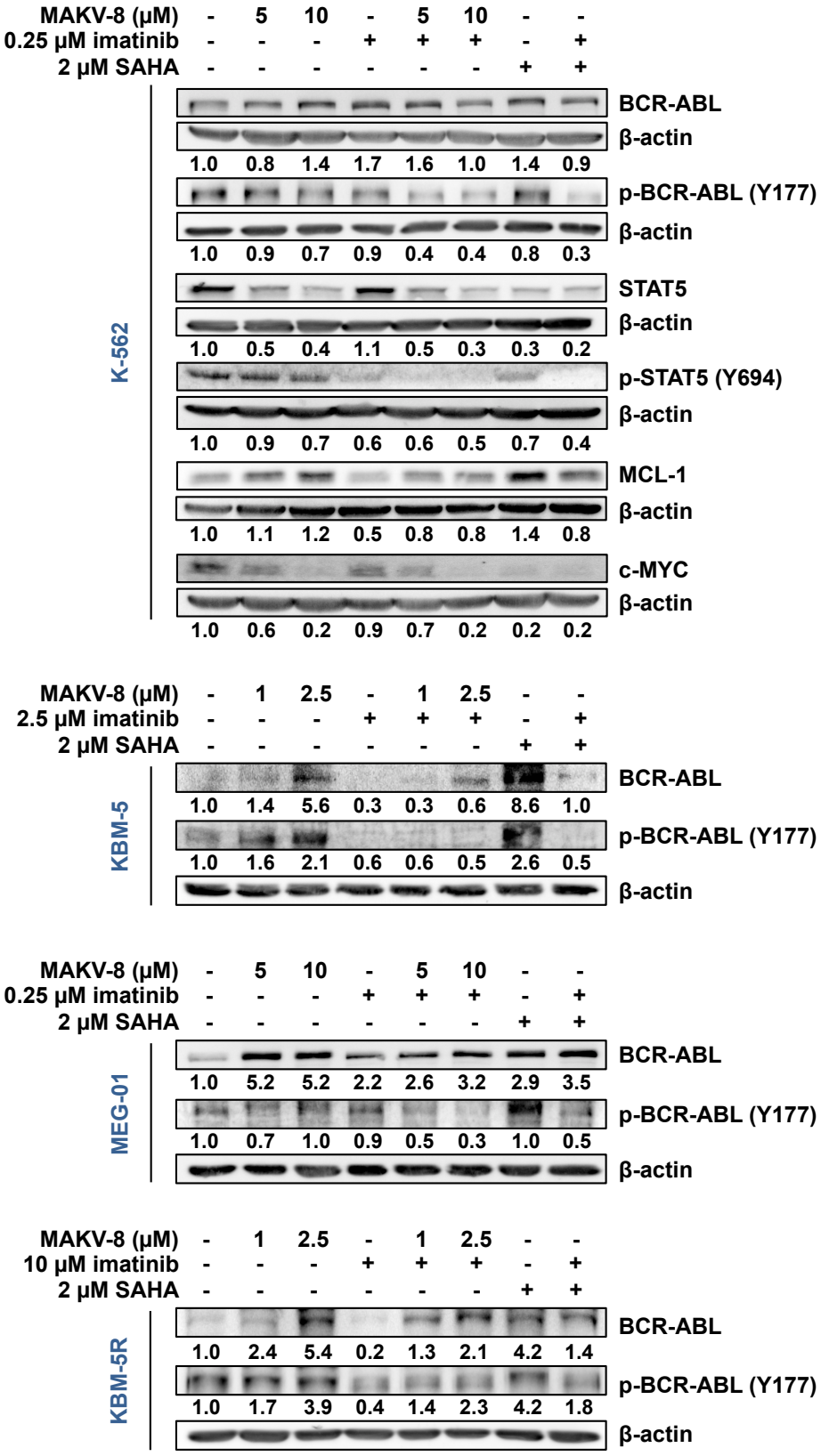

Figure 49: Effect of MAKV-8-imatinib co-treatments on proteins implicated in BCR-ABL-dependent signaling pathways in imatinib-sensitive and -resistant CML cells.

CML cells were cultured with either MAKV-8 or imatinib alone, or in combination for 24 hours. The expression level of proteins was assessed by western blot, with β-actin as loading control. SAHA was used as a reference HDACi. Quantification values are indicated underneath corresponding blots that are representative of three independent experiments.

1.10. MAKV-8 and imatinib co-treatment reduces CML stem cell population

The oncogenic transcription factor c-MYC was reported to play an important role in LSC survival that appears to be implicated in TKi resistance and relapse in leukemic patients (Venton *et al.*, 2016). Accordingly, c-MYC mRNA expression level is significantly up-regulated in LSCs versus HSCs from patients (Figure 50A).

Elevated ALDH activity is an established marker for the identification of hematopoietic stem cells. Since we previously demonstrated that MAKV-8 strongly reduced c-MYC expression, we sought to evaluate by flow cytometry whether a 24-hour treatment with 10 µM MAKV-8 plus 0.25 µM imatinib could decrease ALDH-positive population in K-562 cell line, which are known to have a substantial proportion of cells with cancer stem-like characteristics. Results show that the percentage of ALDH+ cells is lowered from 50% in untreated cells to 24 and 30% in cells treated with MAKV-8 and imatinib, respectively. After MAKV-8-imatinib co-treatments, the reduction is further enhanced, reaching 15%. In contrast, SAHA fails to reduce the proportion of ALDH+ cells. When cells are concomitantly treated with SAHA and imatinib, the percentage of ALDH+ cells decreases to 30%, indicating that combination with MAKV-8 and imatinib is more efficient to reduce the cancer stem cell population. The percentage of ALDH+ cells treated with DEAB, a specific inhibitor of ALDH activity, is close to 0% as expected (Figure 50B).

In conclusion, the combination of MAKV-8-imatinib reduced BCR-ABL phosphorylation, as well as the expression of downstream targets that play a critical role in CML proliferation and survival. In addition, this therapeutic approach effectively decreased the LSC population.

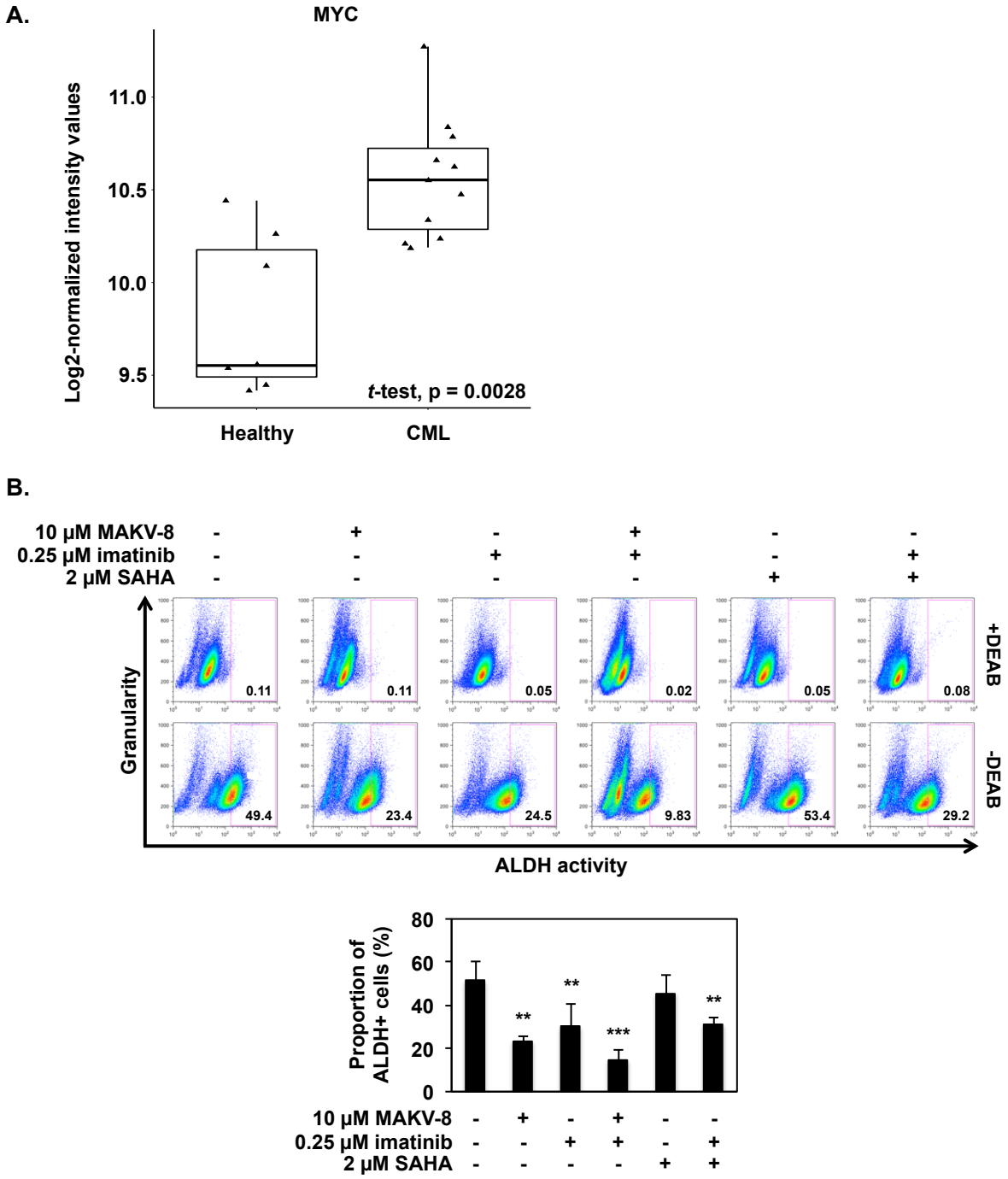

Figure 50: Effect of co-treatments with MAKV-8 and imatinib on ALDH activity in K-562 cells. (A) Boxplots illustrating fold change (log2) of c-MYC mRNA expression in $CD34^{+}CD38^{-}$ stem cells isolated from healthy (n=7) and CML (n=11) patients (represented by triangles). Results were analyzed by Welch *t*-test. (B) K-562 cells were treated with either MAKV-8 or imatinib alone, or in combination for 24 hours. Cells were labeled with Aldefluor™ in presence or absence of the ALDH inhibitor DEAB and analyzed by flow cytometry. The gate for ALDH+ cells was determined by comparison to the DEAB control and showed the brightly fluorescent ALDH population versus granularity. SAHA was used as a reference HDACi. Representative dot plots where the percentage of ALDH+ cells is indicated (upper panel) and quantifications (lower panel) corresponding to the mean ± SD of three independent experiments are presented. Results were analyzed by a one-way ANOVA with **, *** indicating $p < 0.01$, $p < 0.001$, respectively.

2. Characterization of the anticancer properties of MAKV-15, a new hydroxamate-based selective HDAC6i

The compound MAKV-15 given by the group of Guy Bormans, is a derivative of the HDAC6i tubastatin A and was originally published in the same paper (Butler *et al.*, 2010). These compounds differ in the position of the nitrogen atom on the ring associated with a change in the inhibitory potency towards HDAC6 (Figure 20), based on the IC_{50} values found in the paper (15 nM for tubastatin A *vs.* 1.4 nM for MAKV-15).

2.1. *In vitro* inhibitory potential of MAKV-15 and tubastatin A on HDAC isoenzymes

To compare the results found in the literature concerning MAKV-15 and tubastatin A, we assessed their inhibitory potential against HDAC activities *in vitro*, using a fluorimetric HDAC activity assay with either total proteins as a source of HDAC, or recombinant HDAC1 or HDAC6. The analysis reveals that the concentration of MAKV-15 required to inhibit 50 % of total HDAC activity is 7.2 µM. In addition, MAKV-15 has an IC_{50} inhibitory activity against HDAC1 and HDAC6 of 380 nM and 30 nM, respectively, whereas IC_{50} values of tubastatin A against the same enzymes are 2.9 µM and 0.8 µM, respectively (Figure 51). Based on the ratio between IC_{50} values against HDAC1 versus HDAC6, both compounds show selectivity towards HDAC6 but MAKV-15 has a higher potency of about 3 times.

A.

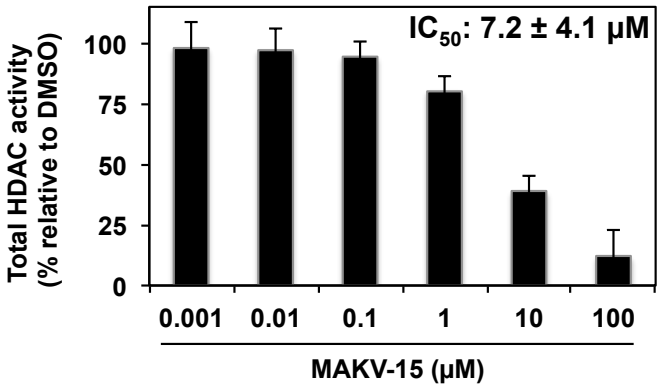

B.

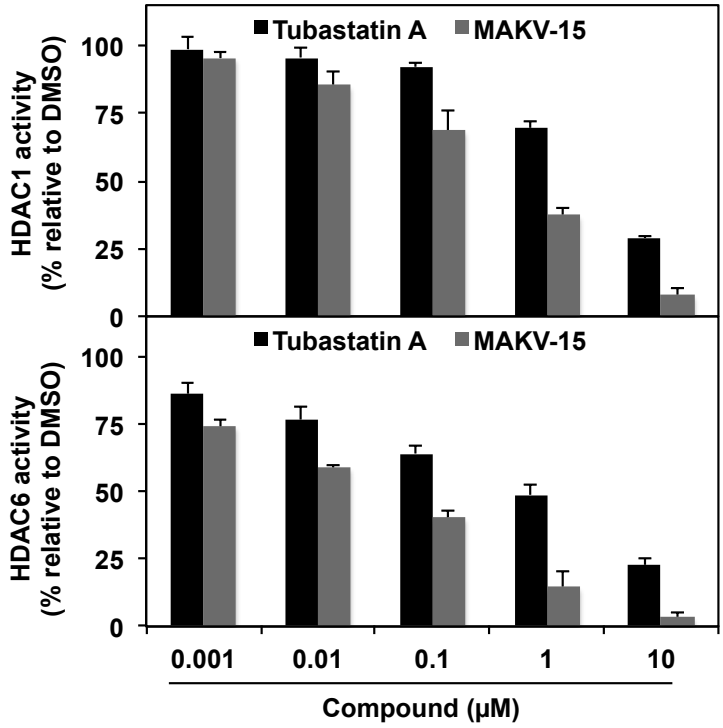

C.

Compound	IC_{50} HDAC1 (nM)	IC_{50} HDAC6 (nM)	IC_{50} ratio (HDAC1/HDAC6)
Tubastatin A	2913±323	751±142	3.9
MAKV-15	379.8±82.3	28.8±7.6	13.2

Figure 51: Effect of MAKV-15 and tubastatin A on the activity of total HDAC and HDAC isoenzymes.

In vitro HDAC activity assays were performed with increasing concentrations of MAKV-15 and tubastatin A. Relative activities of (A) total HDAC, (B) HDAC1 and HDAC6 were determined by comparison to the vehicle, and (C) IC_{50} values for each HDAC activities were calculated using nonlinear regression from Prism software. Results correspond to mean ± SD of at least three independent experiments. IC_{50}: concentration inhibiting 50% of enzymatic activity.

In silico, MAKV-15 displays favorable druglikeness parameters and a low predicted risk of toxicity similar to HDAC6i already used in clinical trials (*i.e.* ACY-1215 and ACY-241) (Table 12). For instance, MAKV-15 has low lipophilicity, as characterized by an octanol-water partition coefficient Log *P* lower than 5, which is a major criterion for orally active drugs. The molecular flexibility of MAKV-15 for membrane permeation, as defined by the number of rotatable bonds, and its drug transport properties predicted by topological polar surface area are favorable, as well as its intestinal absorption parameter and plasma protein binding potential, predicting a good bioavailability (Table 12).

Table 12: *In silico* prediction of the MAKV-15 druglikeness and oral bioavailability based on Lipinski's Rule of Five extended with Ghose filter and on Veber's Rule.

Method	**Parameter (unit)**	**Values**				
		Theoretical	**MAKV-15**	**Tubastatin A**	**ACY-1215**	**ACY-241**
Lipinski's rule of five	Volume (Å^3)	NA	309.93	309.93	398.21	416.47
	Log*P*	≤5	2.71	2.71	-0.07	4.31
	MW (Da)	≤500	335.41	335.41	436.5	467.96
	n-OHNH	≤5	2	2	3	3
	n-ON	≤10	5	5	9	8
Ghose filter	n-atoms	20≤ x ≤70	25	25	32	33
Veber's Rule	n-rotb	≤10	3	3	11	11
	TPSA (Å^2)	≤140	57.5	57.5	118.62	107.45
Absorption	BBBP	0.1≤ MA ≤2	0.53	0.44	0.17	0.36
	IA (%)	≥70	94.49	94.49	92.23	93.44
	PPB (%)	<90	54.91	55.67	87.23	86.14
Toxicity	Rat	NA	Negative	Negative	Negative	Negative
	Mouse	NA	Negative	Negative	Negative	Negative

BBBP: blood-brain barrier penetration; IA: intestinal absorption; MA: middle absorption; Log*P*: octanol-water partition coefficient; MW: molecular weight; n-: number of; OHNH: hydrogen bond donors; ON: hydrogen bond acceptors; rotb: rotatable bonds; NA: not applicable; PPB: plasma protein binding; TPSA: topological polar surface area.

2.2. *In cellulo* study of MAKV-15 and tubastatin A

2.2.1. Study of MAKV-15 in CML cells

2.2.1.1. MAKV-15 acts as a potent HDAC6i in CML cells

In order to determine the inhibitory profile of MAKV-15 and tubastatin A *in cellulo*, we next analyzed by western blot the effect of increasing concentrations of compounds on the acetylation levels of histone H4 and α-tubulin. In K-562 cells, tubastatin A induces the acetylation of histone H4 and α-tubulin observed from 1 and 5 µM, respectively, and the maximal acetylation level is reached between 15 and 25 µM for both proteins. By comparison, MAKV-15 induces the acetylation of histone H4 and α-tubulin detected from 1 µM for both proteins. For histone H4, the maximal acetylation level is reached between 15 and 25 µM, while it is reached between 5 and 15 µM for α-tubulin (Figure 52A). Since EC_{50} values against acetyl α-tubulin and acetyl histone H4 are 35 and 25 µM, respectively for tubastatin A, and 4 and 17 µM, respectively for MAKV-15 (Figure 52A), MAKV-15 displays an increased selectivity against HDAC6 of around 4 times whereas tubastatin A acts similarly on both targets.

Additionally, kinetic analysis of histone H4 and α-tubulin acetylation status shows that MAKV-15 at 5 µM induces only a strong increase of α-tubulin acetylation peaking between 4 and 24 hours, whereas 25 µM tubastatin A induces the acetylation of α-tubulin and histone H4 noted after 1 hour and peaking between 8 and 24 hours (Figure 52B).

In conclusion, MAKV-15 acts as a more potent HDACi than its parent compound and displays an increased selectivity against HDAC6 *vs.* HDAC1 *in vitro* and *in cellulo*.

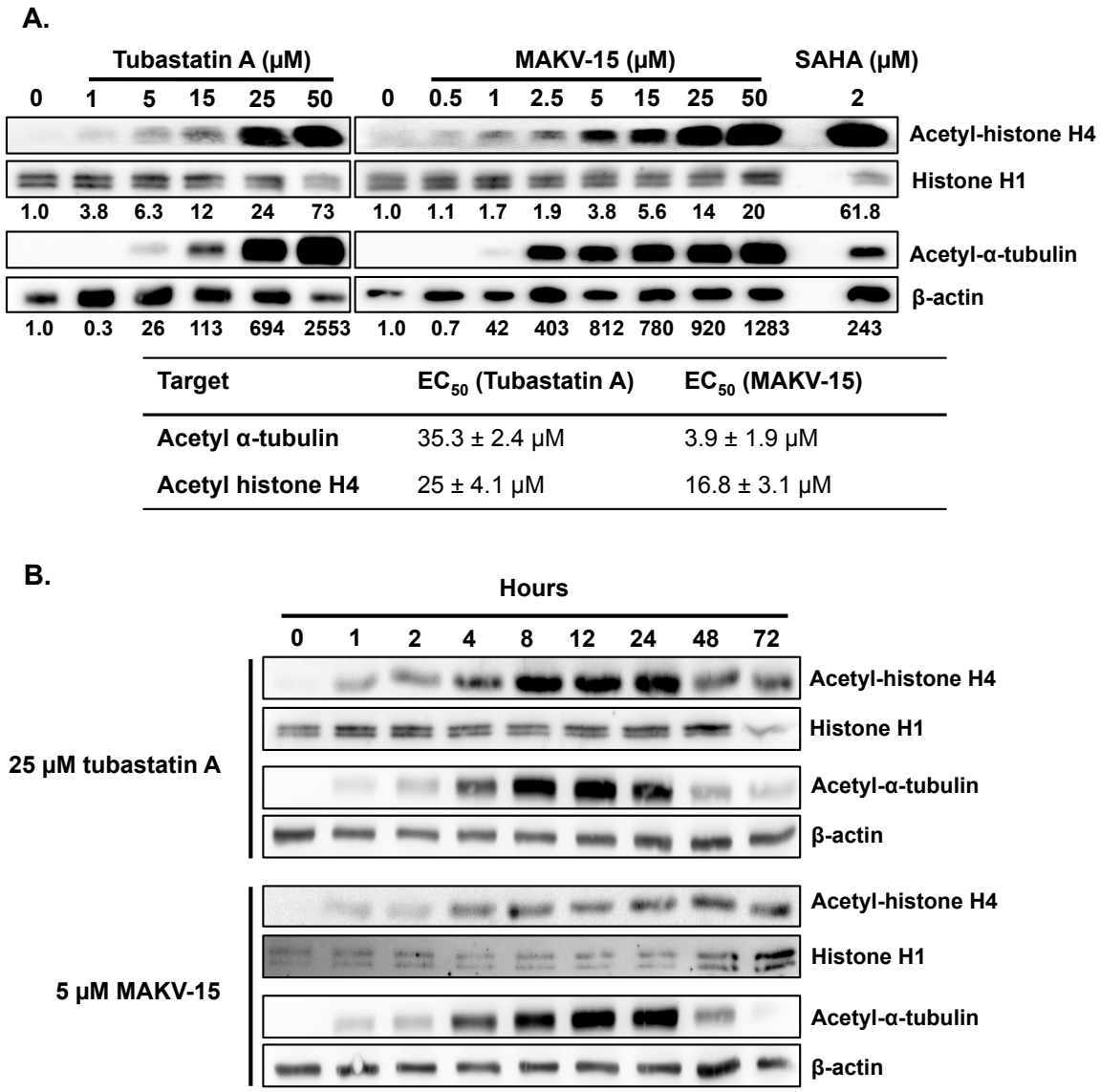

Target	EC_{50} (Tubastatin A)	EC_{50} (MAKV-15)
Acetyl α-tubulin	35.3 ± 2.4 μM	3.9 ± 1.9 μM
Acetyl histone H4	25 ± 4.1 μM	16.8 ± 3.1 μM

Figure 52: Effect of MAKV-15 and tubastatin A on the acetylation of histone H4 and α-tubulin in K-562 cells.

K-562 cells were treated with (A) increasing concentrations of MAKV-15 or tubastatin A for 24 hours, and (B) 25 μM tubastatin A or 5 μM MAKV-15 for the indicated period of time. Acetylation of histone H4 and α-tubulin was assessed by western blot, with β-actin and histone H1 as loading control for α-tubulin and histone H4, respectively. SAHA was used as a reference HDACi. Quantification values are indicated underneath corresponding blots that are representative of three independent experiments. EC_{50} values (*i.e.* 50% of the maximum effect) were determined using prism software and represent the mean ± SD of three independent experiments.

2.2.1.2. Selectively inhibiting HDAC6 is insufficient to reduce CML cell proliferation and viability

We further evaluated whether treatments with MAKV-15 and tubastatin A exert anticancer properties. K-562 cells were incubated with increasing concentrations of compounds, and their proliferation and viability were assessed after up to 72 hours of

treatment using a Trypan blue assay. Results demonstrate that MAKV-15 and tubastatin A both generate similar effects on cell proliferation and viability. Inhibition of the proliferation is detected from 33.3 µM MAKV-15 or tubastatin A after 24 hours, while an increase of cell death is observed from 33.3 µM MAKV15 or tubastatin A after 48 hours. After 24 hours of treatment with 100 µM MAKV-15 or tubastatin A, cell viability is reduced of 30% or 45%, respectively (Figure 53).

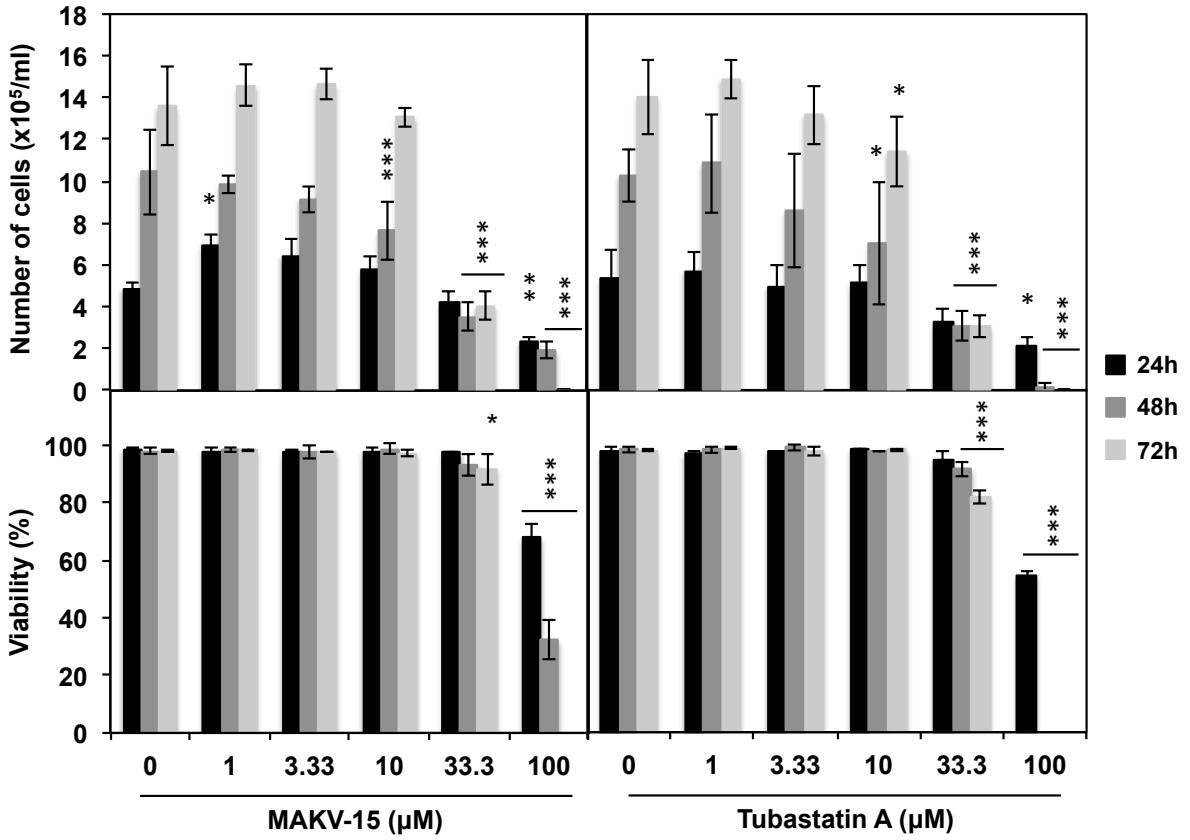

Figure 53: Effect of MAKV-15 and tubastatin A on K-562 cell proliferation and viability.
K-562 cells were treated with increasing concentrations of MAKV-15 or tubastatin A for up to 72 hours, and cell proliferation and viability were assessed based on the Trypan Blue exclusion method. Results correspond to mean ± SD of three independent experiments and were analyzed by a two-way ANOVA with *, **, *** indicating $p < 0.05$, $p < 0.01$, $p < 0.001$, respectively.

2.2.1.3. High concentrations of MAKV-15 induce cell cycle arrest and apoptotic cell death in CML cells

As treatment of cells with high concentrations of MAKV-15 and tubastatin A hampers K-562 cell proliferation, the effect of compounds on the cell cycle distribution was studied by flow cytometry after 24 hours of treatment. Globally, cells progressively accumulate in G_1

phase in a time and concentration-dependent manner. After a treatment with 25 µM MAKV-15 or tubastatin A, 71 or 62% of cells accumulate in G_1 phase, respectively (Figure 54A).

Despite the lack of acute cytotoxicity of those compounds, the prolonged cell cycle arrest is followed by apoptotic cell death, as observed by nuclear morphology analysis, reaching about 20 and 100% of mortality after 72 hours of treatment with 50 and 100 µM MAKV-15, or 25 and 50 µM tubastatin A, respectively (Figure 54B). Of note, cell death experiments were only performed twice because the concentrations of MAKV-15 and tubastatin A needed to observe apoptosis induction will not be used in further experiments.

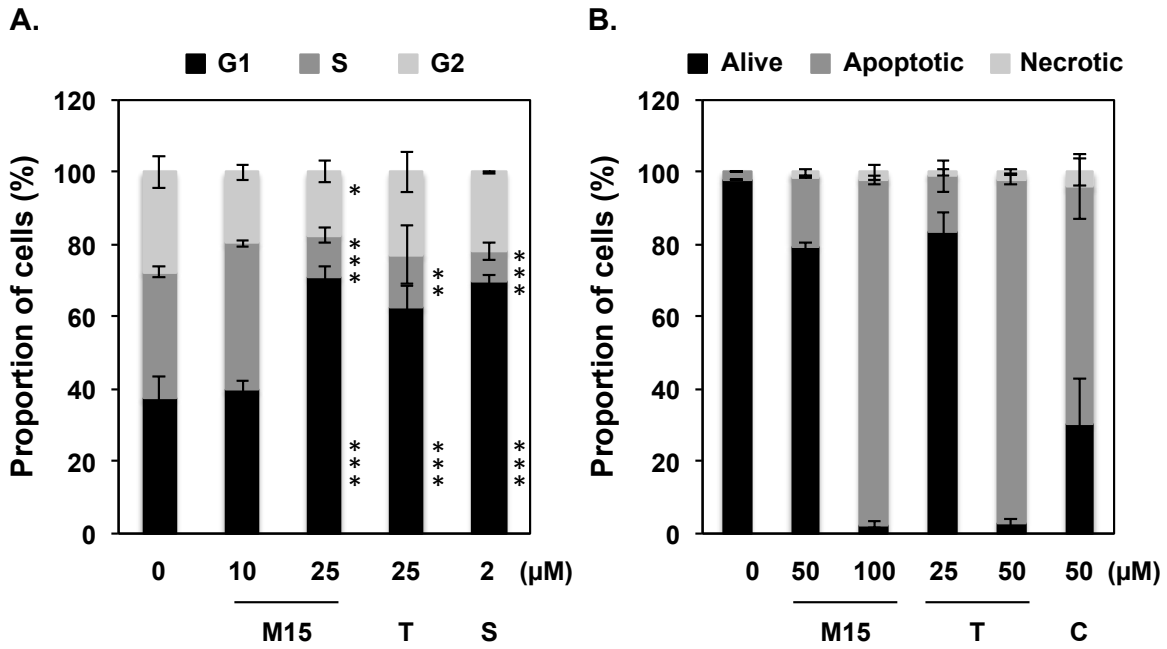

Figure 54: Effect of MAKV-15 and tubastatin A on K-562 cell cycle (A) and cell death (B).
(A) K-562 cells were treated with the indicated concentrations of MAKV-15 (M15) or tubastatin A (T) for 24 hours. Distribution of cells in the three phases of cell cycle was obtained after their staining with propidium iodide and analysis by flow cytometry. SAHA (S) was used as a standard HDACi. Results correspond to mean ± SD of three independent experiments and were analyzed by two-way ANOVA with *, **, *** indicating $p < 0.05$, $p < 0.01$, $p < 0.001$, respectively. (B) K-562 cells were treated with the indicated concentrations of MAKV-15 (M15) or tubastatin A (T) for 72 hours. The study of nuclear morphology was performed by fluorescence microscopy after Hoechst-propidium iodide staining. Cisplatin (C) was used as positive control for apoptosis induction. Results correspond to mean ± SD of two independent experiments.

In conclusion, since the reduction of proliferation and the induction of K-562 cell death occur only at concentrations for which acetylation of histones is induced, MAKV-15 anticancer properties seem to be unrelated to the HDAC6 inhibition.

2.2.2. Study of MAKV-15 in MM cells

2.2.2.1. MAKV-15 acts as a potent HDAC6i in MM cells

Two HDAC6i, ACY-1215 (Rocilinostat) and ACY-241 (Citarinostat), are undergoing clinical trials for the treatment of MM, usually in combination treatments with the proteasome inhibitor bortezomib, or an immunomodulatory agent such as dexamethasone (www.clinicaltrials.gov). Since ACY-1215 reportedly presents a more potent *in vitro* selectivity against HDAC6 of about 10 times compared to HDAC1, HDAC2 and HDAC3 (Santo *et al.*, 2012), we aimed to assess the inhibitory profile of this compound in our cell model (*i.e.* U266 cells) by evaluating by western blot its effect on the acetylation levels of histone H4 and α-tubulin. ACY-1215 induces the acetylation of α-tubulin and histone H4 detected from 0.1 and 1 µM, respectively, and the maximal acetylation level is reached at 10 µM for both proteins (Figure 55A). Nevertheless, EC_{50} values against acetyl α-tubulin and acetyl histone H4 are 3.1 µM and 4.5 µM, respectively.

To determine whether MAKV-15 and tubastatin A were selective HDAC6i in the MM cell lines U-266 and MOLP-8, their effects were evaluated by western blot on acetylation of α-tubulin and histone H4. In both cell lines, MAKV-15 induces an increase in the acetylation of α-tubulin and histone H4 in a concentration-dependent manner, observed from 0.25 and 5 µM, respectively. By comparison, tubastatin A induces the acetylation of histone H4 and α-tubulin noted from 1 µM for both proteins (Figure 55A and B). Surprisingly, EC_{50} values determined for MAKV-15 against acetylated protein targets are within the same range of concentrations in U-266 cells. In MOLP-8 cells, EC_{50} values against acetyl α-tubulin and acetyl histone H4 are 25.5 and 11.5 µM, respectively for tubastatin A, and 3 and 22.5 µM, respectively for MAKV-15. Based on EC_{50} values, MAKV-15 displays selectivity for HDAC6 of around 7 times in MOLP-8 cells.

Additionally, kinetic analysis of histone H4 and α-tubulin acetylation status shows that MAKV-15 at 1 µM only induces a time-dependent increase in α-tubulin acetylation, whereas 10 µM tubastatin A induces the acetylation of α-tubulin and histone H4 after 1 hour, with a peak occurring between 8 and 24 hours for acetyl-α-tubulin or being maintained at later time for acetyl-histone H4 (Figure 55C).

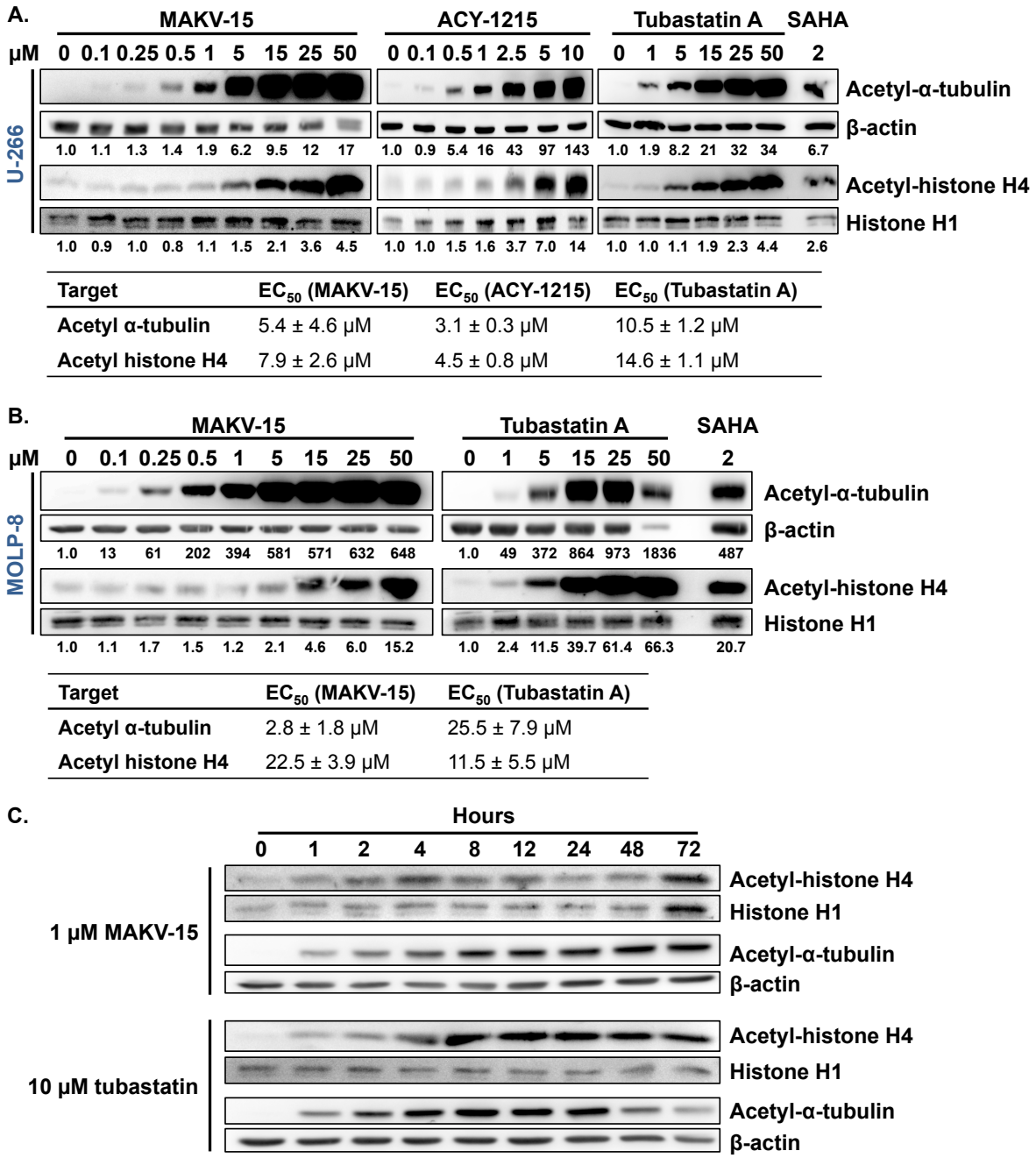

Target	EC_{50} (MAKV-15)	EC_{50} (ACY-1215)	EC_{50} (Tubastatin A)
Acetyl α-tubulin	5.4 ± 4.6 µM	3.1 ± 0.3 µM	10.5 ± 1.2 µM
Acetyl histone H4	7.9 ± 2.6 µM	4.5 ± 0.8 µM	14.6 ± 1.1 µM

Target	EC_{50} (MAKV-15)	EC_{50} (Tubastatin A)
Acetyl α-tubulin	2.8 ± 1.8 µM	25.5 ± 7.9 µM
Acetyl histone H4	22.5 ± 3.9 µM	11.5 ± 5.5 µM

Figure 55: Effect of MAKV-15, ACY-1215, and tubastatin A on the acetylation of histone H4 and α-tubulin in U-266 and MOLP-8 cells.

(A) U-266 cells were treated with increasing concentrations of MAKV-15, ACY-1215, or tubastatin A for 24 hours. (B and C) MOLP-8 cells were treated with (B) increasing concentrations of MAKV-15 or tubastatin A for 24 hours, and (C) 10 µM tubastatin A or 1 µM MAKV-15 for the indicated period of time. Acetylation of histone H4 and α-tubulin was assessed by western blot, with histone H1 and β-actin as loading control, respectively. SAHA was used as a reference HDACi. Quantification values are indicated underneath corresponding blots that are representative of three (or two for MAKV-15 and tubastatin A in U-266 cells) independent experiments. EC_{50} values (*i.e.* 50% of the maximum effect) were determined using prism software and represent the mean ± SD of three (or two for MAKV-15 and tubastatin A in U-266 cells) independent experiments.

2.2.2.2. Selectively inhibiting HDAC6 is insufficient to reduce MM cell proliferation and viability

We further evaluated whether treatments with MAKV-15, ACY-1215 ant tubastatin A exert anticancer properties against MM cells. A Trypan blue exclusion test was performed to assess their effect on proliferation and viability of U-266 and MOLP-8 cells incubated with increasing concentrations of compounds for up to 72 hours. Our results demonstrate that MAKV-15 and tubastatin A generate similar effects on U-266 and MOLP-8 cell proliferation and viability but starting at different concentrations. In U-266, decreased proliferation is noted after 72 hours of treatment with MAKV-15 and tubastatin A starting from a concentration of 5 and 1 µM, respectively, whereas cell death is induced at 50 µM MAKV-15 and 15 µM tubastatin A. By comparison, a 72-hour treatment with ACY-1215 inhibits proliferation and triggers cell death from 1 and 5 µM, respectively. After 48 hours of treatment with 10 µM ACY-1215 or 72 hours of treatment with 25 µM tubastatin A, cell viability is reduced of 60%, whereas MAKV-15 at concentrations up to 50 µM fails to induce more than 35% reduction of cell viability (Figure 56A). In MOLP-8 cells, inhibition of proliferation is detected from 5 µM MAKV15 or 1 µM tubastatin A, while an increase of cell death is observed from 15 µM MAKV15 or 5 µM tubastatin A after 72 hours. After 48 hours of treatment with 25 µM MAKV-15 or tubastatin A, cell viability is reduced of 30 or 55%, respectively (Figure 56B).

In conclusion, MAKV-15 shows a higher selectivity towards HDAC6 in MM cells compared to K-562 CML cells. Since the reduction of proliferation and the induction of MM cell death occur only at concentrations for which acetylation of histones is induced, MAKV-15 anticancer properties seem to be unrelated to the HDAC6 inhibition.

Additionally, the selectivity of MAKV-15 against HDAC6 is higher than that of ACY-1215 in our cell models, accompanied by lower MAKV-15-mediated toxicity compared to ACY-1215.

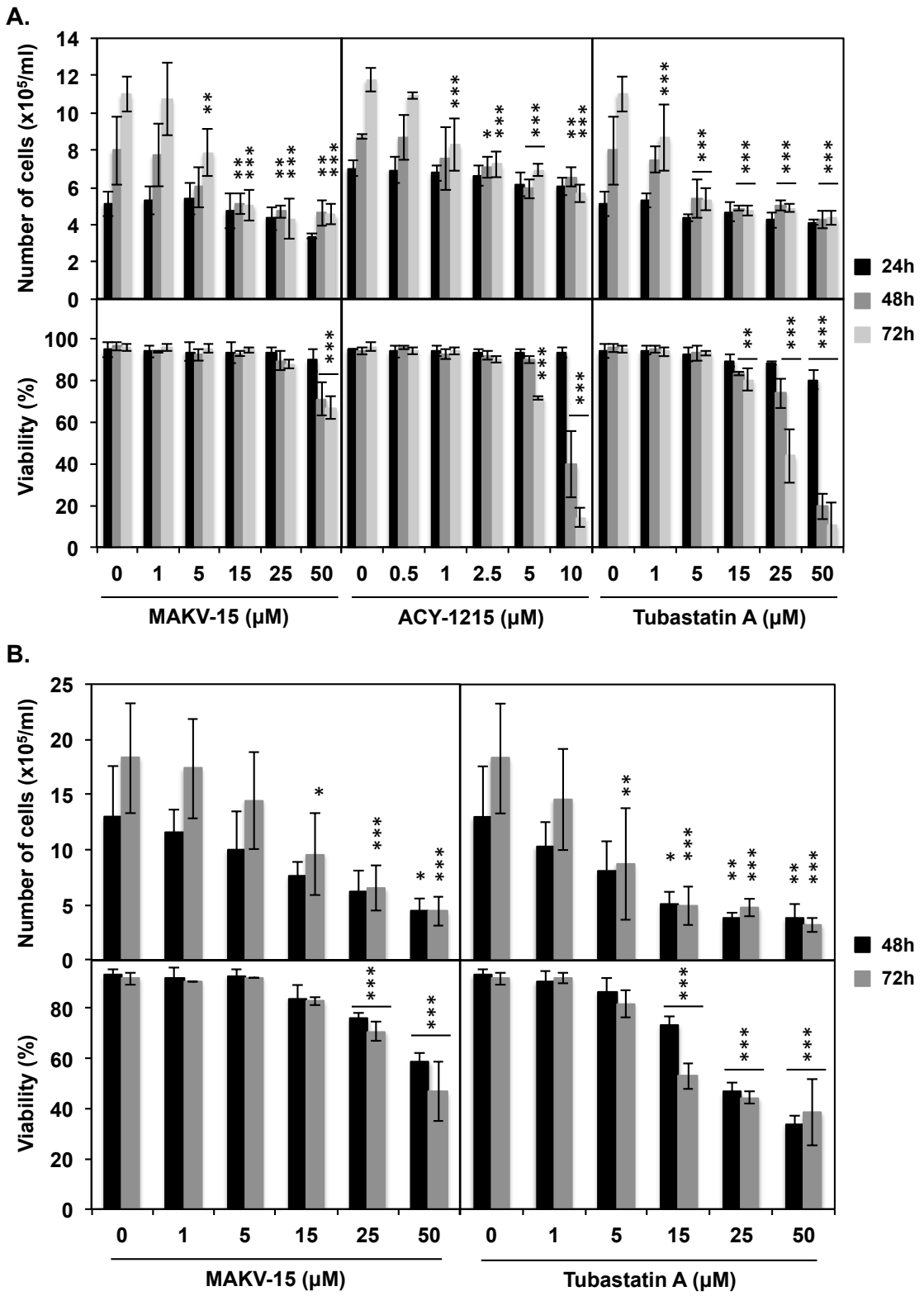

Figure 56: Effect of MAKV-15, ACY-1215, and tubastatin A on proliferation and viability of U-266 and MOLP-8 cells.

(A) U-266 cells were treated with increasing concentrations of MAKV-15, ACY-1215 or tubastatin A for up to 72 hours and (B) MOLP-8 cells were treated with increasing concentrations of MAKV-15 or tubastatin A for 48 and 72 hours. Cell proliferation and viability were assessed based on the Trypan Blue exclusion method. Results correspond to mean ± SD of three independent experiments and were analyzed by a two-way ANOVA with *, **, *** indicating $p < 0.05$, $p < 0.01$, $p < 0.001$, respectively.

The present findings provide a rationale to further assess the potential of hydroxamate-based HDAC6i in combination treatments as a novel therapeutic approach for MM.

2.2.2.3. HDAC6i in combination with bortezomib in MM

Inhibition of the proteasome leads to an accumulation of poly-ubiquitinated proteins, which can be reversed when the aggresome pathway, an alternative way to clear misfolded proteins, is activated. Since HDAC6 is implicated in several steps of the aggresome pathway (Ouyang *et al.*, 2012), we sought to test by nuclear morphology analysis whether combination treatments with bortezomib and MAKV-15 or tubastatin A displayed at least an additional effect on cell death. In that purpose, MOLP-8 cells were treated with increasing concentrations of bortezomib, MAKV-15 or tubastatin A for 48 and 72 hours (Figure 57A), or co-treated with 5 µM MAKV-15 or tubastatin A and 5 nM bortezomib for 72 hours (Figure 57B). To focus only on the impact of HDAC6 inhibition in combination treatment with bortezomib, we used MAKV-15 concentrations for which we observed only an induction of acetyl-α-tubulin, by comparison with tubastatin A that acts as a pan-HDACi. The reduction of viability mediated by the co-treatments is more important than the one triggered by each compound alone at 48 (data not showed) and 72 hours (Figure 57B), with a diminution of 30 and 60% of living cells after a 72-hour treatment with bortezomib in combination with MAKV-15 and tubastatin A, respectively.

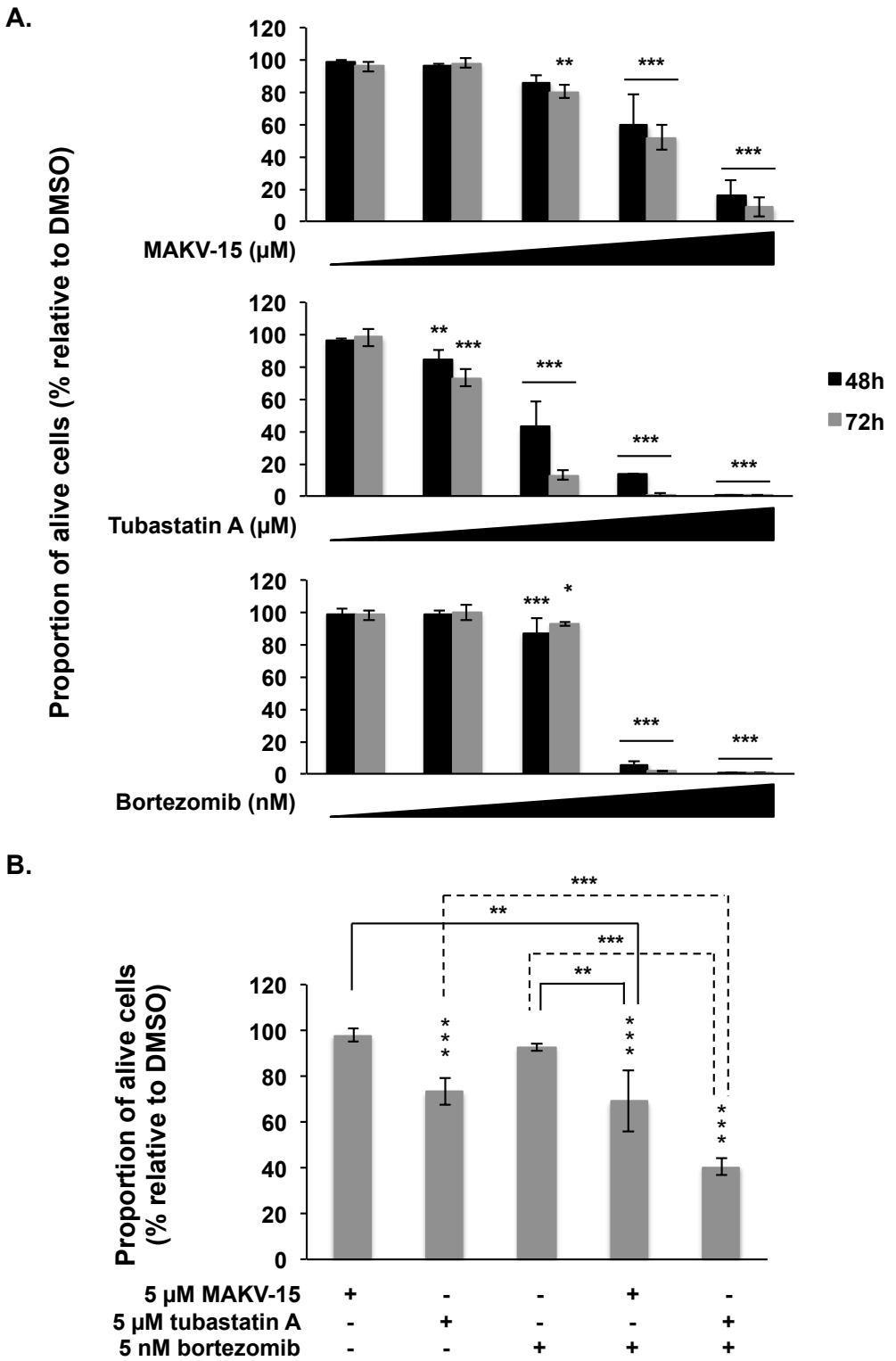

Figure 57: Effect of co-treatment with MAKV-15 or tubastatin A, and bortezomib on MOLP-8 cell death.

MOLP-8 cells were treated with (A) increasing concentrations of MAKV-15 (1, 5, 15, 25, 50 µM), tubastatin A (1, 5, 15, 25, 50 µM) or bortezomib (1, 2.5, 5, 10, 25 nM**)** for 48 and 72 hours, or (B) a combination of 5 µM MAKV-15 or tubastatin A and 5 nM bortezomib for 72 hours. The study of nuclear morphology was performed by fluorescence microscopy after Hoechst-PI staining. Results correspond to mean ± SD of three independent experiments and were analyzed by a two-way ANOVA with *, **, *** indicating $p < 0.05$, $p < 0.01$, $p < 0.001$, respectively.

We further assessed by western blot whether an increased accumulation of poly-ubiquitinated proteins was observed in MOLP-8 cells treated with MAKV-15 or tubastatin A, and bortezomib alone or in combination for 24 and 48 hours. By comparison to treatments with MAKV-15 or tubastatin A alone, bortezomib treatment stimulates the accumulation of poly-ubiquitinated proteins only after 24 hours. Co-treatment with MAKV-15 and bortezomib further enhances poly-ubiquitinated protein accumulation, whereas the increase of poly-ubiquitinated proteins observed after tubastatin A-bortezomib co-treatment is similar to treatment with bortezomib alone after 24 hours. After 48 hours, both co-treatments result in the accumulation of poly-ubiquitinated proteins (Figure 58).

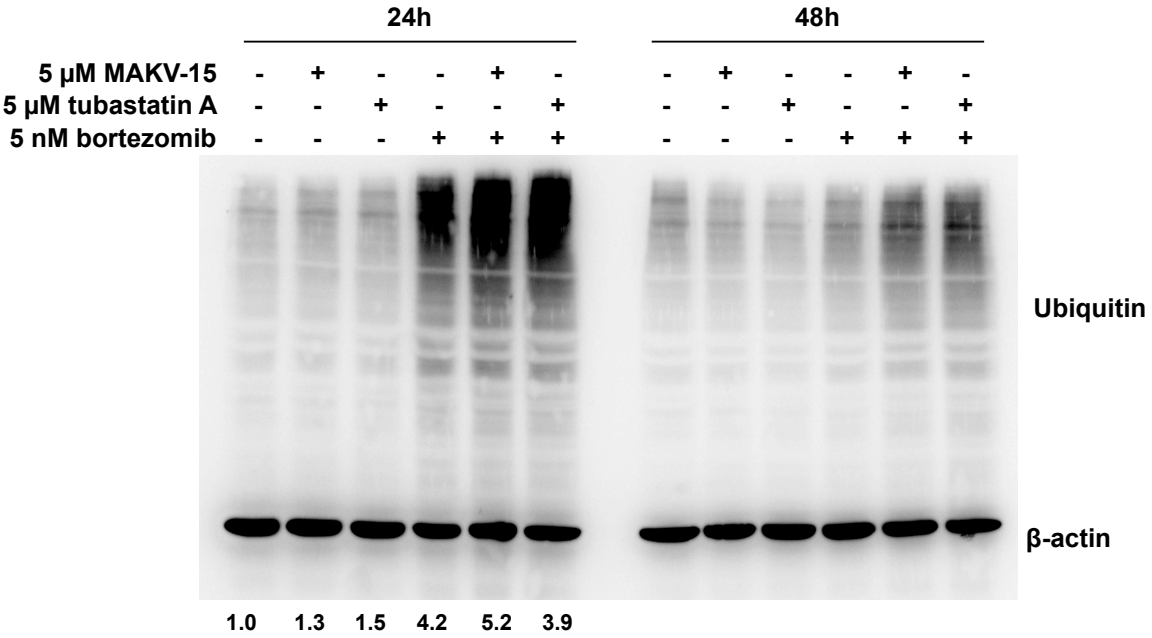

Figure 58: Effect of co-treatments bortezomib-MAKV-15 or tubastatin A on the accumulation of poly-ubiquitinated proteins in MOLP-8 cells.
MOLP-8 cells were treated with two concentrations of MAKV-15, 5 µM tubastatin A or 5 nM bortezomib, or co-treated for 24 and 48 hours. The accumulation of poly-ubiquitinated proteins was assessed by western blot, with β-actin as loading control. Quantification values are indicated underneath corresponding blots that are representative of three independent experiments.

In conclusion, a potentiation of the anticancer effects accompanied with a stronger accumulation of poly-ubiquitinated proteins are observed in MOLP-8 cells concomitantly treated with MAKV-15 and bortezomib.

2.2.2.4. HDAC6i in a tri-therapy for MM

Despite a moderate induction of cell death by MAKV-15-bortezomib co-treatments, we expect that this bi-therapy provokes the saturation of misfolded protein elimination pathways. This could then lead to decreased acquired cell resistance to commonly used chemotherapies and a sensitization to a third compound.

2.2.2.4.1. Screening of chemotherapeutical compounds for efficient tri-therapies in combination with HDAC6i and bortezomib

In the literature, various drugs are currently evaluated for the treatment of MM, mostly in combination treatments. Initially, we selected three drugs (*i.e.* cisplatin, dexamethasone, and doxorubicin) in concentrations found in the literature and the study of nuclear morphology allowed to assess their effects on cell viability when combined with MAKV-15 or tubastatin A, and bortezomib. Since tri-therapies with MAKV-15 fail to induce a pronounced decrease of living cell percentage, the investigations for those compounds were stopped (Annex A6).

Deregulated activation of mTOR signaling pathway is considered to be associated with drug resistance and poor prognosis in many cancers including MM. Furthermore, various studies have highlighted that inhibition of the PI3K-AKT-mTOR axis could be a promising strategy for MM therapy (Han *et al.*, 2015). Therefore, we evaluated the effect of a tri-therapy combining MAKV-15 or tubastatin A, bortezomib and rapamycin, an inhibitor of the mTOR pathway, on MOLP-8 cell viability by nuclear morphology analysis. The concentration of rapamycin used in our experiments (*i.e.* 0.1 µM) was chosen based on the literature. After 72 hours of treatment, living cell percentage is strikingly lowered by the combination of MAKV-15 or tubastatin A with bortezomib and rapamycin compared with each reagent alone. Nevertheless, only a mild decrease in cell viability is obtained after addition of MAKV-15 or tubastatin A to the combination bortezomib-rapamycin since the latter already induces a reduction of 89% of alive cells, which is close to maximal effect (Figure 59). Noteworthy, such tri-therapy is only effective in MOLP-8 cells but not in the other MM cell lines tested (data not shown).

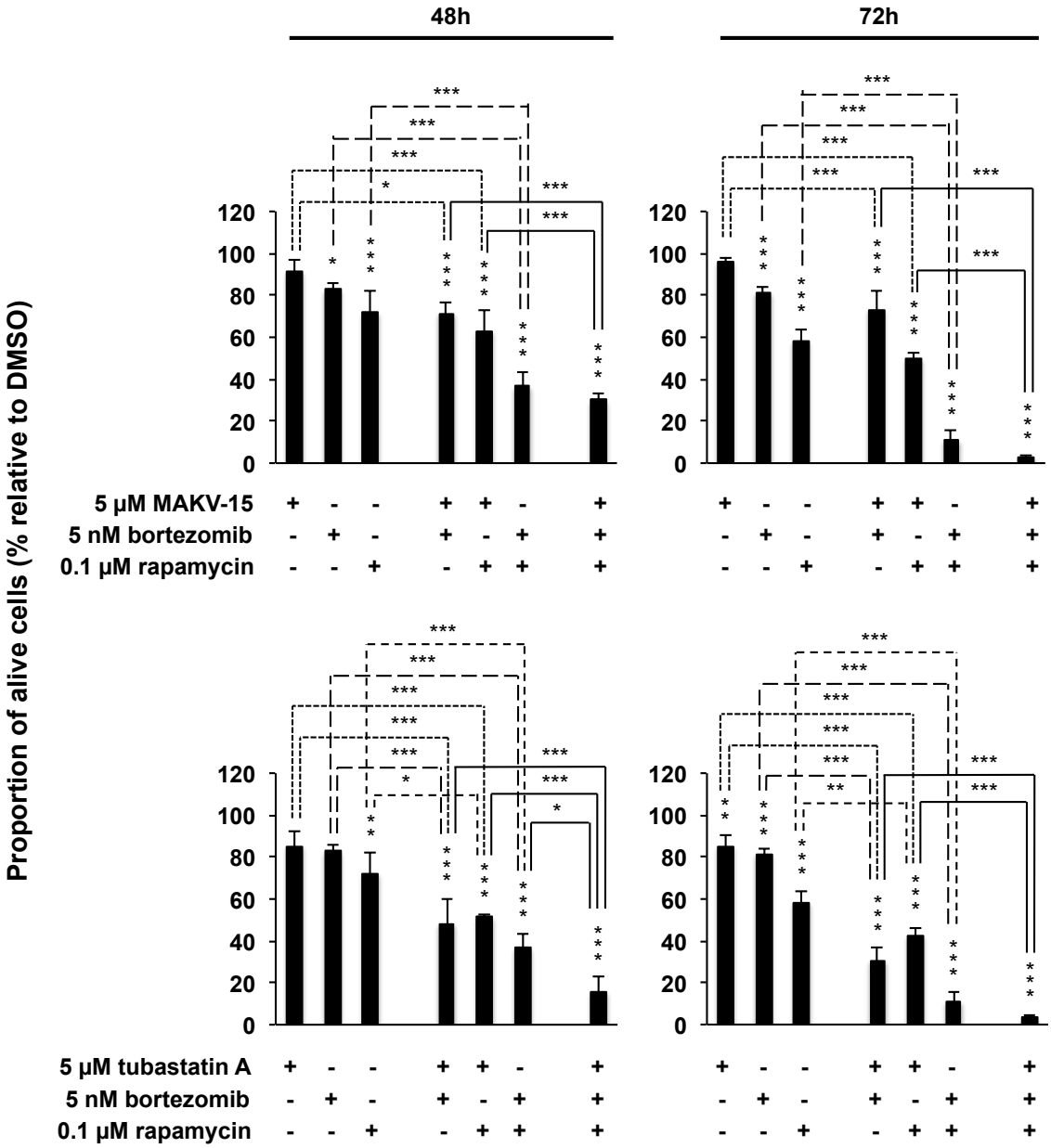

Figure 59: Effect of co-treatments with bortezomib, rapamycin and MAKV-15 or tubastatin A on MOLP-8 cell death.

MOLP-8 cells were co-treated with 5 nM bortezomib, 0.1 µM rapamycin and 5 µM MAKV-15 or tubastatin A for 48 hours. The study of nuclear morphology was performed by fluorescence microscopy after Hoechst-PI staining. Results correspond to mean ± SD of three independent experiments and were analyzed by a one-way ANOVA with *, **, *** indicating $p < 0.05$, $p < 0.01$, $p < 0.001$, respectively.

2.2.2.4.2. BCL-2 family protein inhibitors as a third compound for efficient tri-therapies in combination with HDAC6i and bortezomib

Accumulating evidence has demonstrated the importance of the pro-survival BCL-2 family proteins in the maintenance of MM cell viability, implying that potent inhibitors of BCL-2 family proteins would be clinically effective (Gong *et al.*, 2016; Touzeau *et al.*, 2018).

Therefore, we have further assessed the potency of a tri-therapy on a panel of MM cell lines representative of various cytogenetic backgrounds. Based on their differential sensitivity to each tested inhibitor, selected cells have been co-treated with HDAC6i, bortezomib, and BCL-2 family protein inhibitors, and the anticancer activity evaluated.

The constitutive expression levels of various proteins were first assessed by western blot in a panel of 10 MM cell lines to evaluate the differential sensitivity to each tested inhibitor. All cells express HDAC6, albeit with highly distinct abundance (Figure 60), suggesting that they could be variably responsive to MAKV-15. Since MM cell lines are generally characterized by an increased ER stress due to the excessive antibody production, the expression level of GRP78 was studied as a marker of the ER stress intensity, which could be predictive to differential sensitivities of the cells towards bortezomib. Results show that all cell lines express GRP78 at diverse levels (Figure 60). Finally, we investigated expression levels of BCL-2 family proteins. These results demonstrate that more or less all cells express MCL-1 whereas some cell lines do not express BCL-2 or BCL-xL (Figure 60), implying that they do not rely on the same anti-apoptotic family member for their survival and might be differentially responsive to selective inhibitors.

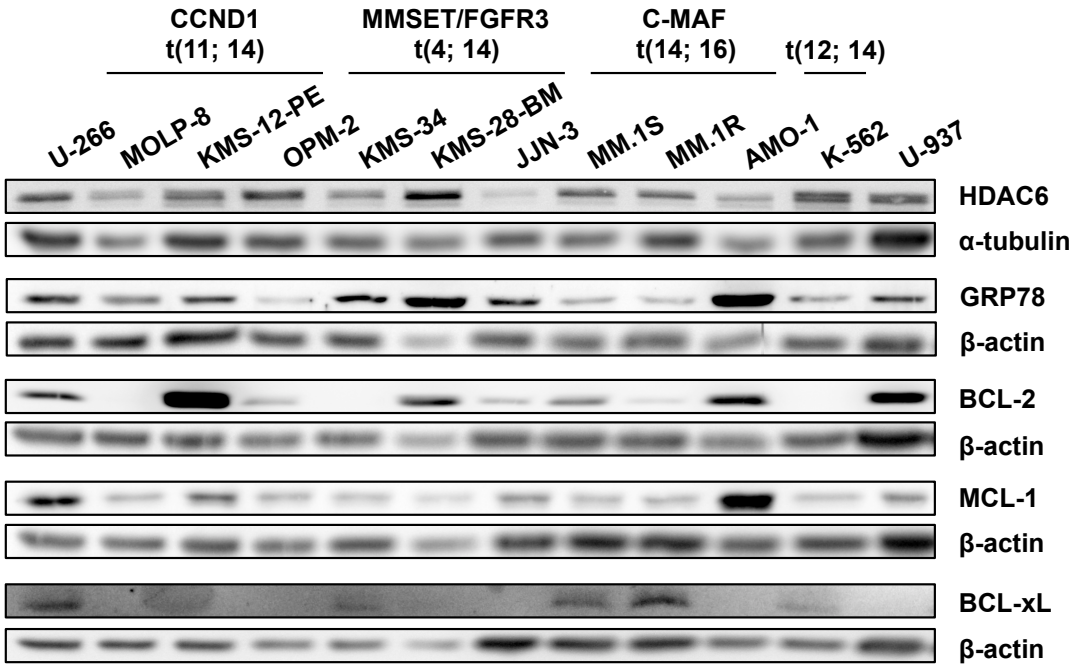

Figure 60: Evaluation of the constitutive expression level of five proteins in 10 MM cell lines.
The expression levels of HDAC6, GRP78, BCL-2, MCL-1 and BCL-xL were assessed in various MM cell lines by western blot, with α-tubulin or β-actin as loading controls. K-562 (CML) and U-937 (histiocytic lymphoma) cell lines were use as reference. Blots are representative of three independent experiments. CCND1: cyclin D1; FGFR: fibroblast growth factor receptor; MMSET: multiple myeloma SET domain; t: translocation.

We then tested whether MM cell lines respond to MAKV-15-mediated HDAC6 inhibition. To study the inhibitory profile of MAKV-15 in MM cell lines, we analyzed its effect on the acetylation levels of histone H4 and α-tubulin by western blot. The 10 MM cell lines were treated for 8, 24 and 48 hours with a MAKV-15 concentration for which we observed a selective inhibition of HDAC6 in MOLP-8 and U-266 cells. Surprisingly, while most cell lines display a profile of response similar to the one observed in MOLP-8 cells (*i.e.* a strong induction of acetyl-α-tubulin associated with a weak or no increase of histone H4 acetylation), a subset of cell lines present a weaker response (*e.g.* KMS-34) or fail to respond to MAKV-15 (*e.g.* KMS-12-PE) (Figure 61). Of note, the cell lines that do not respond to MAKV-15-induced HDAC6 inhibition are also unresponsive to SAHA treatment.

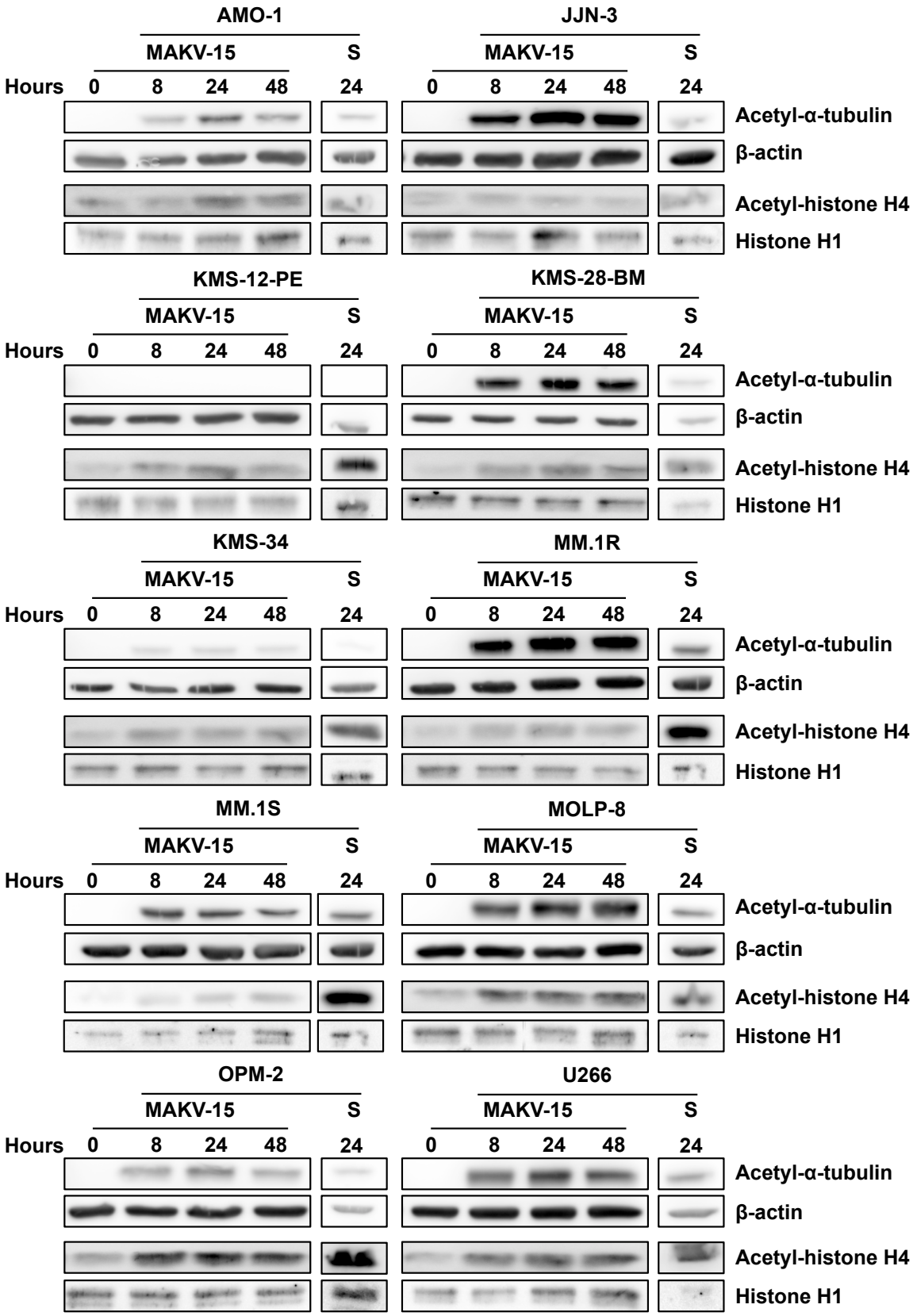

Figure 61: Effect of MAKV-15 on the acetylation of histone H4 and α-tubulin in MM cell lines. MM cells were treated with 5 µM MAKV-15 for the indicated time points. Acetylation of histone H4 and α-tubulin was assessed by western blot, with β-actin and histone H1 as loading control for α-tubulin and histone H4, respectively. SAHA (S, 2 µM) was used as a reference HDACi. Blots are representative of two independent experiments.

Finally, we evaluated by nuclear morphology analysis whether a tri-therapy combining MAKV-15 compared to FDA-approved ACY-1215, bortezomib, and BCL-2 family protein inhibitors could be effective against MM cell lines. The optimal concentration of bortezomib, ABT-199 (BCL-2 inhibitor), A1210477 and S63845 (MCL-1 inhibitor) used in combination with HDAC6i was preliminarily determined by treating each MM cell lines with increasing concentrations of compounds for 48 hours and selecting concentrations that induces low cell toxicity, *i.e.* less than 10-20% of cell death (Annex A7). Since viability of MM cell was not markedly impacted by simultaneous treatment with the three types of compounds for 48 hours (data not shown), we chose 5 MM cell lines for which preliminary results seemed promising and tested tri-therapies for 72 hours keeping the same concentrations of compounds.

Tri-therapies with MAKV-15 do not substantially affect KMS-28BM cell viability, with maximum decrease of 41% of alive cells. In AMO-1 and JJN-3 cell lines, the effect observed on cell viability upon treatment with three compounds is close to those obtained after combination of bortezomib and BCL-2 family proteins inhibitors. Indeed, addition of MAKV-15 further reduces cell viability of maximum 14 and 22% in AMO-1 and JJN-3 cells, respectively, reaching 28 and 37% of living cells following tri-therapies with ABT-199. Conversely, combinations of three inhibitors strikingly decrease MOLP-8 and U-266 cell viability, and a loss of 87 and 100% of living cells occurs after tri-therapies with ABT-199. Nevertheless, close to maximal effect is already observed after co-treatments with bortezomib and BCL-2 family proteins inhibitors in U-266 cells. By comparison, tri-therapies with the reference HDAC6i ACY-1215 display results similar to those obtained with MAKV-15. Furthermore, combinations with BCL-2 or MCL-1 inhibitors appear to produce comparable effects on MM cell viability, considering that ABT-199 alone is slightly more efficient at reducing the percentage of living cells compared to A1210477 and S63845 alone (Figure 62).

In conclusion, MAKV-15 acts as a selective HDAC6i in a subset of MM cell lines, since it preferentially increases HDAC6 substrate acetylation in comparison to a non-HDAC6 substrate. Furthermore, the variety of responses to tri-therapies highlights the heterogeneity among MM cell lines and suggests distinct mechanisms of action.

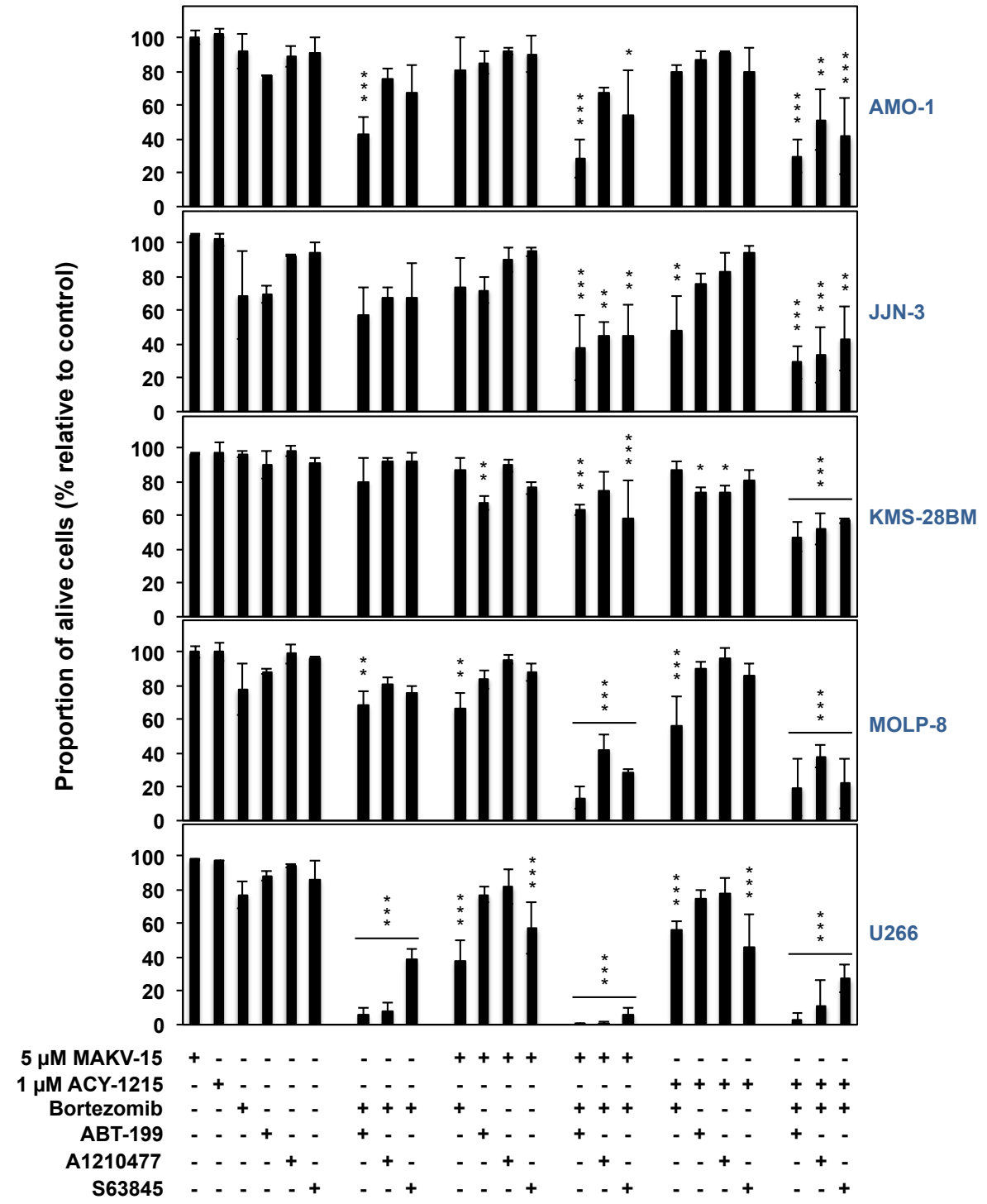

Figure 62: Effects of tri-therapies with HDAC6i, proteasome inhibitor, and BCL-2 family protein inhibitors on MM cell death.

MM cells were co-treated for 72 hours with indicated compounds at concentrations determined in Annex A7. The study of nuclear morphology was performed by fluorescence microscopy after Hoechst-PI staining. Results correspond to mean ± SD of three independent experiments and were analyzed by a one-way ANOVA with *, **, *** indicating $p < 0.05$, $p < 0.01$, $p < 0.001$, respectively.

Discussion

Epigenetic alterations, like changes of the HDAC-modulated acetylation status of proteins, are implicated in carcinogenesis. Since these modifications are dynamically regulated and potentially reversible, HDACs represent an interesting target in anticancer therapy. Research for HDACi allowed the identification of new natural and synthetic compounds displaying promising inhibitory potential against HDAC enzymatic activities (Seidel *et al.*, 2012a; Seidel *et al.*, 2012b). To date, several HDACi have been clinically tested and most of them are broad-spectrum or pan-HDACi. Nevertheless, the inhibition of multiple HDAC activities is associated with diverse side effects and mutagenicity (Subramanian *et al.*, 2010). Consequently, research is now focusing on the discovery and characterization of more potent and selective HDACi with anticancer properties.

1. Characterization of the anticancer properties of a new hydroxamate-based pan-HDACi: MAKV-8

Kozikowski *et al.* reported MAKV-8 as a potent HDACi *in vitro* with anti-proliferative activity against pancreatic cancer cell lines (Kozikowski *et al.*, 2008). Accordingly, we show here that MAKV-8 displays inhibitory potential against HDACs *in vitro* and *in cellulo*, as well as anticancer properties when used alone or in combination with imatinib against CML.

Despite a fairly good overall *in silico* profile, some structural modifications could be necessary to improve the drug likeness parameters of MAKV-8. Importantly, *in silico* predictions should be critically considered due to potentially different pharmacokinetic properties of compounds *in vivo*. For instance, poor pharmacokinetics is associated with pan-HDACi comprising a hydroxamic acid as a ZBG due to rapid degradation and clearance *in vivo* (Zhang *et al.*, 2018). The physicochemical and pharmacokinetic properties of MAKV-8, possessing a hydroxamic acid with a pK_a value of 8.91, may be affected by the protonated state of compound under varying pH conditions (Manallack *et al.*, 2013). In addition, MAKV-8, whose chemical name is tert-butyl N-[3-(3-{[6-(hydroxycarbamoyl)hexyl]carbamoyl}-1,2-oxazol-5-yl)phenyl]carbamate, could behave as a pro-drug. Indeed, the carbamate group, displaying the capability to permeate cell membranes (Ghosh *et al.*, 2015), undergoes a rapid cleavage within cells (Wolfe *et al.*, 2012). MAKV-8 is also a weak substrate of CYP3A4, an oxidizing enzyme responsible for the deactivation of many drugs (Ogu *et al.*, 2000).

Noteworthy, the metabolism of imatinib by CYP3A4 should not be influenced by co-medication since MAKV-8 is not predicted to be a modulator of cytochrome CYP3A4 activity.

In vitro, MAKV-8 acts as a pan-HDACi, inhibiting HDAC1, HDAC6 and total HDAC activities with a potency about 10 times higher than SAHA. In line with these observations, docking studies suggest efficient interactions of MAKV-8 with the ligand-binding pockets of all tested HDAC isoenzymes, associated with higher binding affinities compared to SAHA. Importantly, such predictions do not totally reflect the biological reality since they do not take into consideration the abundance of the different HDAC isoforms *in cellulo*. For instance, HDAC1 and HDAC2, which are particularly involved in the regulation of gene expression through the modulation of histone acetylation levels (Moser *et al.*, 2014), were reported to be highly expressed in the K-562 CML cell model (Uhlen *et al.*, 2010). Accordingly, we further highlighted in this study that HDAC1 and HDAC2 are also up-regulated in LSCs versus HSCs from patients. Therefore, considering that HDAC1 and 2 inhibitions strongly impact the transcription of genes coding for proteins essential for tumor cell survival (Chen *et al.*, 2019), using HDACi such as MAKV-8 for CML treatment may represent a promising therapeutic interest.

In CML cells, MAKV-8 induces the acetylation of histone H4 and α-tubulin from low micromolar concentrations, witnessing the inhibition of multiple HDAC activities. Interestingly, the reference pan-HDACi SAHA displays comparable EC_{50} values against acetyl histone H4 and acetyl α-tubulin, whereas the EC_{50} values for MAKV-8 towards both targets differ moderately. Furthermore, the addition of imatinib to pan-HDACi treatment dissimilarly modulates MAKV-8- and SAHA-mediated HDAC inhibition, which may suggest distinct HDAC inhibitory properties. The acetylation level of α-tubulin is reduced after SAHA-imatinib combination compared to treatment with SAHA alone, whereas cells treated with MAKV-8 alone or combined with imatinib display a similar acetylated α-tubulin level. Such result may be explained by imatinib-stimulated SAHA degradation or export if those processes are distinct between MAKV-8 and SAHA. In addition, a small conformational change in HDAC6 may affect preferentially SAHA-HDAC6 interaction since the binding affinity of SAHA for HDAC6 is weaker compared to MAKV-8. Conversely, the addition of imatinib to either MAKV-8 or SAHA treatments enhances histone H4 acetylation levels compared to that obtained with compounds alone, which may suggest increased import of the HDACi in the nucleus or induced activity of HATs targeting lysines on histone H4. Notably,

nilotinib was reported to down-regulate HDAC1, HDAC2 and HDAC4 protein expression in hepatic stellate cells (Shaker *et al.*, 2013). Compared to SAHA, MAKV-8-mediated acetylation of specific histone and non-histone protein targets may result in improvement of HDACi-related anticancer activities. Altogether, pan-HDACi MAKV-8 seems to be an attractive drug candidate to consider for further investigations in CML therapies.

Similar to SAHA, prolonged exposure of CML cells (*i.e.* K-562, KBM-5 and MEG-01 cells) to MAKV-8 reduces proliferation, accompanied by a concentration- and time-dependent cell cycle arrest in G_1 and/or G_2/M phases in K-562 cells. The double blockage in G_1 and G_2/M phases of the cell cycle with the highest MAKV-8 concentrations has already been reported for other HDACi (Liu *et al.*, 2010; Xu *et al.*, 2014) and may be due for instance to (*i*) HDACi-induced cyclin B1 degradation (Prystowsky *et al.*, 2013), (*ii*) loss of HDAC1 substrate Eg5, a mitosis-related protein that plays a critical role in bipolar spindle formation (Nalawansha *et al.*, 2017), or (*iii*) HDACi-mediated down-regulation of cell-division cycle protein (cdc)20 transcription and expression, preventing the completion of cell division in asynchronous cells that already passed G_1/S restriction point and continued to cycle until reaching mitosis (Iacomino *et al.*, 2006). Since the accumulation of cells in G_2/M phase is decreased between 24 and 48 hours, the premature exit from defective mitosis, and not the cycle arrest in G_1 phase, might be required for MAKV-8-induced apoptosis. Accordingly, HDACi-induced aberrant mitosis engenders rapid onset of cell death, which appears to considerably contribute to the cytotoxicity of these drugs (Warrener *et al.*, 2003). In agreement with these features, the colony-forming capacity of CML cells is significantly reduced upon exposure with MAKV-8 alone or in combination with imatinib, confirming compounds-mediated impairment of CML replicative ability in a 3D model.

In imatinib-sensitive and -resistant BCR-ABL-positive CML cell models, apoptotic cell death is triggered upon concomitant treatment with MAKV-8 and imatinib, with combination index values below 1 indicating synergism. In line with our findings, treatment with SAHA, alone and in combination with TKi has previously been reported to synergistically induce apoptosis in CML cell lines (Nimmanapalli *et al.*, 2003; Fiskus *et al.*, 2006a). Furthermore, MAKV-8 in combination with imatinib also impairs tumor growth of xenografted CML cells in zebrafish. Notably, a moderate cytotoxicity is observed in a subset of healthy models (*i.e.* non-proliferating PBMCs, RPMI-1788 cells and platelets) exposed to the same combination treatment whereas proliferating PBMCs and $CD34^+$ cells are very sensitive to such therapy.

Since the mortality of proliferating healthy cells is related to prolonged MAKV-8 exposure, the selectivity of the combination towards cancer cells could be improved by testing other treatment schedules. A weak toxicity of compounds towards normal cells compared to cancerous cells has been described for many HDACi (Marks *et al.*, 2007; Cea *et al.*, 2011). Nevertheless, Zhang *et al.* describe a significant activity of panobinostat against normal hematopoietic progenitors *in cellulo*, and panobinostat-associated moderate inhibition of normal blood cell counts, as well as BM stem and progenitor populations *in vivo* (Zhang *et al.*, 2010). Altogether, our results show that MAKV-8 could provide a strategy for overcoming imatinib resistance and support the use of pan-HDACi in combination with TKi for the treatment of CML.

Interestingly, the differences of response between the three CML cell lines may be first explained by the presence of distinct BCR-ABL transcripts: K-562 and KBM-5 cells possess the b3a2 transcript, whereas MEG-01 cells express the b2a2 transcript (Beran *et al.*, 1993; Withey *et al.*, 2005). One study reported that patients with the b2a2 transcript had a slower molecular response with inferior response rates to imatinib and poorer long-term outcome (Jain *et al.*, 2016). Additionally, the CML cell lines, although representing the same pathological phenotype, show characteristics in their protein expression profile that suggest different phenotype leukemia subclasses, highlighting inter-patient variability (Fontana *et al.*, 2007). Finally, although the three cell lines are derived from patients in CML blastic phase, K-562, KBM-5 and MEG-01 cells may engage into different hematopoietic differentiation pathways.

The MAKV-8 derivatives possessing a shorter linker (MAKV-6 and -7) inhibit HDACs with a lower potency than MAKV-8, and the derived molecules without a hydroxamate group (MAKV-10 and -12) do not act as HDACi either *in vitro* or *in cellulo*. Our results confirm that the presence of the hydroxamate group and the length of the linker chain are important for designing of new HDACi (Kozikowski *et al.*, 2008). Accordingly, docking analyses show moderate binding of MAKV-8 derivatives to HDAC6 isoenzyme, with lower affinity than MAKV-8. Treatment with MAKV-6 and -7 also leads to inhibited proliferation and increased mortality, but fails to induce α-tubulin acetylation, suggesting that the observed anticancer effects are mainly caused by the inhibition of HDACs targeting histones. Analogously, it was reported that HDACi-induced α-tubulin acetylation does not affect mitosis (Xu *et al.*, 2007).

MAKV-8 treatment triggers ER stress in K-562 cells at low concentrations and short durations, as evidenced by the up-regulation of proteins related to UPR such as GRP78. Since HDACs have been previously described to modulate GRP78 acetylation (Kahali *et al.*, 2012), HDAC inhibition following MAKV-8 treatment could result in strong GRP78 acetylation and selective activation of the UPR, as similarly reported for other HDACi (Rao *et al.*, 2010). Furthermore, MAKV-8-mediated inhibition of HDAC6, which is important in the clearance of misfolded proteins, could thus lead to the formation and accumulation of protein aggregates, and the induction of ER stress (Bruning *et al.*, 2015).

Simultaneously to ER stress, the induction of MAKV-8-mediated autophagy is revealed by the conversion of LC3-I to LC3-II and decreased SQSTM1 expression level, as well as the appearance of autophagy-related vesicles. It has been shown that pan-HDACi both promote the initiation and block the maturation phases of autophagy by inhibiting class I-IIa and class IIb HDACs, respectively (Koeneke *et al.*, 2015). Notably, the swollen cytoplasm observed in MAKV-8-treated K-562 cells could reflect an ongoing cell differentiation process. Accordingly, the acetylation of GATA-1 directly stimulates GATA-1-dependent transcription of genes involved in erythropoiesis (Yang *et al.*, 2012), a process that requires autophagy induction (J. Zhang *et al.*, 2015). Autophagy may also participate in the observed sensitization to imatinib as down-regulation of pro-autophagic beclin 1 expression partly prevents cell death induced by co-treatments. Nevertheless, LC3-II and p62 expression levels are not markedly impacted by BECN1 knockdown, suggesting the involvement of another mechanism, such as the induction of non-canonical autophagy independent of beclin 1 expression (Wong *et al.*, 2010), or the sufficient abundance of the remaining protein to stimulate autophagy. We hypothesize that the interaction between the BH3 only domain of beclin 1 and pro-survival family member BCL-xL is lost in BECN1-silenced cells, freeing the latter that may reduce apoptotic induction *via* the prevention of BAX-BAK oligomerization in the outer mitochondrial membrane (Yip *et al.*, 2008). Noteworthy, one study has shown that impairing autophagy significantly enhances the anticancer activity of SAHA, therefore emerging as an attractive strategy to treat imatinib-refractory CML patients failing conventional therapy (Carew *et al.*, 2007).

Finally, treatment with MAKV-8 weakly induces the appearance of DSB at a time (*i.e.* 24 hours) where no cell death is observed. Some studies support the notion that HDACi can disrupt DNA repair through multiple mechanisms such as acetylation of Ku70 (Cohen *et al.*, 2004) and down-regulation of DNA repair proteins (J.H. Lee *et al.*, 2010), which may result in accumulation of excessive DNA damage and activation of apoptosis. Since H2AX

phosphorylation does not occur in concomitance with histone acetylation, as previously reported (Gaymes *et al.*, 2006), MAKV-8-related induction of DNA damage is most probably the consequence of DNA fragmentation during apoptosis. Accordingly, MAKV-8-mediated increase in phosphorylated histone H2AX is almost completely abrogated upon exposure to the caspase inhibitor Z-VAD-FMK, which is surprisingly comparable to the results obtained with cisplatin, a well-known DNA damaging agent. Since the catalytic activity of PARP-1 is responsible for mediating multiple DNA damage repair pathways, one of the earliest events in the DNA damage response is the recruitment of PARP-1 to diverse types of DNA lesions (Ray Chaudhuri *et al.*, 2017). Upon Z-VAD-FMK-mediated inhibition of caspases, uncleaved PARP-1 may participate in DNA damage repair, providing a hypothesis for the disappearance of γ-H2AX. Consequently, we cannot conclude whether MAKV-8-dependent activation of apoptosis result predominantly from DNA damage or precedes them. Furthermore, it is possible that the MAKV-8-mediated accumulation of excessive DNA damage results from ER stress and/or autophagy, especially considering the order of events (see summary in Figure 63).

Collectively, our work does not exclude that MAKV-8-related mechanisms could be implicated in its anticancer effect, but further studies must be performed. We hypothesized that MAKV-8-induced ER stress would rapidly stimulate an autophagic response in an attempt to restore homeostasis. For instance, IRE1 activation may trigger autophagy either through XBP1 mRNA splicing leading to BECN1 transcriptional activation (Margariti *et al.*, 2013), or c-Jun N-terminal kinase (JNK) phosphorylation resulting in disruption of the inhibitory interaction between beclin 1 and BCL-2/BCL-xL (Verfaillie *et al.*, 2010). Upon prolonged ER stress caused by failure of cells to recover, apoptosis might occur following increased DDIT3 mRNA levels (Verfaillie *et al.*, 2010) or ER stress-related blockage of cell cycle progression (Brewer *et al.*, 1999). In addition, HDACi-mediated alteration of DNA repair mechanisms may further enhance apoptosis induction.

Mechanistically, a decrease in BCR-ABL kinase activity is observed after MAKV-8-imatinib co-treatment, which most likely explains the diminution of STAT5 phosphorylation, as well as the drop in c-MYC and MCL-1 expression. Previous reports indicate that SAHA down-regulates BCR-ABL mRNA and protein levels in two CML cell models (Nimmanapalli *et al.*, 2003), which could be implicated in synergistic anti-leukemic interactions involving TKi (Fiskus *et al.*, 2006a). By inhibiting HDAC6, treatment with pan-HDACi could lead to the disruption of HSP90α chaperone association with BCR-ABL, provoking its poly-

ubiquitination and degradation by the proteasome (Bali *et al.*, 2005). Surprisingly, MAKV-8 rather augments BCR-ABL expression level in our cell models, implying the involvement of other regulatory mechanisms. For instance, HDAC1 inhibition reportedly results in increased acetyl histone H4 levels in BCR-ABL promoter region, subsequently up-regulating the level of BCR-ABL transcript (Brusa *et al.*, 2006). Noteworthy, BCR-ABL overexpression has been associated with enhanced, rather than reduced, imatinib sensitivity (Modi *et al.*, 2007).

Furthermore, BCR-ABL downstream targets play a critical role in the pathogenesis of CML (Ceballos *et al.*, 2000; Hoelbl *et al.*, 2006; Warsch *et al.*, 2012). Similar to our observations, HDACi-mediated potentiation of TKi cytotoxicity has been related to STAT5 inhibition in BCR-ABL-positive cells (Nguyen *et al.*, 2011). As previously described, imatinib-mediated down-regulation of anti-apoptotic MCL-1 expression, whose up-regulation was induced by MAKV-8, could potentiate HDACi-mediated apoptosis in CML cells (Inoue *et al.*, 2008). In addition, c-MYC has been recently reported as an important target to selectively eliminate CML LSCs (Abraham *et al.*, 2016). Accordingly, human LSCs display increased c-MYC mRNA level compared to HSCs. Along with lowering c-MYC expression, treatment with MAKV-8 potently decreased the ALDH+ cell proportion, which was further enhanced upon co-treatment with imatinib. Interestingly, concomitant SAHA and imatinib treatment was less effective at reducing the ALDH+ cell population, despite a similar decrease of c-MYC expression. Since c-MYC is not the only transcription factor essential for LSC survival (Houshmand *et al.*, 2019), MAKV-8 and SAHA may target different proteins implicated in LSC maintenance due to distinct HDAC inhibitory profiles. Although TKi such as imatinib eradicate most CML cells, they are largely ineffective against the reservoir of quiescent LSCs (Zhou *et al.*, 2015). Conversely, imatinib was able to moderately diminish the ALDH+ cell proportion in our cell model. Our results demonstrate that partnering imatinib with MAKV-8, which targets key hematopoietic stem cell molecular effectors, may represent an effective strategy to overcome LSC resistance to TKi, thereby offering the opportunity to improve disease outcomes for CML patients.

In summary, the present findings suggest that treatment with MAKV-8 contributes to the strong sensitization of imatinib-sensitive and -resistant CML cells, including LSCs, towards imatinib cytotoxicity, hence providing a rational basis to further study the potency of MAKV-8 and imatinib as a combination therapy against CML.

2. Characterization of the anticancer properties of a new hydroxamate-based selective HDAC6i: MAKV-15

Improved knowledge about the functions of isoenzyme HDAC6 in physiological and pathological conditions has been associated with a growing interest for this deacetylase. Research has thus intensified in order to discover more potent and selective HDAC6i, two even reaching clinical trials for the treatment of MM. In the future, the recently reported crystal structure of the two deacetylase domains of HDAC6 will most likely allow the successful structure-based design of selective HDAC6i with novel chemical properties and enable the determination of essential structure-activity relationships.

As already mentioned, the mechanisms underlying the negative regulation of HDAC6 expression are still globally unknown and deserve to be investigated. In this perspective, an improved knowledge of the (post)-transcriptional and (post)-translational mechanisms regulating HDAC6 gene expression would allow the development of new strategies for the modulation of HDAC6 functions rather than its catalytic inhibition. In addition, getting a full picture of the acetylome regulated by HDAC6 would enable a better understanding of its roles and therapeutic potential.

Selective HDAC6 inhibition is not associated with severe cytotoxicity (Gaisina *et al.*, 2016). Accordingly, HDAC6 KO mice do not go through an abnormal development nor develop problems in important organ functions, suggesting that HDAC6 inhibition would not cause major side effects (Li *et al.*, 2013). Therefore, the advent of novel specific HDAC6i may justify the rational of using HDAC6 as a preferred synergistic target in combinatorial therapies with natural and synthetic compounds for the improvement of clinical cancer treatment. For instance, simultaneous inhibition of proteasome and HDAC6 activities, resulting in the accumulation of misfolded proteins, has been proposed as a new strategy in cancer therapy to synergistically induce cell death in MM (Hideshima *et al.*, 2016), and many additional solid cancers. There is no doubt that such approaches based on combination with HDAC6i represent promising anticancer therapeutic strategies that will be further developed in a near future and be beneficial to cancer patients. Furthermore, selectively inhibiting HDAC6 may be considered as a potential immuno-modulatory option since it has been described to participate in the regulation of immune-related pathways in melanoma (Lienlaf *et al.*, 2016).

Finally, HDAC6 has been recognized as a promising target in several additional disorders, such as inflammation, autoimmune diseases, and neurodegeneration (Falkenberg *et al.*, 2014).

For instance, HDAC6i in Alzheimer's disease have been demonstrated to induce the degradation of tubule-associated unit (Tau) *via* the alteration of HDAC6-HSP90α interaction, and the subsequent restoration of β-amyloid-induced damages (Seidel *et al.*, 2015). Consequently, the advancement in HDAC6 targeting may also ameliorate ongoing therapies for those pathologies.

2.1. CML cells

In vitro, MAKV-15 acts as a more potent and selective HDAC6i than its parent compound. Accordingly, in CML, MAKV-15 increases preferentially the acetylation of the HDAC6 substrate α-tubulin in comparison to a non-HDAC6 substrate (i.e. histone H4), whereas tubastatin A fails to display any selectivity. The modest inhibitory selectivity of MAKV-15 for HDAC6 is comparable to the solo HDAC6i in clinical trial, ACY-1215 (Santo *et al.*, 2012). Even though the selectivity of tubastatin A is around 1000 times towards HDAC6 in the original paper (Butler *et al.*, 2010), the selectivity of this compound drops down to about 50 times against HDAC6 in the paper of Wagner *et al.* when authors perform *in vitro* HDAC activity assays using different substrates compared to the initial paper. Moreover, in the second paper, tubastatin A induces histone H4 and α-tubulin acetylation at levels comparable to the pan-HDACi SAHA, which indicates a lack of selectivity *in cellulo* (Wagner *et al.*, 2013). Similarly, our *in vitro* and *in cellulo* results confirm that tubastatin A is not a selective HDAC6i. The discrepancy concerning the HDAC inhibitory profile of tubastatin A may be due to the variety of cell models used to study its effects. Furthermore, verification of tubastatin A-mediated HDAC6 selectivity is not investigated in numerous papers, which raises doubt as to whether the observed effects are HDAC6 related or occur due to off-target effects.

It appears that the selective inhibition of HDAC6 activity in K-562 cells is not sufficient to reduce cancer cell proliferation. Accordingly, Depetter *et al.* reported that all HDAC6i tested (*i.e.* tubastatin A, tubacin and tubathian A) failed to display any anticancer properties when used in an HDAC6-selective manner (Depetter *et al.*, 2019). Nevertheless, higher concentrations of MAKV-15 and tubastatin A induce an accumulation of cells in G_1 phase of the cell cycle, leading to a decrease of cell proliferation and an induction of apoptotic cell death.

2.2. MM cells

MM is a hematological malignancy currently treated with proteasome inhibitors such as bortezomib (Field-Smith *et al.*, 2006). However, resistance and recurrence occur, leading to the research of new treatments or co-treatments. Since HDAC6 is involved in the aggresome pathway (Seidel *et al.*, 2015), HDAC6i have been commonly tested for the treatment of MM, usually in combination treatments with a proteasome inhibitor (Santo *et al.*, 2012) (www.acetylon.com). The rational underlying this therapy is a simultaneous inhibition of both pathways, provoking a stronger accumulation of misfolded proteins and cell death (Mishima *et al.*, 2015).

Since all cells from a panel of 10 MM cell lines constitutively express HDAC6, we expected that they would all be responsive to MAKV-15. Nevertheless, while MAKV-15 displays an HDAC6 inhibitory selectivity in most MM cell lines, increasing preferentially the acetylation levels of α-tubulin compared to histone H4, a subset of cell lines surprisingly present a weaker response or fail to respond to MAKV-15. Notably, the responsiveness to HDAC6i does not appear to be related to HDAC6 protein abundance among the different MM cell lines. Interestingly, the selectivity of MAKV-15 against HDAC6 is higher than the one observed with ACY-1215 in U-266 cells. Treatments of selected MM cell lines (*i.e.* MOLP-8 and U-266 cells) with MAKV-15 and tubastatin A show similar results in MM cells than in CML cells as selective inhibition of HDAC6 activity is insufficient to generate anticancer responses. Nevertheless, decreased cell proliferation and the induction of apoptotic cell death are observed with higher concentrations of the two compounds, as well as concentrations of bortezomib in the nanomolar range, which is consistent with data from the literature (Hideshima *et al.*, 2001). By comparison, ACY-1215 displays stronger toxicity than MAKV-15. Accordingly, treatment with low micromolar concentrations of ACY-1215 reportedly reduced viability in various MM cell lines (Santo *et al.*, 2012; Mishima *et al.*, 2015).

A potentiation of the anticancer effects accompanied with a stronger accumulation of poly-ubiquitinated proteins are observed in MOLP-8 cells concomitantly treated with MAKV-15 or tubastatin A, and bortezomib. However, tri-therapies with common chemotherapeutic drugs or rapamycin results in a percentage of dead cells similar to that obtained with the combination HDAC(6)i-bortezomib or bortezomib-rapamycin, respectively.

Tri-therapies with BCL-2 family protein inhibitors do not display similar efficiency in the 5 MM cell lines tested. Cell lines with the t(11;14) translocation are the most sensitive to tri-therapies, despite distinct expression levels of the pro-survival BCL-2 family members. According to Morales *et al*., the expression pattern of such proteins does not predict (co-)

dependency for MM survival (Morales *et al.*, 2011). Notably, plasma cells harboring the t(11;14) translocation have been reportedly associated with high BCL-2 and low MCL-1 and BCL-xL expression levels (Touzeau *et al.*, 2018). In addition, our results demonstrate that tri-therapies with BCL-2 and MCL-1 inhibitors give comparable cell death percentage in all MM cell lines. Data on the importance of BCL-2 family members for MM survival are controversial. Some studies support the notion that MCL-1 is essential for human myeloma cell viability *in vitro* (Gong *et al.*, 2016), and show that its overexpression *in vivo* is in relation with relapse and shorter survival (Wuilleme-Toumi *et al.*, 2005). Conversely, other studies demonstrate that MM is a heterogeneous disease concerning BCL-2, BCL-xL or MCL-1 dependence, MM cell lines and patient samples either monolithically relying on one anti-apoptotic BCL-2 family member or characterized by co-dependency (Touzeau *et al.*, 2016). Furthermore, MCL-1 dependency appears to be influenced by the microenvironment such as the secretion of survival cytokine IL-6 by BMSCs (Gupta *et al.*, 2017). The discrepancy between our results and data from the literature highlight the diversity between MM cell lines.

Conclusions and Perspectives

1. Characterization of the anticancer properties of a new hydroxamate-based pan-HDACi: MAKV-8

In CML cells, MAKV-8-mediated inhibition of multiple HDAC activities results in a broad range of potentially interconnected biological responses, including stimulation of ER stress and autophagy, generation of DSBs, cell cycle arrest and apoptosis induction (Figure 63A). Furthermore, MAKV-8 in combination with imatinib generates synergistic anti-cancer effects against CML cells by lowering the expression and/or phosphorylation of BCR-ABL and its downstream targets such as c-MYC and STAT5, which leads to the induction of apoptotic cell death, and the reduction of LSC fraction (Figure 63B).

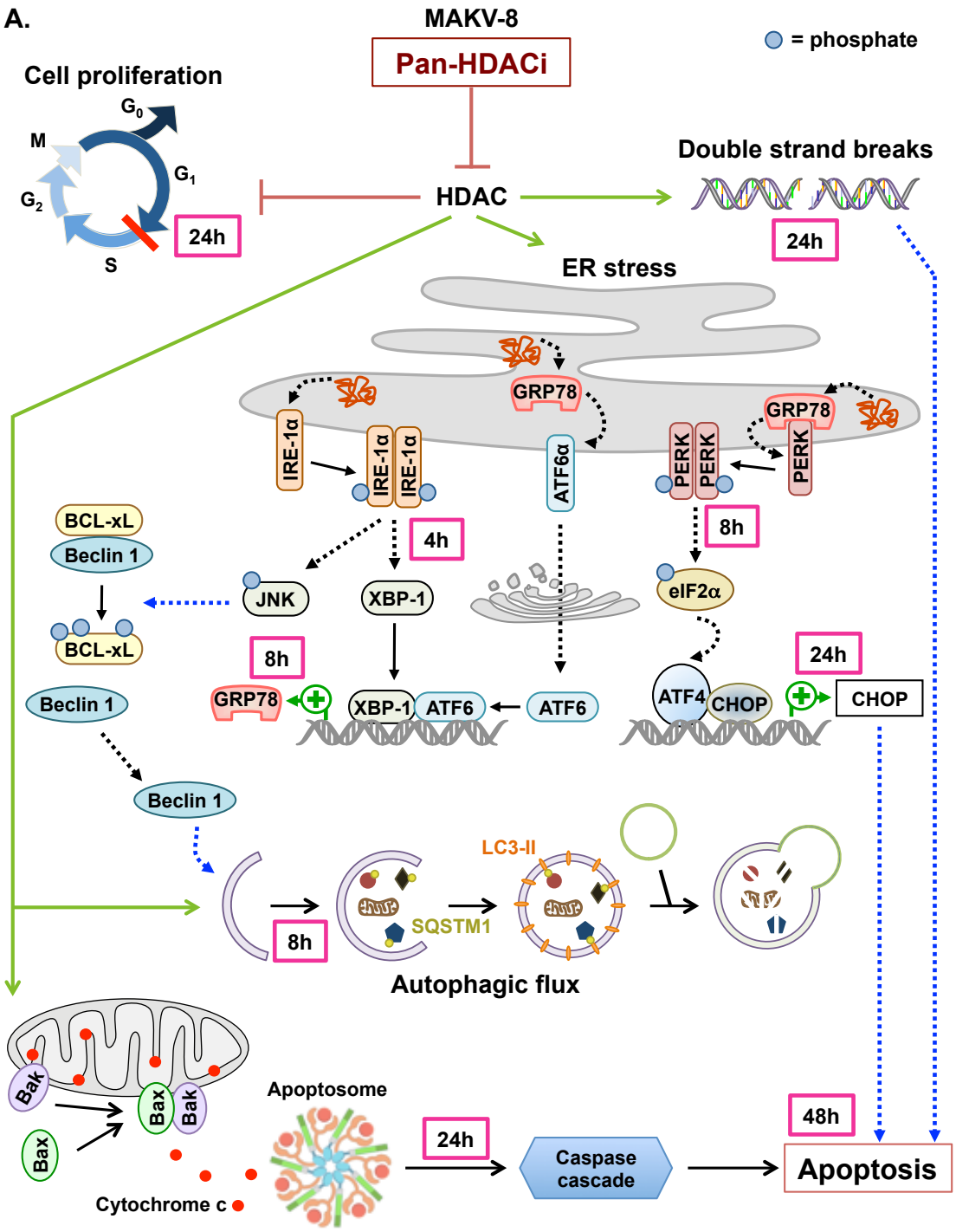

Figure 63: Mechanisms of action of MAKV-8 in combination with imatinib in CML cells.
The blue arrows represent hypothetic mechanisms of action that would need further investigations. ALDH: aldehyde dehydrogenase, ATF: activating transcription factor, BAK: BCL-2 homologous antagonist/killer, BAX: BCL-2-associated X protein, BCL: B-cell lymphoma, BCR-ABL: breakpoint cluster region-Abelson murine leukemia viral oncogene homolog 1, CHOP: CCAAT/enhancer-binding protein homologous protein, CML: chronic myeloid leukemia, eIF: eukaryotic initiation factor, ER: endoplasmic reticulum, GRP: glucose-regulated protein, HDAC: histone deacetylase, HDACi: HDAC inhibitor, IRE: inositol-requiring enzyme, JNK: c-Jun N-terminal kinase, LC: MT-associated protein 1 light chain, PERK: protein kinase RNA-like ER kinase, SQSTM: sequestosome, STAT: signal transducer and activator of transcription, TKi: tyrosine kinase inhibitor, XBPs: spliced X-box binding protein.

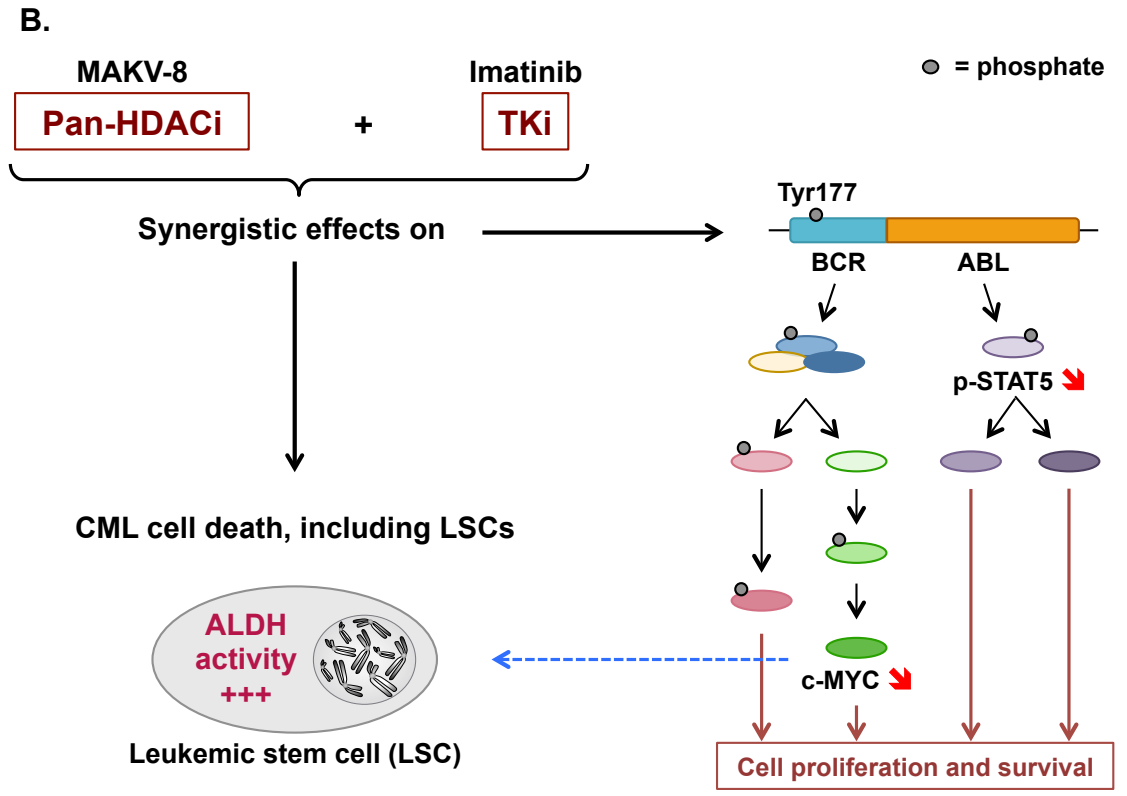

Figure 63 (continued)

Perspectives

To further address the mechanisms of action underlying the combinations, the effect of ER stress inhibition by siRNA-mediated silencing of genes coding for GRP78 or one of UPR sensor pathways (*i.e.* PERK, ATF6 or IRE1) would be studied on the synergistic cell death induced by MAKV-8-imatinib treatments. Since HDACi reportedly stimulate ROS generation (Robert *et al.*, 2012), we could also determine whether MAKV-8 enhances ROS production in cells *via* labeling with cell-permeant 2',7' dichlorodihydrofluorescein diacetate, a reduced form of fluorescein, and test their implication in combination-mediated CML cell death. Additionally, cancer-related metabolic pathways could be assessed upon treatment with MAKV-8 and imatinib using consumables developed for Seahorse XFp Analyzer (Agilent). Indeed, it has been reported that resistance to imatinib is associated to specific metabolic signature including highly glycolytic metabolic phenotype (Kominsky *et al.*, 2009). Furthermore, systematic analysis of dynamic changes of the proteome, acetyl- or phosphoproteome, and transcriptome upon treatment with MAKV-8 alone or in combination with imatinib could be performed by mass spectrometry and microarray, respectively, to evaluate the mechanisms related to the synergy.

The structure-activity relationship of MAKV-8 must be evaluated with quantitative structure-activity relationship (QSAR) modeling in order to improve the selectivity ratio for compound-induced toxicity in cancer versus healthy cells by modifying MAKV-8 chemical structure. In addition, the reasons (*e.g.* pharmacokinetic properties) leading to the *in cellulo* loss of MAKV-8-improved HDAC inhibition observed *in vitro* by comparison to SAHA should be determined.

The anticancer properties of MAKV-8 in combination with second or third generation TKi such as ponatinib should be tested in KBM-5 cells carrying the T315I mutation.

Finally, tumor growth could be visualized thanks to xenografted fluorescent primary CML cells in zebrafish or severe combined immunodeficient (SCID) mice.

2. Characterization of the anticancer properties of a new hydroxamate-based selective HDAC6i: MAKV-15

The selective inhibition of HDAC6 with low MAKV-15 concentrations is insufficient to generate anticancer effects. Since HDAC6 is involved in the aggresome pathway, a simultaneous inhibition of proteasome and aggresome pathways provoke a stronger accumulation of misfolded proteins and cell death, providing the rationale underlying bortezomib-HDAC6i combination therapy in MM cells. Additionally, this bi-therapy could lead to decreased acquired cell resistance to commonly used chemotherapies and a sensitization to a third compound, such as inhibitors of Bcl-2 family proteins (Figure 64).

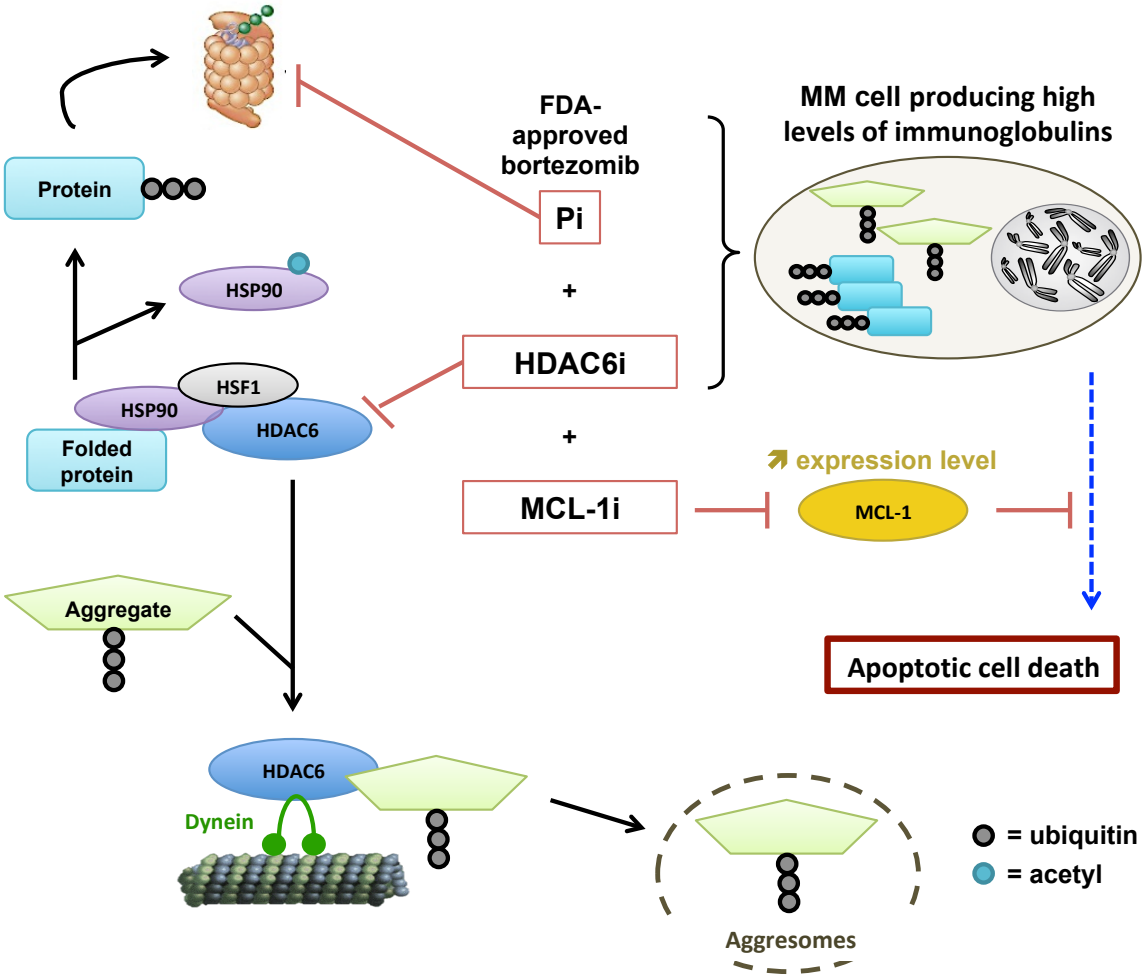

Figure 64: Mechanisms of action of MAKV-15 in combination with bortezomib in MM cells. The blue arrow represents one hypothetic mechanism of action that will need to be further studied. HDAC: histone deacetylase, HDACi: HDAC inhibitor, HSF: heat shock factor, HSP: heat shock protein, MM: multiple myeloma, Pi: proteasome inhibitor.

Perspectives

The effects of the tri-therapy (MAKV-15-bortezomib-BCL-2 family protein inhibitors) on the type cell death induced in MM cell lines could be further assessed *via* the analysis of PS exposure using flow cytometry. The toxicity of tri-therapies should be studied on MM cell lines by comparison with normal PBMCs from healthy donors. To determine whether co-treatments display a synergistic effect on cell mortality, the combination index should be calculated using the CompuSyn software. If so, the clonogenic tumor potential could be evaluated by colony formation assay.

To determine the mechanisms of action underlying the most promising tri-therapies, the effects of co-treatments could first be investigated on proteins implicated in cell death pathways. Western blotting and caspase activity assays could be performed to analyze caspase activation. The expression of pro- and anti-apoptotic proteins such as BCL-2 family proteins and IAPs could also be analyzed. The impact of combinations could then be examined on the expression of key proteins of critical signaling pathways in MM for survival or the development of drug resistance, especially towards bortezomib. Such key proteins are represented by the oncogenic transcription factors c-MYC and interferon regulatory factor (IRF)4, interacting with each other to generate an autoregulatory circuit and enhance their expression in MM cells, mediate the expression of genes associated with MM cell proliferation, survival and drug resistance (Bat-Erdene *et al.*, 2016). Another factor is XBP1, which is crucial for the development of terminally differentiated plasma cells and has been implicated in the development of resistance to chemotherapy with bortezomib (Gambella *et al.*, 2014). Moreover, the effect of combinations could be studied on AKT/mTOR, Wnt/β-catenin, Notch or Hedgehog pathways, which are aberrantly activated in MM.

The effect of compounds alone or in combination could also be evaluated on cell proliferation and viability following the modulation of HDAC6 expression, either by siRNA-mediated silencing or using HDAC6-overexpressing plasmids. Furthermore, the impact of IL-6, an essential cytokine for MM development, could be determined on anticancer processes by co-treating IL-6 non-producing cells in presence or absence of this cytokine or measuring IL-6 production in U-266 after co-treatments.

MM cells are characterized by excessive protein synthesis resulting in chronic ER stress, which is adaptively alleviated by the three pathways of the UPR to support cellular homeostasis and survival. However, extended ER stress can also lead to apoptosis (Ri, 2016). In this context, we could assess whether our compounds develop an anti-tumor effect in co-

treatments by increasing ER stress and/or modulating UPR. The expression level of GRP78 could be analyzed as a marker of ER stress. Moreover, the activation of UPR sensor pathways including PERK/eIF2α/ATF4; ATF6; as well as the amount of spliced XBP1 mRNA could be assessed. Components of the ER stress machinery may constitute clinically relevant druggable targets for the induction of immunogenic cell death (ICD) (Kepp *et al.*, 2013), which is a process generating a series of spatiotemporally defined signals that activate the immune response to detect and eliminate tumor cells. Among them, the three critical marks of ICD, *i.e.* high mobility group box (HMGB)1 release, calreticulin exposure and ATP secretion, could be measured as a starting point to determine whether the compounds used in combination treatments could potentially induce ICD.

Finally, the potency of co-treatments could be assessed in *in vivo* models. Since interactions between BM microenvironment and malignant plasma cells are essential for tumor progression *via* IL-6 secretion for example (Manier *et al.*, 2012), MM cell lines would first be co-cultured with BMSCs generated from MM patient samples. Then, we would evaluate proliferation and viability, as well as the clonogenic potential, of plasma cells derived from MM patient BM or blood samples and separated into tumor (CD138+) and nontumor (CD138-) fractions. Finally, tumor growth could be visualized thanks to xenografted fluorescent MM cell lines and primary MM cells in zebrafish or SCID mice.

3. "Take home" message

Altogether, our results demonstrate that HDACi alone or in combination with targeted drug therapies display interesting therapeutic potential in CML and MM, especially using pan and HDAC6-selective inhibitors, respectively.

In my opinion, the most promising combination to potentially reach clinical trials would be that with the selective HDAC6i, bortezomib and a third compound in MM. Despite efficient reduction of stem cell population by MAKV-8-imatinib combination, suggesting fewer patients with resistance and relapse, MAKV-8-associated toxicity in healthy models makes its use in clinics very unlikely. Nevertheless, improving MAKV-8 structure to increase its selectivity against cancer cells may be of great therapeutic interest. Conversely, specific HDAC6i are associated with less adverse events. Furthermore, MM is still an incurable disease in most patients, necessitating an urgent discovery and development of novel therapeutic strategies, whereas CML is manageable in many patients thanks to first-, second-, and third-generation TKi.

References

Abbas, T. and Dutta A. (2009). "*p21 in cancer: intricate networks and multiple activities*." Nat Rev Cancer 9(6): 400-414.

Abraham, S. A., Hopcroft L. E., Carrick E., Drotar M. E., Dunn K., Williamson A. J., Korfi K., Baquero P., Park L. E., Scott M. T., Pellicano F., Pierce A., Copland M., Nourse C., Grimmond S. M., Vetrie D., Whetton A. D. and Holyoake T. L. (2016). "*Dual targeting of p53 and c-MYC selectively eliminates leukaemic stem cells*." Nature 534(7607): 341-346.

Abramson, H. N. (2016). "*Kinase inhibitors as potential agents in the treatment of multiple myeloma*." Oncotarget 7(49): 81926-81968.

Adams, C. J., Kopp M. C., Larburu N., Nowak P. R. and Ali M. M. U. (2019). "*Structure and Molecular Mechanism of ER Stress Signaling by the Unfolded Protein Response Signal Activator IRE1*." Front Mol Biosci 6: 11.

Afifi, S., Michael A., Azimi M., Rodriguez M., Lendvai N. and Landgren O. (2015). "*Role of Histone Deacetylase Inhibitors in Relapsed Refractory Multiple Myeloma: A Focus on Vorinostat and Panobinostat*." Pharmacotherapy 35(12): 1173-1188.

Ahamed, M., Vermeulen K., Schnekenburger M., Moltzau L. R., Levy F. O., Marton J., Froeyen M., Olberg D. E., Diederich M. and Bormans G. (2016). "*Synthesis, Enzyme Assays and Molecular Docking Studies of Fluorinated Bioisosteres of Santacruzamate A as Potential HDAC Tracers*." Letters in Drug Design & Discovery 13: 1-11.

Al Baghdadi, T., Abonour R. and Boswell H. S. (2012). "*Novel combination treatments targeting chronic myeloid leukemia stem cells*." Clin Lymphoma Myeloma Leuk 12(2): 94-105.

Aldana-Masangkay, G. I., Rodriguez-Gonzalez A., Lin T., Ikeda A. K., Hsieh Y. T., Kim Y. M., Lomenick B., Okemoto K., Landaw E. M., Wang D., Mazitschek R., Bradner J. E. and Sakamoto K. M. (2011a). "*Tubacin suppresses proliferation and induces apoptosis of acute lymphoblastic leukemia cells*." Leuk Lymphoma 52(8): 1544-1555.

Aldana-Masangkay, G. I. and Sakamoto K. M. (2011b). "*The role of HDAC6 in cancer*." J Biomed Biotechnol 2011: 875824.

Alzrigat, M., Parraga A. A. and Jernberg-Wiklund H. (2018). "*Epigenetics in multiple myeloma: From mechanisms to therapy*." Semin Cancer Biol 51: 101-115.

Ammanamanchi, S. and Brattain M. G. (2004). "*Restoration of transforming growth factor-beta signaling through receptor RI induction by histone deacetylase activity inhibition in breast cancer cells*." J Biol Chem 279(31): 32620-32625.

An, X., Tiwari A. K., Sun Y., Ding P. R., Ashby C. R., Jr. and Chen Z. S. (2010). "*BCR-ABL tyrosine kinase inhibitors in the treatment of Philadelphia chromosome positive chronic myeloid leukemia: a review*." Leuk Res 34(10): 1255-1268.

Ankathil, R., Azlan H., Dzarr A. A. and Baba A. A. (2018). "*Pharmacogenetics and the treatment of chronic myeloid leukemia: how relevant clinically? An update*." Pharmacogenomics.

Annicotte, J. S., Iankova I., Miard S., Fritz V., Sarruf D., Abella A., Berthe M. L., Noel D., Pillon A., Iborra F., Dubus P., Maudelonde T., Culine S. and Fajas L. (2006). "*Peroxisome proliferator-activated receptor gamma regulates E-cadherin expression and inhibits growth and invasion of prostate cancer*." Mol Cell Biol 26(20): 7561-7574.

Apperley, J. F. (2015). "*Chronic myeloid leukaemia*." Lancet 385(9976): 1447-1459.

Arber, D. A., Orazi A., Hasserjian R., Thiele J., Borowitz M. J., Le Beau M. M., Bloomfield C. D., Cazzola M. and Vardiman J. W. (2016). "*The 2016 revision to the World Health Organization classification of myeloid neoplasms and acute leukemia*." Blood 127(20): 2391-2405.

Atadja, P. (2009). "*Development of the pan-DAC inhibitor panobinostat (LBH589): successes and challenges*." Cancer Lett 280(2): 233-241.

Aviles-Vazquez, S., Chavez-Gonzalez A., Hidalgo-Miranda A., Moreno-Lorenzana D., Arriaga-Pizano L., Sandoval-Esquivel M. A., Ayala-Sanchez M., Aguilar R., Alfaro-Ruiz L. and Mayani H. (2017). "*Global gene expression profiles of hematopoietic stem and progenitor cells from patients with chronic myeloid leukemia: the effect of in vitro culture with or without imatinib*." Cancer Med 6(12): 2942-2956.

Ayer, D. E. (1999). "*Histone deacetylases: transcriptional repression with SINers and NuRDs*." Trends Cell Biol 9(5): 193-198.

Azuma, K., Urano T., Horie-Inoue K., Hayashi S., Sakai R., Ouchi Y. and Inoue S. (2009). "*Association of estrogen receptor alpha and histone deacetylase 6 causes rapid deacetylation of tubulin in breast cancer cells*." Cancer Res 69(7): 2935-2940.

Bai, J., Lei Y., An G. L. and He L. (2015). "*Down-regulation of deacetylase HDAC6 inhibits the melanoma cell line A375.S2 growth through ROS-dependent mitochondrial pathway*." PLoS One 10(3): e0121247.

Balabanov, S., Braig M. and Brummendorf T. H. (2014). "*Current aspects in resistance against tyrosine kinase inhibitors in chronic myelogenous leukemia*." Drug Discov Today Technol 11: 89-99.

Balasubramanian, S., Verner E. and Buggy J. J. (2009). "*Isoform-specific histone deacetylase inhibitors: the next step?*" Cancer Lett 280(2): 211-221.

Bali, P., Pranpat M., Bradner J., Balasis M., Fiskus W., Guo F., Rocha K., Kumaraswamy S., Boyapalle S., Atadja P., Seto E. and Bhalla K. (2005). "*Inhibition of histone deacetylase 6 acetylates and disrupts the chaperone function of heat shock protein 90: a novel basis for antileukemia activity of histone deacetylase inhibitors*." J Biol Chem 280(29): 26729-26734.

Balliu, M., Guandalini L., Romanelli M. N., D'Amico M. and Paoletti F. (2015). "*HDAC-inhibitor (S)-8 disrupts HDAC6-PP1 complex prompting A375 melanoma cell growth arrest and apoptosis*." J Cell Mol Med 19(1): 143-154.

Bamodu, O. A., Kuo K. T., Yuan L. P., Cheng W. H., Lee W. H., Ho Y. S., Chao T. Y. and Yeh C. T. (2018). "*HDAC inhibitor suppresses proliferation and tumorigenicity of drug-resistant chronic myeloid leukemia stem cells through regulation of hsa-miR-196a targeting BCR/ABL1*." Exp Cell Res 370(2): 519-530.

Banerjee, T. and Chakravarti D. (2011). "*A peek into the complex realm of histone phosphorylation*." Mol Cell Biol 31(24): 4858-4873.

Banreti, A., Sass M. and Graba Y. (2013). "*The emerging role of acetylation in the regulation of autophagy*." Autophagy 9(6): 819-829.

Bartolomei, G., Leutert M., Manzo M., Baubec T. and Hottiger M. O. (2016). "*Analysis of Chromatin ADP-Ribosylation at the Genome-wide Level and at Specific Loci by ADPr-ChAP*." Mol Cell 61(3): 474-485.

Bat-Erdene, A., Miki H., Oda A., Nakamura S., Teramachi J., Amachi R., Tenshin H., Hiasa M., Iwasa M., Harada T., Fujii S., Sogabe K., Kagawa K., Yoshida S., Endo I., Aihara K. and Abe M. (2016). "*Synergistic targeting of Sp1, a critical transcription factor for myeloma cell growth and survival, by panobinostat and proteasome inhibitors*." Oncotarget 7(48): 79064-79075.

Batchu, S. N., Brijmohan A. S. and Advani A. (2016). "*The therapeutic hope for HDAC6 inhibitors in malignancy and chronic disease*." Clin Sci (Lond) 130(12): 987-1003.

Batova, A., Shao L. E., Diccianni M. B., Yu A. L., Tanaka T., Rephaeli A., Nudelman A. and Yu J. (2002). "*The histone deacetylase inhibitor AN-9 has selective toxicity to acute leukemia and drug-resistant primary leukemia and cancer cell lines*." Blood 100(9): 3319-3324.

Bazzaro, M., Lin Z., Santillan A., Lee M. K., Wang M. C., Chan K. C., Bristow R. E., Mazitschek R., Bradner J. and Roden R. B. (2008). "*Ubiquitin proteasome system stress underlies synergistic killing of ovarian cancer cells by bortezomib and a novel HDAC6 inhibitor*." Clin Cancer Res 14(22): 7340-7347.

Becker, N. (2011). "*Epidemiology of multiple myeloma*." Recent Results Cancer Res 183: 25-35.

Beran, M., Pisa P., O'Brien S., Kurzrock R., Siciliano M., Cork A., Andersson B. S., Kohli V. and Kantarjian H. (1993). "*Biological properties and growth in SCID mice of a new myelogenous leukemia cell line (KBM-5) derived from chronic myelogenous leukemia cells in the blastic phase*." Cancer Res 53(15): 3603-3610.

Berger, S. L. (2007). "*The complex language of chromatin regulation during transcription*." Nature 447(7143): 407-412.

Bertos, N. R., Gilquin B., Chan G. K., Yen T. J., Khochbin S. and Yang X. J. (2004). "*Role of the tetradecapeptide repeat domain of human histone deacetylase 6 in cytoplasmic retention*." J Biol Chem 279(46): 48246-48254.

Bertrand, P. (2010). "*Inside HDAC with HDAC inhibitors*." Eur J Med Chem 45(6): 2095-2116.

Bhatnagar, N., Li X., Chen Y., Zhou X., Garrett S. H. and Guo B. (2009). "*3,3'-diindolylmethane enhances the efficacy of butyrate in colon cancer prevention through down-regulation of survivin*." Cancer Prev Res (Phila) 2(6): 581-589.

Bixby, D. and Talpaz M. (2009). "*Mechanisms of resistance to tyrosine kinase inhibitors in chronic myeloid leukemia and recent therapeutic strategies to overcome resistance*." Hematology Am Soc Hematol Educ Program: 461-476.

Blum, K. A., Advani A., Fernandez L., Van Der Jagt R., Brandwein J., Kambhampati S., Kassis J., Davis M., Bonfils C., Dubay M., Dumouchel J., Drouin M., Lucas D. M., Martell R. E. and Byrd J. C. (2009). "*Phase II study of the histone deacetylase inhibitor MGCD0103 in patients with previously treated chronic lymphocytic leukaemia*." Br J Haematol 147(4): 507-514.

Bodiford, A., Bodge M., Talbott M. S. and Reddy N. M. (2014). "*Profile of belinostat for the treatment of relapsed or refractory peripheral T-cell lymphoma*." Onco Targets Ther 7: 1971-1977.

Bolden, J. E., Peart M. J. and Johnstone R. W. (2006). "*Anticancer activities of histone deacetylase inhibitors*." Nat Rev Drug Discov 5(9): 769-784.

Bose, P., Park H., Al-Khafaji J. and Grant S. (2013). "*Strategies to circumvent the T315I gatekeeper mutation in the Bcr-Abl tyrosine kinase*." Leuk Res Rep 2(1): 18-20.

Boyault, C., Gilquin B., Zhang Y., Rybin V., Garman E., Meyer-Klaucke W., Matthias P., Muller C. W. and Khochbin S. (2006). "*HDAC6-p97/VCP controlled polyubiquitin chain turnover*." EMBO J 25(14): 3357-3366.

Boyault, C., Sadoul K., Pabion M. and Khochbin S. (2007a). "*HDAC6, at the crossroads between cytoskeleton and cell signaling by acetylation and ubiquitination*." Oncogene 26(37): 5468-5476.

Boyault, C., Zhang Y., Fritah S., Caron C., Gilquin B., Kwon S. H., Garrido C., Yao T. P., Vourc'h C., Matthias P. and Khochbin S. (2007b). "*HDAC6 controls major cell response pathways to cytotoxic accumulation of protein aggregates*." Genes Dev 21(17): 2172-2181.

Bradbury, C. A., Khanim F. L., Hayden R., Bunce C. M., White D. A., Drayson M. T., Craddock C. and Turner B. M. (2005). "*Histone deacetylases in acute myeloid leukaemia show a distinctive pattern of expression that changes selectively in response to deacetylase inhibitors*." Leukemia 19(10): 1751-1759.

Brewer, J. W., Hendershot L. M., Sherr C. J. and Diehl J. A. (1999). "*Mammalian unfolded protein response inhibits cyclin D1 translation and cell-cycle progression*." Proc Natl Acad Sci U S A 96(15): 8505-8510.

Bruning, A. and Juckstock J. (2015). "*Misfolded proteins: from little villains to little helpers in the fight against cancer*." Front Oncol 5: 47.

Brusa, G., Zuffa E., Mancini M., Benvenuti M., Calonghi N., Barbieri E. and Santucci M. A. (2006). "*P210 Bcr-abl tyrosine kinase interaction with histone deacetylase 1 modifies histone H4 acetylation and chromatin structure of chronic myeloid leukaemia haematopoietic progenitors*." Br J Haematol 132(3): 359-369.

Bu, Q., Cui L., Li J., Du X., Zou W., Ding K. and Pan J. (2014). "*SAHA and S116836, a novel tyrosine kinase inhibitor, synergistically induce apoptosis in imatinib-resistant chronic myelogenous leukemia cells*." Cancer Biol Ther 15(7): 951-962.

Burgess, R. J., Zhou H., Han J. and Zhang Z. (2010). "*A role for Gcn5 in replication-coupled nucleosome assembly*." Mol Cell 37(4): 469-480.

Butler, K. V., Kalin J., Brochier C., Vistoli G., Langley B. and Kozikowski A. P. (2010). "*Rational design and simple chemistry yield a superior, neuroprotective HDAC6 inhibitor, tubastatin A*." J Am Chem Soc 132(31): 10842-10846.

Campos, E. I., Fillingham J., Li G., Zheng H., Voigt P., Kuo W. H., Seepany H., Gao Z., Day L. A., Greenblatt J. F. and Reinberg D. (2010). "*The program for processing newly synthesized histones H3.1 and H4*." Nat Struct Mol Biol 17(11): 1343-1351.

Cao, S. S. and Kaufman R. J. (2012). "*Unfolded protein response*." Curr Biol 22(16): R622-626.

Carew, J. S., Nawrocki S. T., Kahue C. N., Zhang H., Yang C., Chung L., Houghton J. A., Huang P., Giles F. J. and Cleveland J. L. (2007). "*Targeting autophagy augments the anticancer activity of the histone deacetylase inhibitor SAHA to overcome Bcr-Abl-mediated drug resistance*." Blood 110(1): 313-322.

Carvalho, B. S. and Irizarry R. A. (2010). "*A framework for oligonucleotide microarray preprocessing*." Bioinformatics 26(19): 2363-2367.

Cea, M., Soncini D., Fruscione F., Raffaghello L., Garuti A., Emionite L., Moran E., Magnone M., Zoppoli G., Reverberi D., Caffa I., Salis A., Cagnetta A., Bergamaschi M., Casciaro S., Pierri I., Damonte G., Ansaldi F., Gobbi M., Pistoia V., Ballestrero A., Patrone F., Bruzzone S. and Nencioni A. (2011). "*Synergistic interactions between HDAC and sirtuin inhibitors in human leukemia cells*." PLoS One 6(7): e22739.

Ceballos, E., Delgado M. D., Gutierrez P., Richard C., Muller D., Eilers M., Ehinger M., Gullberg U. and Leon J. (2000). "*c-Myc antagonizes the effect of p53 on apoptosis and p21WAF1 transactivation in K562 leukemia cells*." Oncogene 19(18): 2194-2204.

Chateauvieux, S., Morceau F., Dicato M. and Diederich M. (2010). "*Molecular and therapeutic potential and toxicity of valproic acid*." J Biomed Biotechnol 2010.

Chen, P. B., Hung J. H., Hickman T. L., Coles A. H., Carey J. F., Weng Z., Chu F. and Fazzio T. G. (2013). "*Hdac6 regulates Tip60-p400 function in stem cells*." Elife 2: e01557.

Chen, Q., Yue F., Li W., Zou J., Xu T., Huang C., Zhang Y., Song K., Huang G., Xu G., Huang H., Li J. and Liu L. (2015). "*Potassium Bisperoxo(1,10-phenanthroline)oxovanadate (bpV(phen)) Induces Apoptosis and Pyroptosis and Disrupts the P62-HDAC6 Protein Interaction to Suppress the Acetylated Microtubule-dependent Degradation of Autophagosomes*." J Biol Chem 290(43): 26051-26058.

Chen, S., Owens G. C., Makarenkova H. and Edelman D. B. (2010). "*HDAC6 regulates mitochondrial transport in hippocampal neurons*." PLoS One 5(5): e10848.

Chen, S. H., Chow J. M., Hsieh Y. Y., Lin C. Y., Hsu K. W., Hsieh W. S., Chi W. M., Shabangu B. M. and Lee C. H. (2019). "*HDAC1,2 Knock-Out and HDACi Induced Cell Apoptosis in Imatinib-Resistant K562 Cells*." Int J Mol Sci 20(9).

Chhabra, S. (2017). "*Novel Proteasome Inhibitors and Histone Deacetylase Inhibitors: Progress in Myeloma Therapeutics*." Pharmaceuticals (Basel) 10(2).

Chou, T. C. (2006). "*Theoretical basis, experimental design, and computerized simulation of synergism and antagonism in drug combination studies*." Pharmacol Rev 58(3): 621-681.

Chou, T. C. (2010). "*Drug combination studies and their synergy quantification using the Chou-Talalay method*." Cancer Res 70(2): 440-446.

Choudhary, C., Weinert B. T., Nishida Y., Verdin E. and Mann M. (2014). "*The growing landscape of lysine acetylation links metabolism and cell signalling*." Nat Rev Mol Cell Biol 15(8): 536-550.

Chuang, M. J., Wu S. T., Tang S. H., Lai X. M., Lai H. C., Hsu K. H., Sun K. H., Sun G. H., Chang S. Y., Yu D. S., Hsiao P. W., Huang S. M. and Cha T. L. (2013). "*The HDAC inhibitor LBH589 induces ERK-dependent prometaphase arrest in prostate cancer via HDAC6 inactivation and down-regulation*." PLoS One 8(9): e73401.

Cilloni, D. and Saglio G. (2012). "*Molecular pathways: BCR-ABL*." Clin Cancer Res 18(4): 930-937.

Clapier, C. R. and Cairns B. R. (2009). "*The biology of chromatin remodeling complexes*." Annu Rev Biochem 78: 273-304.

Clocchiatti, A., Florean C. and Brancolini C. (2011). "*Class IIa HDACs: from important roles in differentiation to possible implications in tumourigenesis*." J Cell Mol Med 15(9): 1833-1846.

Cohen, H. Y., Lavu S., Bitterman K. J., Hekking B., Imahiyerobo T. A., Miller C., Frye R., Ploegh H., Kessler B. M. and Sinclair D. A. (2004). "*Acetylation of the C terminus of Ku70 by CBP and PCAF controls Bax-mediated apoptosis*." Mol Cell 13(5): 627-638.

Cortes, J. E., Apperley J. F., DeAngelo D. J., Deininger M. W., Kota V. K., Rousselot P. and Gambacorti-Passerini C. (2018a). "*Management of adverse events associated with bosutinib treatment of chronic-phase chronic myeloid leukemia: expert panel review*." J Hematol Oncol 11(1): 143.

Cortes, J. E., Gambacorti-Passerini C., Deininger M. W., Mauro M. J., Chuah C., Kim D. W., Dyagil I., Glushko N., Milojkovic D., le Coutre P., Garcia-Gutierrez V., Reilly L., Jeynes-Ellis A., Leip E., Bardy-Bouxin N., Hochhaus A. and Brummendorf T. H. (2018b). "*Bosutinib Versus Imatinib for Newly Diagnosed Chronic Myeloid Leukemia: Results From the Randomized BFORE Trial*." J Clin Oncol 36(3): 231-237.

Cottini, F. and Anderson K. (2015). "*Novel therapeutic targets in multiple myeloma*." Clin Adv Hematol Oncol 13(4): 236-248.

Crazzolara, R., Johrer K., Johnstone R. W., Greil R., Kofler R., Meister B. and Bernhard D. (2002). "*Histone deacetylase inhibitors potently repress CXCR4 chemokine receptor expression and function in acute lymphoblastic leukaemia*." Br J Haematol 119(4): 965-969.

Czabotar, P. E., Lessene G., Strasser A. and Adams J. M. (2014). "*Control of apoptosis by the BCL-2 protein family: implications for physiology and therapy*." Nat Rev Mol Cell Biol 15(1): 49-63.

Dai, Y., Chen S., Venditti C. A., Pei X. Y., Nguyen T. K., Dent P. and Grant S. (2008). "*Vorinostat synergistically potentiates MK-0457 lethality in chronic myelogenous leukemia cells sensitive and resistant to imatinib mesylate*." Blood 112(3): 793-804.

Dasari, S. and Tchounwou P. B. (2014). "*Cisplatin in cancer therapy: molecular mechanisms of action*." Eur J Pharmacol 740: 364-378.

de Ruijter, A. J., van Gennip A. H., Caron H. N., Kemp S. and van Kuilenburg A. B. (2003). "*Histone deacetylases (HDACs): characterization of the classical HDAC family*." Biochem J 370(Pt 3): 737-749.

Depetter, Y., Geurs S., De Vreese R., Goethals S., Vandoorn E., Laevens A., Steenbrugge J., Meyer E., de Tullio P., Bracke M., D'Hooghe M. and De Wever O. (2019). "*Selective pharmacological inhibitors of HDAC6 reveal biochemical activity but functional tolerance in cancer models*." Int J Cancer 145(3): 735-747.

Deribe, Y. L., Wild P., Chandrashaker A., Curak J., Schmidt M. H., Kalaidzidis Y., Milutinovic N., Kratchmarova I., Buerkle L., Fetchko M. J., Schmidt P., Kittanakom S., Brown K. R., Jurisica I., Blagoev B., Zerial M., Stagljar I. and Dikic I. (2009). "*Regulation of epidermal growth factor receptor trafficking by lysine deacetylase HDAC6*." Sci Signal 2(102): ra84.

Deskin, B., Lasky J., Zhuang Y. and Shan B. (2016). "*Requirement of HDAC6 for activation of Notch1 by TGF-beta1*." Sci Rep 6: 31086.

Di Fulvio, S., Azakir B. A., Therrien C. and Sinnreich M. (2011). "*Dysferlin interacts with histone deacetylase 6 and increases alpha-tubulin acetylation*." PLoS One 6(12): e28563.

Ding, G., Liu H. D., Huang Q., Liang H. X., Ding Z. H., Liao Z. J. and Huang G. (2013). "*HDAC6 promotes hepatocellular carcinoma progression by inhibiting P53 transcriptional activity*." FEBS Lett 587(7): 880-886.

Ding, N., Ping L., Feng L., Zheng X., Song Y. and Zhu J. (2014). "*Histone deacetylase 6 activity is critical for the metastasis of Burkitt's lymphoma cells*." Cancer Cell Int 14(1): 139.

Dong, S., Ma X., Wang Z., Han B., Zou H., Wu Z., Zang Y. and Zhuang L. (2017). "*YY1 promotes HDAC1 expression and decreases sensitivity of hepatocellular carcinoma cells to HDAC inhibitor*." Oncotarget 8(25): 40583-40593.

Duensing, T. D. and Watson S. R. (2018). "*Assessment of Apoptosis (Programmed Cell Death) by Flow Cytometry*." Cold Spring Harb Protoc 2018(1): pdb prot093807.

Duvic, M., Talpur R., Ni X., Zhang C., Hazarika P., Kelly C., Chiao J. H., Reilly J. F., Ricker J. L., Richon V. M. and Frankel S. R. (2007). "*Phase 2 trial of oral vorinostat (suberoylanilide hydroxamic acid, SAHA) for refractory cutaneous T-cell lymphoma (CTCL)*." Blood 109(1): 31-39.

Falkenberg, K. J. and Johnstone R. W. (2014). "*Histone deacetylases and their inhibitors in cancer, neurological diseases and immune disorders*." Nat Rev Drug Discov 13(9): 673-691.

Fang, T. J., Lin Y. Z., Liu C. C., Lin C. H., Li R. N., Wu C. C., Ou T. T., Tsai W. C. and Yen J. H. (2016). "*Methylation and gene expression of histone deacetylases 6 in systemic lupus erythematosus*." Int J Rheum Dis 19(10): 968-973.

Farre, J. C. and Subramani S. (2016). "*Mechanistic insights into selective autophagy pathways: lessons from yeast*." Nat Rev Mol Cell Biol 17(9): 537-552.

Field-Smith, A., Morgan G. J. and Davies F. E. (2006). "*Bortezomib (Velcadetrade mark) in the Treatment of Multiple Myeloma*." Ther Clin Risk Manag 2(3): 271-279.

Fierz, B., Chatterjee C., McGinty R. K., Bar-Dagan M., Raleigh D. P. and Muir T. W. (2011). "*Histone H2B ubiquitylation disrupts local and higher-order chromatin compaction*." Nat Chem Biol 7(2): 113-119.

Fiskus, W., Pranpat M., Balasis M., Bali P., Estrella V., Kumaraswamy S., Rao R., Rocha K., Herger B., Lee F., Richon V. and Bhalla K. (2006a). "*Cotreatment with vorinostat (suberoylanilide hydroxamic acid) enhances activity of dasatinib (BMS-354825) against imatinib mesylate-sensitive or imatinib mesylate-resistant chronic myelogenous leukemia cells*." Clin Cancer Res 12(19): 5869-5878.

Fiskus, W., Pranpat M., Bali P., Balasis M., Kumaraswamy S., Boyapalle S., Rocha K., Wu J., Giles F., Manley P. W., Atadja P. and Bhalla K. (2006b). "*Combined effects of novel tyrosine kinase inhibitor AMN107 and histone deacetylase inhibitor LBH589 against Bcr-Abl-expressing human leukemia cells*." Blood 108(2): 645-652.

Fiskus, W., Wang Y., Joshi R., Rao R., Yang Y., Chen J., Kolhe R., Balusu R., Eaton K., Lee P., Ustun C., Jillella A., Buser C. A., Peiper S. and Bhalla K. (2008). "*Cotreatment with vorinostat enhances activity of MK-0457 (VX-680) against acute and chronic myelogenous leukemia cells*." Clin Cancer Res 14(19): 6106-6115.

Florean, C., Schnekenburger M., Grandjenette C., Dicato M. and Diederich M. (2011). "*Epigenomics of leukemia: from mechanisms to therapeutic applications*." Epigenomics 3(5): 581-609.

Folmer, F., Orlikova B., Schnekenburger M., Dicato M. and Diederich M. (2010). "*Naturally occurring regulators of histone acetylation/deacetylation*." Current Nutrition & Food Science 6: 78-99.

Fontana, S., Alessandro R., Barranca M., Giordano M., Corrado C., Zanella-Cleon I., Becchi M., Kohn E. C. and De Leo G. (2007). "*Comparative proteome profiling and functional analysis of chronic myelogenous leukemia cell lines*." J Proteome Res 6(11): 4330-4342.

Friedmann, D. R., Aguilar A., Fan J., Nachury M. V. and Marmorstein R. (2012). "*Structure of the alpha-tubulin acetyltransferase, alphaTAT1, and implications for tubulin-specific acetylation*." Proc Natl Acad Sci U S A 109(48): 19655-19660.

Friedmann, D. R. and Marmorstein R. (2013). "*Structure and mechanism of non-histone protein acetyltransferase enzymes*." FEBS J 280(22): 5570-5581.

Furukawa, Y. and Kikuchi J. (2016). "*Epigenetic mechanisms of cell adhesion-mediated drug resistance in multiple myeloma*." Int J Hematol 104(3): 281-292.

Fusco, C., Micale L., Augello B., Mandriani B., Pellico M. T., De Nittis P., Calcagni A., Monti M., Cozzolino F., Pucci P. and Merla G. (2014). "*HDAC6 mediates the acetylation of TRIM50*." Cell Signal 26(2): 363-369.

Fusco, C., Micale L., Egorov M., Monti M., D'Addetta E. V., Augello B., Cozzolino F., Calcagni A., Fontana A., Polishchuk R. S., Didelot G., Reymond A., Pucci P. and Merla G. (2012). "*The E3-ubiquitin ligase TRIM50 interacts with HDAC6 and p62, and promotes the sequestration and clearance of ubiquitinated proteins into the aggresome*." PLoS One 7(7): e40440.

Gaisina, I. N., Tueckmantel W., Ugolkov A., Shen S., Hoffen J., Dubrovskyi O., Mazar A., Schoon R. A., Billadeau D. and Kozikowski A. P. (2016). "*Identification of HDAC6-Selective Inhibitors of Low Cancer Cell Cytotoxicity*." ChemMedChem 11(1): 81-92.

Galluzzi, L., Senovilla L., Vitale I., Michels J., Martins I., Kepp O., Castedo M. and Kroemer G. (2012). "*Molecular mechanisms of cisplatin resistance*." Oncogene 31(15): 1869-1883.

Gambella, M., Rocci A., Passera R., Gay F., Omede P., Crippa C., Corradini P., Romano A., Rossi D., Ladetto M., Boccadoro M. and Palumbo A. (2014). "*High XBP1 expression is a marker of better outcome in multiple myeloma patients treated with bortezomib*." Haematologica 99(2): e14-16.

Gammoh, N., Lam D., Puente C., Ganley I., Marks P. A. and Jiang X. (2012). "*Role of autophagy in histone deacetylase inhibitor-induced apoptotic and nonapoptotic cell death*." Proc Natl Acad Sci U S A 109(17): 6561-6565.

Gao, S., Mobley A., Miller C., Boklan J. and Chandra J. (2008). "*Potentiation of reactive oxygen species is a marker for synergistic cytotoxicity of MS-275 and 5-azacytidine in leukemic cells*." Leuk Res 32(5): 771-780.

Gao, Y. S., Hubbert C. C., Lu J., Lee Y. S., Lee J. Y. and Yao T. P. (2007). "*Histone deacetylase 6 regulates growth factor-induced actin remodeling and endocytosis*." Mol Cell Biol 27(24): 8637-8647.

Gao, Y. S., Hubbert C. C. and Yao T. P. (2010). "*The microtubule-associated histone deacetylase 6 (HDAC6) regulates epidermal growth factor receptor (EGFR) endocytic trafficking and degradation*." J Biol Chem 285(15): 11219-11226.

Garcia-Gutierrez, V. and Hernandez-Boluda J. C. (2019). "*Tyrosine Kinase Inhibitors Available for Chronic Myeloid Leukemia: Efficacy and Safety*." Front Oncol 9: 603.

Gardner, K. E., Allis C. D. and Strahl B. D. (2011). "*Operating on chromatin, a colorful language where context matters*." J Mol Biol 409(1): 36-46.

Gaymes, T. J., Padua R. A., Pla M., Orr S., Omidvar N., Chomienne C., Mufti G. J. and Rassool F. V. (2006). "*Histone deacetylase inhibitors (HDI) cause DNA damage in leukemia cells: a mechanism for leukemia-specific HDI-dependent apoptosis?*" Mol Cancer Res 4(8): 563-573.

Ghose, A. K., Viswanadhan V. N. and Wendoloski J. J. (1999). "*A knowledge-based approach in designing combinatorial or medicinal chemistry libraries for drug discovery. 1. A qualitative and quantitative characterization of known drug databases*." J Comb Chem 1(1): 55-68.

Ghosh, A. K. and Brindisi M. (2015). "*Organic carbamates in drug design and medicinal chemistry*." J Med Chem 58(7): 2895-2940.

Giles, F., Fischer T., Cortes J., Garcia-Manero G., Beck J., Ravandi F., Masson E., Rae P., Laird G., Sharma S., Kantarjian H., Dugan M., Albitar M. and Bhalla K. (2006). "*A phase I study of intravenous LBH589, a novel cinnamic hydroxamic acid analogue histone deacetylase inhibitor, in patients with refractory hematologic malignancies*." Clin Cancer Res 12(15): 4628-4635.

Giorgi, C., Baldassari F., Bononi A., Bonora M., De Marchi E., Marchi S., Missiroli S., Patergnani S., Rimessi A., Suski J. M., Wieckowski M. R. and Pinton P. (2012). "*Mitochondrial Ca(2+) and apoptosis*." Cell Calcium 52(1): 36-43.

Gong, J. N., Khong T., Segal D., Yao Y., Riffkin C. D., Garnier J. M., Khaw S. L., Lessene G., Spencer A., Herold M. J., Roberts A. W. and Huang D. C. (2016). "*Hierarchy for targeting pro-survival BCL2 family proteins in multiple myeloma: pivotal role of MCL1*." Blood.

Govindan, M. V. (2010). "*Recruitment of cAMP-response element-binding protein and histone deacetylase has opposite effects on glucocorticoid receptor gene transcription*." J Biol Chem 285(7): 4489-4510.

Gradilone, S. A., Radtke B. N., Bogert P. S., Huang B. Q., Gajdos G. B. and LaRusso N. F. (2013). "*HDAC6 inhibition restores ciliary expression and decreases tumor growth*." Cancer Res 73(7): 2259-2270.

Gregoretti, I. V., Lee Y. M. and Goodson H. V. (2004). "*Molecular evolution of the histone deacetylase family: functional implications of phylogenetic analysis*." J Mol Biol 338(1): 17-31.

Gryder, B. E., Sodji Q. H. and Oyelere A. K. (2012). "*Targeted cancer therapy: giving histone deacetylase inhibitors all they need to succeed*." Future Med Chem 4(4): 505-524.

Gu, S., Liu Y., Zhu B., Ding K., Yao T. P., Chen F., Zhan L., Xu P., Ehrlich M., Liang T., Lin X. and Feng X. H. (2016). "*Loss of alpha-Tubulin Acetylation Is Associated with TGF-beta-induced Epithelial-Mesenchymal Transition*." J Biol Chem 291(10): 5396-5405.

Gupta, V. A., Matulis S. M., Conage-Pough J. E., Nooka A. K., Kaufman J. L., Lonial S. and Boise L. H. (2017). "*Bone marrow microenvironment-derived signals induce Mcl-1 dependence in multiple myeloma*." Blood 129(14): 1969-1979.

Haggarty, S. J., Koeller K. M., Wong J. C., Grozinger C. M. and Schreiber S. L. (2003). "*Domain-selective small-molecule inhibitor of histone deacetylase 6 (HDAC6)-mediated tubulin deacetylation*." Proc Natl Acad Sci U S A 100(8): 4389-4394.

Hai, Y. and Christianson D. W. (2016). "*Histone deacetylase 6 structure and molecular basis of catalysis and inhibition*." Nat Chem Biol 12(9): 741-747.

Halkidou, K., Gaughan L., Cook S., Leung H. Y., Neal D. E. and Robson C. N. (2004). "*Upregulation and nuclear recruitment of HDAC1 in hormone refractory prostate cancer*." Prostate 59(2): 177-189.

Han, K., Xu X., Xu Z., Chen G., Zeng Y., Zhang Z., Cao B., Kong Y., Tang X. and Mao X. (2015). "*SC06, a novel small molecule compound, displays preclinical activity against multiple myeloma by disrupting the mTOR signaling pathway*." Sci Rep 5: 12809.

Han, Y., Jeong H. M., Jin Y. H., Kim Y. J., Jeong H. G., Yeo C. Y. and Lee K. Y. (2009). "*Acetylation of histone deacetylase 6 by p300 attenuates its deacetylase activity*." Biochem Biophys Res Commun 383(1): 88-92.

Hao, R., Nanduri P., Rao Y., Panichelli R. S., Ito A., Yoshida M. and Yao T. P. (2013). "*Proteasomes activate aggresome disassembly and clearance by producing unanchored ubiquitin chains*." Mol Cell 51(6): 819-828.

Harada, T., Hideshima T. and Anderson K. C. (2016). "*Histone deacetylase inhibitors in multiple myeloma: from bench to bedside*." Int J Hematol 104(3): 300-309.

Hauschild, A., Trefzer U., Garbe C., Kaehler K. C., Ugurel S., Kiecker F., Eigentler T., Krissel H., Schott A. and Schadendorf D. (2008). "*Multicenter phase II trial of the histone deacetylase inhibitor pyridylmethyl-N-{4-[(2-aminophenyl)-carbamoyl]-benzyl}-carbamate in pretreated metastatic melanoma*." Melanoma Res 18(4): 274-278.

Hawkes, N. A., Otero G., Winkler G. S., Marshall N., Dahmus M. E., Krappmann D., Scheidereit C., Thomas C. L., Schiavo G., Erdjument-Bromage H., Tempst P. and Svejstrup J. Q. (2002). "*Purification and characterization of the human elongator complex*." J Biol Chem 277(4): 3047-3052.

He, D., Guo X., Zhang E., Zi F., Chen J., Chen Q., Lin X., Yang L., Li Y., Wu W., Yang Y., He J. and Cai Z. (2016). "*Quercetin induces cell apoptosis of myeloma and displays a synergistic effect with dexamethasone in vitro and in vivo xenograft models*." Oncotarget 7(29): 45489-45499.

Hellebrekers, D. M., Castermans K., Vire E., Dings R. P., Hoebers N. T., Mayo K. H., Oude Egbrink M. G., Molema G., Fuks F., van Engeland M. and Griffioen A. W. (2006). "*Epigenetic regulation of tumor endothelial cell anergy: silencing of intercellular adhesion molecule-1 by histone modifications*." Cancer Res 66(22): 10770-10777.

Hideshima, T., Qi J., Paranal R. M., Tang W., Greenberg E., West N., Colling M. E., Estiu G., Mazitschek R., Perry J. A., Ohguchi H., Cottini F., Mimura N., Gorgun G., Tai Y. T., Richardson P. G., Carrasco R. D., Wiest O., Schreiber S. L., Anderson K. C. and Bradner J. E. (2016). "*Discovery of selective small-molecule HDAC6 inhibitor for overcoming proteasome inhibitor resistance in multiple myeloma*." Proc Natl Acad Sci U S A 113(46): 13162-13167.

Hideshima, T., Richardson P., Chauhan D., Palombella V. J., Elliott P. J., Adams J. and Anderson K. C. (2001). "*The proteasome inhibitor PS-341 inhibits growth, induces apoptosis, and overcomes drug resistance in human multiple myeloma cells*." Cancer Res 61(7): 3071-3076.

Hodawadekar, S. C. and Marmorstein R. (2007). "*Chemistry of acetyl transfer by histone modifying enzymes: structure, mechanism and implications for effector design*." Oncogene 26(37): 5528-5540.

Hoelbl, A., Kovacic B., Kerenyi M. A., Simma O., Warsch W., Cui Y., Beug H., Hennighausen L., Moriggl R. and Sexl V. (2006). "*Clarifying the role of Stat5 in lymphoid development and Abelson-induced transformation*." Blood 107(12): 4898-4906.

Holohan, C., Van Schaeybroeck S., Longley D. B. and Johnston P. G. (2013). "*Cancer drug resistance: an evolving paradigm*." Nat Rev Cancer 13(10): 714-726.

Hou, H., Zhao L., Chen W., Li J., Zuo Q., Zhang G., Zhang X. and Li X. (2015). "*Expression and significance of cortactin and HDAC6 in human prostatic foamy gland carcinoma*." Int J Exp Pathol 96(4): 248-254.

Houshmand, M., Simonetti G., Circosta P., Gaidano V., Cignetti A., Martinelli G., Saglio G. and Gale R. P. (2019). "*Chronic myeloid leukemia stem cells*." Leukemia 33(7): 1543-1556.

Hrzenjak, A., Moinfar F., Kremser M. L., Strohmeier B., Staber P. B., Zatloukal K. and Denk H. (2006). "*Valproate inhibition of histone deacetylase 2 affects differentiation and decreases proliferation of endometrial stromal sarcoma cells*." Mol Cancer Ther 5(9): 2203-2210.

Hubbert, C., Guardiola A., Shao R., Kawaguchi Y., Ito A., Nixon A., Yoshida M., Wang X. F. and Yao T. P. (2002). "*HDAC6 is a microtubule-associated deacetylase*." Nature 417(6887): 455-458.

Iacomino, G., Medici M. C., Napoli D. and Russo G. L. (2006). "*Effects of histone deacetylase inhibitors on p55CDC/Cdc20 expression in HT29 cell line*." J Cell Biochem 99(4): 1122-1131.

Inoue, S., Walewska R., Dyer M. J. and Cohen G. M. (2008). "*Downregulation of Mcl-1 potentiates HDACi-mediated apoptosis in leukemic cells*." Leukemia 22(4): 819-825.

Iwata, A., Riley B. E., Johnston J. A. and Kopito R. R. (2005). "*HDAC6 and microtubules are required for autophagic degradation of aggregated huntingtin*." J Biol Chem 280(48): 40282-40292.

Jabbour, E. and Kantarjian H. (2018). "*Chronic myeloid leukemia: 2018 update on diagnosis, therapy and monitoring*." Am J Hematol 93(3): 442-459.

Jabbour, E. J., Cortes J. E. and Kantarjian H. M. (2013). "*Resistance to tyrosine kinase inhibition therapy for chronic myelogenous leukemia: a clinical perspective and emerging treatment options*." Clin Lymphoma Myeloma Leuk 13(5): 515-529.

Jain, P., Kantarjian H., Patel K. P., Gonzalez G. N., Luthra R., Kanagal Shamanna R., Sasaki K., Jabbour E., Romo C. G., Kadia T. M., Pemmaraju N., Daver N., Borthakur G., Estrov Z., Ravandi F., O'Brien S. and Cortes J. (2016). "*Impact of BCR-ABL transcript type on outcome in patients with chronic-phase CML treated with tyrosine kinase inhibitors*." Blood 127(10): 1269-1275.

Jia, X., Zheng Y., Guo Y. and Chen K. (2019). "*Sodium butyrate and panobinostat induce apoptosis of chronic myeloid leukemia cells via multiple pathways*." Mol Genet Genomic Med 7(5): e613.

Jin, Y., Yao Y., Chen L., Zhu X., Jin B., Shen Y., Li J., Du X., Lu Y., Jiang S. and Pan J. (2016). "*Depletion of gamma-catenin by Histone Deacetylase Inhibition Confers Elimination of CML Stem Cells in Combination with Imatinib*." Theranostics 6(11): 1947-1962.

Jochems, J., Teegarden S. L., Chen Y., Boulden J., Challis C., Ben-Dor G. A., Kim S. F. and Berton O. (2015). "*Enhancement of stress resilience through histone deacetylase 6-mediated regulation of glucocorticoid receptor chaperone dynamics*." Biol Psychiatry 77(4): 345-355.

Jones, P., Altamura S., De Francesco R., Gallinari P., Lahm A., Neddermann P., Rowley M., Serafini S. and Steinkuhler C. (2008). "*Probing the elusive catalytic activity of vertebrate class IIa histone deacetylases*." Bioorg Med Chem Lett 18(6): 1814-1819.

Jung, H. Y., Jung J. S., Whang Y. M. and Kim Y. H. (2013). "*RASSF1A Suppresses Cell Migration through Inactivation of HDAC6 and Increase of Acetylated alpha-Tubulin*." Cancer Res Treat 45(2): 134-144.

Jung, K. H., Noh J. H., Kim J. K., Eun J. W., Bae H. J., Chang Y. G., Kim M. G., Park W. S., Lee J. Y., Lee S. Y., Chu I. S. and Nam S. W. (2012). "*Histone deacetylase 6 functions as a tumor suppressor by activating c-Jun NH2-terminal kinase-mediated beclin 1-dependent autophagic cell death in liver cancer*." Hepatology 56(2): 644-657.

Kabat, G. C., Wu J. W., Moore S. C., Morton L. M., Park Y., Hollenbeck A. R. and Rohan T. E. (2013). "*Lifestyle and dietary factors in relation to risk of chronic myeloid leukemia in the NIH-AARP Diet and Health Study*." Cancer Epidemiol Biomarkers Prev 22(5): 848-854.

Kahali, S., Sarcar B., Prabhu A., Seto E. and Chinnaiyan P. (2012). "*Class I histone deacetylases localize to the endoplasmic reticulum and modulate the unfolded protein response*." FASEB J 26(6): 2437-2445.

Kalin, J. H. and Bergman J. A. (2013). "*Development and therapeutic implications of selective histone deacetylase 6 inhibitors*." J Med Chem 56(16): 6297-6313.

Kalin, J. H., Butler K. V., Akimova T., Hancock W. W. and Kozikowski A. P. (2012). "*Second-generation histone deacetylase 6 inhibitors enhance the immunosuppressive effects of Foxp3+ T-regulatory cells*." J Med Chem 55(2): 639-651.

Kaluza, D., Kroll J., Gesierich S., Yao T. P., Boon R. A., Hergenreider E., Tjwa M., Rossig L., Seto E., Augustin H. G., Zeiher A. M., Dimmeler S. and Urbich C. (2011). "*Class IIb HDAC6 regulates endothelial cell migration and angiogenesis by deacetylation of cortactin*." EMBO J 30(20): 4142-4156.

Kamemura, K., Ito A., Shimazu T., Matsuyama A., Maeda S., Yao T. P., Horinouchi S., Khochbin S. and Yoshida M. (2008). "*Effects of downregulated HDAC6 expression on the proliferation of lung cancer cells*." Biochem Biophys Res Commun 374(1): 84-89.

Kaneko, M., Imaizumi K., Saito A., Kanemoto S., Asada R., Matsuhisa K. and Ohtake Y. (2017). "*ER Stress and Disease: Toward Prevention and Treatment*." Biol Pharm Bull 40(9): 1337-1343.

Kanno, K., Kanno S., Nitta H., Uesugi N., Sugai T., Masuda T., Wakabayashi G. and Maesawa C. (2012). "*Overexpression of histone deacetylase 6 contributes to accelerated migration and invasion activity of hepatocellular carcinoma cells*." Oncol Rep 28(3): 867-873.

Kassambara, A. (2018). ggpubr: 'ggplot2' Based Publication Ready Plots.

Kawaguchi, Y., Kovacs J. J., McLaurin A., Vance J. M., Ito A. and Yao T. P. (2003). "*The deacetylase HDAC6 regulates aggresome formation and cell viability in response to misfolded protein stress*." Cell 115(6): 727-738.

Kepp, O., Menger L., Vacchelli E., Locher C., Adjemian S., Yamazaki T., Martins I., Sukkurwala A. Q., Michaud M., Senovilla L., Galluzzi L., Kroemer G. and Zitvogel L. (2013). "*Crosstalk between ER stress and immunogenic cell death*." Cytokine Growth Factor Rev 24(4): 311-318.

Kerr, E., Holohan C., McLaughlin K. M., Majkut J., Dolan S., Redmond K., Riley J., McLaughlin K., Stasik I., Crudden M., Van Schaeybroeck S., Fenning C., O'Connor R., Kiely P., Sgobba M., Haigh D., Johnston P. G. and Longley D. B. (2012). "*Identification of an acetylation-dependant Ku70/FLIP complex that regulates FLIP expression and HDAC inhibitor-induced apoptosis*." Cell Death Differ 19(8): 1317-1327.

Kerr, J. F., Wyllie A. H. and Currie A. R. (1972). "*Apoptosis: a basic biological phenomenon with wide-ranging implications in tissue kinetics*." Br J Cancer 26(4): 239-257.

Khan, S. N. and Khan A. U. (2010). "*Role of histone acetylation in cell physiology and diseases: An update*." Clin Chim Acta 411(19-20): 1401-1411.

Kim, B. S., Bae E., Kim Y. J., Ahn K. S., Park J., Rhee J. Y., Lee Y. Y., Kim Y., Lee D., Kim B. K. and Yoon S. S. (2007). "*Combination of SK-7041, one of novel histone deacetylase inhibitors, and STI571-induced synergistic apoptosis in chronic myeloid leukemia*." Anticancer Drugs 18(6): 641-647.

Kim, H. S., Shen Q. and Nam S. W. (2015). "*Histone Deacetylases and Their Regulatory MicroRNAs in Hepatocarcinogenesis*." J Korean Med Sci 30(10): 1375-1380.

Kim, I. A., No M., Lee J. M., Shin J. H., Oh J. S., Choi E. J., Kim I. H., Atadja P. and Bernhard E. J. (2009). "*Epigenetic modulation of radiation response in human cancer cells with activated EGFR or HER-2 signaling: potential role of histone deacetylase 6*." Radiother Oncol 92(1): 125-132.

Kimura, A., Matsubara K. and Horikoshi M. (2005). "*A decade of histone acetylation: marking eukaryotic chromosomes with specific codes*." J Biochem 138(6): 647-662.

Kinner, A., Wu W., Staudt C. and Iliakis G. (2008). "*Gamma-H2AX in recognition and signaling of DNA double-strand breaks in the context of chromatin*." Nucleic Acids Res 36(17): 5678-5694.

Koeneke, E., Witt O. and Oehme I. (2015). "*HDAC Family Members Intertwined in the Regulation of Autophagy: A Druggable Vulnerability in Aggressive Tumor Entities*." Cells 4(2): 135-168.

Kolesnikov, N., Hastings E., Keays M., Melnichuk O., Tang Y. A., Williams E., Dylag M., Kurbatova N., Brandizi M., Burdett T., Megy K., Pilicheva E., Rustici G., Tikhonov A., Parkinson H., Petryszak R., Sarkans U. and Brazma A. (2015). "*ArrayExpress update--simplifying data submissions*." Nucleic Acids Res 43(Database issue): D1113-1116.

Kominsky, D. J., Klawitter J., Brown J. L., Boros L. G., Melo J. V., Eckhardt S. G. and Serkova N. J. (2009). "*Abnormalities in glucose uptake and metabolism in imatinib-resistant human BCR-ABL-positive cells*." Clin Cancer Res 15(10): 3442-3450.

Kouzarides, T. (2007). "*Chromatin modifications and their function*." Cell 128(4): 693-705.

Kovacs, J. J., Murphy P. J., Gaillard S., Zhao X., Wu J. T., Nicchitta C. V., Yoshida M., Toft D. O., Pratt W. B. and Yao T. P. (2005). "*HDAC6 regulates Hsp90 acetylation and chaperone-dependent activation of glucocorticoid receptor*." Mol Cell 18(5): 601-607.

Kozikowski, A. P., Tapadar S., Luchini D. N., Kim K. H. and Billadeau D. D. (2008). "*Use of the nitrile oxide cycloaddition (NOC) reaction for molecular probe generation: a new class of enzyme selective histone deacetylase inhibitors (HDACIs) showing picomolar activity at HDAC6*." J Med Chem 51(15): 4370-4373.

Kramer, O. H., Mahboobi S. and Sellmer A. (2014). "*Drugging the HDAC6-HSP90 interplay in malignant cells*." Trends Pharmacol Sci 35(10): 501-509.

Kroemer, G. (2015). "*Autophagy: a druggable process that is deregulated in aging and human disease*." J Clin Invest 125(1): 1-4.

Kumagai, T., Wakimoto N., Yin D., Gery S., Kawamata N., Takai N., Komatsu N., Chumakov A., Imai Y. and Koeffler H. P. (2007). "*Histone deacetylase inhibitor, suberoylanilide hydroxamic acid (Vorinostat, SAHA) profoundly inhibits the growth of human pancreatic cancer cells*." Int J Cancer 121(3): 656-665.

Kumar, S. K., Rajkumar V., Kyle R. A., van Duin M., Sonneveld P., Mateos M. V., Gay F. and Anderson K. C. (2017). "*Multiple myeloma*." Nat Rev Dis Primers 3: 17046.

Lagger, G., O'Carroll D., Rembold M., Khier H., Tischler J., Weitzer G., Schuettengruber B., Hauser C., Brunmeir R., Jenuwein T. and Seiser C. (2002). "*Essential function of histone deacetylase 1 in proliferation control and CDK inhibitor repression*." EMBO J 21(11): 2672-2681.

Lahm, A., Paolini C., Pallaoro M., Nardi M. C., Jones P., Neddermann P., Sambucini S., Bottomley M. J., Lo Surdo P., Carfi A., Koch U., De Francesco R., Steinkuhler C. and

Gallinari P. (2007). "*Unraveling the hidden catalytic activity of vertebrate class IIa histone deacetylases*." Proc Natl Acad Sci U S A 104(44): 17335-17340.

Lam, H. C., Cloonan S. M., Bhashyam A. R., Haspel J. A., Singh A., Sathirapongsasuti J. F., Cervo M., Yao H., Chung A. L., Mizumura K., An C. H., Shan B., Franks J. M., Haley K. J., Owen C. A., Tesfaigzi Y., Washko G. R., Quackenbush J., Silverman E. K., Rahman I., Kim H. P., Mahmood A., Biswal S. S., Ryter S. W. and Choi A. M. (2013). "*Histone deacetylase 6-mediated selective autophagy regulates COPD-associated cilia dysfunction*." J Clin Invest 123(12): 5212-5230.

Lam, K. and Zhang D. E. (2012). "*RUNX1 and RUNX1-ETO: roles in hematopoiesis and leukemogenesis*." Front Biosci (Landmark Ed) 17: 1120-1139.

Leder, A. and Leder P. (1975). "*Butyric acid, a potent inducer of erythroid differentiation in cultured erythroleukemic cells*." Cell 5(3): 319-322.

Lee, J. H., Choy M. L. and Marks P. A. (2012). "*Mechanisms of resistance to histone deacetylase inhibitors*." Adv Cancer Res 116: 39-86.

Lee, J. H., Choy M. L., Ngo L., Foster S. S. and Marks P. A. (2010). "*Histone deacetylase inhibitor induces DNA damage, which normal but not transformed cells can repair*." Proc Natl Acad Sci U S A 107(33): 14639-14644.

Lee, J. H., Mahendran A., Yao Y., Ngo L., Venta-Perez G., Choy M. L., Kim N., Ham W. S., Breslow R. and Marks P. A. (2013). "*Development of a histone deacetylase 6 inhibitor and its biological effects*." Proc Natl Acad Sci U S A 110(39): 15704-15709.

Lee, J. Y., Koga H., Kawaguchi Y., Tang W., Wong E., Gao Y. S., Pandey U. B., Kaushik S., Tresse E., Lu J., Taylor J. P., Cuervo A. M. and Yao T. P. (2010a). "*HDAC6 controls autophagosome maturation essential for ubiquitin-selective quality-control autophagy*." EMBO J 29(5): 969-980.

Lee, J. Y., Nagano Y., Taylor J. P., Lim K. L. and Yao T. P. (2010b). "*Disease-causing mutations in parkin impair mitochondrial ubiquitination, aggregation, and HDAC6-dependent mitophagy*." J Cell Biol 189(4): 671-679.

Lee, K. K. and Workman J. L. (2007). "*Histone acetyltransferase complexes: one size doesn't fit all*." Nat Rev Mol Cell Biol 8(4): 284-295.

Lee, S. M., Bae J. H., Kim M. J., Lee H. S., Lee M. K., Chung B. S., Kim D. W., Kang C. D. and Kim S. H. (2007). "*Bcr-Abl-independent imatinib-resistant K562 cells show aberrant protein acetylation and increased sensitivity to histone deacetylase inhibitors*." J Pharmacol Exp Ther 322(3): 1084-1092.

Lee, S. W., Yang J., Kim S. Y., Jeong H. K., Lee J., Kim W. J., Lee E. J. and Kim H. S. (2015). "*MicroRNA-26a induced by hypoxia targets HDAC6 in myogenic differentiation of embryonic stem cells*." Nucleic Acids Res 43(4): 2057-2073.

Lee, Y. S., Lim K. H., Guo X., Kawaguchi Y., Gao Y., Barrientos T., Ordentlich P., Wang X. F., Counter C. M. and Yao T. P. (2008). "*The cytoplasmic deacetylase HDAC6 is required for efficient oncogenic tumorigenesis*." Cancer Res 68(18): 7561-7569.

Levy, J. M. M., Towers C. G. and Thorburn A. (2017). "*Targeting autophagy in cancer*." Nat Rev Cancer 17(9): 528-542.

Li, D., Sun X., Zhang L., Yan B., Xie S., Liu R., Liu M. and Zhou J. (2014). "*Histone deacetylase 6 and cytoplasmic linker protein 170 function together to regulate the motility of pancreatic cancer cells*." Protein Cell 5(3): 214-223.

Li, D., Xie S., Ren Y., Huo L., Gao J., Cui D., Liu M. and Zhou J. (2011). "*Microtubule-associated deacetylase HDAC6 promotes angiogenesis by regulating cell migration in an EB1-dependent manner*." Protein Cell 2(2): 150-160.

Li, L. and Yang X. J. (2015). "*Tubulin acetylation: responsible enzymes, biological functions and human diseases*." Cell Mol Life Sci 72(22): 4237-4255.

Li, S., Liu X., Chen X., Zhang L. and Wang X. (2015). "*Histone deacetylase 6 promotes growth of glioblastoma through inhibition of SMAD2 signaling*." Tumour Biol 36(12): 9661-9665.

Li, Y., Shin D. and Kwon S. H. (2013). "*Histone deacetylase 6 plays a role as a distinct regulator of diverse cellular processes*." FEBS J 280(3): 775-793.

Li, Z. Y., Zhang C., Zhang Y., Chen L., Chen B. D., Li Q. Z., Zhang X. J. and Li W. P. (2017). "*A novel HDAC6 inhibitor Tubastatin A: Controls HDAC6-p97/VCP-mediated ubiquitination-autophagy turnover and reverses Temozolomide-induced ER stress-tolerance in GBM cells*." Cancer Lett 391: 89-99.

Lienlaf, M., Perez-Villarroel P., Knox T., Pabon M., Sahakian E., Powers J., Woan K. V., Lee C., Cheng F., Deng S., Smalley K. S., Montecino M., Kozikowski A., Pinilla-Ibarz J., Sarnaik A., Seto E., Weber J., Sotomayor E. M. and Villagra A. (2016). "*Essential role of HDAC6 in the regulation of PD-L1 in melanoma*." Mol Oncol 10(5): 735-750.

Lim, J. A. and Juhnn Y. S. (2016). "*Isoproterenol increases histone deacetylase 6 expression and cell migration by inhibiting ERK signaling via PKA and Epac pathways in human lung cancer cells*." Exp Mol Med 48(1): e204.

Lin, K., Zhang Q., Liu Z., Yang S., Lin Y., Wen C. and Zheng Y. (2015). "*Effects of suberoylanilide hydroxamic acid on rat cytochrome P450 enzyme activities*." Int J Clin Exp Pathol 8(5): 5584-5590.

Lindholm, D., Korhonen L., Eriksson O. and Koks S. (2017). "*Recent Insights into the Role of Unfolded Protein Response in ER Stress in Health and Disease*." Front Cell Dev Biol 5: 48.

Linev, A. J., Ivanov H. J., Zhelyazkov I. G., Ivanova H., Goranova-Marinova V. S. and Stoyanova V. K. (2018). "*Mutations Associated with Imatinib Mesylate Resistance - Review*." Folia Med (Plovdiv) 60(4): 617-623.

Lipinski, C. A. (2004). "*Lead- and drug-like compounds: the rule-of-five revolution*." Drug Discov Today Technol 1(4): 337-341.

Liu, J., Gu J., Feng Z., Yang Y., Zhu N., Lu W. and Qi F. (2016). "*Both HDAC5 and HDAC6 are required for the proliferation and metastasis of melanoma cells*." J Transl Med 14: 7.

Liu, K. P., Zhou D., Ouyang D. Y., Xu L. H., Wang Y., Wang L. X., Pan H. and He X. H. (2013). "*LC3B-II deacetylation by histone deacetylase 6 is involved in serum-starvation-induced autophagic degradation*." Biochem Biophys Res Commun 441(4): 970-975.

Liu, N., Wang C., Wang L., Gao L., Cheng H., Tang G., Hu X. and Wang J. (2016). "*Valproic acid enhances the antileukemic effect of cytarabine by triggering cell apoptosis*." Int J Mol Med 37(6): 1686-1696.

Liu, W., Fan L. X., Zhou X., Sweeney W. E., Jr., Avner E. D. and Li X. (2012). "*HDAC6 regulates epidermal growth factor receptor (EGFR) endocytic trafficking and degradation in renal epithelial cells*." PLoS One 7(11): e49418.

Liu, Y., Cao Y., Zhang W., Bergmeier S., Qian Y., Akbar H., Colvin R., Ding J., Tong L., Wu S., Hines J. and Chen X. (2012). "*A small-molecule inhibitor of glucose transporter 1 downregulates glycolysis, induces cell-cycle arrest, and inhibits cancer cell growth in vitro and in vivo*." Mol Cancer Ther 11(8): 1672-1682.

Liu, Y. and Gray N. S. (2006). "*Rational design of inhibitors that bind to inactive kinase conformations*." Nat Chem Biol 2(7): 358-364.

Liu, Y., Li L. and Min J. (2016). "*Structural biology: HDAC6 finally crystal clear*." Nat Chem Biol 12(9): 660-661.

Liu, Y., Salvador L. A., Byeon S., Ying Y., Kwan J. C., Law B. K., Hong J. and Luesch H. (2010). "*Anticolon cancer activity of largazole, a marine-derived tunable histone deacetylase inhibitor*." J Pharmacol Exp Ther 335(2): 351-361.

Lopez-Iglesias, A. A., Gonzalez-Mendez L., San-Segundo L., Herrero A. B., Hernandez-Garcia S., Martin-Sanchez M., Gutierrez N. C., Paino T., Aviles P., Mateos M. V., San-Miguel J. F., Garayoa M. and Ocio E. M. (2016). "*Synergistic DNA-damaging effect in multiple myeloma with the combination of zalypsis, bortezomib and dexamethasone*." Haematologica.

Losson, H., Schnekenburger M., Dicato M. and Diederich M. (2016). "*Natural Compound Histone Deacetylase Inhibitors (HDACi): Synergy with Inflammatory Signaling Pathway Modulators and Clinical Applications in Cancer*." Molecules 21(11).

Lu, S. and Wang J. (2013). "*The resistance mechanisms of proteasome inhibitor bortezomib*." Biomark Res 1(1): 13.

Luu, T. H., Morgan R. J., Leong L., Lim D., McNamara M., Portnow J., Frankel P., Smith D. D., Doroshow J. H., Wong C., Aparicio A., Gandara D. R. and Somlo G. (2008). "*A phase II trial of vorinostat (suberoylanilide hydroxamic acid) in metastatic breast cancer: a California Cancer Consortium study*." Clin Cancer Res 14(21): 7138-7142.

Lv, Z., Weng X., Du C., Zhang C., Xiao H., Cai X., Ye S., Cheng J., Ding C., Xie H., Zhou L., Wu J. and Zheng S. (2016). "*Downregulation of HDAC6 promotes angiogenesis in hepatocellular carcinoma cells and predicts poor prognosis in liver transplantation patients*." Mol Carcinog 55(5): 1024-1033.

Macho, A., Decaudin D., Castedo M., Hirsch T., Susin S. A., Zamzami N. and Kroemer G. (1996). "*Chloromethyl-X-Rosamine is an aldehyde-fixable potential-sensitive fluorochrome for the detection of early apoptosis*." Cytometry 25(4): 333-340.

Manallack, D. T., Prankerd R. J., Yuriev E., Oprea T. I. and Chalmers D. K. (2013). "*The significance of acid/base properties in drug discovery*." Chem Soc Rev 42(2): 485-496.

Manier, S., Sacco A., Leleu X., Ghobrial I. M. and Roccaro A. M. (2012). "*Bone marrow microenvironment in multiple myeloma progression*." J Biomed Biotechnol 2012: 157496.

Manni, S., Carrino M., Manzoni M., Gianesin K., Nunes S. C., Costacurta M., Tubi L. Q., Macaccaro P., Taiana E., Cabrelle A., Barila G., Martines A., Zambello R., Bonaldi L., Trentin L., Neri A., Semenzato G. and Piazza F. (2017). "*Inactivation of CK1alpha in multiple myeloma empowers drug cytotoxicity by affecting AKT and beta-catenin survival signaling pathways*." Oncotarget 8(9): 14604-14619.

Marcato, P., Dean C. A., Giacomantonio C. A. and Lee P. W. (2011). "*Aldehyde dehydrogenase: its role as a cancer stem cell marker comes down to the specific isoform*." Cell Cycle 10(9): 1378-1384.

Marcus, A. I., Zhou J., O'Brate A., Hamel E., Wong J., Nivens M., El-Naggar A., Yao T. P., Khuri F. R. and Giannakakou P. (2005). "*The synergistic combination of the farnesyl transferase inhibitor lonafarnib and paclitaxel enhances tubulin acetylation and requires a functional tubulin deacetylase*." Cancer Res 65(9): 3883-3893.

Margariti, A., Li H., Chen T., Martin D., Vizcay-Barrena G., Alam S., Karamariti E., Xiao Q., Zampetaki A., Zhang Z., Wang W., Jiang Z., Gao C., Ma B., Chen Y. G., Cockerill G., Hu Y., Xu Q. and Zeng L. (2013). "*XBP1 mRNA splicing triggers an autophagic response in endothelial cells through BECLIN-1 transcriptional activation*." J Biol Chem 288(2): 859-872.

Marks, P. A. and Breslow R. (2007). "*Dimethyl sulfoxide to vorinostat: development of this histone deacetylase inhibitor as an anticancer drug*." Nat Biotechnol 25(1): 84-90.

Marlow, L. A., Bok I., Smallridge R. C. and Copland J. A. (2015). "*RhoB upregulation leads to either apoptosis or cytostasis through differential target selection*." Endocr Relat Cancer 22(5): 777-792.

Marquard, L., Gjerdrum L. M., Christensen I. J., Jensen P. B., Sehested M. and Ralfkiaer E. (2008). "*Prognostic significance of the therapeutic targets histone deacetylase 1, 2, 6 and acetylated histone H4 in cutaneous T-cell lymphoma*." Histopathology 53(3): 267-277.

Massaro, F., Molica M. and Breccia M. (2018). "*Ponatinib: A Review of Efficacy and Safety*." Curr Cancer Drug Targets 18(9): 847-856.

Matsuda, Y., Yamauchi T., Hosono N., Uzui K., Negoro E., Morinaga K., Nishi R., Yoshida A., Kimura S., Maekawa T. and Ueda T. (2016). "*Combination of panobinostat with ponatinib synergistically overcomes imatinib-resistant CML cells*." Cancer Sci 107(7): 1029-1038.

Matthias, P., Yoshida M. and Khochbin S. (2008). "*HDAC6 a new cellular stress surveillance factor*." Cell Cycle 7(1): 7-10.

Mazumder, A., Lee J. Y., Talhi O., Cerella C., Chateauvieux S., Gaigneaux A., Hong C. R., Kang H. J., Lee Y., Kim K. W., Kim D. W., Shin H. Y., Dicato M., Bachari K., Silva A. M. S., Orlikova-Boyer B. and Diederich M. (2018). "*Hydroxycoumarin OT-55 kills CML cells alone or in synergy with imatinib or Synribo: Involvement of ER stress and DAMP release*." Cancer Lett 438: 197-218.

Meenakshi Sundaram, D. N., Jiang X., Brandwein J. M., Valencia-Serna J., Remant K. C. and Uludag H. (2019). "*Current outlook on drug resistance in chronic myeloid leukemia (CML) and potential therapeutic options*." Drug Discov Today 24(7): 1355-1369.

Miller, K. M., Tjeertes J. V., Coates J., Legube G., Polo S. E., Britton S. and Jackson S. P. (2010). "*Human HDAC1 and HDAC2 function in the DNA-damage response to promote DNA nonhomologous end-joining*." Nat Struct Mol Biol 17(9): 1144-1151.

Misawa, T., Takahama M., Kozaki T., Lee H., Zou J., Saitoh T. and Akira S. (2013). "*Microtubule-driven spatial arrangement of mitochondria promotes activation of the NLRP3 inflammasome*." Nat Immunol 14(5): 454-460.

Mishima, Y., Santo L., Eda H., Cirstea D., Nemani N., Yee A. J., O'Donnell E., Selig M. K., Quayle S. N., Arastu-Kapur S., Kirk C., Boise L. H., Jones S. S. and Raje N. (2015). "*Ricolinostat (ACY-1215) induced inhibition of aggresome formation accelerates carfilzomib-induced multiple myeloma cell death*." Br J Haematol 169(3): 423-434.

Miyake, Y., Keusch J. J., Wang L., Saito M., Hess D., Wang X., Melancon B. J., Helquist P., Gut H. and Matthias P. (2016). "*Structural insights into HDAC6 tubulin deacetylation and its selective inhibition*." Nat Chem Biol 12(9): 748-754.

Miyata, Y., Nakamoto H. and Neckers L. (2013). "*The therapeutic target Hsp90 and cancer hallmarks*." Curr Pharm Des 19(3): 347-365.

Modesitt, S. C., Sill M., Hoffman J. S., Bender D. P. and Gynecologic Oncology G. (2008). "*A phase II study of vorinostat in the treatment of persistent or recurrent epithelial ovarian or primary peritoneal carcinoma: a Gynecologic Oncology Group study*." Gynecol Oncol 109(2): 182-186.

Modi, H., McDonald T., Chu S., Yee J. K., Forman S. J. and Bhatia R. (2007). "*Role of BCR/ABL gene-expression levels in determining the phenotype and imatinib sensitivity of transformed human hematopoietic cells*." Blood 109(12): 5411-5421.

Morales, A. A., Kurtoglu M., Matulis S. M., Liu J., Siefker D., Gutman D. M., Kaufman J. L., Lee K. P., Lonial S. and Boise L. H. (2011). "*Distribution of Bim determines Mcl-1 dependence or codependence with Bcl-xL/Bcl-2 in Mcl-1-expressing myeloma cells*." Blood 118(5): 1329-1339.

Moreno, D. A., Scrideli C. A., Cortez M. A., de Paula Queiroz R., Valera E. T., da Silva Silveira V., Yunes J. A., Brandalise S. R. and Tone L. G. (2010). "*Differential expression of HDAC3, HDAC7 and HDAC9 is associated with prognosis and survival in childhood acute lymphoblastic leukaemia*." Br J Haematol 150(6): 665-673.

Moriya, S., Komatsu S., Yamasaki K., Kawai Y., Kokuba H., Hirota A., Che X. F., Inazu M., Gotoh A., Hiramoto M. and Miyazawa K. (2015). "*Targeting the integrated networks of aggresome formation, proteasome, and autophagy potentiates ER stressmediated cell death in multiple myeloma cells*." Int J Oncol 46(2): 474-486.

Morotti, A., Cilloni D., Messa F., Arruga F., Defilippi I., Carturan S., Catalano R., Rosso V., Chiarenza A., Pilatrino C., Guerrasio A., Taulli R., Bracco E., Pautasso M., Baraban D., Gottardi E. and Saglio G. (2006). "*Valproate enhances imatinib-induced growth arrest and apoptosis in chronic myeloid leukemia cells*." Cancer 106(5): 1188-1196.

Moser, M. A., Hagelkruys A. and Seiser C. (2014). "*Transcription and beyond: the role of mammalian class I lysine deacetylases*." Chromosoma 123(1-2): 67-78.

Mrakovcic, M., Kleinheinz J. and Frohlich L. F. (2019). "*p53 at the Crossroads between Different Types of HDAC Inhibitor-Mediated Cancer Cell Death*." Int J Mol Sci 20(10).

Mughal, T. I., Radich J. P., Deininger M. W., Apperley J. F., Hughes T. P., Harrison C. J., Gambacorti-Passerini C., Saglio G., Cortes J. and Daley G. Q. (2016). "*Chronic myeloid leukemia: reminiscences and dreams*." Haematologica 101(5): 541-558.

Nagai, T., Ikeda M., Chiba S., Kanno S. and Mizuno K. (2013). "*Furry promotes acetylation of microtubules in the mitotic spindle by inhibition of SIRT2 tubulin deacetylase*." J Cell Sci 126(Pt 19): 4369-4380.

Nalawansha, D. A., Gomes I. D., Wambua M. K. and Pflum M. K. H. (2017). "*HDAC Inhibitor-Induced Mitotic Arrest Is Mediated by Eg5/KIF11 Acetylation*." Cell Chem Biol 24(4): 481-492 e485.

Namdar, M., Perez G., Ngo L. and Marks P. A. (2010). "*Selective inhibition of histone deacetylase 6 (HDAC6) induces DNA damage and sensitizes transformed cells to anticancer agents*." Proc Natl Acad Sci U S A 107(46): 20003-20008.

Nawrocki, S. T., Carew J. S., Pino M. S., Highshaw R. A., Andtbacka R. H., Dunner K., Jr., Pal A., Bornmann W. G., Chiao P. J., Huang P., Xiong H., Abbruzzese J. L. and McConkey D. J. (2006). "*Aggresome disruption: a novel strategy to enhance bortezomib-induced apoptosis in pancreatic cancer cells*." Cancer Res 66(7): 3773-3781.

Nestal de Moraes, G., Souza P. S., Costas F. C., Vasconcelos F. C., Reis F. R. and Maia R. C. (2012). "*The Interface between BCR-ABL-Dependent and -Independent Resistance Signaling Pathways in Chronic Myeloid Leukemia*." Leuk Res Treatment 2012: 671702.

Nguyen, T., Dai Y., Attkisson E., Kramer L., Jordan N., Nguyen N., Kolluri N., Muschen M. and Grant S. (2011). "*HDAC inhibitors potentiate the activity of the BCR/ABL kinase inhibitor KW-2449 in imatinib-sensitive or -resistant BCR/ABL+ leukemia cells in vitro and in vivo*." Clin Cancer Res 17(10): 3219-3232.

Nimmanapalli, R., Fuino L., Stobaugh C., Richon V. and Bhalla K. (2003). "*Cotreatment with the histone deacetylase inhibitor suberoylanilide hydroxamic acid (SAHA) enhances imatinib-induced apoptosis of Bcr-Abl-positive human acute leukemia cells*." Blood 101(8): 3236-3239.

Nogues, L., Reglero C., Rivas V., Salcedo A., Lafarga V., Neves M., Ramos P., Mendiola M., Berjon A., Stamatakis K., Zhou X. Z., Lu K. P., Hardisson D., Mayor F., Jr. and Penela P. (2016). "*G Protein-coupled Receptor Kinase 2 (GRK2) Promotes Breast Tumorigenesis Through a HDAC6-Pin1 Axis*." EBioMedicine 13: 132-145.

Ogu, C. C. and Maxa J. L. (2000). "*Drug interactions due to cytochrome P450*." Proc (Bayl Univ Med Cent) 13(4): 421-423.

Okabe, S., Tauchi T., Kimura S., Maekawa T., Kitahara T., Tanaka Y. and Ohyashiki K. (2014). "*Combining the ABL1 kinase inhibitor ponatinib and the histone deacetylase inhibitor vorinostat: a potential treatment for BCR-ABL-positive leukemia*." PLoS One 9(2): e89080.

Olzmann, J. A., Li L., Chudaev M. V., Chen J., Perez F. A., Palmiter R. D. and Chin L. S. (2007). "*Parkin-mediated K63-linked polyubiquitination targets misfolded DJ-1 to aggresomes via binding to HDAC6*." J Cell Biol 178(6): 1025-1038.

Ota, S., Zhou Z. Q., Romero M. P., Yang G. and Hurlin P. J. (2016). "*HDAC6 deficiency or inhibition blocks FGFR3 accumulation and improves bone growth in a model of achondroplasia*." Hum Mol Genet 25(19): 4227-4243.

Ouyang, H., Ali Y. O., Ravichandran M., Dong A., Qiu W., MacKenzie F., Dhe-Paganon S., Arrowsmith C. H. and Zhai R. G. (2012). "*Protein aggregates are recruited to aggresome by histone deacetylase 6 via unanchored ubiquitin C termini*." J Biol Chem 287(4): 2317-2327.

Ozaki, T., Wu D., Sugimoto H., Nagase H. and Nakagawara A. (2013). "*Runt-related transcription factor 2 (RUNX2) inhibits p53-dependent apoptosis through the collaboration with HDAC6 in response to DNA damage*." Cell Death Dis 4: e610.

Pai, M. T., Tzeng S. R., Kovacs J. J., Keaton M. A., Li S. S., Yao T. P. and Zhou P. (2007). "*Solution structure of the Ubp-M BUZ domain, a highly specific protein module that recognizes the C-terminal tail of free ubiquitin*." J Mol Biol 370(2): 290-302.

Palijan, A., Fernandes I., Bastien Y., Tang L., Verway M., Kourelis M., Tavera-Mendoza L. E., Li Z., Bourdeau V., Mader S., Yang X. J. and White J. H. (2009). "*Function of histone deacetylase 6 as a cofactor of nuclear receptor coregulator LCoR*." J Biol Chem 284(44): 30264-30274.

Pane, F., Intrieri M., Quintarelli C., Izzo B., Muccioli G. C. and Salvatore F. (2002). "*BCR/ABL genes and leukemic phenotype: from molecular mechanisms to clinical correlations*." Oncogene 21(56): 8652-8667.

Park, J. H., Kim S. H., Choi M. C., Lee J., Oh D. Y., Im S. A., Bang Y. J. and Kim T. Y. (2008). "*Class II histone deacetylases play pivotal roles in heat shock protein 90-mediated proteasomal degradation of vascular endothelial growth factor receptors*." Biochem Biophys Res Commun 368(2): 318-322.

Park, S. J., Kim J. K., Bae H. J., Eun J. W., Shen Q., Kim H. S., Shin W. C., Yang H. D., Lee E. K., You J. S., Park W. S., Lee J. Y. and Nam S. W. (2014). "*HDAC6 sustains growth stimulation by prolonging the activation of EGF receptor through the inhibition of rabaptin-5-mediated early endosome fusion in gastric cancer*." Cancer Lett 354(1): 97-106.

Parmigiani, R. B., Xu W. S., Venta-Perez G., Erdjument-Bromage H., Yaneva M., Tempst P. and Marks P. A. (2008). "*HDAC6 is a specific deacetylase of peroxiredoxins and is involved in redox regulation*." Proc Natl Acad Sci U S A 105(28): 9633-9638.

Peinado, H., Ballestar E., Esteller M. and Cano A. (2004). "*Snail mediates E-cadherin repression by the recruitment of the Sin3A/histone deacetylase 1 (HDAC1)/HDAC2 complex*." Mol Cell Biol 24(1): 306-319.

Peng, U., Wang Z., Pei S., Ou Y., Hu P., Liu W. and Song J. (2017). "*ACY-1215 accelerates vemurafenib induced cell death of BRAF-mutant melanoma cells via induction of ER stress and inhibition of ERK activation*." Oncol Rep 37(2): 1270-1276.

Petruccelli, L. A., Dupere-Richer D., Pettersson F., Retrouvey H., Skoulikas S. and Miller W. H., Jr. (2011). "*Vorinostat induces reactive oxygen species and DNA damage in acute myeloid leukemia cells*." PLoS One 6(6): e20987.

Pluemsampant, S., Safronova O. S., Nakahama K. and Morita I. (2008). "*Protein kinase CK2 is a key activator of histone deacetylase in hypoxia-associated tumors*." Int J Cancer 122(2): 333-341.

Pogue, S. L., Taura T., Bi M., Yun Y., Sho A., Mikesell G., Behrens C., Sokolovsky M., Hallak H., Rosenstock M., Sanchez E., Chen H., Berenson J., Doyle A., Nock S. and Wilson D. S. (2016). "*Targeting Attenuated Interferon-alpha to Myeloma Cells with a CD38 Antibody Induces Potent Tumor Regression with Reduced Off-Target Activity*." PLoS One 11(9): e0162472.

Prystowsky, M., Feeney K., Kawachi N., Montagna C., Willmott M., Wasson C., Antkowiak M., Loudig O. and Parish J. (2013). "*Inhibition of Plk1 and Cyclin B1 expression results in panobinostat-induced G(2) delay and mitotic defects*." Sci Rep 3: 2640.

Puccetti, E. and Ruthardt M. (2004). "*Acute promyelocytic leukemia: PML/RARalpha and the leukemic stem cell*." Leukemia 18(7): 1169-1175.

Qian, D. Z., Kachhap S. K., Collis S. J., Verheul H. M., Carducci M. A., Atadja P. and Pili R. (2006). "*Class II histone deacetylases are associated with VHL-independent regulation of hypoxia-inducible factor 1 alpha*." Cancer Res 66(17): 8814-8821.

Qin, H. T., Li H. Q. and Liu F. (2017). "*Selective histone deacetylase small molecule inhibitors: recent progress and perspectives*." Expert Opin Ther Pat 27(5): 621-636.

Qu, X., Yu J., Bhagat G., Furuya N., Hibshoosh H., Troxel A., Rosen J., Eskelinen E. L., Mizushima N., Ohsumi Y., Cattoretti G. and Levine B. (2003). "*Promotion of tumorigenesis by heterozygous disruption of the beclin 1 autophagy gene*." J Clin Invest 112(12): 1809-1820.

R Development Core Team (2010). R: A language and environment for statistical computing, R Foundation for Statistical Computing.

Raab, M. S., Podar K., Breitkreutz I., Richardson P. G. and Anderson K. C. (2009). "*Multiple myeloma*." Lancet 374(9686): 324-339.

Rada-Iglesias, A., Enroth S., Ameur A., Koch C. M., Clelland G. K., Respuela-Alonso P., Wilcox S., Dovey O. M., Ellis P. D., Langford C. F., Dunham I., Komorowski J. and Wadelius C. (2007). "*Butyrate mediates decrease of histone acetylation centered on transcription start sites and down-regulation of associated genes*." Genome Res 17(6): 708-719.

Rajkumar, S. V., Dimopoulos M. A., Palumbo A., Blade J., Merlini G., Mateos M. V., Kumar S., Hillengass J., Kastritis E., Richardson P., Landgren O., Paiva B., Dispenzieri A., Weiss B., LeLeu X., Zweegman S., Lonial S., Rosinol L., Zamagni E., Jagannath S., Sezer O., Kristinsson S. Y., Caers J., Usmani S. Z., Lahuerta J. J., Johnsen H. E., Beksac M., Cavo M., Goldschmidt H., Terpos E., Kyle R. A., Anderson K. C., Durie B. G. and Miguel J. F. (2014). "*International Myeloma Working Group updated criteria for the diagnosis of multiple myeloma*." Lancet Oncol 15(12): e538-548.

Ramalingam, S. S., Belani C. P., Ruel C., Frankel P., Gitlitz B., Koczywas M., Espinoza-Delgado I. and Gandara D. (2009). "*Phase II study of belinostat (PXD101), a histone deacetylase inhibitor, for second line therapy of advanced malignant pleural mesothelioma*." J Thorac Oncol 4(1): 97-101.

Rampalli, S., Pavithra L., Bhatt A., Kundu T. K. and Chattopadhyay S. (2005). "*Tumor suppressor SMAR1 mediates cyclin D1 repression by recruitment of the SIN3/histone deacetylase 1 complex*." Mol Cell Biol 25(19): 8415-8429.

Rao, R., Nalluri S., Kolhe R., Yang Y., Fiskus W., Chen J., Ha K., Buckley K. M., Balusu R., Coothankandaswamy V., Joshi A., Atadja P. and Bhalla K. N. (2010). "*Treatment with panobinostat induces glucose-regulated protein 78 acetylation and endoplasmic reticulum stress in breast cancer cells*." Mol Cancer Ther 9(4): 942-952.

Rauzan, M., Chuah C. T., Ko T. K. and Ong S. T. (2017). "*The HDAC inhibitor SB939 overcomes resistance to BCR-ABL kinase Inhibitors conferred by the BIM deletion polymorphism in chronic myeloid leukemia*." PLoS One 12(3): e0174107.

Ray Chaudhuri, A. and Nussenzweig A. (2017). "*The multifaceted roles of PARP1 in DNA repair and chromatin remodelling*." Nat Rev Mol Cell Biol 18(10): 610-621.

Reed, S. M. and Quelle D. E. (2014). "*p53 Acetylation: Regulation and Consequences*." Cancers (Basel) 7(1): 30-69.

Regna, N. L., Vieson M. D., Luo X. M., Chafin C. B., Puthiyaveetil A. G., Hammond S. E., Caudell D. L., Jarpe M. B. and Reilly C. M. (2016). "*Specific HDAC6 inhibition by ACY-738 reduces SLE pathogenesis in NZB/W mice*." Clin Immunol 162: 58-73.

Ri, M. (2016). "*Endoplasmic-reticulum stress pathway-associated mechanisms of action of proteasome inhibitors in multiple myeloma*." Int J Hematol 104(3): 273-280.

Richardson, P. G., Moreau P., Laubach J. P., Maglio M. E., Lonial S. and San-Miguel J. (2017). "*Deacetylase inhibitors as a novel modality in the treatment of multiple myeloma*." Pharmacol Res 117: 185-191.

Richon, V. M., Sandhoff T. W., Rifkind R. A. and Marks P. A. (2000). "*Histone deacetylase inhibitor selectively induces p21WAF1 expression and gene-associated histone acetylation*." Proc Natl Acad Sci U S A 97(18): 10014-10019.

Riester, D., Hildmann C., Grunewald S., Beckers T. and Schwienhorst A. (2007). "*Factors affecting the substrate specificity of histone deacetylases*." Biochem Biophys Res Commun 357(2): 439-445.

Ritchie, M. E., Phipson B., Wu D., Hu Y., Law C. W., Shi W. and Smyth G. K. (2015). "*limma powers differential expression analyses for RNA-sequencing and microarray studies*." Nucleic Acids Res 43(7): e47.

Robert, C. and Rassool F. V. (2012). "*HDAC inhibitors: roles of DNA damage and repair*." Adv Cancer Res 116: 87-129.

Rodriguez-Gonzalez, A., Lin T., Ikeda A. K., Simms-Waldrip T., Fu C. and Sakamoto K. M. (2008). "*Role of the aggresome pathway in cancer: targeting histone deacetylase 6-dependent protein degradation*." Cancer Res 68(8): 2557-2560.

Rosato, R. R., Almenara J. A., Maggio S. C., Coe S., Atadja P., Dent P. and Grant S. (2008). "*Role of histone deacetylase inhibitor-induced reactive oxygen species and DNA damage in LAQ-824/fludarabine antileukemic interactions*." Mol Cancer Ther 7(10): 3285-3297.

Rosik, L., Niegisch G., Fischer U., Jung M., Schulz W. A. and Hoffmann M. J. (2014). "*Limited efficacy of specific HDAC6 inhibition in urothelial cancer cells*." Cancer Biol Ther 15(6): 742-757.

Rossari, F., Minutolo F. and Orciuolo E. (2018). "*Past, present, and future of Bcr-Abl inhibitors: from chemical development to clinical efficacy*." J Hematol Oncol 11(1): 84.

Roychowdhury, S. and Talpaz M. (2011). "*Managing resistance in chronic myeloid leukemia*." Blood Rev 25(6): 279-290.

RStudio Team (2015). RStudio: Integrated Development for R.

Ryu, H. W., Shin D. H., Lee D. H., Choi J., Han G., Lee K. Y. and Kwon S. H. (2017a). "*HDAC6 deacetylates p53 at lysines 381/382 and differentially coordinates p53-induced apoptosis*." Cancer Lett 391: 162-171.

Ryu, H. W., Won H. R., Lee D. H. and Kwon S. H. (2017b). "*HDAC6 regulates sensitivity to cell death in response to stress and post-stress recovery*." Cell Stress Chaperones 22(2): 253-261.

Sadakierska-Chudy, A., Kostrzewa R. M. and Filip M. (2015). "*A comprehensive view of the epigenetic landscape part I: DNA methylation, passive and active DNA demethylation pathways and histone variants*." Neurotox Res 27(1): 84-97.

Sadoul, K., Wang J., Diagouraga B. and Khochbin S. (2011). "*The tale of protein lysine acetylation in the cytoplasm*." J Biomed Biotechnol 2011: 970382.

Saji, S., Kawakami M., Hayashi S., Yoshida N., Hirose M., Horiguchi S., Itoh A., Funata N., Schreiber S. L., Yoshida M. and Toi M. (2005). "*Significance of HDAC6 regulation via estrogen signaling for cell motility and prognosis in estrogen receptor-positive breast cancer*." Oncogene 24(28): 4531-4539.

Sakuma, T., Uzawa K., Onda T., Shiiba M., Yokoe H., Shibahara T. and Tanzawa H. (2006). "*Aberrant expression of histone deacetylase 6 in oral squamous cell carcinoma*." Int J Oncol 29(1): 117-124.

Sano, R. and Reed J. C. (2013). "*ER stress-induced cell death mechanisms*." Biochim Biophys Acta 1833(12): 3460-3470.

Santo, L., Hideshima T., Kung A. L., Tseng J. C., Tamang D., Yang M., Jarpe M., van Duzer J. H., Mazitschek R., Ogier W. C., Cirstea D., Rodig S., Eda H., Scullen T., Canavese M., Bradner J., Anderson K. C., Jones S. S. and Raje N. (2012). "*Preclinical activity, pharmacodynamic, and pharmacokinetic properties of a selective HDAC6 inhibitor, ACY-1215, in combination with bortezomib in multiple myeloma*." Blood 119(11): 2579-2589.

Schindler, T., Bornmann W., Pellicena P., Miller W. T., Clarkson B. and Kuriyan J. (2000). "*Structural mechanism for STI-571 inhibition of abelson tyrosine kinase*." Science 289(5486): 1938-1942.

Schnekenburger, M., Florean C., Dicato M. and Diederich M. (2016). "*Epigenetic alterations as a universal feature of cancer hallmarks and a promising target for personalized treatments*." Curr Top Med Chem 16(7): 745-776.

Schnekenburger, M., Morceau F., Henry E., Blasius R., Dicato M., Trentesaux C. and Diederich M. (2006). "*Transcriptional and post-transcriptional regulation of glutathione S-transferase P1 expression during butyric acid-induced differentiation of K562 cells*." Leuk Res 30(5): 561-568.

Scott, M. T., Korfi K., Saffrey P., Hopcroft L. E., Kinstrie R., Pellicano F., Guenther C., Gallipoli P., Cruz M., Dunn K., Jorgensen H. G., Cassels J. E., Hamilton A., Crossan A., Sinclair A., Holyoake T. L. and Vetrie D. (2016). "*Epigenetic Reprogramming Sensitizes CML Stem Cells to Combined EZH2 and Tyrosine Kinase Inhibition*." Cancer Discov 6(11): 1248-1257.

Seidel, C., Florean C., Schnekenburger M., Dicato M. and Diederich M. (2012a). "*Chromatin-modifying agents in anti-cancer therapy*." Biochimie 94(11): 2264-2279.

Seidel, C., Schnekenburger M., Dicato M. and Diederich M. (2012b). "*Histone deacetylase modulators provided by Mother Nature*." Genes Nutr 7(3): 357-367.

Seidel, C., Schnekenburger M., Dicato M. and Diederich M. (2014). "*Antiproliferative and proapoptotic activities of 4-hydroxybenzoic acid-based inhibitors of histone deacetylases*." Cancer Lett 343(1): 134-146.

Seidel, C., Schnekenburger M., Dicato M. and Diederich M. (2015). "*Histone deacetylase 6 in health and disease*." Epigenomics 7(1): 103-118.

Seigneurin-Berny, D., Verdel A., Curtet S., Lemercier C., Garin J., Rousseaux S. and Khochbin S. (2001). "*Identification of components of the murine histone deacetylase 6 complex: link between acetylation and ubiquitination signaling pathways*." Mol Cell Biol 21(23): 8035-8044.

Senft, D. and Ronai Z. A. (2015). "*UPR, autophagy, and mitochondria crosstalk underlies the ER stress response*." Trends Biochem Sci 40(3): 141-148.

Seto, E. and Yoshida M. (2014). "*Erasers of histone acetylation: the histone deacetylase enzymes*." Cold Spring Harb Perspect Biol 6(4): a018713.

Shaker, M. E., Ghani A., Shiha G. E., Ibrahim T. M. and Mehal W. Z. (2013). "*Nilotinib induces apoptosis and autophagic cell death of activated hepatic stellate cells via inhibition of histone deacetylases*." Biochim Biophys Acta 1833(8): 1992-2003.

Shan, B., Yao T. P., Nguyen H. T., Zhuo Y., Levy D. R., Klingsberg R. C., Tao H., Palmer M. L., Holder K. N. and Lasky J. A. (2008). "*Requirement of HDAC6 for transforming growth factor-beta1-induced epithelial-mesenchymal transition*." J Biol Chem 283(30): 21065-21073.

Sibbesen, N. A., Kopp K. L., Litvinov I. V., Jonson L., Willerslev-Olsen A., Fredholm S., Petersen D. L., Nastasi C., Krejsgaard T., Lindahl L. M., Gniadecki R., Mongan N. P., Sasseville D., Wasik M. A., Iversen L., Bonefeld C. M., Geisler C., Woetmann A. and Odum N. (2015). "*Jak3, STAT3, and STAT5 inhibit expression of miR-22, a novel tumor suppressor microRNA, in cutaneous T-Cell lymphoma*." Oncotarget 6(24): 20555-20569.

Singh, S. S., Vats S., Chia A. Y., Tan T. Z., Deng S., Ong M. S., Arfuso F., Yap C. T., Goh B. C., Sethi G., Huang R. Y., Shen H. M., Manjithaya R. and Kumar A. P. (2018). "*Dual role of autophagy in hallmarks of cancer*." Oncogene 37(9): 1142-1158.

Song, S., Tan J., Miao Y. and Zhang Q. (2018). "*Crosstalk of ER stress-mediated autophagy and ER-phagy: Involvement of UPR and the core autophagy machinery*." J Cell Physiol 233(5): 3867-3874.

Spange, S., Wagner T., Heinzel T. and Kramer O. H. (2009). "*Acetylation of non-histone proteins modulates cellular signalling at multiple levels*." Int J Biochem Cell Biol 41(1): 185-198.

Steele, N. L., Plumb J. A., Vidal L., Tjornelund J., Knoblauch P., Rasmussen A., Ooi C. E., Buhl-Jensen P., Brown R., Evans T. R. and DeBono J. S. (2008). "*A phase 1 pharmacokinetic and pharmacodynamic study of the histone deacetylase inhibitor belinostat in patients with advanced solid tumors*." Clin Cancer Res 14(3): 804-810.

Stein, B. and Smith B. D. (2010). "*Treatment options for patients with chronic myeloid leukemia who are resistant to or unable to tolerate imatinib*." Clin Ther 32(5): 804-820.

Su, J. M., Li X. N., Thompson P., Ou C. N., Ingle A. M., Russell H., Lau C. C., Adamson P. C. and Blaney S. M. (2011). "*Phase 1 study of valproic acid in pediatric patients with refractory solid or CNS tumors: a children's oncology group report*." Clin Cancer Res 17(3): 589-597.

Subramanian, C., Jarzembowski J. A., Opipari A. W., Jr., Castle V. P. and Kwok R. P. (2011). "*HDAC6 deacetylates Ku70 and regulates Ku70-Bax binding in neuroblastoma*." Neoplasia 13(8): 726-734.

Subramanian, S., Bates S. E., Wright J. J., Espinoza-Delgado I. and Piekarz R. L. (2010). "*Clinical Toxicities of Histone Deacetylase Inhibitors*." Pharmaceuticals (Basel) 3(9): 2751-2767.

Tandon, N., Ramakrishnan V. and Kumar S. K. (2016). "*Clinical use and applications of histone deacetylase inhibitors in multiple myeloma*." Clin Pharmacol 8: 35-44.

Taylor, R. C., Cullen S. P. and Martin S. J. (2008). "*Apoptosis: controlled demolition at the cellular level*." Nat Rev Mol Cell Biol 9(3): 231-241.

Thompson, P. A., Kantarjian H. M. and Cortes J. E. (2015). "*Diagnosis and Treatment of Chronic Myeloid Leukemia in 2015*." Mayo Clin Proc 90(10): 1440-1454.

Tokesi, N., Lehotzky A., Horvath I., Szabo B., Olah J., Lau P. and Ovadi J. (2010). "*TPPP/p25 promotes tubulin acetylation by inhibiting histone deacetylase 6*." J Biol Chem 285(23): 17896-17906.

Toropainen, S., Vaisanen S., Heikkinen S. and Carlberg C. (2010). "*The down-regulation of the human MYC gene by the nuclear hormone 1alpha,25-dihydroxyvitamin D3*

is associated with cycling of corepressors and histone deacetylases." J Mol Biol 400(3): 284-294.

Touzeau, C., Maciag P., Amiot M. and Moreau P. (2018). "*Targeting Bcl-2 for the treatment of multiple myeloma*." Leukemia 32(9): 1899-1907.

Touzeau, C., Ryan J., Guerriero J., Moreau P., Chonghaile T. N., Le Gouill S., Richardson P., Anderson K., Amiot M. and Letai A. (2016). "*BH3 profiling identifies heterogeneous dependency on Bcl-2 family members in multiple myeloma and predicts sensitivity to BH3 mimetics*." Leukemia 30(3): 761-764.

Traynor, A. M., Dubey S., Eickhoff J. C., Kolesar J. M., Schell K., Huie M. S., Groteluschen D. L., Marcotte S. M., Hallahan C. M., Weeks H. R., Wilding G., Espinoza-Delgado I. and Schiller J. H. (2009). "*Vorinostat (NSC# 701852) in patients with relapsed non-small cell lung cancer: a Wisconsin Oncology Network phase II study*." J Thorac Oncol 4(4): 522-526.

Trott, O. and Olson A. J. (2010). "*AutoDock Vina: improving the speed and accuracy of docking with a new scoring function, efficient optimization, and multithreading*." J Comput Chem 31(2): 455-461.

Uhlen, M., Oksvold P., Fagerberg L., Lundberg E., Jonasson K., Forsberg M., Zwahlen M., Kampf C., Wester K., Hober S., Wernerus H., Bjorling L. and Ponten F. (2010). "*Towards a knowledge-based Human Protein Atlas*." Nat Biotechnol 28(12): 1248-1250.

Van Damme, M., Crompot E., Meuleman N., Mineur P., Bron D., Lagneaux L. and Stamatopoulos B. (2012). "*HDAC isoenzyme expression is deregulated in chronic lymphocytic leukemia B-cells and has a complex prognostic significance*." Epigenetics 7(12): 1403-1412.

Veber, D. F., Johnson S. R., Cheng H. Y., Smith B. R., Ward K. W. and Kopple K. D. (2002). "*Molecular properties that influence the oral bioavailability of drug candidates*." J Med Chem 45(12): 2615-2623.

Venton, G., Perez-Alea M., Baier C., Fournet G., Quash G., Labiad Y., Martin G., Sanderson F., Poullin P., Suchon P., Farnault L., Nguyen C., Brunet C., Ceylan I. and Costello R. T. (2016). "*Aldehyde dehydrogenases inhibition eradicates leukemia stem cells while sparing normal progenitors*." Blood Cancer J 6(9): e469.

Verdel, A., Curtet S., Brocard M. P., Rousseaux S., Lemercier C., Yoshida M. and Khochbin S. (2000). "*Active maintenance of mHDA2/mHDAC6 histone-deacetylase in the cytoplasm*." Curr Biol 10(12): 747-749.

Verdin, E. and Ott M. (2015). "*50 years of protein acetylation: from gene regulation to epigenetics, metabolism and beyond*." Nat Rev Mol Cell Biol 16(4): 258-264.

Verfaillie, T., Salazar M., Velasco G. and Agostinis P. (2010). "*Linking ER Stress to Autophagy: Potential Implications for Cancer Therapy*." Int J Cell Biol 2010: 930509.

Voelter-Mahlknecht, S. and Mahlknecht U. (2003). "*Cloning and structural characterization of the human histone deacetylase 6 gene*." Int J Mol Med 12(1): 87-93.

Vogl, D. T., Raje N., Jagannath S., Richardson P., Hari P., Orlowski R., Supko J. G., Tamang D., Yang M., Jones S. S., Wheeler C., Markelewicz R. J. and Lonial S. (2017). "*Ricolinostat, the First Selective Histone Deacetylase 6 Inhibitor, in Combination with Bortezomib and Dexamethasone for Relapsed or Refractory Multiple Myeloma*." Clin Cancer Res.

Wagner, F. F., Wesmall yi U. M., Lewis M. C. and Holson E. B. (2013). "*Small molecule inhibitors of zinc-dependent histone deacetylases*." Neurotherapeutics 10(4): 589-604.

Wahaib, K., Beggs A. E., Campbell H., Kodali L. and Ford P. D. (2016). "*Panobinostat: A histone deacetylase inhibitor for the treatment of relapsed or refractory multiple myeloma*." Am J Health Syst Pharm 73(7): 441-450.

Wang, L., Xiang S., Williams K. A., Dong H., Bai W., Nicosia S. V., Khochbin S., Bepler G. and Zhang X. (2012). "*Depletion of HDAC6 enhances cisplatin-induced DNA damage and apoptosis in non-small cell lung cancer cells*." PLoS One 7(9): e44265.

Wang, Y. C., Peterson S. E. and Loring J. F. (2014). "*Protein post-translational modifications and regulation of pluripotency in human stem cells*." Cell Res 24(2): 143-160.

Wang, Z., Hu P., Tang F. and Xie C. (2016a). "*HDAC6-mediated EGFR stabilization and activation restrict cell response to sorafenib in non-small cell lung cancer cells*." Med Oncol 33(5): 50.

Wang, Z., Qin G. and Zhao T. C. (2014). "*HDAC4: mechanism of regulation and biological functions*." Epigenomics 6(1): 139-150.

Wang, Z., Tang F., Hu P., Wang Y., Gong J., Sun S. and Xie C. (2016b). "*HDAC6 promotes cell proliferation and confers resistance to gefitinib in lung adenocarcinoma*." Oncol Rep 36(1): 589-597.

Warrener, R., Beamish H., Burgess A., Waterhouse N. J., Giles N., Fairlie D. and Gabrielli B. (2003). "*Tumor cell-selective cytotoxicity by targeting cell cycle checkpoints*." FASEB J 17(11): 1550-1552.

Warsch, W., Grundschober E., Berger A., Gille L., Cerny-Reiterer S., Tigan A. S., Hoelbl-Kovacic A., Valent P., Moriggl R. and Sexl V. (2012). "*STAT5 triggers BCR-ABL1 mutation by mediating ROS production in chronic myeloid leukaemia*." Oncotarget 3(12): 1669-1687.

Watabe, M. and Nakaki T. (2011). "*Protein kinase CK2 regulates the formation and clearance of aggresomes in response to stress*." J Cell Sci 124(Pt 9): 1519-1532.

Watanabe, Y. and Tanaka M. (2011). "*p62/SQSTM1 in autophagic clearance of a non-ubiquitylated substrate*." J Cell Sci 124(Pt 16): 2692-2701.

Wei, D., Lu T., Ma D., Yu K., Zhang T., Xiong J., Wang W., Zhang Z., Fang Q. and Wang J. (2018). "*Synergistic activity of imatinib and AR-42 against chronic myeloid leukemia cells mainly through HDAC1 inhibition*." Life Sci 211: 224-237.

Wei, G., Rafiyath S. and Liu D. (2010). "*First-line treatment for chronic myeloid leukemia: dasatinib, nilotinib, or imatinib*." J Hematol Oncol 3: 47.

Weisberg, E., Manley P. W., Cowan-Jacob S. W., Hochhaus A. and Griffin J. D. (2007). "*Second generation inhibitors of BCR-ABL for the treatment of imatinib-resistant chronic myeloid leukaemia*." Nat Rev Cancer 7(5): 345-356.

Wen, Y. D., Perissi V., Staszewski L. M., Yang W. M., Krones A., Glass C. K., Rosenfeld M. G. and Seto E. (2000). "*The histone deacetylase-3 complex contains nuclear receptor corepressors*." Proc Natl Acad Sci U S A 97(13): 7202-7207.

Westendorf, J. J., Zaidi S. K., Cascino J. E., Kahler R., van Wijnen A. J., Lian J. B., Yoshida M., Stein G. S. and Li X. (2002). "*Runx2 (Cbfa1, AML-3) interacts with histone deacetylase 6 and represses the p21(CIP1/WAF1) promoter*." Mol Cell Biol 22(22): 7982-7992.

Whetstine, J. R., Ceron J., Ladd B., Dufourcq P., Reinke V. and Shi Y. (2005). "*Regulation of tissue-specific and extracellular matrix-related genes by a class I histone deacetylase*." Mol Cell 18(4): 483-490.

Whittaker, S. J., Demierre M. F., Kim E. J., Rook A. H., Lerner A., Duvic M., Scarisbrick J., Reddy S., Robak T., Becker J. C., Samtsov A., McCulloch W. and Kim Y. H. (2010). "*Final results from a multicenter, international, pivotal study of romidepsin in refractory cutaneous T-cell lymphoma*." J Clin Oncol 28(29): 4485-4491.

Wickstrom, S. A., Masoumi K. C., Khochbin S., Fassler R. and Massoumi R. (2010). "*CYLD negatively regulates cell-cycle progression by inactivating HDAC6 and increasing the levels of acetylated tubulin*." EMBO J 29(1): 131-144.

Wilson, A. J., Byun D. S., Popova N., Murray L. B., L'Italien K., Sowa Y., Arango D., Velcich A., Augenlicht L. H. and Mariadason J. M. (2006). "*Histone deacetylase 3 (HDAC3) and other class I HDACs regulate colon cell maturation and p21 expression and are deregulated in human colon cancer*." J Biol Chem 281(19): 13548-13558.

Wilson, N. R. and Hochstrasser M. (2016). "*The Regulation of Chromatin by Dynamic SUMO Modifications*." Methods Mol Biol 1475: 23-38.

Withey, J. M., Marley S. B., Kaeda J., Harvey A. J., Crompton M. R. and Gordon M. Y. (2005). "*Targeting primary human leukaemia cells with RNA interference: Bcr-Abl targeting inhibits myeloid progenitor self-renewal in chronic myeloid leukaemia cells*." Br J Haematol 129(3): 377-380.

Witt, O., Deubzer H. E., Milde T. and Oehme I. (2009). "*HDAC family: What are the cancer relevant targets?*" Cancer Lett 277(1): 8-21.

Wolfe, A. L., Duncan K. K., Parelkar N. K., Weir S. J., Vielhauer G. A. and Boger D. L. (2012). "*A novel, unusually efficacious duocarmycin carbamate prodrug that releases no residual byproduct*." J Med Chem 55(12): 5878-5886.

Wong, C. H., Iskandar K. B., Yadav S. K., Hirpara J. L., Loh T. and Pervaiz S. (2010). "*Simultaneous induction of non-canonical autophagy and apoptosis in cancer cells by ROS-dependent ERK and JNK activation*." PLoS One 5(4): e9996.

Woyach, J. A., Kloos R. T., Ringel M. D., Arbogast D., Collamore M., Zwiebel J. A., Grever M., Villalona-Calero M. and Shah M. H. (2009). "*Lack of therapeutic effect of the histone deacetylase inhibitor vorinostat in patients with metastatic radioiodine-refractory thyroid carcinoma*." J Clin Endocrinol Metab 94(1): 164-170.

Wu, R., Lu Z., Cao Z. and Zhang Y. (2011). "*Zinc chelation with hydroxamate in histone deacetylases modulated by water access to the linker binding channel*." J Am Chem Soc 133(16): 6110-6113.

Wu, Y., Song S. W., Sun J., Bruner J. M., Fuller G. N. and Zhang W. (2010). "*IIp45 inhibits cell migration through inhibition of HDAC6*." J Biol Chem 285(6): 3554-3560.

Wuilleme-Toumi, S., Robillard N., Gomez P., Moreau P., Le Gouill S., Avet-Loiseau H., Harousseau J. L., Amiot M. and Bataille R. (2005). "*Mcl-1 is overexpressed in multiple myeloma and associated with relapse and shorter survival*." Leukemia 19(7): 1248-1252.

Xargay-Torrent, S., Lopez-Guerra M., Saborit-Villarroya I., Rosich L., Campo E., Roue G. and Colomer D. (2011). "*Vorinostat-induced apoptosis in mantle cell lymphoma is mediated by acetylation of proapoptotic BH3-only gene promoters*." Clin Cancer Res 17(12): 3956-3968.

Xiong, Y. and Guan K. L. (2012). "*Mechanistic insights into the regulation of metabolic enzymes by acetylation*." J Cell Biol 198(2): 155-164.

Xu, W. S., Parmigiani R. B. and Marks P. A. (2007). "*Histone deacetylase inhibitors: molecular mechanisms of action*." Oncogene 26(37): 5541-5552.

Xu, X. D., Yang L., Zheng L. Y., Pan Y. Y., Cao Z. F., Zhang Z. Q., Zhou Q. S., Yang B. and Cao C. (2014). "*Suberoylanilide hydroxamic acid, an inhibitor of histone deacetylase, suppresses vasculogenic mimicry and proliferation of highly aggressive pancreatic cancer PaTu8988 cells*." BMC Cancer 14: 373.

Yan, J., Seibenhener M. L., Calderilla-Barbosa L., Diaz-Meco M. T., Moscat J., Jiang J., Wooten M. W. and Wooten M. C. (2013). "*SQSTM1/p62 interacts with HDAC6 and regulates deacetylase activity*." PLoS One 8(9): e76016.

Yang, P. H., Zhang L., Zhang Y. J., Zhang J. and Xu W. F. (2013). "*HDAC6: physiological function and its selective inhibitors for cancer treatment*." Drug Discov Ther 7(6): 233-242.

Yang, T., Jian W., Luo Y., Fu X., Noguchi C., Bungert J., Huang S. and Qiu Y. (2012). "*Acetylation of histone deacetylase 1 regulates NuRD corepressor complex activity*." J Biol Chem 287(48): 40279-40291.

Yang, X., Li L., Liang J., Shi L., Yang J., Yi X., Zhang D., Han X., Yu N. and Shang Y. (2013). "*Histone acetyltransferase 1 promotes homologous recombination in DNA repair by facilitating histone turnover*." J Biol Chem 288(25): 18271-18282.

Yip, K. W. and Reed J. C. (2008). "*Bcl-2 family proteins and cancer*." Oncogene 27(50): 6398-6406.

Yoshida, N., Omoto Y., Inoue A., Eguchi H., Kobayashi Y., Kurosumi M., Saji S., Suemasu K., Okazaki T., Nakachi K., Fujita T. and Hayashi S. (2004). "*Prediction of prognosis of estrogen receptor-positive breast cancer with combination of selected estrogen-regulated genes*." Cancer Sci 95(6): 496-502.

Yuan, H. and Marmorstein R. (2013). "*Histone acetyltransferases: Rising ancient counterparts to protein kinases*." Biopolymers 99(2): 98-111.

Zhang, B., Strauss A. C., Chu S., Li M., Ho Y., Shiang K. D., Snyder D. S., Huettner C. S., Shultz L., Holyoake T. and Bhatia R. (2010). "*Effective targeting of quiescent chronic myelogenous leukemia stem cells by histone deacetylase inhibitors in combination with imatinib mesylate*." Cancer Cell 17(5): 427-442.

Zhang, J., Wu K., Xiao X., Liao J., Hu Q., Chen H., Liu J. and An X. (2015). "*Autophagy as a regulatory component of erythropoiesis*." Int J Mol Sci 16(2): 4083-4094.

Zhang, L., Liu N., Xie S., He X., Zhou J., Liu M. and Li D. (2014). "*HDAC6 regulates neuroblastoma cell migration and may play a role in the invasion process*." Cancer Biol Ther 15(11): 1561-1570.

Zhang, L., Liu S., Liu N., Zhang Y., Liu M., Li D., Seto E., Yao T. P., Shui W. and Zhou J. (2015). "*Proteomic identification and functional characterization of MYH9, Hsc70, and DNAJA1 as novel substrates of HDAC6 deacetylase activity*." Protein Cell 6(1): 42-54.

Zhang, L., Zhang J., Jiang Q., Zhang L. and Song W. (2018). "*Zinc binding groups for histone deacetylase inhibitors*." J Enzyme Inhib Med Chem 33(1): 714-721.

Zhang, X., Yang L., Liu X., Nie Z., Wang X., Pan Y. and Luo J. (2017). "*Research on the epigenetic regulation mechanism of the PTPN6 gene in advanced chronic myeloid leukaemia*." Br J Haematol 178(5): 728-738.

Zhang, X., Yuan Z., Zhang Y., Yong S., Salas-Burgos A., Koomen J., Olashaw N., Parsons J. T., Yang X. J., Dent S. R., Yao T. P., Lane W. S. and Seto E. (2007). "*HDAC6 modulates cell motility by altering the acetylation level of cortactin*." Mol Cell 27(2): 197-213.

Zhang, Y., Zhang M., Dong H., Yong S., Li X., Olashaw N., Kruk P. A., Cheng J. Q., Bai W., Chen J., Nicosia S. V. and Zhang X. (2009). "*Deacetylation of cortactin by SIRT1 promotes cell migration*." Oncogene 28(3): 445-460.

Zhang, Z., Yamashita H., Toyama T., Sugiura H., Omoto Y., Ando Y., Mita K., Hamaguchi M., Hayashi S. and Iwase H. (2004). "*HDAC6 expression is correlated with better survival in breast cancer*." Clin Cancer Res 10(20): 6962-6968.

Zheng, K., Jiang Y., He Z., Kitazato K. and Wang Y. (2017). "*Cellular defence or viral assist: the dilemma of HDAC6*." J Gen Virol 98(3): 322-337.

Zhou, H. and Xu R. (2015). "*Leukemia stem cells: the root of chronic myeloid leukemia*." Protein Cell 6(6): 403-412.

Zhou, J., Vos C. C., Gjyrezi A., Yoshida M., Khuri F. R., Tamanoi F. and Giannakakou P. (2009). "*The protein farnesyltransferase regulates HDAC6 activity in a microtubule-dependent manner*." J Biol Chem 284(15): 9648-9655.

Zou, H., Wu Y., Navre M. and Sang B. C. (2006). "*Characterization of the two catalytic domains in histone deacetylase 6*." Biochem Biophys Res Commun 341(1): 45-50.

Zuo, Q., Wu W., Li X., Zhao L. and Chen W. (2012). "*HDAC6 and SIRT2 promote bladder cancer cell migration and invasion by targeting cortactin*." Oncol Rep 27(3): 819-824.

ANNEXES

Annex A1: Effect of the co-treatment with MAKV-8 and imatinib on K-562 cell proliferation and viability

Results show that the co-treatment MAKV-8-imatinib has no effect on K-562 cell proliferation and viability after 24 hours of incubation (Figure A1).

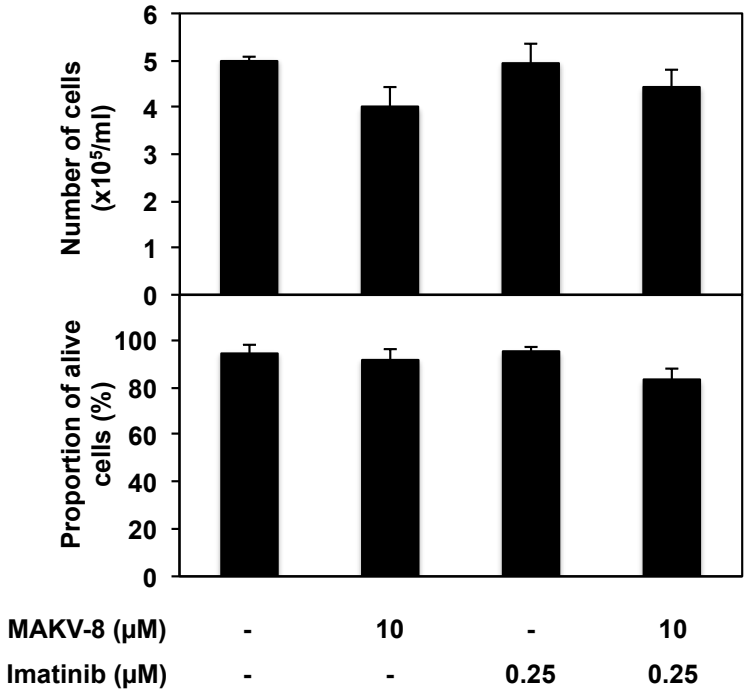

Figure A1: Effect of MAKV-8-imatinib co-treatment on K-562 cell proliferation and viability. K-562 cells were treated with MAKV-8 and imatinib alone, or in combination for 24 hours. Cell proliferation and viability were assessed based on the Trypan Blue exclusion method. Results correspond the to mean ± SD of three independent experiments.

Annex A2: Determination of the imatinib concentration to use in co-treatments for colony formation assays

Colony formation assays with imatinib-sensitive and -resistant CML cells were performed in the presence of increasing concentrations of imatinib. Results demonstrate that cologenic capacities of cells is significantly reduced by compound from a concentration of 0.25 µM for K-562 and MEG-01 cells, 0.5 µM for KBM-5 cells, and 1 µM for KBM-5R cells (Figure A2).

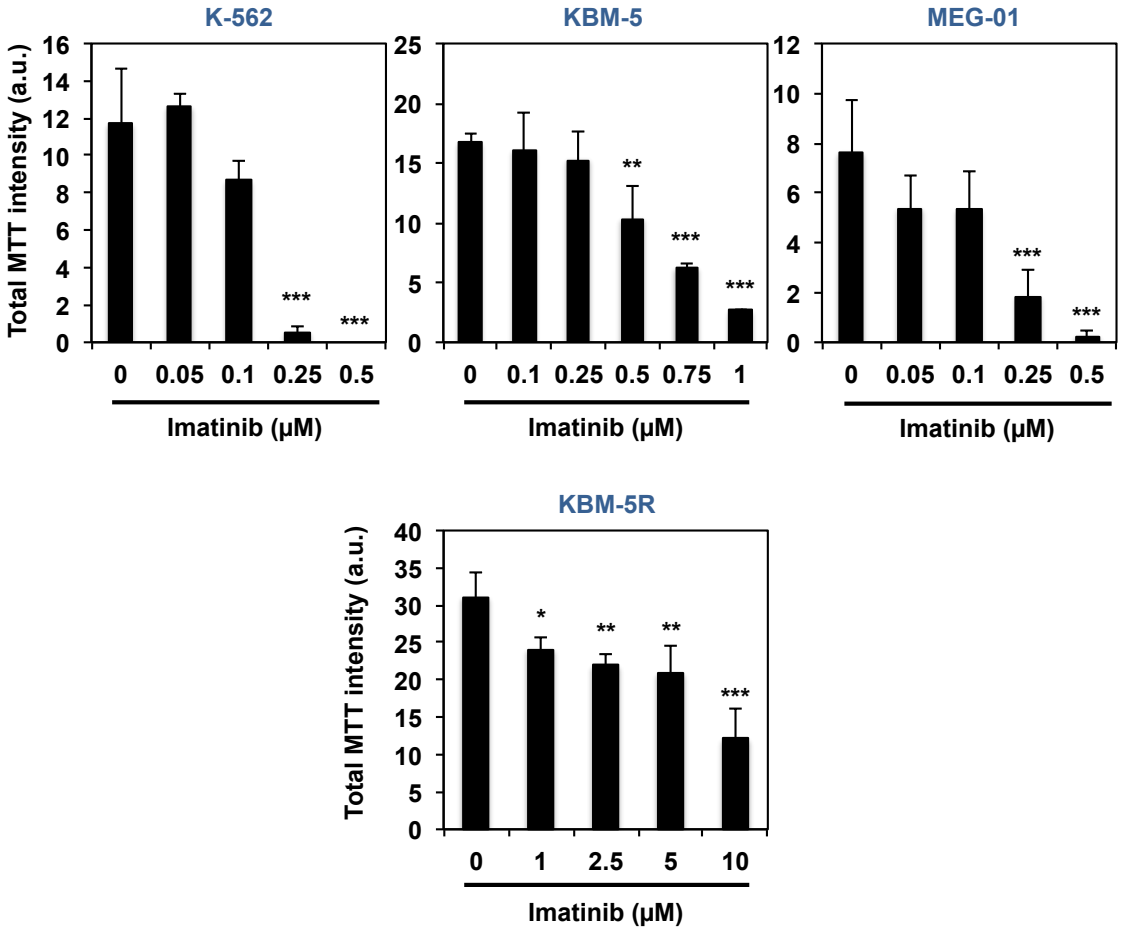

Figure A2: Effect of MAKV-8 on imatinib-sensitive and -resistant CML colony formation capacity.

Cells were grown in the presence of increasing concentrations of imatinib for 10 days and colony formation was then scored. Results correspond to the mean of total MTT intensity ± SD of three independent experiments and were analyzed by a one-way ANOVA with **, *** indicating $p < 0.01$, $p < 0.001$, respectively.

Annex A3: Panel of zebrafish pictures

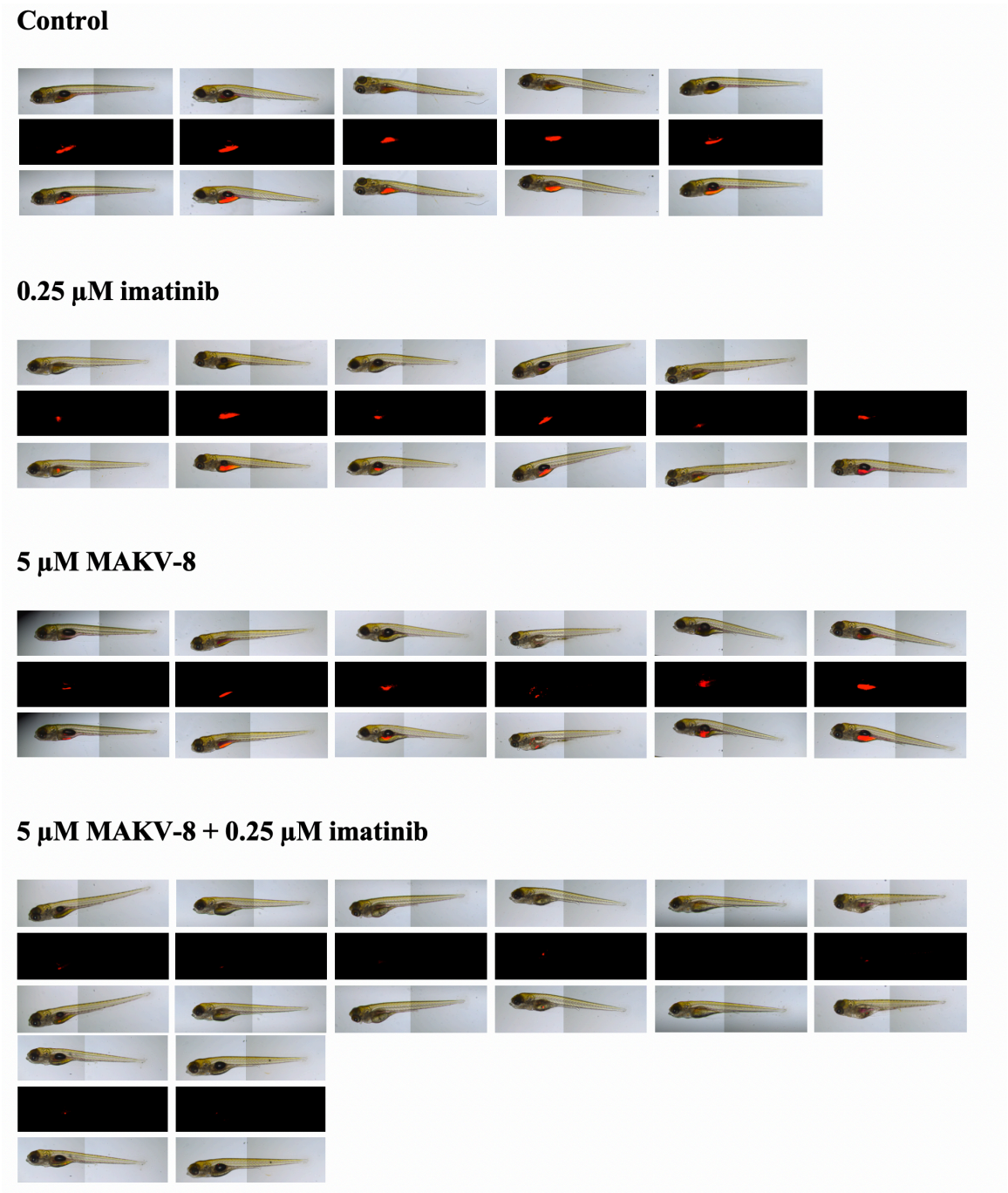

Figure A3: Effect of MAKV-8-imatinib co-treatment on tumor growth in zebrafish.
K-562 cells were treated as indicated in the figure for 24 hours, labeled with fluorescent dye and then injected in the zebrafish yolk sac. All zebrafish pictures for each condition are shown. Upper, middle and lower pictures represent bright field, red fluorescence and merge, respectively.

Annex A4: Determination of the imatinib concentration to use in co-treatments in imatinib-resistant cell lines

Imatinib-resistant K-562 and KBM-5 cell lines were treated with increasing concentrations of imatinib and the induction of cell death was assessed by the analysis of nuclear morphology. K-562R and KBM-5R cells started to die after a treatment with 10 µM imatinib, reaching 25 and 15% of cell mortality after 48 hours, respectively (Figure A4).

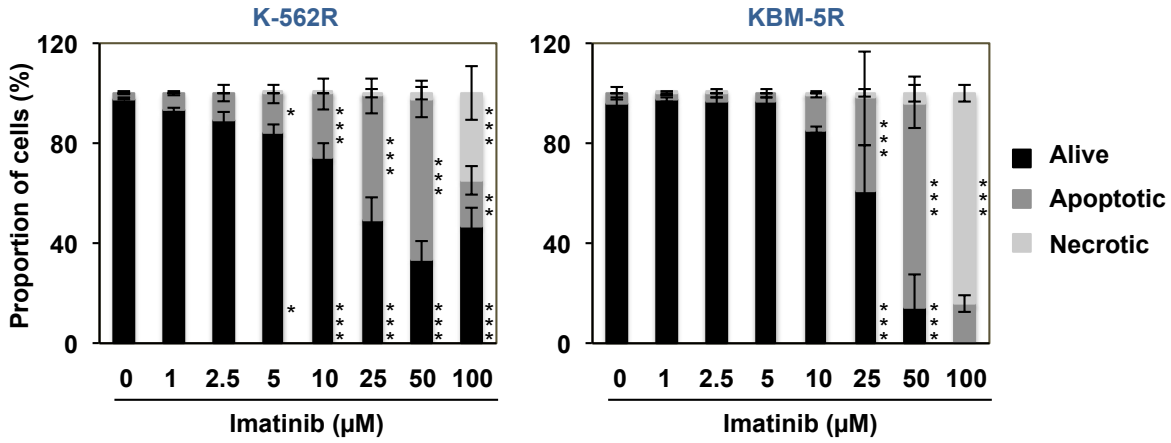

Figure A4: Effect of imatinib on K-562R and KBM-5R cell death.
K-562R and KBM-5R cells were treated with increasing concentrations of imatinib for 48 hours. The study of nuclear morphology was performed by fluorescence microscopy after Hoechst-propidium iodide staining. Results correspond to the mean ± SD of three independent experiments and were analyzed by a one-way ANOVA with *, **, *** indicating $p < 0.05$, $p < 0.01$, $p < 0.001$, respectively.

Annex A5: Evaluation of the blastogenic response of PHA/IL-2-stimulated PBMCs

By comparison to non-stimulated PBMCs, population of PBMCs stimulated with PHA and IL-2 displays augmented size, as translated by increased FSC-H value (Figure A5).

Upon CFSE staining, intensity of fluorescent signal is halved between two daughter cells after cell division. Accordingly, CFSE-stained non-stimulated PBMCs that did not proliferate are highly fluorescent by comparison to unstained PBMCs. In both instances, one peak only is detected whereas the CFSE-stained stimulated PBMCs give several peaks depending on the number of cell divisions (Figure A5).

The CD3 antigen is bound to the membranes of all mature T-cells. Accordingly, the population of stimulated PBMCs compared to non-stimulated PBMCs is enriched with T-cell lymphocytes since the proportion of cells weakly fluorescent after labeling with anti-CD3 antibody disappears (Figure A5).

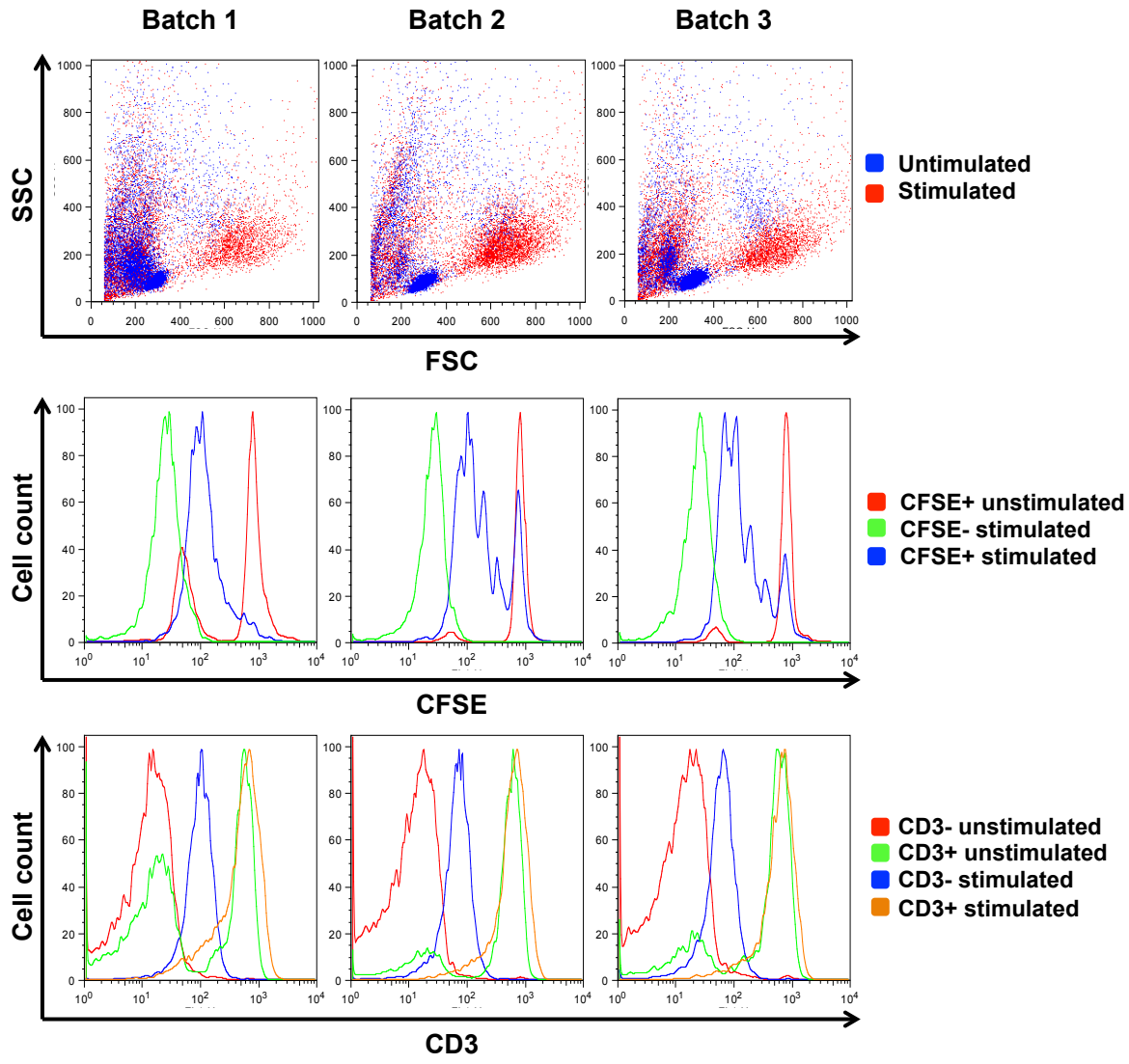

Figure A5: Evaluation of the blastogenic response of PHA/IL-2-stimulated PBMCs.
For each batch, PBMCs stimulated with phytohaemoagglutinin (PHA) and interleukin (IL)-2 or non-stimulated were stained with or without 5,6- carboxyfluorescein diacetate succinimidyl ester (CFSE+ or CFSE-, respectively) or labeled with or without FITC-conjugated mouse anti-human CD (cluster of differenciation)3 (CD3+ or CD3-, respectively). Morphological cellular changes associated with cell activation were monitored by assessment of FSC-H versus SSC-H parameters; proliferation of T-cell lymphocytes and the purity of the T-cell lymphocytic proliferating population were determined by assessment of CFSE and anti-CD3-associated intensity of fluorescence, respectively.

Annex A6: Screening of chemotherapeutical compounds for efficient tri-therapies in combination with HDAC6i and bortezomib

MOLP-8 cells were treated with a HDAC6i (5 µM MAKV-15) or HDACi (tubastatin A), a proteasome inhibitor (5 nM bortezomib) and an appropriate concentration of a common chemotherapeutic agent (*i.e.* 1 µM cisplatin, 1 µM dexamethasone, and 0.1µM doxorubicin), or treated simultaneously with the three types of compounds for 48 hours.

All tested tri-therapies induced a rate of MOLP-8 apoptotic cell death similar to the one obtained with the combination HDAC(6)i-bortezomib. Moreover, the effect on cell death is more important after a co-treatment with tubastatin A (Figure A6). Since two experiments gave the same results, investigations for those compounds in tri-therapies were stopped.

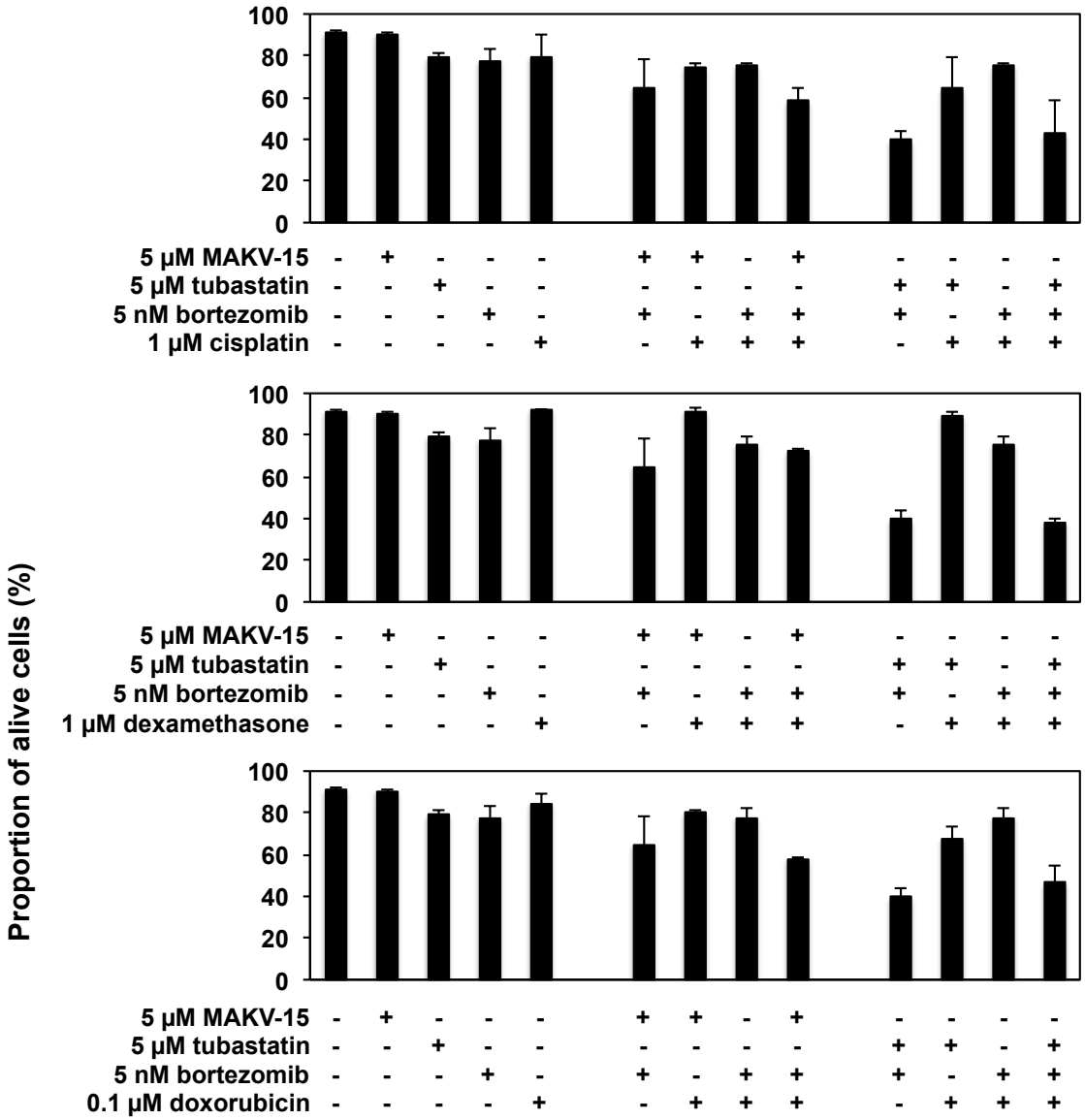

Figure A6: Effect of co-treatment with MAKV-15 or tubastatin A, bortezomib and a third drug on MOLP-8 cell death.

MOLP-8 cells were treated simultaneously with 5 µM MAKV-15 or tubastatin A, 5 nM bortezomib and a third drug (*i.e.* 1 µM cisplatin, 1 µM dexamethasone, or 0.1 µM doxorubicin) for 48 hours. The study of nuclear morphology was performed by fluorescence microscopy after Hoechst-PI staining. Results correspond to the mean ± SD of two independent experiments.

Annex A7: Determination of the concentration of BCL-2 family protein and proteasome inhibitors to use in co-treatments

Ten MM cell lines were treated with increasing concentrations of the proteasome inhibitor bortezomib (2.5, 5 nM, except for MM.1S, MM.1R and OPM-2: 1, 2.5, 5 nM), BCL-2 inhibitor ABT199 (0.001, 0.005, 0.01, 0.05, 0.1, 0.5, 1, 5, 10 µM), and MCL-1 inhibitors A1210477 (0.1, 0.5, 1, 5, 10 µM) and S63845 (0.001, 0.005, 0.01, 0.05, 0.1, 0.5, 1, 5, 10 µM) for 48 hours (Figure A7). Cell counting based on nuclear morphology analysis allowed to determine the optimal concentration of the inhibitors to use in co-treatments in each MM cell line (Table A1).

A.

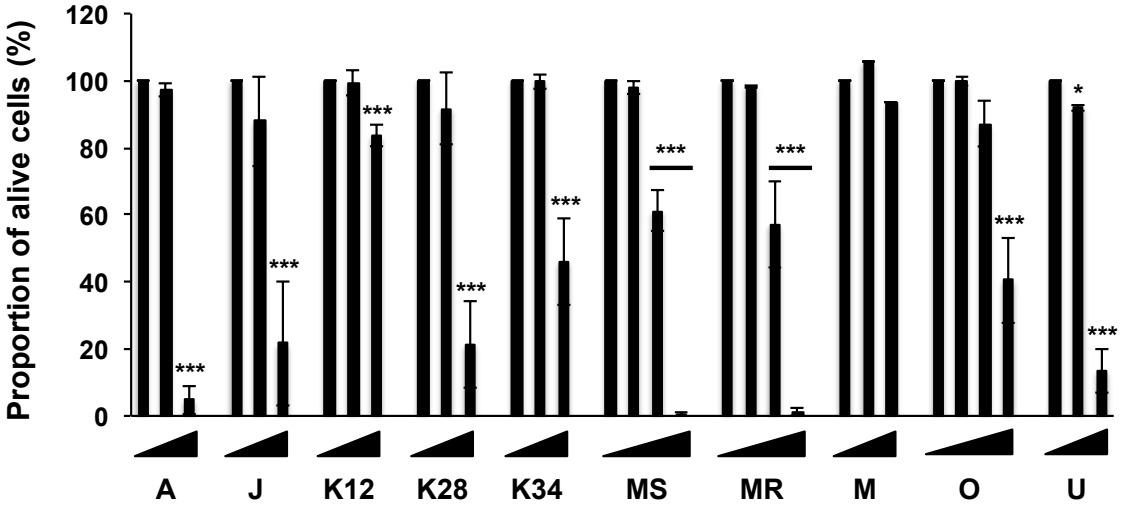

Figure A7: Effect of bortezomib, ABT199, A1210477 and S63845 on MM cell death.
MM cells were treated with increasing concentrations (black triangles) of (A) bortezomib, (B) ABT199, (C) A1210477 and (D) S63845 for 48 hours. The study of nuclear morphology was performed by fluorescence microscopy after Hoechst-PI staining. Results correspond to the mean ± SD of three independent experiments and were analyzed by a one-way ANOVA with *, **, *** indicating $p < 0.05$, $p < 0.01$, $p < 0.001$, respectively.

B.

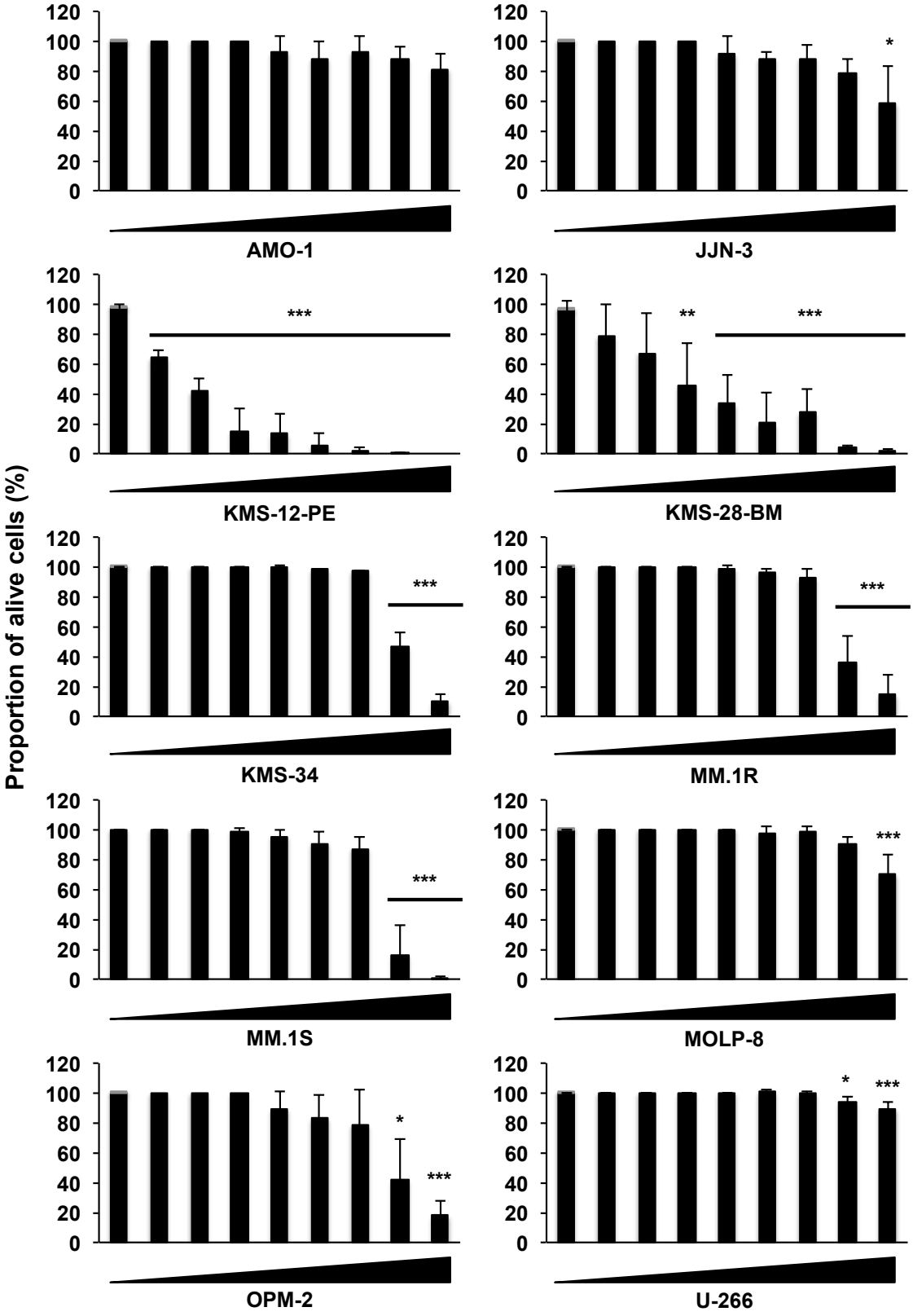

Figure A7 (continued)

C.

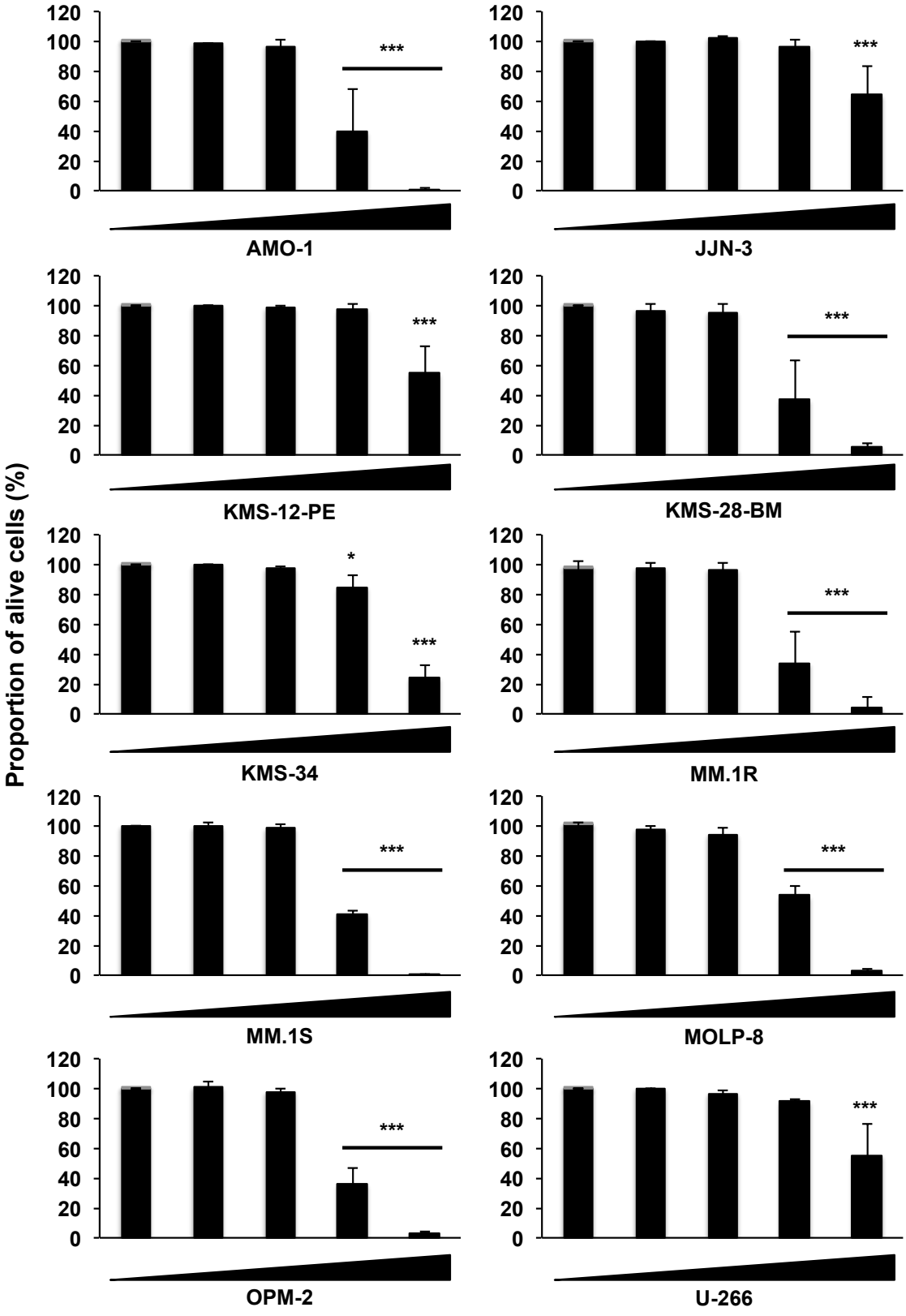

Figure A7 (continued)

D.

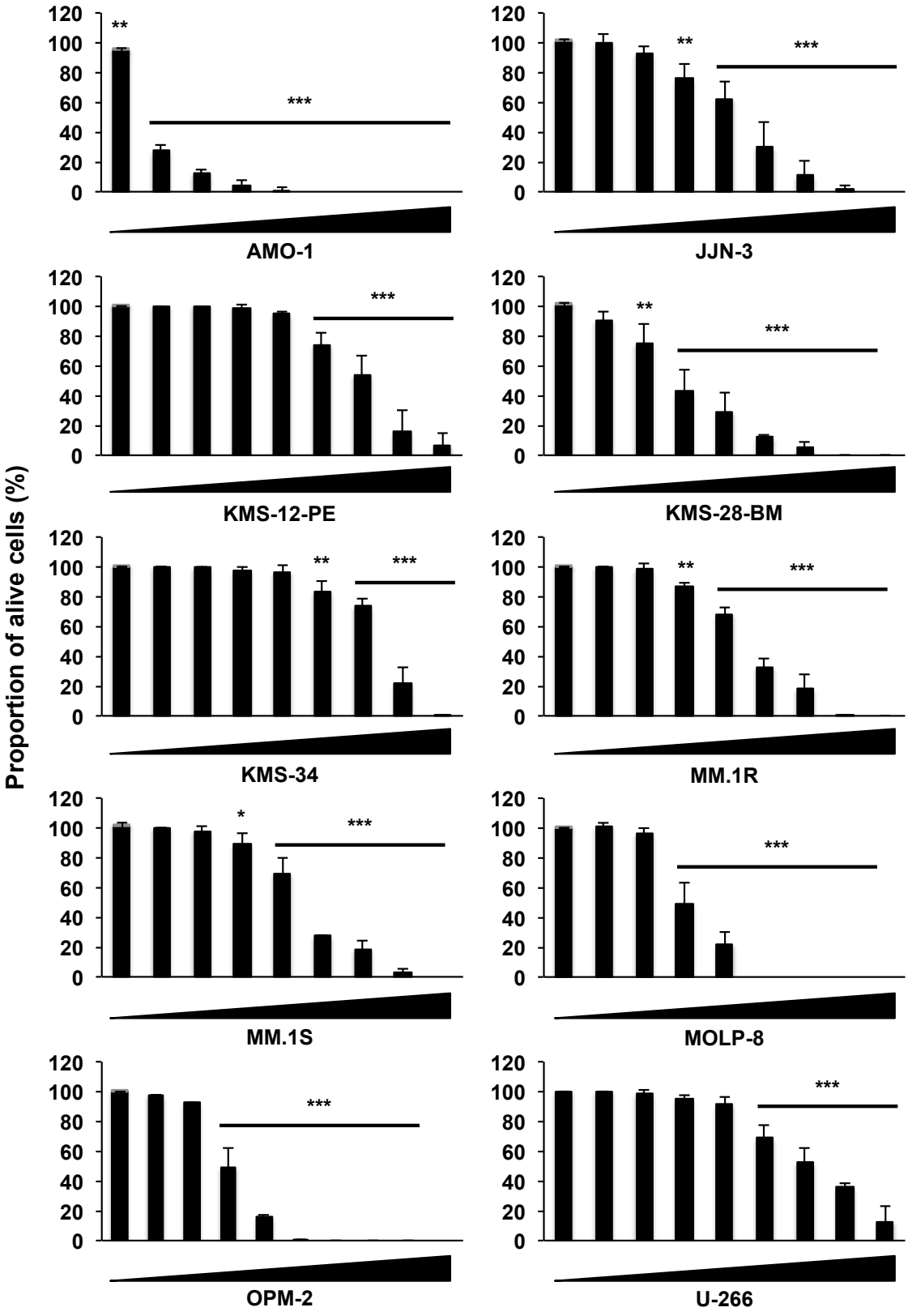

Figure A7 (continued)

Table A1: Concentrations of compounds to use in co-treatment in MM cell lines.

The chosen concentrations induce low cell mortality, *i.e.* less than 10-20% of cell death.

Cell line	ABT-199 (µM)	A1210477 (µM)	S63845 (µM)	Bortezomib (nM)
AMO-1	5	1	0.001	2.5
JJN-3	1	5	0.01	2.5
KMS-12-PE	0.001	5	0.1	2.5
KMS-28-BM	0.005	1	0.005	2.5
KMS-34	1	1	0.5	2.5
MM.1S	1	1	0.05	1
MM.1R	1	1	0.05	1
MOLP-8	5	1	0.01	5
OPM-2	1	1	0.01	2.5
U-266	5	5	0.1	2.5

Annex A8: Publications

Review

Manon Lernoux, Michael Schnekenburger, Mario Dicato, Marc Diederich. Anti-cancer effects of naturally derived compounds targeting histone deacetylase 6-related pathways, Pharmacological Research (2018) 129: 337-356.

Manon Lernoux, Michael Schnekenburger, Mario Dicato, Marc Diederich. Epigenetic mechanisms underlying therapeutic effects of HDAC inhibitors in chronic myeloid leukemia, Biochemical Pharmacology (2019): 113698.

Research papers

Manon Lernoux, Michael Schnekenburger, Hélène Losson, Koen Vermeulen, Hyunggu Hahn, Déborah Gérard, Jin-Young Lee, Aloran Mazumder, Muneer Ahamed, Christo Christov, Dong-Wook Kim, Mario Dicato, Guy Bormans, Byung-Woo Han, Marc Diederich. Novel HDAC inhibitor MAKV-8 and imatinib synergistically kill chronic myeloid leukemia cells via inhibition of BCR-ABL/MYC-signaling: effect on imatinib resistance and stem cells, Clinical Epigenetics (submitted).

Hélène Losson, Manon Lernoux, Jin-Young Lee, Aloran Mazumder, Carole Seidel, Mario Dicato, Gilbert Kirsch, Byung Woo Han, Michael Schnekenburger, Marc Diederich. The HDAC6 inhibitor 7b induces BCR-ABL ubiquitination and downregulation and synergizes with imatinib to trigger apoptosis in chronic myeloid leukemia, Pharmacological Research (submitted).

Extended abstract

Michael Schnekenburger, Hélène Losson, Manon Lernoux, Cristina Florean, Mario Dicato, Marc Diederich. Natural Compounds as Epigenetic Modulators in Cancer, Proceedings (2019) 11, 30.

Pharmacological Research 129 (2018) 337–356

Contents lists available at ScienceDirect

Pharmacological Research

journal homepage: www.elsevier.com/locate/yphrs

Review

Anti-cancer effects of naturally derived compounds targeting histone deacetylase 6-related pathways

Manon Lernoux[a], Michael Schnekenburger[a], Mario Dicato[a], Marc Diederich[b,*]

[a] Laboratory of Molecular and Cellular Biology of Cancer, Kirchberg Hospital, 9, Edward Steichen Street, L-2540 Luxembourg, Luxembourg
[b] Department of Pharmacy, Research Institute of Pharmaceutical Sciences, College of Pharmacy, Seoul National University, 1 Gwanak-ro, Gwanak-gu, 08826, South Korea

ARTICLE INFO

Article history:
Received 1 June 2017
Received in revised form 2 October 2017
Accepted 6 November 2017
Available online 11 November 2017

ABSTRACT

Alterations of the epigenetic machinery, affecting multiple biological functions, represent a major hallmark enabling the development of tumors. Among epigenetic regulatory proteins, histone deacetylase (HDAC)6 has emerged as an interesting potential therapeutic target towards a variety of diseases including cancer. Accordingly, this isoenzyme regulates many vital cellular regulatory processes and pathways essential to physiological homeostasis, as well as tumor multistep transformation involving initiation, promotion, progression and metastasis. In this review, we will consequently discuss the critical implications of HDAC6 in distinct mechanisms relevant to physiological and cancerous conditions, as well as

Abbreviations: ALL, acute lymphoblastic leukemia; AML, acute myeloid leukemia; AP, activator protein; AR, androgen receptor; BAX, Bcl-2-associated X protein; Bcl, B-cell lymphoma; BUZ, ubiquitin-binding domain; CDK, cyclin-dependent kinase; CLIP, cytoplasmic linker protein; CLL, chronic lymphocytic leukemia; CTCL, cutaneous T-cell lymphoma; CYLD, cylindromatosis; DD, deacetylase domain; DMB, dynein motor binding; DNMT, DNA methyltransferase; EA, ellagic acid; EB, end binding protein; EC, endothelial cell; EGCG, (−)-epigallocatechin-3-gallate; EGFR, epidermal growth factor receptor; EMT, epithelial-to-mesenchymal transition; ER, estrogen receptor; ERK, extracellular signal-regulated kinase; ERST, endoplasmic reticulum stress-tolerance; FADD, Fas-associated protein with death domain; FDA, Food and Drug Administration; FLICE, FADD-like IL-1 β-converting enzyme; FLIP, FLICE inhibitory protein; GBM, glioblastoma; GR, glucocorticoid receptor; GSK, glycogen synthase kinase; HAT, histone acetyltransferase; HCC, hepatocellular carcinoma; HDAC, histone deacetylase; HDAC6i, HDAC6 inhibitor; HDACi, HDAC inhibitor; HIF, hypoxia-inducible factor; HMGN, high mobility group nucleosomal binding domain; HSF, heat shock transcription factor; HSP, heat shock protein; ICD, immunogenic cell death; IIp, invasion inhibitory protein; IL, interleukin; JAK, Janus kinase; LCoR, ligand-dependent nuclear receptor co-repressor; MAPK, mitogen-activated protein kinase; MM, multiple myeloma; MMP, matrix metalloproteinase; MST, mammalian STE20-like kinase; MT, microtubule; mTOR, mammalian target of rapamycin; NES, nuclear export signal; NLS, nuclear localization signal; Nrf, nuclear factor erythroid 2-related factor; PI3K, phosphoinositide 3-kinase; PKA, protein kinase A; PP, protein phosphatase; Prx, peroxiredoxin; PTEN, phosphatase and tensin homolog; PTM, post-translational modification; RhoB, Ras homolog family member B; RUNX, runt-related transcription factor; SAHA, suberoylanilide hydroxamic acid; SE14, cytoplasmic retention domain; SFN, sulforaphane; SIRT, sirtuin; SMRT, silencing mediator for retinoid or thyroid-hormone receptor; SRSF, serine and arginine rich splicing factor; STAT, signal transducer and activator of transcription; Tau, tubule-associated unit; TGF, transforming growth factor; TPA, 12-*O*-tetradecanoylphorbol-13-acetate; TPPP, tubulin polymerization-promoting protein; TSA, trichostatin A; TSG, tumor suppressor gene; UA, ursolic acid; UDCA, ursodeoxycholic acid; VCP, valosin-containing protein; VEGF, vascular endothelial growth factor; VEGFR, VEGF receptor; ZBG, zinc binding group.

* Corresponding author at: Department of Pharmacy, Research Institute of Pharmaceutical Sciences, College of Pharmacy, Seoul National University, 1 Gwanak-ro, Gwanak-gu, Seoul, 08826, South Korea.
E-mail address: marcdiederich@snu.ac.kr (M. Diederich).

https://doi.org/10.1016/j.phrs.2017.11.004
1043-6618/© 2017 Elsevier Ltd. All rights reserved.

Chemical compounds studied in this article:
FK228 (PubChem CID: 5352062)
PXD101 (PubChem CID: 6918638)
SAHA (PubChem CID: 5311)
LBH-589 (PubChem CID: 6918837)
tubacin (PubChem CID: 6675804)
tubastatin A (PubChem CID: 49850262)
ACY-1215 (PubChem CID: 53340666)
ACY-241 (PubChem CID: 53340426)
(−)-epigallocatechin-3-gallate (PubChem CID: 65064)
aceroside VIII (PubChem CID: 21637600)
curcumin (PubChem CID: 969516)
ellagic acid (PubChem CID: 5281855)
genistein (PubChem CID: 5280961)
20(S)-Rh2 (PubChem CID: 119307)
salirepol (PubChem CID: 188287)
butyrate (PubChem CID: 264)
sulforaphane (PubChem CID: 5350)
trichostatin A (PubChem CID: 444732)
ursodeoxycholic acid (PubChem CID: 31401)
ursolic acid (PubChem CID: 64945)

Keywords:
HDAC6
HDAC6 inhibitors
Natural compounds
Cancer hallmarks
Cancer therapy

the anticancer properties of synthetic, natural and natural-derived compounds through the modulation of HDAC6-related pathways.

© 2017 Elsevier Ltd. All rights reserved.

Contents

1. Introduction 338
2. The isoenzyme HDAC6: a unique deacetylase 339
3. HDAC6 in cancer 339
3.1. Tumor progression 339
3.2. Angiogenesis 339
3.3. Epithelial-to-mesenchymal transition 340
3.4. Aggressiveness: migration, invasion and metastasis 340
3.5. Cancer resistance to therapeutic agents 341
4. Natural and hemi-synthetic compounds with anti-cancer properties targeting HDAC6 341
4.1. (−)-epigallocatechin-3-gallate 343
4.2. Aceroside VIII 344
4.3. Butyrate 344
4.4. Curcumin 345
4.5. Ellagic acid 346
4.6. Genistein 346
4.7. Ginsenosides 346
4.8. NBM-T-BBX-OS01 347
4.9. Salirepol 348
4.10. Sulforaphane 348
4.11. Trichostatin A 348
4.12. Ursodeoxycholic acid 349
4.13. Ursolic acid 350
4.14. Vanillate-based compounds 350
5. Critical consideration and future perspectives 350
Conflict of interest 351
Acknowledgements 351
Appendix A. Supplementary data 351
References 351

1. Introduction

Tumorigenesis is a multistep process whereby normal cells are transformed into malignant cells leading to an abnormal tissue growth. Such transformational events are associated with major biological changes shared by most neoplastic cells called hallmarks of cancer (see for review [1]). It is now widely accepted that besides mutations, the deregulation of epigenetic mechanisms, referring to heritable changes in gene expression that do not involve DNA sequence modifications, participate in the acquisition of the underlying causes of the cancer hallmarks [2].

Growing evidence highlight the essential role of lysine acetylation of histone and non-histone proteins in the coordination of

highly regulated cell functions. The acetylation status of lysine residues results from a balance between the addition and removal of the acetyl group by histone acetyltransferases (HATs) and histone deacetylases (HDACs), respectively. Initially, HATs and HDACs were considered to target only histones; however, acetylomic studies in various cell models revealed that such enzymes control the acetylation of a large and continuously growing list of many non-histone targets in different cellular compartments [3]. Accordingly, lysine acetylation is a major post-translational modification (PTM) regulating many cytoplasmic and nuclear protein functions including enzymatic activity, subcellular localization and protein–protein interactions, and affecting a wide variety of vital cellular processes such as pluripotency, cellular signaling, protein turnover, cell differentiation and cell survival [4–6].

Since Mother Nature is an inexhaustible source of therapeutic scaffolds, medicinal chemistry extensively focused on the discovery of natural compounds or derivatives with anti-cancer properties, such as the modulation of enzymes with epigenetic activities [7–11]. In this review, we will focus on the epigenetic regulatory protein HDAC6, which has become an interesting and relevant pharmacological target for cancer therapy thanks to its unique structure and multiple physiological functions, as well as its implication in cancer progression [12,13].

2. The isoenzyme HDAC6: a unique deacetylase

Over the past few years, there has been a significantly increasing interest for HDAC6 due to its critical role in multiple biological functions through deacetylase-dependent and -independent mechanisms regulating many vital cellular regulatory processes essential to normal and tumor cell growth, migration, and death. Despite its implication in cell homeostasis, the regulation, substrate interactions and specific functions of HDAC6 are not totally unraveled yet [14].

The deacetylase HDAC6 is a structurally unique isoenzyme of the HDAC family because it harbors two functional active sites (Fig. 1). This enzyme presents specific protein domains: a nuclear localization signal (NLS) rich in arginine and lysine sequences; a leucine-rich nuclear export signal (NES); two functional catalytic sites, deacetylase domain (DD)1 and 2 [15]; a cytoplasmic retention signal called SE14, which is a repeated sequence of eight consecutive Ser-Glu tetradecapeptides [16]; and a zinc finger ubiquitin binding domain (BUZ) [17] that binds polyubiquitinated misfolded proteins through the C-terminal Gly–Gly residues of ubiquitin [18]. Similar to the metalloenzymes of classes I, II and IV, HDAC6 possesses a zinc ion at the bottom of its catalytic pocket, which is required for the deacetylation reaction.

Up to now, it was controversial whether both DD1 and DD2 of HDAC6 were fully functional. Initial studies reported both domains as catalytically active toward histone substrates, with only DD2 displaying tubulin deacetylase activity [20], whereas more recent studies suggested that only DD2 was catalytically active [21]. In 2016, crystallographic structures of both catalytic domains of zebrafish HDAC6, and of human DD2 were reported. The two catalytic domains are structurally highly conserved with a similar active site. Both DD1 and DD2 are functional, although DD1 has a weaker activity and displays much more stringent selectivity towards substrates bearing C-terminal acetyl-lysine residues [22,23]. Despite several dissimilarities between zebrafish and human HDAC6 proteins, an overall analysis revealed that the structure of zebrafish HDAC6 is a valid model to characterize the human enzyme [24].

Multiple levels of regulation are required to achieve well-tuned HDAC6 activity: *(i)* specific HDAC6 localization within the cell, *(ii)* PTMs such as phosphorylation and acetylation by specific kinases or HAT, respectively [25], and *(iii)* direct or indirect interactions of HDAC6 to various partners, such as the membrane-associated protein dysferlin [26], invasion inhibitory protein (IIp)45 [27], tubulin polymerization-promoting protein/p25 (TPPP/p25) [28] or farnesyltransferase [29]. Unlike other members of the lysine deacetylase family, HDAC6 does not modify histones but controls the acetylation status of many non-histone substrates, such as chaperones (*e.g.* heat shock protein (HSP)90α) and cytoskeletal proteins (*e.g.* α-tubulin and cortactin) [3]. Consequently, HDAC6 plays a critical role in many cellular processes, which are summarized in Fig. 2 [12,13,25,30].

3. HDAC6 in cancer

Nowadays, it is well established that HDAC6 exerts functions in various disease processes, such as in neurodegenerative and chronic diseases [13], in viral infections by affecting viral replication [31] or in autoimmune diseases *via* its capacity to decrease the immunosuppressive potential of regulatory T-cells [32]. In this review, we will focus on the critical implications of HDAC6 in diverse mechanisms related to cancer including tumor initiation, development and metastasis [33,34]. HDAC6 expression is up- or down-regulated in several cancer subtypes (Table 1) in which it can play a role as tumor inducer or suppressor depending on cancer type and stage [12,35]. In cancer, aberrant HDAC6 overexpression correlates with advanced cancer stages and increased neoplastic transformation [30,36].

3.1. Tumor progression

It has been demonstrated that HDAC6 regulates cell proliferation at distinct cell-cycle phases. HDAC6 interacts with and is inhibited by the deubiquitinating enzyme cylindromatosis (CYLD) at the perinuclear region, significantly delaying the G1-to-S-phase transition, and in the midbody where it regulates the rate of cytokinesis in a deubiquitinase-independent manner [37]. Moreover, HDAC6 regulates the c-Raf-protein phosphatase (PP)1-extracellular signal-regulated kinase (ERK) signaling pathway and inhibition of HDAC6 activity contributes to early M-phase cell-cycle transition arrest *via* sustained ERK activation in prostate cancer [38]. Additionally, cancer developmental steps such as the sustained activation of growth factor signaling and cellular proliferation are achieved through the modulation of specific HDAC6-related pathways [39–41].

3.2. Angiogenesis

HDAC6 is implicated in various mechanisms underlying angiogenesis, which is an essential process for tumor progression and metastatic spread. First, HDAC6, whose mRNA and protein expression levels are up-regulated by hypoxia in endothelial cells (ECs) [42], increases hypoxia-inducible factor (HIF)-1α stability in cancer cells *via* direct deacetylation, and also indirectly through the modulation of HSP90α chaperone function [43]. HIF-1α protein accumulation stimulates its transcriptional activity towards target genes promoting angiogenesis such as vascular endothelial growth factor (VEGF) [44]. Additionally, HDAC6-mediated HSP90α deacetylation ensures adequate binding to VEGF receptor (VEGFR)-1 or VEGFR-2, which transduces angiogenic signaling upon VEGF-A stimulation [45]. Furthermore, pro-angiogenic effects of HDAC6 in ECs are achieved *via* HDAC6-modulated (*i*) stimulation of membrane ruffling at the leading edge to promote cell polarization, (*ii*) regulation of EC migration and generation of capillary-like structures in a microtubule (MT) end binding protein (EB)1-dependent manner [46], and (*iii*) deacetylation of the actin-remodeling protein cortactin, which is necessary for EC migration and sprouting [42].

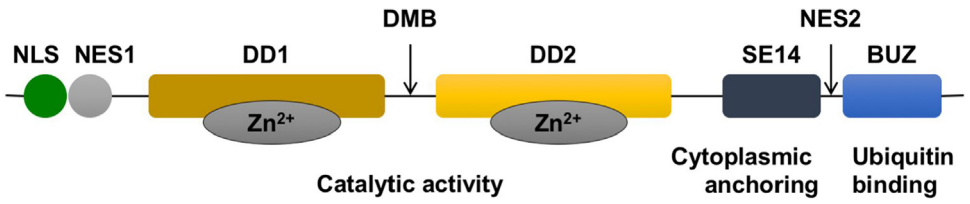

Fig. 1. Schematic structure of histone deacetylase 6.
Figure adapted from [19]. DD: deacetylase domain; DMB; dynein motor binding; NLS: nuclear localization sequence; NES: nuclear export sequence; SE14: cytoplasmic retention domain; BUZ: ubiquitin binding domain.

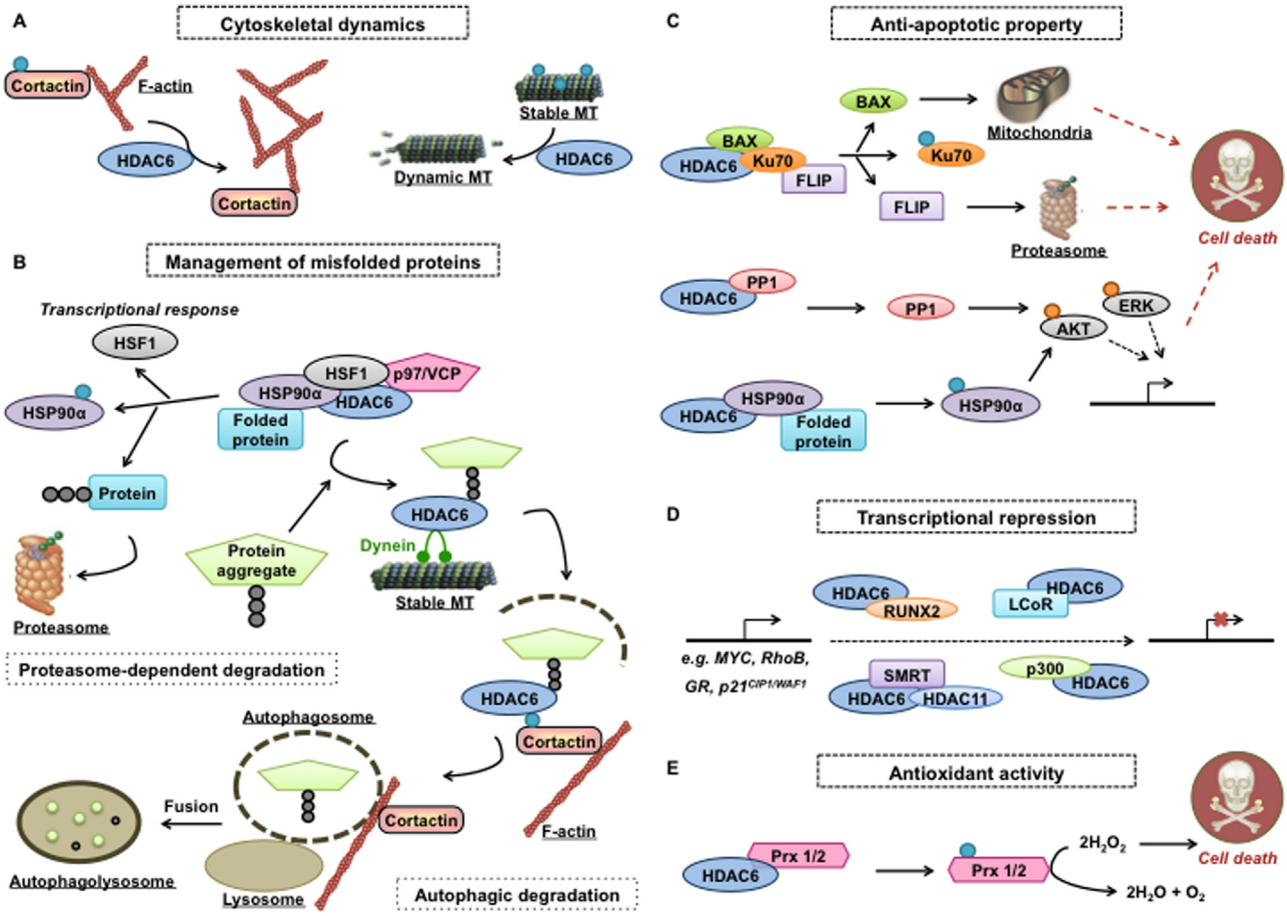

Fig. 2. Physiological roles of HDAC6.
Histone deacetylase (HDAC)6 is involved in (A) cell division and migration by participating in F-actin assembly and microtubule (MT) dynamic through the regulation of the acetylation of cortactin and α-tubulin, respectively, and in (B) protein degradation that is either proteasome-independent by forming aggresomes or proteasome-dependent based on the acetylation status of the chaperone heat shock protein (HSP)90α. (C) HDAC6 possesses anti-apoptotic properties by deacetylating Ku70, which sequesters Bcl-2-associated X protein (BAX) and Fas-associated death domain protein (FADD)-like interleukin-1β-converting enzyme (FLICE) inhibitory protein (FLIP), as well as playing a role in the phosphoinositide 3-kinase (PI3K)/AKT and mitogen-activated protein kinase (MAPK)/extracellular signal-regulated kinase (ERK) signaling pathways. (D) HDAC6 participates in gene regulation through the formation of various transcriptional repressor complexes. Finally, (E) HDAC6 is implicated in redox regulation *via* the deacetylation of peroxiredoxin (Prx)1/2. ● acetyl, ● ubiquitin, ● phosphate. GR: glucocorticoid receptor; HSF: heat shock transcription factor; LCoR: ligand-dependent nuclear receptor co-repressor; PP: protein phosphatase; RhoB: Ras homolog family member B; RUNX: runt-related transcription factor; SMRT: silencing mediator for retinoid or thyroid-hormone receptors; VCP: valosin-containing protein.

Surprisingly, hypoxia-induced suppression of HDAC6 promotes angiogenesis in hepatocellular carcinoma (HCC) by significantly up-regulating HIF-1α/VEGF-A expression levels [47].

3.3. Epithelial-to-mesenchymal transition

Type-3 epithelial-to-mesenchymal (EMT) transition is a hallmark of metastatic cancer, promoting tumor cell motility and invasiveness [48]. Transforming growth factor (TGF)β-mediated EMT induction is accompanied with HDAC6-dependent loss of α-tubulin acetylation, supporting that HDAC6 represents a key regulator of this process [49]. In non-small cell lung cancer, HDAC6 regulates the TGFβ-induced Notch-1 signaling cascade activation *via* deacetylation of HSP90α [50], whereas in lung adenocarcinoma, HDAC6 interplays with the TGFβ-SMAD3 signaling cascade and is required for the maximal expression of various TGFβ-induced EMT markers, such as the proteins E-cadherin and vimentin [51].

3.4. Aggressiveness: migration, invasion and metastasis

Thanks to its influence on the acetylation status of α-tubulin and other cytoskeletal proteins such as cortactin (reviewed by Boy-

Table 1
HDAC6 expression is deregulated in various cancer subtypes.

Cancer	Expression-comments	Reference
ALL	Overexpressed – expression increased in advanced stage	[169,170]
AML	Overexpressed relative to adult	[169]
Brain cancer	Overexpressed	[35]
Breast cancer	Overexpressed – correlated with better or poor prognosis	[53,171,172]
Cholangiocarcinoma	Overexpressed	[173]
CLL	Overexpressed – correlated with longer survival	[174]
CTCL	Overexpressed – correlated with longer survival	[175]
GBM	Overexpressed	[40]
HCC	Overexpressed – expression increased in advanced stage – under expressed	[41,47,57,176]
Lung adenocarcinoma	Overexpressed	[63]
Melanoma	Overexpressed	[177]
Oral squamous cell carcinoma	Overexpressed – expression increased in advanced stage	[178,179]
Ovarian cancer	Overexpressed – expression increased in advanced stage	[35,180]
Pancreatic cancer	Overexpressed	[59]
Urothelial cancer	Overexpressed	[181]

ALL: acute lymphoblastic leukemia, AML: acute myeloid leukemia, CLL: chronic lymphocytic leukemia, CTCL: cutaneous T-cell lymphoma, GBM: glioblastoma, HCC: hepatocellular carcinoma.

ault et al. [52]), HDAC6 promotes cell motility and contributes to the invasiveness and metastasis of many cancers [53–57]. In other types of cancer, HDAC6 stimulates cancer cell aggressiveness by acting synergistically with other partners such as sirtuin (SIRT)2 in bladder cancer [58], cytoplasmic linker protein (CLIP)-170 in pancreatic cancer cells [59], HDAC5 in melanoma cells [60], and estrogen receptor (ER)α ligand in ERα-positive breast cancer cells [61]. Interestingly, stress signals can stimulate the migration of cancer cells by stimulating *HDAC6* gene transcription through a protein kinase A (PKA)/Epac/ERK-dependent signaling pathway in lung and other cancer cells [62]. Conversely, HDAC6 inhibition or depletion increases acetylated α-tubulin levels [24], which enhance MT stability and reduce cancer cell growth and migration [15].

3.5. Cancer resistance to therapeutic agents

HDAC6 is implicated in cancer cell resistance to various chemotherapeutic agents. HDAC6 overexpression, resulting in epidermal growth factor receptor (EGFR) stabilization and activation, confers resistance to the EGFR inhibitor gefitinib in lung adenocarcinoma [63], and to the VEGF inhibitor sorafenib in non-small lung cancer cells [64]. Furthermore, the balance of HDAC6-p97/valosin-containing protein (VCP) influences HDAC6-facilitated autophagic clearance of ubiquitinated misfolded proteins, which is crucial to endoplasmic reticulum stress-tolerance (ERST)-associated temozolomide resistance in glioma [65]. In contrast, HDAC6 inhibition or depletion sensitizes cancer cells to chemotherapeutic compounds such as doxorubicin and etoposide in transformed but not in normal cells [66,67], to paclitaxel [68] and cisplatin [69] in non-small cell lung cancer and to vincristine and bortezomib in acute lymphoblastic leukemia (ALL) [70].

4. Natural and hemi-synthetic compounds with anti-cancer properties targeting HDAC6

Over the years, HDAC inhibitors (HDACi) have become a promising strategy for the treatment of malignancies [12,71]. A multitude of these HDACi were discovered in Nature whereas derivatives have been synthesized by rational design or the modification of natural compounds [72]. The inhibition of HDAC enzymes in cancer cells results in various anti-cancer properties through unforeseeable pleiotropic epigenetic mechanisms [73–76]. Notably, the Food and Drug Administration (FDA)-approved compounds (Fig. 3) are class I selective [FK-228 (**1**) and PXD-101 (**2**)] or pan-HDACi [suberoylanilide hydroxamic acid (SAHA, **3**) and LBH-589 (**4**)].

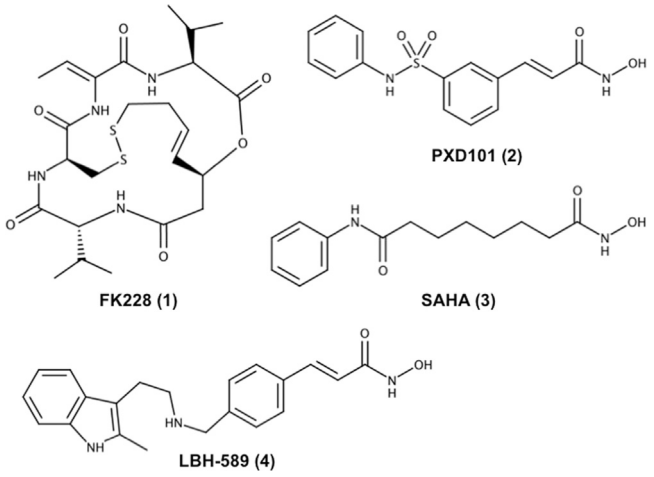

Fig. 3. Molecular structures of Food and Drug Administration-approved histone deacetylase inhibitors. SAHA: suberoylanilide hydroxamic acid.

Nowadays, an increasing number of investigations are focusing on the development of HDACi selective for one class or even for a single isoform [77,78], to target cancer cells more precisely and avoid side effects [36,77]. Considering its unique physiological function and structure, as well as its implication in cancer progression, HDAC6 became an interesting pharmacological target for cancer therapy [34]. Diverse HDAC6 inhibitors (HDAC6i) have been synthetized with the hope of designing a highly selective and potent compound, with suitable pharmacological properties (Table 2). Up to now, only tubacin (**5**) and its derivative tubastatin A (**6**) were intensively reported in the literature as selective HDAC6i (Fig. 4). Since the hydroxamate-based tubacin (**5**) possesses non-drug-like properties, only tubastatin A (**6**) is considered as a promising anti-cancer drug [79]. Additionally, the hydroxamic acid-based compounds ACY-241 (Citarinostat, **7**) and ACY-1215 (Rocilinostat, **8**) are currently undergoing clinical trials conducted by Acetylon Pharmaceuticals, Inc. (Fig. 4) to test their efficacy either as single agents or in combination treatments in patients with multiple myeloma (MM) [80] and other malignancies (www.clinicaltrials.gov).

In addition to synthetic molecules, many natural compounds from terrestrial [10,81] and marine origins [11] were described to act as epigenetic modulators. Some of these compounds exert their anti-cancer effects through HDAC6 modulation, either by inhibiting HDAC6 catalytic activity or regulating HDAC6 protein expression (Table 3).

Table 2
Non-exhaustive list of HDAC6 inhibitors.

Chemical class	Inhibitors	IC_{50}[a] (nM)	Type of cancer (cell lines)[b]	Reference
Hydroxamates	(*E*)-*N*-hydroxy-4-(2-styrylthiazol-4-yl)butanamide	199	Cervix cancer (HeLa)	[182]
	2-benzazolyl-4-Piperazin-1-yl-sulfonylbenzenecarbohydroxamic acids	100–1000	Lung cancer (HCC4017 and HCC4018)	[183]
	3-aroylindole derivatives	64.5	Hematologic (RPMI8226) and solid (A549, HCT116 and PC3) cancers	[184]
	4-(aminomethyl)-*N*-hydroxybenzamide derivatives	20–490	Cervix cancer (HeLa)	[185]
	A452	ND	Colorectal cancer (HCT116, RKO, SW620 and HT29)	[186,187]
	ACY-1083	3	ND	[188]
	ACY-738	1.7	ND	[189]
	ACY-775	7.5	ND	[190]
	Aminopyrrolidinone-based inhibitors	17–1070	ND	[191]
	Azaindolylsulfonamides	5.2–280	Solid cancers (KB, H460, PC3, HSC3, HONE1, A549, MCF7, TSGH, MKN45, HT29, and HCT116)	[192]
	Biarryl inhibitors	<0.2–16	Pancreatic cancer (BxPC3, HupT3, Panc0403, Mia Paca2 and SU8686)	[193]
	Bicyclic-cap containing inhibitors	1.2–8305	ND	[194]
	Bromophenylalanine-containing inhibitors	470–6760	ND	[195]
	C-3 substituted vorinostat derivative	8000	ND	[196]
	C1A	479	Hematologic (ARH77 and KMS11) and solid (HCT116, A2780, IGROV1, MDAMB435, T47D, MCF7, Ishikawa, A431, A549, SHSY5Y, Kelly, SKNAS, BE2C, LNCap and DU145) cancers	[197]
	Capless inhibitors	4–1360	Cervix cancer (HeLa)	[198]
	CAY10603	0.002	Pancreatic cancer (BxPC3, HupT3, MiaPaCa2, Panc0403 and SU8686) and lung adenocarcinoma (A549 and HCC827)	[63,199]
	Chiral 3,4-dihydroquinoxalin-2(1*H*)-one	10–310	Bladder cancer (T24)	[200]
	Citarinostat (ACY-241)	2.6	MM (H929, MM1S and U266) and solid cancer (MiaPaCa2, TOV21G, A2780, MDAMB231 and T47D)	[201,202]
	Compounds containing a phenylisoxazole as a cap group	0.002−72.2	Pancreatic cancer (BxPC3, HupT3, MiaPaCa2, Panc0403 and SU8686)	[199]
	Compound containing Boc and cyclopentyl groups	26	ND	[203]
	Cyclic alpha3beta-tetrapeptides analog	39	T-cell leukemia (Jurkat)	[204]
	γ-lactam based inhibitors	0.8–6.6	Solid cancers (Caco2, PC3, MDAMB231, ACHN, HCT15, NCIH23, NUGC3 and LOXIMVI)	[187]
	HPOB	56	Solid cancers (LNCaP, U87, and A549)	[66]
	Isoxazole-based inhibitors	0.6–1510	Pancreatic cancer (BxPC3, Panc1 and L36PL)	[165]
	KA1010	8	ND	[205]
	N-Hydroxy-4-(2-methoxy-5-(methyl(2-methylquinazolin-4-yl)amino)phenoxy)butanamide	17	Hematologic (U266, RPMI8226, K562, MV411 and Romas) and solid (A2780s, SKOV3, SKBR3, HepG2, H460, A549, HT29 and HCT116) cancers	[206]
	Nexturastat A	5	Melanoma (B16)	[207]
	NK84	ND	Ovarian cancer (SKOV3, TOV21G and ES2)	[180,208]
	Non-natural macrocyclic inhibitors	0.4–75	Solid cancers (HCT116 and NCIH460)	[209]
	Oxazole	59	Hematologic (HL60) and solid (HeLa) cancers	[210]
	Piperazine-2,5-dione aryl hydroxamates	110–170	Bladder cancer (T24)	[200]
	Pteroate hydroxamate	17.6	Solid cancers (HeLa and KB)	[211]
	Pyridylalanine-based inhibitors	1580–6700	Solid cancers (HCT116 and MCF7)	[212]
	Pyrimidinedione derivatives	12.4	Colorectal cancer (HCT116)	[213]
	Pyrrole- and benzene-based inhibitors bearing the *tert*-butylcarbamate group at the CAP moiety	10–30	Hematologic (U937 and K562) and solid (H1299, A549, HCT116, HT29, LAN5, SHSY5Y, M14, MCF7, HEY, U87, Panc1, PC3 and SKOV3) cancers	[214]
	Quinazoline- 4-one derivatives	8–1920	ND	[215]
	Ricolinostat (ACY-1215)	4.7	Relapsed or refractory MM (*e.g.* MM1S and RPMI8226), BRAF-mutant melanoma (*e.g.* A375), (Non-Hodgkin)-lymphoma (*e.g.* OCILy10)[c]	[80,216–223]
	Ring-opened tetrahydro-γ-carbolines	ND	Solid cancers (A549, HCT116, and PC3)	[224]
	ST80	910	Breast cancer (SKBR3) and leukemia (HL60, Kasumi1, NB4, THP1, K562, U937 and Jurkat)	[225,226]
	Tetrahydrocarboline derivatives	0.8–4.9	ND	[32]
	Triazolylphenyl-based inhibitor	1.9	Pancreatic cancer (BxPC3, HupT3, MiaPaCa2, Panc0403 and SU8686)	[227]
	Tubacin	4	Hematologic (*e.g.* Jurkat and RPMI8226) and solid cancer (*e.g.* MDAMB231)[c]	[20,70,228,229]
	Tubastatin A	15	Hematologic (*e.g.* MOLT4) and solid cancer (*e.g.* MDAMB231, A172, and U87)[c]	[65,79]
	Tubathian A et B	1.9−3.7	ND	[230]
	WT161	0.4	MM (RPMI8226, MM1S, ANBL6, ANBL6-V5R, H929, U266, OPM2 and KMS11)	[166]
Benzamide	4-(acylaminomethyl)-*N*-hydrobenzamide 1a	19	Cervix cancer (HeLa)	[185]
Others	AK-14	12800	Cervix cancer (HeLa)	[231]

Table 2 (*Continued*)

Chemical class	Inhibitors	IC_{50}[a] (nM)	Type of cancer (cell lines)[b]	Reference
	Compounds bearing 3-hydroxypyridin-2-thione as ZBG	306–2390	Prostate cancer (DU145 and LNCap) and T-cell leukemia (Jurkat)	[232]
	Compound bearing a trifluoromethylketone ZBG	70	Colon carcinoma (HCT116)	[233]
	Compound containing a cycohephyl cap group and thiol ZBG	23	ND	[234]
	Compound containing mercaptoacetamide ZBG	2.7–2010	ND	[235]
	Isoxazole derivatives with substituted mercaptoacetamide ZBG	260–280	ND	[236]
	Naphthoquinone	5540–15600	Leukemia (MV411, Kasumi1, and Reh)	[237]
	Thiolate analogues	23–3860	Solid cancers (HCT116 and MCF7)	[238]
	Vanillate derivatives	200–20000	Solid cancers (MDAMB231, MCF7, PC3 and LNCaP)	[164]

MM: multiple myeloma, ND: not determined, ZBG: zinc binding group.
[a] IC (inhibitory concentration)$_{50}$ of the compounds towards HDAC6 were determined based on *in vitro* assays.
[b] Cancer cell lines on which biological activities of the compound have been evaluated.
[c] Besides the selected cell models, the compound has been studied in a broad panel of cancer cell lines.

Table 3
Natural compounds with anticancer properties through HDAC6 modulations.

Name of the compound	Type of HDAC6 modulation	Cancer type[a]	Comments	Ref.
(−)-epigallocatechin-3-gallate (combined with Am80)	Down-regulation of protein level	Lung cancer, myeloid leukemia	Potential posttranscriptional regulations and stimulation of HDAC6 degradation.	[91]
Aceroside VIII	Inhibition of catalytic activity	Colon cancer	Enhancement of the efficacy of other HDAC6i.	[95]
Butyrate derivative (B-R2B)	Inhibition of catalytic activity	Leukemia, cervical cancer	Localization at the entrance of the active pocket of HDAC6.	[101]
Curcumin	Down-regulation of protein level	Colon cancer	Potential contribution of HDAC6 reduced expression to the regulation of the TSG *DLEC1* transcriptional activity.	[108]
		Neuro-blastoma, leukemia	ND	[109,110]
Ellagic acid	Down-regulation of protein level	Oral cancer	Significant blockage of AKT activation and subsequent decrease of HIF-1α and VEGF expression.	[114]
Genistein	Down-regulation of protein level	Prostate cancer	Decreased HDAC6 expression potentially due to transcriptional repression. Subsequent reduction of hyperacetylated HSP90α chaperone activity leading to increased AR ubiquitination and probable proteasome-mediated degradation.	[119]
Ginsenoside 20(S)-Rh2	Down-regulation of protein level	Chronic and acute myeloid leukemia	Possible involvement in apoptosis induction through activation of the MAPK signaling pathway.	[121]
NBM-T-BBX-OS01	Down-regulation of protein level	Lung cancer	Disruption of HSP90α-cyclin D1/CDK4 interaction leading to G1 cell cycle arrest.	[129]
Salirepol	Inhibition of catalytic activity (*in vitro*)	ND	ND	[132]
Sulforaphane (SFN)	Down-regulation of protein level	Prostate cancer	Contribution of two distinct pathways to the effect of HDAC6 in mediating SFN-induced cytotoxicity (presence *versus* absence of AR).	[143–145]
		Colon cancer	Unexpected decrease of acetylated α-tubulin.	[140,142]
Trichostatin A	Inhibition of catalytic activity	Numerous cancer types	Modulation of a broad range of HDAC6-related signaling pathways.	[149–151]
Ursodeoxycholic acid (UDCA)	Up-regulation of protein level	Colon cancer	Important role of HDAC6 increased expression in UDCA-induced senescence.	[159]
Ursolic acid (UA)	Down-regulation of protein level	Skin cancer	Involvement of HDAC6 decreased expression in UA-mediated Nrf2 expression induction resulting in the rescue of TPA-induced transformation in epidermal cells.	[162]
Vanillate-based compounds	Inhibition of catalytic activity	Prostate cancer	Decreased cell proliferation and cell death induction. Modulation of microtubular architecture. Reduction of AR-HSP90α interaction resulting in decreased AR protein levels and target gene expression.	[164]

AR: androgen receptor; CDK: cyclin-dependent kinase; HDAC6: histone deacetylase 6; HDAC6i: HDAC6 inhibitor; HIF: hypoxia-inducible factor; HSP: heat shock protein; ND: not determined; Nrf: nuclear factor erythroid 2-related factor; TPA: 12-*O*-tetradecanoylphorbol-13-acetate; TSG: tumor suppressor gene; VEGF: vascular endothelial growth factor.
[a] Cancers on which biological activities of the compound have been evaluated.

4.1. (−)-epigallocatechin-3-gallate

The catechin (−)-epigallocatechin-3-gallate (EGCG, **9**) is the most abundant and active flavone-3-ol polyphenol of green tea plants (*Camellia sinensis*), but is also found in apple skin, plums and onions (Fig. 5). Before absorption, EGCG (**9**) is subjected to a gut microbiota-mediated degradation pathway in which it undergoes extensive biotransformations, such as hydrolysis.

The green tea catechins possess numerous pharmacotherapeutic properties such as anti-inflammatory, anti-oxidative,

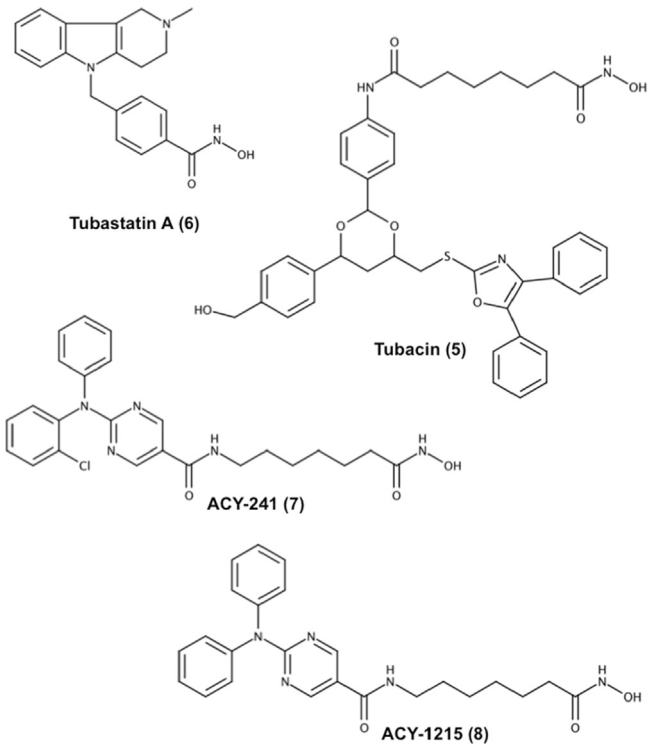

Fig. 4. Molecular structures of selected histone deacetylase 6 inhibitors.

anti-carcinogenic, anti-microbial, anti-obesity and anti-diabetic activities [82]. More specifically, beneficial anti-cancer activities including anti-oxidant, anti-inflammatory, anti-proliferative, anti-invasive, anti-angiogenic and pro-apoptotic properties were described [83] after treatment of a variety of cancer cells, such as adrenal, bladder, breast, cervical, colorectal, esophageal, gastric, liver, lung, oral, ovarian, pancreatic, prostate and skin cancer cells [84] with EGCG (**9**).

A large number of cell-based studies proposed various mechanisms for EGCG-mediated cancer signaling and metabolic pathway modulations [85]. EGCG (**9**) induces cell cycle arrest *via* alteration of cell cycle regulatory protein expression. Treatment of human pancreatic cancer cells by EGCG (**9**) caused cell cycle arrest in G1 phase through up-regulation of $p21^{CIP1/WAF1}$ and $p27^{KIP1}$ expression, and down-regulation of cyclin D1, cyclin-dependent kinase (CDK)4 and CDK6 protein expression levels [86]. In addition, induction of apoptosis can be mainly associated with EGCG (**9**)-mediated regulation of different pro-apoptotic and anti-apoptotic proteins. Furthermore, EGCG (**9**) exhibits anti-angiogenic activities in various experimental tumor models through blocking ERK and AKT phosphorylation, which inhibits HIF-1α synthesis and therefore decreases the expression of VEGF [87,88]. Notably, EGCG (**9**) has the highest free radical scavenging ability among common phenolic compounds.

Many reports have highlighted the effects of EGCG on the epigenetic machinery that might account for its anti-cancer activities. Green tea polyphenols reduce the activity and protein expression of class I HDACs in prostate cancer cells *via* their increased proteasomal degradation, leading to G0/G1 phase cell cycle arrest and apoptosis induction [8,89].

Interestingly, EGCG (**9**) synergizes with conventional anti-cancer compounds [90]. For instance, combining EGCG (**9**) with the synthetic retinoid Am80 induces synergistic apoptotic cell death in lung cancer cells by reducing HDAC4, 5 and 6 protein levels and altering the acetylation levels of non-histone proteins, such as p53 and α-tubulin. Authors suggest that the combination diminishes HDAC protein levels through post-transcriptional regulations and the stimulation of their degradation. In addition, EGCG (**9**) accentuates Am80-triggered differentiation of human myeloid leukemia cells into granulocytes, along with reduction of HDAC4 and 6 protein levels [91].

4.2. Aceroside VIII

Aceroside VIII (**10**) is a diarylheptanoid isolated from the bark of *Betula platyphylla* (Betulaceae). The healing properties of bark and its extracts from several species belonging to the genus *Betula* have been widely used in traditional medicine (Fig. 5). More specifically, *Betula platyphylla* possesses anti-inflammatory, anti-oxidant and anti-cancer effects [92]. Nevertheless, bioactive compounds, such as aceroside VIII (**10**), are ubiquitously synthetized by this species family, so further investigations are required to determine which effects of the extracts could be mediated by aceroside VIII (**10**) [93].

Aceroside VIII (**10**) is known for its anti-fibrotic effects as it demonstrates significant dose-dependent inhibitory activity towards the proliferation of immortalized hepatic stellar cells, considered to play a fundamental role in the pathogenesis of liver fibrosis [94]. Recently, studies have shown that aceroside VIII (**10**) also plays a role in colon cancer cells, by selectively inhibiting HDAC6 catalytic activity and enhancing the efficacy of other HDAC6i through a mechanism yet to be discovered [95].

4.3. Butyrate

Butyrate (**11**) is a short-chain fatty acid generated during gut flora-mediated fermentation of dietary fibers, which are indigestible food ingredients (Fig. 5). In the colon, butyrate (**11**) provides energy to colonic bacteria. Notably, it is also present in cheese and butter.

Initially, butyrate (**11**) was described as an unusually potent inducer of erythroid differentiation in cultured erythroleukemic cells [96]. Treatment of cultured leukemia cells with butyrate (**11**) was then reported to inhibit classes I, IIa and IV HDAC activity, causing rapid histone hyperacetylation in leukemia cells [97].

Up to now, multiple studies have demonstrated that butyrate (**11**) possesses pleiotropic anti-cancer effects in various models including cell cycle arrest, inhibition of proliferation, inflammation and oxidative stress, modulation of detoxification potential, and induction of differentiation and apoptotic cell death [98,99]. Possible mechanisms of butyrate (**11**)-mediated chemoprevention include transcription induction of detoxifying enzymes such as glutathione *S*-transferases [73], as well as inhibition of HDACs.

Although butyrate (**11**) does not directly target class IIb HDACs, HDAC6 is required for the accumulation of serine- and arginine-rich splicing factor (SRSF)2 protein in response to butyrate (**11**) treatment, which then leads to overexpression of $p21^{CIP1/WAF1}$ and induction of senescence in lung carcinoma cell lines. HDAC6 is possibly involved in the accumulation of an acetylated and non-phosphorylated form of SRSF2 *via* inhibition of its proteasomal degradation through a direct or indirect mechanism [100]. Otherwise, derivatives of phenyl butyrate were designed by *in silico* methods to identify a novel compound with HDAC6 inhibitory activity. The derivative named B-R2 B specifically inhibits HDAC6 *in vitro* and in cancer cells in a non-competitive manner *via* its localization at the entrance of the active pocket of HDAC6. The compound then blocks the passage of the substrate unable to reach the HDAC6 binding site. Furthermore, treatments with micromolar amounts of B-R2 B decrease the viability of leukemia and cervical cancer cells [101].

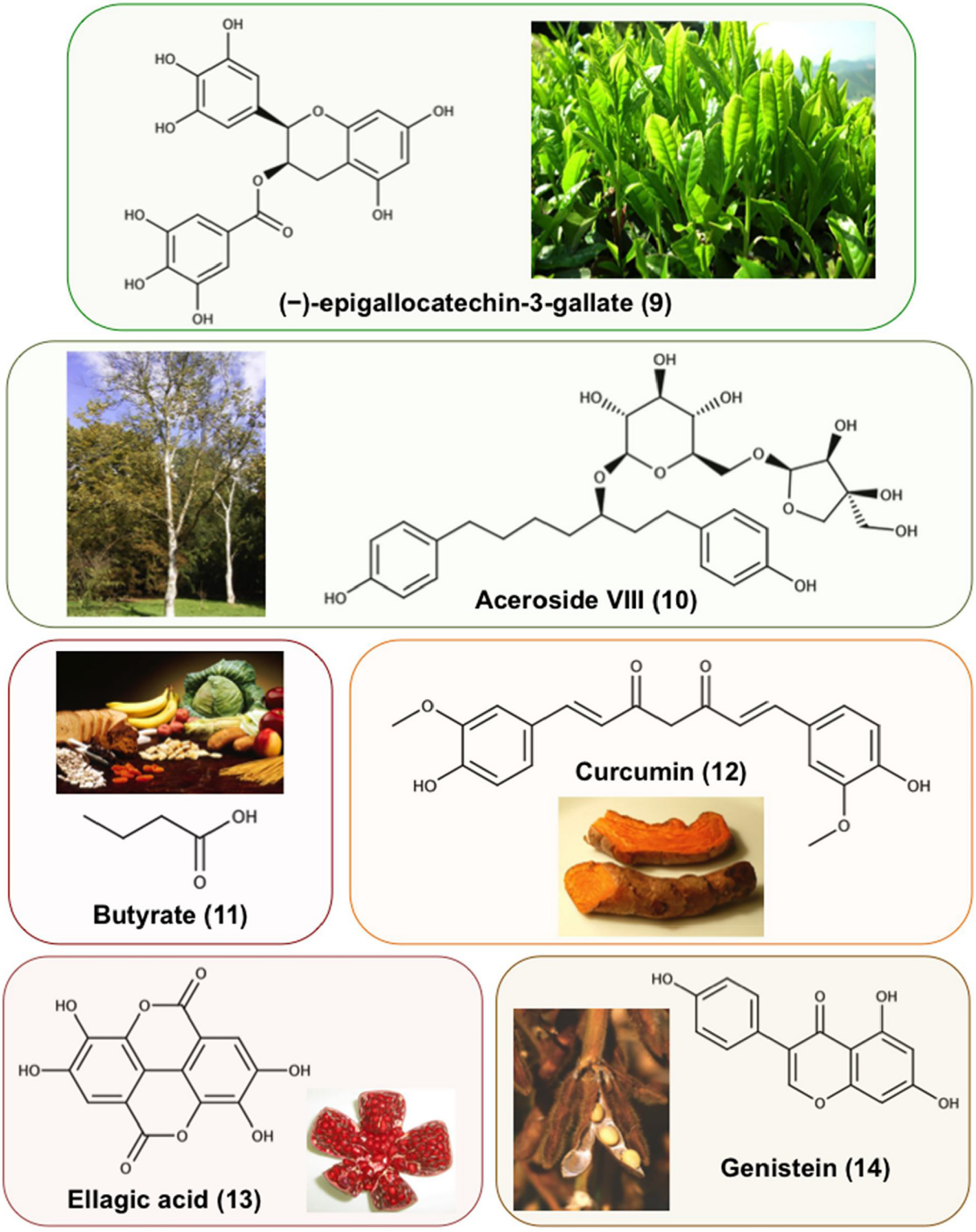

Fig. 5. Natural histone deacetylase inhibitors and corresponding terrestrial sources. (−)-epigallocatechin-3-gallate (**9**) from *Camellia sinensis*; aceroside VIII (**10**) from *Betula platyphylla;* butyrate (**11**) derived from dietary fibers; curcumin (**12**) from *Curcuma longa*; ellagic acid (**13**) from *Punica granatum*; genistein (**14**) from *Glycine max*.

4.4. Curcumin

Curcumin (**12**) is an active dietary polyphenol extracted from the root of the plant turmeric *Curcuma longa* (Fig. 5). This yellow-colored pigment has been widely used in traditional medicine, and consumed as a common food spice in culinary traditions. Curcumin (**12**) has been associated with well-known biological and pharmacological properties such as anti-oxidant, anti-inflammatory, anti-microbial, and anti-tumor properties [102]. Accumulating evidence present this well-tolerated phytochemical as potent agent in both prophylaxis and treatment of several types of cancer since it targets numerous molecular signaling pathways involved in carcinogenesis [103,104].

These anti-cancer properties may result from epigenetic changes triggered by curcumin (**12**), an epigenetically active compound selectively modulating the expression of genes implicated in cancer death and progression (reviewed in [105]). More specifically, curcumin (**12**) can be considered as a class I HDAC inhibitor or protein expression modulator. For instance, curcumin (**12**) reduces B-cell lymphoma proliferation and induces apoptosis by down-regulating HDAC1, 3, and 8 protein expression levels, which is associated with an up-regulation of acetylated histone H4 protein expression [106]. In addition, the HDAC inhibitory activity of curcumin (**12**) reduces double strand break repair thus increasing DNA damage sensitivity. Curcumin (**12**) inhibits homologous recombination and subsequent DNA repair processing, presumably by promoting the degradation of Rad52 recombinase in a process dependent on HDAC inhibition [107].

In colon cancer cells, curcumin (**12**)-mediated epigenetic regulation of the tumor suppressor gene (TSG) *DLEC1* transcriptional activity leads to the suppression of anchorage-independent cell growth. Upon treatment with curcumin (**12**), a significant reduction of HDAC6 protein expression accompanied by reduced HDAC4, 5, and 8 protein levels suggests that histone modifications may contribute to the regulation of *DLEC1* transcriptional activity. Moreover, CpG methylation of the *DLEC1* promoter is decreased due to curcumin (**12**)-induced reduction of protein expression of DNA methyltransferases (DNMTs) in a concentration-dependent manner [108]. Similarly, curcumin (**12**) down-regulates HDAC6 overexpression in human neuroblastoma [109] and leukemia cells [110] *via* mechanisms that still need to be investigated.

4.5. Ellagic acid

Ellagic acid (EA, **13**), an anti-oxidant polyphenol, is found as a naturally occurring hydrolysis product of ellagitannins in many vegetables and fruits, like pomegranate (*Punica granatum*) whose juice is considered as highly cancer preventive [111] (Fig. 5).

EA (**13**) possesses many pharmacological activities, especially anti-tumor properties. Accordingly, EA (**13**) notably prevents the development of diverse cancers, such as colon, prostate, breast, pancreatic and bladder cancer *in vitro* and *in vivo* [81,112]. EA (**13**) exerts its chemotherapeutic properties through the regulation of multiple subcellular signaling pathways implicated in tumor growth and metastasis prevention, by inhibiting tumor cell proliferation, promoting apoptosis and neutralizing the interaction of carcinogens with DNA. Moreover, EA (**13**) abrogates inflammation, angiogenesis, and drug-resistance processes [112,113].

Recently, this dietary compound has been reported to abrogate hypoxia-driven angiogenesis *via* the suppression of phosphoinositide 3-kinase (PI3K)/AKT/mammalian target of rapamycin (mTOR) and mitogen-activated protein kinase (MAPK) signaling cascades, preventing HIF-1α translocation to the nucleus and inhibiting VEGF/VEGFR-2-mediated signaling. In addition, EA (**13**) treatment down-regulates hypoxia-induced HDAC6 overexpression, significantly blocking AKT activation and subsequently decreasing HIF-1α and VEGF expression [114]. Those results show for the first time the modulatory effects of dietary EA (**13**) on HDAC expression.

4.6. Genistein

The isoflavone genistein (**14**) was isolated in 1899 from the dyer's broom, *Genista tinctoria* (Fig. 5). Nevertheless, the predominant form naturally occurring in plants is the 7-*O*-beta-D-glucoside form of genistein (**14**), namely genistin, which is abundantly found in soybeans (*Glycine max.*), lupine *(Lupinus albus),* kudzu (*Pueraria lobata*) and psoralea (*Psoralea corylifolia*). Upon ingestion, genistin undergoes hydrolysis to be converted to genistein (**14**), which is absorbed in the intestine and responsible for the biological activities.

Genistein (**14**) is the major anti-cancer constituent of soybean, whose consumption reduces the risk of development of several types of cancer. Accordingly, it prevents, delays or blocks multiple steps of carcinogenesis *in vitro* and *in vivo* by targeting pleiotropic cellular mechanisms relevant in oxidative stress management, angiogenesis, cell cycle regulation, and apoptosis [115]. Nevertheless, this phytochemical is not only associated with desired chemopreventive virtues against cancer, but also with unexpected and potentially dangerous consequences of its uses for treatment. The "good" and the "bad" effects of the biological activities of genistein (**14**) strongly depend upon the dose applied and its main molecular targets in the different types of cancer [116,117].

Due to structural similarities with estrogens, this phytoestrogen primarily targets estrogen receptors and possesses estrogen-like properties. In addition to estrogen receptors, genistein (**14**) main targets include tyrosine kinase and topoisomerase II, whose inhibition is essential for genistein (**14**) cytotoxic activity [118]. The anti-estrogenic activity of genistein (**14**) can also be mediated *via* a decrease in HDAC6 protein expression and the subsequent inhibition of HDAC6-HSP90α co-chaperone function, which is required to stabilize androgen receptor (AR) protein. Prostatic cancer cells treated with genistein (**14**) exhibit hyperacetylated HSP90α with reduced chaperone activity, resulting in increased AR ubiquitination and probable proteasome-mediated degradation [119]. Since HDAC6 has been identified as a positively regulated gene by estrogen in estradiol-treated breast cancer cells, the phytoestrogen genistein (**14**) likely down-regulates HDAC6 protein expression through transcriptional repression [119].

4.7. Ginsenosides

Panax ginseng, belonging to the Araliaceae family, is one of the most widely used herbal medicines and is reported to have a wide range of therapeutic and preventive activities including vasorelaxation, anti-oxidation, anti-inflammation and anti-cancer effects. Ginsenosides are triterpene saponins considered to be the major pharmacologically active components of *P. ginseng* roots and rhizomes (Fig. 6). They appear to be responsible for the majority of the whole ginseng extract activities, but purified individual ginsenosides may have specific pharmacological mechanisms of action due to their different chemical structures [120]. Ginsenosides are generally divided into two groups based on their chemical structures: protopanaxatriols and protopanaxadiols [121].

Rh2 is a protopanaxadiol-type ginsenoside and two stereoisomeric forms, 20(S)- and 20(R)-Rh2, were selectively isolated. 20(S)-Rh2 (**15**) induces cell cycle arrest and apoptosis in various cancers. For instance, 20(S)-Rh2 (**15**) could suppress proliferation, promote apoptosis and inhibit metastasis of liver carcinoma cells by down-regulating β-catenin through glycogen synthase kinase (GSK)-3β activation [122]. Additionally, 20(S)-Rh2 (**15**) effectively targets interleukin (IL)-6-induced Janus kinase (JAK)2/signal transducer and activator of transcription (STAT)3 pathway leading to the inhibition of STAT3 phosphorylation, and suppresses the expression of matrix metalloproteinases (MMPs), including MMP-1, -2, and -9, resulting in the inhibition of human colorectal cancer cell invasion [123].

Ginsenosides can also exhibit their potential as chemotherapeutic agents through modulation of epigenetic processes. The inhibitory effect of ginsenoside Rh2 on the migratory ability of liver carcinoma cells is presumed to occur by the recruitment of HDAC4 and the resulting inhibition of activator protein (AP)-1 transcription factors, in order to reduce MMP-3 gene and protein expression levels [124].

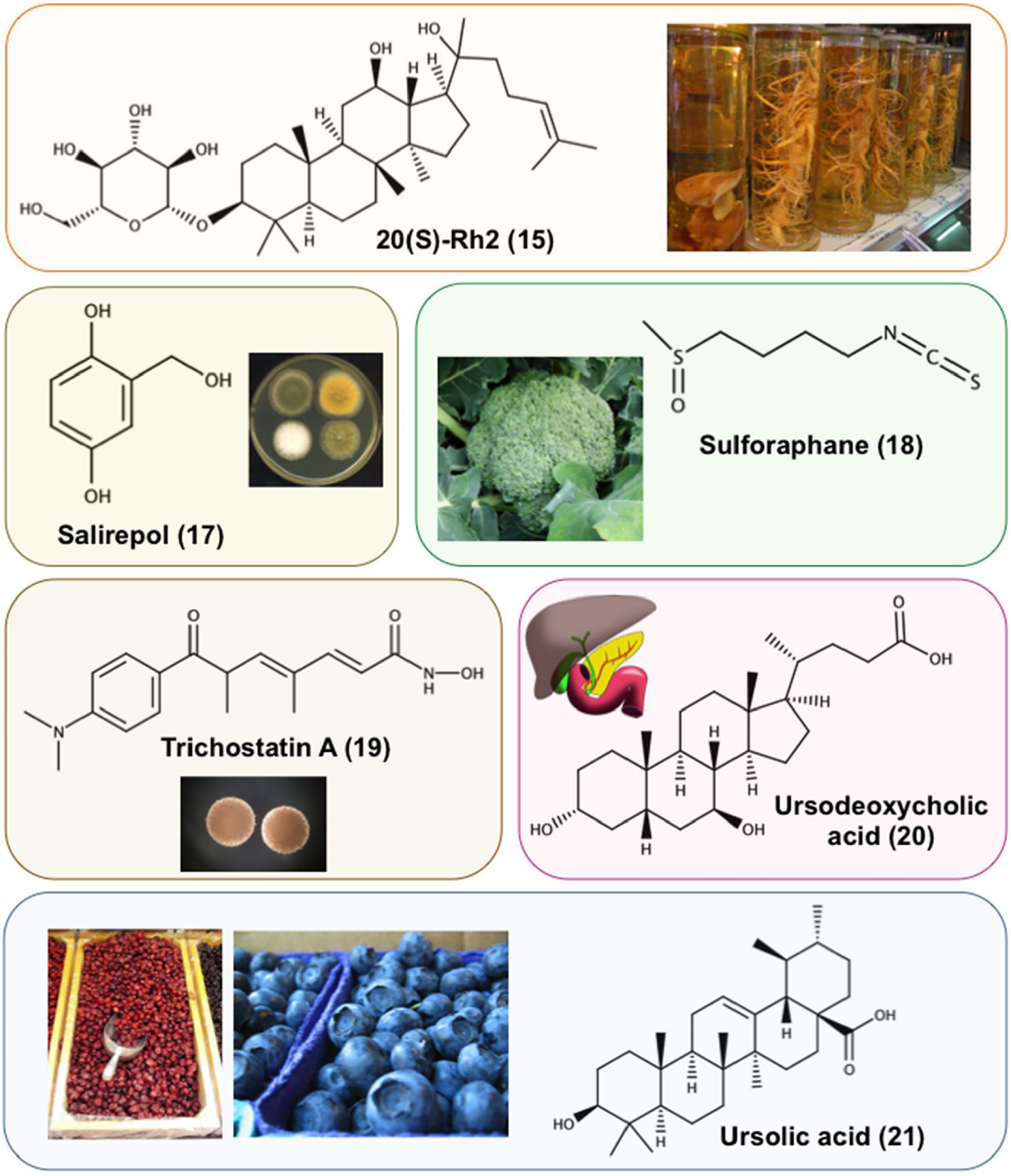

Fig. 6. Natural histone deacetylase inhibitors and corresponding terrestrial or marine sources. 20(S)-Rh2 (15) from Panax ginseng; salirepol (17) from Aspergillus genus; sulforaphane (18) from Brassica oleracea; trichostatin A (19) from Streptomyces hygroscopicus; ursodeoxycholic acid (20) from primary bile acid; ursolic acid (21) from Vaccinium myrtillus and Vaccinium oxycoccos.

In chronic and acute myeloid leukemia cells, 20(S)-Rh2 (**15**) was also described to inhibit cancer cell growth, accompanied with a G0/G1 cell cycle arrest, p16 and p21 up-regulation, as well as cyclin D1 and CDK4 down-regulation. In the same models, 20(s)-Rh2 (**15**) induces B-cell lymphoma (Bcl)-2 down-regulation and apoptotic cell death, whereas this drug is only moderately toxic in healthy bone marrow stromal cells. Furthermore, authors reported that 20(S)-Rh2 (**15**) also reduces tumor growth *in vivo*. Interestingly, treatments with 20(S)-Rh2 (**15**) significantly decrease HDAC activity concomitantly to HDAC6 down-regulation in tumor cells *in vitro* as well as *in vivo* [121]. Authors suggest that HDAC6 down-regulation could possibly play a role in the anti-tumor properties of 20(S)-Rh2 (**15**) *via* the activation of the MAPK signaling pathway and the subsequent increase of caspase-3 cleavage, resulting in apoptosis induction [121].

4.8. NBM-T-BBX-OS01

Osthole is an O-methylated coumarin found in plants such as *Cnidium monnieri*, *Angelica archangelica* and *Angelica pubescens*.

Osthole demonstrates multiple pharmacological properties including immunomodulatory, anti-microbial, and anti-cancer activities through the modulation of diverse signal transduction pathways [125]. This compound has served as the lead compound for the synthesis of other anti-cancer derivatives such as NBM-T-BMX-OS01 (BMX) [126], which targets VEGFR signaling to regulate vascular endothelial cell remodeling, leading to the inhibition of tumor angiogenesis. Another series of osthole derivatives showed potent activity against nuclear HDACs *in vitro* and in cellular assays [127,128].

Recently, NBM-T-BBX-OS01 (TBBX, **16**), a semisynthetic derivative of osthole (Fig. 7), was described to provoke lung cancer cell growth arrest in G1 phase, associated with decreased cyclin D1, CDK2 and CDK4 protein levels and transcriptional up-regulation of $p21^{Waf1/Cip1}$ protein expression level. Upon TBBX (**16**) treatment, the down-regulation of HDAC6 protein levels, rather than a direct inhibition of HDAC6 activity, caused an attenuation of the HDAC6-HSP90α signaling pathway. Consequently, the disrupted interaction of HSP90α with cyclin D1 and CDK4 triggered their proteasomal degradation. Accordingly, ectopic expression of HDAC6 rescues TBBX (**16**)-induced G1 cell cycle arrest [129].

4.9. Salirepol

Salirepol (**17**) is a 2,5-dihydroxybenzyl alcohol, also named gentisyl alcohol (Fig. 6). It has been found in a marine isolate of the fungus *Aspergillus* and was reported to display a potent antibacterial activity against the methicillin-resistant and multi-drug-resistant *Staphylococcus aureus* [130].

Upon extraction from *Penicillium concentricum*, this compound has also showed moderate and weak anti-proliferative activities against colon and breast cancer cells, with IC_{50} values of 6.4 and 17.1 μM, respectively [131].

Recently, salirepol (**17**) was reported for the first time to be present in *Penicillium griseofulvum* extracts thanks to a mass spectrometry-based assay optimized for bio-guided identification of HDACi in fungi. Since this fungal compound showed a 14-fold selectivity towards HDAC6 (IC_{50} = 3.4 μM) *versus* HDAC1 (IC_{50} = 76.4 μM) *in vitro* [132], further investigations will determine the biological activities of salirepol (**17**) and whether it displays *in vivo* selectivity of towards HDAC6, potentially associated with chemotherapeutic properties.

4.10. Sulforaphane

Isolated in 1992, sulforaphane (SFN, **18**) is a dietary isothiocyanate derived from a naturally occurring precursor, glucoraphanin, mainly present in Brassicaceae or "cruciferous" vegetables such as broccoli (*Brassica oleracea*), broccoli sprouts and cabbage (Fig. 6). Upon food intake, the release of endogenous myrosinase enzymes induces the hydrolysis of glucoraphanin into bioactive substances such as SFN (**18**).

Initially, Zhang et al. [133] identified SFN (**18**) as a potent anti-carcinogenic agent through the induction of phase-II detoxification enzymes such as quinone reductase and glutathione *S*-transferase. Up to now, this phytochemical interfered with several hallmarks of cancer thanks to its pleiotropic activities [134]. Accordingly, it induces cell cycle arrest and apoptosis in various cancer models [135]. Furthermore, numerous studies have also reported SFN (**18**) as an interesting potential chemopreventive compound, since its consumption is associated with lower risks of developing bladder [136], pancreatic [137] and prostate cancers [138]. At the molecular level, one potential role of SFN (**18**) in cancer prevention and therapy consists in the activation of the transcription factor nuclear factor erythroid 2-related factor (Nrf)2, the master regulator of cellular redox homeostasis [139].

SFN (**18**)-promoted anti-cancer effects may also be associated with the inhibition of HDAC activities. *In vitro* studies and *in silico* modeling hypothesize that SFN (**18**)-mediated inhibition of HDAC activity is due to its binding to cysteine in the cell in order to fit within the active site of HDACs [140]. In colon cancer cells, treatment with SFN (**18**) induces the acetylation of lysine on various positions within histones H3 and H4 in a dose-dependent manner, associated with an inhibition of HDAC activity and an increase of HDAC protein turnover [141,142].

Particularly, SFN (**18**) decreases HDAC6 protein levels in various prostatic cancer cells by a yet unknown mechanism. Depending on the presence or absence of AR in the considered cell lines, two distinct pathways contribute to the effect of HDAC6 in mediating SFN (**18**)-induced cytotoxicity. In AR-positive prostate cancer cells, HDAC6 down-regulation enhances HSP90α acetylation, resulting in the disruption of HSP90α-AR interaction associated with AR degradation and reduced expression of AR target genes [143,144]. In AR-negative cells, HDAC6 inhibition stabilizes the MT network, thereby disrupting α-tubulin polymerization and ultimately contributing to mitotic cell cycle arrest. Importantly, HDAC6 overexpression reversed SFN (**18**)-induced cytotoxicity [145].

Studies performed in colon cancer cells reported a similar decrease of HDAC6 protein levels after treatment with SFN (**18**) [140,142]. Nevertheless, Dickinson, et al. [140] showed that this decrease was not correlated to an expected increase of acetylated α-tubulin since treated cells rather showed a decreased level of α-tubulin acetylation. Further investigations will be necessary to clarify this discrepancy.

4.11. Trichostatin A

Trichostatin A (TSA, **19**), a common non-selective HDACi, was first isolated in 1976 from the metabolites of strains of *Streptomyces hygroscopicus* (Fig. 6) and identified as a derivative of a primary hydroxamic acid due to the presence of a free or glycosylated hydroxamate group [146]. The (*S*) enantiomer of TSA (**19**) is unnatural and initially reported to be biologically inactive [147]. More recently, (*S*)-TSA was reported to act *in vitro* as a moderate selective HDAC6i, whereas (*R*)-TSA is a pan-HDACi [24].

Initial studies revealed that the potent HDAC inhibitory activity of TSA (**19**) promoted differentiation and cell cycle arrest of transformed cells, accompanied with histone hyperacetylation [147]. Over the years, TSA (**19**) became a promising compound for the treatment of different cancer subtypes thanks to its pharmacotherapeutic potential at various stages of tumor initiation and progression. For example, this HDACi blocks tumor survival pathways by inducing transcription of TSGs such as p53 and $p21^{CIP1/WAF1}$ [148].

Anti-cancer activities of TSA (**19**), such as tumor growth arrest and cell death induction, can be associated with the modulation of a broad range of HDAC6-related signaling pathways. Upon HDAC6 inhibition by TSA (**19**), (*i*) chromatin-remodeling protein high mobility group nucleosomal binding domain (HMGN)2 acetylation at Lys2 blocks STAT5A-mediated gene transcription, leading to inhibition of cancer growth [149] and (*ii*) phosphatase and tensin homolog (PTEN) acetylation at K163 induces its membrane translocation and activation, which significantly contributes to inhibition of tumors without PTEN mutations or deletions [150]. Moreover, TSA (**19**)-mediated HDAC6 inhibition results in increased levels of acetylated tumor-suppressor mammalian STE20-like kinase (MST)1, abolishing its degradation in a chaperone-mediated autophagy manner, which is normally required for the promotion of breast cancer growth [151]. Additionally, alteration of mTOR phosphorylation status following HDAC6 inhibition by TSA (**19**) decreased autophagy induction, while markedly enhancing bortezomib-induced apoptosis in head and neck squamous cell

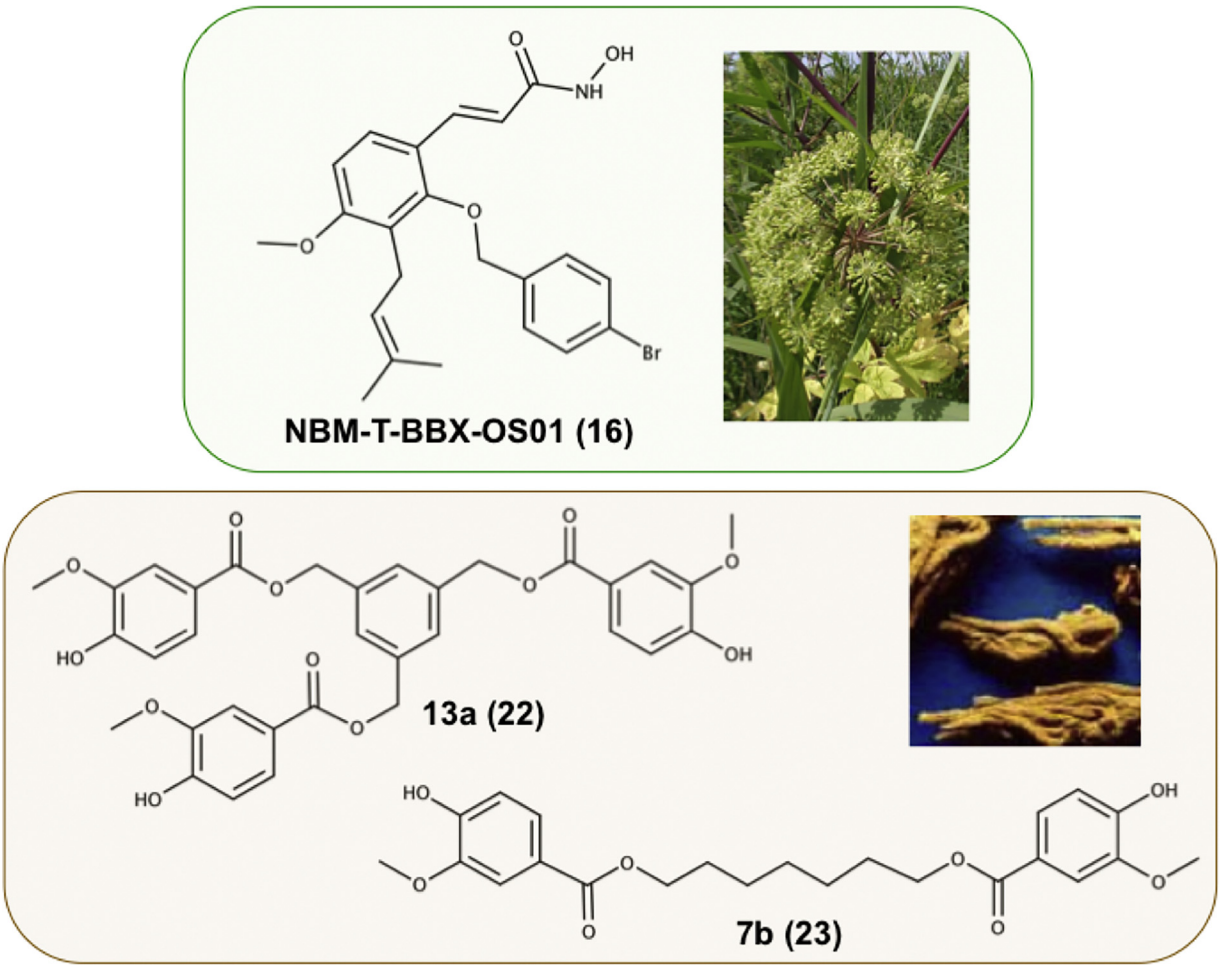

Fig. 7. Semi-synthetic histone deacetylase inhibitors. NBM-T-BBX-OS01 (**16**) is a derivative of osthole from *Angelica archangelica*; 13a (**22**) and 7b (**23**) are derivatives of vanillic acid from *Angelica sinensis*.

carcinoma cells [152]. Furthermore, TSA (**19**) decreases HDAC6-mediated α-tubulin deacetylation [153], affecting MT-associated processes such as cell motility and metastasis formation.

Interestingly, TSA (**19**) also displays anti-cancer effects in combination treatments through the inhibition of the catalytic activity of HDAC6. For instance, TSA (**19**) in combination with C6-ceramide, a cell-permeable lipid molecule, exerts highly synergistic anti-tumor effects through the disruption of HDAC6/PP1/α-tubulin complex, promoting α-tubulin acetylation and activating PP1, which then leads to AKT dephosphorylation and eventually causes cancer cell death in *in vitro* and *in vivo* models [154].

4.12. Ursodeoxycholic acid

Bile acids are polar derivatives of cholesterol that are excreted into the digestive tract where they aid in the emulsification and absorption of dietary fats. They have been implicated in the pathogenesis of many diseases, particularly colon cancer. Considered as a tertiary bile acid, ursodeoxycholic acid (UDCA, **20**) is metabolized by the hepatocytes through the 11β-hydroxysteroid dehydrogenase 1-mediated reduction of the reabsorbed primary bile acid intermediate 7-oxolithocholic acid [155] (Fig. 6).

UDCA (**20**) is predominantly used in the clinic for the treatment of primary biliary cirrhosis thanks to its growth suppressing activity accompanied with cytoprotective properties. Additionally, this bile acid is the most commonly drug investigated for primary sclerosing cholangitis, a chronic cholestatic liver disease associated with both hepatobiliary and colorectal malignancies, potentially resulting in liver cirrhosis and its complications [156].

Recent evidence suggests that UDCA (**20**) exhibits chemopreventive properties [157]. For instance, UDCA (**20**) impacts the oncogenic signaling pathways driving the multistep process of colon cancer development, such as the EGFR/MAPK pathway. In colorectal adenocarcinoma cells, UDCA (**20**) treatment suppresses EGFR/MAPK signaling in a process enhanced by the presence of the TSG caveolin-1, a negative regulator of the Ras-p42/44 MAPK kinase cascade. UCDA (**20**) promotes calveolin-1-facilitated endocytosis of EGFR, as well as the recruitment of c-Cbl E3 ligase to the receptor, which subsequently leads to its ubiquitination and degradation. Moreover, UDCA (**20**) causes the reduction of EGF-induced ERK1/2 activity, suggesting direct negative regulatory effects on the EGFR-MAPK pathway [158].

In human colon cancer cells, treatment with UCDA (**20**) induces a modest increase in HDAC activity, accompanied with reduced levels of acetylated histones. The UCDA (**20**)-mediated promotion of histone deacetylation clearly establishes that UDCA (**20**) is not an HDACi. Nevertheless, this bile acid stimulates differentiation and senescence of colon cancer cells, which is essential for the colon cancer prevention. Interestingly, HDAC6 expression is up-regulated in human colon cancer cells treated with UDCA (**20**) and appears to play an important role in UDCA (**20**)-induced senescence [159].

4.13. Ursolic acid

Ursolic acid (UA, **21**), a well-known naturally synthetized pentacyclic triterpenoid, is found in abundance in blueberries (*e.g. Vaccinium myrtillus*), cranberries (*e.g. Vaccinium oxycoccos*) and apple peels (Fig. 6). Through multiple effects on the cellular proteome and signalome, UA (**21**) has a positive impact on numerous cancer types, mainly by decreasing cell density, but also diminishing cell viability and increasing cell death (reviewed in [160]).

Molecularly speaking, treatment with UA (**21**) induces leukemia cell death partially through increasing acetylation of histone H3 and inhibition of HDAC activity [161]. In addition, 12-*O*-tetradecanoylphorbol-13-acetate (TPA)-induced transformation in epidermal cells is rescued by UA (**21**)-mediated Nrf2 expression induction. To do so, UA (**21**) alters the methylation status of the Nrf2 promoter *via* the negative regulation of the expression of epigenetic modification enzymes, including HDAC6, potentially contributing to prevention of skin cancer [162].

4.14. Vanillate-based compounds

Natural vanillin, a phenolic aldehyde, is the major constituent of several essential plant oils, principally *Vanilla planifolia*, *Vanilla tahitensis,* and *Vanilla pompona*. It is used as the principal flavor and aromatic component worldwide, and is commonly found in processed foods, beverages, and pharmaceutical products as well as in perfume industry [163]. Vanillin presents anti-tumor potential *via* anti-oxidant, anti-invasive, anti-metastatic, and anti-angiogenic activities in differing models. Vanillin has numerous molecular targets implying several biological processes implicated in cancer such as cell proliferation and cell cycle; DNA damage, oxidative and stress response; apoptosis; invasion and metastasis [163].

The highest amount of vanillic acid, an oxidized form of vanillin, is extracted from the root of *Angelica sinensis*. Notably, two derivatives of vanillic acid, 13a (**22**) and 7b (**23**), which are di- and tri-vanillate-based polyphenols, respectively (Fig. 7), have been reported as selective HDAC6i *in vitro* and *in cellulo*. Furthermore, compounds 13a (**22**) and 7b (**23**) decrease the proliferation of prostate cancer cell lines in 2D and 3D cell culture conditions [164]. In the same models, these vanillate-based compounds modulate microtubular architecture through increased α-tubulin acetylation, diminishing the migration potential of tumor cells. Moreover, 13a (**22**) and 7b (**23**) reduce cell cycle progression with an accumulation of cells in S and G2/M phases associated with a reduction of cyclin A2, cyclin D1 and CDK1 protein levels. Subsequently, treatments with 13a (**22**) and 7b (**23**) induce prostate cancer cell death with a differential toxicity compared to non-cancerous prostate cells. Finally, in AR-positive prostate cancer cells, these molecules strongly decrease AR protein levels and target gene expression *via* HDAC6 inhibition-mediated HSP90α hyperacetylation leading to the reduction of AR-HSP90α interaction [164].

Remarkably, synthetic analogues of 13a (**22**) and 7b (**23**) without vanillic acid moieties lack inhibitory selectivity against HDAC6 activity. Nonetheless, they still have been described as pan-HDACi [6]. Such findings bring critical information for structure-activity relationship analyses, especially considering that they also have structural similarities with curcumin (see part 4.2.3.), enabling some insightful comparison between their respective actions against cancer cells.

5. Critical consideration and future perspectives

Disruptions of the functional acetylation pattern contribute to tumorigenesis and can be triggered by various mechanisms such as aberrant activation or overexpression of HDAC isoforms, which thus represent interesting therapeutic targets.

Improved knowledge about the functions of isoenzyme HDAC6 in physiological and pathological conditions has been associated with a growing interest for this deacetylase. Research has thus intensified in order to discover more potent and selective HDAC6i, two even reaching clinical trials for the treatment of MM. However, further pharmacodynamic studies will enable the evaluation of their potential side effects and to determine whether they present a better benefit *versus* risk balance than other non-selective approved HDACi. Such aspects have also to be considered for any further HDAC6i undergoing pre-clinical evaluations.

In the future, the recently reported crystal structure of the two deacetylase domains of HDAC6 will most likely allow the successful structure-based design of selective HDAC6i with novel chemical properties and enable the determination of essential structure-activity relationships. Nonetheless, an increased structural knowledge of HDAC6 is required and could allow determining how the different HDAC6 domains are inter-connected and whether they play a role in substrate recognition and specificity, as well as their impact on the modulation of the catalytic activity of HDAC6.

Bioactive principles obtained from natural sources, or compounds derived from scaffolds provided by Mother Nature have gained considerable popularity, particularly as anti-cancer drugs. However, only few HDAC6i have been discovered so far. It would thus be of considerable interest to assess the selectivity of well-known or newly discovered natural compounds towards HDAC6 activity and/or protein expression in order to determine whether they could display their anti-cancer properties through regulation of HDAC6-dependent mechanisms, yet to be elucidated.

As already mentioned, the mechanisms underlying compound-mediated negative regulation of HDAC6 expression are still globally unknown and deserve to be investigated. In this perspective, elucidating the upstream pathways regulating HDAC6 expression and catalytic activity could lead to new efficient therapeutic strategies against specific diseases in which HDAC6 plays a critical role by targeting various axes implicating this deacetylase. Similarly, an improved knowledge of the (post)-transcriptional and (post)-translational mechanisms regulating HDAC6 gene expression would allow the development of new strategies for the modulation of HDAC6 functions rather than its catalytic inhibition. In addition, getting a full picture of the acetylome regulated by HDAC6 would also enable a better understanding of its roles and therapeutic potential.

Selective HDAC6 inhibition is not associated with severe cytotoxicity [66,165]. Therefore, the advent of novel specific HDAC6i may justify the rational of using HDAC6 as a preferred synergistic target in combinatorial therapies with natural and synthetic compounds for the improvement of clinical cancer treatment. For instance, simultaneous inhibition of proteasome and HDAC6 activities, resulting in the accumulation of misfolded proteins, has been proposed as a new strategy in cancer therapy to synergistically induce cell death in MM [166], and many additional solid cancers. Notably, cells could be differentially dependent on the HDAC6-regulated aggresome pathway to eliminate proteins, which would result in various responses of the cells to this combination treatment. Nevertheless, there is no doubt that such approaches based on combination with HDAC6i represent promising anti-cancer therapeutic strategies that will be further developed in a near future and be beneficial to cancer patients.

Although HDAC6 is the major deacetylase regulating α-tubulin and cortactin acetylation levels, such substrates are also targeted by SIRT2 and SIRT1, respectively. Accordingly, another potential attractive opportunity is the combination of selective inhibitors or the development of dual inhibitors against HDAC6 and SIRT1 or

SIRT2 deacetylases. Such approaches could overcome the limitations of a single target antitumor drug and potentiate the effect of selective HDAC6 inhibition by improved targeting of shared substrates and associated signaling pathways.

Furthermore, selectively inhibiting HDAC6 may be considered as a potential immuno-modulatory option since it has been described to participate in the regulation of immune-related pathways in melanoma [167]. Of note, the immuno-modulatory effects observed with selective HDAC6i are similar to those obtained with pan-HDACi. Nonetheless, further investigations are granted to identify the precise role(s) of HDAC6 in the immune response, especially in the context of cancer subtypes presenting altered HDAC expression profiles. Particularly, it would be of interest to establish how HDAC6 may regulate the expression of co-stimulatory/inhibitory molecules or its potential influence on the different immune cell populations. In that sense, future investigations will reveal the level of neo-antigen formation after treatment of selected cancer types by HDACi in general and particularly by HDAC6i. Indeed, perturbation of the cancer cell acetylome could trigger *de novo* protein expression potentially contributing to a better recognition of the (dying) cancer by dendritic cells or macrophages. Although the induction of immunogenic cell death (ICD) was described for pan-HDACi, the impact of HDAC6i remains largely to be investigated. Ultimately, this approach should determine the contribution of HDAC6i to trigger ICD and the full benefit of using HDAC6i alone or in combination for anti-cancer immunotherapies.

Finally, HDAC6 has been recognized as a promising target in several additional disorders, such as inflammation, autoimmune diseases, and neurodegeneration [168]. For instance, HDAC6i in Alzheimer's disease have been demonstrated to induce the degradation of tubule-associated unit (Tau) *via* the alteration of HDAC6-HSP90α interaction, and the subsequent restoration of β-amyloid-induced damages [12]. Consequently, the advancement in HDAC6 targeting may also ameliorate ongoing therapies for those pathologies. Accordingly, the identification of the causes and mechanisms linked to HDAC6 deregulations in those diseases, as well as HDAC6-specific roles in their development and maintenance, may lead to major progresses in the research towards personalized therapies.

Conflict of interest

The authors declare no conflicts of interest.

Acknowledgements

ML is recipient of a Télévie Luxembourg fellowship. This work was supported by Télévie Luxembourg, the «Recherche Cancer et Sang» foundation and «Recherches Scientifiques Luxembourg» association. The authors thank «Een Häerz fir Kriibskrank Kanner» association and the Action Lions "Vaincre le Cancer" for generous support. MD is supported by the NRF by the MEST of Korea for Tumor Microenvironment GCRC2012-0001184 grant.

Appendix A. Supplementary data

Supplementary data associated with this article can be found, in the online version, at https://doi.org/10.1016/j.phrs.2017.11.004.

References

[1] D. Hanahanand, R.A. Weinberg, Hallmarks of cancer: the next generation, Cell 144 (2011) 646–674.
[2] M. Schnekenburger, C. Florean, M. Dicato, M. Diederich, Epigenetic alterations as a universal feature of cancer hallmarks and a promising target for personalized treatments, Curr. Top. Med. Chem. 16 (2016) 745–776.
[3] S. Spange, T. Wagner, T. Heinzel, O.H. Kramer, Acetylation of non-histone proteins modulates cellular signalling at multiple levels, Int. J. Biochem. Cell Biol. 41 (2009) 185–198.
[4] C. Choudhary, C. Kumar, F. Gnad, M.L. Nielsen, M. Rehman, T.C. Walther, J.V. Olsen, M. Mann, Lysine acetylation targets protein complexes and co-regulates major cellular functions, Science 325 (2009) 834–840.
[5] Y.C. Wang, S.E. Peterson, J.F. Loring, Protein post-translational modifications and regulation of pluripotency in human stem cells, Cell Res. 24 (2014) 143–160.
[6] C. Seidel, M. Schnekenburger, M. Dicato, M. Diederich, Antiproliferative and proapoptotic activities of 4-hydroxybenzoic acid-based inhibitors of histone deacetylases, Cancer Lett. 343 (2014) 134–146.
[7] T.M. Hardyand, T.O. Tollefsbol, Epigenetic diet: impact on the epigenome and cancer, Epigenomics 3 (2011) 503–518.
[8] F. Vahid, H. Zand, E. Nosrat-Mirshekarlou, R. Najafi, A. Hekmatdoost, The role dietary of bioactive compounds on the regulation of histone acetylases and deacetylases: a review, Gene 562 (2015) 8–15.
[9] C. Seidel, M. Schnekenburger, M. Dicato, M. Diederich, Histone deacetylase modulators provided by Mother Nature, Genes Nutr. 7 (2012) 357–367.
[10] M. Schnekenburger, M. Dicato, M. Diederich, Plant-derived epigenetic modulators for cancer treatment and prevention, Biotechnol. Adv. 32 (2014) 1123–1132.
[11] M. Schnekenburger, M. Dicato, M. Diederich, Epigenetic modulators from The Big Blue: a treasure to fight against cancer, Cancer Lett. 351 (2014) 182–197.
[12] C. Seidel, M. Schnekenburger, M. Dicato, M. Diederich, Histone deacetylase 6 in health and disease, Epigenomics 7 (2015) 103–118.
[13] S.N. Batchu, A.S. Brijmohan, A. Advani, The therapeutic hope for HDAC6 inhibitors in malignancy and chronic disease, Clin. Sci. 130 (2016) 987–1003.
[14] L. Zhang, S. Liu, N. Liu, Y. Zhang, M. Liu, D. Li, E. Seto, T.P. Yao, W. Shui, J. Zhou, Proteomic identification and functional characterization of MYH9 Hsc70, and DNAJA1 as novel substrates of HDAC6 deacetylase activity, Protein Cell 6 (2015) 42–54.
[15] C. Hubbert, A. Guardiola, R. Shao, Y. Kawaguchi, A. Ito, A. Nixon, M. Yoshida, X.F. Wang, T.P. Yao, HDAC6 is a microtubule-associated deacetylase, Nature 417 (2002) 455–458.
[16] N.R. Bertos, B. Gilquin, G.K. Chan, T.J. Yen, S. Khochbin, X.J. Yang, Role of the tetradecapeptide repeat domain of human histone deacetylase 6 in cytoplasmic retention, J. Biol. Chem. 279 (2004) 48246–48254.
[17] D. Seigneurin-Berny, A. Verdel, S. Curtet, C. Lemercier, J. Garin, S. Rousseaux, S. Khochbin, Identification of components of the murine histone deacetylase 6 complex: link between acetylation and ubiquitination signaling pathways, Mol. Cell. Biol. 21 (2001) 8035–8044.
[18] M.T. Pai, S.R. Tzeng, J.J. Kovacs, M.A. Keaton, S.S. Li, T.P. Yao, P. Zhou, Solution structure of the Ubp-M BUZ domain, a highly specific protein module that recognizes the C-terminal tail of free ubiquitin, J. Mol. Biol. 370 (2007) 290–302.
[19] Y. Li, D. Shin, S.H. Kwon, Histone deacetylase 6 plays a role as a distinct regulator of diverse cellular processes, FEBS J. 280 (2013) 775–793.
[20] S.J. Haggarty, K.M. Koeller, J.C. Wong, C.M. Grozinger, S.L. Schreiber, Domain-selective small-molecule inhibitor of histone deacetylase 6 (HDAC6)-mediated tubulin deacetylation, Proc. Natl. Acad. Sci. U. S. A. 100 (2003) 4389–4394.
[21] H. Zou, Y. Wu, M. Navre, B.C. Sang, Characterization of the two catalytic domains in histone deacetylase 6, Biochem. Biophys. Res. Commun. 341 (2006) 45–50.
[22] Y. Haiand, D.W. Christianson, Histone deacetylase 6 structure and molecular basis of catalysis and inhibition, Nat. Chem. Biol. 12 (2016) 741–747.
[23] Y. Liu, L. Li, J. Min, Structural biology: HDAC6 finally crystal clear, Nat. Chem. Biol. 12 (2016) 660–661.
[24] Y. Miyake, J.J. Keusch, L. Wang, M. Saito, D. Hess, X. Wang, B.J. Melancon, P. Helquist, H. Gut, P. Matthias, Structural insights into HDAC6 tubulin deacetylation and its selective inhibition, Nat. Chem. Biol. 12 (2016) 748–754.
[25] O.H. Kramer, S. Mahboobi, A. Sellmer, Drugging the HDAC6-HSP90 interplay in malignant cells, Trends Pharmacol. Sci. 35 (2014) 501–509.
[26] S. Di Fulvio, B.A. Azakir, C. Therrien, M. Sinnreich, Dysferlin interacts with histone deacetylase 6 and increases alpha-tubulin acetylation, PLoS One 6 (2011) e28563.
[27] Y. Wu, S.W. Song, J. Sun, J.M. Bruner, G.N. Fuller, W. Zhang, Ilp45 inhibits cell migration through inhibition of HDAC6, J. Biol. Chem. 285 (2010) 3554–3560.
[28] N. Tokesi, A. Lehotzky, I. Horvath, B. Szabo, J. Olah, P. Lau, J. Ovadi, TPPP/p25 promotes tubulin acetylation by inhibiting histone deacetylase 6, J. Biol. Chem. 285 (2010) 17896–17906.
[29] J. Zhou, C.C. Vos, A. Gjyrezi, M. Yoshida, F.R. Khuri, F. Tamanoi, P. Giannakakou, The protein farnesyltransferase regulates HDAC6 activity in a microtubule-dependent manner, J. Biol. Chem. 284 (2009) 9648–9655.
[30] G.I. Aldana-Masangkayand, K.M. Sakamoto, The role of HDAC6 in cancer, J. Biomed. Biotechnol. 2011 (2011) 875824.
[31] K. Zheng, Y. Jiang, Z. He, K. Kitazato, Y. Wang, Cellular defence or viral assist: the dilemma of HDAC6, J. Gen. Virol. 98 (2017) 322–337.

[32] J.H. Kalin, K.V. Butler, T. Akimova, W.W. Hancock, A.P. Kozikowski, Second-generation histone deacetylase 6 inhibitors enhance the immunosuppressive effects of Foxp3+ T-regulatory cells, J. Med. Chem. 55 (2012) 639–651.
[33] Y.S. Lee, K.H. Lim, X. Guo, Y. Kawaguchi, Y. Gao, T. Barrientos, P. Ordentlich, X.F. Wang, C.M. Counter, T.P. Yao, The cytoplasmic deacetylase HDAC6 is required for efficient oncogenic tumorigenesis, Cancer Res. 68 (2008) 7561–7569.
[34] P.H. Yang, L. Zhang, Y.J. Zhang, J. Zhang, W.F. Xu, HDAC6: physiological function and its selective inhibitors for cancer treatment, Drug Discov. Ther. 7 (2013) 233–242.
[35] A.J. de Ruijter, A.H. van Gennip, H.N. Caron, S. Kemp, A.B. van Kuilenburg, Histone deacetylases (HDACs): characterization of the classical HDAC family, Biochem. J. 370 (2003) 737–749.
[36] A. Bruningand, J. Juckstock, Misfolded proteins: from little villains to little helpers in the fight against cancer, Front. Oncol. 5 (2015) 47.
[37] S.A. Wickstrom, K.C. Masoumi, S. Khochbin, R. Fassler, R. Massoumi, CYLD negatively regulates cell-cycle progression by inactivating HDAC6 and increasing the levels of acetylated tubulin, EMBO J. 29 (2010) 131–144.
[38] M.J. Chuang, S.T. Wu, S.H. Tang, X.M. Lai, H.C. Lai, K.H. Hsu, K.H. Sun, G.H. Sun, S.Y. Chang, D.S. Yu, P.W. Hsiao, S.M. Huang, T.L. Cha, The HDAC inhibitor LBH589 induces ERK-dependent prometaphase arrest in prostate cancer via HDAC6 inactivation and down-regulation, PLoS One 8 (2013) e73401.
[39] L. Nogues, C. Reglero, V. Rivas, A. Salcedo, V. Lafarga, M. Neves, P. Ramos, M. Mendiola, A. Berjon, K. Stamatakis, X.Z. Zhou, K.P. Lu, D. Hardisson, F. Mayor Jr., P. Penela, G protein-coupled receptor kinase 2 (GRK2) promotes Breast tumorigenesis through a HDAC6-Pin1 axis, EBioMedicine 13 (2016) 132–145.
[40] S. Li, X. Liu, X. Chen, L. Zhang, X. Wang, Histone deacetylase 6 promotes growth of glioblastoma through inhibition of SMAD2 signaling, Tumour Biol. 36 (2015) 9661–9665.
[41] G. Ding, H.D. Liu, Q. Huang, H.X. Liang, Z.H. Ding, Z.J. Liao, G. Huang, HDAC6 promotes hepatocellular carcinoma progression by inhibiting P53 transcriptional activity, FEBS Lett. 587 (2013) 880–886.
[42] D. Kaluza, J. Kroll, S. Gesierich, T.P. Yao, R.A. Boon, E. Hergenreider, M. Tjwa, L. Rossig, E. Seto, H.G. Augustin, A.M. Zeiher, S. Dimmeler, C. Urbich, Class IIb HDAC6 regulates endothelial cell migration and angiogenesis by deacetylation of cortactin, EMBO J. 30 (2011) 4142–4156.
[43] H.W. Ryu, H.R. Won, D.H. Lee, S.H. Kwon, HDAC6 regulates sensitivity to cell death in response to stress and post-stress recovery, Cell Stress Chaperones 22 (2017) 253–261.
[44] D.Z. Qian, S.K. Kachhap, S.J. Collis, H.M. Verheul, M.A. Carducci, P. Atadja, R. Pili, Class II histone deacetylases are associated with VHL-independent regulation of hypoxia-inducible factor 1 alpha, Cancer Res. 66 (2006) 8814–8821.
[45] J.H. Park, S.H. Kim, M.C. Choi, J. Lee, D.Y. Oh, S.A. Im, Y.J. Bang, T.Y. Kim, Class II histone deacetylases play pivotal roles in heat shock protein 90-mediated proteasomal degradation of vascular endothelial growth factor receptors, Biochem. Biophys. Res. Commun. 368 (2008) 318–322.
[46] D. Li, S. Xie, Y. Ren, L. Huo, J. Gao, D. Cui, M. Liu, J. Zhou, Microtubule-associated deacetylase HDAC6 promotes angiogenesis by regulating cell migration in an EB1-dependent manner, Protein Cell 2 (2011) 150–160.
[47] Z. Lv, X. Weng, C. Du, C. Zhang, H. Xiao, X. Cai, S. Ye, J. Cheng, C. Ding, H. Xie, L. Zhou, J. Wu, S. Zheng, Downregulation of HDAC6 promotes angiogenesis in hepatocellular carcinoma cells and predicts poor prognosis in liver transplantation patients, Mol. Carcinog. 55 (2016) 1024–1033.
[48] J.H. Kalinand, J.A. Bergman, Development and therapeutic implications of selective histone deacetylase 6 inhibitors, J. Med. Chem. 56 (2013) 6297–6313.
[49] S. Gu, Y. Liu, B. Zhu, K. Ding, T.P. Yao, F. Chen, L. Zhan, P. Xu, M. Ehrlich, T. Liang, X. Lin, X.H. Feng, Loss of alpha-tubulin acetylation is associated with TGF-beta-induced epithelial-Mesenchymal transition, J. Biol. Chem. 291 (2016) 5396–5405.
[50] B. Deskin, J. Lasky, Y. Zhuang, B. Shan, Requirement of HDAC6 for activation of Notch1 by TGF-beta1, Sci. Rep. 6 (2016) 31086.
[51] B. Shan, T.P. Yao, H.T. Nguyen, Y. Zhuo, D.R. Levy, R.C. Klingsberg, H. Tao, M.L. Palmer, K.N. Holder, J.A. Lasky, Requirement of HDAC6 for transforming growth factor-beta1-induced epithelial-mesenchymal transition, J. Biol. Chem. 283 (2008) 21065–21073.
[52] C. Boyault, K. Sadoul, M. Pabion, S. Khochbin, HDAC6, at the crossroads between cytoskeleton and cell signaling by acetylation and ubiquitination, Oncogene 26 (2007) 5468–5476.
[53] S. Saji, M. Kawakami, S. Hayashi, N. Yoshida, M. Hirose, S. Horiguchi, A. Itoh, N. Funata, S.L. Schreiber, M. Yoshida, M. Toi, Significance of HDAC6 regulation via estrogen signaling for cell motility and prognosis in estrogen receptor-positive breast cancer, Oncogene 24 (2005) 4531–4539.
[54] H. Hou, L. Zhao, W. Chen, J. Li, Q. Zuo, G. Zhang, X. Zhang, X. Li, Expression and significance of cortactin and HDAC6 in human prostatic foamy gland carcinoma, Int. J. Exp. Pathol. 96 (2015) 248–254.
[55] N. Ding, L. Ping, L. Feng, X. Zheng, Y. Song, J. Zhu, Histone deacetylase 6 activity is critical for the metastasis of Burkitt's lymphoma cells, Cancer Cell Int. 14 (2014) 139.
[56] L. Zhang, N. Liu, S. Xie, X. He, J. Zhou, M. Liu, D. Li, HDAC6 regulates neuroblastoma cell migration and may play a role in the invasion process, Cancer. Biol. Ther. 15 (2014) 1561–1570.
[57] K. Kanno, S. Kanno, H. Nitta, N. Uesugi, T. Sugai, T. Masuda, G. Wakabayashi, C. Maesawa, Overexpression of histone deacetylase 6 contributes to accelerated migration and invasion activity of hepatocellular carcinoma cells, Oncol. Rep. 28 (2012) 867–873.
[58] Q. Zuo, W. Wu, X. Li, L. Zhao, W. Chen, HDAC6 and SIRT2 promote bladder cancer cell migration and invasion by targeting cortactin, Oncol. Rep. 27 (2012) 819–824.
[59] D. Li, X. Sun, L. Zhang, B. Yan, S. Xie, R. Liu, M. Liu, J. Zhou, Histone deacetylase 6 and cytoplasmic linker protein 170 function together to regulate the motility of pancreatic cancer cells, Protein Cell 5 (2014) 214–223.
[60] J. Liu, J. Gu, Z. Feng, Y. Yang, N. Zhu, W. Lu, F. Qi, Both HDAC5 and HDAC6 are required for the proliferation and metastasis of melanoma cells, J. Transl. Med. 14 (7) (2016) C6.
[61] K. Azuma, T. Urano, K. Horie-Inoue, S. Hayashi, R. Sakai, Y. Ouchi, S. Inoue, Association of estrogen receptor alpha and histone deacetylase 6 causes rapid deacetylation of tubulin in breast cancer cells, Cancer Res. 69 (2009) 2935–2940.
[62] J.A. Limand, Y.S. Juhnn, Isoproterenol increases histone deacetylase 6 expression and cell migration by inhibiting ERK signaling via PKA and Epac pathways in human lung cancer cells, Exp. Mol. Med. 48 (2016) e204.
[63] Z. Wang, F. Tang, P. Hu, Y. Wang, J. Gong, S. Sun, C. Xie, HDAC6 promotes cell proliferation and confers resistance to gefitinib in lung adenocarcinoma, Oncol. Rep. 36 (2016) 589–597.
[64] Z. Wang, P. Hu, F. Tang, C. Xie, HDAC6-mediated EGFR stabilization and activation restrict cell response to sorafenib in non-small cell lung cancer cells, Med. Oncol. 33 (2016) 50.
[65] Z.Y. Li, C. Zhang, Y. Zhang, L. Chen, B.D. Chen, Q.Z. Li, X.J. Zhang, W.P. Li, A novel HDAC6 inhibitor tubastatin A: controls HDAC6-p97/VCP-mediated ubiquitination-autophagy turnover and reverses temozolomide-induced ER stress-tolerance in GBM cells, Cancer Lett. 391 (2017) 89–99.
[66] J.H. Lee, A. Mahendran, Y. Yao, L. Ngo, G. Venta-Perez, M.L. Choy, N. Kim, W.S. Ham, R. Breslow, P.A. Marks, Development of a histone deacetylase 6 inhibitor and its biological effects, Proc. Natl. Acad. Sci. U. S. A. 110 (2013) 15704–15709.
[67] M. Namdar, G. Perez, L. Ngo, P.A. Marks, Selective inhibition of histone deacetylase 6 (HDAC6) induces DNA damage and sensitizes transformed cells to anticancer agents, Proc. Natl. Acad. Sci. U. S. A. 107 (2010) 20003–20008.
[68] A.I. Marcus, J. Zhou, A. O'Brate, E. Hamel, J. Wong, M. Nivens, A. El-Naggar, T.P. Yao, F.R. Khuri, P. Giannakakou, The synergistic combination of the farnesyl transferase inhibitor lonafarnib and paclitaxel enhances tubulin acetylation and requires a functional tubulin deacetylase, Cancer Res. 65 (2005) 3883–3893.
[69] L. Wang, S. Xiang, K.A. Williams, H. Dong, W. Bai, S.V. Nicosia, S. Khochbin, G. Bepler, X. Zhang, Depletion of HDAC6 enhances cisplatin-induced DNA damage and apoptosis in non-small cell lung cancer cells, PLoS One 7 (2012) e44265.
[70] G.I. Aldana-Masangkay, A. Rodriguez-Gonzalez, T. Lin, A.K. Ikeda, Y.T. Hsieh, Y.M. Kim, B. Lomenick, K. Okemoto, E.M. Landaw, D. Wang, R. Mazitschek, J.E. Bradner, K.M. Sakamoto, Tubacin suppresses proliferation and induces apoptosis of acute lymphoblastic leukemia cells, Leukemia Lymphoma 52 (2011) 1544–1555.
[71] C. Florean, M. Schnekenburger, C. Grandjenette, M. Dicato, M. Diederich, Epigenomics of leukemia: from mechanisms to therapeutic applications, Epigenomics 3 (2011) 581–609.
[72] H. Losson, M. Schnekenburger, M. Dicato, M. Diederich, Natural compound histone deacetylase inhibitors (HDACi): synergy with inflammatory signaling pathway modulators and clinical applications in cancer, Molecules 21 (2016).
[73] M. Schnekenburger, F. Morceau, E. Henry, R. Blasius, M. Dicato, C. Trentesaux, M. Diederich, Transcriptional and post-transcriptional regulation of glutathione S-transferase P1 expression during butyric acid-induced differentiation of K562 cells, Leuk. Res. 30 (2006) 561–568.
[74] T. Kumagai, N. Wakimoto, D. Yin, S. Gery, N. Kawamata, N. Takai, N. Komatsu, A. Chumakov, Y. Imai, H.P. Koeffler, Histone deacetylase inhibitor, suberoylanilide hydroxamic acid (Vorinostat, SAHA) profoundly inhibits the growth of human pancreatic cancer cells, Int. J. Cancer 121 (2007) 656–665.
[75] N. Bhatnagar, X. Li, Y. Chen, X. Zhou, S.H. Garrett, B. Guo, 3,3'-diindolylmethane enhances the efficacy of butyrate in colon cancer prevention through down-regulation of survivin, Cancer Prev. Res. 2 (2009) 581–589.
[76] S. Xargay-Torrent, M. Lopez-Guerra, I. Saborit-Villarroya, L. Rosich, E. Campo, G. Roue, D. Colomer, Vorinostat-induced apoptosis in mantle cell lymphoma is mediated by acetylation of proapoptotic BH3-only gene promoters, Clin. Cancer Res. 17 (2011) 3956–3968.
[77] C. Seidel, C. Florean, M. Schnekenburger, M. Dicato, M. Diederich, Chromatin-modifying agents in anti-cancer therapy, Biochimie 94 (2012) 2264–2279.
[78] S. Balasubramanian, E. Verner, J.J. Buggy, Isoform-specific histone deacetylase inhibitors: the next step? Cancer Lett. 280 (2009) 211–221.
[79] K.V. Butler, J. Kalin, C. Brochier, G. Vistoli, B. Langley, A.P. Kozikowski, Rational design and simple chemistry yield a superior, neuroprotective HDAC6 inhibitor, tubastatin A, J. Am. Chem. Soc. 132 (2010) 10842–10846.
[80] D.T. Vogl, N. Raje, S. Jagannath, P. Richardson, P. Hari, R. Orlowski, J.G. Supko, D. Tamang, M. Yang, S.S. Jones, C. Wheeler, R.J. Markelewicz, S. Lonial, Ricolinostat, the first selective histone deacetylase 6 inhibitor, in

combination with bortezomib and dexamethasone for relapsed or refractory multiple myeloma, Clin. Cancer Res. 23 (2017) 3307–3315.
[81] Z. Huang, Q. Huang, L. Ji, Y. Wang, X. Qi, L. Liu, Z. Liu, L. Lu, Epigenetic regulation of active Chinese herbal components for cancer prevention and treatment: a follow-up review, Pharmacol. Res. 114 (2016) 1–12.
[82] B. Rashidi, M. Malekzadeh, M. Goodarzi, A. Masoudifar, H. Mirzaei, Green tea and its anti-angiogenesis effects, Biomed. Pharmacother.=Biomed. Pharmacother. 89 (2017) 949–956.
[83] Y. Shirakami, M. Shimizu, H. Moriwaki, Cancer chemoprevention with green tea catechins: from bench to bed, Curr. Drug Targets 13 (2012) 1842–1857.
[84] R.Y. Gan, H.B. Li, Z.Q. Sui, H. Corke, Absorption, metabolism, anti-Cancer effect and molecular targets of epigallocatechin gallate (EGCG): an updated review, Crit. Rev. Food Sci Nutr. (2016) 1–18.
[85] C.S. Yangand, H. Wang, Cancer preventive activities of tea catechins, Molecules 21 (2016).
[86] S. Shankar, G. Suthakar, R.K. Srivastava, Epigallocatechin-3-gallate inhibits cell cycle and induces apoptosis in pancreatic cancer, Front. Biosci. 12 (2007) 5039–5051.
[87] Y. Shirakami, M. Shimizu, S. Adachi, H. Sakai, T. Nakagawa, Y. Yasuda, H. Tsurumi, Y. Hara, H. Moriwaki, (−)-Epigallocatechin gallate suppresses the growth of human hepatocellular carcinoma cells by inhibiting activation of the vascular endothelial growth factor-vascular endothelial growth factor receptor axis, Cancer Sci. 100 (2009) 1957–1962.
[88] Q. Zhang, X. Tang, Q. Lu, Z. Zhang, J. Rao, A.D. Le, Green tea extract and (−)-epigallocatechin-3-gallate inhibit hypoxia- and serum-induced HIF-1alpha protein accumulation and VEGF expression in human cervical carcinoma and hepatoma cells, Mol. Cancer Ther. 5 (2006) 1227–1238.
[89] V.S. Thakur, K. Gupta, S. Gupta, Green tea polyphenols causes cell cycle arrest and apoptosis in prostate cancer cells by suppressing class I histone deacetylases, Carcinogenesis 33 (2012) 377–384.
[90] H. Fujiki, E. Sueoka, T. Watanabe, M. Suganuma, Synergistic enhancement of anticancer effects on numerous human cancer cell lines treated with the combination of EGCG, other green tea catechins, and anticancer compounds, J. Cancer Res. Clin. Oncol. 141 (2015) 1511–1522.
[91] Y. Oya, A. Mondal, A. Rawangkan, S. Umsumarng, K. Iida, T. Watanabe, M. Kanno, K. Suzuki, Z. Li, H. Kagechika, K. Shudo, H. Fujiki, M. Suganuma, Down-regulation of histone deacetylase 4, −5 and −6 as a mechanism of synergistic enhancement of apoptosis in human lung cancer cells treated with the combination of a synthetic retinoid, Am80 and green tea catechin, J. Nutr. Biochem. 42 (2017) 7–16.
[92] E.M. Ju, S.E. Lee, H.J. Hwang, J.H. Kim Antioxidant and, anticancer activity of extract from Betula platyphylla var. japonica, Life Sci. 74 (2004) 1013–1026.
[93] S. Rastogi, M.M. Pandey, A. Kumar Singh Rawat, Medicinal plants of the genus Betula–traditional uses and a phytochemical-pharmacological review, J. Ethnopharmacol. 159 (2015) 62–83.
[94] M. Lee, J.H. Park, D.S. Min, H. Yoo, J.H. Park, Y.C. Kim, S.H. Sung, Antifibrotic activity of diarylheptanoids from Betula platyphylla toward HSC-T6 cells, Biosci. Biotechnol. Biochem. 76 (2012) 1616–1620.
[95] H.W. Ryu, D.H. Lee, D.H. Shin, S.H. Kim, S.H. Kwon, Aceroside VIII is a new natural selective HDAC6 inhibitor that synergistically enhances the anticancer activity of HDAC inhibitor in HT29 cells, Planta Med. 81 (2015) 222–227.
[96] A. Lederand, P. Leder, Butyric acid: a potent inducer of erythroid differentiation in cultured erythroleukemic cells, Cell 5 (1975) 319–322.
[97] L. Sealyand, R. Chalkley, The effect of sodium butyrate on histone modification, Cell 14 (1978) 115–121.
[98] M.C. Myzakand, R.H. Dashwood, Histone deacetylases as targets for dietary cancer preventive agents: lessons learned with butyrate, diallyl disulfide, and sulforaphane, Curr. Drug Targets 7 (2006) 443–452.
[99] D. Scharlau, A. Borowicki, N. Habermann, T. Hofmann, S. Klenow, C. Miene, U. Munjal, K. Stein, M. Glei, Mechanisms of primary cancer prevention by butyrate and other products formed during gut flora-mediated fermentation of dietary fibre, Mutat. Res. 682 (2009) 39–53.
[100] V. Edmond, C. Brambilla, E. Brambilla, S. Gazzeri, B. Eymin, SRSF2 is required for sodium butyrate-mediated p21(WAF1) induction and premature senescence in human lung carcinoma cell lines, ABBV Cell Cycle 10 (2011) 1968–1977.
[101] R.R. Alberto, S.L. Yudibeth, F.M. Jonathan, F.M. Raul, C.L. Cristina, V.M. Ismael, R.M. Cecilia, B. Martiniano, M. Martinez-Archundia, T.J. Guadalupe, B.M. Elvia, C.B. Jose, Design, synthesis and biological evaluation of a phenyl butyric acid derivative, N-(4-chlorophenyl)-4-phenylbutanamide: a HDAC6 inhibitor with anti-proliferative activity on cervix cancer and leukemia cells, Anticancer Agents Med. Chem. 17 (2017) 1441–1454.
[102] S. Tejada, A. Manayi, M. Daglia, S.F. Nabavi, A. Sureda, Z. Hajheydari, O. Gortzi, H. Pazoki-Toroudi, S.M. Nabavi, Wound Healing Effects of Curcumin: A Short Review, Curr. Pharm. Biotechnol. 17 (2016) 1002–1007.
[103] A. Shehzad, F. Wahid, Y.S. Lee, Curcumin in cancer chemoprevention: molecular targets, pharmacokinetics, bioavailability, and clinical trials, Arch. Pharm. 343 (2010) 489–499.
[104] A. Duvoix, R. Blasius, S. Delhalle, M. Schnekenburger, F. Morceau, E. Henry, M. Dicato, M. Diederich, Chemopreventive and therapeutic effects of curcumin, Cancer Lett. 223 (2005) 181–190.
[105] M.H. Teiten, M. Dicato, M. Diederich, Curcumin as a regulator of epigenetic events, Mol. Nutr. Food Res. 57 (2013) 1619–1629.
[106] H.L. Liu, Y. Chen, G.H. Cui, J.F. Zhou, Curcumin, a potent anti-tumor reagent, is a novel histone deacetylase inhibitor regulating B-NHL cell line Raji proliferation, Acta Pharmacol. Sin. 26 (2005) 603–609.
[107] S.H. Wang, P.Y. Lin, Y.C. Chiu, J.S. Huang, Y.T. Kuo, J.C. Wu, C.C. Chen, Curcumin-Mediated HDAC inhibition suppresses the DNA damage response and contributes to increased DNA damage sensitivity, PLoS One 10 (2015) e0134110.
[108] Y. Guo, L. Shu, C. Zhang, Z.Y. Su, A.N. Kong, Curcumin inhibits anchorage-independent growth of HT29 human colon cancer cells by targeting epigenetic restoration of the tumor suppressor gene DLEC1, Biochem. Pharmacol. 94 (2015) 69–78.
[109] H.C. Huang, D. Tang, K. Xu, Z.F. Jiang, Curcumin attenuates amyloid-beta-induced tau hyperphosphorylation in human neuroblastoma SH-SY5Y cells involving PTEN/Akt/GSK-3beta signaling pathway, J. Recept. Signal Transduct. Res. 34 (2014) 26–37.
[110] R. Sarkar, A. Mukherjee, S. Mukherjee, R. Biswas, J. Biswas, M. Roy, Curcumin augments the efficacy of antitumor drugs used in leukemia by modulation of heat shock proteins via HDAC6, J. Environ. Pathol. Toxicol. Oncol. 33 (2014) 247–263.
[111] C. Vlachojannis, B.F. Zimmermann, S. Chrubasik-Hausmann, Efficacy and safety of pomegranate medicinal products for cancer, Evid.-based Complem. Altern. Med.: eCAM 2015 (2015) 258598.
[112] C. Ceci, L. Tentori, M.G. Atzori, P.M. Lacal, E. Bonanno, M. Scimeca, R. Cicconi, M. Mattei, M.G. de Martino, G. Vespasiani, R. Miano, G. Graziani, Ellagic acid inhibits bladder cancer invasiveness and In vivo tumor growth, Nutrients 8 (2016).
[113] H.M. Zhang, L. Zhao, H. Li, H. Xu, W.W. Chen, L. Tao, Research progress on the anticarcinogenic actions and mechanisms of ellagic acid, Cancer Biol. Med. 11 (2014) 92–100.
[114] J. Kowshik, H. Giri, T.K. Kishore, R. Kesavan, R.N. Vankudavath, G.B. Reddy, M. Dixit, S. Nagini, Ellagic acid inhibits VEGF/VEGFR2, PI3K/Akt and MAPK signaling cascades in the hamster cheek pouch carcinogenesis model, Anticancer Agents Med. Chem. 14 (2014) 1249–1260.
[115] S. Banerjee, Y. Li, Z. Wang, F.H. Sarkar, Multi-targeted therapy of cancer by genistein, Cancer Lett. 269 (2008) 226–242.
[116] I.M. Rietjens, A.M. Sotoca, J. Vervoort, J. Louisse, Mechanisms underlying the dualistic mode of action of major soy isoflavones in relation to cell proliferation and cancer risks, Mol. Nutr. Food Res. 57 (2013) 100–113.
[117] M. Russo, G.L. Russo, M. Daglia, P.D. Kasi, S. Ravi, S.F. Nabavi, S.M. Nabavi, Understanding genistein in cancer: the good and the bad effects: a review, Food Chem. 196 (2016) 589–600.
[118] A.A. Ganaiand, H. Farooqi, Bioactivity of genistein: a review of in vitro and in vivo studies, Biomed. Pharmacother.=Biomed. Pharmacother. 76 (2015) 30–38.
[119] S. Basak, D. Pookot, E.J. Noonan, R. Dahiya, Genistein down-regulates androgen receptor by modulating HDAC6-Hsp90 chaperone function, Mol. Cancer Ther. 7 (2008) 3195–3202.
[120] J.M. Lu, Q. Yao, C. Chen, Ginseng compounds: an update on their molecular mechanisms and medical applications, Curr. Vasc. Pharmacol. 7 (2009) 293–302.
[121] Z.H. Liu, J. Li, J. Xia, R. Jiang, G.W. Zuo, X.P. Li, Y. Chen, W. Xiong, D.L. Chen, Ginsenoside 20(s)-Rh2 as potent natural histone deacetylase inhibitors suppressing the growth of human leukemia cells, Chem. Biol. Interact. 242 (2015) 227–234.
[122] Q. Shi, X. Shi, G. Zuo, W. Xiong, H. Li, P. Guo, F. Wang, Y. Chen, J. Li, D.L. Chen, Anticancer effect of 20(S)-ginsenoside Rh2 on HepG2 liver carcinoma cells: activating GSK-3beta and degrading beta-catenin, Oncol. Rep. 36 (2016) 2059–2070.
[123] S. Han, A.J. Jeong, H. Yang, K. Bin Kang, H. Lee, E.H. Yi, B.H. Kim, C.H. Cho, J.W. Chung, S.H. Sung, S.K. Ye, Ginsenoside 20(S)-Rh2 exerts anti-cancer activity through targeting IL-6-induced JAK2/STAT3 pathway in human colorectal cancer cells, J. Ethnopharmacol. 194 (2016) 83–90.
[124] Q. Shi, J. Li, Z. Feng, L. Zhao, L. Luo, Z. You, D. Li, J. Xia, G. Zuo, D. Chen, Effect of ginsenoside Rh2 on the migratory ability of HepG2 liver carcinoma cells: recruiting histone deacetylase and inhibiting activator protein 1 transcription factors, Mol. Med. Rep. 10 (2014) 1779–1785.
[125] Z.R. Zhang, W.N. Leung, H.Y. Cheung, C.W. Chan, Osthole a review on its bioactivities, pharmacological properties, and potential as alternative medicine, Evid.-based Complem. Altern. Med.: eCAM 2015 (2015) 919616.
[126] H.Y. Yang, Y.F. Hsu, P.T. Chiu, S.J. Ho, C.H. Wang, C.C. Chi, Y.H. Huang, C.F. Lee, Y.S. Li, G. Ou, M.J. Hsu, Anti-cancer activity of an osthole derivative, NBM-T-BMX-O: targeting vascular endothelial growth factor receptor signaling and angiogenesis, PLoS One 8 (2013) e81592.
[127] W.J. Huang, C.C. Chen, S.W. Chao, S.S. Lee, F.L. Hsu, Y.L. Lu, M.F. Hung, C.I. Chang, Synthesis of N-hydroxycinnamides capped with a naturally occurring moiety as inhibitors of histone deacetylase, ChemMedChem 5 (2010) 598–607.
[128] W.J. Huang, C.C. Chen, S.W. Chao, C.C. Yu, C.Y. Yang, J.H. Guh, Y.C. Lin, C.I. Kuo, P. Yang, C.I. Chang, Synthesis and evaluation of aliphatic-chain hydroxamates capped with osthole derivatives as histone deacetylase inhibitors, Eur. J. Med. Chem. 46 (2011) 4042–4049.
[129] J.T. Pai, C.Y. Hsu, K.T. Hua, S.Y. Yu, C.Y. Huang, C.N. Chen, C.H. Liao, M.S. Weng, NBM-T-BBX-OS01, semisynthesized from osthole, induced G1 growth arrest through HDAC6 inhibition in lung cancer cells, Molecules 20 (2015) 8000–8019.

[130] Y. Li, X. Li, B.W. Son, Antibacterial and radical scavenging epoxycyclohexenones and aromatic polyols from a marine isolate of the fungus Aspergillus, Nat. Prod. Sci. 11 (2005) 136–138.
[131] T. Ali, M. Inagaki, H.B. Chai, T. Wieboldt, C. Rapplye, L.H. Rakotondraibe, Halogenated compounds from directed fermentation of penicillium concentricum, an endophytic fungus of the liverwort trichocolea tomentella, J. Nat. Prod. 80 (2017) 1397–1403.
[132] V. Zwick, P.M. Allard, L. Ory, C.A. Simoes-Pires, L. Marcourt, K. Gindro, J.L. Wolfender, M. Cuendet, UHPLC-MS-based HDAC assay applied to bio-guided microfractionation of fungal extracts, Phytochem. Anal.: PCA 28 (2017) 93–100.
[133] Y. Zhang, P. Talalay, C.G. Cho, G.H. Posner, A major inducer of anticarcinogenic protective enzymes from broccoli: isolation and elucidation of structure, Proc. Natl. Acad. Sci. U. S. A. 89 (1992) 2399–2403.
[134] M. Russo, C. Spagnuolo, G.L. Russo, K. Skalicka-Wozniak, M. Daglia, E. Sobarzo-Sanchez, S.F. Nabavi, S.M. Nabavi, Nrf2 targeting by sulforaphane: a potential therapy for cancer treatment, Crit. Rev. Food Sci. Nutr. (2016) 1–15.
[135] J.D. Clarke, R.H. Dashwood, E. Ho, Multi-targeted prevention of cancer by sulforaphane, Cancer Lett. 269 (2008) 291–304.
[136] A. Leone, G. Diorio, W. Sexton, M. Schell, M. Alexandrow, J.W. Fahey, N.B. Kumar, Sulforaphane for the chemoprevention of bladder cancer: molecular mechanism targeted approach, Oncotarget 8 (2017) 35412–35424.
[137] S.A. Ganai, R. Rashid, E. Abdullah, M. Altaf, Plant derived inhibitor Sulforaphane in combinatorial therapy against therapeutically challenging Pancreatic Cancer, Anticancer Agents Med. Chem. 17 (2016) 365–373.
[138] S.A. Ganai, Histone deacetylase inhibitor sulforaphane: the phytochemical with vibrant activity against prostate cancer, Biomed. Pharmacother.=Biomed. Pharmacother. 81 (2016) 250–257.
[139] K.M. Holmstrom, R.V. Kostov, A.T. Dinkova-Kostova, The multifaceted role of Nrf2 in mitochondrial function, Curr. Opin. Toxicol. 1 (2016) 80–91.
[140] S.E. Dickinson, J.J. Rusche, S.L. Bec, D.J. Horn, J. Janda, S.H. Rim, C.L. Smith, G.T. Bowden, The effect of sulforaphane on histone deacetylase activity in keratinocytes: differences between in vitro and in vivo analyses, Mol. Carcinog. 54 (2015) 1513–1520.
[141] M.C. Myzak, P.A. Karplus, F.L. Chung, R.H. Dashwood, A novel mechanism of chemoprotection by sulforaphane: inhibition of histone deacetylase, Cancer Res. 64 (2004) 5767–5774.
[142] P. Rajendran, A.I. Kidane, T.W. Yu, W.M. Dashwood, W.H. Bisson, C.V. Lohr, E. Ho, D.E. Williams, R.H. Dashwood, HDAC turnover: ctIP acetylation and dysregulated DNA damage signaling in colon cancer cells treated with sulforaphane and related dietary isothiocyanates, Epigenetics 8 (2013) 612–623.
[143] L. Gaoand, J. Alumkal, Epigenetic regulation of androgen receptor signaling in prostate cancer, Epigenetics 5 (2010) 100–104.
[144] A. Gibbs, J. Schwartzman, V. Deng, J. Alumkal, Sulforaphane destabilizes the androgen receptor in prostate cancer cells by inactivating histone deacetylase 6, Proc. Natl. Acad. Sci. U. S. A. 106 (2009) 16663–16668.
[145] J.D. Clarke, A. Hsu, Z. Yu, R.H. Dashwood, E. Ho, Differential effects of sulforaphane on histone deacetylases, cell cycle arrest and apoptosis in normal prostate cells versus hyperplastic and cancerous prostate cells, Mol. Nutr. Food Res. 55 (2011) 999–1009.
[146] N. Tsuji, M. Kobayashi, K. Nagashima, Y. Wakisaka, K. Koizumi, A new antifungal antibiotic: trichostatin, J. Antibiotics 29 (1976) 1–6.
[147] M. Yoshida, M. Kijima, M. Akita, T. Beppu, Potent and specific inhibition of mammalian histone deacetylase both in vivo and in vitro by trichostatin A, J. Biol. Chem. 265 (1990) 17174–17179.
[148] M. Dickinson, R.W. Johnstone, H.M. Prince, Histone deacetylase inhibitors: potential targets responsible for their anti-cancer effect, Invest. New Drugs 28 (Suppl 1) (2010) S3–S20.
[149] T.R. Medler, J.M. Craig, A.A. Fiorillo, Y.B. Feeney, J.C. Harrell, C.V. Clevenger, HDAC6 deacetylates HMGN2 to regulate stat5a activity and Breast cancer growth, Mol. Cancer Res.: MCR 14 (2016) 994–1008.
[150] Z. Meng, L.F. Jia, Y.H. Gan, PTEN activation through K163 acetylation by inhibiting HDAC6 contributes to tumour inhibition, Oncogene 35 (2016) 2333–2344.
[151] L. Li, R. Fang, B. Liu, H. Shi, Y. Wang, W. Zhang, X. Zhang, L. Ye, Deacetylation of tumor-suppressor MST1 in Hippo pathway induces its degradation through HBXIP-elevated HDAC6 in promotion of breast cancer growth, Oncogene 35 (2016) 4048–4057.
[152] I. Changand, C.Y. Wang, Inhibition of HDAC6 protein enhances bortezomib-induced apoptosis in head and neck squamous cell carcinoma (HNSCC) by reducing autophagy, J. Biol. Chem. 291 (2016) 18199–18209.
[153] A. Matsuyama, T. Shimazu, Y. Sumida, A. Saito, Y. Yoshimatsu, D. Seigneurin-Berny, H. Osada, Y. Komatsu, N. Nishino, S. Khochbin, S. Horinouchi, M. Yoshida, In vivo destabilization of dynamic microtubules by HDAC6-mediated deacetylation, EMBO J. 21 (2002) 6820–6831.
[154] Q.Y. Zhu, Z. Wang, C. Ji, L. Cheng, Y.L. Yang, J. Ren, Y.H. Jin, Q.J. Wang, X.J. Gu, Z.G. Bi, G. Hu, Y. Yang, C6-ceramide synergistically potentiates the anti-tumor effects of histone deacetylase inhibitors via AKT dephosphorylation and alpha-tubulin hyperacetylation both in vitro and in vivo, Cell. Death. Dis. 2 (2011) e117.
[155] A. Odermatt, T. Da Cunha, C.A. Penno, C. Chandsawangbhuwana, C. Reichert, A. Wolf, M. Dong, M.E. Baker, Hepatic reduction of the secondary bile acid 7-oxolithocholic acid is mediated by 11beta-hydroxysteroid dehydrogenase 1, Biochem. J. 436 (2011) 621–629.
[156] F. Saffioti, K.S. Gurusamy, N. Hawkins, C.D. Toon, E. Tsochatzis, B.R. Davidson, D. Thorburn, Pharmacological interventions for primary sclerosing cholangitis: an attempted network meta-analysis, Cochrane Database syst. Rev. 3 (2017) CD011343.
[157] S.M. Centuoriand, J.D. Martinez, Differential regulation of EGFR-MAPK signaling by deoxycholic acid (DCA) and ursodeoxycholic acid (UDCA) in colon cancer, Dig. Dis. Sci. 59 (2014) 2367–2380.
[158] R. Feldmanand, J.D. Martinez, Growth suppression by ursodeoxycholic acid involves caveolin-1 enhanced degradation of EGFR, Biochim. Biophys. Acta 1793 (2009) 1387–1394.
[159] S. Akare, S. Jean-Louis, W. Chen, D.J. Wood, A.A. Powell, J.D. Martinez, Ursodeoxycholic acid modulates histone acetylation and induces differentiation and senescence, Int. J. Cancer 119 (2006) 2958–2969.
[160] K.M. Weh, J. Clarke, L.A. Kresty, Cranberries and cancer: an update of preclinical studies evaluating the cancer inhibitory potential of cranberry and cranberry derived constituents, Antioxidants 5 (2016).
[161] I.H. Chen, M.C. Lu, Y.C. Du, M.H. Yen, C.C. Wu, Y.H. Chen, C.S. Hung, S.L. Chen, F.R. Chang, Y.C. Wu, Cytotoxic triterpenoids from the stems of Microtropis japonica, J. Nat. Prod. 72 (2009) 1231–1236.
[162] H. Kim, C.N. Ramirez, Z.Y. Su, A.N. Kong, Epigenetic modifications of triterpenoid ursolic acid in activating Nrf2 and blocking cellular transformation of mouse epidermal cells, J. Nutr. Biochem. 33 (2016) 54–62.
[163] D.P. Bezerra, A.K. Soares, D.P. de Sousa, Overview of the role of vanillin on redox status and cancer development, Oxid. Med. Cell. Longevity 2016 (2016) 9734816.
[164] C. Seidel, M. Schnekenburger, A. Mazumder, M.H. Teiten, G. Kirsch, M. Dicato, M. Diederich, 4-Hydroxybenzoic acid derivatives as HDAC6-specific inhibitors modulating microtubular structure and HSP90alpha chaperone activity against prostate cancer, Biochem. Pharmacol. 99 (2016) 31–52.
[165] I.N. Gaisina, W. Tueckmantel, A. Ugolkov, S. Shen, J. Hoffen, O. Dubrovskyi, A. Mazar, R.A. Schoon, D. Billadeau, A.P. Kozikowski, Identification of HDAC6-Selective inhibitors of low cancer cell cytotoxicity, ChemMedChem 11 (2016) 81–92.
[166] T. Hideshima, J. Qi, R.M. Paranal, W. Tang, E. Greenberg, N. West, M.E. Colling, G. Estiu, R. Mazitschek, J.A. Perry, H. Ohguchi, F. Cottini, N. Mimura, G. Gorgun, Y.T. Tai, P.G. Richardson, R.D. Carrasco, O. Wiest, S.L. Schreiber, K.C. Anderson, J.E. Bradner, Discovery of selective small-molecule HDAC6 inhibitor for overcoming proteasome inhibitor resistance in multiple myeloma, Proc. Natl. Acad. Sci. U. S. A. 113 (2016) 13162–13167.
[167] M. Lienlaf, P. Perez-Villarroel, T. Knox, M. Pabon, E. Sahakian, J. Powers, K.V. Woan, C. Lee, F. Cheng, S. Deng, K.S. Smalley, M. Montecino, A. Kozikowski, J. Pinilla-Ibarz, A. Sarnaik, E. Seto, J. Weber, E.M. Sotomayor, A. Villagra, Essential role of HDAC6 in the regulation of PD-L1 in melanoma, Mol. Oncol. 10 (2016) 735–750.
[168] K.J. Falkenbergand, R.W. Johnstone, Histone deacetylases and their inhibitors in cancer: neurological diseases and immune disorders, Nat. Rev. Drug Discov. 13 (2014) 673–691.
[169] C.A. Bradbury, F.L. Khanim, R. Hayden, C.M. Bunce, D.A. White, M.T. Drayson, C. Craddock, B.M. Turner, Histone deacetylases in acute myeloid leukaemia show a distinctive pattern of expression that changes selectively in response to deacetylase inhibitors, Leukemia 19 (2005) 1751–1759.
[170] D.A. Moreno, C.A. Scrideli, M.A. Cortez, R. de Paula Queiroz, E.T. Valera, V. da Silva Silveira, J.A. Yunes, S.R. Brandalise, L.G. Tone, Differential expression of HDAC3, HDAC7 and HDAC9 is associated with prognosis and survival in childhood acute lymphoblastic leukaemia, Br. J. Haematol. 150 (2010) 665–673.
[171] Z. Zhang, H. Yamashita, T. Toyama, H. Sugiura, Y. Omoto, Y. Ando, K. Mita, M. Hamaguchi, S. Hayashi, H. Iwase, HDAC6 expression is correlated with better survival in breast cancer, Clin. Cancer Res. 10 (2004) 6962–6968.
[172] N. Yoshida, Y. Omoto, A. Inoue, H. Eguchi, Y. Kobayashi, M. Kurosumi, S. Saji, K. Suemasu, T. Okazaki, K. Nakachi, T. Fujita, S. Hayashi, Prediction of prognosis of estrogen receptor-positive breast cancer with combination of selected estrogen-regulated genes, Cancer Sci. 95 (2004) 496–502.
[173] S.A. Gradilone, B.N. Radtke, P.S. Bogert, B.Q. Huang, G.B. Gajdos, N.F. LaRusso, HDAC6 inhibition restores ciliary expression and decreases tumor growth, Cancer Res. 73 (2013) 2259–2270.
[174] M. Van Damme, E. Crompot, N. Meuleman, P. Mineur, D. Bron, L. Lagneaux, B. Stamatopoulos, HDAC isoenzyme expression is deregulated in chronic lymphocytic leukemia B-cells and has a complex prognostic significance, Epigenetics 7 (2012) 1403–1412.
[175] L. Marquard, L.M. Gjerdrum, I.J. Christensen, P.B. Jensen, M. Sehested, E. Ralfkiaer, Prognostic significance of the therapeutic targets histone deacetylase 1, 2, 6 and acetylated histone H4 in cutaneous T-cell lymphoma, Histopathology 53 (2008) 267–277.
[176] K.H. Jung, J.H. Noh, J.K. Kim, J.W. Eun, H.J. Bae, Y.G. Chang, M.G. Kim, W.S. Park, J.Y. Lee, S.Y. Lee, I.S. Chu, S.W. Nam, Histone deacetylase 6 functions as a tumor suppressor by activating c-Jun NH2-terminal kinase-mediated beclin 1-dependent autophagic cell death in liver cancer, Hepatology 56 (2012) 644–657.
[177] J. Bai, Y. Lei, G.L. An, L. He, Down-regulation of deacetylase HDAC6 inhibits the melanoma cell line A375. S2 growth through ROS-dependent mitochondrial pathway, PLoS One 10 (2015) e0121247.
[178] T. Sakuma, K. Uzawa, T. Onda, M. Shiiba, H. Yokoe, T. Shibahara, H. Tanzawa, Aberrant expression of histone deacetylase 6 in oral squamous cell carcinoma, Int. J. Oncol. 29 (2006) 117–124.

[179] O. Witt, H.E. Deubzer, T. Milde, I. Oehme, HDAC family: what are the cancer relevant targets? Cancer Lett. 277 (2009) 8–21.
[180] M. Bazzaro, Z. Lin, A. Santillan, M.K. Lee, M.C. Wang, K.C. Chan, R.E. Bristow, R. Mazitschek, J. Bradner, R.B. Roden, Ubiquitin proteasome system stress underlies synergistic killing of ovarian cancer cells by bortezomib and a novel HDAC6 inhibitor, Clin. Cancer Res. 14 (2008) 7340–7347.
[181] L. Rosik, G. Niegisch, U. Fischer, M. Jung, W.A. Schulz, M.J. Hoffmann, Limited efficacy of specific HDAC6 inhibition in urothelial cancer cells, Cancer. Biol. Ther. 15 (2014) 742–757.
[182] J. Yoo, S.J. Kim, D. Son, H. Seo, S.Y. Baek, C.Y. Maeng, C. Lee, I.S. Kim, Y.H. Jung, S.M. Lee, H.J. Park, Computer-aided identification of new histone deacetylase 6 selective inhibitor with anti-sepsis activity, Eur. J. Med. Chem. 116 (2016) 126–135.
[183] L. Wang, M. Kofler, G. Brosch, J. Melesina, W. Sippl, E.D. Martinez, J. Easmon, 2-Benzazolyl-4-Piperazin-1-Ylsulfonylbenzenecarbohydroxamic acids as novel selective histone deacetylase-6 inhibitors with antiproliferative activity, PLoS One 10 (2015) e0134556.
[184] H.Y. Lee, J.F. Lee, S. Kumar, Y.W. Wu, W.C. HuangFu, M.J. Lai, Y.H. Li, H.L. Huang, F.C. Kuo, C.J. Hsiao, C.C. Cheng, C.R. Yang, J.P. Liou, 3-Aroylindoles display antitumor activity in vitro and in vivo: effects of N1-substituents on biological activity, Eur. J. Med. Chem. 125 (2017) 1268–1278.
[185] C. Blackburn, C. Barrett, J. Chin, K. Garcia, K. Gigstad, A. Gould, J. Gutierrez, S. Harrison, K. Hoar, C. Lynch, R.S. Rowland, C. Tsu, J. Ringeling, H. Xu, Potent histone deacetylase inhibitors derived from 4-(aminomethyl)-N-hydroxybenzamide with high selectivity for the HDAC6 isoform, J. Med. Chem. 56 (2013) 7201–7211.
[186] H.W. Ryu, D.H. Shin, D.H. Lee, J. Choi, G. Han, K.Y. Lee, S.H. Kwon, HDAC6 deacetylates p53 at lysines 381/382 and differentially coordinates p53-induced apoptosis, Cancer Lett. 391 (2017) 162–171.
[187] E. Choi, C. Lee, J.E. Park, J.J. Seo, M. Cho, J.S. Kang, H.M. Kim, S.K. Park, K. Lee, G. Han, Structure and property based design, synthesis and biological evaluation of gamma-lactam based HDAC inhibitors, Bioorg. Med. Chem. Lett. 21 (2011) 1218–1221.
[188] K. Krukowski, J. Ma, O. Golonzhka, G.O. Laumet, T. Gutti, J.H. van Duzer, R. Mazitschek, M.B. Jarpe, C.J. Heijnen, A. Kavelaars, HDAC6 inhibition effectively reverses chemotherapy-induced peripheral neuropathy, Pain 158 (2017) 1126–1137.
[189] J. Jochems, S.L. Teegarden, Y. Chen, J. Boulden, C. Challis, G.A. Ben-Dor, S.F. Kim, O. Berton, Enhancement of stress resilience through histone deacetylase 6-mediated regulation of glucocorticoid receptor chaperone dynamics, Biol. Psychiatry 77 (2015) 345–355.
[190] J. Jochems, J. Boulden, B.G. Lee, J.A. Blendy, M. Jarpe, R. Mazitschek, J.H. Van Duzer, S. Jones, O. Berton, Antidepressant-like properties of novel HDAC6-selective inhibitors with improved brain bioavailability, Neuropsychopharmacology 39 (2014) 389–400.
[191] X. Lin, W. Chen, Z. Qiu, L. Guo, W. Zhu, W. Li, Z. Wang, W. Zhang, Z. Zhang, Y. Rong, M. Zhang, L. Yu, S. Zhong, R. Zhao, X. Wu, J.C. Wong, G. Tang, Design and synthesis of orally bioavailable aminopyrrolidinone histone deacetylase 6 inhibitors, J. Med. Chem. 58 (2015) 2809–2820.
[192] H.Y. Lee, A.C. Tsai, M.C. Chen, P.J. Shen, Y.C. Cheng, C.C. Kuo, S.L. Pan, Y.M. Liu, J.F. Liu, T.K. Yeh, J.C. Wang, C.Y. Chang, J.Y. Chang, J.P. Liou, Azaindolylsulfonamides, with a more selective inhibitory effect on histone deacetylase 6 activity, exhibit antitumor activity in colorectal cancer HCT116 cells, J. Med. Chem. 57 (2014) 4009–4022.
[193] A.P. Kozikowski, Y. Chen, A.M. Gaysin, D.N. Savoy, D.D. Billadeau, K.H. Kim, Chemistry, biology, and QSAR studies of substituted biaryl hydroxamates and mercaptoacetamides as HDAC inhibitors-nanomolar-potency inhibitors of pancreatic cancer cell growth, ChemMedChem 3 (2008) 487–501.
[194] S. Shen, V. Benoy, J.A. Bergman, J.H. Kalin, M. Frojuello, G. Vistoli, W. Haeck, L. Van Den Bosch, A.P. Kozikowski, Bicyclic-capped histone deacetylase 6 inhibitors with improved activity in a model of axonal charcot-marie-Tooth disease, ACS Chem. Neurosci. 7 (2016) 240–258.
[195] S. Schafer, L. Saunders, E. Eliseeva, A. Velena, M. Jung, A. Schwienhorst, A. Strasser, A. Dickmanns, R. Ficner, S. Schlimme, W. Sippl, E. Verdin, M. Jung, Phenylalanine-containing hydroxamic acids as selective inhibitors of class IIb histone deacetylases (HDACs), Bioorg. Med. Chem. 16 (2008) 2011–2033.
[196] S.E. Choi, S.V. Weerasinghe, M.K. Pflum, The structural requirements of histone deacetylase inhibitors: suberoylanilide hydroxamic acid analogs modified at the C3 position display isoform selectivity, Bioorg. Med. Chem. Lett. 21 (2011) 6139–6142.
[197] M. Kaliszczak, S. Trousil, O. Aberg, M. Perumal, Q.D. Nguyen, E.O. Aboagye, A novel small molecule hydroxamate preferentially inhibits HDAC6 activity and tumour growth, Br. J. Cancer 108 (2013) 342–350.
[198] F.F. Wagner, D.E. Olson, J.P. Gale, T. Kaya, M. Weiwer, N. Aidoud, M. Thomas, E.L. Davoine, B.C. Lemercier, Y.L. Zhang, E.B. Holson, Potent and selective inhibition of histone deacetylase 6 (HDAC6) does not require a surface-binding motif, J. Med. Chem. 56 (2013) 1772–1776.
[199] A.P. Kozikowski, S. Tapadar, D.N. Luchini, K.H. Kim, D.D. Billadeau, Use of the nitrile oxide cycloaddition (NOC) reaction for molecular probe generation: a new class of enzyme selective histone deacetylase inhibitors (HDACIs) showing picomolar activity at HDAC6, J. Med. Chem. 51 (2008) 4370–4373.
[200] D.V. Smil, S. Manku, Y.A. Chantigny, S. Leit, A. Wahhab, T.P. Yan, M. Fournel, C. Maroun, Z. Li, A.M. Lemieux, A. Nicolescu, J. Rahil, S. Lefebvre, A. Panetta, J.M. Besterman, R. Deziel, Novel HDAC6 isoform selective chiral small molecule histone deacetylase inhibitors, Bioorg. Med. Chem. Lett. 19 (2009) 688–692.
[201] P. Huang, I. Almeciga-Pinto, M. Jarpe, J.H. van Duzer, R. Mazitschek, M. Yang, S.S. Jones, S.N. Quayle, Selective HDAC inhibition by ACY-241 enhances the activity of paclitaxel in solid tumor models, Oncotarget 8 (2017) 2694–2707.
[202] B.J. North, I. Almeciga-Pinto, D. Tamang, M. Yang, S.S. Jones, S.N. Quayle, Enhancement of pomalidomide anti-tumor response with ACY-241, a selective HDAC6 inhibitor, PLoS One 12 (2017) e0173507.
[203] P.K. Gupta, R.C. Reid, L. Liu, A.J. Lucke, S.A. Broomfield, M.R. Andrews, M.J. Sweet, D.P. Fairlie, Inhibitors selective for HDAC6 in enzymes and cells, Bioorg. Med. Chem. Lett. 20 (2010) 7067–7070.
[204] C.A. Olsenand, M.R. Ghadiri, Discovery of potent and selective histone deacetylase inhibitors via focused combinatorial libraries of cyclic alpha3beta-tetrapeptides, J. Med. Chem. 52 (2009) 7836–7846.
[205] J.D. Ellis, D.A. Neil, N.G. Inston, E. Jenkinson, M.T. Drayson, P. Hampson, S.J. Shuttleworth, A.R. Ready, M. Cobbold, Inhibition of histone deacetylase 6 reveals a potent immunosuppressant effect in models of transplantation, Transplantation 100 (2016) 1667–1674.
[206] Z. Yang, T. Wang, F. Wang, T. Niu, Z. Liu, X. Chen, C. Long, M. Tang, D. Cao, X. Wang, W. Xiang, Y. Yi, L. Ma, J. You, L. Chen, Discovery of selective histone deacetylase 6 inhibitors using the quinazoline as the cap for the treatment of cancer, J. Med. Chem. 59 (2016) 1455–1470.
[207] J.A. Bergman, K. Woan, P. Perez-Villarroel, A. Villagra, E.M. Sotomayor, A.P. Kozikowski, Selective histone deacetylase 6 inhibitors bearing substituted urea linkers inhibit melanoma cell growth, J. Med. Chem. 55 (2012) 9891–9899.
[208] S.M. Sternson, J.C. Wong, C.M. Grozinger, S.L. Schreiber, Synthesis of 7200 small molecules based on a substructural analysis of the histone deacetylase inhibitors trichostatin and trapoxin, Org. Lett. 3 (2001) 4239–4242.
[209] L. Auzzas, A. Larsson, R. Matera, A. Baraldi, B. Deschenes-Simard, G. Giannini, W. Cabri, G. Battistuzzi, G. Gallo, A. Ciacci, L. Vesci, C. Pisano, S. Hanessian, Non-natural macrocyclic inhibitors of histone deacetylases: design, synthesis, and activity, J. Med. Chem. 53 (2010) 8387–8399.
[210] J. Senger, J. Melesina, M. Marek, C. Romier, I. Oehme, O. Witt, W. Sippl, M. Jung, Synthesis and biological investigation of oxazole hydroxamates as highly selective histone deacetylase 6 (HDAC6) inhibitors, J. Med. Chem. 59 (2016) 1545–1555.
[211] Q.H. Sodji, J.R. Kornacki, J.F. McDonald, M. Mrksich, A.K. Oyelere, Design and structure activity relationship of tumor-homing histone deacetylase inhibitors conjugated to folic and pteroic acids, Eur. J. Med. Chem. 96 (2015) 340–359.
[212] S. Schafer, L. Saunders, S. Schlimme, V. Valkov, J.M. Wagner, F. Kratz, W. Sippl, E. Verdin, M. Jung, Pyridylalanine-containing hydroxamic acids as selective HDAC6 inhibitors, ChemMedChem 4 (2009) 283–290.
[213] Y.M. Liu, H.Y. Lee, M.J. Lai, S.L. Pan, H.L. Huang, F.C. Kuo, M.C. Chen, J.P. Liou, Pyrimidinedione-mediated selective histone deacetylase 6 inhibitors with antitumor activity in colorectal cancer HCT116 cells, Org. Biomol. Chem. 13 (2015) 10226–10235.
[214] S. Valente, D. Trisciuoglio, M. Tardugno, R. Benedetti, D. Labella, D. Secci, C. Mercurio, R. Boggio, S. Tomassi, S. Di Maro, E. Novellino, L. Altucci, D. Del Bufalo, A. Mai, S. Cosconati, tert-Butylcarbamate-containing histone deacetylase inhibitors: apoptosis induction, cytodifferentiation, and antiproliferative activities in cancer cells, ChemMedChem 8 (2013) 800–811.
[215] C.W. Yu, P.T. Chang, L.W. Hsin, J.W. Chern, Quinazolin-4-one derivatives as selective histone deacetylase-6 inhibitors for the treatment of Alzheimer's disease, J. Med. Chem. 56 (2013) 6775–6791.
[216] L. Santo, T. Hideshima, A.L. Kung, J.C. Tseng, D. Tamang, M. Yang, M. Jarpe, J.H. van Duzer, R. Mazitschek, W.C. Ogier, D. Cirstea, S. Rodig, H. Eda, T. Scullen, M. Canavese, J. Bradner, K.C. Anderson, S.S. Jones, N. Raje, Preclinical activity, pharmacodynamic, and pharmacokinetic properties of a selective HDAC6 inhibitor, ACY-1215, in combination with bortezomib in multiple myeloma, Blood 119 (2012) 2579–2589.
[217] U. Peng, Z. Wang, S. Pei, Y. Ou, P. Hu, W. Liu, J. Song, ACY-1215 accelerates vemurafenib induced cell death of BRAF-mutant melanoma cells via induction of ER stress and inhibition of ERK activation, Oncol. Rep. 37 (2017) 1270–1276.
[218] J.E. Amengual, P. Johannet, M. Lombardo, K. Zullo, D. Hoehn, G. Bhagat, L. Scotto, X. Jirau-Serrano, D. Radeski, J. Heinen, H. Jiang, S. Cremers, Y. Zhang, S. Jones, O.A. O'Connor, Dual targeting of protein degradation pathways with the selective HDAC6 inhibitor ACY-1215 and bortezomib is synergistic in lymphoma, Clin. Cancer Res. 21 (2015) 4663–4675.
[219] J.E. Amengual, S.A. Prabhu, M. Lombardo, K. Zullo, P.M. Johannet, Y. Gonzalez, L. Scotto, X.J. Serrano, Y. Wei, J. Duong, R. Nandakumar, S. Cremers, A. Verma, O. Elemento, O.A. O'Connor, Mechanisms of acquired drug resistance to the HDAC6 selective inhibitor ricolinostat reveals rational drug-drug combination with ibrutinib, Clin. Cancer Res. 23 (2016) 3084–3096.
[220] A.J. Yee, W.I. Bensinger, J.G. Supko, P.M. Voorhees, J.G. Berdeja, P.G. Richardson, E.N. Libby, E.E. Wallace, N.E. Birrer, J.N. Burke, D.L. Tamang, M. Yang, S.S. Jones, C.A. Wheeler, R.J. Markelewicz, N.S. Raje, Ricolinostat plus lenalidomide, and dexamethasone in relapsed or refractory multiple myeloma: a multicentre phase 1b trial, Lancet Oncol. 17 (2016) 1569–1578.
[221] D.S. Das, A. Das, A. Ray, Y. Song, M.K. Samur, N.C. Munshi, D. Chauhan, K.C. Anderson, Blockade of deubiquitylating enzyme USP1 inhibits DNA repair and triggers apoptosis in multiple myeloma cells, Clin. Cancer Res. (2017).
[222] G. Dasmahapatra, H. Patel, J. Friedberg, S.N. Quayle, S.S. Jones, S. Grant, In vitro and in vivo interactions between the HDAC6 inhibitor ricolinostat (ACY1215) and the irreversible proteasome inhibitor carfilzomib in non-Hodgkin lymphoma cells, Mol. Cancer Ther. 13 (2014) 2886–2897.

[223] Y. Mishima, L. Santo, H. Eda, D. Cirstea, N. Nemani, A.J. Yee, E. O'Donnell, M.K. Selig, S.N. Quayle, S. Arastu-Kapur, C. Kirk, L.H. Boise, S.S. Jones, N. Raje, Ricolinostat (ACY-1215) induced inhibition of aggresome formation accelerates carfilzomib-induced multiple myeloma cell death, Br. J. Haematol. 169 (2015) 423–434.
[224] K. Nepali, H.Y. Lee, M.J. Lai, R. Ojha, T.Y. Wu, G.X. Wu, M.C. Chen, J.P. Liou, Ring-opened tetrahydro-gamma-carbolines display cytotoxicity and selectivity with histone deacetylase isoforms, Eur. J. Med. Chem. 127 (2017) 115–127.
[225] G.K. Scott, C. Marx, C.E. Berger, L.R. Saunders, E. Verdin, S. Schafer, M. Jung, C.C. Benz, Destabilization of ERBB2 transcripts by targeting 3' untranslated region messenger RNA associated HuR and histone deacetylase-6, Mol. Cancer Res.: MCR 6 (2008) 1250–1258.
[226] B. Hackanson, L. Rimmele, M. Benkisser, M. Abdelkarim, M. Fliegauf, M. Jung, M. Lubbert, HDAC6 as a target for antileukemic drugs in acute myeloid leukemia, Leuk. Res. 36 (2012) 1055–1062.
[227] Y. Chen, M. Lopez-Sanchez, D.N. Savoy, D.D. Billadeau, G.S. Dow, A.P. Kozikowski, A series of potent and selective, triazolylphenyl-based histone deacetylases inhibitors with activity against pancreatic cancer cells and Plasmodium falciparum, J. Med. Chem. 51 (2008) 3437–3448.
[228] T. Hideshima, J.E. Bradner, J. Wong, D. Chauhan, P. Richardson, S.L. Schreiber, K.C. Anderson, Small-molecule inhibition of proteasome and aggresome function induces synergistic antitumor activity in multiple myeloma, Proc. Natl. Acad. Sci. U. S. A. 102 (2005) 8567–8572.
[229] S. Komatsu, S. Moriya, X.F. Che, T. Yokoyama, N. Kohno, K. Miyazawa, Combined treatment with SAHA, bortezomib, and clarithromycin for concomitant targeting of aggresome formation and intracellular proteolytic pathways enhances ER stress-mediated cell death in breast cancer cells, Biochem. Biophys. Res. Commun. 437 (2013) 41–47.
[230] R. De Vreese, T. Verhaeghe, T. Desmet, M. D'Hooghe, Potent and selective HDAC6 inhibitory activity of N-(4-hydroxycarbamoylbenzyl)-1,2,4,9-tetrahydro-3-thia-9-azafluorenes as novel sulfur analogues of Tubastatin A, Chem. Commun. 49 (2013) 3775–3777.
[231] L. Goracci, N. Deschamps, G.M. Randazzo, C. Petit, C. Dos Santos Passos, P.A. Carrupt, C. Simoes-Pires, A. Nurisso, A rational approach for the identification of non-Hydroxamate HDAC6-Selective inhibitors, Sci. Rep. 6 (2016) 29086.
[232] V. Patil, Q.H. Sodji, J.R. Kornacki, M. Mrksich, A.K. Oyelere, 3-Hydroxypyridin-2-thione as novel zinc binding group for selective histone deacetylase inhibition, J. Med. Chem. 56 (2013) 3492–3506.
[233] J.M. Ontoria, S. Altamura, A. Di Marco, F. Ferrigno, R. Laufer, E. Muraglia, M.C. Palumbi, M. Rowley, R. Scarpelli, C. Schultz-Fademrecht, S. Serafini, C. Steinkuhler, P. Jones, Identification of novel, selective, and stable inhibitors of class II histone deacetylases. Validation studies of the inhibition of the enzymatic activity of HDAC4 by small molecules as a novel approach for cancer therapy, J. Med. Chem. 52 (2009) 6782–6789.
[234] T. Suzuki, A. Kouketsu, Y. Itoh, S. Hisakawa, S. Maeda, M. Yoshida, H. Nakagawa, N. Miyata, Highly potent and selective histone deacetylase 6 inhibitors designed based on a small-molecular substrate, J. Med. Chem. 49 (2006) 4809–4812.
[235] A.P. Kozikowski, Y. Chen, A. Gaysin, B. Chen, M.A. D'Annibale, C.M. Suto, B.C. Langley, Functional differences in epigenetic modulators-superiority of mercaptoacetamide-based histone deacetylase inhibitors relative to hydroxamates in cortical neuron neuroprotection studies, J. Med. Chem. 50 (2007) 3054–3061.
[236] J.H. Kalin, H. Zhang, S. Gaudrel-Grosay, G. Vistoli, A.P. Kozikowski, Chiral mercaptoacetamides display enantioselective inhibition of histone deacetylase 6 and exhibit neuroprotection in cortical neuron models of oxidative stress, ChemMedChem 7 (2012) 425–439.
[237] E.S. Inks, B.J. Josey, S.R. Jesinkey, C.J. Chou, A novel class of small molecule inhibitors of HDAC6, ACS Chem. Biol. 7 (2012) 331–339.
[238] T. Itoh, A. Suzuki, N. Kouketsu, S. Suzuki, M. Maeda, H. Nakagawa, N. Miyata, Design, synthesis, structure–selectivity relationship, and effect on human cancer cells of a novel series of histone deacetylase 6-selective inhibitors, J. Med. Chem. 50 (2007) 5425–5438.

Contents lists available at ScienceDirect

Biochemical Pharmacology

journal homepage: http://ees.elsevier.com

Review

Epigenetic mechanisms underlying the therapeutic effects of HDAC inhibitors in chronic myeloid leukemia

Manon Lernoux [a], Michael Schnekenburger [a], Mario Dicato [a], Marc Diederich [b,]

[a] Laboratoire de Biologie Moléculaire et Cellulaire du Cancer, Hôpital Kirchberg 9, rue Edward Steichen, L-2540 Luxembourg, Luxembourg
[b] College of Pharmacy, Seoul National University, 1 Gwanak-ro, Gwanak-gu, Seoul 08826, South Korea

ARTICLE INFO

Keywords
Cancer
Histone acetylation
Targeted treatment
Personalized medicine

ABSTRACT

Chronic myeloid leukemia (CML) is a hematological disorder caused by the oncogenic BCR-ABL fusion protein in more than 90% of patients. Despite the striking improvements in the management of CML patients since the introduction of tyrosine kinase inhibitors (TKis), the appearance of TKi resistance and side effects lead to treatment failure, justifying the need of novel therapeutic approaches. Histone deacetylase inhibitors (HDACis), able to modulate gene expression patterns and important cellular signaling pathways through the regulation of the acetylation status of both histone and non-histone protein targets, have been reported to display promising anti-leukemic properties alone or in combination with TKis. This review summarizes pre-clinical and clinical studies that investigated the mechanisms underlying the anticancer potential of HDACis and discusses the rationale for a combination of HDACis with TKis as a therapeutic option in CML.

1. Introduction

Chronic myeloid leukemia (CML) is a well-characterized hematological malignancy displaying abnormal accumulation of clonal pluripotent hematopoietic stem cells in peripheral blood, bone marrow and spleen. In over 95% of CML patients, leukemogenesis is caused by the reciprocal translocation t(9;22)(q34;11) between the breakpoint cluster region (*BCR*) and Abelson murine leukemia viral oncogene homolog 1 (*ABL*) genes known as the Philadelphia chromosome. The resulting oncogenic BCR-ABL fusion protein, *via* its abnormal constitutive tyrosine kinase activity, stimulates a variety of oncogenic signaling pathways leading to the disruption of key cellular processes. The introduction of first-generation tyrosine kinase inhibitors (TKis) against CML strikingly improved the management of patients and the disease outcome. Nevertheless, clinical resistance of BCR-ABL-positive leukemia to currently used TKis justifies the need for alternative or additional treatments, including the design of second or third generation TKis and their combination with other drugs.

Since aberrant functional acetylation landscapes due to the activation or overexpression of histone deacetylases (HDACs) are associated with the development of numerous cancers including CML [1], this family of epigenetic enzymes became a promising target for developing new anticancer therapeutic strategies. Accordingly, numerous histone deacetylase inhibitors (HDACis) have been developed in the last years and HDAC isoenzyme inhibition leads to hyperacetylation of histone and non-histone proteins, resulting in anticancer effects through many multiple molecular mechanisms. Besides regimens using HDACis as a single agent, a growing number of ongoing clinical trials use HDACis in combination with classical chemotherapeutic agents in order to improve anticancer activities.

The importance of HDAC isoforms in CML initiation and progression has led researchers to study the therapeutic potential of HDACis alone or in combination with TKis. In this review, we will focus on the *in cellulo* and *in vivo* anti-leukemic properties of TKi-HDACi combinations in CML therapy.

2. Chronic myeloid leukemia

2.1. Classification of leukemia

The term *leukemia* describes abnormal proliferation and development of one or more cell lines in the bone marrow. The broad classification of leukemia is still based on the cell origin (myeloid *versus* lymphoid) and the rapidity of the clinical course (acute *versus* chronic), resulting in four main types of leukemia. In chronic leukemia, slow progressive accumulation (rather than proliferation) of cells in the bone marrow is observed and peripheral tissues predominate. Replacement of the normal hematopoietic tissue in the bone marrow by tumor cells can occur before the onset of overt leukemia.

Corresponding author at: Department of Pharmacy, College of Pharmacy, Seoul National University, 1 Gwanak-ro, Gwanak-gu, Seoul 08826, South Korea.
E-mail address: marcdiederich@snu.ac.kr (M. Diederich)

https://doi.org/10.1016/j.bcp.2019.113698
Received 1 October 2019; Accepted 5 November 2019
Available online xxx
0006-2952/© 2019.

UNCORRECTED PROOF

CML is a hematological disorder characterized by an abnormal accumulation of clonal pluripotent hematopoietic stem cells in peripheral blood, bone marrow, and the spleen. Patients with CML consequently display symptoms such as anemia, extreme blood granulocytosis with immaturity, basophilia, thrombocytosis, and splenomegaly. Without treatment, CML ultimately progresses from a chronic phase that is primarily asymptomatic and characterized by an increase in granulocytes, to an accelerated phase, with a rapid expansion of granulocytes and terminal blast crisis that resembles acute leukemia, leading to metastasis, organ failure, and death [2].

2.2. Epidemiology

Worldwide, 1.2 to 1.5 million people are currently living with CML. In the United States, CML has an incidence of 1 2 cases per 100,000 adults, and accounts for approximately 15% of newly diagnosed cases of leukemia in adults [3]. While the number of patients diagnosed each year has stayed relatively constant, survival rates have more than doubled owing to advances in treatment.

The associated risk factors that may affect CML initiation include age (increased risk after 65 years of age), gender (higher genetic predisposition in males), obesity, and heavy exposure to radiation [4].

2.3. Pathophysiology

In 95% of patients, CML pathogenesis is driven by a cytogenetic abnormality known as the Philadelphia chromosome resulting from the reciprocal translocation, t(9;22)(q34;11), between *BCR* and the *ABL* genes (Fig. 1). The resulting *BCR-ABL* fusion gene is translated into different BCR-ABL proteins that vary in size and pathogenicity depending on the location of the breakpoint in the *BCR* gene. Three breakpoint cluster regions in the *BCR* gene have been described to date: major (M BCR; p210), minor (m-BCR; p230), and micro (-BCR; p190) [5]. The majority of patients with CML display breakpoints in exon a2 of the *ABL* gene and either in exons 13 (b2) or 14 (b3) of the *BCR* gene, resulting in fusion genes that are transcribed either to a b2a2 or b3a2 mRNA. The final product of this genetic rearrangement is a 210-kDa cytoplasmic fusion protein that is essential and sufficient for the malignant transformation of CML. Less frequently, CML is induced by atypical BCR-ABL transcripts, involving for instance, *ABL* exon a3 instead of a2 or transcripts with an e1a2, e19a2, or e6a2 junction [6].

The oncogenic BCR-ABL protein, displaying abnormal constitutive tyrosine kinase activity, interacts with a variety of effector proteins involved in oncogenic pathways, which leads to the disruption of key cellular processes (Fig. 1). Among these effectors, signal transducer and activator of transcription (STAT)5 is a transcription factor aberrantly activated through BCR-ABL-mediated constitutive phosphorylation, which then up-regulates the expression of B-cell lymphoma (BCL)-extra large (BCL-xL) and myeloid cell leukemia (MCL)-1, two anti-apoptotic BCL-2 family members. Another effector is growth factor receptor-bound protein 2 (GRB2) that binds to a tyrosine-phosphorylated site of BCR-ABL *via* its SH2 domain. The BCR-ABL/GRB2 complex recruits Son of sevenless (SOS) that induces the activation of GRB2-associated binding protein 2 (GAB2). Consequently, the GRB2/GAB2/SOS complex causes constitutive activation of phosphoinositide 3-kinase (PI3K) and Ras signaling pathways. The latter stimulates the activation of mitogen-activated protein kinase (MAPK) proteins, which results in the up-regulation of c-MYC expression. This proto-oncogene then regulates the expression of survivin, a member of the inhibitor of apoptosis (IAP) family that inhibits caspase activation, thereby leading to a negative regulation of apoptosis [7]. Subsequently, the activation of these signaling pathways leads to uncontrolled cell proliferation, impaired transcriptional activity, decreased adherence of leukemia cells to the bone marrow stroma, malignant expansion of hematopoietic stem cell populations, and stimulated survival of tumor cells owing to a reduced apoptotic response to mutagenic stimuli [8,9].

2.4. Current treatments

The development of TKis, including imatinib, more than 10 years ago helped transform Philadelphia chromosome-positive CML from a life-threatening disease to, in most cases, a chronic condition when managed with appropriate treatments (Novartis, Basel, Switzerland).

2.4.1. First-generation inhibitor: Imatinib

Imatinib has a typical bisarylanilino core comprising a phenyl ring and a pyridine-pyrimidine moiety, containing a benzamide-piperazine group in the *meta*-position of the aniline-type nitrogen atom [10]. Imatinib is a type II TKi that only binds to the inactive state of BCR-ABL, which is characterized by a specific DFG (Asp-Phe-Gly)-out conformation of the unphosphorylated activation loop, in which the DFG motif is being folded away from the conformation required for ATP phosphate transfer. Imatinib interactions with BCR-ABL are mediated by (*i*) a unique hydrogen bond donor acceptor pair and hydrophobic tail moiety that form van der Waals interactions with the hydrophobic site of BCR-ABL, also referred to as the allosteric site , that is directly adjacent to the ATP binding pocket created by the DFG-out conformation and (*ii*) a head group that extends to the adenine region and forms a single hydrogen bond with the kinase hinge residue [11,12]. Notably, imatinib is most efficacious in the chronic phase of CML when most patients achieve durable complete cytogenetic responses.

Nevertheless, such therapeutic regimens are associated with TKi resistance and severe side effects, which represent barriers to effective treatments. Clinical resistance to imatinib can be elicited by various BCR-ABL-dependent and -independent mechanisms. The BCR-ABL-dependent mechanisms include selection of sub-clones containing point mutations within the BCR-ABL kinase domain that impede imatinib binding, and the over-expression or amplification of the *BCR-ABL* gene. The BCR-ABL-independent mechanisms involve factors influencing the intracellular concentration of imatinib (*e.g.* alterations in drug influx and efflux) and activation of BCR-ABL independent pathways [13,14]. Furthermore, the quiescent population of leukemic stem cells (LSCs) constitutes a possible reservoir for the development of therapeutic resistance or disease progression through escape mechanisms of altered self-renewal, differentiation, and survival [14,15].

Therefore, it is critical to explore novel therapeutic approaches to address these limitations [2]. The need for alternative or additional treatment for imatinib-resistant BCR-ABL-positive leukemia has guided the design of second generation TKis (see chapters 2.4.2. and 2.4.3. for more details) [16]. Additionally, treatment of cancerous cells with imatinib combined with another drug such as HDACis could sensitize cells to the cell killing effects of imatinib and allow the diminution of the concentration of each compound, thus reducing side effects.

2.4.2. Second-generation inhibitors: dasatinib, nilotinib, and bosutinib

Dasatinib is a smaller TKi than imatinib, establishing fewer interactions with its targets, and binding BCR-ABL with great versatility, in both active and inactive conformations. Nevertheless, the inactive DFG-out conformation has higher entropy than the DFG-in active conformation, which is thus preferentially inhibited by dasatinib. Conversely, nilotinib binds to the DFG-out inactive conformation of the BCR-ABL protein [10]. *In vitro*, dasatinib and nilotinib display 325-fold and 10- to 50-fold greater potency against native BCR-ABL,

UNCORRECTED PROOF

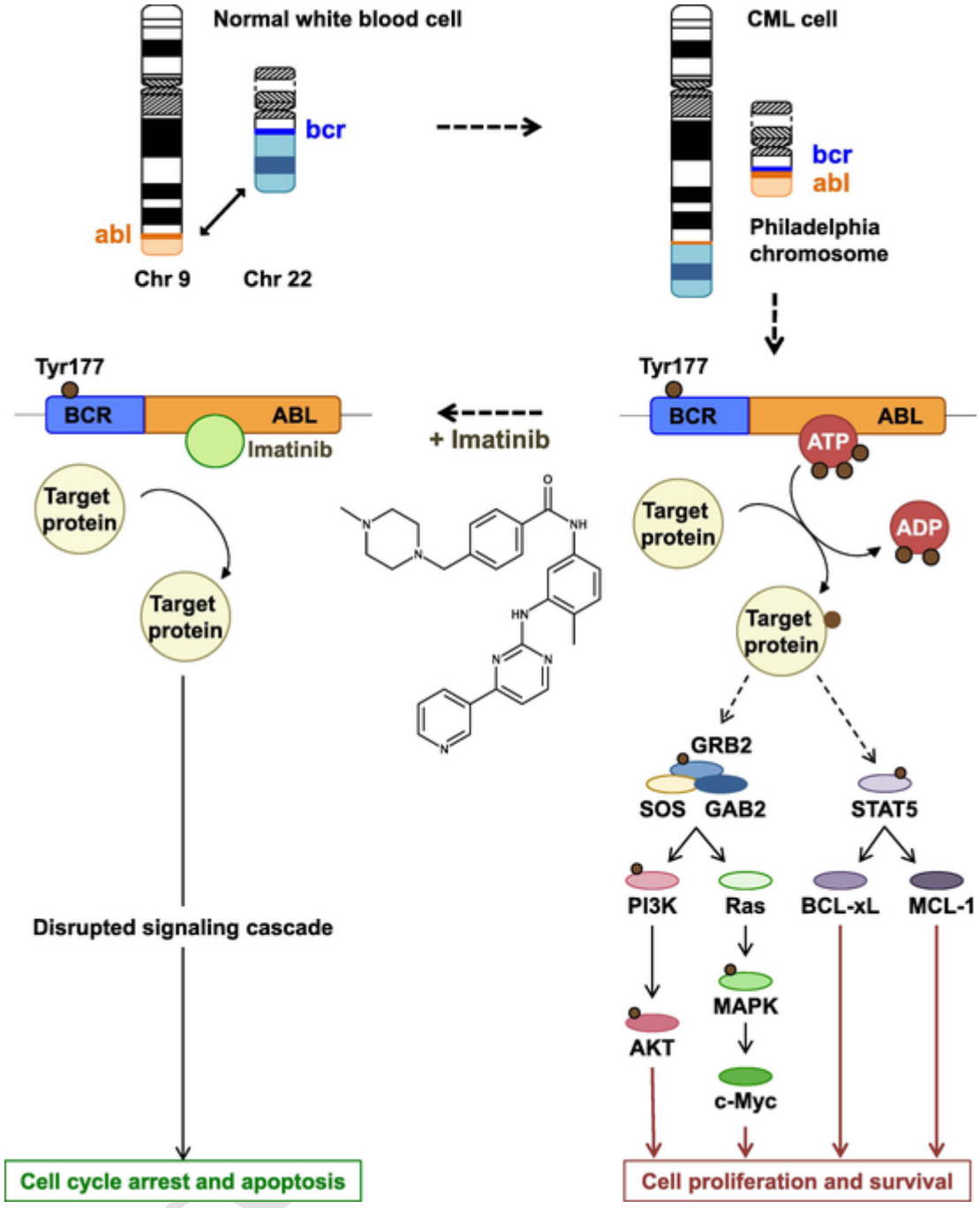

Fig. 1. CML pathogenesis and effect of treatment with tyrosine kinase inhibitor imatinib. Breakpoint cluster region-Abelson murine leukemia viral oncogene homolog 1 (BCR-ABL) dependent signaling pathways are activated upon phosphorylation of the tyrosine (Tyr) 177 of BCR-ABL. Growth factor receptor-bound protein 2 (GRB2), phosphorylated by BCR-ABL, is associated with the Son of sevenless (SOS) and GRB2-associated-binding protein 2 (GAB2), leading to the activation of phosphatidylinositol 3-kinase (PI3K) and Ras signaling pathways. The latter is responsible of the expression of c-MYC gene via mitogen-activated protein kinases (MAPK). BCR-ABL also induces phosphorylation of signal transducer and activator of transcription 5 (STAT5), which is responsible for the expression of BCL-xL and MCL-1 genes. These BCR-ABL dependent signaling pathways are implicated in cell proliferation and survival. Imatinib induces cell cycle arrest and apoptotic cell death by preventing the binding of BCR-ABL target proteins (*e.g.* GRB2 and STAT5) at the active site.

respectively, in comparison to imatinib, as well as activity against all currently described imatinib-resistant BCR-ABL mutations except T315I [17]. Therefore, dasatinib and nilotinib are Food and Drug Administration (FDA)-approved for the second-line treatment of CML, *i.e.* for the treatment of patients with chronic or accelerated phase CML associated with resistance or intolerance to prior therapy, including imatinib. Despite this, dasatinib and nilotinib-insensitive BCR-ABL mutations have been identified *in vitro* [18].

Bosutinib is a potent dual SRC/ABL kinase inhibitor with considerable activity against BCR-ABL and most imatinib-resistant BCR-ABL kinase domain mutants except T315I and V299L [19]. Bosutinib is approved for the treatment of CML patients who previouslyreceived at least one TKi and where imatinib and other second-generation TKis are not considered suitable therapeutic options. Bosutinib is also used in patients with resistance or intolerance to prior

therapies. More recently, bosutinib was approved as a first-line therapy in patients with newly diagnosed chronic-phase CML [20].

2.4.3. Third-generation inhibitor: Ponatinib

To date, the only approved third-generation TKi is ponatinib, a dual SRC/ABL inhibitor designed to overcome the gatekeeper T315I mutation. Ponatinib is indicated for the treatment of CML in every phase that is disease resistant and/or intolerant to dasatinib and nilotinib and for patients for whom imatinib is not indicated anymore, or for patients with T315I mutation [21]. Structurally, ponatinib closely overlaps nilotinib despite several differences such as the insertion of an ethynyl linker to accommodate the isoleucine side chain without any steric interference also in the inactive conformation [10].

3. Acetylation of histone and non-histone proteins

Growing evidence highlights the essential role of lysine acetylation of histone and non-histone proteins in the coordination of highly regulated cell functions. This post-translational modification (PTM) neutralizes the positive charge of the -amino group of lysine residues or introduces steric hindrance, resulting in the modulation of protein interactions with nucleic acids or with other proteins [1,22]. In addition, acetylation can regulate enzymatic activity of the lysine residues involved in catalysis by influencing their interactions with regulatory proteins and their access to substrates, or through allosteric regulation [23].

As previously mentioned, an equilibrium between the addition and removal of acetyl groups by histone acetyl transferases (HATs) and HDACs, respectively, establishes the acetylation status of lysine residues in various protein substrates (Fig. 2). HAT enzymes catalyze the transfer of an acetyl moiety from acetyl coenzyme A to lysine residues of target proteins [24]. Since acetyl coenzyme A is a key metabolic intermediate in essential carbon catabolic pathways, protein acetylation connects the metabolism to cellular signaling pathways [23].

Initially, HATs and HDACs were believed to exclusively modulate the acetylation level of histone tails. Nevertheless, mass spectrometry-based investigations of the acetylome in different cell models showed that such enzymes also target a wide and continuously growing list of non-histone proteins in various cellular compartments [23,25]. Accordingly, lysine acetylation is a crucial PTM affecting numerous nuclear and cytoplasmic protein functions and is regulating a large variety of vital cellular processes [23,26,27].

4. Histone deacetylases

4.1. Classification

In mammals, 18 HDACs were identified and subdivided into four classes according to their catalytic activity, sequence similarity, and cellular localization (Table 1). Class I includes HDAC1, 2, 3, and 8; class II is divided into two subclasses: subclass IIa corresponds to HDAC4, 5, 7, and 9 and subclass IIb encompasses HDAC6 and 10; class III contains seven members, sirtuins (SIRT) 1 to 7; and class IV comprises only HDAC11 [28,29].

Classes I, II, and IV metalloenzymes possess a zinc ion at the bottom of their catalytic pocket essential for the deacetylation reaction whereas class III isoforms, or sirtuins, depend on the cofactor nicotinamide adenine dinucleotide (NAD^+) for their catalytic activity. Members of classes I and IIa are characterized by a single deacetylase domain at their C-terminus, whereas class IIb enzymes, HDAC6 and 10, also present a second deacetylase domain on their N-terminus that is only active in HDAC6 [29,30].

Class I and II HDACs show high similarity to yeast reduced potassium dependency 3 (Rpd3) and yeast histone deacetylase 1 (Hda1), respectively [31]. Ubiquitously expressed class I enzymes are mainly detected in the nucleus of cells owing to the presence of a nuclear localization signal. Except HDAC9 and HDAC10, class II isoenzymes possess both a nuclear localization signal and a nuclear export signal, conferring them the remarkable capability to shuttle between the nucleus and the cytoplasm. Notably, the expression of class IIa HDAC is tissue-specific. The only member of class IV, HDAC11, is homologous to class I and II HDACs. Class III members, known as sirtuins by analogy with the yeast silent information regulator 2 (Sir2), can be located either in the nucleus, mitochondria, or cytoplasm [1,31].

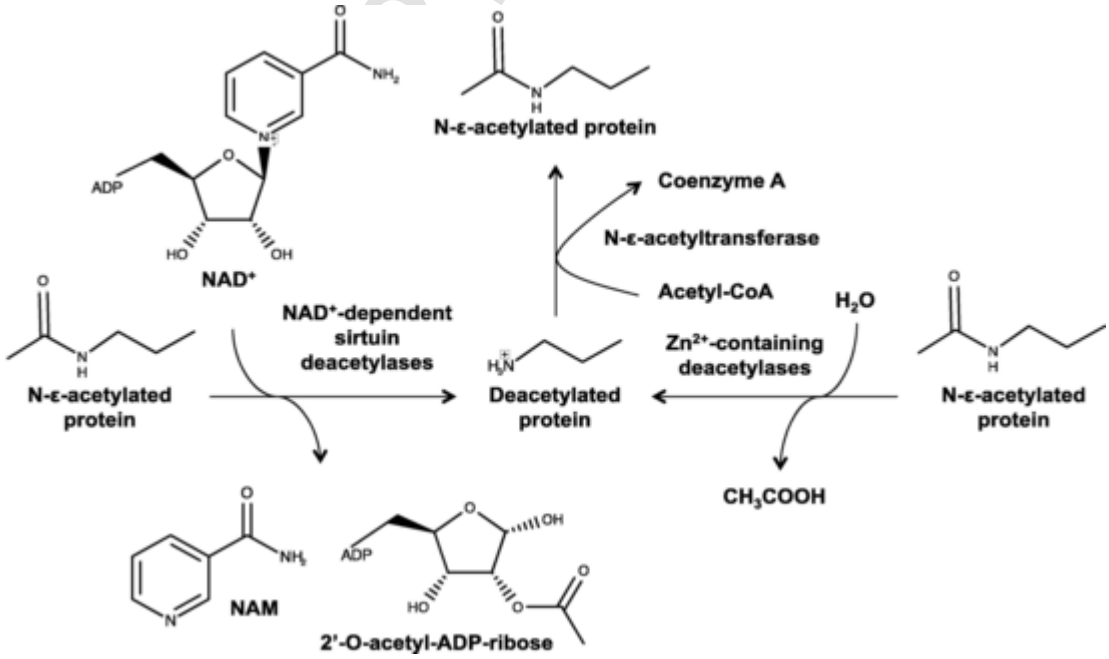

Fig. 2. Mechanisms of protein HDAC-mediated deacetylation and HAT-mediated acetylation. ADP: adenosine diphosphate; CoA: coenzyme A; NAD^+: nicotinamide adenine dinucleotide; NAM: nicotinamide.

Table 1
Classification of HDAC isoenzymes.

Family	Class	Protein (*S. cerevisiae*)	Subclass	Protein (human)	Cellular localization	Chromosomal localization
Histone deacetylase	I	Rpd3, Hos1, Hos2, Hos3	NA	HDAC1	Nuclear	1p34
				HDAC2	Nuclear	6q21
				HDAC3	Nuclear	5q31
				HDAC8	Mainly nuclear	Xq13
	II	Hda1	Class IIa	HDAC4	Nucleo-cytoplasmic shuttle	2q37.3
				HDAC5		17q21
				HDAC7		12q13.1
				HDAC9	Nuclear	7p21.1
			Class IIb	HDAC6	Mainly cytoplasmic	Xp11.23
				HDAC10	Nuclear and cytoplasmic	22q13.31
	IV		NA	HDAC11	Nuclear	3p25.1
Sir2 regulator	III	Sir2, Hst1, Hst2, Hst3, Hst4	I	SIRT1	Mainly nuclear	10q21.3
				SIRT2	Nuclear and cytoplasmic	19q13
				SIRT3	Mitochondrial	11p15.5
			II	SIRT4	Mitochondrial	12q
			III	SIRT5	Mitochondrial	6p23
			IV	SIRT6	Nuclear	19p13.3
				SIRT7	Mainly nuclear	17q25

Hda: yeast histone deacetylase, HDAC: histone deacetylase, NA: non-applicable, Rpd: yeast reduced potassium dependency, Sir: yeast silent information regulator, SIRT: sirtuin.

4.2. Regulation of HDAC activities

HDAC expression and enzymatic activities are highly regulated at the transcriptional, post-transcriptional, translational, and post-translational levels. Two well-characterized mechanisms of HDAC regulation are protein protein interactions within stable large multi-subunit complexes and PTMs such as phosphorylation, sumoylation, acetylation, ubiquitination, glycosylation, and S-nitrosylation. Moreover, the regulation of some HDAC activities includes also subcellular localization, alternative RNA splicing, proteolytic processing, and availability of metabolic cofactors [29,32].

Examples of HDAC regulation by protein protein interaction were reported in studies on class I HDACs. For instance, at least three distinct multi-protein complexes called the CoREST, the NuRD, and the Sin3 complexes function as recruitment platforms for HDAC1 and HDAC2 [33]. In addition, HDAC3 exists in a complex constituted of silencing mediator for retinoid or thyroid-hormone receptor (SMRT) and nuclear receptor co-repressor (N-CoR) [34].

All HDACs possess phosphorylation sites targeted by specific kinases and their phosphorylation status affects enzymatic activity as well as protein complex formation. It is the most extensively studied PTM controlling HDAC functionality. Regarding class I HDACs, phosphorylation enhances HDAC1-3 activities, but inhibits HDAC8 [28,29]. The enzymatic activity of phosphorylated class IIa HDAC4 is modulated partly through subcellular localization, as the binding of 14 3-3 proteins to phosphorylated HDAC4 results in its cytoplasmic sequestration [35].

4.3. HDACs and cancer

Disruption of the functional acetylation pattern contributes to tumorigenesis. Accordingly, overexpression of HDACs is usually detected in cancer, resulting in a global hypoacetylation. Alternatively, mutations in the sequences encoding HDAC isoforms are detected in different cancer subtypes leading to a loss of function of the mutated isoform or a disruption of its cellular localization [36]. A third mechanism involves fusion proteins responsible for an aberrant recruitment of HDACs to target gene promoters, leading to deregulation of gene transcription that may involve both an abnormal silencing of tumor suppressor genes and activation of developmental genes that sustain cancer progression. Moreover, aberrant activation or overexpression of HDACs promotes tumorigenesis *via* the arrest of normal hematopoietic cell differentiation [1,37].

Class IIa HDACs reportedly display a weak catalytic activity *in vitro*, and their presence in complexes with other HDACs suggests a recruitment function [38,39]. Therefore, the following chapters will describe some examples of the implications of class I HDACs in tumorigenesis.

4.3.1. Cellular proliferation

Cyclin-dependent kinase inhibitor 1A (CDKN1A, p21) promotes cell-cycle arrest primarily by binding to and inhibiting cyclin/cyclin-dependent kinase (CDK) complexes [40]. Multiple HDACs repress p21 transcription through deacetylation of histones H3 and H4 in its promoter region [41]. In normal development, targeted loss of HDAC1 causes early embryonic lethality because of a lack of prolif-

UNCORRECTED PROOF

eration caused by increased p21 expression. Despite a concomitant increase in HDAC2 and HDAC3 expression, disruption of HDAC1 in early embryonic development cannot be compensated [42]. Many cancer cell types overexpress HDAC1, HDAC2, and/or HDAC3 as compared to the normal counterpart, which correlates with inhibited p21 expression [43 45].

Additionally, the loss of tumor suppressor scaffold/matrix attachment region binding protein 1 (SMAR1) in cancer correlates with overexpression of the cell-cycle activator cyclin D1. Tumor suppressor SMAR1 normally binds the cyclin D1 promoter and recruits the HDAC1/mSin3 repression complex, causing reduced cyclin D1 expression through histone deacetylation and restrained cell growth [46].

Furthermore, HDAC1-containing complexes interact with and induce deacetylation of the tumor suppressor p53 at C-terminal lysine residues K320, K373 and K382, strongly reducing p53 stability and transcriptional activity, thereby reversing p53-mediated cell growth arrest, senescence and apoptosis [47].

Finally, HDAC1 is associated with Sp1/Sp3 at the promoter of transforming growth factor receptor I (TGF- RI), decreasing the acetylation levels of histones H3 and H4. The associated loss of TGF- RI expression, frequently observed in many cancer types, renders cancer cells unresponsive to TGF and allows for unfettered cell growth [48].

4.3.2. Hematopoietic differentiation

Chromosomal translocations in leukemia and lymphoma often result in an aberrant HDAC recruitment to regulatory regions of promoters, preventing the appropriate expression of target genes involved in differentiation. For instance, the oncogenic fusion protein promyelocytic leukemia (PML)-retinoic acid receptor (RAR) resulting from the t(15;17) translocation is the main driver of acute promyelocytic leukemia (APL) development. Accordingly, different class I HDAC-containing repressor complexes associate with PML-RAR , which leads to the blockage of physiological all trans retinoic acid (t-RA) signaling, thereby preventing complete remission [49]. Additionally, the chimeric protein runt-related transcription factor (RUNX)1-ETO, product of the t(8;21) translocation, interacts with HDAC1-3 as well as the co-repressors mSin3a, SMRT and N-CoR, preventing transcription of target genes implicated in myeloid differentiation, thus allowing for continued proliferation of undifferentiated progenitor cells and initiation of acute myeloid leukemia (AML) [50].

4.3.3. Angiogenesis and metastasis

Hypoxic regions of tumors increase HDAC1 expression and activity, resulting in enhanced angiogenesis *via* the repression of the tumor suppressor genes p53 and von Hippel Lindau (VHL), accompanied by the induction of genes promoting new vessel formation such as hypoxia-inducible factor (HIF)-1 and vascular endothelial growth factor (VEGF) [51].

Class I HDACs are involved in the loss of extracellular matrix-related gene expression. For instance, HDAC1 inhibits the expression of cystatin, a peptidase inhibitor that suppresses tumor invasion [52]. In addition, the repressor Snail recruits HDAC1 and HDAC2, as well as the co-repressor mSin3A to the E-cadherin promoter, directly silencing its gene expression, which is essential to lower cell cell adhesion and stimulate the invasiveness of cells [53]. Similarly, the HDAC3 and peroxisome proliferator-activated receptor (PPAR) complex repress E-cadherin gene transcription through binding to its promoter in prostate cancer cells [54]. Furthermore, HDACis down-regulate the expression of the C-X-C chemokine receptor (CXCR)4 in acute lymphocytic leukemia (ALL) cells, resulting in impaired cell migration [55]. Importantly, the HDACi-mediated increase in intercellular adhesion molecule (ICAM)1 expression on tumor-derived endothelial cells prevents the escape of tumor cells from the immune response by restoring leukocyte-vessel wall interactions and leukocyte infiltration into the tumors [56].

5. HDAC inhibitors

Owing to the reversible nature of epigenetic modifications, considerable efforts have been undertaken to generate small molecules inhibiting proteins involved in epigenetic regulation like HDACs. Thus, over the years, HDACis have become a promising strategy for the treatment of multiple malignancies [1,30].

5.1. Classification and structure

Based on their chemical structures, HDACis were initially sub-divided into five classes, namely hydroxamic acids, carboxylates (short-chain fatty acids), benzamides, depsipeptides and cyclic peptides [57,58]. Moreover, a long list of other compounds with a broad range of chemical structures was reported to inhibit HDAC activities. A multitude of these HDACis were discovered in nature, whereas derivatives have been synthesized by rational design or the modification of natural compounds [59].

Although most of them are pan-HDACis (*i.e.* targeting multiple non-sirtuin HDACs), an increasing number of molecules are designed to be selective for one class or even for a single isoform [37].

Three domains characterize the prototypical pharmacophoric model shared by HDACis (Fig. 3): the zinc binding group that is a metal-binding moiety that chelates the catalytic Zn ion; the hydrophobic linker region that mimics the substrate s lysine chain and fits the catalytic site channel; and the cap group that blocks the access of the substrate to the active site by targeting the channel rim, mainly responsible for HDAC isoform selectivity [57]. HDACis mainly exert their inhibitory effect by chelating the zinc cofactor at the active site of the enzyme. HDACi specificity arises not only from

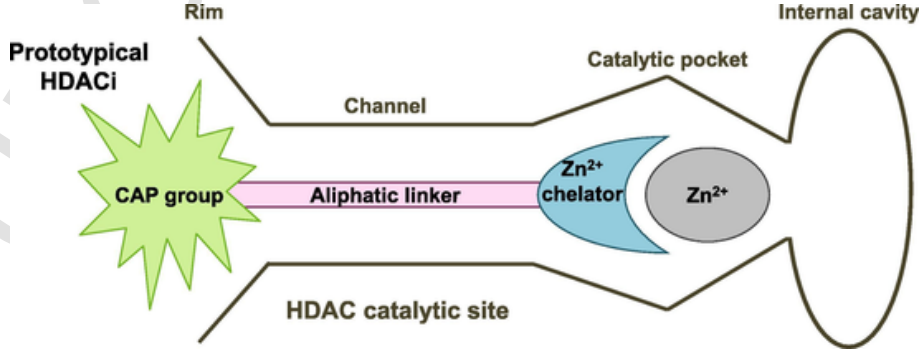

Fig. 3. Prototypical pharmacophoric model of HDAC inhibitors (HDACi).

UNCORRECTED PROOF

interactions with residues in the cap region, which is adjacent to the catalytic site [57,60], but also from - interactions [61].

5.2. Consequences of HDAC inhibition

The inhibition of HDAC enzymes in cancer cells leads to hyper-acetylation of histone and non-histone proteins, resulting in various anti-cancer properties through many different mechanisms (Fig. 4) [62]. Interestingly, deacetylation of histones H3 and H4 was reported in genomic regions close to transcription start sites of genes down-regulated upon HDACi exposure, suggesting that such thera-

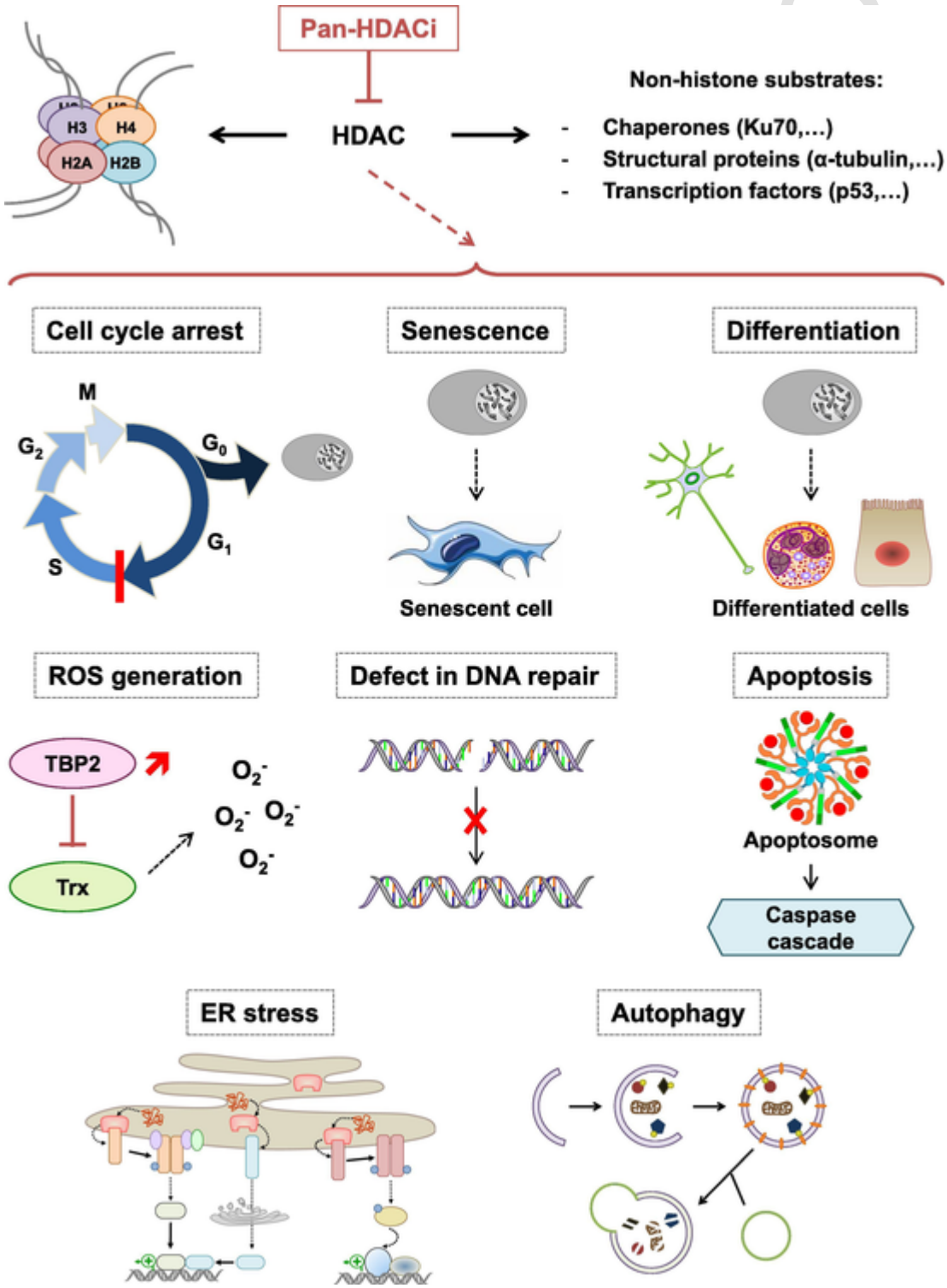

Fig. 4. Anticancer activity of HDAC inhibitors. Through the inhibition of HDACs targeting numerous histone and non-histone proteins, pan-HDAC inhibitors (HDACi) display many anti-cancer properties. Trx: thioredoxin; TBP: Trx binding protein.

peutic compounds may display additional mechanisms of action [63].

Some HDACis display the potency to restore impaired differentiation processes in certain tumor types [64], whereas others inhibit aberrant cell-cycle progression through an increase in p21 expression [65]. In addition, several HDACis induce apoptotic cell death *via* the restoration of apoptotic pathways, and the transcriptional induction or inhibition of pro-apoptotic (*e.g.* BIM) or anti-apoptotic (*e.g.* survivin) proteins, respectively [66,67].

Furthermore, DNA damage induction involved in HDACi toxicity in transformed cells has been associated with reactive oxygen species (ROS) generation [68]. Accordingly, HDAC inhibition may result in the up-regulation of thioredoxin (Trx) binding protein (TBP)2, which binds and inhibits the activity of the ROS antioxidant scavenger Trx [69]. Lethal consequences of ROS production may be strengthened by HDACis that interfere with DNA repair processes *via* the acetylation or transcriptional down-regulation of DNA repair proteins such as Ku70 or RAD50, respectively [70].

Finally, some HDACis promote endoplasmic reticulum (ER) stress *via* 78 kDa glucose-regulated protein (GRP78) acetylation [71] or disruption of the aggresome pathway [72]. These compounds also induce autophagy by inhibiting mammalian target of rapamycin (mTOR) [62] or acetylating autophagy-related proteins (ATGs) [73]. Thus, the type of response induced by HDACis in cancer cells seems to depend on the HDAC inhibitory profile, the concentration and the time of exposure to the inhibitor. Notably, HDACis usually target preferentially cancer cells with moderate effects on normal cells [26].

5.3. Most common HDACis

Many pan-HDACis have been developed in the last years, some of which have entered clinical trials and are currently investigated in different phases against a variety of diseases, including different types of cancer (reviewed in [74]). Hematological malignancies reacted well to most of the pan-HDACis already tested clinically, but the efficacy on solid tumors was disappointingly poor and was also associated with intolerable side effects [75].

Besides studies using HDACis as a single agent, a growing number of completed or ongoing clinical trials employ HDACis in combination with other chemotherapeutic drugs in order to achieve improved anticancer activities [37]. Thus, the combination of classical anticancer agents with epigenetic modulators appears to be a promising future strategy against cancer [30].

5.3.1. "Short-chain fatty acid" family: Sodium butyrate and valproic acid

Within the class of short-chain fatty acids, the two most characterized HDACis are sodium 4-phenylbutyrate and valproic acid [37]. The first is derived from sodium butyrate, a prototype compound of the short-chain fatty acid family initially reported to induce differentiation in cultured erythroleukemic cells [76] and whose short half-life limits its therapeutic application [1]. Sodium 4-phenylbutyrate shows selective toxicity for leukemia cells against healthy blood cells [77] and underwent a phase II trial for the treatment of pediatric brain tumors (www.clinicaltrials.gov). VPA, a branched derivative of valeric acid, is commonly used for its antiepileptic properties [78] and shows selective inhibition against class I and IIa HDACs. Moreover, valproic acid induces differentiation in AML cells and increases responsiveness of CML and promyelocytic leukemia cell lines to cytarabine [79]. This compound was tested in a phase I trial for the treatment of solid tumors and central nervous system tumors [80], and in a phase II trial for treatments in combination with 5-azacytidine in hematological malignancies [74].

5.3.2. "Benzamide" family: MS-275 and MGCD103

The group of benzamides, a class of molecules showing specificity for class I HDACs, comprises mainly MS-275 (Entinostat) and MGCD0103 (Mocetinostat) [37]. Both of them have entered clinical trials against hematological malignancies and some solid tumors. Indeed, MS-275 and MGCD0103 were evaluated in two clinical phase II trials for the treatment of patients with refractory chronic lymphocytic leukemia and metastatic melanoma, respectively [81,82]. Moreover, MS-275 was used together with 5-azacytidine to improve cytotoxicity in AML and acute lymphocytic leukemia [83]. Interestingly, MGCD0103 possesses two main advantages: an oral mode of administration and a long half-life, the latter allowing less frequent drug administration but preventing dose escalation or re-treatment [37]. Treatment with MS-275 did not achieve any objective responses. However, MS-275 could be evaluated as part of a combination therapy to enhance its efficacy [74].

5.3.3. "Hydroxamic acid" family: SAHA, PXD101, and LBH589

The group of hydroxamate-based HDACis contains several compounds tested in clinical trials. Suberoylanilide hydroxamic acid (SAHA; vorinostat) is a pan-HDACi approved by the FDA in 2006 for the treatment of cutaneous T-cell lymphoma [84]. Moreover, SAHA has been tested in phase II clinical trials against numerous solid cancer types, including breast cancer [85], non-small cell lung cancer [86], ovarian epithelial cancer [87], primary peritoneal cavity cancer, and thyroid cancer [88]. Two other compounds belonging to the class of hydroxamic acids recently obtained FDA approval; PXD101 (belinostat) was approved in 2014 for the treatment of patients with relapsed or refractory peripheral T-cell lymphoma [89], whereas LBH589 (panobinostat) was approved in 2015 for patients with multiple myeloma who received at least two prior regimens including the proteasome inhibitor bortezomib and an immunomodulatory agent [90,91]. In addition, both LBH-589 and PXD101 have undergone different phase clinical trials for the treatment of solid and non-solid tumors [92 94].

5.3.4. "Depsipeptide" family: FK228

The depsipeptide FK228 (romidepsin), an epigenetic drug from natural origin, received FDA approval in 2009 for the treatment of cutaneous T-cell lymphoma based on two studies sponsored by Gloucester Pharmaceuticals Incorporated and the National Cancer Institute, which highlighted the benefits of using FK228, including a response rate of approximately 35%, the duration of the response, and low and reversible toxicity [95]. Notably, FK228 has undergone phase II clinical trials for various solid cancers including metastatic breast cancer, metastatic renal cell carcinoma, ovarian epithelial or peritoneal cavity cancer, prostate cancer, and small cell lung cancer [37].

The four compounds that have received FDA approval (Fig. 5) are class I selective (FK-228) or pan-HDAC inhibitors (SAHA, LBH-589, and PXD-101).

6. HDAC inhibitors and CML

The regulation of HDAC1 and 2 is essential in maintaining CML cell survival [96]. Alteration of the normal balance between HATs and HDACs, partly owing to the up-regulation of class I HDACs, leads to aberrant acetylation status of apoptosis-related non-histone proteins p53 and Ku70, which promotes BCR-ABL-independent imatinib resistance [97]. Accordingly, the HDACi AR-42 may increase the sensitivity of CML cells to imatinib and reverse imatinib resistance by regulating HDAC1 expression, which is up-regulated in imatinib-resistant cells [98]. Furthermore, low protein tyrosine phosphatase non-receptor type 6 (PTPN6) expression level, correlated

UNCORRECTED PROOF

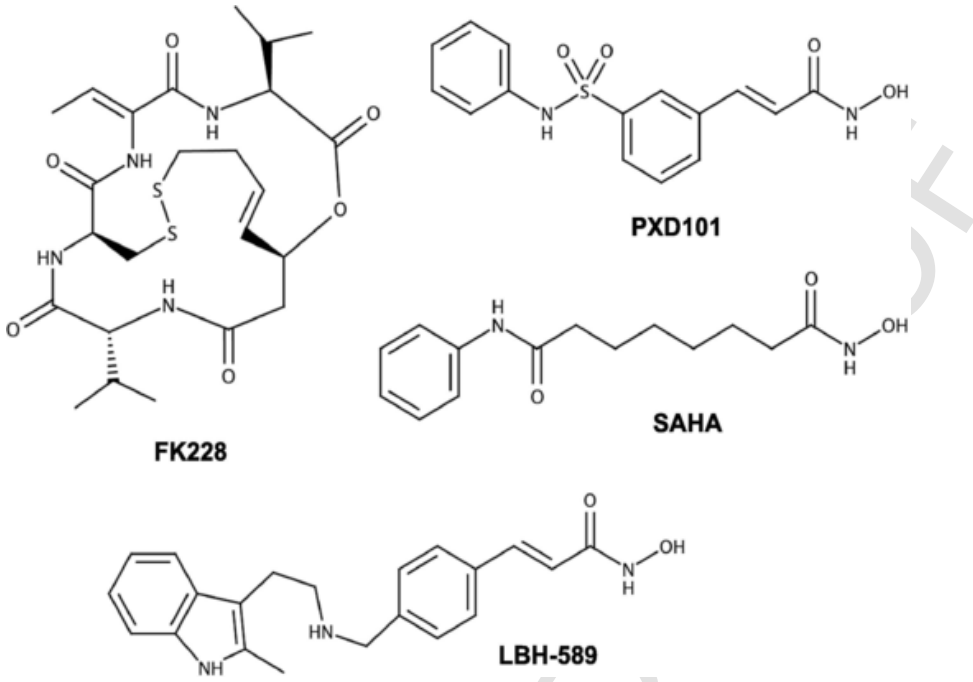

Fig. 5. Molecular structures of Food and Drug Administration-approved HDAC inhibitors. SAHA: suberoylanilide hydroxamic acid.

with CML progression and observed in cell lines and patients with advanced phase CML, results from its regulation by HDAC1 through direct binding [99].

Mechanistically, HDACi-mediated heat shock protein (HSP)90 hyperacetylation leads to the inhibition of the interaction between this chaperone and BCR-ABL, thereby promoting BCR-ABL proteasomal degradation [100]. Some HDACis also reduce the ratio of anti-apoptotic exon 3- to pro-apoptotic exon 4-containing BIM transcripts in CML cell lines and primary CML progenitors with the BIM deletion polymorphism, inducing apoptotic cell death and restoring TKI-sensitivity [101]. Finally, HDACis target the AKT-mammalian target of rapamycin (mTOR) signaling pathway, down-regulating the level of phosphorylated eukaryotic initiation factor (eIF)4E that participates in the translation of tumor-associated proteins such as c-MYC, cyclin D1, and MCL-1 [102].

It has already been shown that combining HDACis with TKis or dual BCR-ABL and Aurora kinase inhibitors synergistically induce anti-CML effects like induction of apoptosis in imatinib-sensitive and -resistant CML cells, as well as primary cells from patients expressing wild-type and imatinib-resistant mutant forms of BCR-ABL [103 106]. Noteworthy, cell mortality is not increased in normal cells incubated with such co-treatments [107]. In addition, HDACi-TKi combination induces apoptosis in pro-B Ba/F3 murine cells expressing either wild-type BCR-ABL in an ectopic manner, or the imatinib-resistant T315I and E255K point-mutated BCR-ABL [108]. Such combination also exhibited antitumor activity *in vivo* [109], significantly prolonging the survival of mice xenografted with imatinib-resistant BCR-ABL^{+} leukemic cells [107].

HDACis in combination with TKis exert anticancer properties through various mechanisms. First, their synergistic effect involves reduction of cyclin D1 levels, as well as induction of p21 and p27 expression [108,110]. Additionally, such therapies enhance the activation of mitochondria-dependent caspase cascades [111], ROS generation and DNA damage induction [107], accompanied by up-regulated and decreased expression of BIM and anti-apoptosis proteins, such as MCL-1 and X-linked inhibitor of apoptosis protein (XIAP), respectively [111]. Finally, combined treatments induce stronger depletion of BCR-ABL, p-Crk-like protein (p-CrkL), p-STAT5, p-ERK1/2, c-MYC, and BCL-xL levels [108,112].

TKi-HDACi combinations display also the potential to eliminate LSCs responsible for TKi resistance [113] by up-regulating hsa-miR-196a expression [114] or suppressing -catenin, which displays a -catenin-independent role in survival and self-renewal of LSCs [115]. Interestingly, therapeutic activity against LSCs was reproduced in *in vivo* mice models [114].

7. Conclusion and perspectives

A growing number of studies highlight the anti-leukemic properties of broad-spectrum or pan-HDACis, alone or in combination with TKis. Nevertheless, the inhibition of multiple HDAC activities is associated with diverse side effects and mutagenicity [116]. Consequently, research is now focusing on the discovery and characterization of more potent and selective HDACis with anticancer properties. Since class I HDACs and HDAC6 appear to be involved in CML pathogenesis, combining TKis with inhibitors specifically targeting these isoenzymes could still result in improved anticancer properties while lowering adverse effects. For instance, in addition to TKi-mediated inhibition of BCR-ABL activity, treatment with HDAC6i could lead to the disruption of HSP90 chaperone association with BCR-ABL, provoking its poly-ubiquitination and degradation by the proteasome [117]. This rational would be of particular interest in the case of BCR-ABL-dependent imatinib resistance.

To further decipher the mechanisms of action underlying the anti-leukemic effect of the TKi-HDACi combinations, potential reprogramming of cancer-related metabolic pathways could be assessed. Indeed, HDAC inhibition has been reported to increase acetylation levels of tumor suppressor p53 and numerous transcription factors (*e.g.* HIF-1 and c-MYC) involved in the regulation of cancer metabolism, leading to increased or decreased protein stability, respectively [118]. Moreover, HDACis in combination with TKis strongly reduce the expression of c-MYC, which targets the gene of lactate dehydrogenase A that catalyze the conversion of pyruvate to lactate. Interestingly, a deletion of such enzyme significantly inhibited the function of both stem cells and progenitor cells during hematopoiesis [119],

UNCORRECTED PROOF

which may at least partly explain the importance of c-MYC in LSC persistence [120].

The immunomodulatory effects exerted by HDACis have been extensively described [121]. In addition, a recent study has demonstrated that initiation of TKi treatment is accompanied by the restoration of natural killer and T cell-mediated immune surveillance in CML patients, implying that TKis also plays a role in the immune response [122]. Combining both therapeutic compounds may result in enhanced immunogenicity of cancer cells and immune system re-activation. Furthermore, c-MYC has been reported to directly bind the promoter region of CD47, a receptor that inhibits phagocytosis of cancer cells by macrophages and dendritic cells, thereby up-regulating CD47 mRNA and cell-surface protein expression [123].

Acknowledgments

ML is supported by a grant from Télévie Luxemburg. Research at LBMCC is supported by the Recherche Cancer et Sang foundation; Recherches Scientifiques Luxembourg ; Een Haerz fir kriibskrank Kanner ; Action LIONS Vaincre le Cancer ; and Télévie Luxembourg. Research at SNU is supported by National Research Foundation (NRF) [Grant Number 019R1A2C1009231] and by a grant from the MEST of Korea for Tumor Microenvironment Global Core Research Center (GCRC) [Grant Number 2011-0030001]. Support from Brain Korea (BK21) PLUS program and Creative-Pioneering Researchers Program at Seoul National University [Funding number: 370C-20160062] are acknowledged.

References

[1] C. Florean, M. Schnekenburger, C. Grandjenette, M. Dicato, M. Diederich, Epigenomics of leukemia: from mechanisms to therapeutic applications, Epigenomics 3 (5) (2011) 581 609.
[2] P.A. Thompson, H.M. Kantarjian, J.E. Cortes, Diagnosis and Treatment of Chronic Myeloid Leukemia in 2015, Mayo Clinic Proceedings 90 (10) (2015) 1440 1454.
[3] E. Jabbour, H. Kantarjian, Chronic myeloid leukemia: 2018 update on diagnosis, therapy and monitoring, Am J Hematol 93 (3) (2018) 442 459.
[4] G.C. Kabat, J.W. Wu, S.C. Moore, L.M. Morton, Y. Park, A.R. Hollenbeck, T.E. Rohan, Lifestyle and dietary factors in relation to risk of chronic myeloid leukemia in the NIH-AARP Diet and Health Study, Cancer Epidemiol Biomarkers Prev 22 (5) (2013) 848 854.
[5] T.I. Mughal, J.P. Radich, M.W. Deininger, J.F. Apperley, T.P. Hughes, C.J. Harrison, C. Gambacorti-Passerini, G. Saglio, J. Cortes, G.Q. Daley, Chronic myeloid leukemia: reminiscences and dreams, Haematologica 101 (5) (2016) 541 558.
[6] F. Pane, M. Intrieri, C. Quintarelli, B. Izzo, G.C. Muccioli, F. Salvatore, BCR/ABL genes and leukemic phenotype: from molecular mechanisms to clinical correlations, Oncogene 21 (56) (2002) 8652 8667.
[7] D. Cilloni, G. Saglio, Molecular pathways: BCR-ABL, Clin Cancer Res 18 (4) (2012) 930 937.
[8] P. Bose, H. Park, J. Al-Khafaji, S. Grant, Strategies to circumvent the T315I gatekeeper mutation in the Bcr-Abl tyrosine kinase, Leuk Res Rep 2 (1) (2013) 18 20.
[9] J.F. Apperley, Chronic myeloid leukaemia, Lancet 385 (9976) (2015) 1447 1459.
[10] F. Rossari, F. Minutolo, E. Orciuolo, Past, present, and future of Bcr-Abl inhibitors: from chemical development to clinical efficacy, J Hematol Oncol 11 (1) (2018) 84.
[11] Y. Liu, N.S. Gray, Rational design of inhibitors that bind to inactive kinase conformations, Nat Chem Biol 2 (7) (2006) 358 364.
[12] T. Schindler, W. Bornmann, P. Pellicena, W.T. Miller, B. Clarkson, J. Kuriyan, Structural mechanism for STI-571 inhibition of abelson tyrosine kinase, Science 289 (5486) (2000) 1938 1942.
[13] G. Nestal de Moraes, P.S. Souza, F.C. Costas, F.C. Vasconcelos, F.R. Reis, R.C. Maia, The Interface between BCR-ABL-Dependent and -Independent Resistance Signaling Pathways in Chronic Myeloid Leukemia, Leuk Res Treatment 2012 (2012) 671702.
[14] S. Roychowdhury, M. Talpaz, Managing resistance in chronic myeloid leukemia, Blood Rev 25 (6) (2011) 279 290.
[15] H. Zhou, R. Xu, Leukemia stem cells: the root of chronic myeloid leukemia, Protein Cell 6 (6) (2015) 403 412.
[16] E. Weisberg, P.W. Manley, S.W. Cowan-Jacob, A. Hochhaus, J.D. Griffin, Second generation inhibitors of BCR-ABL for the treatment of imatinib-resistant chronic myeloid leukaemia, Nat Rev Cancer 7 (5) (2007) 345 356.
[17] G. Wei, S. Rafiyath, D. Liu, First-line treatment for chronic myeloid leukemia: dasatinib, nilotinib, or imatinib, J Hematol Oncol 3 (2010) 47.
[18] B. Stein, B.D. Smith, Treatment options for patients with chronic myeloid leukemia who are resistant to or unable to tolerate imatinib, Clin Ther 32 (5) (2010) 804 820.
[19] J.E. Cortes, C. Gambacorti-Passerini, M.W. Deininger, M.J. Mauro, C. Chuah, D.W. Kim, I. Dyagil, N. Glushko, D. Milojkovic, P. le Coutre, V. Garcia-Gutierrez, L. Reilly, A. Jeynes-Ellis, E. Leip, N. Bardy-Bouxin, A. Hochhaus, T.H. Brummendorf, Bosutinib Versus Imatinib for Newly Diagnosed Chronic Myeloid Leukemia: Results From the Randomized BFORE Trial, J Clin Oncol 36 (3) (2018) 231 237.
[20] J.E. Cortes, J.F. Apperley, D.J. DeAngelo, M.W. Deininger, V.K. Kota, P. Rousselot, C. Gambacorti-Passerini, Management of adverse events associated with bosutinib treatment of chronic-phase chronic myeloid leukemia: expert panel review, J Hematol Oncol 11 (1) (2018) 143.
[21] F. Massaro, M. Molica, M. Breccia, Ponatinib: A Review of Efficacy and Safety, Curr Cancer Drug Targets 18 (9) (2018) 847 856.
[22] S.C. Hodawadekar, R. Marmorstein, Chemistry of acetyl transfer by histone modifying enzymes: structure, mechanism and implications for effector design, Oncogene 26 (37) (2007) 5528 5540.
[23] C. Choudhary, B.T. Weinert, Y. Nishida, E. Verdin, M. Mann, The growing landscape of lysine acetylation links metabolism and cell signalling, Nature Reviews. Molecular Cell Biology 15 (8) (2014) 536 550.
[24] K. Sadoul, J. Wang, B. Diagouraga, S. Khochbin, The tale of protein lysine acetylation in the cytoplasm, Journal of Biomedicine & Biotechnology 2011 (2011) 970382.
[25] S. Spange, T. Wagner, T. Heinzel, O.H. Kramer, Acetylation of non-histone proteins modulates cellular signalling at multiple levels, The International Journal of Biochemistry & Cell Biology 41 (1) (2009) 185 198.
[26] C. Seidel, M. Schnekenburger, M. Dicato, M. Diederich, Antiproliferative and proapoptotic activities of 4-hydroxybenzoic acid-based inhibitors of histone deacetylases, Cancer Letters 343 (1) (2014) 134 146.
[27] Y.C. Wang, S.E. Peterson, J.F. Loring, Protein post-translational modifications and regulation of pluripotency in human stem cells, Cell Research 24 (2) (2014) 143 160.
[28] A.J. de Ruijter, A.H. van Gennip, H.N. Caron, S. Kemp, A.B. van Kuilenburg, Histone deacetylases (HDACs): characterization of the classical HDAC family, The Biochemical Journal 370 (Pt 3) (2003) 737 749.
[29] E. Seto, M. Yoshida, Erasers of histone acetylation: the histone deacetylase enzymes, Cold Spring Harbor Perspectives in Biology 6 (4) (2014) a018713.
[30] C. Seidel, M. Schnekenburger, M. Dicato, M. Diederich, Histone deacetylase 6 in health and disease, Epigenomics 7 (1) (2015) 103 118.
[31] I.V. Gregoretti, Y.M. Lee, H.V. Goodson, Molecular evolution of the histone deacetylase family: functional implications of phylogenetic analysis, Journal of Molecular Biology 338 (1) (2004) 17 31.
[32] N. Sengupta, E. Seto, Regulation of histone deacetylase activities, J Cell Biochem 93 (1) (2004) 57 67.
[33] D.E. Ayer, Histone deacetylases: transcriptional repression with SINers and NuRDs, Trends Cell Biol 9 (5) (1999) 193 198.
[34] Y.D. Wen, V. Perissi, L.M. Staszewski, W.M. Yang, A. Krones, C.K. Glass, M.G. Rosenfeld, E. Seto, The histone deacetylase-3 complex contains nuclear receptor corepressors, Proc Natl Acad Sci U S A 97 (13) (2000) 7202 7207.
[35] Z. Wang, G. Qin, T.C. Zhao, HDAC4: mechanism of regulation and biological functions, Epigenomics 6 (1) (2014) 139 150.
[36] A. Clocchiatti, C. Florean, C. Brancolini, Class IIa HDACs: from important roles in differentiation to possible implications in tumourigenesis, Journal of Cellular and Molecular Medicine 15 (9) (2011) 1833 1846.
[37] C. Seidel, C. Florean, M. Schnekenburger, M. Dicato, M. Diederich, Chromatin-modifying agents in anti-cancer therapy, Biochimie 94 (11) (2012) 2264 2279.
[38] P. Jones, S. Altamura, R. De Francesco, P. Gallinari, A. Lahm, P. Neddermann, M. Rowley, S. Serafini, C. Steinkuhler, Probing the elusive catalytic activity of vertebrate class IIa histone deacetylases, Bioorg Med Chem Lett 18 (6) (2008) 1814 1819.
[39] A. Lahm, C. Paolini, M. Pallaoro, M.C. Nardi, P. Jones, P. Neddermann, S. Sambucini, M.J. Bottomley, P. Lo Surdo, A. Carfi, U. Koch, R. De Francesco, C. Steinkuhler, P. Gallinari, Unraveling the hidden catalytic activity of vertebrate class IIa histone deacetylases, Proc Natl Acad Sci U S A 104 (44) (2007) 17335 17340.
[40] T. Abbas, A. Dutta, p21 in cancer: intricate networks and multiple activities, Nat Rev Cancer 9 (6) (2009) 400 414.
[41] V.M. Richon, T.W. Sandhoff, R.A. Rifkind, P.A. Marks, Histone deacetylase inhibitor selectively induces p21WAF1 expression and gene-associated histone acetylation, Proc Natl Acad Sci U S A 97 (18) (2000) 10014 10019.
[42] G. Lagger, D. O Carroll, M. Rembold, H. Khier, J. Tischler, G. Weitzer, B. Schuettengruber, C. Hauser, R. Brunmeir, T. Jenuwein, C. Seiser, Essential function of histone deacetylase 1 in proliferation control and CDK inhibitor repression, EMBO J 21 (11) (2002) 2672 2681.
[43] K. Halkidou, L. Gaughan, S. Cook, H.Y. Leung, D.E. Neal, C.N. Robson, Upregulation and nuclear recruitment of HDAC1 in hormone refractory prostate cancer, Prostate 59 (2) (2004) 177 189.
[44] A. Hrzenjak, F. Moinfar, M.L. Kremser, B. Strohmeier, P.B. Staber, K. Zatloukal, H. Denk, Valproate inhibition of histone deacetylase 2 affects differentiation and decreases proliferation of endometrial stromal sarcoma cells, Mol Cancer Ther 5 (9) (2006) 2203 2210.
[45] A.J. Wilson, D.S. Byun, N. Popova, L.B. Murray, K. L Italien, Y. Sowa, D. Arango, A. Velcich, L.H. Augenlicht, J.M. Mariadason, Histone deacetylase 3 (HDAC3) and other class I HDACs regulate colon cell maturation and p21 expression and are deregulated in human colon cancer, J Biol Chem 281 (19) (2006) 13548 13558.
[46] S. Rampalli, L. Pavithra, A. Bhatt, T.K. Kundu, S. Chattopadhyay, Tumor suppressor SMAR1 mediates cyclin D1 repression by recruitment of the SIN3/histone deacetylase 1 complex, Mol Cell Biol 25 (19) (2005) 8415 8429.

UNCORRECTED PROOF

[47] S.M. Reed, D.E. Quelle, p53 Acetylation: Regulation and Consequences, Cancers (Basel) 7 (1) (2014) 30 69.
[48] S. Ammanamanchi, M.G. Brattain, Restoration of transforming growth factor-beta signaling through receptor RI induction by histone deacetylase activity inhibition in breast cancer cells, J Biol Chem 279 (31) (2004) 32620 32625.
[49] E. Puccetti, M. Ruthardt, Acute promyelocytic leukemia: PML/RARalpha and the leukemic stem cell, Leukemia 18 (7) (2004) 1169 1175.
[50] K. Lam, D.E. Zhang, RUNX1 and RUNX1-ETO: roles in hematopoiesis and leukemogenesis, Front Biosci (Landmark Ed) 17 (2012) 1120 1139.
[51] S. Pluemsampant, O.S. Safronova, K. Nakahama, I. Morita, Protein kinase CK2 is a key activator of histone deacetylase in hypoxia-associated tumors, Int J Cancer 122 (2) (2008) 333 341.
[52] J.R. Whetstine, J. Ceron, B. Ladd, P. Dufourcq, V. Reinke, Y. Shi, Regulation of tissue-specific and extracellular matrix-related genes by a class I histone deacetylase, Mol Cell 18 (4) (2005) 483 490.
[53] H. Peinado, E. Ballestar, M. Esteller, A. Cano, Snail mediates E-cadherin repression by the recruitment of the Sin3A/histone deacetylase 1 (HDAC1)/HDAC2 complex, Mol Cell Biol 24 (1) (2004) 306 319.
[54] J.S. Annicotte, I. Iankova, S. Miard, V. Fritz, D. Sarruf, A. Abella, M.L. Berthe, D. Noel, A. Pillon, F. Iborra, P. Dubus, T. Maudelonde, S. Culine, L. Fajas, Peroxisome proliferator-activated receptor gamma regulates E-cadherin expression and inhibits growth and invasion of prostate cancer, Mol Cell Biol 26 (20) (2006) 7561 7574.
[55] R. Crazzolara, K. Johrer, R.W. Johnstone, R. Greil, R. Kofler, B. Meister, D. Bernhard, Histone deacetylase inhibitors potently repress CXCR4 chemokine receptor expression and function in acute lymphoblastic leukaemia, Br J Haematol 119 (4) (2002) 965 969.
[56] D.M. Hellebrekers, K. Castermans, E. Vire, R.P. Dings, N.T. Hoebers, K.H. Mayo, M.G. Oude Egbrink, G. Molema, F. Fuks, M. van Engeland, A.W. Griffioen, Epigenetic regulation of tumor endothelial cell anergy: silencing of intercellular adhesion molecule-1 by histone modifications, Cancer Res 66 (22) (2006) 10770 10777.
[57] Y. Li, D. Shin, S.H. Kwon, Histone deacetylase 6 plays a role as a distinct regulator of diverse cellular processes, The FEBS Journal 280 (3) (2013) 775 793.
[58] P.H. Yang, L. Zhang, Y.J. Zhang, J. Zhang, W.F. Xu, HDAC6: physiological function and its selective inhibitors for cancer treatment, Drug Discoveries & Therapeutics 7 (6) (2013) 233 242.
[59] H. Losson, M. Schnekenburger, M. Dicato, M. Diederich, Natural Compound Histone Deacetylase Inhibitors (HDACi): Synergy with Inflammatory Signaling Pathway Modulators and Clinical Applications in Cancer, Molecules 21 (11) (2016).
[60] P. Bertrand, Inside HDAC with HDAC inhibitors, European Journal of Medicinal Chemistry 45 (6) (2010) 2095 2116.
[61] M. Ahamed, K. Vermeulen, M. Schnekenburger, L.R. Moltzau, F.O. Levy, J. Marton, M. Froeyen, D.E. Olberg, M. Diederich, G. Bormans, Synthesis, Enzyme Assays and Molecular Docking Studies of Fluorinated Bioisosteres of Santacruzamate A as Potential HDAC Tracers, Letters in Drug Design & Discovery 13 (2016) 1 11.
[62] M. Mrakovcic, J. Kleinheinz, L.F. Frohlich, p53 at the Crossroads between Different Types of HDAC Inhibitor-Mediated Cancer Cell Death, Int J Mol Sci 20 (10) (2019).
[63] A. Rada-Iglesias, S. Enroth, A. Ameur, C.M. Koch, G.K. Clelland, P. Respuela-Alonso, S. Wilcox, O.M. Dovey, P.D. Ellis, C.F. Langford, I. Dunham, J. Komorowski, C. Wadelius, Butyrate mediates decrease of histone acetylation centered on transcription start sites and down-regulation of associated genes, Genome Res 17 (6) (2007) 708 719.
[64] M. Schnekenburger, F. Morceau, E. Henry, R. Blasius, M. Dicato, C. Trentesaux, M. Diederich, Transcriptional and post-transcriptional regulation of glutathione S-transferase P1 expression during butyric acid-induced differentiation of K562 cells, Leukemia Research 30 (5) (2006) 561 568.
[65] T. Kumagai, N. Wakimoto, D. Yin, S. Gery, N. Kawamata, N. Takai, N. Komatsu, A. Chumakov, Y. Imai, H.P. Koeffler, Histone deacetylase inhibitor, suberoylanilide hydroxamic acid (Vorinostat, SAHA) profoundly inhibits the growth of human pancreatic cancer cells, Int J Cancer 121 (3) (2007) 656 665.
[66] N. Bhatnagar, X. Li, Y. Chen, X. Zhou, S.H. Garrett, B. Guo, 3,3 -diindolylmethane enhances the efficacy of butyrate in colon cancer prevention through down-regulation of survivin, Cancer Prevention Research 2 (6) (2009) 581 589.
[67] S. Xargay-Torrent, M. Lopez-Guerra, I. Saborit-Villarroya, L. Rosich, E. Campo, G. Roue, D. Colomer, Vorinostat-induced apoptosis in mantle cell lymphoma is mediated by acetylation of proapoptotic BH3-only gene promoters, Clin Cancer Res 17 (12) (2011) 3956 3968.
[68] R.R. Rosato, J.A. Almenara, S.C. Maggio, S. Coe, P. Atadja, P. Dent, S. Grant, Role of histone deacetylase inhibitor-induced reactive oxygen species and DNA damage in LAQ-824/fludarabine antileukemic interactions, Mol Cancer Ther 7 (10) (2008) 3285 3297.
[69] W.S. Xu, R.B. Parmigiani, P.A. Marks, Histone deacetylase inhibitors: molecular mechanisms of action, Oncogene 26 (37) (2007) 5541 5552.
[70] K.M. Miller, J.V. Tjeertes, J. Coates, G. Legube, S.E. Polo, S. Britton, S.P. Jackson, Human HDAC1 and HDAC2 function in the DNA-damage response to promote DNA nonhomologous end-joining, Nat Struct Mol Biol 17 (9) (2010) 1144 1151.
[71] R. Rao, S. Nalluri, R. Kolhe, Y. Yang, W. Fiskus, J. Chen, K. Ha, K.M. Buckley, R. Balusu, V. Coothankandaswamy, A. Joshi, P. Atadja, K.N. Bhalla, Treatment with panobinostat induces glucose-regulated protein 78 acetylation and endoplasmic reticulum stress in breast cancer cells, Mol Cancer Ther 9 (4) (2010) 942 952.
[72] S.T. Nawrocki, J.S. Carew, M.S. Pino, R.A. Highshaw, R.H. Andtbacka, K. Dunner Jr., A. Pal, W.G. Bornmann, P.J. Chiao, P. Huang, H. Xiong, J.L. Abbruzzese, D.J. McConkey, Aggresome disruption: a novel strategy to enhance bortezomib-induced apoptosis in pancreatic cancer cells, Cancer Res 66 (7) (2006) 3773 3781.
[73] A. Banreti, M. Sass, Y. Graba, The emerging role of acetylation in the regulation of autophagy, Autophagy 9 (6) (2013) 819 829.
[74] M. Schnekenburger, C. Florean, M. Dicato, M. Diederich, Epigenetic alterations as a universal feature of cancer hallmarks and a promising target for personalized treatments, Current Topics in Medicinal Chemistry 16 (7) (2016) 745 776.
[75] A. Bruning, J. Juckstock, Misfolded proteins: from little villains to little helpers in the fight against cancer, Frontiers in Oncology 5 (2015) 47.
[76] A. Leder, P. Leder, Butyric acid, a potent inducer of erythroid differentiation in cultured erythroleukemic cells, Cell 5 (3) (1975) 319 322.
[77] A. Batova, L.E. Shao, M.B. Diccianni, A.L. Yu, T. Tanaka, A. Rephaeli, A. Nudelman, J. Yu, The histone deacetylase inhibitor AN-9 has selective toxicity to acute leukemia and drug-resistant primary leukemia and cancer cell lines, Blood 100 (9) (2002) 3319 3324.
[78] S. Chateauvieux, F. Morceau, M. Dicato, M. Diederich, Molecular and therapeutic potential and toxicity of valproic acid, Journal of Biomedicine & Biotechnology 2010 (2010).
[79] N. Liu, C. Wang, L. Wang, L. Gao, H. Cheng, G. Tang, X. Hu, J. Wang, Valproic acid enhances the antileukemic effect of cytarabine by triggering cell apoptosis, International Journal of Molecular Medicine 37 (6) (2016) 1686 1696.
[80] J.M. Su, X.N. Li, P. Thompson, C.N. Ou, A.M. Ingle, H. Russell, C.C. Lau, P.C. Adamson, S.M. Blaney, Phase 1 study of valproic acid in pediatric patients with refractory solid or CNS tumors: a children s oncology group report, Clin Cancer Res 17 (3) (2011) 589 597.
[81] K.A. Blum, A. Advani, L. Fernandez, R. Van Der Jagt, J. Brandwein, S. Kambhampati, J. Kassis, M. Davis, C. Bonfils, M. Dubay, J. Dumouchel, M. Drouin, D.M. Lucas, R.E. Martell, J.C. Byrd, Phase II study of the histone deacetylase inhibitor MGCD0103 in patients with previously treated chronic lymphocytic leukaemia, Br J Haematol 147 (4) (2009) 507 514.
[82] A. Hauschild, U. Trefzer, C. Garbe, K.C. Kaehler, S. Ugurel, F. Kiecker, T. Eigentler, H. Krissel, A. Schott, D. Schadendorf, Multicenter phase II trial of the histone deacetylase inhibitor pyridylmethyl-N-{4-[(2-aminophenyl)-carbamoyl]-benzyl}-carbamate in pretreated metastatic melanoma, Melanoma Research 18 (4) (2008) 274 278.
[83] S. Gao, A. Mobley, C. Miller, J. Boklan, J. Chandra, Potentiation of reactive oxygen species is a marker for synergistic cytotoxicity of MS-275 and 5-azacytidine in leukemic cells, Leukemia Research 32 (5) (2008) 771 780.
[84] M. Duvic, R. Talpur, X. Ni, C. Zhang, P. Hazarika, C. Kelly, J.H. Chiao, J.F. Reilly, J.L. Ricker, V.M. Richon, S.R. Frankel, Phase 2 trial of oral vorinostat (suberoylanilide hydroxamic acid, SAHA) for refractory cutaneous T-cell lymphoma (CTCL), Blood 109 (1) (2007) 31 39.
[85] T.H. Luu, R.J. Morgan, L. Leong, D. Lim, M. McNamara, J. Portnow, P. Frankel, D.D. Smith, J.H. Doroshow, C. Wong, A. Aparicio, D.R. Gandara, G. Somlo, A phase II trial of vorinostat (suberoylanilide hydroxamic acid) in metastatic breast cancer: a California Cancer Consortium study, Clin Cancer Res 14 (21) (2008) 7138 7142.
[86] A.M. Traynor, S. Dubey, J.C. Eickhoff, J.M. Kolesar, K. Schell, M.S. Huie, D.L. Groteluschen, S.M. Marcotte, C.M. Hallahan, H.R. Weeks, G. Wilding, I. Espinoza-Delgado, J.H. Schiller, Vorinostat (NSC# 701852) in patients with relapsed non-small cell lung cancer: a Wisconsin Oncology Network phase II study, Journal of Thoracic Oncology : Official Publication of the International Association for the Study of Lung Cancer 4 (4) (2009) 522 526.
[87] S.C. Modesitt, M. Sill, J.S. Hoffman, D.P. Bender, G., Gynecologic Oncology, A phase II study of vorinostat in the treatment of persistent or recurrent epithelial ovarian or primary peritoneal carcinoma: a Gynecologic Oncology Group study, Gynecologic Oncology 109 (2) (2008) 182 186.
[88] J.A. Woyach, R.T. Kloos, M.D. Ringel, D. Arbogast, M. Collamore, J.A. Zwiebel, M. Grever, M. Villalona-Calero, M.H. Shah, Lack of therapeutic effect of the histone deacetylase inhibitor vorinostat in patients with metastatic radioiodine-refractory thyroid carcinoma, The Journal of Clinical Endocrinology and Metabolism 94 (1) (2009) 164 170.
[89] A. Bodiford, M. Bodge, M.S. Talbott, N.M. Reddy, Profile of belinostat for the treatment of relapsed or refractory peripheral T-cell lymphoma, OncoTargets and Therapy 7 (2014) 1971 1977.
[90] P. Atadja, Development of the pan-DAC inhibitor panobinostat (LBH589): successes and challenges, Cancer Letters 280 (2) (2009) 233 241.
[91] K. Wahaib, A.E. Beggs, H. Campbell, L. Kodali, P.D. Ford, Panobinostat: A histone deacetylase inhibitor for the treatment of relapsed or refractory multiple myeloma, American Journal of Health-System Pharmacy : AJHP : Official Journal of the American Society of Health-System Pharmacists 73 (7) (2016) 441 450.
[92] F. Giles, T. Fischer, J. Cortes, G. Garcia-Manero, J. Beck, F. Ravandi, E. Masson, P. Rae, G. Laird, S. Sharma, H. Kantarjian, M. Dugan, M. Albitar, K. Bhalla, A phase I study of intravenous LBH589, a novel cinnamic hydroxamic acid analogue histone deacetylase inhibitor, in patients with refractory hematologic malignancies, Clin Cancer Res 12 (15) (2006) 4628 4635.
[93] S.S. Ramalingam, C.P. Belani, C. Ruel, P. Frankel, B. Gitlitz, M. Koczywas, I. Espinoza-Delgado, D. Gandara, Phase II study of belinostat (PXD101), a histone deacetylase inhibitor, for second line therapy of advanced malignant pleural mesothelioma, Journal of Thoracic Oncology : Official Publication of the International Association for the Study of Lung Cancer 4 (1) (2009) 97 101.
[94] N.L. Steele, J.A. Plumb, L. Vidal, J. Tjornelund, P. Knoblauch, A. Rasmussen, C.E. Ooi, P. Buhl-Jensen, R. Brown, T.R. Evans, J.S. DeBono, A phase 1 pharmacokinetic and pharmacodynamic study of the histone deacetylase inhibitor belinostat in patients with advanced solid tumors, Clin Cancer Res 14 (3) (2008) 804 810.
[95] S.J. Whittaker, M.F. Demierre, E.J. Kim, A.H. Rook, A. Lerner, M. Duvic, J. Scarisbrick, S. Reddy, T. Robak, J.C. Becker, A. Samtsov, W. McCulloch, Y.H.

UNCORRECTED PROOF

Kim, Final results from a multicenter, international, pivotal study of romidepsin in refractory cutaneous T-cell lymphoma, J Clin Oncol 28 (29) (2010) 4485 4491.
[96] S.H. Chen, J.M. Chow, Y.Y. Hsieh, C.Y. Lin, K.W. Hsu, W.S. Hsieh, W.M. Chi, B.M. Shabangu, C.H. Lee, HDAC1,2 Knock-Out and HDACi Induced Cell Apoptosis in Imatinib-Resistant K562 Cells, Int J Mol Sci 20 (9) (2019).
[97] S.M. Lee, J.H. Bae, M.J. Kim, H.S. Lee, M.K. Lee, B.S. Chung, D.W. Kim, C.D. Kang, S.H. Kim, Bcr-Abl-independent imatinib-resistant K562 cells show aberrant protein acetylation and increased sensitivity to histone deacetylase inhibitors, J Pharmacol Exp Ther 322 (3) (2007) 1084 1092.
[98] D. Wei, T. Lu, D. Ma, K. Yu, T. Zhang, J. Xiong, W. Wang, Z. Zhang, Q. Fang, J. Wang, Synergistic activity of imatinib and AR-42 against chronic myeloid leukemia cells mainly through HDAC1 inhibition, Life Sci 211 (2018) 224 237.
[99] X. Zhang, L. Yang, X. Liu, Z. Nie, X. Wang, Y. Pan, J. Luo, Research on the epigenetic regulation mechanism of the PTPN6 gene in advanced chronic myeloid leukaemia, Br J Haematol 178 (5) (2017) 728 738.
[100] R. Nimmanapalli, L. Fuino, C. Stobaugh, V. Richon, K. Bhalla, Cotreatment with the histone deacetylase inhibitor suberoylanilide hydroxamic acid (SAHA) enhances imatinib-induced apoptosis of Bcr-Abl-positive human acute leukemia cells, Blood 101 (8) (2003) 3236 3239.
[101] M. Rauzan, C.T. Chuah, T.K. Ko, S.T. Ong, The HDAC inhibitor SB939 overcomes resistance to BCR-ABL kinase Inhibitors conferred by the BIM deletion polymorphism in chronic myeloid leukemia, PLoS One 12 (3) (2017) e0174107.
[102] X. Jia, Y. Zheng, Y. Guo, K. Chen, Sodium butyrate and panobinostat induce apoptosis of chronic myeloid leukemia cells via multiple pathways, Mol Genet Genomic Med 7 (5) (2019) e613.
[103] Y. Dai, S. Chen, C.A. Venditti, X.Y. Pei, T.K. Nguyen, P. Dent, S. Grant, Vorinostat synergistically potentiates MK-0457 lethality in chronic myelogenous leukemia cells sensitive and resistant to imatinib mesylate, Blood 112 (3) (2008) 793 804.
[104] W. Fiskus, Y. Wang, R. Joshi, R. Rao, Y. Yang, J. Chen, R. Kolhe, R. Balusu, K. Eaton, P. Lee, C. Ustun, A. Jillella, C.A. Buser, S. Peiper, K. Bhalla, Cotreatment with vorinostat enhances activity of MK-0457 (VX-680) against acute and chronic myelogenous leukemia cells, Clin Cancer Res 14 (19) (2008) 6106 6115.
[105] Y. Matsuda, T. Yamauchi, N. Hosono, K. Uzui, E. Negoro, K. Morinaga, R. Nishi, A. Yoshida, S. Kimura, T. Maekawa, T. Ueda, Combination of panobinostat with ponatinib synergistically overcomes imatinib-resistant CML cells, Cancer Sci 107 (7) (2016) 1029 1038.
[106] A. Morotti, D. Cilloni, F. Messa, F. Arruga, I. Defilippi, S. Carturan, R. Catalano, V. Rosso, A. Chiarenza, C. Pilatrino, A. Guerrasio, R. Taulli, E. Bracco, M. Pautasso, D. Baraban, E. Gottardi, G. Saglio, Valproate enhances imatinib-induced growth arrest and apoptosis in chronic myeloid leukemia cells, Cancer 106 (5) (2006) 1188 1196.
[107] T. Nguyen, Y. Dai, E. Attkisson, L. Kramer, N. Jordan, N. Nguyen, N. Kolluri, M. Muschen, S. Grant, HDAC inhibitors potentiate the activity of the BCR/ABL kinase inhibitor KW-2449 in imatinib-sensitive or -resistant BCR/ABL+ leukemia cells in vitro and in vivo, Clin Cancer Res 17 (10) (2011) 3219 3232.
[108] W. Fiskus, M. Pranpat, P. Bali, M. Balasis, S. Kumaraswamy, S. Boyapalle, K. Rocha, J. Wu, F. Giles, P.W. Manley, P. Atadja, K. Bhalla, Combined effects of novel tyrosine kinase inhibitor AMN107 and histone deacetylase inhibitor LB-H589 against Bcr-Abl-expressing human leukemia cells, Blood 108 (2) (2006) 645 652.
[109] S. Okabe, T. Tauchi, S. Kimura, T. Maekawa, T. Kitahara, Y. Tanaka, K. Ohyashiki, Combining the ABL1 kinase inhibitor ponatinib and the histone deacetylase inhibitor vorinostat: a potential treatment for BCR-ABL-positive leukemia, PLoS One 9 (2) (2014) e89080.
[110] B.S. Kim, E. Bae, Y.J. Kim, K.S. Ahn, J. Park, J.Y. Rhee, Y.Y. Lee, Y. Kim, D. Lee, B.K. Kim, S.S. Yoon, Combination of SK-7041, one of novel histone deacetylase inhibitors, and STI571-induced synergistic apoptosis in chronic myeloid leukemia, Anticancer Drugs 18 (6) (2007) 641 647.
[111] Q. Bu, L. Cui, J. Li, X. Du, W. Zou, K. Ding, J. Pan, SAHA and S116836, a novel tyrosine kinase inhibitor, synergistically induce apoptosis in imatinib-resistant chronic myelogenous leukemia cells, Cancer Biol Ther 15 (7) (2014) 951 962.
[112] W. Fiskus, M. Pranpat, M. Balasis, P. Bali, V. Estrella, S. Kumaraswamy, R. Rao, K. Rocha, B. Herger, F. Lee, V. Richon, K. Bhalla, Cotreatment with vorinostat (suberoylanilide hydroxamic acid) enhances activity of dasatinib (BMS-354825) against imatinib mesylate-sensitive or imatinib mesylate-resistant chronic myelogenous leukemia cells, Clin Cancer Res 12 (19) (2006) 5869 5878.
[113] T. Al Baghdadi, R. Abonour, H.S. Boswell, Novel combination treatments targeting chronic myeloid leukemia stem cells, Clinical lymphoma, myeloma, & Leukemia 12 (2) (2012) 94 105.
[114] O.A. Bamodu, K.T. Kuo, L.P. Yuan, W.H. Cheng, W.H. Lee, Y.S. Ho, T.Y. Chao, C.T. Yeh, HDAC inhibitor suppresses proliferation and tumorigenicity of drug-resistant chronic myeloid leukemia stem cells through regulation of hsa-miR-196a targeting BCR/ABL1, Exp Cell Res 370 (2) (2018) 519 530.
[115] Y. Jin, Y. Yao, L. Chen, X. Zhu, B. Jin, Y. Shen, J. Li, X. Du, Y. Lu, S. Jiang, J. Pan, Depletion of gamma-catenin by Histone Deacetylase Inhibition Confers Elimination of CML Stem Cells in Combination with Imatinib, Theranostics 6 (11) (2016) 1947 1962.
[116] S. Subramanian, S.E. Bates, J.J. Wright, I. Espinoza-Delgado, R.L. Piekarz, Clinical Toxicities of Histone Deacetylase Inhibitors, Pharmaceuticals 3 (9) (2010) 2751 2767.
[117] P. Bali, M. Pranpat, J. Bradner, M. Balasis, W. Fiskus, F. Guo, K. Rocha, S. Kumaraswamy, S. Boyapalle, P. Atadja, E. Seto, K. Bhalla, Inhibition of histone deacetylase 6 acetylates and disrupts the chaperone function of heat shock protein 90: a novel basis for antileukemia activity of histone deacetylase inhibitors, J Biol Chem 280 (29) (2005) 26729 26734.
[118] F. Chiaradonna, C. Cirulli, R. Palorini, G. Votta, L. Alberghina, New Insights into the Connection Between Histone Deacetylases, Cell Metabolism, and Cancer, Antioxid Redox Signal 23 (1) (2015) 30 50.
[119] Y.H. Wang, W.J. Israelsen, D. Lee, V.W.C. Yu, N.T. Jeanson, C.B. Clish, L.C. Cantley, M.G. Vander Heiden, D.T. Scadden, Cell-state-specific metabolic dependency in hematopoiesis and leukemogenesis, Cell 158 (6) (2014) 1309 1323.
[120] G. Venton, M. Perez-Alea, C. Baier, G. Fournet, G. Quash, Y. Labiad, G. Martin, F. Sanderson, P. Poullin, P. Suchon, L. Farnault, C. Nguyen, C. Brunet, I. Ceylan, R.T. Costello, Aldehyde dehydrogenases inhibition eradicates leukemia stem cells while sparing normal progenitors, Blood Cancer J 6 (9) (2016) e469.
[121] A.C. West, M.J. Smyth, R.W. Johnstone, The anticancer effects of HDAC inhibitors require the immune system, Oncoimmunology 3 (1) (2014) e27414.
[122] A. Hughes, A.S.M. Yong, Immune Effector Recovery in Chronic Myeloid Leukemia and Treatment-Free Remission, Front Immunol 8 (2017) 469.
[123] E.K. Curran, J. Godfrey, J. Kline, Mechanisms of Immune Tolerance in Leukemia and Lymphoma, Trends Immunol 38 (7) (2017) 513 525.

UNCORRECTED PROOF

Manuscript
Click here to access/download;Manuscript;Lernoux et al_Text_MD.docx
Click here to view linked References

Novel HDAC inhibitor MAKV-8 and imatinib synergistically kill chronic myeloid leukemia cells via inhibition of BCR-ABL/MYC-signaling: effect on imatinib resistance and stem cells

Manon Lernoux[1], Michael Schnekenburger[1], Hélène Losson[1], Koen Vermeulen[2], Hyunggu Hahn[3], Déborah Gérard[1], Jin-Young Lee[3], Aloran Mazumder[3], Muneer Ahamed[2], Christo Christov[4], Dong-Wook Kim[5], Mario Dicato[1], Guy Bormans[2], Byung-Woo Han[3*], Marc Diederich[3*]

[1]Laboratoire de Biologie Moléculaire et Cellulaire du Cancer, Hôpital Kirchberg, 9, rue Edward Steichen, L-2540 Luxembourg, Luxembourg

[2]Laboratory for Radiopharmaceutical Research, Department of Pharmaceutical and Pharmacological Sciences, KU Leuven, Leuven, Belgium

[3]Department of Pharmacy, College of Pharmacy, Seoul National University, 1 Gwanak-ro, Gwanak-gu, Seoul, 08826, Korea

[4]Faculté de Médecine, Université de Lorraine, Nancy, France

[5]Seoul St. Mary's Hospital, Leukemia Research Institute, the Catholic University of Korea, Seoul Korea

Corresponding authors:

*Marc Diederich. Tel: +82-2-880-8919; E-mail address: marcdiederich@snu.ac.kr; and Byung-Woo Han. Tel: +82-2-880-7898, E-mail: bwhan@snu.ac.kr. Department of Pharmacy, College of Pharmacy, Seoul National University, Building 29 Room 223, 1 Gwanak-ro, Gwanak-gu, Seoul, 08826, Korea.

Abstract

Background: Chronic myeloid leukemia (CML) pathogenesis is mainly driven by the oncogenic breakpoint cluster region-Abelson murine leukemia viral oncogene homolog 1 (BCR-ABL) fusion protein. Since BCR-ABL displays abnormal constitutive tyrosine kinase activity, therapies using tyrosine kinase inhibitors (TKis) such as imatinib represent a major breakthrough for the outcome of CML patients. Nevertheless, the development of TKi resistance and the persistence of leukemia stem cells (LSCs) remain barriers to cure the disease, justifying the development of novel therapeutic approaches. Since the activity of histone deacetylase (HDAC) is deregulated in numerous cancers including CML, pan-HDAC inhibitors may represent promising therapeutic regimens for the treatment of CML cells in combination with TKi.

Results: We assessed the anti-leukemic activity of a novel hydroxamate-based pan-HDAC inhibitor MAKV-8, which complied with the Lipinski's "rule of 5", in various CML cells alone or in combination with imatinib. We validated the *in vitro* HDAC-inhibitory potential of MAKV-8 and demonstrated efficient binding to the ligand-binding pocket of HDAC isoenzymes. *In cellulo*, MAKV-8 significantly induced target protein acetylation, displayed cytostatic and cytotoxic properties, and triggered concomitant ER stress/protective autophagy leading to canonical caspase-dependent apoptosis. Considering the specific upregulation of selected HDACs in LSCs from CML patients, we investigated the differential toxicity of a co-treatment with MAKV-8 and imatinib in CML versus healthy cells. We also showed that beclin-1 knockdown prevented MAKV-8-imatinib combination-induced apoptosis. Moreover, MAKV-8 and imatinib co-treatment synergistically reduced BCR-ABL-related signaling pathways involved in CML cell growth and survival. Since our results showed that LSCs from CML patients overexpressed c-MYC, importantly MAKV-8-imatinib co-treatment reduced c-

MYC levels and the LSC population. . *In vivo*, tumor growth of xenografted K-562 cells in zebrafish was completely abrogated upon combined treatment with MAKV-8 and imatinib. Conclusions: Collectively, the present findings show that combinations HDAC inhibitor-imatinib are likely to overcome drug resistance in CML pathology.

Keywords: epigenetic regulation; tyrosine kinase inhibitor; computational docking; autophagy; apoptosis; endoplasmic reticulum stress

Background

Chronic myeloid leukemia (CML) is a clonal myeloproliferative malignancy accounting for 15% of newly diagnosed leukemia cases in adults (1). CML pathogenesis is mainly driven by the translocation t(9;22)(q34;11) between the breakpoint cluster region (*BCR*) and the Abelson murine leukemia viral oncogene homolog 1 (*ABL*) genes. The resulting fusion gene is translated into the oncogenic BCR-ABL protein with abnormal constitutive tyrosine kinase activity, which stimulates tumor cell proliferation and survival (2). Accordingly, BCR-ABL-positive CML patients are currently treated with tyrosine kinase inhibitors (TKis) including imatinib. TKis effectively block downstream BCR-ABL signaling pathways and eliminate most CML cells (3). Nevertheless, such therapeutic regimens are associated with severe side effects, as well as the development of TKi resistance, partly due to the reservoir of TKi-insensitive quiescent leukemic stem cells (LSCs) (4, 5). Therefore, novel therapeutic approaches are required to overcome these limitations and effectively cure CML patients. Combining imatinib with epigenetic modulators has emerged as a promising strategy for improving anti-leukemic therapy. Accordingly, TKi-HDACi combinations have been shown to induce synergistic anti-CML effects and LSC eradication (6).

Histone deacetylases (HDACs) catalyze the removal of acetyl groups from lysine residues

of various histones and non-histone protein targets. They thus act as important regulators of gene expression and are implicated in a plethora of cellular processes (7). Nowadays, it is established that aberrant activation or overexpression of HDAC isoenzymes trigger disruptions of the functional acetylation landscape, therefore contributing to the development of numerous cancers including CML (8, 9). Since HDACs are considered to be attractive targets for cancer prevention and therapy, pan-HDAC inhibitors (HDACis) represent a powerful class of epigenetically active therapeutic drugs that have already demonstrated promising anti-cancer activities in pre-clinical studies and are undergoing clinical trials for many cancers (10, 11). Four HDACis have achieved Food and Drug Administration approval: class I selective- (FK-228) or pan-HDACis [suberoylanilide hydroxamic acid (SAHA), PXD-101, and LBH-589] (12). In particular, SAHA has been repeatedly reported to enhance the cytotoxicity of various chemotherapeutic drugs including TKis such as imatinib (13), and dasatinib (14).

MAKV-8, characterized by a linker of 6-methylene units and a CAP group with arylisoxazole, has been initially reported to display an IC_{50} value of 2 pM towards HDAC3 and HDAC6 *in vitro*, and its anti-proliferative activity against pancreatic cancer cells was similar to that of SAHA (15). However, its HDAC-inhibitory properties were never tested *in cellulo* and the molecular mechanism through which MAKV-8 exhibits anti-cancer effects has not been characterized. In this study, we demonstrated that the pan-HDACi MAKV-8 displays anti-leukemic properties alone and in combination with imatinib, which are likely to lower the burden of resistance in CML pathology.

Results

In vitro HDAC inhibition by MAKV-8

First, we assessed the *in vitro* HDAC inhibitory potential of MAKV-8 using SAHA as a reference compound (Fig. 1). MAKV-8 inhibited total HDAC, as well as recombinant HDAC1

and HDAC6 deacetylase activities with IC_{50} values of 5.8, 2.6 and 11.4nM, respectively, suggesting the inhibition of multiple deacetylase activities. Notably, about 10% of the total HDAC activity remained with 2μM SAHA or 0.1μM MAKV-8 (Fig. 2A).

In silico prediction of the drug-likeness characteristics of MAKV-8

In silico predictions showed that MAKV-8 had low lipophilicity, as characterized by a miLog*P* coefficient below 5 and a $logD_{7.4}$ of 2.8, which is a major criterion for orally active drugs. This compound expressed a topological polar surface area of 142.79 combined with a molecular weight of 446.5 Da; further 4 and 10 hydrogen bond donors and acceptors, respectively, were recognized. These parameters imply free diffusion over the cell membrane. Interestingly, MAKV-8 displayed a favorable intestinal absorption parameter and plasma protein binding potential compared to PXD-101, predicting a good bioavailability (Table 1). Altogether, MAKV-8 displayed favorable drug-likeness parameters and a low predicted toxicity risk, similar to FDA-approved pan-HDACis.

Table 1: *In silico* predictions of MAKV-8 druglikeness and oral bioavailability.

Method	**Parameter (unit)**	**Values**				
		Theoretical	**MAKV-8**	**SAHA**	**PXD-101**	**LBH-589**
Lipinski's rule of five	Volume ($Å^3$)	NA	411.02	255.64	266.11	330.62
	miLog*P*	≤5	3.49	2.47	2.19	3.19
	MW (Da)	≤500	446.5	264.32	318.35	349.43
	n-OHNH	≤5	4	3	3	4
	n-ON	≤10	10	5	6	5
Ghose filter	n-atoms	20≤ x ≤70	32	19	22	26
Veber's Rule	n-rotb	≤10	12	8	5	7
	TPSA ($Å^2$)	≤140	142.79	78.42	95.5	77.14

Absorption	BBBP	0.1≤ MA ≤2	0.12	0.22	0.18	1.16
	IA (%)	≥70	76.68	84.53	89.94	89.23
	PPB (%)	<90	82.82	72.16	94.26	78.3
Toxicity	Rat	NA	Negative	Negative	Negative	Negative

BBBP: blood-brain barrier penetration; IA: intestinal absorption; MA: middle absorption; miLogP: octanol-water partition coefficient; MW: molecular weight; n-atoms: number of atoms; n-OHNH: number of hydrogen bond donors; n-ON: number of hydrogen bond acceptors; n-rotb: number of rotatable bonds; NA: not applicable; PPB: plasma protein binding; TPSA: topological polar surface area.

MAKV-8 efficiently binds to the ligand-binding pocket of HDAC isoenzymes

A docking simulation on a panel of human HDAC isoforms frequently associated with tumorigenesis indicated that the hydroxamate group and hydrophobic linker region of MAKV-8 established efficient interactions in the ligand-binding pocket of all HDAC isoenzymes, whereas its CAP group interacted with loops around the ligand-binding pocket (Fig. 2B; Additional file 1: Figure S1). Qualitative molecular analyses demonstrated that MAKV-8 displayed more potent binding affinities than SAHA for all tested HDACs, with average values of -7.1 and -6.2 kcal/mol, respectively, and suggested a moderately different HDAC-inhibitory profile between MAKV-8 and SAHA since binding affinity energy values were similar for certain HDACs and distinct for others (Table 2).

Table 2: Qualitative molecular docking of MAKV-8 against selected HDACs[a].

HDAC (PDB code)	MAKV-8	SAHA
HDAC1 (4BKX)	-6.7	-5.4
HDAC2 (4LY1)	-7.2	-6.7

HDAC3 (4A69)	-6.9	-6.5
HDAC4 (2VQM)	-7.7	-5.6
HDAC6 (5EDU)	-7.2	-6.1
HDAC7 (3C10)	-7.1	-6.0
HDAC8 (3EW8)	-7.0	-6.9
Average	-7.1	-6.2

[a]Binding affinity energy values (kcal/mol) for the indicated Protein Data Bank (PDB) codes were calculated using AutoDock Vina program. SAHA was used as a reference HDACi.

MAKV-8 significantly induced target protein acetylation

To determine whether MAKV-8 acted as an HDACi *in cellulo*, we next analyzed its effect compared to SAHA on the acetylation of histone H4, a nuclear substrate of class I, II, and IV HDACs, and α-tubulin, a cytoplasmic substrate of HDAC6. In K-562 cells, MAKV-8 strongly induced α-tubulin and histone H4 acetylation in a concentration-dependent manner, starting from 5 and 1μM, respectively (Fig. 2C). SAHA increased such protein acetylation in a similar manner to that observed with MAKV-8, albeit at lower concentrations. Noteworthy, EC_{50} values suggested that MAKV-8 displayed increased selectivity against nuclear HDACs targeting histone H4 compared to HDAC6 targeting α-tubulin, whereas SAHA acted similarly on both targets (Table 3). Next, kinetic analysis of α-tubulin and histone H4 acetylation status showed a rapid and time-dependent increase in protein acetylation beginning at 2h after MAKV-8 treatment, with a peak occurring between 8 and 24h. With SAHA, we observed similar effects for acetyl-α-tubulin, but histone H4 acetylation was maintained at a later time (Fig. 2D).

Table 3: EC_{50} values of MAKV-8 and SAHA toward acetylated targets.

Target	EC_{50} (μM)	
	MAKV-8	**SAHA**
Acetyl α-tubulin	12.1 ± 0.9	1.9 ± 0.8
Acetyl histone H4	5.9 ± 1.4	2.6 ± 0.2

Data are presented as the mean ± standard deviation of the effective concentration that induces half-maximal acetylation of protein targets (EC_{50}). Values were calculated after western blot quantification from at least three independent experiments. Concentrations of compounds near the EC_{50} values have been used for subsequent experiments.

MAKV-8 displayed cytotoxic properties in CML cells

We further evaluated whether MAKV-8 treatments exert anti-CML properties. MAKV-8 inhibited the growth of CML cell lines (*i.e.*, K-562, KBM-5, and MEG-01) starting at about 3µM, and cell death was triggered beginning at 10µM after 48h of treatment (Fig. 2E). Accordingly, the replicative ability of CML cells in a 3D model was strongly reduced by MAKV-8, beginning at 5µM in K-562 and MEG-01 cells and 10µM in KBM-5 cells (Fig. 2F). Notably, MAKV-8 exposure also enhanced α-tubulin and histone H4 acetylation in KBM-5 and MEG-01 cells, which generalized our findings concerning MAKV-8-mediated inhibition of multiple HDAC activities in CML cells (Fig. 2G).

MAKV-8 derivatives were less potent than their parent compound

To gain insight into the relationship between MAKV-8 structure and deacetylase-inhibiting activities, we tested the HDAC-inhibitory potential of four MAKV-8 derivatives (Fig. 1). *In vitro*, IC_{50} values for MAKV-6 and -7 against total HDAC activities were in the low µM range (Table 4), indicating that compounds were less potent than MAKV-8, whereas MAKV-10 and -12 failed to inhibit HDAC activities with concentrations up to 100µM (Additional file 1: Figure

S2). Compared to MAKV-8, docking analysis showed weaker binding affinities of the derivatives to HDAC6; MAKV-6 and -7 could not bind properly to its ligand-binding pocket, whereas MAKV-10 and -12 moderate binding did not allow suitable interactions with the zinc atom (Fig. 2H; Table 5). We confirmed these results in K-562 cells by showing that MAKV-6 and -7 increased histone H4 acetylation only at the highest concentrations and failed to increase α-tubulin acetylation, suggesting that HDACs targeting histones were preferentially inhibited, but with a much lower potency than MAKV-8. Conversely, MAKV-10 and -12 did not augment protein target acetylation levels even at the highest concentrations tested (Fig. 2I). After 48h of treatment with MAKV-8 derivatives, we detected a reduction in K-562 cell proliferation starting at 5µM MAKV-6 or 10µM MAKV-7 and a decrease of cell viability starting at 25µM MAKV-6 or -7. In contrast, neither MAKV-10 nor -12 impacted K-562 cell proliferation and viability (Fig. 2I), suggesting that MAKV-8 anti-cancer effects are associated with the inhibition of HDACs targeting histones.

Table 4: *In vitro* HDAC-inhibitory activity of MAKV-8 and derived compounds.

Compounds	IC_{50} values against total HDAC activity (nM)
MAKV-6	1,050 ± 220
MAKV-7	22,000 ± 25,200
MAKV-8	5.8 ± 3.8
MAKV-10	>100,000
MAKV-12	>100,000

Data are presented as the mean ± standard deviation of the concentration inhibiting 50% (IC_{50}) of the HDAC activity. Values were calculated from at least three independent experiments, or two independent experiments for MAKV-10 and MAKV-12. HDAC: histone deacetylase.

Table 5: Qualitative molecular docking of MAKV-8 derivatives against HDAC6.

Compounds	Binding affinity (kcal/mol)[a]
MAKV-6	-5.9
MAKV-7	-6.4
MAKV-8	-7.2
MAKV-10	-6.9
MAKV-12	-6.1

[a]Binding affinity energy values for Protein Data Bank (PDB) code 5EDU were calculated using AutoDock Vina program.

MAKV-8 induced cell cycle arrest and apoptotic cell death in CML cells

Next, we further characterized MAKV-8 anti-cancer properties. Since MAKV-8 treatment hampered CML cell proliferation, we studied its effects on cell cycle distribution, which revealed a time-dependent accumulation of cells in the G1 phase, which was comparable to results obtained with SAHA (Fig. 3A).

Nuclear morphology analyses showed that MAKV-8 mainly triggered a time- and dose-dependent increase in apoptotic cells, which was completely prevented upon treatment with the pan-caspase inhibitor z-VAD-FMK (Fig. 3B). In addition, cleavage of pro-caspases 3, 7, 8 and 9, and poly (ADP-ribose) polymerase (PARP)-1 was consistent with caspase-dependent apoptosis induction (Fig. 3C).

MAKV-8 triggered ER stress, autophagic flux, and DNA damage

Since the inhibition of cell cycle progression could result from endoplasmic reticulum (ER) stress-induced unfolded protein response (UPR) activation (16), we analyzed 78 kDa glucose-regulated protein (GRP78) expression levels in K-562 cells upon treatments with MAKV-8

compared to thapsigargin. GRP78 expression was upregulated after 8h of treatment and accompanied by increased ATF6 expression, as well as phosphorylated protein kinase RNA-like ER kinase (PERK) and eukaryotic initiation factor (eIF)2α levels (Fig. 4A). Accordingly, we also observed enhanced DNA damage-inducible transcript (DDIT)3 mRNA expression after 24h (Fig. 4B) and X-box binding protein (XBP)1 mRNA splicing after 4h (Fig. 4C) upon treatment with 10µM MAKV-8. Altogether, results demonstrate that MAKV-8 activates the UPR signaling.

Modulations of the autophagic machinery, which can be activated by the UPR pathways (17), may contribute to HDACi anti-cancer effects (18). Cell morphology analyses revealed that, unlike control cells, MAKV-8-treated cells displayed a swollen cytoplasm enriched with numerous vacuoles of various sizes (Fig. 4D). Additionally, Cyto-ID®-stained cell quantification showed that the percentage of cells displaying autophagic vesicles, as indicated by the dotted fluorescent pattern, was three times higher in MAKV-8-treated cells compared to control cells presenting a homogeneous signal (Fig. 4E). Furthermore, MAKV-8 treatment stimulated microtubule-associated protein 1 light chain (LC)3-I to LC3-II conversion and reduced p62/sequestosome (SQSTM)1 expression levels. Upon addition of late-phase autophagy inhibitor bafilomycin A1, LC3-II and p62/SQSTM1 accumulation was further enhanced, suggesting that MAKV-8 induced autophagy (Fig. 4F). Accordingly, the study of cellular structures by transmission electron microscopy showed a more extensive autophagocytic vacuolization in MAKV-8-treated cells compared to untreated cells (Fig. 4G).

HDACi treatments reportedly cause DNA damage, including double strand breaks, which partly underlies apoptosis induction (19). Accordingly, we showed that 5µM MAKV-8 enhanced H2AX phosphorylation (γH2AX) levels after 24h; this effect was more pronounced with 10µM MAKV-8 (Fig. 4H), although less important than that observed with cisplatin (20).

Modulation of HDAC expression profiles in CML patients

Despite the outstanding therapeutic results obtained with TKis in CML, the occurrence of imatinib resistance in over 30% of CML patients necessitates the discovery of additional therapeutic approaches. Interestingly, transcriptomic analyses of CML patient data revealed that HDAC1 and HDAC2 mRNA expression levels were significantly upregulated and associated with a trend towards increased HDAC3 mRNA levels in LSCs compared to healthy stem cells (HSCs) (Fig. 5A). The importance of HDAC1 and HDAC2 in tumor cell survival provides a good rational for treating CML cells with imatinib in combination with pan-HDACis (21).

MAKV-8 combined with imatinib displayed synergistic pro-apoptotic activity in imatinib-sensitive and -resistant CML cells

Considering computational docking results, we investigated the anti-leukemic potential of co-treatments with subtoxic concentrations of MAKV-8 and imatinib in imatinib-sensitive and -resistant CML cells. First, we tested whether treatment with imatinib affected MAKV-8-mediated HDAC inhibition. In all CML cells, α-tubulin acetylation was similarly induced after a 24h-exposure to MAKV-8-imatinib co-treatment compared to MAKV-8 treatment alone, whereas acetylated histone H4 levels were further enhanced. In contrast, cells treated with SAHA-imatinib displayed decreased and increased levels of acetylated α-tubulin and histone H4, respectively, compared to SAHA alone (Fig. 5B).

We then evaluated the effect of combinations on CML cell viability. In K-562 cells, MAKV-8-imatinib-mediated reduction in viability was greater than that induced by compounds alone, with a 75%-decrease in living cells after treatment with 10μM MAKV-8 combined with imatinib (Fig. 5C). Combination index (CI) values below 1 indicated synergism for each MAKV-8 concentration combined with imatinib, with the highest MAKV-8 concentration

conferring the maximal effect (Table 6). Additionally, MAKV-8-imatinib co-treatment triggered mitochondrial membrane potential (MMP) loss and increased Annexin V-positive cell proportion, reaching approximately 83% of cells displaying low MMP and Annexin V positivity, respectively, after co-treatments with 10µM MAKV-8 compared to 7 and 20% in untreated cells (Fig. 5D, E). Such co-treatment also caused a stronger cleavage of caspases 3, 8, 9, and PARP-1, indicating more important apoptosis induction than observed with single treatments (Fig. 5F).

We generalized our findings by showing that MAKV-8-imatinib combination also had a synergistic effect on KBM-5 and MEG-01 cell viability, with a reduction of 88 and 69% of living cells, respectively, following co-treatments with the highest MAKV-8 concentration (Fig. 5G, upper panel, Table 6). Additionally, caspase 3 and PARP-1 cleavage highlighted a greater induction of apoptosis in MAKV-8-imatinib co-treated KBM-5 and MEG-01 cells (Fig. 5G, lower panel). Comparatively, co-treatments with 2µM SAHA presented similar results to those obtained after co-treatment with the lowest MAKV-8 concentration in all CML cells (Fig. 5C, G).

In imatinib-resistant KBM-5 (KBM-5R) cells, which began to die in response to a dose between 10 and 25µM imatinib (Additional file 1: Figure S3), the decrease in cell viability was further enhanced by co-treatments compared to treatments with either drug alone, and a synergistic loss of 65% of living cells occurred after a combination with 2.5µM MAKV-8 and 10µM imatinib (Fig. 5H, upper panel; Table 6). Accordingly, PARP-1 cleavage, which indicated the activation of apoptotic pathways, was stronger in co-treated KBM-5R cells (Fig. 5H, lower panel).

Table 6: Combination index (CI) values for treatments with combined MAKV-8-imatinib in imatinib-sensitive and -resistant CML cells.

Cell line	MAKV-8 (μM)	Imatinib (μM)	CI (48 h)[a]
K-562	5	0.25	0.42 ± 0.13
	10	0.25	0.28 ± 0.14
KBM-5	1	2.5	0.46 ± 0.06
	2.5	2.5	0.05 ± 0.03
MEG-01	5	0.25	0.77 ± 0.16
	10	0.25	0.37 ± 0.07
KBM-5R	1	10	1.42 ± 0.58
	2.5	10	0.78 ± 0.16

[a]CI values correspond to the mean ± standard deviation of three independent Hoechst-propidium iodide staining experiments. CML: chronic myeloid leukemia.

Imatinib-MAKV-8 co-treatment induced differential toxicity in healthy cell models compared to CML cells

Next, we evaluated the effect of MAKV-8-imatinib co-treatments on the viability of healthy cell models. In peripheral blood mononuclear cells (PBMCs), we observed a moderate effect with MAKV-8 treatment either alone or in combination, with a maximum decrease of 30% of viable cells after 48h, whereas imatinib alone failed to trigger any cell mortality (Fig. 5I, upper panel; Additional file 1: Figure S4). These results were comparable to those of SAHA (Additional file 1: Figure S4). Although RPMI-1788 cells underwent a reduction of about 55% of living cells following a 48h-treatment with 10µM MAKV-8, the decrease in cell viability was not further enhanced upon addition of imatinib (Fig. 5I, lower panel). Consequently, the ratio of cell death induced by MAKV-8-imatinib co-treatments in cancer versus normal cells attested of a stronger toxicity against cancer cells (Table 7). Finally, MAKV-8 neither alone nor in co-treatments elicited any significant cytotoxicity in platelets (Fig. 5I, right panel; Additional file 1: Figure S4). Altogether, combination of MAKV-8 with imatinib displayed a promising safety profile for healthy cells.

Finally, we investigated the ability of CML cell lines pre-treated with MAKV-8 for 8h to form colonies in the presence of experimentally selected imatinib concentrations (Additional file 1: Figure S5). The combinations exerted more potent effects on reducing colony formation than agents alone in both imatinib-sensitive and -resistant CML cells (Fig. 5J).

Table 7: Selectivity ratio of MAKV-8-imatinib co-treatment for cancer cells versus healthy models.

CML cells	Selectivity ratio	
	PBMCs	RPMI-1788
K-562	5.8	3.9
KBM-5	8.5	9.2
MEG-01	2.2	1.5

Values were calculated from the percentage of cancer cell death *versus* healthy cell death from three independent experiments. PBMCs: peripheral blood mononuclear cells.

Beclin-1 knockdown partially prevented MAKV-8-imatinib combination-induced apoptosis

Since MAKV-8 treatments induced autophagy, we tested whether this process would be implicated in co-treatment-induced synergistic cell death. We knocked down the gene coding for beclin-1 (*BECN1*) (Fig. 6A), and observed after 48h of MAKV-8-imatinib treatment that the proportion of viable K-562 cells was significantly increased from 15 and 20% in cells transfected with or without non-targeting small interfering RNA (siRNA), respectively, to 40% in *BECN1*-silenced cells (Fig. 6B). Finally, decreased PARP-1 cleavage in cells transfected with siRNA targeting BECN1 further confirmed reduced apoptotic rate (Fig. 6B).

MAKV-8 and imatinib co-treatment reduced BCR-ABL-related pathways

BCR-ABL-related signaling pathways result in CML cell growth and survival (22). Accordingly, we examined the effects of MAKV-8-imatinib co-treatment on the expression and phosphorylation of BCR-ABL and downstream targets in K-562 cells. Although such combination did not impact BCR-ABL expression, it led to a drastic decrease in its phosphorylation accompanied by a similar effect on signal transducer and activator of transcription (STAT)5 phosphorylation. Notably, MAKV-8 further downregulated STAT5 protein levels and provoked a striking decrease in c-MYC expression, which was maintained by co-treatment with imatinib. Conversely, myeloid cell leukemia (MCL)-1 expression was not markedly impacted by the combination due to oppositional effects exhibited by each drug (Fig. 6C). Despite a MAKV-8-mediated upregulation in BCR-ABL expression, treatment with MAKV-8 and imatinib decreased BCR-ABL phosphorylation in KBM-5, MEG-01, and KBM5-R cells (Fig. 6D). In all CML cell lines, treatments with SAHA, alone or in combination with imatinib, exhibited results comparable to that of the highest MAKV-8 concentration (Fig. 6C, D).

MAKV-8 and imatinib co-treatment reduced the LSC population and inhibited CML cell growth *in vivo*

The oncogenic transcription factor c-MYC reportedly plays an important role in LSC survival, which is implicated in TKi resistance and relapse in CML patients (23). Moreover, bioinformatic analysis revealed that c-MYC mRNA expression levels were significantly upregulated in LSCs versus HSCs (Fig. 6E).

Since MAKV-8 strongly reduced c-MYC expression (Fig. 6C), we further evaluated whether MAKV-8 treatment, with and without imatinib, could decrease the aldehyde dehydrogenase $(ALDH)^+$ LSC fraction in K-562 cells. The $ALDH^+$ cell percentage was reduced

from 50% in untreated cells to 24 and 30% in MAKV-8- and imatinib-treated cells, respectively, and was further decreased to 15% after MAKV-8-imatinib co-treatment. In contrast, SAHA failed to reduce the $ALDH^+$ cell proportion. When cells were co-treated with SAHA and imatinib, the percentage of $ALDH^+$ cells decreased to 30%, indicating the MAKV-8-imatinib combination was more efficient to reduce LSC population (Fig. 6F).

We finally tested our findings in an *in vivo* setting and demonstrated that combining MAKV-8 with imatinib fully abrogated tumor formation in zebrafish xenografted with K-562 cells, whereas single agents were unable to significantly reduce tumor volumes (Fig. 6G; Additional file 1: Figure S6).

Discussion

In vitro, MAKV-8 acts as a 10-times more potent pan-HDACi than SAHA. Accordingly, docking studies suggest efficient MAKV-8 interactions with the ligand-binding pockets of all tested HDACs, with higher binding affinity in comparison to SAHA. Interestingly, EC_{50} values for MAKV-8 and SAHA towards acetylated protein targets, as well as the different modulations of compounds-mediated HDAC inhibition upon imatinib addition suggest distinct HDAC-inhibitory properties. Compared to SAHA, MAKV-8-mediated acetylation of specific histone and non-histone proteins may result in improved HDACi-related anti-cancer activities. Despite a fairly good overall *in silico* profile, some structural modifications could be necessary to improve MAKV-8 drug-likeness parameters. Nevertheless, the importance of the hydroxamate group and the linker chain length for HDAC-inhibitory activities was confirmed by the results obtained with MAKV-8 derivatives (15). Notably, *in silico* predictions should be critically considered due to potentially different pharmacokinetic properties of compounds *in vivo*. Collectively, MAKV-8 appears to be an attractive drug candidate for further consideration in CML therapies, especially considering that the inhibition of HDAC1 and HDAC2, upregulated

in LSCs versus HSCs from patients, strongly impacts the transcription of proteins essential for tumor cell survival (21),

MAKV-8 treatment triggers ER stress, as evidenced by the upregulation of proteins related to UPR. Since HDACs have been described to modulate GRP78 acetylation (24), MAKV-8-mediated HDAC inhibition could result in GRP78 acetylation and selective UPR activation, as similarly reported for other HDACi (25). Furthermore, MAKV-8-mediated inhibition of HDAC6, which is important for misfolded protein clearance, could thus lead to the accumulation of protein aggregates and ER stress induction (26). Simultaneously to ER stress, MAKV-8 induces autophagy. Pan-HDACi have been shown to promote the initiation and block the maturation phases of autophagy by inhibiting class I-IIa and class IIb HDACs, respectively (27). Autophagy may also participate in imatinib sensitization, as downregulation of pro-autophagic beclin-1 expression partly prevents co-treatment-induced cell death. Conversely, one study showed that impairing autophagy significantly enhanced SAHA anti-cancer activity (28). Finally, MAKV-8 treatment weakly induces the appearance of double strand breaks at a time where no cell death is observed. Since H2AX phosphorylation does not occur in concomitance with histone acetylation, as previously reported (29), MAKV-8-mediated accumulation of excessive DNA damage may result from ER stress and/or autophagy, and this accumulation could lead to apoptosis activation (30). Altogether, our work does not exclude that MAKV-8-related mechanisms could be implicated in its anti-cancer effects, but further studies are required.

In imatinib-sensitive and -resistant BCR-ABL-positive CML cells, synergistic apoptotic cell death is triggered upon MAKV-8-imatinib co-treatment. Accordingly, concomitant treatment with SAHA and TKi has previously been reported to synergistically induce apoptosis in CML cell lines (13, 14). Furthermore, MAKV-8 combined with imatinib also impaired tumor growth of xenografted CML cells in zebrafish. Notably, moderate cytotoxicity was observed in

healthy models exposed to the same co-treatment. A weak toxicity towards normal cells compared to cancerous cells has also been described for many other HDACi (31, 32). Collectively, MAKV-8 could provide a non-toxic strategy for overcoming imatinib resistance, hence providing a rational basis to further study the potency of MAKV-8-imatinib combination for CML therapy.

Mechanistically, lowered BCR-ABL kinase activity is observed after MAKV-8-imatinib co-treatment, which most likely explains the reduction in STAT5 phosphorylation, as well as the drop in c-MYC and MCL-1 expression. Previous reports indicate that SAHA downregulates BCR-ABL mRNA and protein levels in CML cells (13), which could be implicated in synergistic anti-leukemic interactions involving TKis (14). By inhibiting HDAC6, pan-HDACis could disrupt the association of HSP90α with BCR-ABL, provoking its poly-ubiquitination and proteasomal degradation (33). Surprisingly, MAKV-8 rather augments BCR-ABL expression in our cell models, implying the involvement of other regulatory mechanisms. Furthermore, downstream BCR-ABL targets play a critical role in CML pathogenesis (34-36). Similar to our observations, HDACi-mediated potentiation of TKi cytotoxicity has been related to STAT5 inhibition in BCR-ABL-positive cells (37). As previously described, HDACi-related apoptosis induction in CML cells could be enhanced by imatinib-mediated downregulation of anti-apoptotic MCL-1 expression, which was upregulated by MAKV-8 (38). In addition, c-MYC has been recently reported as an important target for selectively eliminating CML LSCs (39). Accordingly, human LSCs displayed increased c-MYC mRNA levels compared to HSCs. Besides lowering c-MYC expression, MAKV-8 treatment potently decreased the $ALDH^+$ cell proportion, which was further enhanced upon co-treatment with imatinib. Altogether, combining imatinib with MAKV-8, which targets key hematopoietic stem cell molecular effectors, may represent an effective strategy to overcome

LSC resistance to TKis, thereby offering the opportunity to improve disease outcomes for CML patients.

Conclusions

We found that compound MAKV-8 acted as a potent pan-HDACi *in vitro* and in various CML cell lines. Furthermore, MAKV-8 alone or in combination with imatinib displayed promising anti-cancer properties in imatinib-sensitive and -resistant BCR-ABL-positive CML cells, whereas only a very moderate toxicity was noted in healthy cell models exposed to the same co-treatment. Mechanistically, the combination MAKV-8-imatinib reduced BCR-ABL expression and phosphorylation, as well as the expression of downstream targets playing a critical role in CML proliferation and survival. In addition, such therapeutic approach effectively decreased LSC population. Altogether, the present findings suggest that treatment with MAKV-8 contributes to a strong sensitization of imatinib-sensitive and -resistant CML cells including LSCs towards imatinib cytotoxicity, hence providing a rational basis to further study the potency of MAKV-8 and imatinib as a combination therapy against CML.

Methods

Cell culture and reagents

The human CML cell lines K-562 (DSMZ Cat# ACC-10, RRID: CVCL_0004) and MEG-01 (DSMZ Cat# ACC-364, RRID: CVCL_0425) were purchased from Deutsche Sammlung für Mikroorganismen und Zellkulturen (Braunschweig, Germany). Human CML KBM-5 cells were kindly provided by Dr. Bharat B. Aggarwal. Imatinib-resistant KBM-5 (KBM-5R) cells were established as previously described (40). The K-562, MEG-01 and KBM-5 cell lines have been authenticated in 2014 using the LGC Standards Cell Line Authentication service (Teddington, United Kingdom). All cells were maintained at 37°C in a humid atmosphere and

5% CO_2 in a culture medium supplemented with 10% heat-inactivated fetal calf serum (FCS; BioWhittaker ®, Lonza, Verviers, Belgium) and 1% (v/v) antibiotic (streptomycin and penicillin) and antimycotic (BioWhittaker®). K-562 and MEG-01 cells were cultured in RPMI 1640 medium (BioWhittaker®). KBM-5 and KBM-5R cells were cultured in IMDM medium (BioWhittaker®).

PBMCs were isolated from the blood of healthy adult human donors obtained from the Red Cross (Luxembourg, Luxembourg) and purified as previously reported (41). Human RPMI-1788 cells (ATCC Cat# CCL-156, RRID: CVCL_2710), which were derived from B lymphocytes, were purchased in 2017 from the American Type Culture Collection (Manassas, Virginia, USA). Platelets from healthy adult human donors were provided by the Red Cross. All healthy models were cultured at 37°C in a humid atmosphere and 5% CO_2 in RPMI 1640 medium (BioWhittaker®) supplemented with 0, 10, or 20% heat-inactivated FCS (BioWhittaker®) for platelets, PBMCs, and RPMI-1788 cells, respectively, and each containing 1% (v/v) antibiotic-antimycotic (BioWhittaker®).

All cell lines have been monthly tested for mycoplasma contamination.

Compound MAKV-8 was synthetized as previously described by Kozikowski *et al*. (compound 3) (15), and compounds MAKV-6, -7, -10, and -12 were derived from the reported synthetic protocol as shown in Additional file 1: Figure S7. The following additional compounds were used in this study: cisplatin in saline solution from Teva Pharmaceutical Industries Ltd. (Wilrijk, Belgium), imatinib and thapsigargin from Sigma-Aldrich (Bornem, Belgium), SAHA from Cayman Bio-connect (Huissen, Netherlands), and z-VAD-FMK from Millipore (Merck, Brussels, Belgium). Except for cisplatin, all compounds were dissolved in dimethylsulfoxide (DMSO).

Computational analysis of public chronic myeloid leukemia datasets

The gene expression microarray datasets E-MTAB-2581 (42) and GSE97562 (43) were downloaded from the ArrayExpress database (44) and the Gene Expression Omnibus repository, respectively. Datasets were normalized using the Robust Multichip Average algorithm from the oligo R package (version 1.48.0) (45) and batch corrected using the function *removeBatchEffect* from the limma R package (version 3.40.2) (46). The *ggboxplot* function from the ggpubr package (version 0.2.1) (47) was used to draw the boxplots in R 3.6.0 (48) and RStudio (49).

In vitro HDAC activity assay

In vitro HDAC activities were measured as previously described (50, 51). IC_{50} values against the various HDAC activities were determined using nonlinear regression in Prism 8.0 software (GraphPad Software, Inc., La Jolla, CA, USA).

Docking studies

Docking studies were carried out as previously reported (52) using the Protein Data Bank (PDB) codes 4BKX, 4LY1, 4A69, 2VQM, 5EDU, 3C10, and 3EW8 corresponding to HDAC1, HDAC2, HDAC3, HDAC4, HDAC6, HDAC7 and HDAC8, respectively. MAKV-6, -7, -8, -10 and -12, and SAHA were drawn using ChemDraw Professional software version 15.0 (PerkinElmer Informatics).

Prediction of _in silico_ drug-likeliness parameters

The web-based Molinspiration Cheminformatics (http://www.molinspiration.com/products.html) and PreADMET ver2.0 (https://preadmet.bmdrc.kr) programs were used to compute compound drug-likeness parameters.

Cell viability and proliferation test

Cell viability and proliferation were evaluated using the Trypan Blue exclusion method (BioWhittaker ®). Cells were processed using a semi-automated image-based cell analyzer (Cedex XS Innovatis, Roche, Luxembourg, Luxembourg), which provided the cell number as well as cell viability based on the fraction of trypan blue-positive cells.

For colony formation assays, 1000 cells were grown in 1mL of semi-solid methylcellulose medium (Methocult H4230, StemCell Technologies Inc., Grenoble, France) supplemented with 10% heat-inactivated FCS (BioWhittaker ®) in 12-well plates. Colonies were detected after 10 days of culturing by adding 5mg/mL 3-(4,5-dimethylthiazol-2-yl)-2,5-diphenyltetrazoliumbromide (MTT) reagent (Sigma-Aldrich) and incubating for 15min at 37°C. Pictures were taken with the GelDoc XR+ System (BioRad, Temse, Belgium), and quantifications were conducted using Image J software (U.S. National Institute of Health, Bethesda, MD, USA).

Protein extractions and western blotting analysis

Cells were lyzed in 10% (v/v) Mammalian Protein Extraction Reagent solution (MPER®; Thermofisher, Erembodegen, Belgium) supplemented with 1× protease inhibitor cocktail (Complete EDTA-free, Roche) according to the manufacturer's instructions. Histone enrichment was performed in acidic conditions as previously described (53). The protein concentration was determined using the Bradford assay (BioRad).

Western blotting was performed as previously described (51) using the following primary antibodies: acetylated α-tubulin (sc-23950, RRID: AB_628409, 1/1000), ATF6 (sc-166659, RRID: AB_2058901, 1/250), c-ABL (sc-23, RRID: AB_626775, 1/1000), caspase 3 (sc-56053, RRID: AB_781826, 1/1000), GRP78 (sc-13968, RRID: AB_2119991, 1/1000), p62/SQSTM1

(sc-28359, RRID: AB_628279, 1/1000), and phosphorylated PERK (sc-32577, RRID: AB_2293243, 1/1000) from Santa Cruz Biotechnology (Boechout, Belgium); phosphorylated H_2AX (05-636, RRID: AB_2755003, 1/500), acetylated histone H4 (06-866, RRID: AB_310270, 1/50000), and histone H1 (05-457, RRID: AB_310843, 1/2000) from Millipore; α-tubulin (CP06, RRID: AB_2617116, 1/5000) from Calbiochem; β-actin (A5441, RRID: AB_476744, 1/20000) and LC3 (L7543, RRID: AB_796155, 1/1000) from Sigma-Aldrich; beclin-1 (3738, RRID: AB_490837, 1/1000), caspase 7 (9494, RRID: AB_2068141, 1/1000), caspase 8 (9746, RRID: AB_2275120, 1/1000), caspase 9 (9502, RRID: AB_2068621, 1/1000), eIF2α (9722, RRID: AB_2230924, 1/2000), MCL-1 (4572, RRID: AB_2281980, 1/1000), PARP-1 (9542, RRID: AB_2160739, 1/1000), PERK (3192, RRID: AB_2095847, 1/1000), phosphorylated BCR (3901, RRID: AB_2063779, 1/1000), phosphorylated eIF2α (3898, RRID not available, 1/2000), STAT5 (9363, RRID: AB_2196923, 1/5000), and phosphorylated STAT5 (9351, RRID: AB_2315225, 1/1000) from Cell Signaling (Leiden, Netherlands); and c-Myc (51-1485GR, RRID: AB_2148606, 1/250) from BD Biosciences (San Jose, CA, USA). Corresponding secondary antibodies were obtained from Santa Cruz Biotechnology. Western blot quantifications were performed with the ImageQuant TL software (GE Healthcare), and corresponding fold change values reported to control are indicated underneath western blot pictures, unless otherwise specified. The EC_{50} values, which represent 50% of the maximum effect, were calculated using Prism 8.0 software.

Cell cycle analyses

Cells were fixed at 4°C for 1h with 70% ethanol and stained for 20min with 1µg/mL propidium iodide in 1× PBS supplemented with 100µg/mL RNase A (Roche). Stained samples were processed through a cytometer (FACS Calibur, BD Biosciences), and data were recorded statistically (10,000 events/sample) using the CellQuest Pro software (BD, Biosciences). The

percentage of cells in each phase of the cycle was finally determined by the Dean-Jet-Fox algorithm using the Flow-Jo 8.8.5 software (Tree Star, Inc., Ashland, OR, USA).

Cell death assessment

Nuclear morphology was evaluated under an IX81 (MT10) fluorescent microscope (Olympus, Aartselaar, Belgium) using the Cell^M software on cells incubated with 1µg/mL Hoechst 33342 (Invitrogen, Tournai, Belgium) for 15min at 37°C and 1µg/mL propidium iodide (Sigma-Aldrich).

Phosphatidylserine exposure was evaluated using the FITC Annexin V Apoptosis Detection Kit I (BD Biosciences) according to the supplier's instructions. Stained samples were processed through a cytometer (FACS Calibur, BD Biosciences), and data were recorded statistically (10,000 events/sample) using the CellQuest Pro software (BD, Biosciences). Data were analyzed using the Flow-Jo 8.8.5 software.

Determination of mitochondrial membrane potential

The MMP was assessed by staining with MitoTracker® Red CMXRos (Invitrogen) according to the manufacturer's protocol. Stained samples (20,000 events/sample) were processed through a cytometer (FACS Calibur, BD Biosciences).

Assessment of gene expression

The total RNA was extracted with the NucleoSpin® RNA Plus Kit (Macherey-Nagel, Hoerdt, France) according to manufacturer's instructions. Reverse transcription and real-time PCR were performed as previously described (54). The following primers (Eurogentec, Liège, Belgium) were used: β-actin (forward 5′-CTCTTCCAGCCTTCCTTCCT-3′, reverse 5′-

AGCACTGTGTTGGCGTACAG-3′); DDIT3 (forward 5′-TGGAAGCCTGGTATGAGGAC-3′, reverse 5′-AAGCAGGGTCAAGAGTGGTG-3′).

XBP1 splicing analysis was performed by end-point PCR as described previously (55) using the following primers (Eurogentec; forward: 5′- GGAGTTAAGACAGCGCTTGG -3', reverse: 5'- ACTGGGTCCAAGTTGTCCAG -3′).

Morphological analysis

After staining cells with the Diff-Quick Stain Kit (Dade Behring S.A., Brussels, Belgium), morphological analyses were performed as previously described (54).

Visualization of autophagic vesicles

For fluorescence microscopy, the Cyto-ID® Autophagy Detection Kit (Enzo Life Science) was used according to the manufacturer's instructions. Stained cells were visualized under an IX81 (MT10) fluorescent microscope.

Transmission electron microscopy was performed as previously described (56).

Evaluation of cellular ALDH activity

Cellular ALDH activity was assessed using the ALDEFLUOR™ kit (StemCell Technologies Inc.) according to the manufacturer's procedure. Diethylaminobenzaldehyde, a specific inhibitor of ALDH activity, was used to differentiate cells with low or high ALDH activity. Stained samples (100,000 events/sample) were processed through a cytometer (FACS Calibur, BD Biosciences).

Transfections

Transfections were carried out with 1.5µL HiPerFect Transfection reagent (Qiagen, Venlo, Netherlands) and 1nM siRNAs (Qiagen) either targeting the human beclin-1 gene [Hs_BECN1_2 (SI00055580)] or non-targeting (AllStars Negative Control) as described elsewhere (57). Treatment compounds were added to the culture medium 24h post-transfection.

Zebrafish cancer cell xenografts

Cancer xenograft assays in zebrafish were performed as previously described (58) using cells stained with 2µM CM-Dil (Invitrogen) and diluted in 1× PBS supplemented with 1% phenol red sodium salt solution.

Statistical analyses

All histograms represent the mean ± standard deviation (SD) of at least 3 independent experiments. Significant differences were determined using one-way or two-way analyses of variance (ANOVA) followed by the Holm-Sidak's multiple comparison tests in the Prism 8.0 software. Variations between patient and Cyto-ID-stained samples were evaluated using two-tailed Welch *t*-test in the R 3.6.0 software and two-tailed paired *t*-test in the Prism 8.0 software, respectively. Statistical significances were evaluated with *p*-values below 0.05 and are represented by the following legend: * $p \leq 0.05$, ** $p \leq 0.01$, *** $p \leq 0.001$. In all experiments, data were presented as the mean ± standard deviation, and results of treated samples were statistically compared to the corresponding vehicle unless otherwise specified.

The CI was calculated according to Chou and Talalay (59) using the Compusyn Software (ComboSyn, Inc., Paramus, NJ, USA). CI values below or above 1 indicate synergism or antagonism, respectively, whereas the effect is determined to be additive when the CI is equal to 1.

List of abbreviations

ABL: Abelson murine leukemia viral oncogene homolog 1, ALDH: aldehyde dehydrogenase, ATF: activating transcription factor, BCR: breakpoint cluster region, CI: combination index, CML: chronic myeloid leukemia, DDIT: DNA damage-inducible transcript, DMSO: dimethylsulfoxide, ER: endoplasmic reticulum, eIF: eukaryotic initiation factor, FCS: fetal calf serum, GRP78: 78 kDa glucose-regulated protein, γH2AX: H2AX phosphorylation, HDAC: histone deacetylase, HDACi: HDAC inhibitor, HSC: healthy stem cell, LC: microtubule-associated protein 1 light chain, LSC: leukemic stem cell, MCL: myeloid cell leukemia, MMP: mitochondrial membrane potential, PARP: poly (ADP-ribose) polymerase, PBMC: peripheral blood mononuclear cell, PDB: Protein Data Bank, PERK: protein kinase RNA-like ER kinase, SAHA: suberoylanilide hydroxamic acid, siRNA: small interfering RNA, SQSTM: sequestosome, STAT: signal transducer and activator of transcription, TKi: tyrosine kinase inhibitor, UPR: unfolded protein response, XBP: X-box binding protein.

Declarations

Ethics approval:

Zebrafish experiments were done with the agreement of the research ethics committee of the College of Pharmacy of Seoul National University.

<

Consent for publication: Not applicable

Availability of data and materials:

The datasets generated and/or analyzed during the current study are available in the Mendeley repository, https://data.mendeley.com/datasets/x25w3bpcyk/draft?a=41167977-f905-442b-9c79-c7dfab18295f.

Competing interests**:** The authors declare that they have no competing interests.

Funding**:** ML, CF and DG were supported by grants from Télévie-Luxembourg. MS was supported by a Waxweiler grant for cancer prevention research from the Action Lions "Vaincre le Cancer". Research at LBMCC is supported by the "Recherche Cancer et Sang" foundation, the "Recherches Scientifiques Luxembourg" (RSL) association, the "Een Häerz fir kriibskrank Kanner" association, the Action LIONS "Vaincre le Cancer" association, and by Télévie-Luxembourg. AM and JYL were supported by the Brain Korea (BK21) PLUS program and RSL. GB, AM and KV received funding from program financing IMIR KU Leuven. The authors thank the "Korea Leukemia Bank" for biomaterial banking and analysis (NRF-2013M3A9B8031236).

Research at SNU was supported by the Tumor Microenvironment Global Core Research Center funded through the National Research Foundation of Korea (NRF) funded by the Ministry of

Science and ICT (Grant number 2011-0030001) (MDie and BWH), by the Creative-Pioneering Researchers Program through Seoul National University (SNU) (Funding Number 370C-20160062) (MDie), by the National Research Foundation [Grant number 2019R1A2C1009231] (MDie) and by Brain Korea (BK21) PLUS program (MDie and BWH).

Authors' contributions

ML carried out the experiments, wrote and edited the paper. MS carried out experiments, conceived and planned the experiments, wrote and edited the paper and helped supervise the project. HL contributed to the experimental setup. KV and MA synthetized the compound. HH carried out docking experiments. DG carried out bioinformatics experiments and edited the paper. JYL carried the setup and out zebrafish xenografts. AM provided the setup and execution of CFAs. CC provided interpretation of TEM and edited the paper. DWK and MDIC discussed the results and contributed to the final version of the manuscript. GB supervised the chemical synthesis and edited the paper. BWH conceived and planned the experiments, wrote and edited the paper and supervised the project. MD conceived and planned the experiments, wrote and edited the paper and supervised the project. All authors provided critical feedback and helped shape the research, analysis and manuscript.

Acknowledgements

No further acknowledgements.

Supplementary information

Additional file 1.docx (5.2MB)

Figure S1: Reaction scheme showing the synthesis of MAKV-6, -7, -8, -10 and -12. Figure S2: Docking of MAKV-8 into human HDAC isoenzymes. Figure S3: Effect of MAKV-8 derived compounds on *in vitro* HDAC6 and total HDAC activities. Figure S4: Effect of imatinib treatment on KBM-5R cell death. Figure S5: Effect of pan-HDACi MAKV-8 and SAHA on healthy model viability. Figure S6: Effect of imatinib treatment on replicative ability of imatinib-sensitive and -resistant CML cells. Figure S7: Panel of zebrafish pictures.

Figure legends

Fig. 1: Chemical structures of MAKV-6, -7, -8, -10 and -12, and the reference HDACi, SAHA. The prototypical pharmacophoric model of an HDACi is constituted by the zinc binding group, the hydrophobic linker region, and the cap group. MAKV-6 and -7 lack the linker portion; MAKV-10 and -12 substitute the hydroxamate group with a methyl ester group and were obtained as synthesis intermediates.

Fig. 2: The potent pan-HDAC inhibitor MAKV-8 displays cytotoxic properties in CML cells. (**A**) *In vitro* HDAC activity assays were conducted with increasing MAKV-8 concentrations. Relative activities of total HDAC, HDAC1, and HDAC6 were determined by comparison to the vehicle, DMSO. (**B**) Docking poses of MAKV-8 (stick model, orange) on the crystal structure of indicated HDAC isoenzymes (white; PDB codes: see Methods section). Numbered residues forming hydrophobic interactions in the binding sites (stick representation) correspond to HDAC1 to HDAC8 from top to bottom. (**C**, **D**) The acetylation levels of HDAC targets were assessed by western blot in K-562 cells treated with (**C**) increasing MAKV-8 concentrations for 24h or (**D**) 15µM MAKV-8 for the indicated time points. (**E**) CML cell

proliferation and viability were evaluated following treatments with increasing MAKV-8 concentrations for up to 72h. **(F)** CML cells were grown in the presence of increasing MAKV-8 concentrations for 10 days, and their colony-forming capacity was scored after MTT addition. Representative pictures (left panel) and corresponding quantifications (right panel) from three independent experiments are provided. (**G**) Histone H4 and α-tubulin acetylation levels were assessed by western blot in KBM-5 and MEG-01 cells treated with increasing MAKV-8 concentrations for 24h. (**H**) Docking poses of MAKV-8 derivatives (stick model) on HDAC6 crystal structure (white; PDB code: 5EDU). Numbered residues forming hydrophobic interactions in the binding sites (stick representation) are indicated. (**B and H**) Zinc atom is shown as a purple sphere; nitrogen and oxygen are colored in blue and red, respectively. (**I**) Histone H4 and α-tubulin acetylation levels were assessed by western blot (upper panel), and cell proliferation and viability were evaluated (lower panel) following treatments of K-562 cells with increasing concentrations of the indicated MAKV-8 derivatives for 24h and up to 72h, respectively. β-actin and histone H1 served as loading controls for α-tubulin and histone H4, respectively. Blots are representative of three independent experiments. SAHA was used as a reference HDACi.

Fig. 3: Treatment with MAKV-8 leads to cell cycle arrest and apoptotic cell death. K-562 cells were treated with MAKV-8 at the indicated time points and concentrations, followed by analyses of (**A**) cell cycle distribution using a range of subtoxic cytostatic MAKV-8 concentrations to focus only on aspects of cell cycle modulation, (**B**) nuclear morphology, and (**C**) caspase and PARP-1 activation. (**B**) Representative pictures (upper panel) and corresponding quantifications (lower panel) from three independent experiments are provided. Where indicated, cells were pre-incubated for 1h with the pan-caspase inhibitor z-VAD-FMK. Cisplatin was used as a positive control for caspase and PARP-1 cleavage. Blots used β-actin

as the loading control and are representative of three independent experiments. SAHA was used as a reference HDACi.

Fig. 4: MAKV-8 treatment induces ER stress, autophagy, and double strand breaks. K-562 cells were treated with the indicated concentrations of MAKV-8 at the indicated time points unless otherwise stated. (**A**) The expression levels of UPR-associated proteins, such as the ER stress marker GRP78, were assessed by western blot. (**B**) DDIT3 mRNA expression levels were quantified by real-time PCR and normalized to β-actin mRNA levels. (**C**) End-point analysis of XBP1 mRNA splicing. (**D**) Cell morphology was analyzed after 48h of treatment using modified GIEMSA staining, and pictures were acquired by bright-field microscopy. (**E**) The appearance of autophagosome-related vesicles was quantified in cells treated with MAKV-8 for 8h. Representative pictures (left panel) and corresponding quantifications (right panel) from three independent experiments are provided. (**F**) After 8h of treatment, the conversion of LC3-I to LC3-II and expression of p62, two autophagic markers, were evaluated by western blot. Where indicated, bafilomycin A_1 was added 2h before the end of treatment. (**G**) Representative images of electron microscopy analysis in indicated CML cell line: (1) phagophores and (2) autophagolysosomes. (**H**) The expression level of γH2AX, the earliest marker for DNA damage localized at double strand breaks, was assessed by western blot. Thapsigargin (T, 4 μM) and cisplatin (C, 50 μM) were used as positive controls for ER stress and double strand break induction, respectively. Blots used β-actin as the loading control, and pictures are representative of three independent experiments.

Fig. 5: The HDACi MAKV-8 combined with imatinib induces synergistic anti-cancer activity in CML cells. (**A**) Boxplots including outliers illustrating fold-change (log2) of HDAC1, HDAC2 and HDAC3 mRNA expression levels in $CD34^+CD38^-$ stem cells isolated

from healthy (n=7) and CML (n=11) patients (represented by triangles). (**B-J**) CML and healthy cells were treated with the indicated concentrations of imatinib alone or in combination with MAKV-8. (**B**) After 24h-incubations, α-tubulin and histone H4 acetylation levels were assessed by western blot, with β-actin and histone H1 as loading controls, respectively. SAHA was used as a reference HDACi. (**C**) Nuclear morphology, (**D**) phosphatidylserine exposure, and (**E**) the mitochondrial membrane potential (MMP) were analyzed in K-562 cells treated for 48h. Representative dot plots (upper panel) and corresponding quantifications (lower panel) from three independent experiments are provided. (**F**) Caspases and PARP-1 cleavage was analyzed in K-562 cells treated for 24h. (**G**) Nuclear morphology (upper panel) and cleavage of caspase 3 and PARP-1 (lower panel) were studied in KBM-5 and MEG-01 cells treated for 48 and 24h, respectively. (**H**) Nuclear morphology (upper panel) and PARP-1 cleavage (lower panel) were evaluated in KBM-5R cells treated for 48 and 24h, respectively. Caspases and PARP-1 cleavage was assessed by western blot using β-actin as the loading control. Cisplatin was used as a positive control for apoptosis induction and MMP disruption. Blots and pictures are representative of three independent experiments. (**I**) Healthy cell models were treated for 48h. Cell viability was assessed based on the Trypan Blue exclusion method for PBMCs, by flow cytometry after Annexin V staining for platelets, and nuclear morphology was examined in RPMI-1788 cells. (**J**) CML cells were pre-treated with MAKV-8 for 8h and then grown in semisolid methylcellulose medium in the presence of imatinib. After 10-day incubations, cell colony-forming capacity was scored after MTT addition. Representative pictures (left panel) and corresponding quantifications (right panel) from three independent experiments are provided.

Fig. 6: Altered BCR-ABL signaling and reduced cancer stem cell population are associated with MAKV-8-imatinib anti-cancer properties.

CML cells were treated with the indicated concentrations of imatinib alone or in combination with MAKV-8. (**A, B**) K-562 cells were transfected with or without the indicated siRNA, then (**A**) the expression level of beclin-1, a protein involved in initiating the autophagic flux, was assessed by western blot 24 and 72h post-transfection, and (**B**) nuclear morphology (upper panel) and cleavage of PARP-1 (lower panel) were analyzed in cells treated for 24 and 48h, respectively. The ratio between the cleaved and uncleaved forms of PARP-1 was determined based on western blot quantification. (**C**, **D**) Protein expression and phosphorylation levels were assessed by western blot in cells treated for 24h. Blots used β-actin as a loading control and are representative of three independent experiments. (**E**) Boxplots illustrating fold-change (log2) of c-MYC mRNA expression in $CD34^{+}CD38^{-}$ stem cells isolated from healthy (n=7) and CML (n=11) patients (represented by triangles). (**F**) Analysis of aldehyde dehydrogenase (ALDH) activity in K-562 cells cultured for 24h and known to present a substantial proportion of cells with cancer stem-like characteristics. Elevated ALDH activity is an established marker for the identification of hematopoietic stem cells. The ALDH inhibitor diethylaminobenzaldehyde (DEAB) was used to distinguish cell subpopulations with low and high ALDH activity. Representative dot plots where the percentage of ALDH+ cells is indicated (upper panel) and corresponding quantifications (lower panel) representative of three independent experiments are presented. SAHA was used as a reference HDACi. (**G**) K-562 cells were treated for 24h, fluorescently labeled, and then injected into the zebrafish yolk sac. Three days post-injection, pictures of 5 to 8 fishes (one representative set of pictures is presented) were taken, and the fluorescence intensity was quantified.

References

1. Jabbour E, Kantarjian H. Chronic myeloid leukemia: 2018 update on diagnosis, therapy and monitoring. Am J Hematol. 2018;93(3):442-59.

2. Apperley JF. Chronic myeloid leukaemia. Lancet. 2015;385(9976):1447-59.

3. Masamoto Y, Kurokawa M. Targeting chronic myeloid leukemia stem cells: can transcriptional program be a druggable target for cancers? Stem Cell Investig. 2018;5:10.

4. Thompson PA, Kantarjian HM, Cortes JE. Diagnosis and Treatment of Chronic Myeloid Leukemia in 2015. Mayo Clin Proc. 2015;90(10):1440-54.

5. Zhou H, Xu R. Leukemia stem cells: the root of chronic myeloid leukemia. Protein Cell. 2015;6(6):403-12.

6. Al Baghdadi T, Abonour R, Boswell HS. Novel combination treatments targeting chronic myeloid leukemia stem cells. Clinical lymphoma, myeloma & leukemia. 2012;12(2):94-105.

7. Seidel C, Florean C, Schnekenburger M, Dicato M, Diederich M. Chromatin-modifying agents in anti-cancer therapy. Biochimie. 2012;94(11):2264-79.

8. Florean C, Schnekenburger M, Grandjenette C, Dicato M, Diederich M. Epigenomics of leukemia: from mechanisms to therapeutic applications. Epigenomics. 2011;3(5):581-609.

9. Lane AA, Chabner BA. Histone deacetylase inhibitors in cancer therapy. J Clin Oncol. 2009;27(32):5459-68.

10. Seidel C, Schnekenburger M, Dicato M, Diederich M. Histone deacetylase modulators provided by Mother Nature. Genes & nutrition. 2012;7(3):357-67.

11. Wagner JM, Hackanson B, Lubbert M, Jung M. Histone deacetylase (HDAC) inhibitors in recent clinical trials for cancer therapy. Clin Epigenetics. 2010;1(3-4):117-36.

12. Schnekenburger M, Florean C, Dicato M, Diederich M. Epigenetic alterations as a universal feature of cancer hallmarks and a promising target for personalized treatments. Current topics in medicinal chemistry. 2016;16(7):745-76.

13. Nimmanapalli R, Fuino L, Stobaugh C, Richon V, Bhalla K. Cotreatment with the histone deacetylase inhibitor suberoylanilide hydroxamic acid (SAHA) enhances imatinib-induced apoptosis of Bcr-Abl-positive human acute leukemia cells. Blood. 2003;101(8):3236-9.

14. Fiskus W, Pranpat M, Balasis M, Bali P, Estrella V, Kumaraswamy S, et al. Cotreatment with vorinostat (suberoylanilide hydroxamic acid) enhances activity of dasatinib (BMS-354825) against imatinib mesylate-sensitive or imatinib mesylate-resistant chronic myelogenous leukemia cells. Clin Cancer Res. 2006;12(19):5869-78.

15. Kozikowski AP, Tapadar S, Luchini DN, Kim KH, Billadeau DD. Use of the nitrile oxide cycloaddition (NOC) reaction for molecular probe generation: a new class of enzyme selective histone deacetylase inhibitors (HDACIs) showing picomolar activity at HDAC6. Journal of medicinal chemistry. 2008;51(15):4370-3.

16. Liu Y, Cao Y, Zhang W, Bergmeier S, Qian Y, Akbar H, et al. A small-molecule inhibitor of glucose transporter 1 downregulates glycolysis, induces cell-cycle arrest, and inhibits cancer cell growth in vitro and in vivo. Mol Cancer Ther. 2012;11(8):1672-82.

17. Song S, Tan J, Miao Y, Zhang Q. Crosstalk of ER stress-mediated autophagy and ER-phagy: Involvement of UPR and the core autophagy machinery. J Cell Physiol. 2018;233(5):3867-74.

18. Gammoh N, Lam D, Puente C, Ganley I, Marks PA, Jiang X. Role of autophagy in histone deacetylase inhibitor-induced apoptotic and nonapoptotic cell death. Proc Natl Acad Sci U S A. 2012;109(17):6561-5.

19. Petruccelli LA, Dupere-Richer D, Pettersson F, Retrouvey H, Skoulikas S, Miller WH, Jr. Vorinostat induces reactive oxygen species and DNA damage in acute myeloid leukemia cells. PLoS One. 2011;6(6):e20987.

20. Galluzzi L, Senovilla L, Vitale I, Michels J, Martins I, Kepp O, et al. Molecular mechanisms of cisplatin resistance. Oncogene. 2012;31(15):1869-83.

21. Chen SH, Chow JM, Hsieh YY, Lin CY, Hsu KW, Hsieh WS, et al. HDAC1,2 Knock-Out and HDACi Induced Cell Apoptosis in Imatinib-Resistant K562 Cells. Int J Mol Sci. 2019;20(9).

22. Apperley JF. CML and tyrosine kinase inhibition: the hope becomes reality. Lancet Haematol. 2015;2(5):e176-7.

23. Venton G, Perez-Alea M, Baier C, Fournet G, Quash G, Labiad Y, et al. Aldehyde dehydrogenases inhibition eradicates leukemia stem cells while sparing normal progenitors. Blood Cancer J. 2016;6(9):e469.

24. Kahali S, Sarcar B, Prabhu A, Seto E, Chinnaiyan P. Class I histone deacetylases localize to the endoplasmic reticulum and modulate the unfolded protein response. FASEB J. 2012;26(6):2437-45.

25. Rao R, Nalluri S, Kolhe R, Yang Y, Fiskus W, Chen J, et al. Treatment with panobinostat induces glucose-regulated protein 78 acetylation and endoplasmic reticulum stress in breast cancer cells. Mol Cancer Ther. 2010;9(4):942-52.

26. Bruning A, Juckstock J. Misfolded proteins: from little villains to little helpers in the fight against cancer. Frontiers in oncology. 2015;5:47.

27. Koeneke E, Witt O, Oehme I. HDAC Family Members Intertwined in the Regulation of Autophagy: A Druggable Vulnerability in Aggressive Tumor Entities. Cells. 2015;4(2):135-68.

28. Carew JS, Nawrocki ST, Kahue CN, Zhang H, Yang C, Chung L, et al. Targeting autophagy augments the anticancer activity of the histone deacetylase inhibitor SAHA to overcome Bcr-Abl-mediated drug resistance. Blood. 2007;110(1):313-22.

29. Gaymes TJ, Padua RA, Pla M, Orr S, Omidvar N, Chomienne C, et al. Histone deacetylase inhibitors (HDI) cause DNA damage in leukemia cells: a mechanism for leukemia-specific HDI-dependent apoptosis? Molecular cancer research : MCR. 2006;4(8):563-73.

30. Lee JH, Choy ML, Ngo L, Foster SS, Marks PA. Histone deacetylase inhibitor induces DNA damage, which normal but not transformed cells can repair. Proc Natl Acad Sci U S A. 2010;107(33):14639-44.

31. Cea M, Soncini D, Fruscione F, Raffaghello L, Garuti A, Emionite L, et al. Synergistic interactions between HDAC and sirtuin inhibitors in human leukemia cells. PLoS One. 2011;6(7):e22739.

32. Marks PA, Breslow R. Dimethyl sulfoxide to vorinostat: development of this histone deacetylase inhibitor as an anticancer drug. Nat Biotechnol. 2007;25(1):84-90.

33. Bali P, Pranpat M, Bradner J, Balasis M, Fiskus W, Guo F, et al. Inhibition of histone deacetylase 6 acetylates and disrupts the chaperone function of heat shock protein 90: a novel basis for antileukemia activity of histone deacetylase inhibitors. J Biol Chem. 2005;280(29):26729-34.

34. Ceballos E, Delgado MD, Gutierrez P, Richard C, Muller D, Eilers M, et al. c-Myc antagonizes the effect of p53 on apoptosis and p21WAF1 transactivation in K562 leukemia cells. Oncogene. 2000;19(18):2194-204.

35. Hoelbl A, Kovacic B, Kerenyi MA, Simma O, Warsch W, Cui Y, et al. Clarifying the role of Stat5 in lymphoid development and Abelson-induced transformation. Blood. 2006;107(12):4898-906.

36. Warsch W, Grundschober E, Berger A, Gille L, Cerny-Reiterer S, Tigan AS, et al. STAT5 triggers BCR-ABL1 mutation by mediating ROS production in chronic myeloid leukaemia. Oncotarget. 2012;3(12):1669-87.

37. Nguyen T, Dai Y, Attkisson E, Kramer L, Jordan N, Nguyen N, et al. HDAC inhibitors potentiate the activity of the BCR/ABL kinase inhibitor KW-2449 in imatinib-sensitive or -resistant BCR/ABL+ leukemia cells in vitro and in vivo. Clin Cancer Res. 2011;17(10):3219-32.

38. Inoue S, Walewska R, Dyer MJ, Cohen GM. Downregulation of Mcl-1 potentiates HDACi-mediated apoptosis in leukemic cells. Leukemia. 2008;22(4):819-25.

39. Abraham SA, Hopcroft LE, Carrick E, Drotar ME, Dunn K, Williamson AJ, et al. Dual targeting of p53 and c-MYC selectively eliminates leukaemic stem cells. Nature. 2016;534(7607):341-6.

40. Mazumder A, Lee JY, Talhi O, Cerella C, Chateauvieux S, Gaigneaux A, et al. Hydroxycoumarin OT-55 kills CML cells alone or in synergy with imatinib or Synribo: Involvement of ER stress and DAMP release. Cancer letters. 2018;438:197-218.

41. Schnekenburger M, Grandjenette C, Ghelfi J, Karius T, Foliguet B, Dicato M, et al. Sustained exposure to the DNA demethylating agent, 2'-deoxy-5-azacytidine, leads to apoptotic cell death in chronic myeloid leukemia by promoting differentiation, senescence, and autophagy. Biochemical pharmacology. 2011;81(3):364-78.

42. Scott MT, Korfi K, Saffrey P, Hopcroft LE, Kinstrie R, Pellicano F, et al. Epigenetic Reprogramming Sensitizes CML Stem Cells to Combined EZH2 and Tyrosine Kinase Inhibition. Cancer Discov. 2016;6(11):1248-57.

43. Aviles-Vazquez S, Chavez-Gonzalez A, Hidalgo-Miranda A, Moreno-Lorenzana D, Arriaga-Pizano L, Sandoval-Esquivel MA, et al. Global gene expression profiles of

hematopoietic stem and progenitor cells from patients with chronic myeloid leukemia: the effect of in vitro culture with or without imatinib. Cancer Med. 2017;6(12):2942-56.

44. Kolesnikov N, Hastings E, Keays M, Melnichuk O, Tang YA, Williams E, et al. ArrayExpress update--simplifying data submissions. Nucleic Acids Res. 2015;43(Database issue):D1113-6.

45. Carvalho BS, Irizarry RA. A framework for oligonucleotide microarray preprocessing. Bioinformatics. 2010;26(19):2363-7.

46. Ritchie ME, Phipson B, Wu D, Hu Y, Law CW, Shi W, et al. limma powers differential expression analyses for RNA-sequencing and microarray studies. Nucleic Acids Res. 2015;43(7):e47.

47. Kassambara A. ggpubr: 'ggplot2' Based Publication Ready Plots. 0.2. ed2018.

48. R Development Core Team. R: A language and environment for statistical computing. R Foundation for Statistical Computing; 2010.

49. RStudio Team. RStudio: Integrated Development for R. 2015.

50. El Amrani M, Lai D, Debbab A, Aly AH, Siems K, Seidel C, et al. Protein kinase and HDAC inhibitors from the endophytic fungus Epicoccum nigrum. J Nat Prod. 2014;77(1):49-56.

51. Seidel C, Schnekenburger M, Dicato M, Diederich M. Antiproliferative and proapoptotic activities of 4-hydroxybenzoic acid-based inhibitors of histone deacetylases. Cancer letters. 2014;343(1):134-46.

52. Schnekenburger M, Goffin E, Lee JY, Jang JY, Mazumder A, Ji S, et al. Discovery and Characterization of R/S-N-3-Cyanophenyl-N'-(6-tert-butoxycarbonylamino-3,4-dihydro-2,2-dimethyl-2H-1- benzopyran-4-yl)urea, a New Histone Deacetylase Class III Inhibitor Exerting Antiproliferative Activity against Cancer Cell Lines. Journal of medicinal chemistry. 2017;60(11):4714-33.

53. Karius T, Schnekenburger M, Ghelfi J, Walter J, Dicato M, Diederich M. Reversible epigenetic fingerprint-mediated glutathione-S-transferase P1 gene silencing in human leukemia cell lines. Biochemical pharmacology. 2011;81(11):1329-42.

54. Grandjenette C, Schnekenburger M, Karius T, Ghelfi J, Gaigneaux A, Henry E, et al. 5-aza-2'-deoxycytidine-mediated c-myc Down-regulation triggers telomere-dependent senescence by regulating human telomerase reverse transcriptase in chronic myeloid leukemia. Neoplasia. 2014;16(6):511-28.

55. Florean C, Kim KR, Schnekenburger M, Kim HJ, Moriou C, Debitus C, et al. Synergistic AML Cell Death Induction by Marine Cytotoxin (+)-1(R), 6(S), 1'(R), 6'(S), 11(R), 17(S)-Fistularin-3 and Bcl-2 Inhibitor Venetoclax. Mar Drugs. 2018;16(12).

56. Lee JY, Mazumder A, Diederich M. Preclinical Assessment of the Bioactivity of the Anticancer Coumarin OT48 by Spheroids, Colony Formation Assays, and Zebrafish Xenografts. J Vis Exp. 2018(136).

57. Seidel C, Schnekenburger M, Mazumder A, Teiten MH, Kirsch G, Dicato M, et al. 4-Hydroxybenzoic acid derivatives as HDAC6-specific inhibitors modulating microtubular structure and HSP90alpha chaperone activity against prostate cancer. Biochemical pharmacology. 2016;99:31-52.

58. Florean C, Schnekenburger M, Lee JY, Kim KR, Mazumder A, Song S, et al. Discovery and characterization of Isofistularin-3, a marine brominated alkaloid, as a new DNA demethylating agent inducing cell cycle arrest and sensitization to TRAIL in cancer cells. Oncotarget. 2016;7(17):24027-49.

59. Chou TC. Theoretical basis, experimental design, and computerized simulation of synergism and antagonism in drug combination studies. Pharmacological reviews. 2006;58(3):621-81.

Figure 1

Click here to access/download;Figure;Lernoux et al_Figure 1.pptx

Figure 1, Lernoux *et al.*

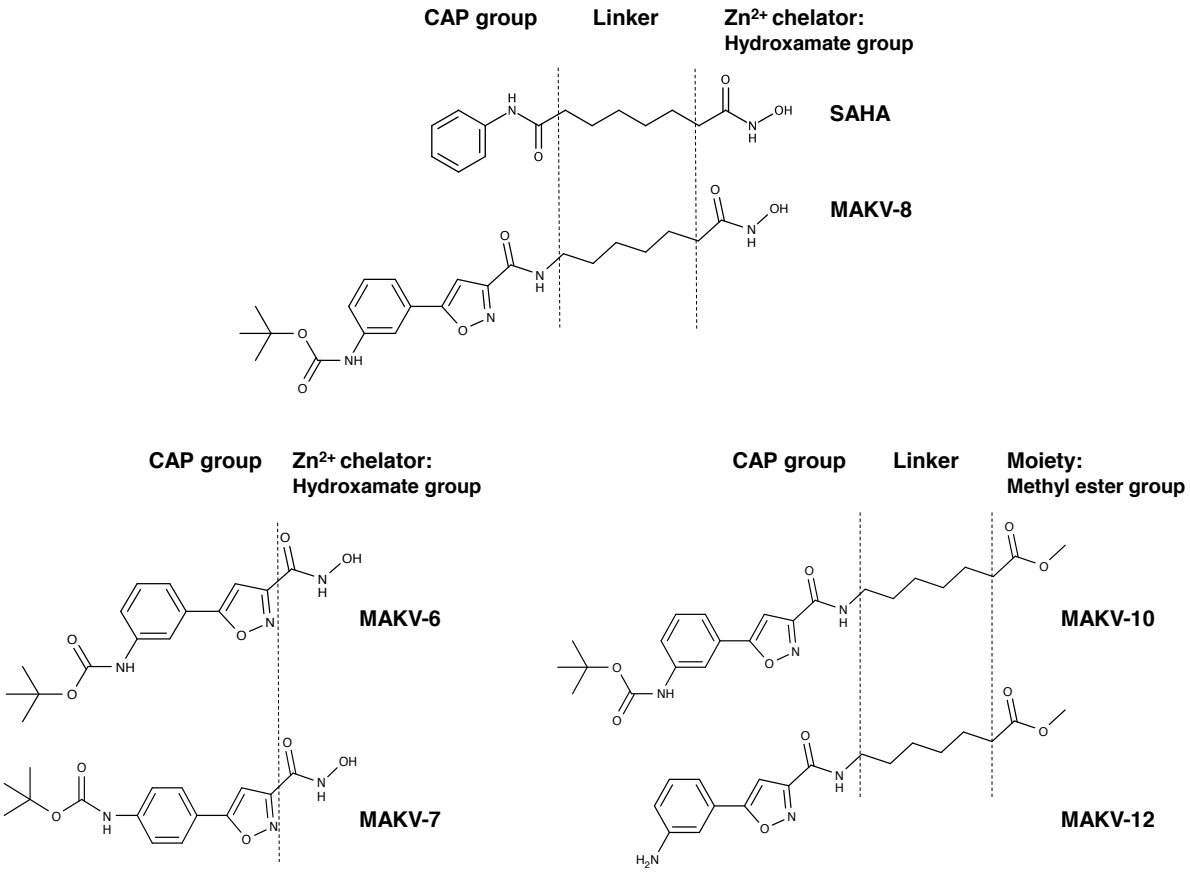

Figure 2

Click here to access/download;Figure;Lernoux et al_Figure 2.pptx

Figure 2, Lernoux *et al.*

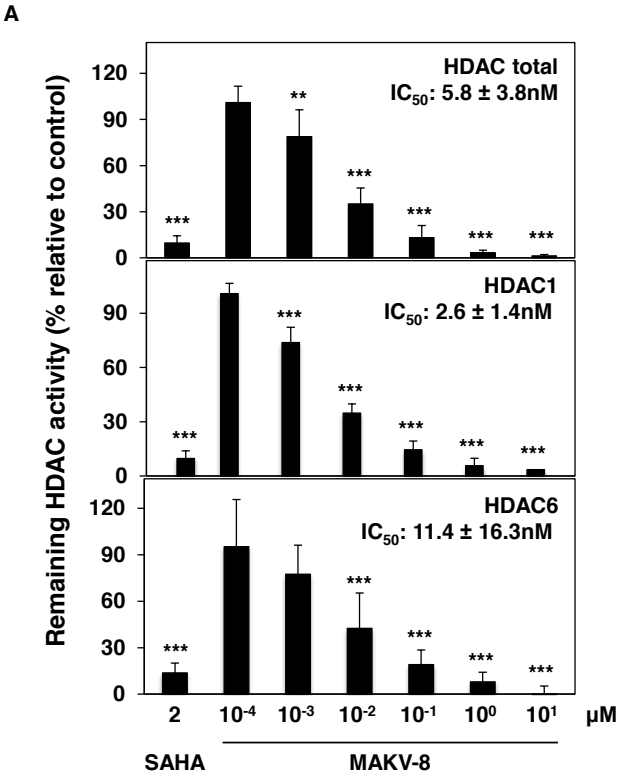

Figure 2, Lernoux *et al.*

B

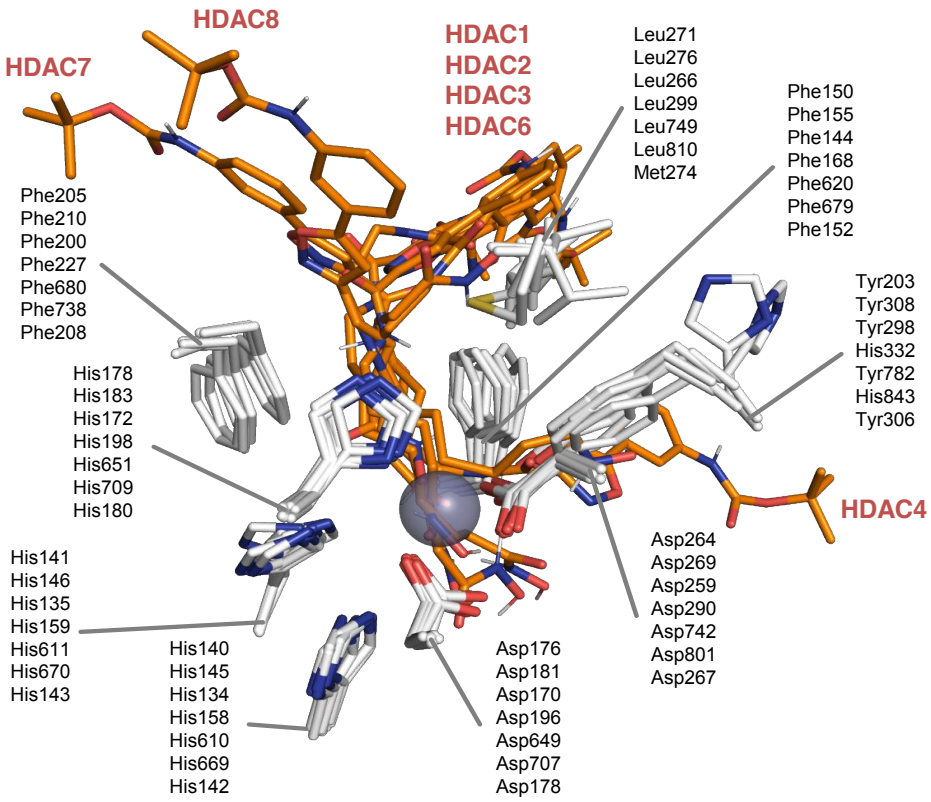

Figure 2, Lernoux *et al.*

C

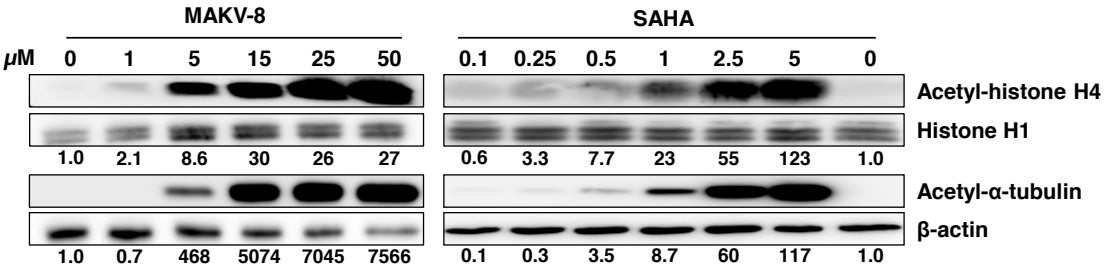

D

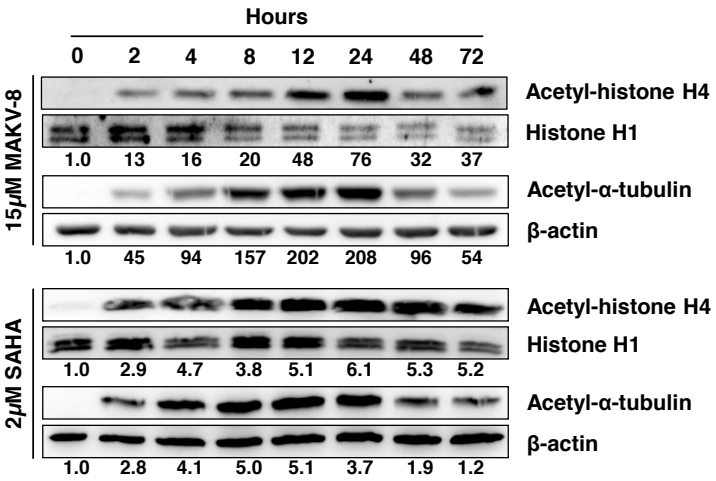

Figure 2, Lernoux *et al.*

E

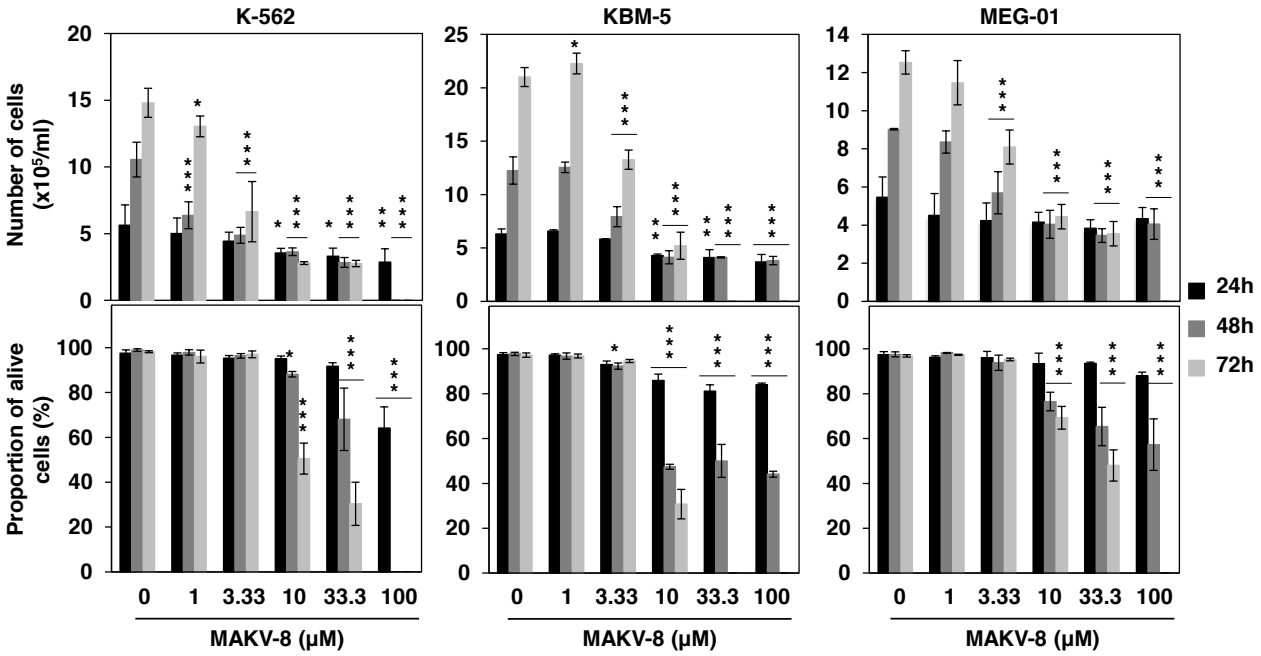

Figure 2, Lernoux *et al.*

F

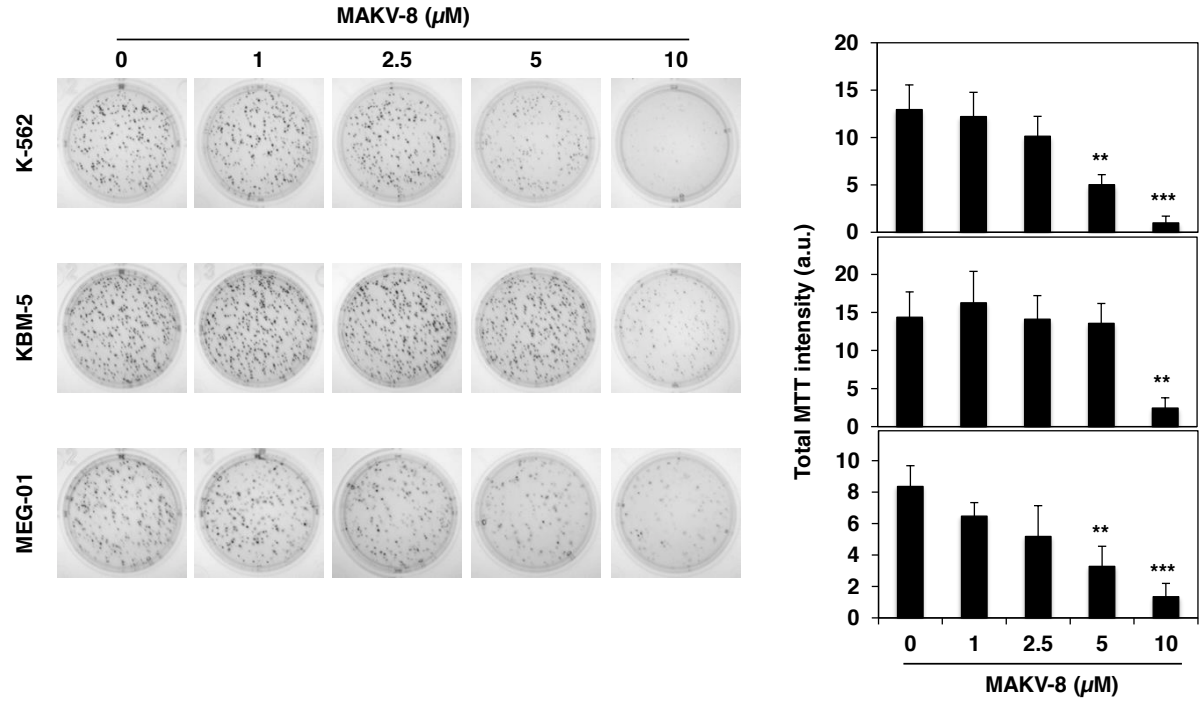

Figure 2, Lernoux *et al.*

G

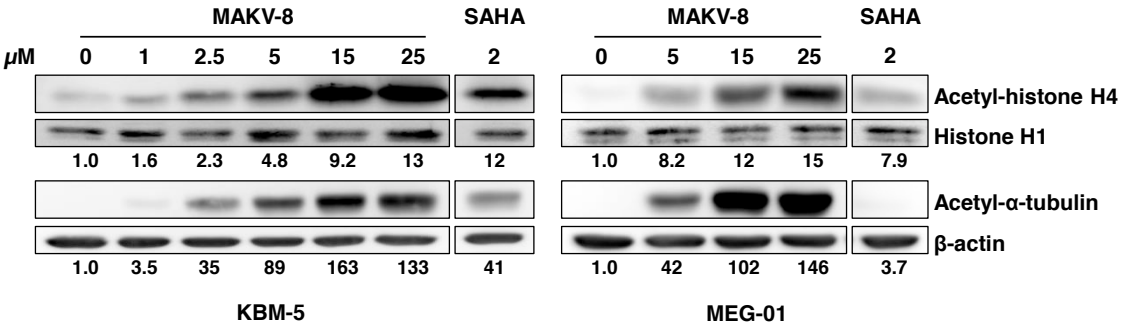

Figure 2, Lernoux *et al.*

H

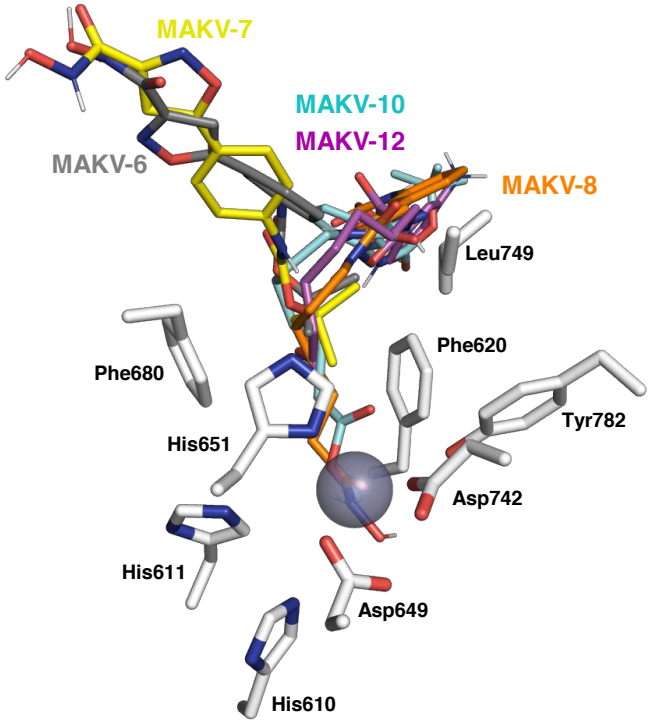

Figure 2, Lernoux *et al.*

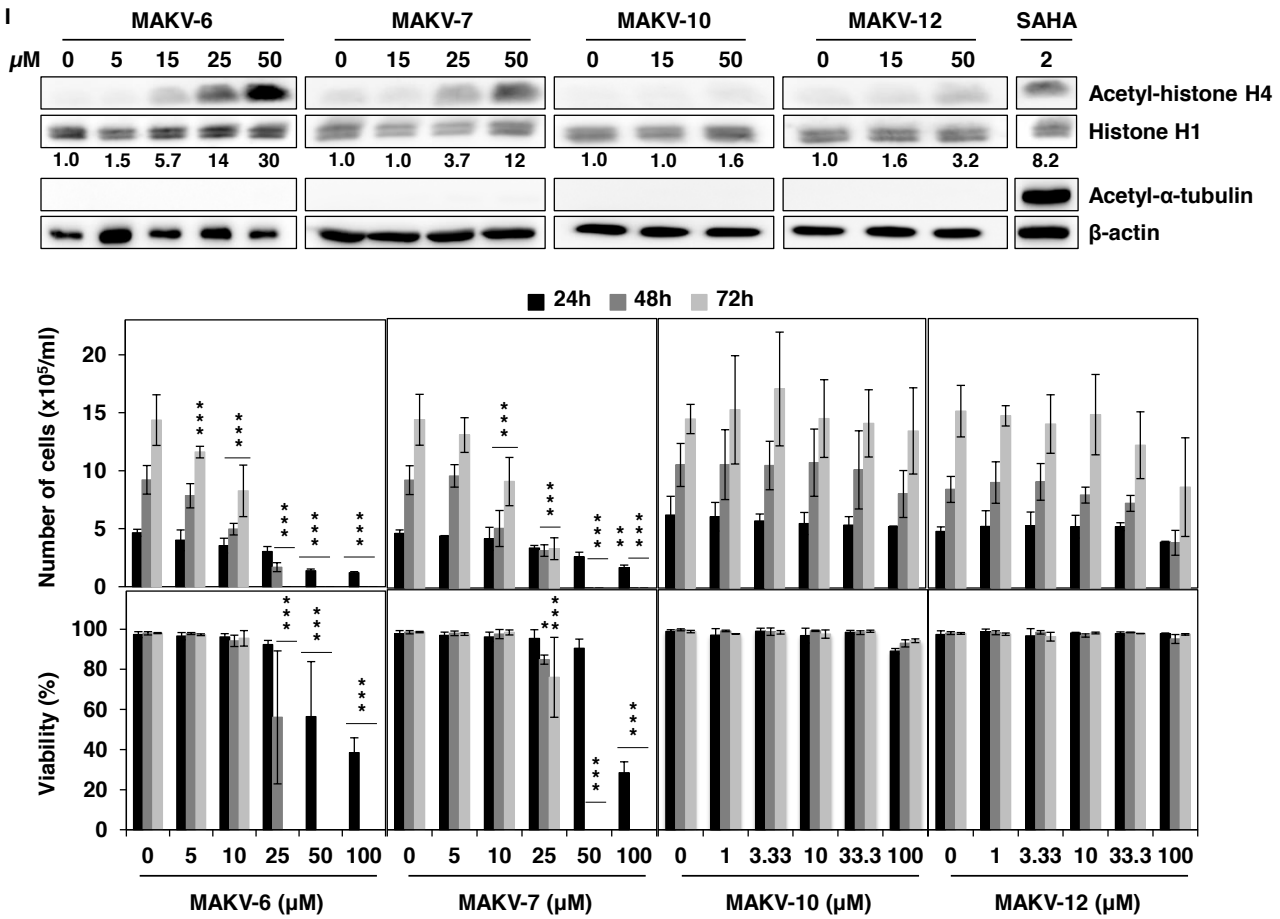

Figure 3

Click here to access/download;Figure;Lernoux et al_Figure 3.pptx

Figure 3, Lernoux *et al.*

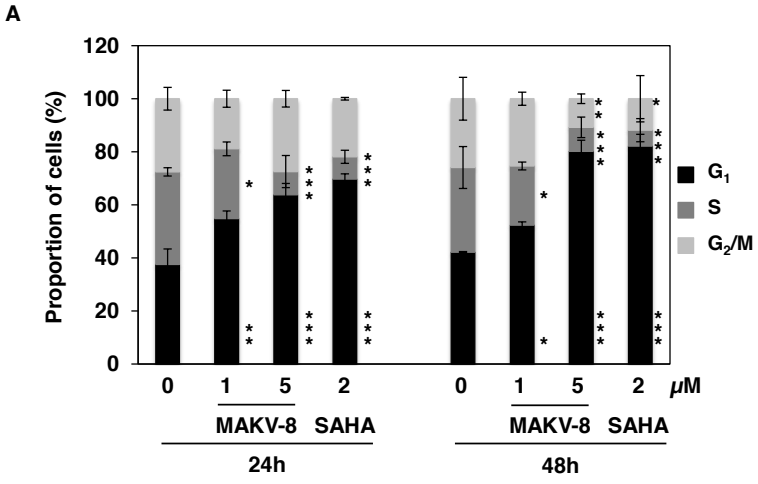

Figure 3, Lernoux *et al.*

B

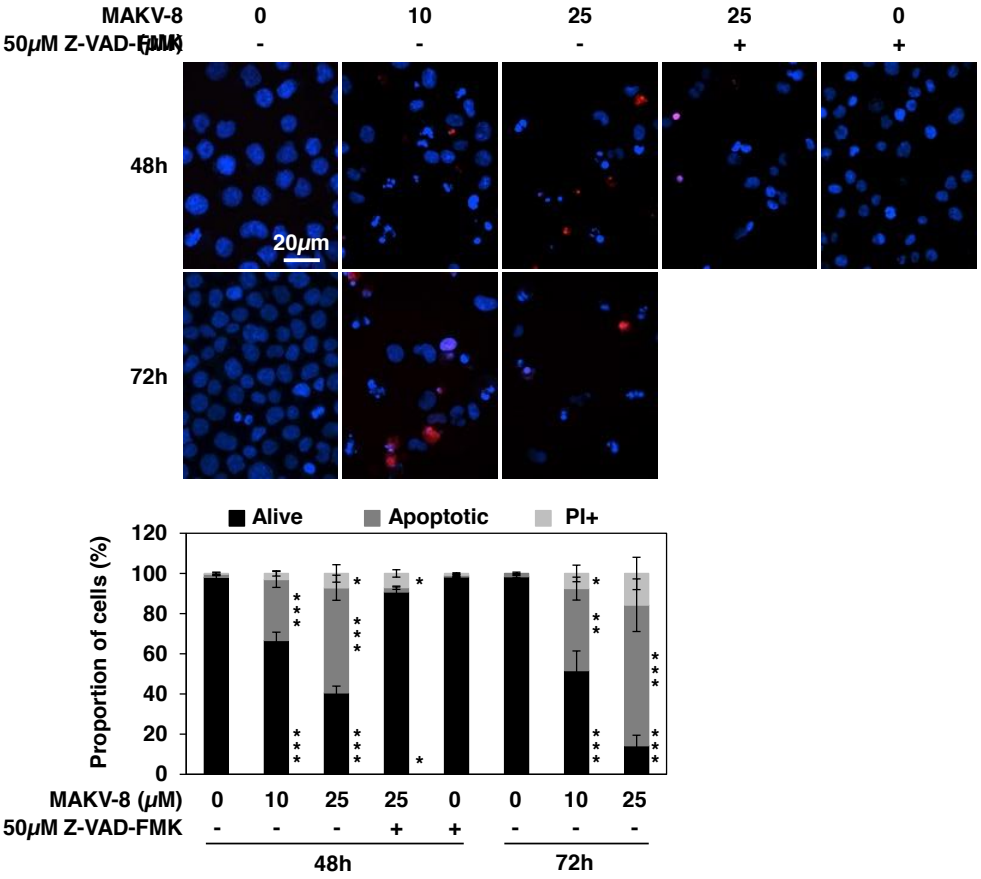

Figure 3, Lernoux *et al.*

C

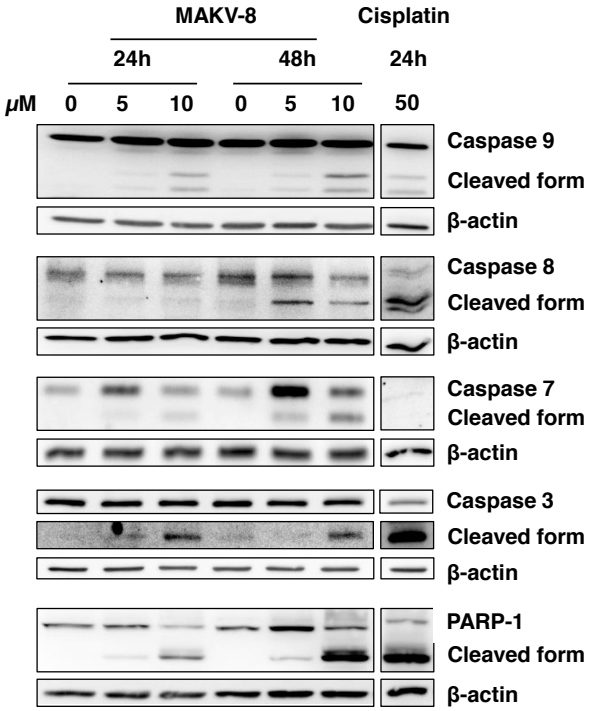

Figure 4

Click here to access/download;Figure;Lernoux et al_Figure 4.pptx

Figure 4, Lernoux *et al.*

A

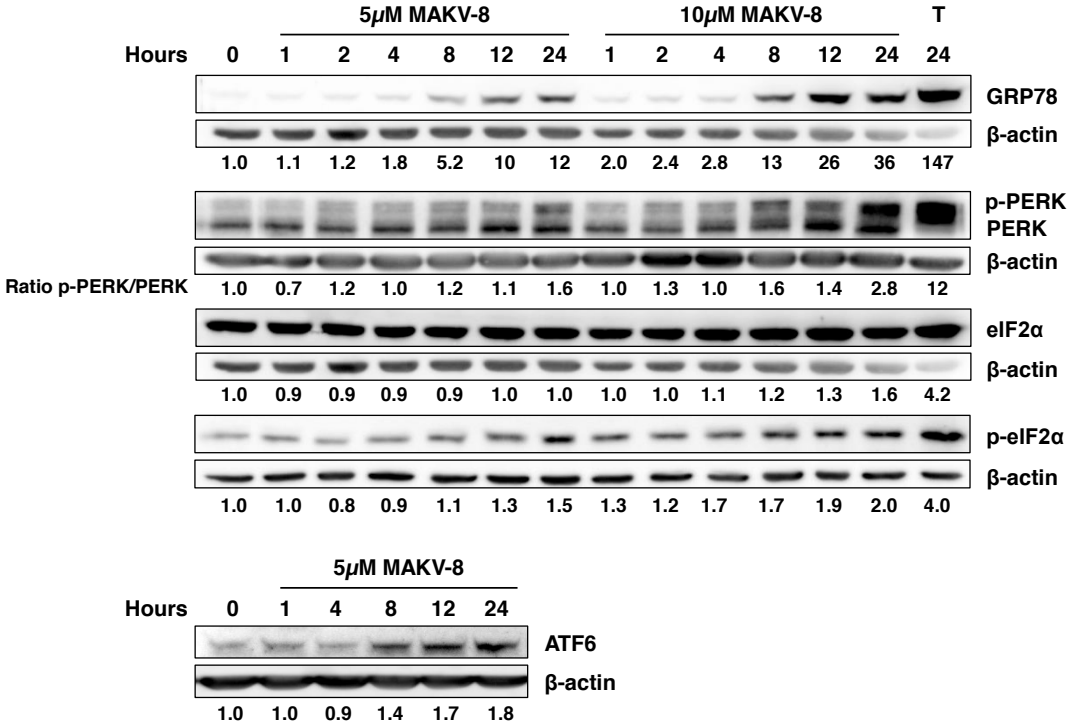

Figure 4, Lernoux *et al.*

B

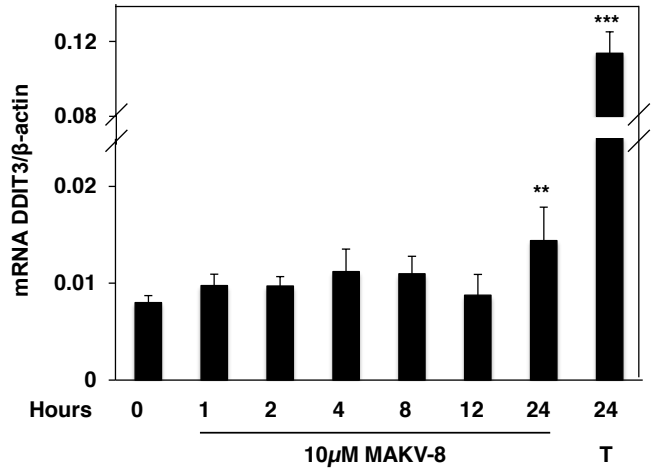

C

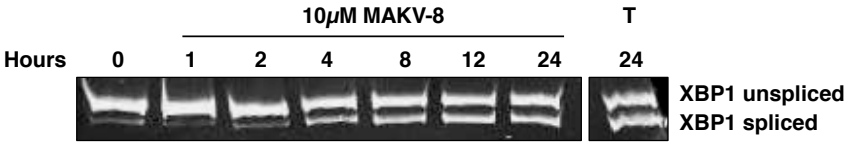

Figure 4, Lernoux *et al.*

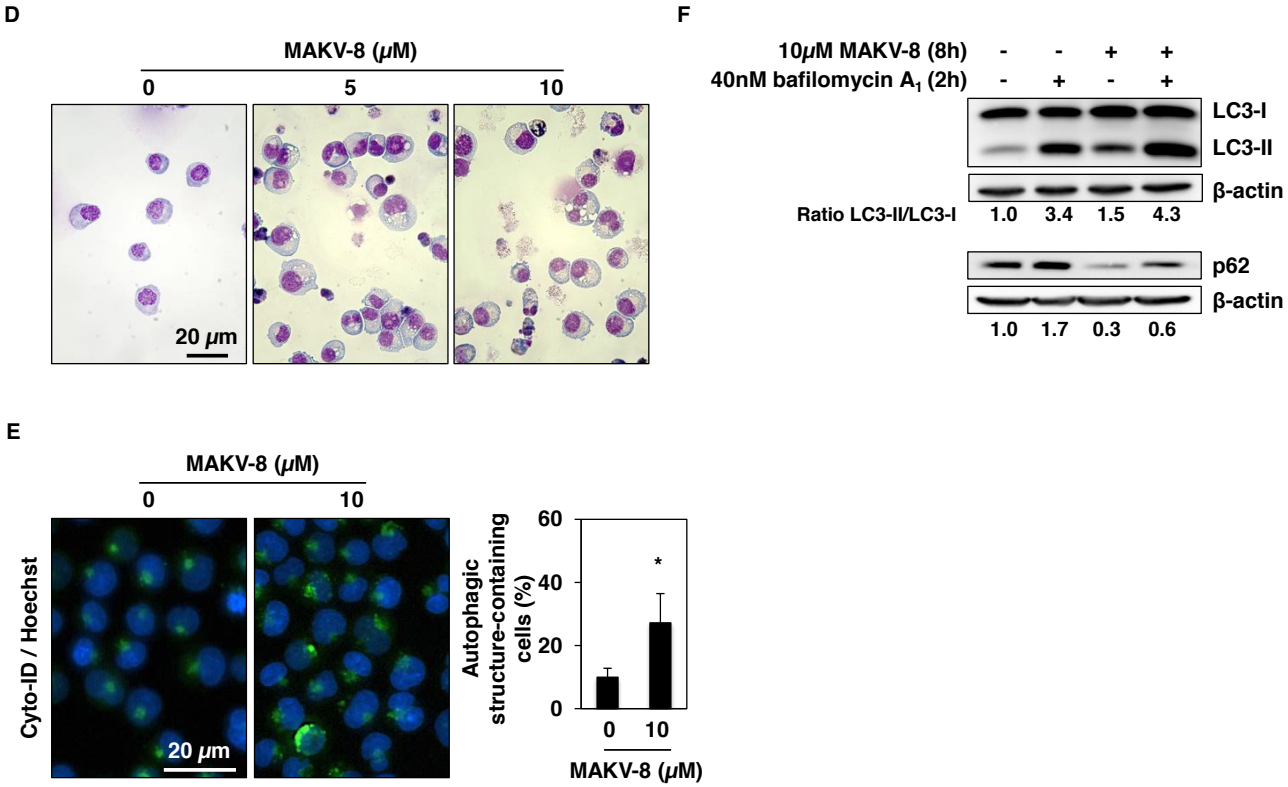

Figure 4, Lernoux *et al.*

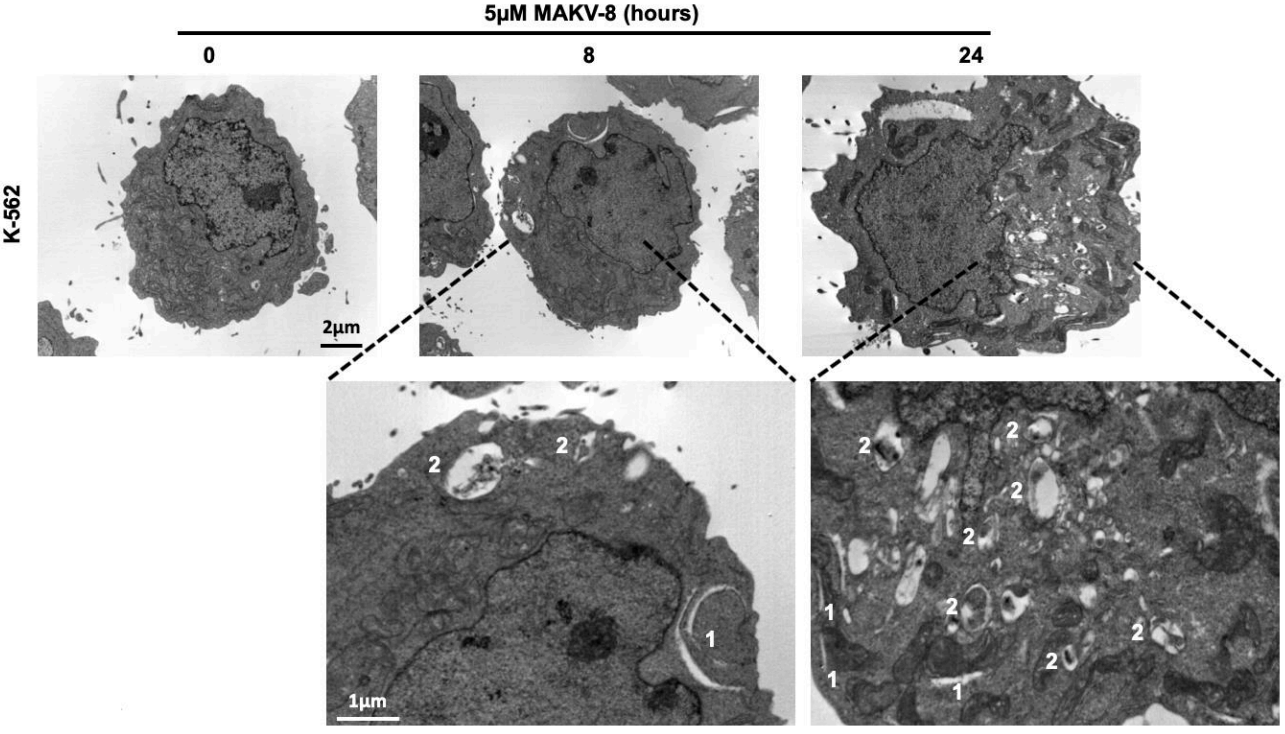

Figure 4, Lernoux *et al.*

G

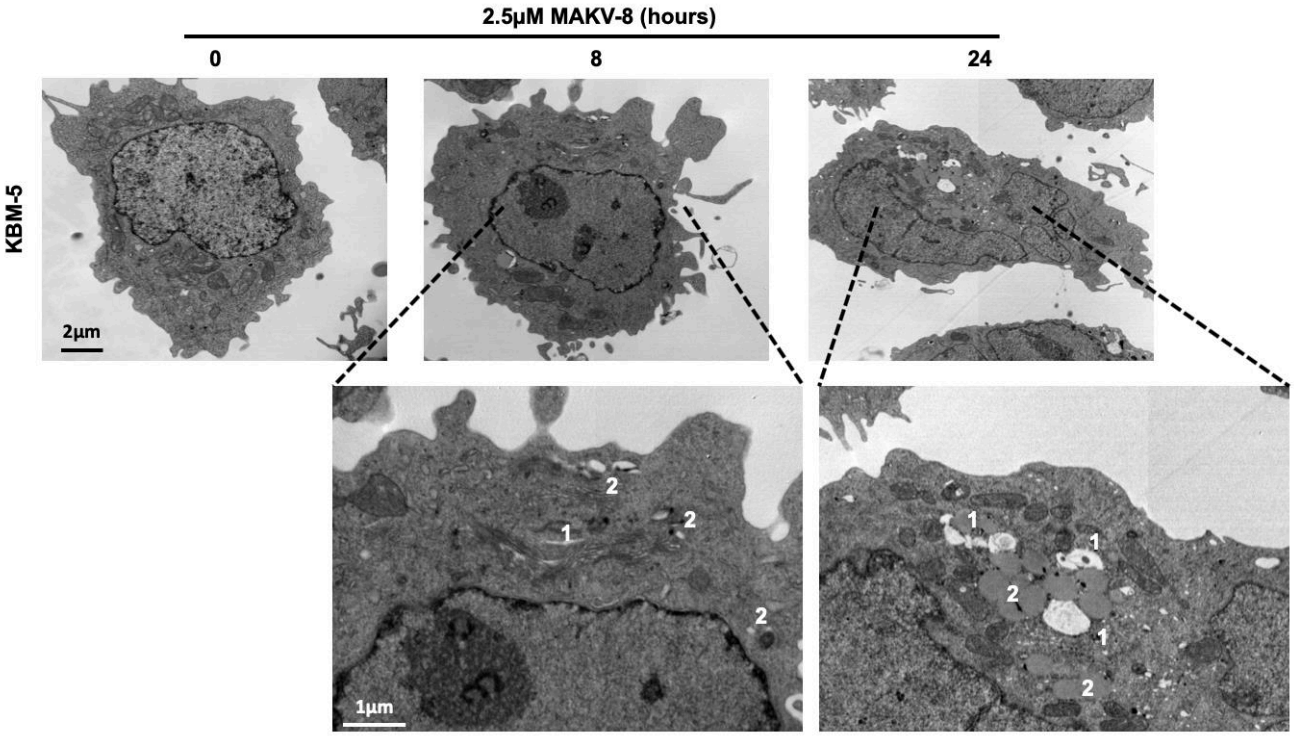

Figure 4, Lernoux *et al.*

G

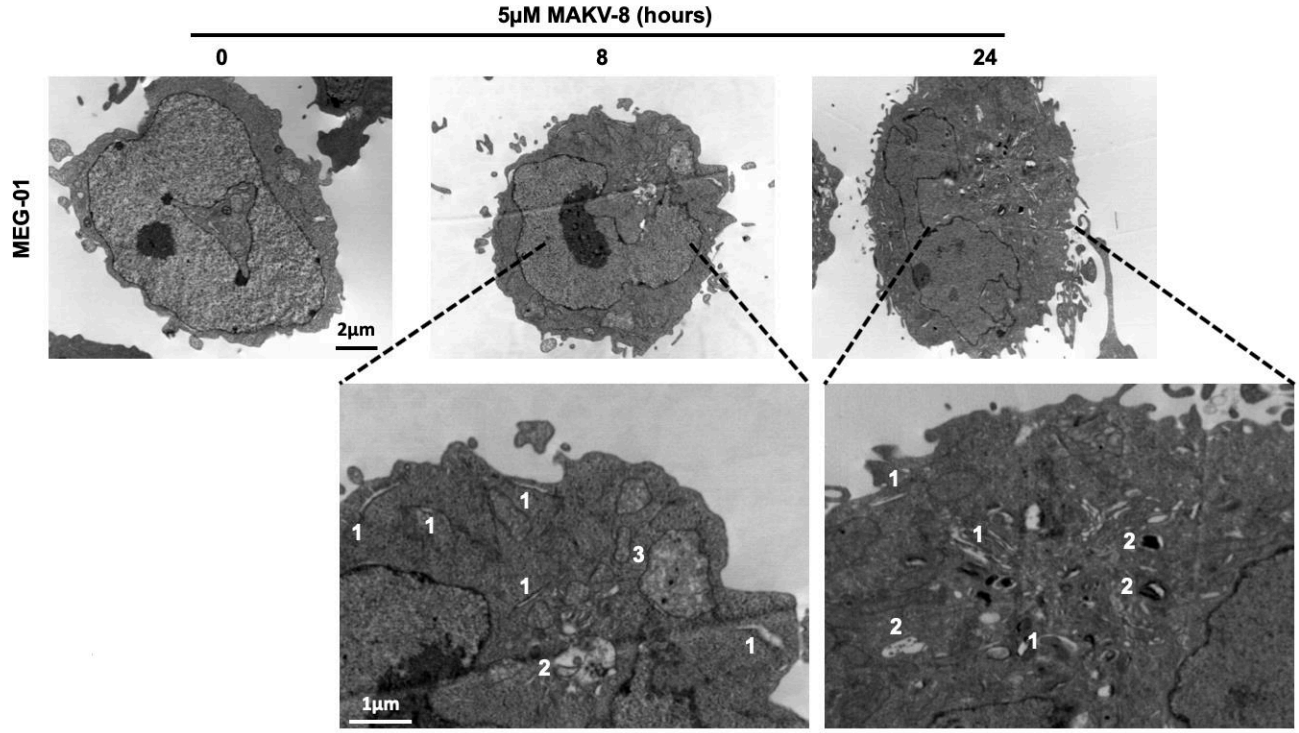

Figure 4, Lernoux *et al.*

H

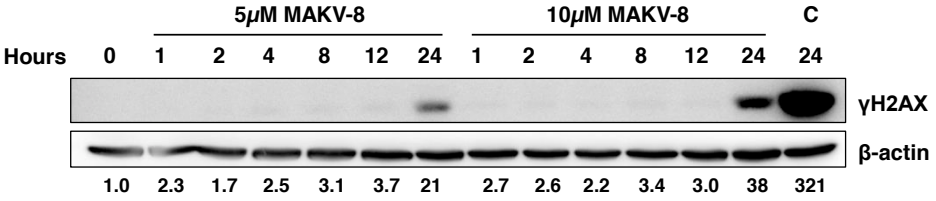

Figure 5

Click here to access/download;Figure;Lernoux et al_Figure 5.pptx

Figure 5, Lernoux *et al.*

A

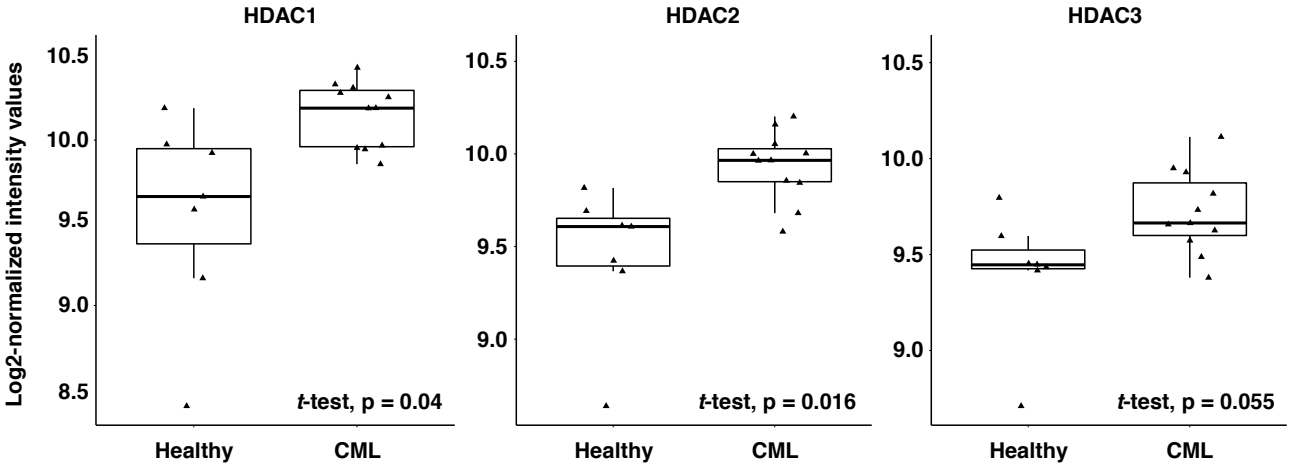

Figure 5, Lernoux *et al.*

B

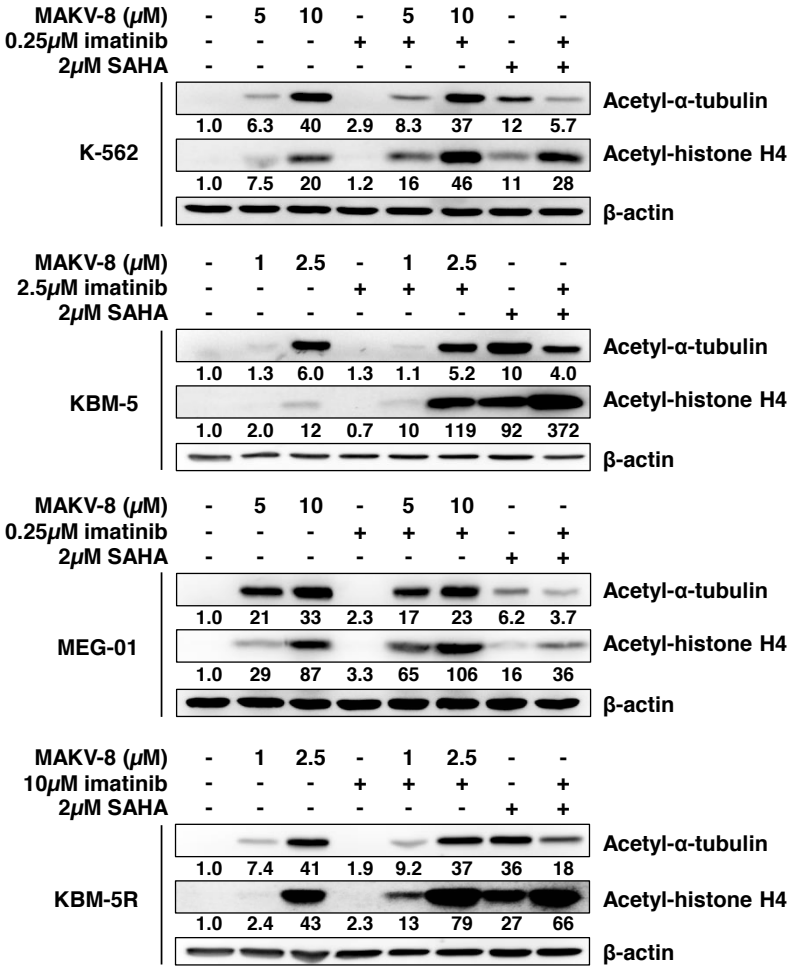

Figure 5, Lernoux *et al.*

C

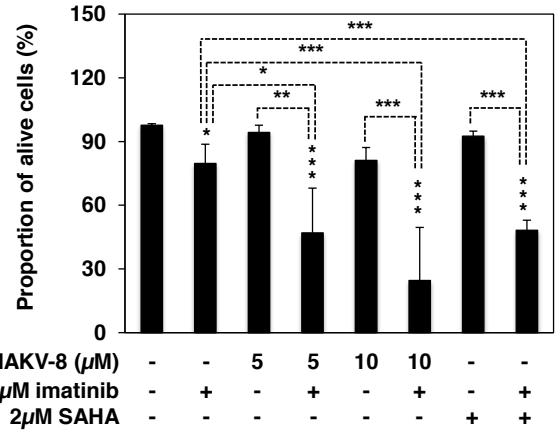

Figure 5, Lernoux *et al.*

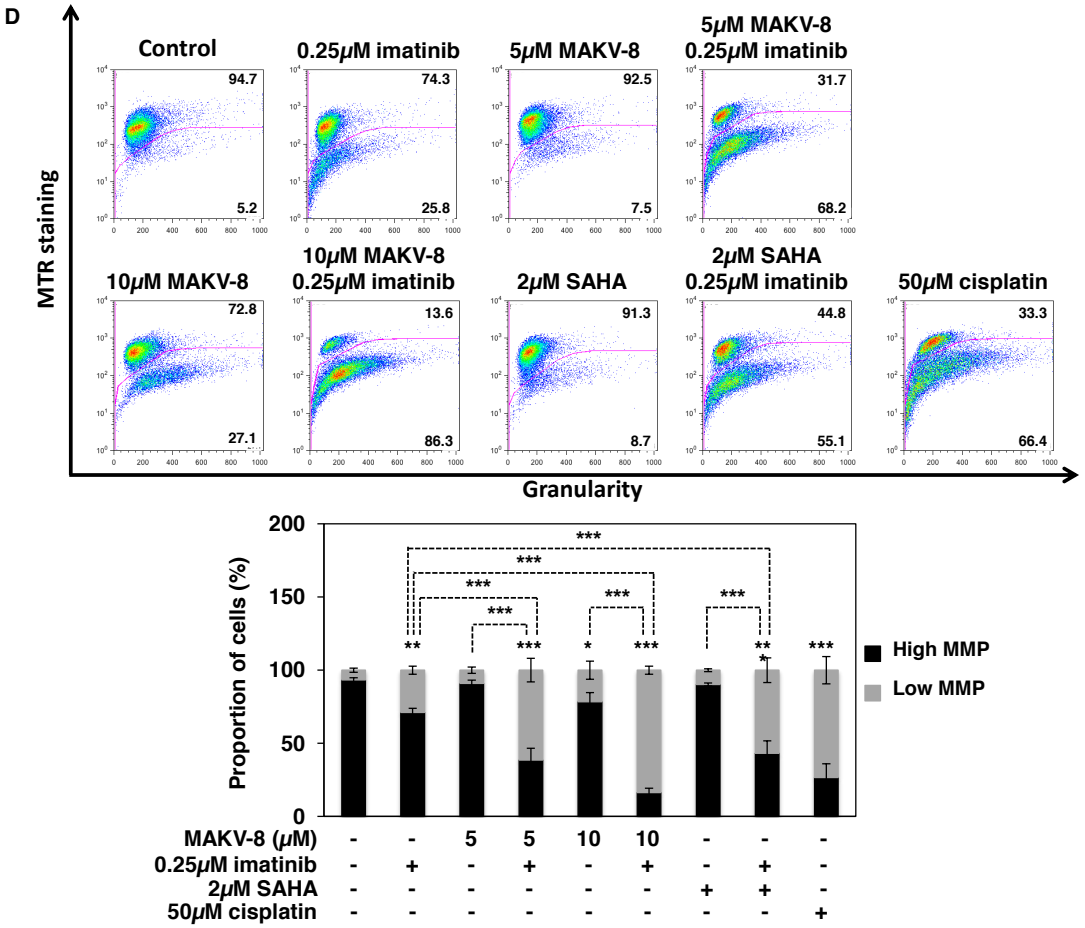

Figure 5, Lernoux *et al.*

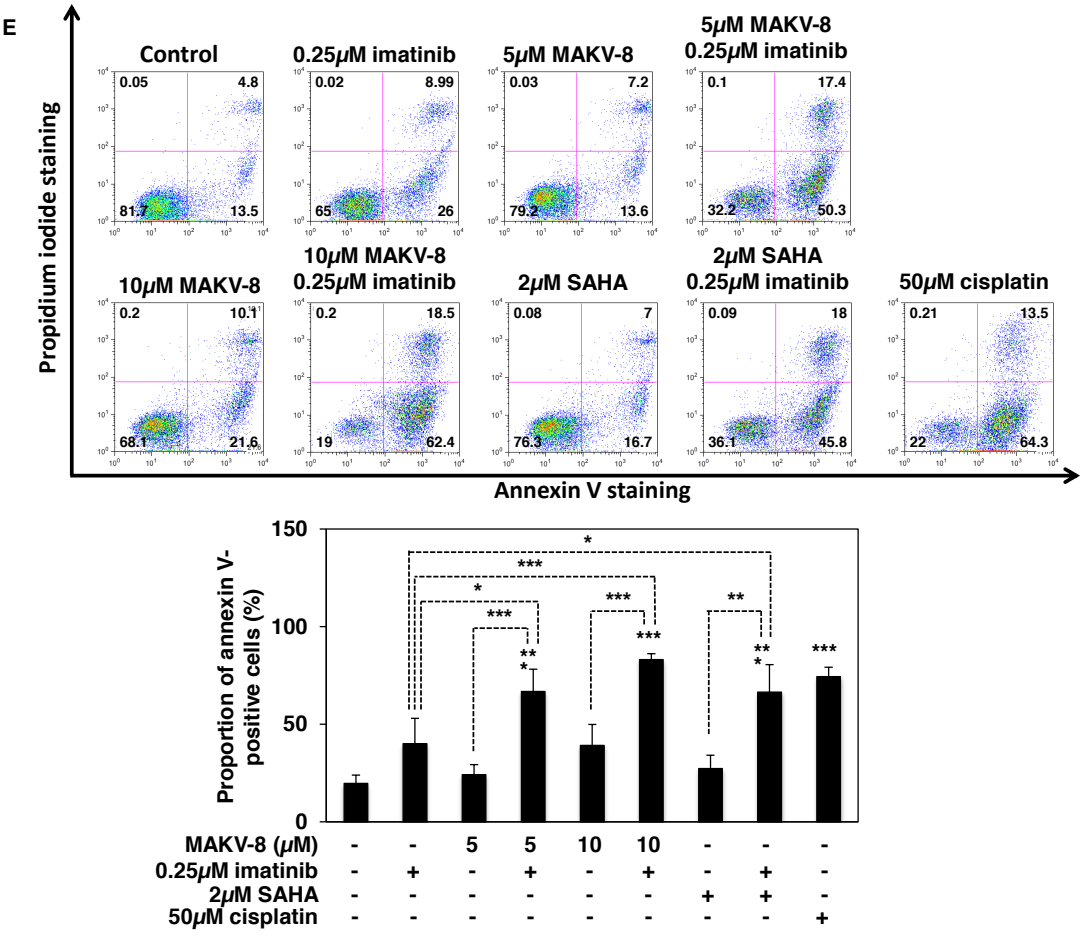

Figure 5, Lernoux *et al.*

F

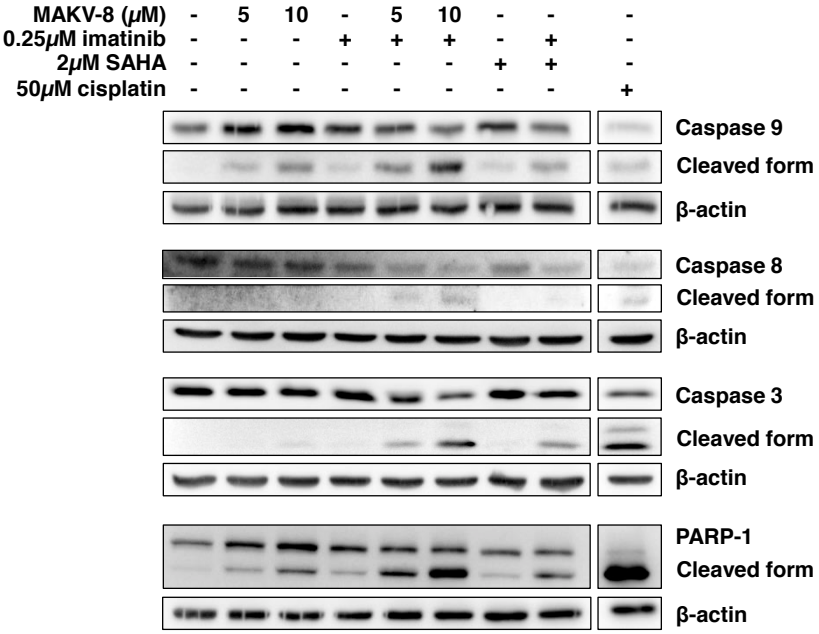

Figure 5, Lernoux *et al.*

G

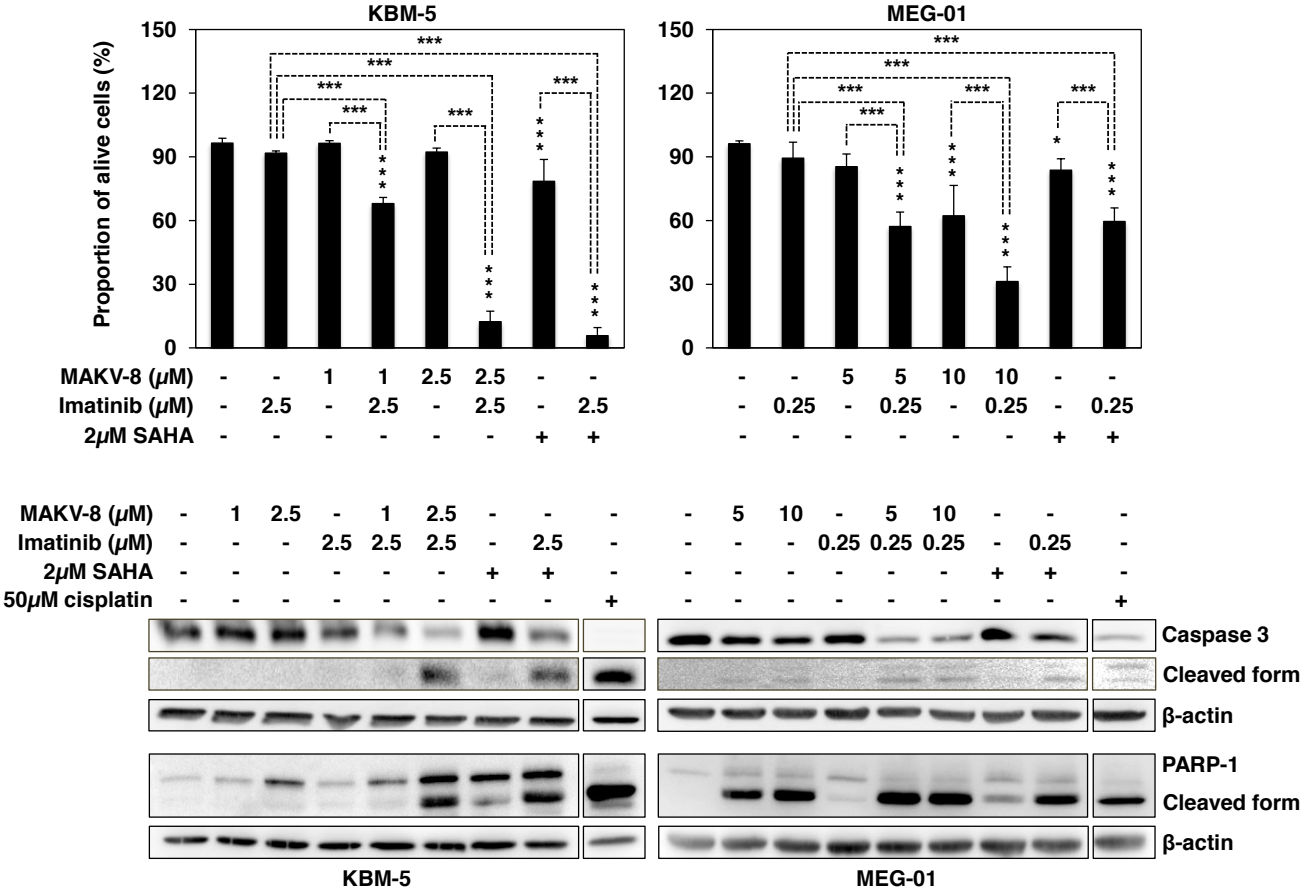

Figure 5, Lernoux *et al.*

H

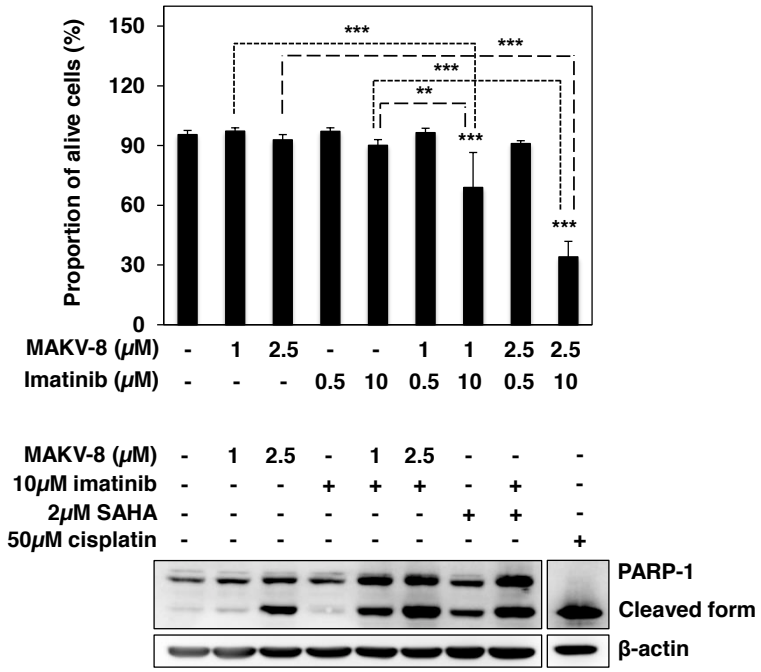

Figure 5, Lernoux *et al.*

I

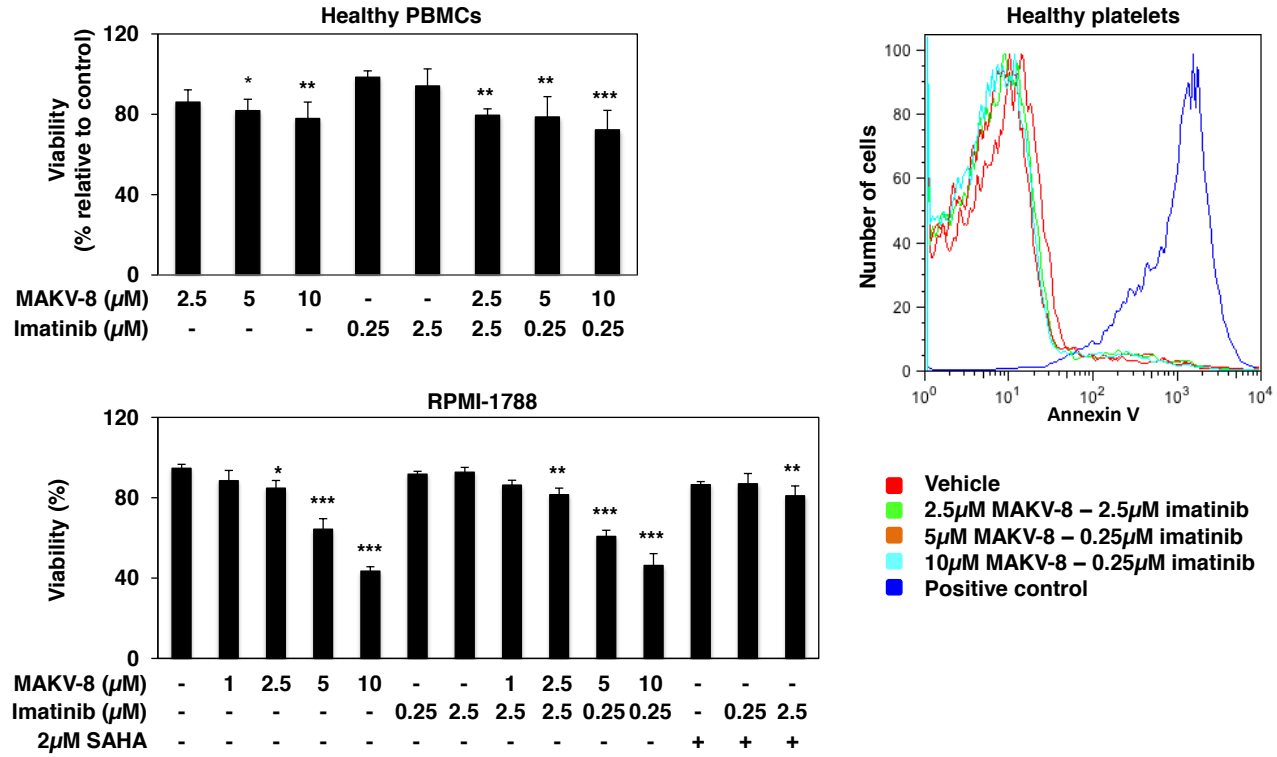

Figure 5, Lernoux *et al.*

J

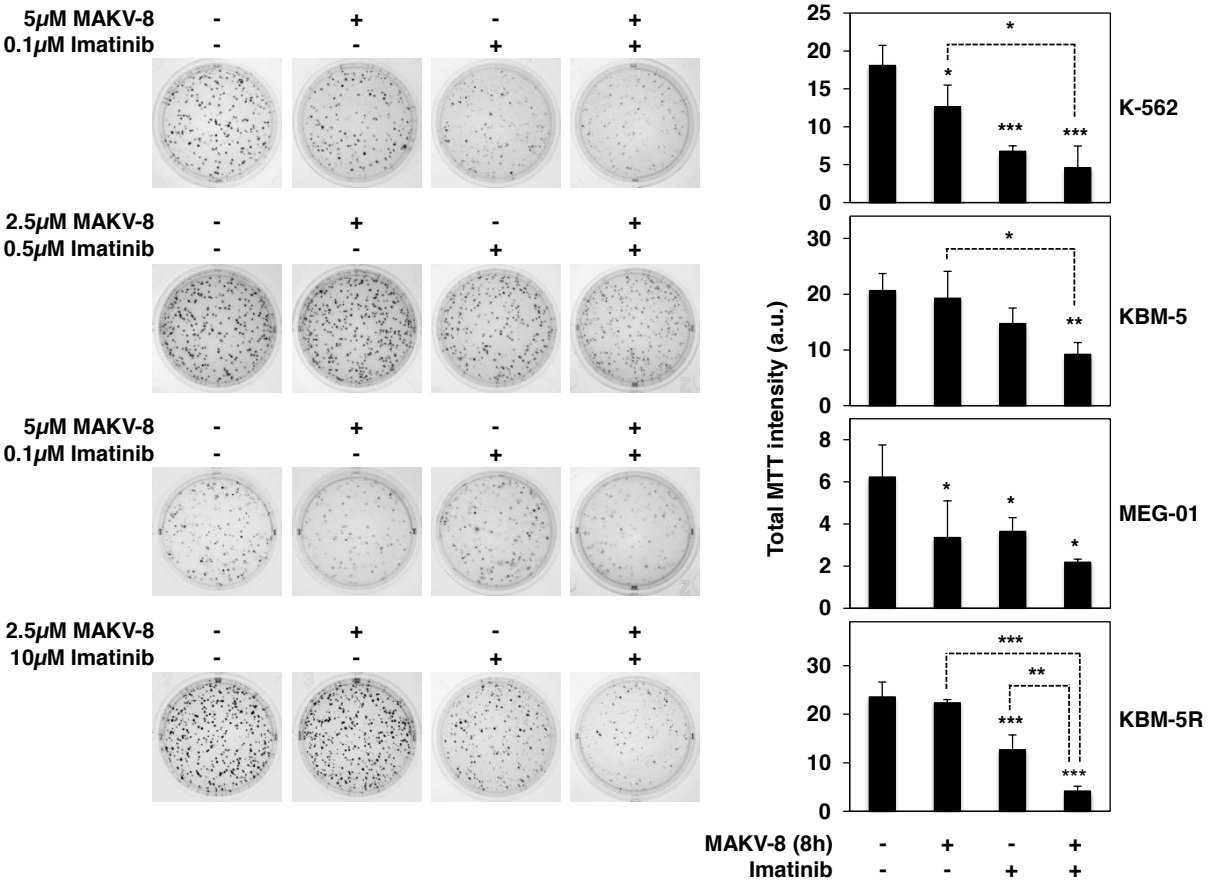

Figure 6

Figure 6, Lernoux *et al.*

Click here to access/download;Figure;Lernoux et al_Figure 6.pptx

A

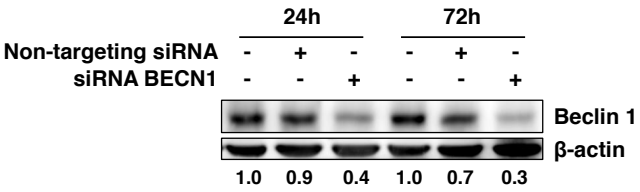

B

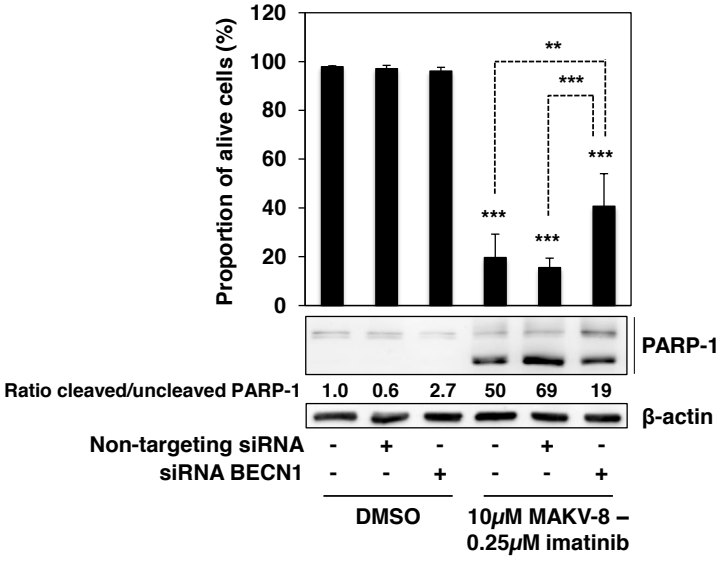

Figure 6, Lernoux *et al.*

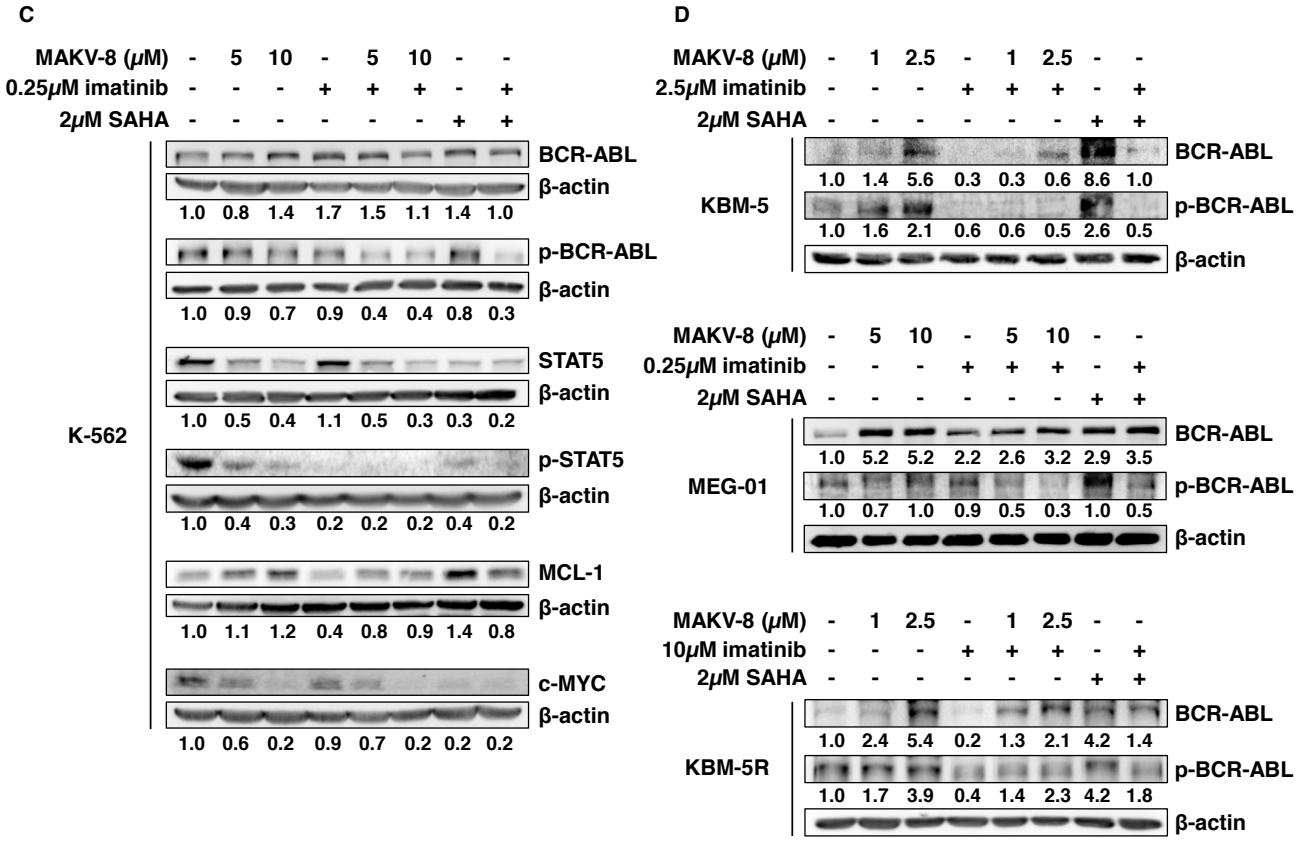

Figure 6, Lernoux *et al.*

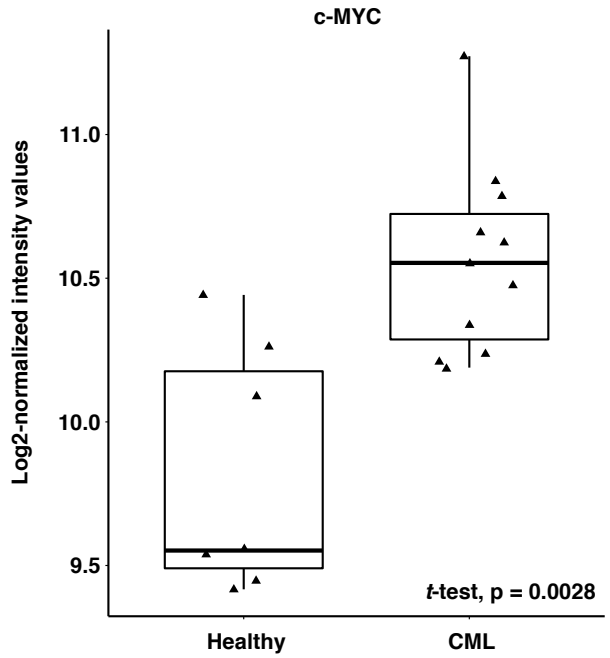

Figure 6, Lernoux *et al.*

F

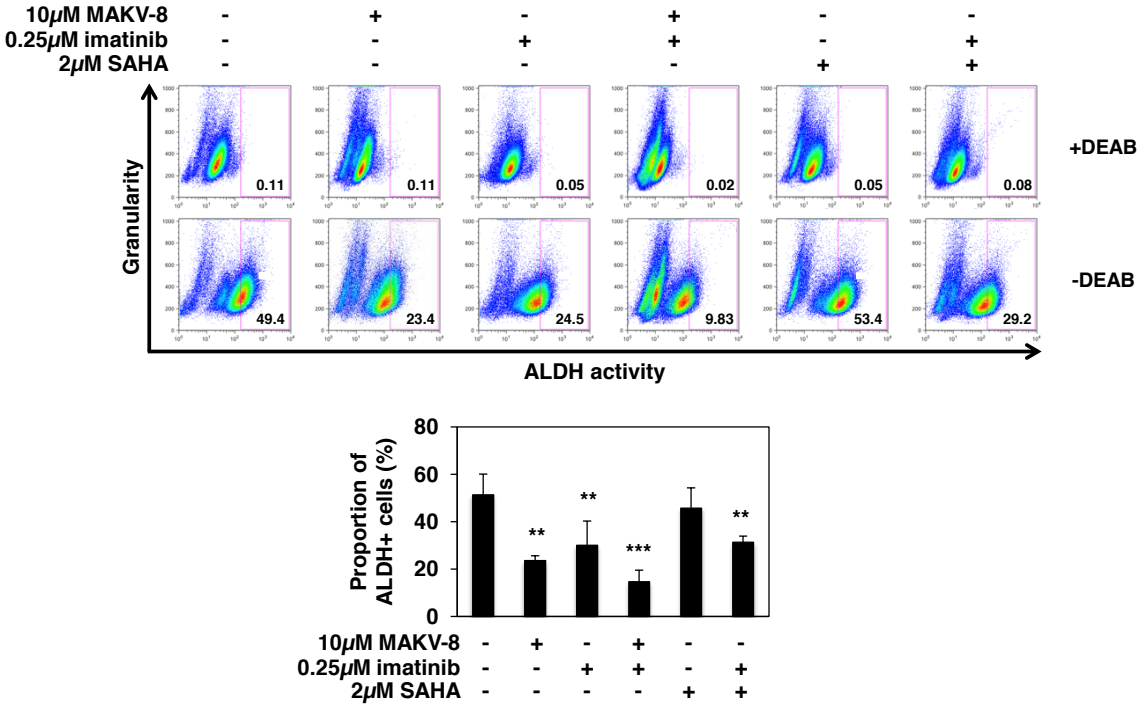

Figure 6, Lernoux *et al.*

G

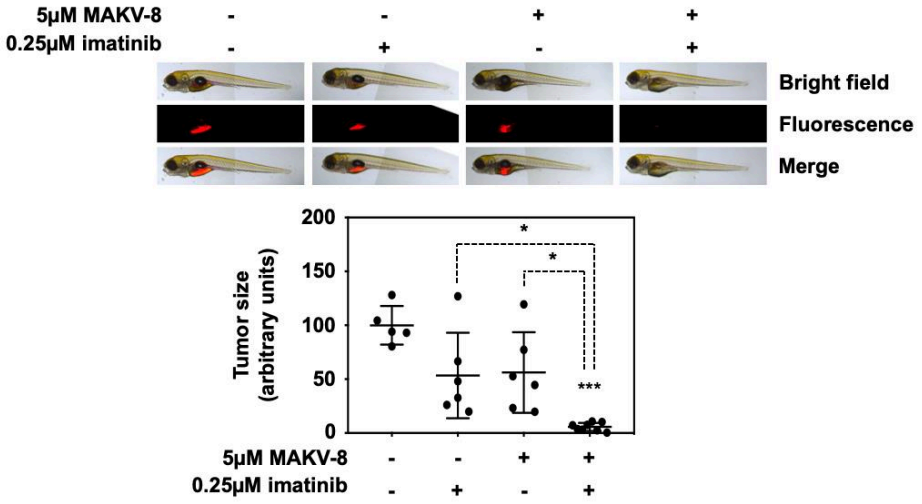

Click here to access/download
Supplementary Material
renamed_3abb3.docx

Aberrant activation or overexpression of histone deacetylase (HDAC) isoenzymes trigger disruptions of the functional acetylation landscape, therefore contributing to the development of numerous cancers. Accordingly, pan- or selective HDAC inhibitors (HDACi) represent a powerful class of epigenetically active therapeutic drugs that have already demonstrated promising anti-cancer properties in pre-clinical studies and are undergoing clinical trials for the therapy of many cancers. The main goal of this project is to develop new therapeutic approaches for the treatment of hematological malignancies combining HDACi to targeted therapies.

In this study, we assessed the anti-cancer activity of the novel hydroxamate-based pan-HDACi MAKV-8, which complied with the Lipinski's "rule of 5", in various chronic myeloid leukemia (CML) cell lines alone or in combination with imatinib. We validated the *in vitro* HDAC inhibitory potential of MAKV-8 and demonstrated efficient binding to the ligand-binding pocket of HDAC isoenzymes by docking analyses. *In cellulo*, MAKV-8 enhanced target protein acetylation, displayed cytostatic and cytotoxic properties, and triggered concomitant ER stress/protective autophagy leading to canonical caspase-dependent apoptosis. Considering the specific up-regulation of selected HDACs in LSCs from CML patients, we investigated the therapeutic potential of MAKV-8 in combination with imatinib against CML cells. First, we highlighted a differential toxicity of a co-treatment with MAKV-8 and imatinib in CML versus healthy cells. We also showed that beclin 1 knockdown prevented MAKV-8-imatinib combination-induced apoptosis. Moreover, MAKV-8 and imatinib co-treatment reduced BCR-ABL-related signaling pathways involved in CML cell growth and survival. Since our results showed that LSCs from CML patients overexpressed c-MYC, MAKV-8-imatinib co-treatment-induced c-MYC down-regulation was importantly accompanied with reduced LSC population. *In vivo*, tumor growth of xenografted K-562 cells in zebrafish was completely abrogated upon combined treatment with MAKV-8 and imatinib.

We also demonstrated that MAKV-15, a new hydroxamate-based compound derived from tubastatin A, acts as a potent and selective HDAC6i *in vitro*. Accordingly, MAKV-15 increases preferentially (about 10 times) the acetylation of the HDAC6 substrate α-tubulin in comparison to a non-HDAC6 substrate *in cellulo*. Interestingly, inhibiting selectively HDAC6 activity is insufficient to trigger any anti-cancer effects. Nevertheless, stronger accumulation of poly-ubiquitinated proteins accompanied with a potentiation of the anti-cancer effects are observed upon co-treatment of multiple myeloma cells with MAKV-15 and bortezomib, suggesting a potential sensitization of cells to a third compound. However, the variety of responses to tri-therapies highlights the heterogeneity among MM cell lines and suggests distinct mechanisms of action that require further investigations.

Collectively, the present findings provide a rational basis to further assess the potential of HDACi in combination treatments as novel therapeutic approaches for hematological malignancies.

Fondation Recherche Cancer & Sang
télévie
LIONS INTERNATIONAL
RSL Recherches Scientifiques Luxembourg